Tata McGraw-Hill

Control Systems

Principles and Design

Second Edition









M Gopal

Copyrighted material



Tata McGraw-Hill

Information contained in this work has been obtained by Tata McGraw-Hill, from sources believed to be reliable. However, neither Tata McGraw-Hill nor its authors guarantee the accuracy or completeness of any information published herein, and neither Tata McGraw-Hill nor its authors shall be responsible for any errors, omissions, or damages arising out of use of this information. This work is published with the understanding that Tata McGraw-Hill and its authors are supplying information but are not attempting to render engineering or other professional services. If such services are required, the assistance of an appropriate professional should be sought.

© 2002, 1997, Tata McGraw-Hill Publishing Company Limited

Eighth reprint 2006
RALYYRBKRQZRY

No part of this publication can be reproduced in any form or by any means without the prior written permission of the publishers

This edition can be exported from India only by the publishers,
Tata McGraw-Hill Publishing Company Limited

ISBN 0-07-048289-6

Published by Tata McGraw-Hill Publishing Company Limited,
7 West Patel Nagar, New Delhi 110 008, Typeset at Script Makers 19,
A1-B DDA Market, Pashchim Vihar, New Delhi 110 063 and printed at
Sai PrintOPack Y-56, Okhla Industrial Area, Phase-II,
New Delhi-110020

Cover: De Unique

The *McGraw-Hill* Companies

Copyrighted material

Contents

Preface to the Second Edition *vi*
Preface to the First Edition *ix*

1. Introduction to the Control Problem **1**
1.1 Control Systems: Terminology and Basic Structure *1*
1.2 The Genesis and Essence of the Feedback Control Theory *13*
1.3 Feedforward-Feedback Control Structure *21*
1.4 Multivariable Control Systems *25*
1.5 Scope and Organization of the Book *33*

2. Dynamic Models and Dynamic Response **37**
2.1 Introduction *37*
2.2 State Variable Models *40*
2.3 Impulse Response Models *46*
2.4 Transfer Function Models *53*
2.5 Models of Disturbances and Standard Test Signals *59*
2.6 Dynamic Response *63*
2.7 Characteristic Parameters of First- and Second-order Models *69*
2.8 Models of Mechanical Systems *77*
2.9 Models of Electrical Circuits *87*
2.10 Models of Thermal Systems *98*
2.11 Models of Hydraulic Systems *107*
2.12 Obtaining Models from Experimental Data *113*
2.13 Systems with Dead-time Elements *114*
2.14 Loading Effects in Interconnected Systems *117*

Copyrighted material

Review Examples 120
Review Questions 130
Problems 131

3. Models of Industrial Control Devices and Systems 141
3.1 Introduction *141*
3.2 Generalized Block Diagram of a Feedback System *142*
3.3 Block Diagram Manipulations *144*
3.4 Signal Flow Graphs and the Mason's Gain Rule *150*
3.5 DC and AC Motors in Control Systems *159*
3.6 Motion Control Systems *175*
3.7 Hydraulic Devices for Motion Control *193*
3.8 Pneumatic Devices for Process Control *203*
Review Examples 211
Review Questions 219
Problems 222

4. Basic Principles of Feedback Control 237
4.1 Introduction *237*
4.2 The Control Objectives *241*
4.3 Feedback Control System Characteristics *251*
4.4 Proportional Mode of Feedback Control *264*
4.5 Integral Mode of Feedback Control *267*
4.6 Derivative Mode of Feedback Control *272*
4.7 Alternative Control Configurations *276*
4.8 Multivariable Control Systems *280*
Review Examples 283
Review Questions 290
Problems 292

5. Concepts of Stability and the Routh Stability Criterion 305
5.1 Introduction *305*
5.2 Bounded-input Bounded-output Stability *307*
5.3 Zero-input Stability *313*
5.4 The Routh Stability Criterion *314*
5.5 Stability Range for a Parameter *327*
Review Examples 329
Review Questions 332
Problems 333

6. The Performance of Feedback Systems 337
6.1 Introduction *337*
6.2 The Performance Specifications *339*

Copyrighted material

6.3 Response of a Standard Second-order System *343*
6.4 Effects of an Additional Zero and an Additional Pole *356*
6.5 Desired Closed-Loop Pole Locations and the Dominance-Condition *363*
6.6 Steady-state Error Constants and System-type Number *366*
6.7 Introduction to Design and Compensation *371*
Review Examples *382*
Review Questions *390*
Problems *392*

7. Compensator Design Using Root Locus Plots **404**
7.1 Introduction *404*
7.2 The Root Locus Concept *405*
7.3 Guidelines for Sketching Root Loci *418*
7.4 Selected Illustrative Root Loci *432*
7.5 Reshaping the Root Locus *443*
7.6 Cascade Lead Compensation *455*
7.7 Cascade Lag Compensation *463*
7.8 Cascade Lag-Lead Compensation *468*
7.9 Minor-Loop Feedback Compensation *472*
7.10 Compensation for Plants with Dominant Complex Poles *477*
7.11 The Root Locus of Systems with Dead-Time *483*
7.12 Sensitivity and the Root Locus *487*
Review Examples *492*
Review Questions *501*
Problems *502*

8. The Nyquist Stability Criterion and Stability Margins **513**
8.1 Introduction *513*
8.2 Development of the Nyquist Criterion *517*
8.3 Selected Illustrative Nyquist Plots *526*
8.4 Stability Margins *536*
8.5 The Bode Plots *544*
8.6 Stability Margins on the Bode Plots *563*
8.7 Stability Analysis of Systems with Dead-Time *566*
8.8 Frequency Response Measurements *571*
Review Examples *577*
Review Questions *583*
Problems *584*

Copyrighted material

9. Feedback System Performance Based on the Frequency Response **593**
9.1 Introduction *593*
9.2 Performance Specifications in Frequency Domain *596*
9.3 Correlation between Frequency-domain and Time-domain Specifications *598*
9.4 Constant-M Circles *608*
9.5 The Nichols Chart *614*
9.6 Sensitivity Analysis in Frequency Domain
Review Examples *626*
Review Questions *629*
Problems *630*

10. Compensator Design Using Bode Plots **638**
10.1 Introduction *638*
10.2 Reshaping the Bode Plot *639*
10.3 Cascade Lead Compensation *649*
10.4 Cascade Lag Compensation *662*
10.5 Cascade Lag-Lead Compensation *670*
10.6 Robust Control Systems *675*
Review Examples *682*
Review Questions *688*
Problems *689*

11. Hardware and Software Implementation of Common Compensators **694**
11.1 Introduction *694*
11.2 Passive Electric Networks *695*
11.3 Operational Amplifier Usage *705*
11.4 Use of Digital Computer as a Compensator Device *708*
11.5 Configuration of the Basic Computer-control Scheme *710*
11.6 Principles of Signal Conversion *712*
11.7 Digital Implementation of Analog Compensators *716*
11.8 Tunable PID Controllers *728*
11.9 Ziegler-Nichols Methods for Controller Tuning *749*
Review Examples *761*
Review Questions *764*
Problems *766*

12. Control System Analysis Using State Variable Methods **773**
12.1 Introduction 773
12.2 Matrices 774

Copyrighted material

12.3 State Variable Representation 779
12.4 Conversion of State Variable Models to Transfer Functions 785
12.5 Conversion of Transfer Functions to Canonical State Variable Models 790
12.6 Solution of State Equations 804
12.7 Concepts of Controllability and Observability 813
12.8 Equivalence between Transfer Function and State Variable Representations 823
Review Examples 828
Review Questions 835
Problems 837

Appendix A: Mathematical Background 846
A.1 Introduction 846
A.2 Functions of a Complex Variable 846
A.3 Laplace Transforms 854
A.4 Table of Transforms 859

Appendix B: MATLAB Environment 861

Appendix C: Control Theory Quiz 898

References 929

Companion Book 938

Answers to Problems 942

Index 961

Copyrighted material

chapter 1

Introduction to the Control Problem

1.1 CONTROL SYSTEMS: TERMINOLOGY AND BASIC STRUCTURE

In recent years, control systems have assumed an increasingly important role in the development and advancement of modern civilization and technology. Practically every aspect of our day-to-day activities is affected by some type of control system. A bathroom toilet tank is a control system. A home-heating system, a refrigerator, an air-conditioner, and an automobile are all control systems. Control systems are indispensable in modern industrial processes. We find control systems in all sectors of industry, such as quality control of manufactured products, automatic assembly line, machine-tool control, space technology and weapon systems, transportation systems, power systems, robotics, and many others. Even such problems as inventory control, and socio-economic systems control may be approached from the theory of feedback control. In this book we will deal with the control of *engineering systems* that are governed by the laws of physics and are therefore called *physical systems*.

In control parlance, the system to be controlled is given various names: *process*, *plant*, and *controlled system* being perhaps the most common. In the so-called process industries (chemicals, petroleum, steam power, fuel, etc.). one repeatedly encounters the need to control temperature, flow rate, liquid-level in vessels, pressure, humidity, chemical composition, and the like; such applications are generally considered *process control* applications. Historically, the wide practical application of control first took place in the process area. Most of the basic concepts were developed and brought to successful realization by the intuitive and experimentally-oriented engineering methods typical of the 1900 to 1940 era.

Copyrighted material

Around the time of the Second World War, the technical needs of military systems—automatic airplane pilots, gun-positioning systems, radar antenna control systems, and the like—led to more scientific approaches in the control engineering field. A comprehensive mathematical theory—the theory of *servomechanism*[1]—aimed mainly at applications wherein the need is to control mechanical motions (position, velocity, or acceleration), was developed around 1940 to 1950. Since this time, the design methods of the process-control area, and the servomechanism area have gradually converged. The terminology of the two areas is also converging. The word 'process' is now in use for all types of controlled systems. Also, irrespective of the area of application, the word 'servomechanism' (or *servo system*) is used for a *command following system* wherein the controlled attribute of the system is required to follow a given command.

Figure 1.1 shows the input–output configuration of a process (or plant). Process *outputs* are the response variables which we require to behave in some specified fashion. Process *inputs* are flows of energy and/or material that cause the process to react or respond. The inputs are classified into *manipulated inputs* (subject to our control) and *disturbance inputs* (undesirable and unavoidable effects beyond our control, generated from outside process-environment, and from within). The presence of the disturbance is one of the main reasons of using control. Clever management of manipulated variables so as to counteract the effects of disturbances is the primary role of the *controller*. Figure 1.2 shows the input–output configuration of a *control system*.

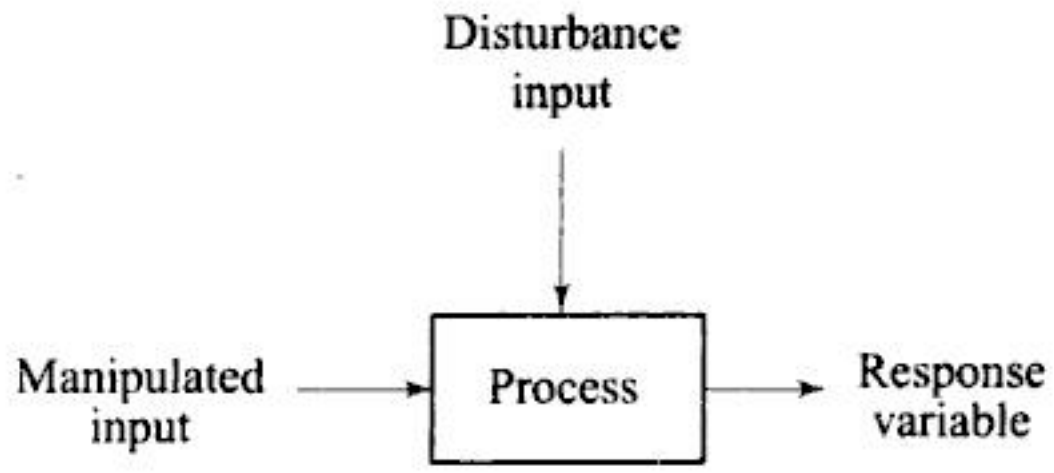


Fig. 1.1 *Process input–output configuration*

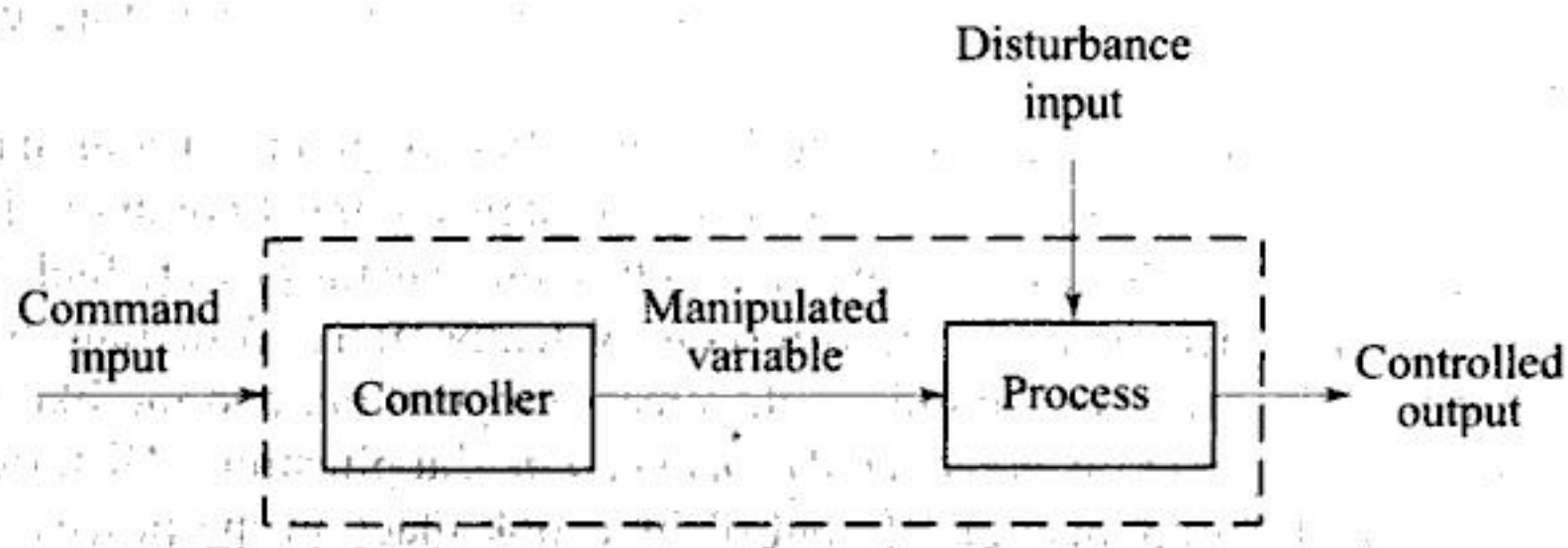


Fig. 1.2 *Input–output configuration of a control system*

1. The word servomechanism originated from the words servant (or slave) and mechanism.

Copyrighted material

When the desired value of the controlled outputs is more or less fixed and the main problem is to reject disturbance effects, the control system is sometimes called a *regulator*. The command input for a regulator becomes a constant and is called *set-point*, which corresponds to the desired value of the controlled output. The set-point may however be changed in time from one constant value to another, and the need for the control of manipulated variables arises from the requirements of both the set-point changes and the disturbance rejection. The control problem is then called *resetting control problem*.

In the *follow-up* or *tracking system*, the controlled output is required to follow or track a time-varying command input. For such systems, the need for the control of manipulated variables arises from the requirements of command-following as well as disturbance rejection.

In the configuration of Fig. 1.3, the controller receives information about the desired value of the controlled output and uses this information as a means of control of the manipulated variables. In contrast to this configuration, the configuration of Fig. 1.4 utilizes measurement of the controlled output in order to compare the actual output with the desired output response. The controller then uses this difference as a means of control of manipulated variables. The configuration of Fig. 1.3 is that of an *open-loop control system* while that of Figure 1.4 is that of *closed-loop control system* or *feedback control system*.

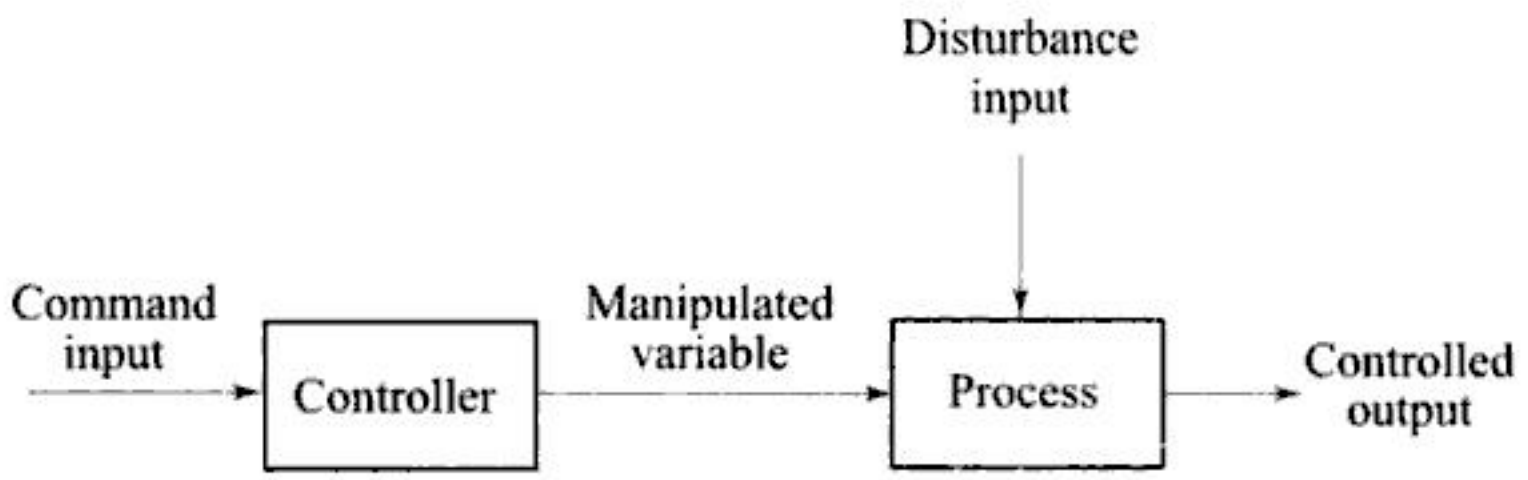


Fig. 1.3 *Input–output configuration of an open-loop control system*

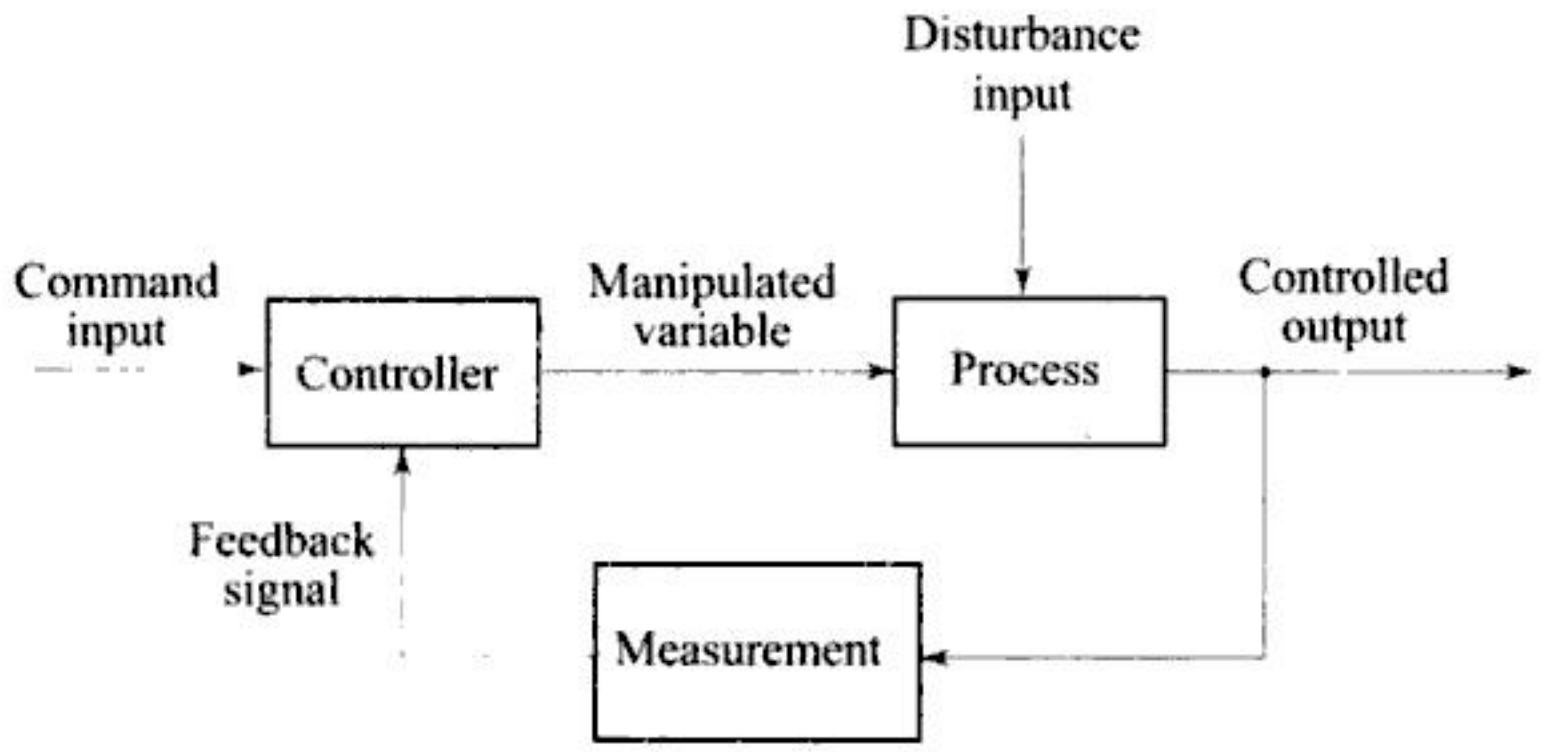


Fig. 1.4 *Input–output configuration of a closed-loop control system*

Copyrighted material



You have either reached a page that is unavailable for viewing or reached your viewing limit for this book.

If because of disturbance, the water level H has decreased, then the float and the points A and B of the lever move down. The inlet valve allows the inflow of water, thus bringing about a gradual growth in the water level H. The inflow of water is stopped automatically whenever the water level reaches the preset height.

The float and linkage in Fig. 1.5a perform the functions of error detection and generation of the correcting signal. This is clear from the geometry of the linkage shown in Fig. 1.5b. For small movements,

$$\frac{AA'}{AC} = \frac{AA'}{AB + BC} = \frac{BB'}{BC} \qquad \text{or} \qquad \frac{e}{l_2 + l_1} = \frac{u}{l_1}$$

Therefore, $$u = \frac{l_1}{l_1 + l_2} e$$

where

e = error signal produced by the float; and

u = control signal produced by the linkage.

The control signal u is thus proportional to the error signal e (*control logic*); the gain $K = \dfrac{l_1}{l_1 + l_2}$ can be varied by shifting the lever axis (point B): the shift of the lever axis towards the float (point A) corresponds to an increase in the gain. The functional block diagram of the toilet tank control system (Fig. 1.5c) has been redrawn in Fig. 1.6, showing the error detector and control logic blocks separately.

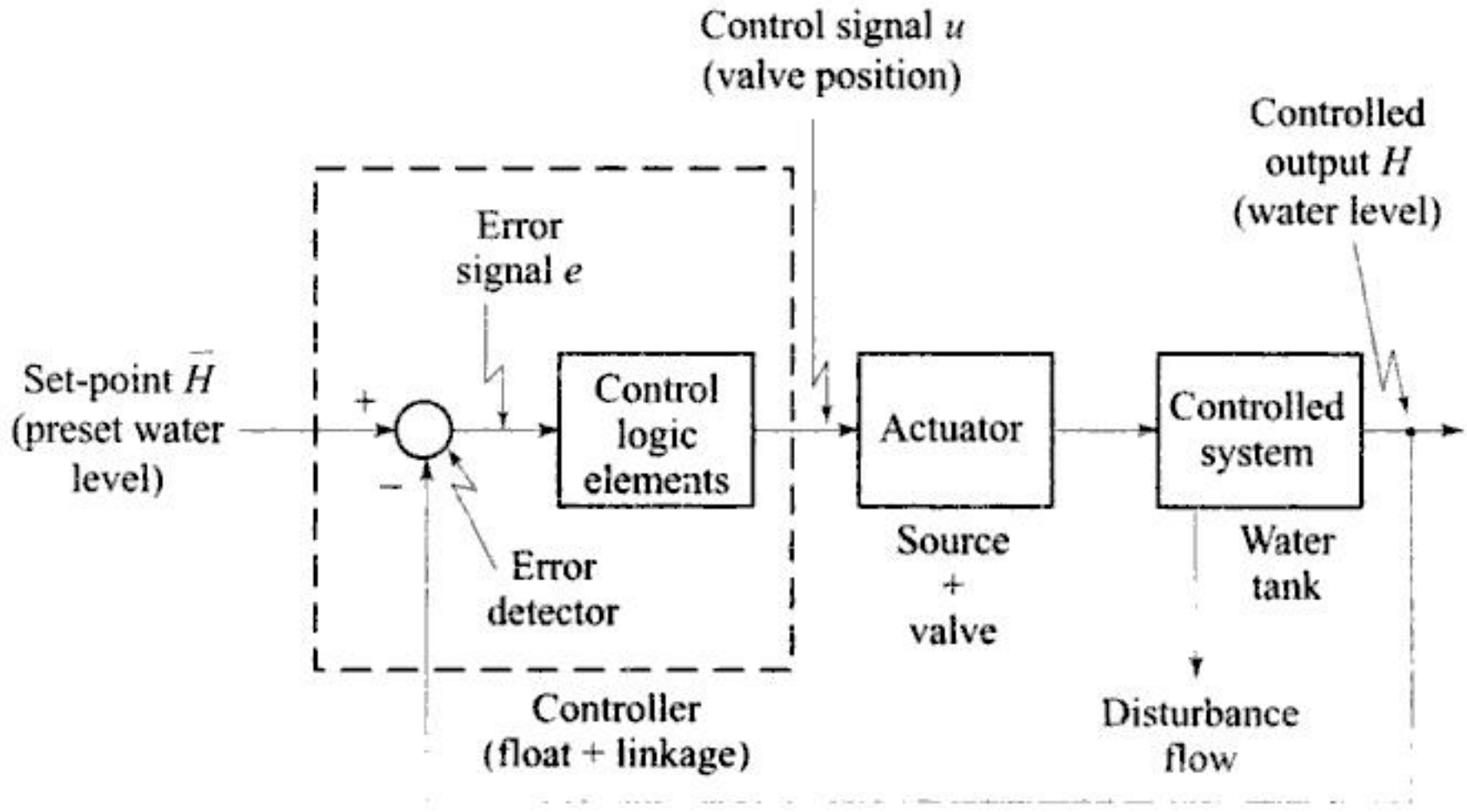


Fig. 1.6 *Functions of controller in control system of Fig. 1.5c*

Although a toilet tank is a very simple mechanism, it has all the ingradients of

Copyrighted material

Example 1.2

Automobile Driving System

The system to be controlled has two inputs (steering, and acceleration/braking) and two controlled outputs (heading, and speed). The two command inputs are the direction of the highway, and speed limits with traffic signals. A block diagram of this two-input, two-output system is shown in Fig. 1.7.

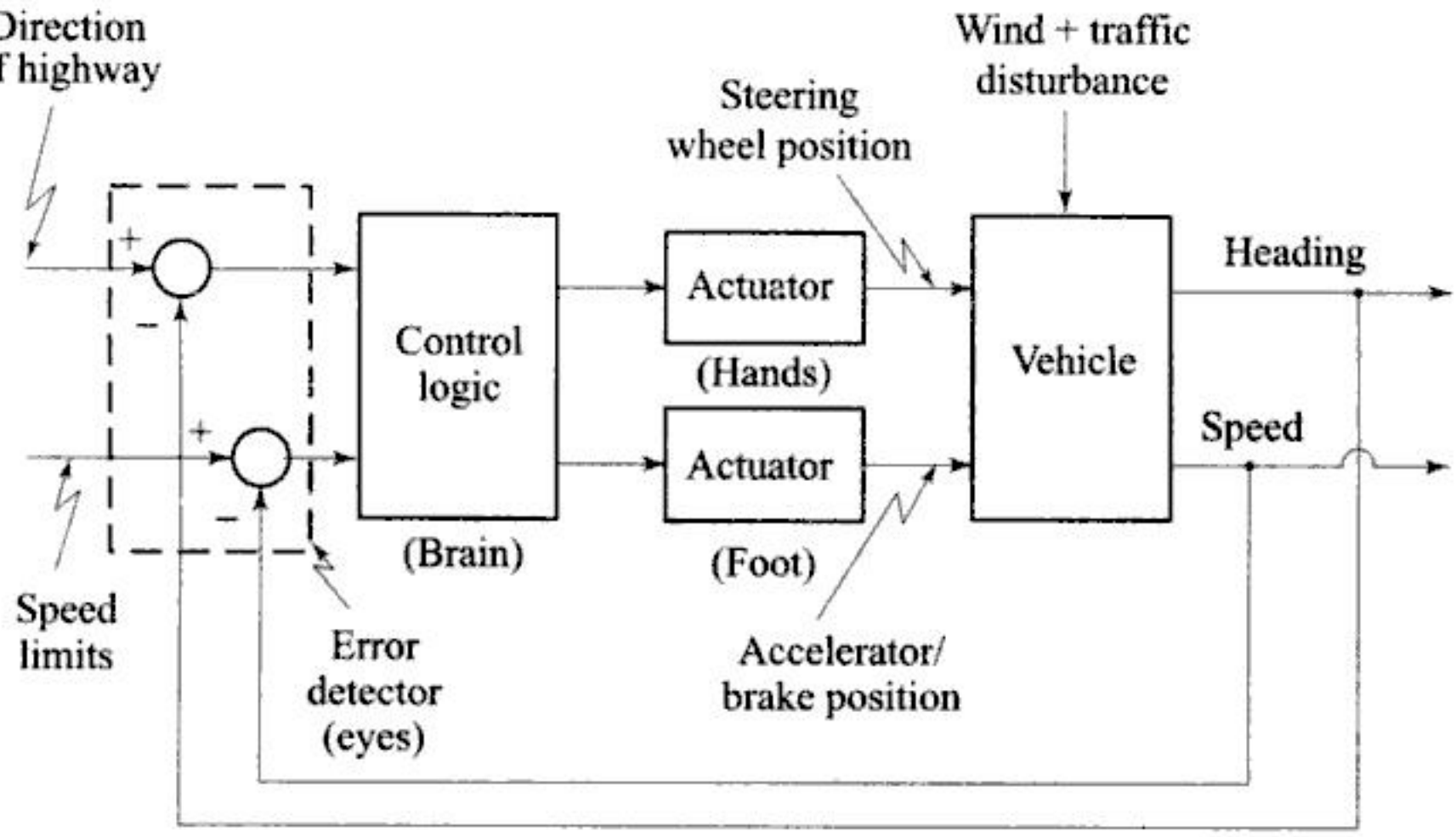


Fig. 1.7 *Automobile driving control system*

Systems with more than one controlled output and command input are called *multivariable* or *multi-input, multi-output* (MIMO) systems. On the other hand, in *single-input, single-output* (SISO) systems, a single output is controlled by single input. In multivariable systems, an input that is meant to control a particular output, also affects the other controlled outputs. This coupling is called *interaction*.

The automobile-driving system is a MIMO system. We can *decouple* this system into two SISO systems for the purpose of design because the interaction is negligible. Steering control affects the heading and not speed, and accelerator control affects the speed and not the heading. However, braking of the vehicle for speed control decreases the side forces at the tyre-road interface for directional control, and with locked wheels the directional control is completely lost. If we consider this interaction negligible, we can consider the vehicle-heading control system as a decoupled SISO system, with no interaction with vehicle-speed control system.

The command inputs for an automobile on the road cannot be constant setpoints. These inputs depend on the traffic and road conditions and vary in an uncontrolled manner. The actual signal inputs to the system are derived by the driver from the actual road and traffic conditions. The human operator subsystem will therefore be a component in the overall control system of the auto-

Copyrighted material

mobile, as shown in Fig. 1.7. The desired course and speed are compared with a measurement of the actual course and speed in order to generate a measurement of the error. The human operator then controls the manipulated variables (steering wheel position, accelerator/brake position) in a manner (control logic) which reduces the absolute error.

▲▲

Comparison of Figs 1.6 and 1.7 gives many common features of the two closed-loop systems. However, the two systems differ clearly in one aspect. In Fig. 1.7, both the feedback of the controlled outputs (actual course, and speed of travel) for comparison with command inputs (desired course, and speed of travel), and the control actions (rotation of steering wheel, and acceleration/braking) take place through the human operator. In Fig. 1.6, the human operator has been replaced by automatic error detecting and correcting devices; both the feedback of the controlled output (actual water level in the tank), and the correcting action (control of the valve position) take place without the need of a human operator. Such systems, therefore, are *automatic closed-loop control systems*. The systems with human operators included into the closed-loop are *man-machine control systems*.

Example 1.3

Hydraulic Power Steering Mechanism

Many automobiles have power steering which utilizes hydraulic amplifiers for the amplification of the force applied to the wheels. A schematic diagram of the hydraulic power steering mechanism is shown in Fig. 1.8a. The command input to the system is the rotation of the steering wheel by the driver and the controlled output is the vehicle heading, in a command-following mode (note that the hydraulic power steering mechanism is a sub-system of the automobile driving system shown in Fig. 1.7).

When the steering wheel is in the zero position, i.e., the cross bar is horizontal, the tyre wheels are directed parallel to the longitudinal axis of the vehicle. For this condition, the spool is in the neutral position and the oil supply to the power cylinder is cutoff. When the steering wheel is turned anti-clockwise through an angle θ_r, the spool is made to move towards right by an amount x with the help of the gear mechanism. The high-pressure oil enters on the left-hand side of the power cylinder causing the power piston and hence the power ram to move towards right by an amount y. Through a proper drive linkage, a torque is applied to the wheels causing a displacement θ of the wheels.

A rigid linkage bar connects the power ram and the movable valve housing. Movement y of the power ram towards the right causes a movement z of the valve housing in such a direction as to seal off the high pressure line.

A simple model of the load on the power piston is shown in Fig. 1.8b. The wheel-and-axle mass M, tyre stiffness K, and viscous friction coefficient B are the parameters of the assumed model. A nominal load is included in the plant

Copyrighted material

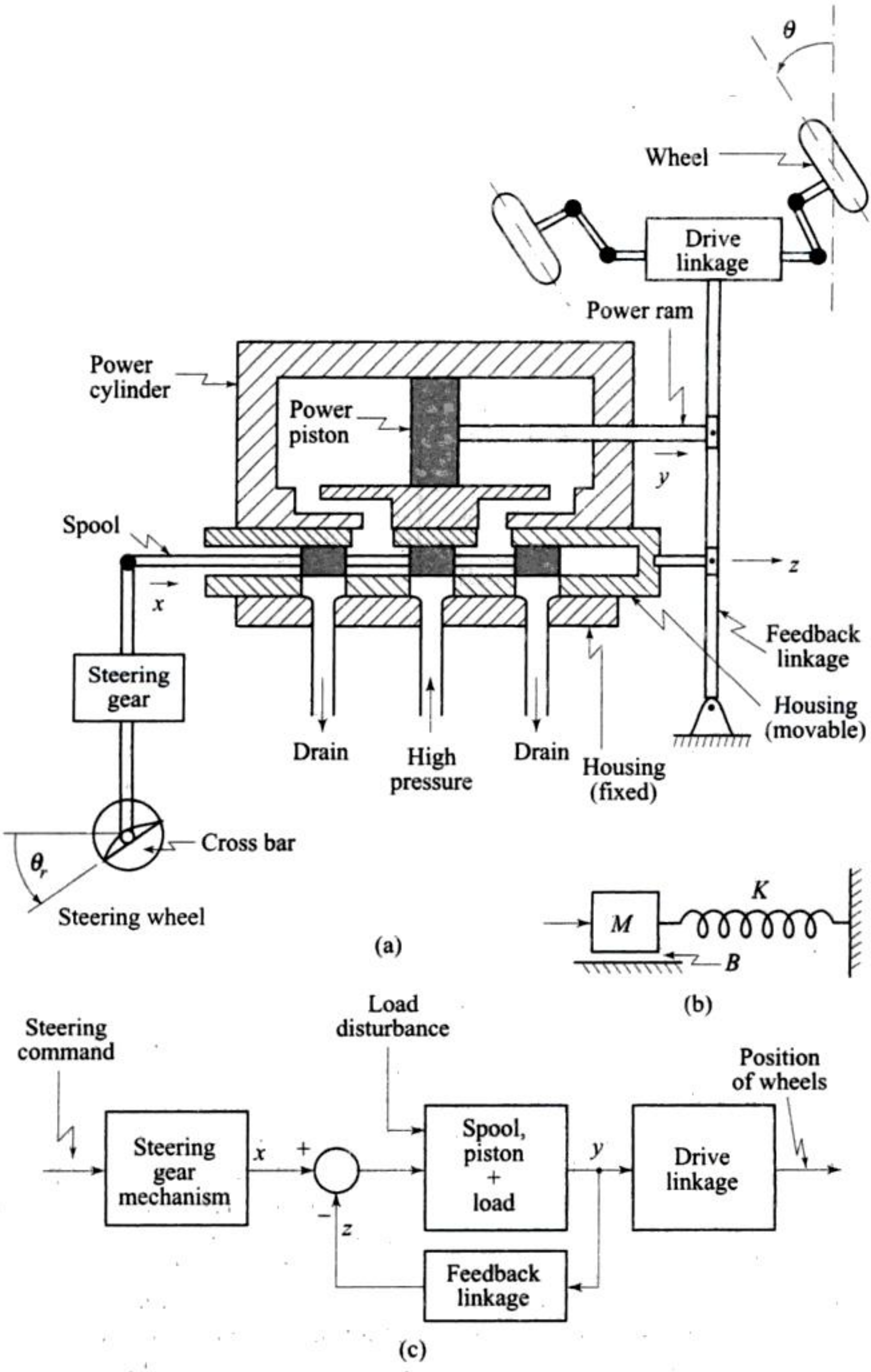


Fig. 1.8 *Hydraulic power steering mechanism*

Copyrighted material

model for the control design. The main disturbance input is the deviation of the load from the nominal estimated value as a result of uncertainty in our estimate, effect of road conditions, and wind power.

Figure 1.8c shows the functional block diagram of the hydraulic power steering mechanism; sub-blocks corresponding to control logic, actuator, etc., have not been shown. Identification of these blocks requires modelling of the system. Detailed study of the system will be taken up in Chapter 3.

Example 1.4

Residential Heating System

In this system, the indoor temperature is the response variable of interest, and it is affected by the main disturbance input—the outdoor temperature. In the scheme of Fig. 1.9, the desired temperature, which is the command-input temperature, is set on a calibrated dial. This positions the valve that admits the steam for circulation through the radiator. The valve dial is calibrated when the environment temperature has certain value. When this value changes significantly, the controlled temperature will deviate from the desired value by a large error and hence precise control will not be realized. The open-loop scheme of Fig. 1.9 is used when performance requirements for heating of a residential building are not very stringent.

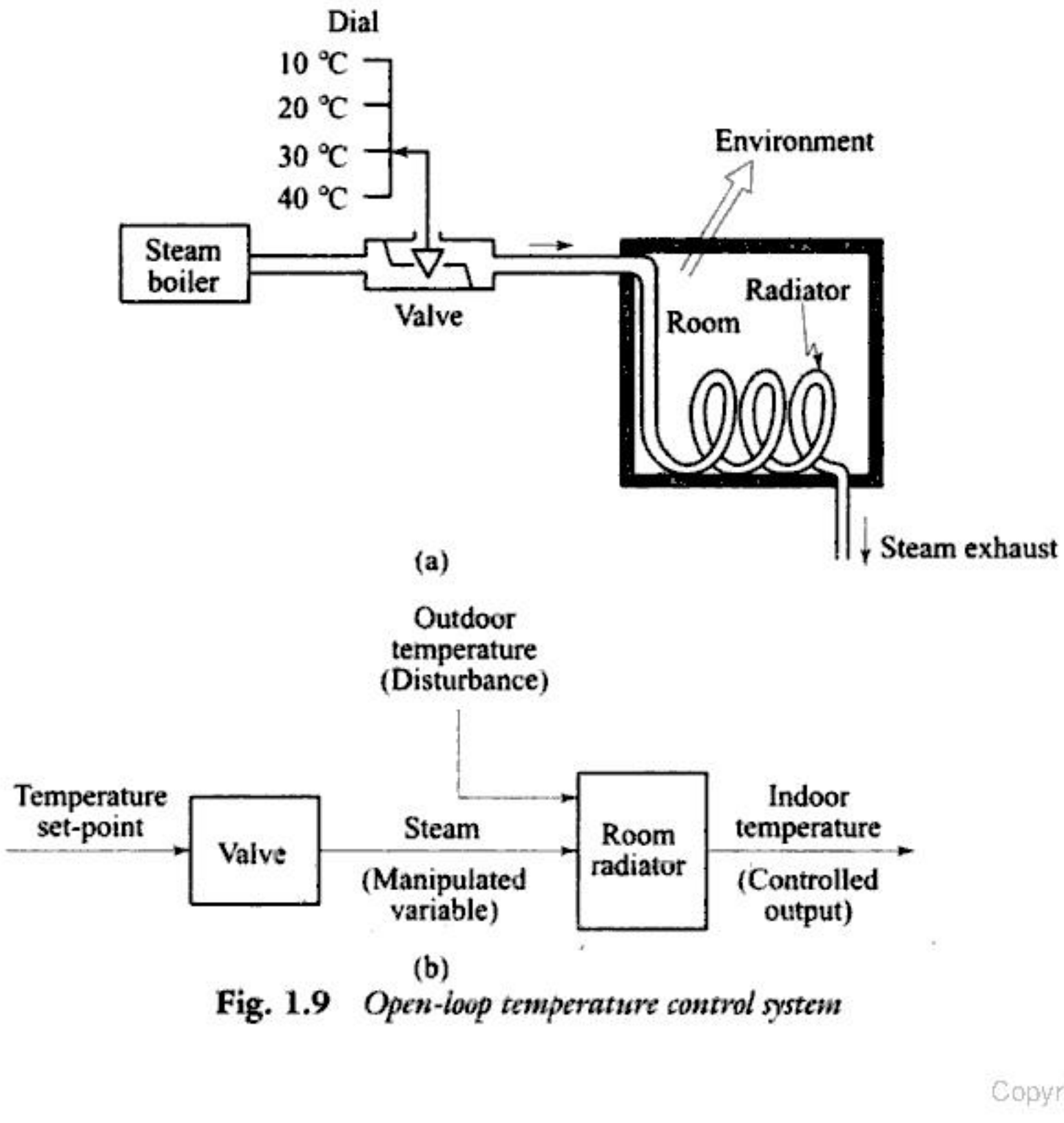


Fig. 1.9 *Open-loop temperature control system*

Copyrighted material

The open-loop control system of Fig. 1.9 can be converted to a closed-loop system by adding the functions of measurement of the controlled temperature, comparison of measured and desired values of the controlled temperature, and control logic to make changes in the heating rate when the desired and measured values differ.

Most residential heating (or cooling) systems utilize one form or another of on–off control. For example, a thermostat with a bimetallic temperature sensor and a snap-action switch to control a simple solenoid-actuated steam valve is often used for this purpose. In a thermostat, two materials with grossly different thermal expansion coefficients are bonded together. When heated, the different expansion rates cause the assembly curve shown in Fig. 1.10a. This effect is used to control power supply to the solenoid (Fig. 1.10b). When the solenoid coil is energized, the plunger becomes magnetized and mutual attraction takes place between the coil and the plunger. If the force required by the load on the plunger does not exceed the force developed by the solenoid, the plunger will pull in. In the temperature control scheme of Fig. 1.10b, position 1 of the switch corresponds to the opening of the steam valve and position 2 corresponds to the closing of the valve.

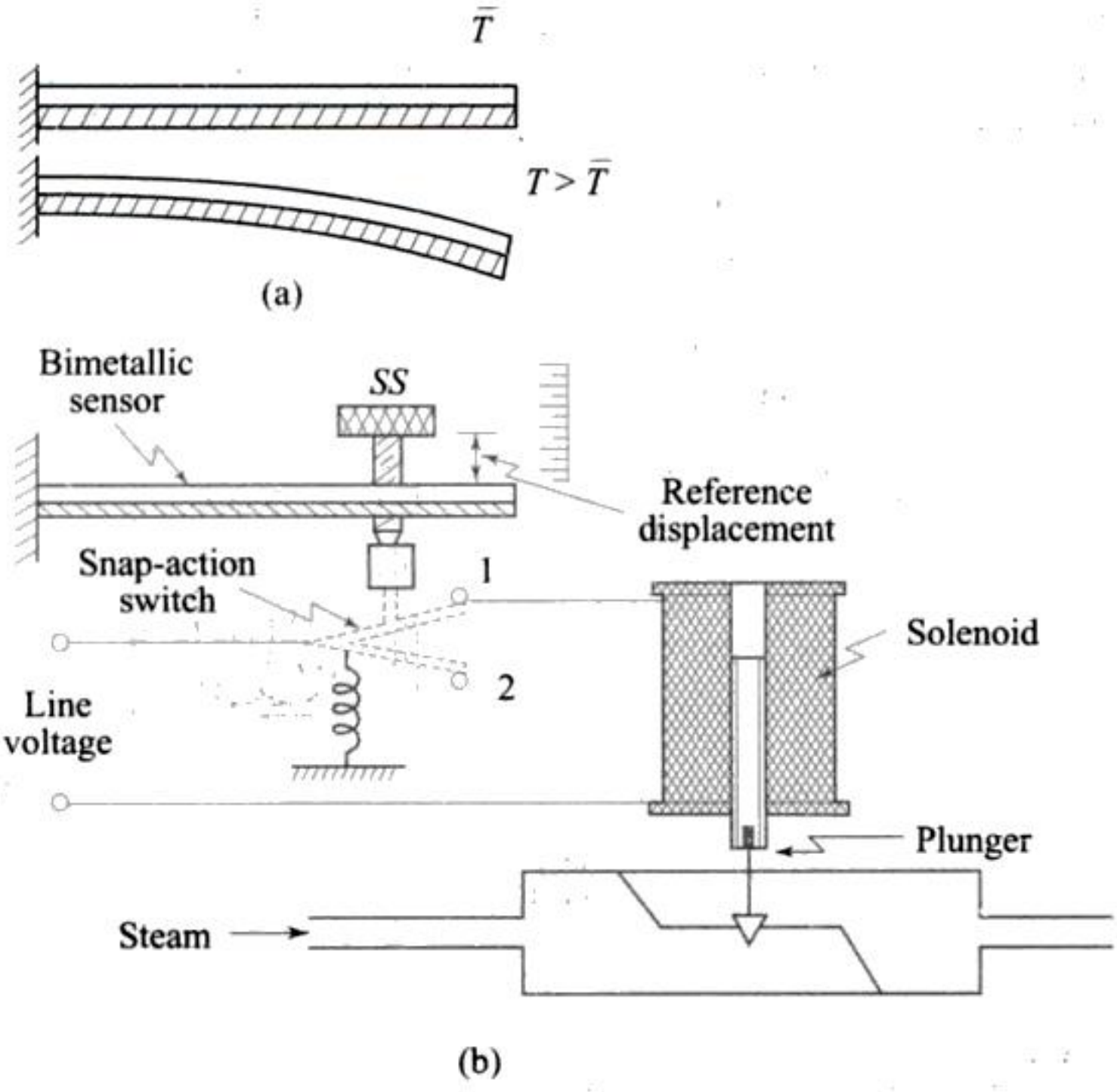


Fig. 1.10 *Closed-loop temperature control system*

The position of the set-screw *SS* (reference displacement) determines the desired temperature $\bar{T}$. The principle of operation of the temperature control

Copyrighted material

system is that the actuator (solenoid + steam valve) is made to operate according to the sequence in which one of the two possible situations specified below has come about at a given time.

- *Situation* 1: The controlled variable T assumes a value below the desired temperature $\overline{T}$, or in other words, the error $e = (\overline{T} - T)$ is positive. In this situation, the snap-action switch is in position 1, the solenoid is in energized state and the steam valve is open. The controlled variable T gradually increases (with the error e decreasing).
- *Situation* 2: The controlled variable T assumes a value above the desired temperature $\overline{T}$, i.e., the error e is negative. In this situation, the bimetallic strip curls, the snap-action switch is thrown to position 2, the solenoid is de-energized, and the steam valve is closed. The controlled variable T is gradually decreasing (the absolute error is also decreasing) due to the heat transfer from the room to the colder surroundings.

Figure 1.11 shows the functional block diagram of the closed-loop temperature control system. Note that the control signal can assume only two values corresponding to the two states of the snap-action switch. The thermostat is serving as the sensing element as well as the controller—it performs the task of automatic reduction of the error to zero, irrespective of the situation created by the disturbance.

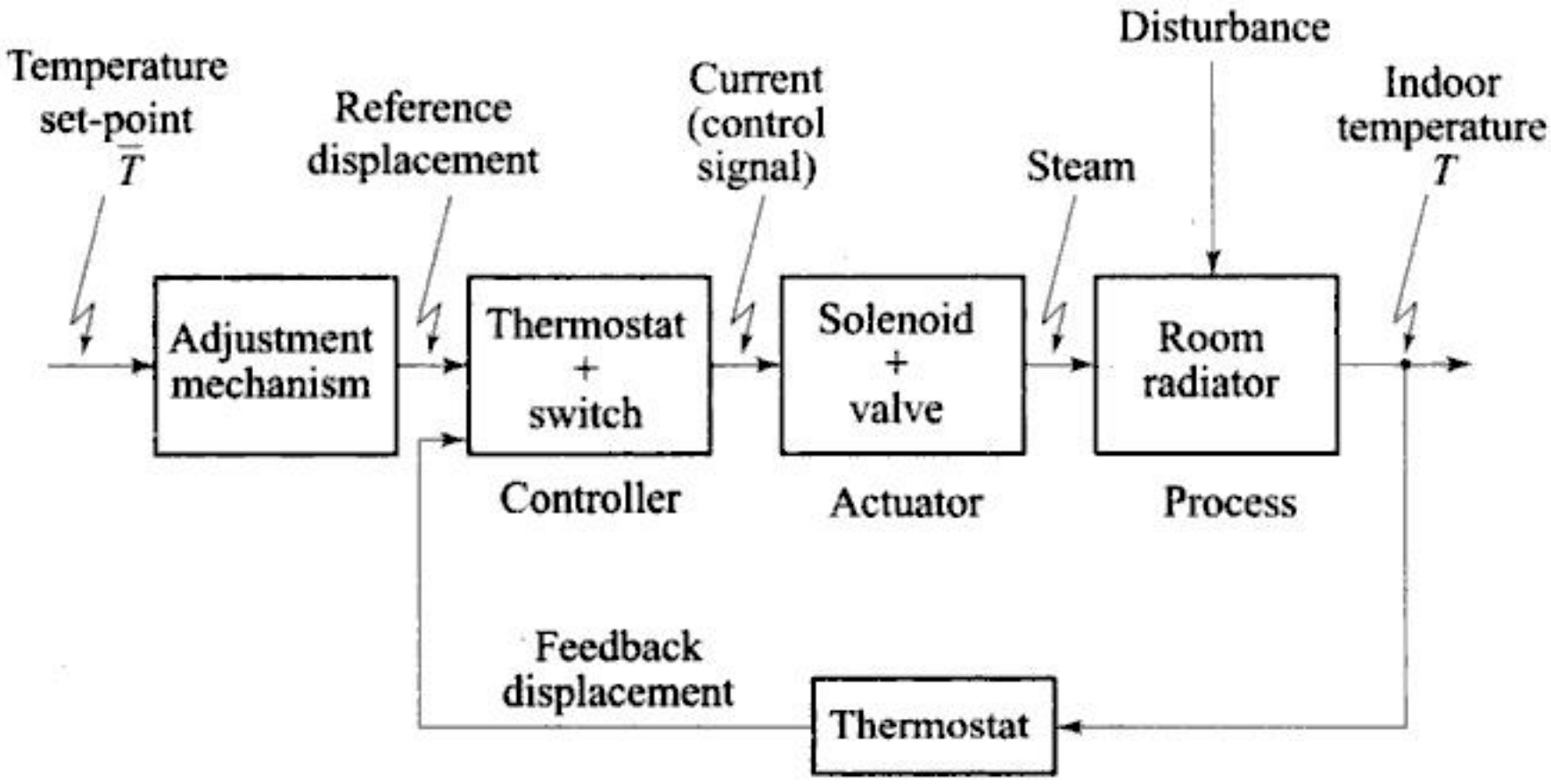


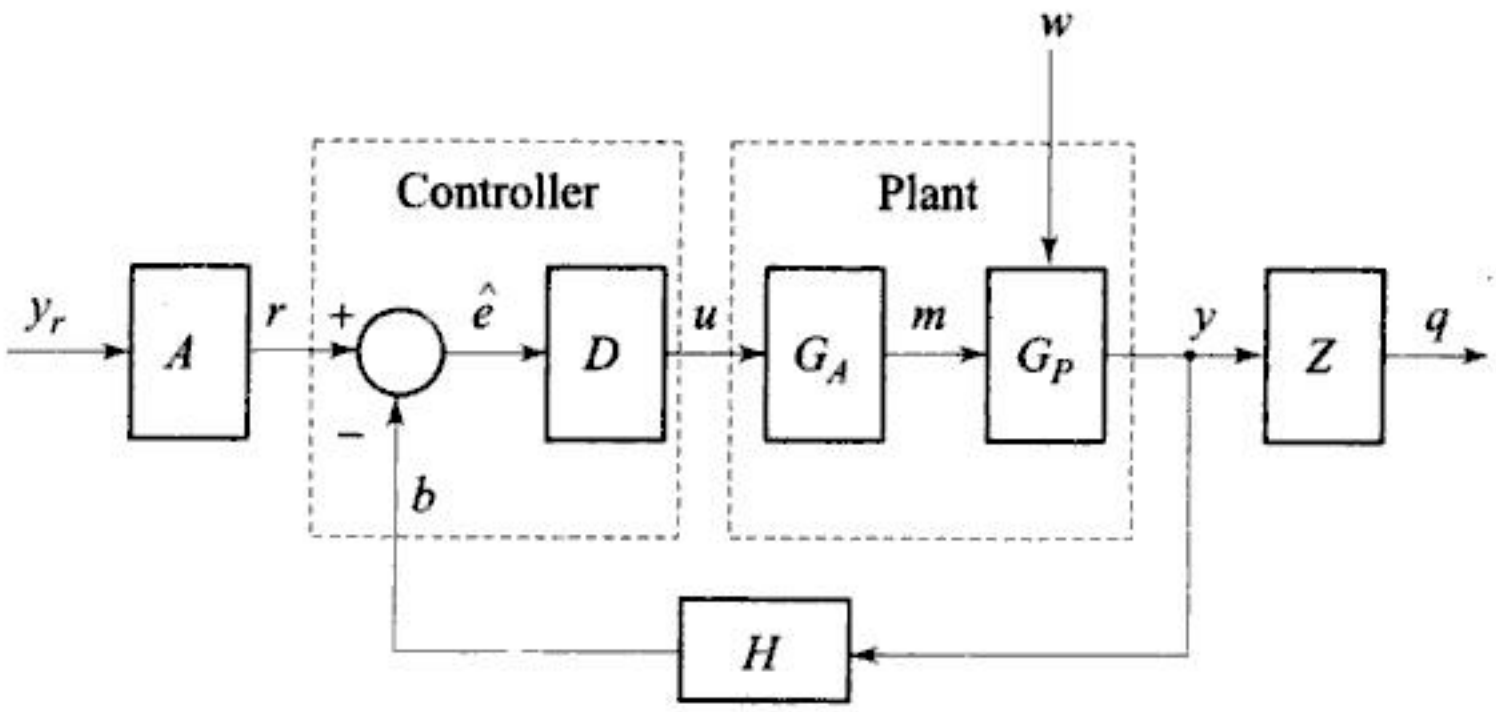
Fig. 1.11 *Functional block diagram of the system of Fig. 1.10*

Basic Structure of a Feedback Control System

The familiar examples of feedback control cited earlier, fit into the basic structure shown in Fig. 1.12 (all functional components identified in Fig. 1.12 do not show up as separate physical elements in Figs 1.6, 1.8, and 1.11).

To understand Fig. 1.12, we begin with the *command signal* y_r—the desired value of the *controlled variable* y. This signal has the same units as the controlled variable, but may or may not exist as an actual physical quantity. For

Copyrighted material



Elements

A : Reference input elements
D : Control logic elements
G_A : Actuator elements (Final control elements)
G_P : Controlled system elements
Z : Indirectly controlled system elements
H : Feedback elements

Signals

b : Feedback signal
y : Controlled variable (output)
w : Disturbance input
$\hat{e}$: Actuating error signal
u : Control signal
m : Manipulated variable
r : Reference input
y_r : Command input
q : Indirectly controlled variable

Fig. 1.12 *Basic structure of a feedback control system*

example in the residential heating system of Fig. 1.10, y_r is the desired room temperature but this is not an actual measurable temperature; it exists only 'mathematically' as the numbers printed on the thermostat dial. In fact, the actual physical input to the control system is a displacement of the set-screw, which is *reference input r* for the residential heating system. The functional block of *reference input elements* represents conversion of the command signal to the reference input signal. In the hydraulic power steering mechanism of Fig. 1.8, the steering gear mechanism corresponds to the reference input elements; it converts the steering command (command input) to the spool displacement (reference input). The reference input element can, when necessary, perform a more sophisticated function such as noise filtering (y_r might be voltage signal contaminated by high-frequency noise).

The *summing junction* is a symbol for the *error detector* which compares the reference input r with the *feedback signal b* and generates a signal $\hat{e} = (r - b)$. The *feedback elements block* is often a sensor for measuring y, but since its functions sometimes include more than simple measurement (e.g., noise filtering), the name feedback element rather than sensing element has been chosen. The signal $\hat{e}$ defines the *actuating error signal*, and not the *system error signal* which is logically defined as $e = (y_r - y)$. Note that r, b and $\hat{e}$ always have exactly the same dimensions.

The *control logic elements block* produces the *control signal u* which has the knowledge about the desired control action. The *controller* is generally

Copyrighted material

thought of as a system that compares the reference input with the feedback signal and is also responsible for suitable control action. In the toilet-tank system of Fig. 1.6, the control logic is simple *proportional control*; the control signal u is proportional to the error signal e. In the residential heating system of Fig. 1.10, the control logic is simple *on-off control*. In general, the control signal is a function of the actuating error signal, which in turn is a function of the reference input r and controlled output y; the functional relationship may therefore be expressed as $u = f(r, y)$. The primary objective set for this book is to study this functional relationship.

The *actuator elements block* (*final control elements*) consists of devices that develop enough torque, pressure, heat, etc. (*manipulated variable* m), to influence the objects under control. Thus, the actuator elements are the 'muscle' of a control system while the control logic elements are the 'brain'.

Disturbance inputs w are the variables over which the designer has no control, and perhaps little information is available on their magnitude, functional form, or time of occurrence. The controlled variable y is influenced by both the manipulated variable m and disturbance w.

In those situations where the quantity q, which we really wish to control, is not used to generate feedback signal, the path from y (the quantity which is used to generate feedback signal) to q is provided through the *indirectly controlled system elements block*. For example, in the hydraulic power steering mechanism of Fig. 1.8, the drive linkage block corresponds to indirectly controlled system elements.

The structure shown in Fig. 1.12 defines the basic types of signals and components necessary for the description of any feedback control system; however it must be adapted to the needs of each specific design. Alternative feedback structures will be introduced in Section 1.3.

1.2 THE GENESIS AND ESSENCE OF THE FEEDBACK CONTROL THEORY

From the simple and familiar examples of automatic control systems presented in Section 1.1, conclusions can be derived regarding the characteristics common to these systems, notwithstanding their manifestable heterogeneity. Automatic control systems share the following general features:

1. The principle of operation of the system uses the feedback idea, i.e., there exists a closed loop: error → manipulated variable → controlled variable → error.
2. The primary objective of the system is error self-nulling.

In all practical control systems, the objective of error self-nulling is required to be realized with a prescribed accuracy (steady-state errors, speed of response, etc.). A demand on accuracy, as we shall shortly see, may result in

Copyrighted material

the loss of *stability*.[2] The reconciliation of the requirements of satisfactory accuracy and adequate stability margin is the principal accomplishment of the feedback control theory. Detailed quantitative study of the effects of feedback on control system performance will be taken up in Chapter 4. The objective of the brief qualitative study in this section is to introduce the basic principles of the feedback control theory.

A brief consideration of the origins of the feedback control theory will be in order here. Examples of feedback control systems have been identified dating back to the third century BC. Ktesibios, a Greek living in Alexandria, is credited with building a self-regulating flow device for use in water clocks. Several examples of feedback control systems appear in windmill designs used by the Dutch in the fifteenth century.

The arrival of the machine age was accompanied by a large increase in the number of control system designs. The development of the steam engine led to the requirement for a speed control device to maintain constant speed in the presence of changes in load torque or steam pressure. In 1788, James Watt of Glasgow developed his now famous flyball governor for this purpose. The principle of the flyball governor is still used for speed control applications.

Analytical tools for control problems were first developed by J. C. Maxwell in 1868. Maxwell utilized a linear differential equation approach and derived stability conditions for a third-order system. In 1876, Edward John Routh was able to determine the stability conditions for higher-order systems. A solution to the stability problem was also obtained by Adolf Hurwitz and reported in 1895. Routh and Hurwitz were unaware of each other's work. In 1911, equivalence of the Routh and Hurwitz criteria was established.

From 1900 to 1940, significant developments occurred in large-scale power generation, aeronautics, chemical industries, and electronics. The development of the vacuum-tube amplifier, in particular, resulted in many analytical techniques for the design of feedback systems.

One of the key problems in electronics, especially since its application to long-distance telephony, was to develop amplifiers with good gain stability. The difficulty stemmed from the considerable scattering of characteristics in the mass-produced electronic tubes and from changes in characteristics taking place in time (e.g., due to emission loss). In 1927, Harold S. Black discovered the negative feedback amplifier as a solution to this problem. Figure 1.13a shows the idea of operation. A potential-dividing resistor delivers a part of the amplifier's output voltage y to the amplifier's input, where it is subtracted from input voltage r. Figure 1.13b gives the equivalent block diagram of the system. It follows from this diagram that

---

2. Stability is a notion that describes whether the system will be able to follow the input command (Chapter 5). In a nonrigorous sense, a system is said to be unstable if its output is out of control or increases without bound.

Copyrighted material

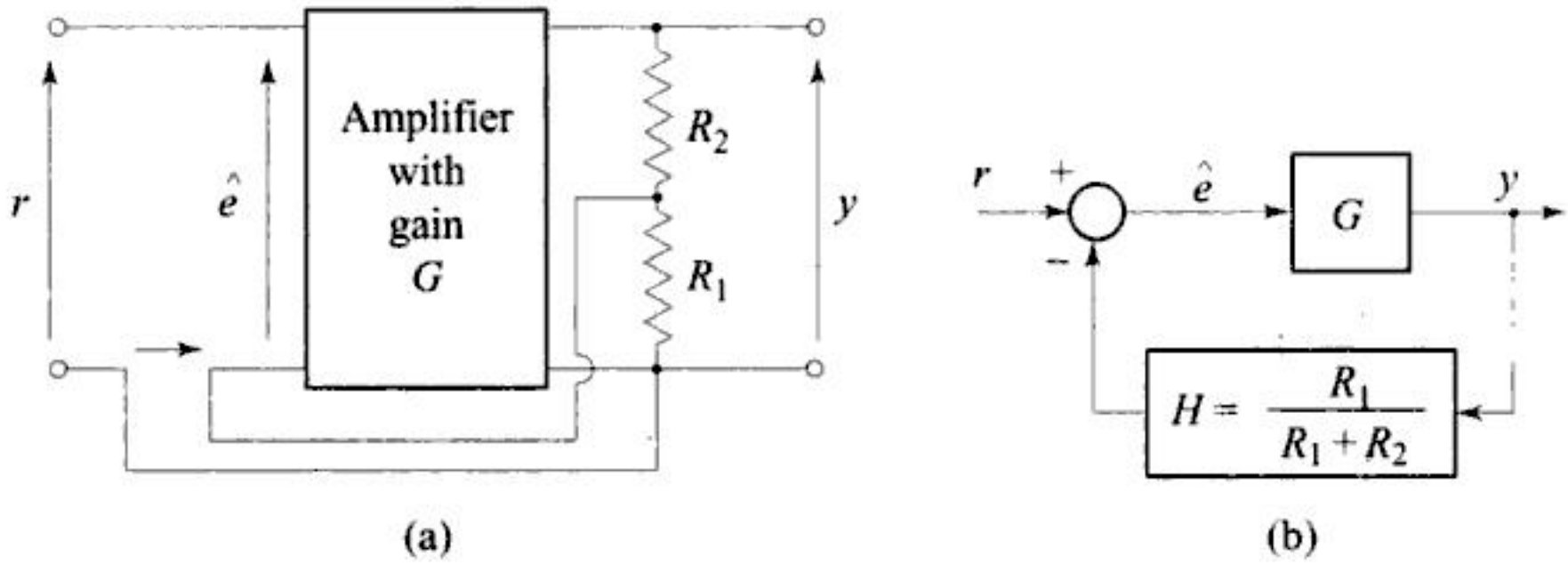


Fig. 1.13 *Amplifier with feedback*

$$y = G(r - Hy)$$

The closed-loop gain

$$M = \frac{y}{r} = \frac{1}{\frac{1}{G} + H}$$

This equation, specifying the relationship between the closed-loop gain M, the open-loop gain G, and the feedback gain H, is crucial for the feedback theory which was developed in electronics (the studies of Harry Nyquist and Hendrik W. Bode in the 1930s) and which relied heavily on the then widely fostered frequency methods of analysis. The most important observation from this equation which determines feedback performance is that

$$M \equiv \frac{1}{H} = \frac{R_1 + R_2}{R_1} \text{ for } \frac{1}{G} \ll H \quad \text{or} \quad GH \gg 1$$

where GH denotes the feedback-loop gain. It follows that under the conditions of strong feedback ($GH \gg 1$), the closed-loop gain M does not depend upon the open-loop gain G; it depends only on the potential-dividing resistor. The gain M is practically constant even if gain G varies to a considerable extent, as long as it remains sufficiently high. Thus, by making use of feedback, it has become possible to convert an amplifier with very high but unsteady gain into an amplifier with a lower but steady gain, and furthermore the higher the gain G, the more steady is M. On the other hand, an excessive increase of G results in the loss of stability. The reconciliation of the requirements of satisfactory performance and adequate stability margins was first the central problem and later the principal accomplishment of the feedback control theory.

During World War II, electronics engineers noticed an analogy between the feedback amplifier and the servomechanism of a radar command post, both in structure and principle of operation, and also with respect to the goal and the basic problem, i.e., reconciliation of the requirements of accuracy and stability. The feedback theory was then successfully applied to the design of servomechanisms, becoming more advanced in the process, and, in this way the *theory* of *servomechanisms* came into being.

Copyrighted material

The application of the theory of servomechanisms to the process industry led to the *feedback control theory*. At about the same time, Norbert Wiener founded *cybernetics* as the new field of study which transplanted elements of the feedback theory to economics, biology and other sciences.

Frequency-response methods have dominated the control systems area since the late 1940s as analysis and design tools. The Nyquist and Bode diagrams became indispensable for assessing closed-loop stability of feedback control systems. Evans' root-locus method brought the complex variable based approach to a fully developed state by 1948. A mature *classical* control systems engineering area thus evolved.

Further advances in control systems engineering resulted from the space programme and associated challenges—launching, maneuvering, guidance, and tracking of space vehicles. The emergence of a *modern* control theory based on state-space ideas is generally traced back to the early 1960s.

After this brief consideration of the origins of the feedback control theory, let us focus our attention on the requirement of reconciling accuracy and stability, which makes the existence of a uniform feedback control theory fully justifiable. We have already considered one example—the electronic amplifier, wherein strong feedback results in insensitivity to variations in parameters of electronic tube. There is however an upper limit on the improvement of performance beyond which stability suffers. In the following we consider more examples.

Example 1.5

Servomechanism for Steering of Antenna

One of the earliest applications of radar tracking was for anti-aircraft fire control, first with guns and later with missiles. Today many civilian applications exist as well, such as satellite-tracking radars, navigation-aiding radars, etc.

The radar scene includes the radar itself, a target, and the transmitted waveform that travels to the target and back. Information about the target's spatial position is first obtained by measuring the changes in the back-scattered waveform relative to the transmitted waveform. The time shift provides information about the target's range, the frequency shift provides information about the target's radial velocity, and the received voltage magnitude and phase provide information about the target's angle[3] [1].

In a typical radar application, it is necessary to point the radar antenna toward the target and follow its movements. The radar sensor detects the error between the antenna axis and the target, and directs the antenna to follow the target. The servomechanism for steering the antenna in response to commands from radar sensor is considered here. The antenna is designed for two inde-

3. The bracketed numbers are keyed to the list of references given at the end of the book.

Copyrighted material

pendent angular motions, one about the vertical axis in which the azimuth angle is varied, and the other about the horizontal axis in which the elevation angle is varied (Fig. 1.14). The servomechanism for steering the antenna is described by two controlled variables—the azimuth angle β and the elevation angle α. The desired values or commands are the azimuth angle β_r and the elevation angle α_r of the target. The feedback control problem involves error self-nulling under conditions of disturbances beyond our control (such as wind power).

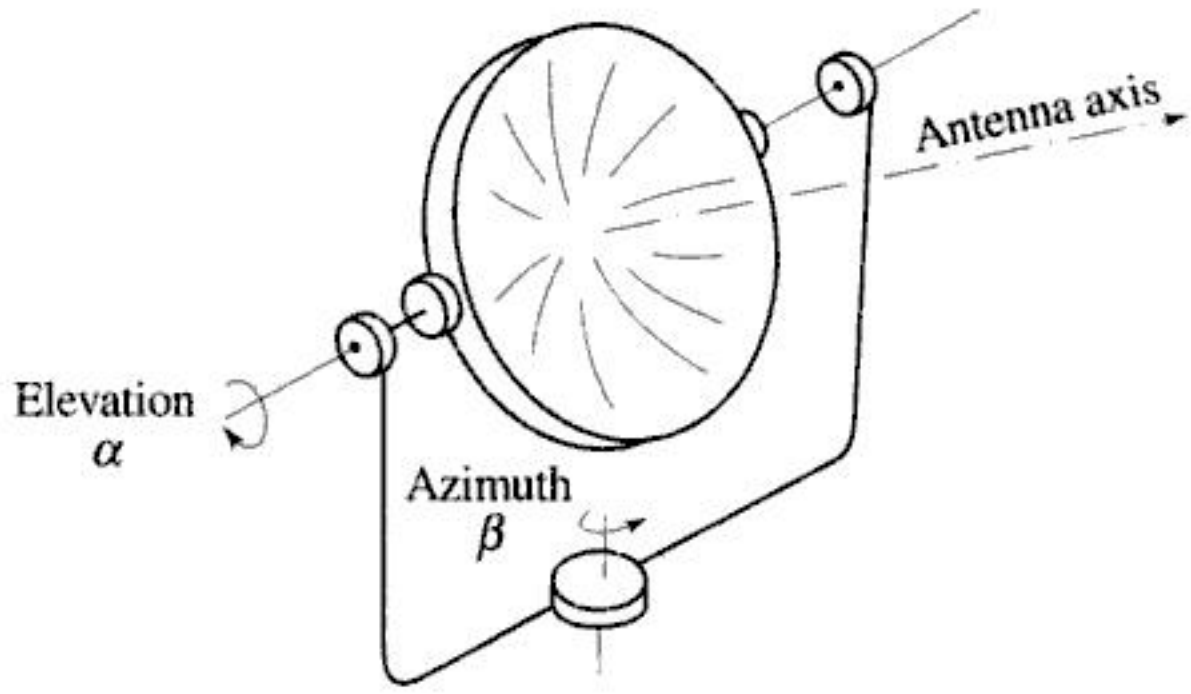


Fig. 1.14 *Antenna configuration*

The control system for steering antenna can be treated as two independent systems—the azimuth-angle servomechanism, and the elevation-angle servomechanism. This is because the interaction effects are usually small. The operational diagram of the azimuth-angle servomechanism is shown in Fig. 1.15. The steering command from the radar sensor which corresponds to the target azimuth angle is compared with the azimuth angle of the antenna axis. The occurrence of the azimuth-angle error causes an error signal to pass through the amplifier, which increases the angular velocity of the servomotor in a direction towards an error reduction. In the scheme of Fig. 1.15, the measurement and processing of signals (calculation of control signal) is digital in

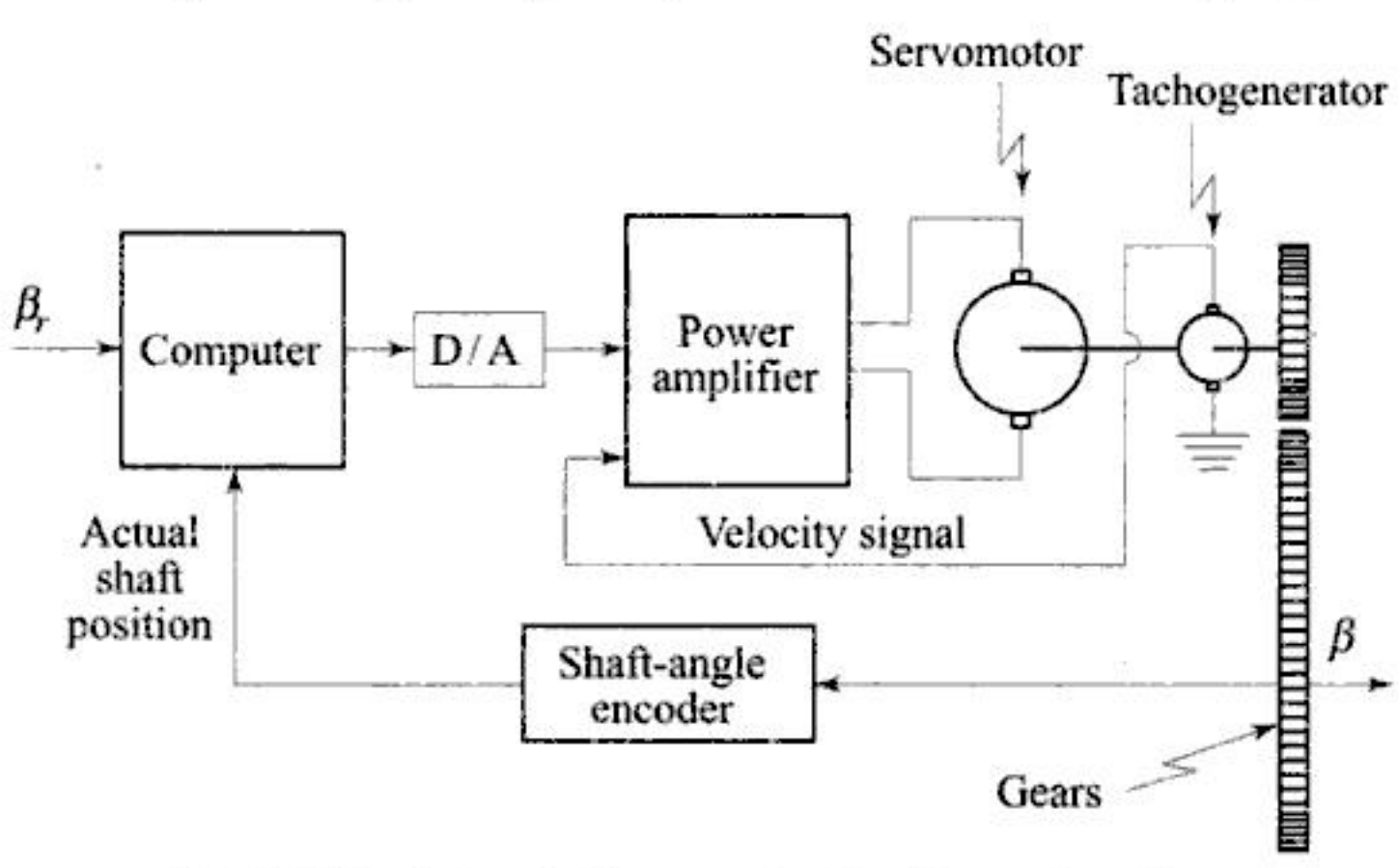


Fig. 1.15 *Azimuthal servomechanism for steering of antenna*

Copyrighted material

nature and is based on proportional control logic. Figure 1.16a gives the functional block diagram of the control system. A simple model of the load (antenna) on the motor is shown in Fig. 1.16b. The moment of inertia J and the viscous friction coefficient B are the parameters of the assumed model. The nominal load is included in the plant model for the control design. The main disturbance input is the deviation of the load from the nominal estimated value as a result of uncertainty in our estimate, effect of wind power, etc.

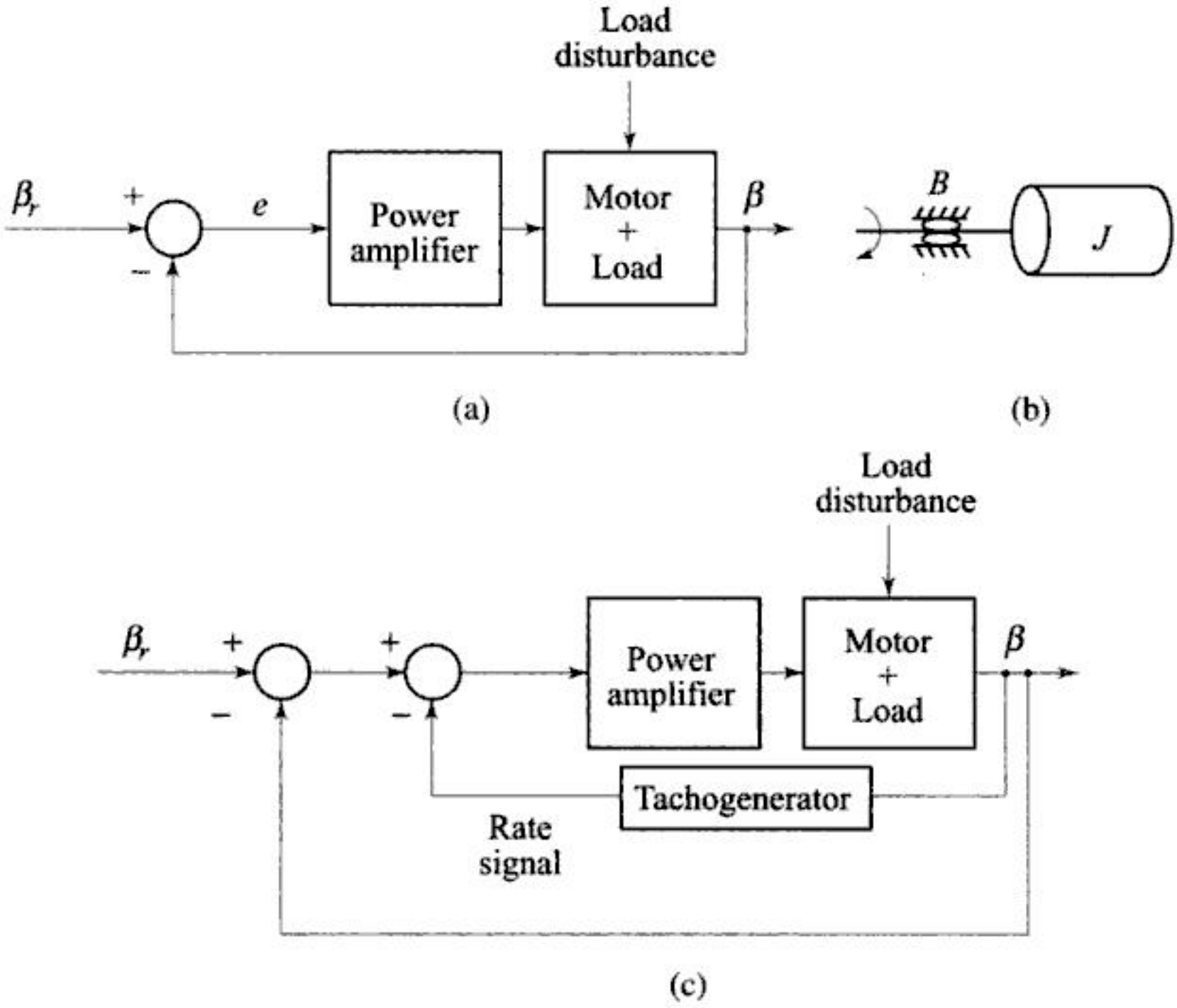


Fig. 1.16 *Functional block diagram of azimuthal servomechanism*

In the tracking system of Fig. 1.16a, the occurrence of error causes the motor to rotate in a direction favouring the dissolution of error. Note that the components of our system cannot respond instantaneously since any real-world system cannot go from one energy level to another in zero time. Thus, in any real-world system there is some kind of dynamic lagging behaviour between the input and the output. In the servosystem of Fig. 1.16a, the control action on the occurrence of the deviation of the controlled output from the desired value (the occurrence of error) will be delayed by the cumulative dynamic lags of the shaft angle encoder, digital computer and digital-to-analog converter, power amplifier, and the servomotor with load. Eventually, however, the trend of the controlled variable deviation from the desired value will be reversed by the action of the amplifier output on the rotation of the motor, returning the

Copyrighted material

controlled variable towards the desired value. Now, if a strong correction (high amplifier gain) is applied (which is desirable from the point of view of control system performance, e.g., strong correction improves the speed of response (Chapter 4)), the controlled variable overshoots the desired value (the 'run-out' of the motor towards an error with the opposite rotation), causing a reversal in the algebraic sign of the system error. Unfortunately, because of system dynamic lags, a reversal of correction does not occur immediately and the amplifier output (acting on 'old' information) is now actually driving the controlled variable in the same direction as it is already going, rather than opposing its excursions, leading to a larger deviation. Eventually, the reversed error does cause a reversed correction but the controlled variable overshoots the desired value in the opposite direction and the correction is again in the wrong direction. The controlled variable is thus driven alternatively in opposite directions before it settles to an equilibrium condition. This oscillatory state is unacceptable as the behaviour of the antenna-steering servomechanism. The considerable amplifier gain, which is necessary if the high accuracies are to be obtained, aggravates the described unfavourable phenomenon.

The occurrence of these oscillatory effects can be controlled by the application of special compensation feedback. When a signal proportional to motor's angular velocity (called the rate signal) is subtracted from the error signal (Fig. 1.16c), the braking process starts sooner before the error reaches a zero value. The 'loop within a loop' (velocity feedback system embedded within a position feedback system) configuration utilized in this application is a classical scheme called *cascade control* in the process field and *minor-loop feedback* (or *state variable feedback*) in servomechanisms.[4]

Example 1.6

Variable Speed dc Drive

Many industrial applications require variable speed drives. For example, variable speed drives are used for pumping duty to vary flow rate or pumping pressure, rolling mills, harbour cranes, rail traction, etc. [2–4].

The variable speed dc drive is the most versatile drive available. The silicon controlled rectifiers (SCR) are almost universally used to control the speed of dc motors because of the considerable benefits that accrue from the compact static controllers supplied directly from the ac mains.

Basically all the dc systems involving the SCR controllers are similar but with different configurations of the devices, different characteristics may be obtained from the controller. Figure 1.17 shows a dc motor driven by a full-wave rectified supply. Armature current of the dc motor is controlled by an SCR which is in turn controlled by the pulses applied by the SCR trigger control circuit.

4. This and other compensation schemes will be discussed in Chapter 4.

Copyrighted material

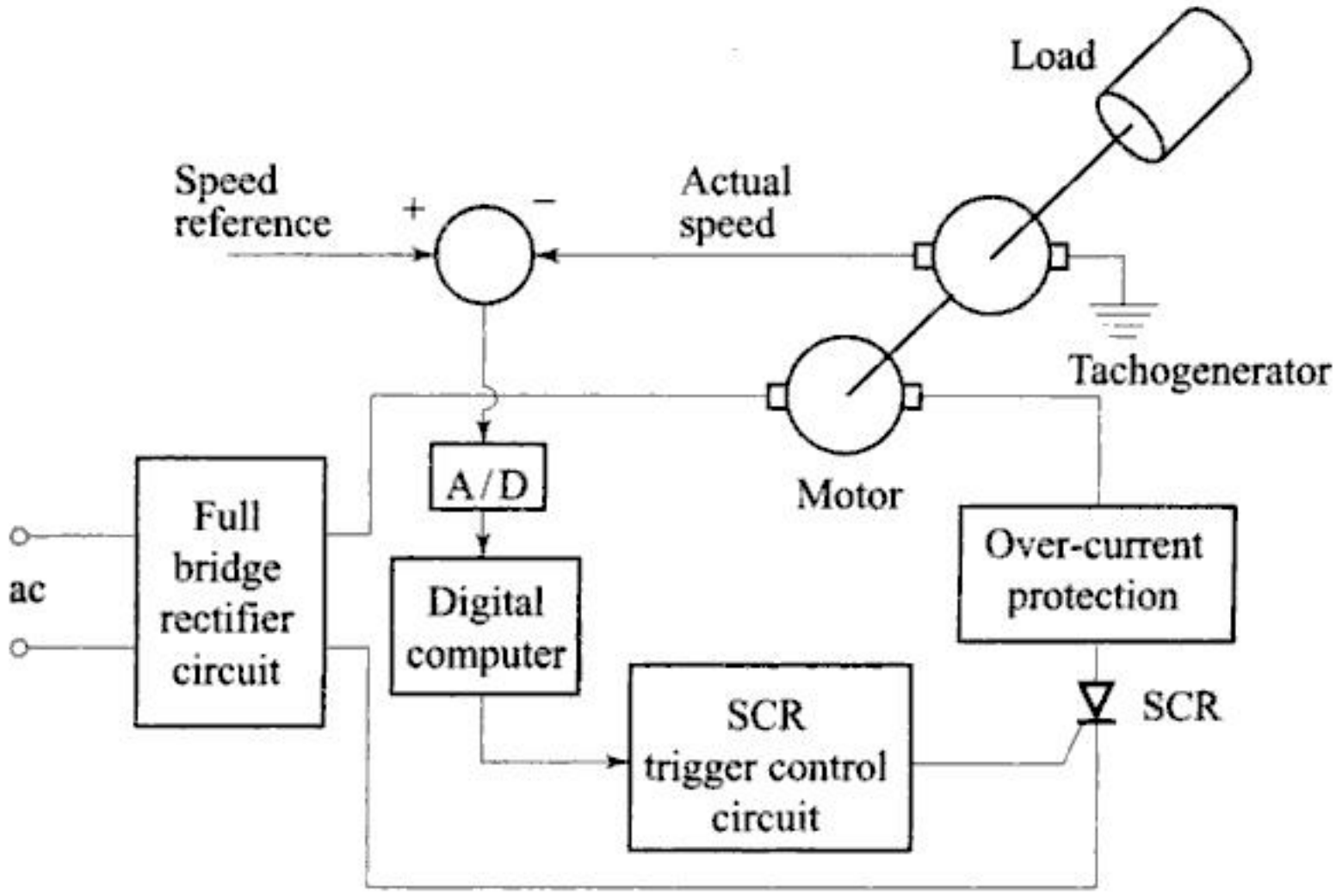


Fig. 1.17 *Variable speed dc drive*

Firing angle of the SCR controls the average armature current which in turn controls the speed of the dc motor. The average armature current (speed) increases as the trigger circuit reduces the delay angle of firing of the SCR, and the average armature current (speed) reduces as the delay angle of firing of the SCR is increased.

In the scheme of Fig. 1.17, the reference voltage which corresponds to the desired speed of the dc motor, is compared with the output voltage of the tachogenerator corresponding to the actual speed of the motor. The occurrence of the error in speed causes an error signal to pass through the trigger circuit which controls the firing angle of the SCR in a direction towards an error reduction. When the processing of the error signal (calculation of the control signal) is based on the proportional control logic, a steady-state error between the actual speed and the desired speed exists (Chapter 4). The occurrence of the steady-state error can be eliminated by generating the control signal with two components: one component proportional to the error signal, and the other proportional to the integral of the error signal. This proportional-integral control logic will be examined in detail in Chapter 4.

▲▲

A point which needs a special mention here is that the presence of disturbances is the main reason for using feedback control. Without disturbances, there is probably no need for feedback control. Table 1.1 gives the details of commonly occurring disturbances in the control system examples considered earlier.

Copyrighted material

Table 1.1 *Disturbances in specific feedback control systems*

Feedback control system	*Disturbance in controlled system*	*Measurement noise*
Bathroom toilet tank	Outflow	Float swaying
Hydraulic power steering mechanism	Vehicle load, resistance to motion	Mechanical vibrations
Residential heating system	Ambient temperature	Mechanical vibrations of bimetallic strip
Servomechanism for steering of antenna	Wind power	Target surface fluctuations
Variable speed dc drive	Variations in load on dc motor	Mechanical vibrations

Other disturbances which affect the performance of control systems are:

(i) uncertainty in our estimate of the hardware parameters of the process and other components of the control system (the estimates of the parameters are used for the design of controller); and
(ii) changes in the parameters taking place in time (due to wear, ageing, environmental effects, etc.), thereby affecting the dynamic characteristics of the system.

As we shall see later in this book, feedback control systems:

(i) greatly reduce the effect on the controlled variable of all external disturbances except those associated with the sensor (measurement system); and
(ii) are tolerant of variations in hardware parameters other than those of the sensor.

The feedback signal coming from the sensor of controlled variable contains useful information related to disturbances (external disturbances and variations in hardware parameters), which is usually of relatively low frequency. It may often include high frequency 'noise' introduced by the measurement sensors. Such noise signals are too fast for the control system to correct; *low-pass filtering* is often needed to allow good control performance.

1.3 FEEDFORWARD-FEEDBACK CONTROL STRUCTURE

This section presents the principle of one of the most profitable control schemes: *feedforward control*. In earlier sections, we studied the principle of

Copyrighted material

feedback control; a very simple technique that compensates for any disturbance affecting the controlled variable. When a disturbance enters the process, the controlled variable deviates from its desired value (set-point) and, on sensing the error, the feedback controller manipulates the process input in a way favouring the dissolution of error. The main limitation of a feedback control system is that in order for it to compensate for disturbances, the controlled variable must first deviate from its desired value. Feedback control acts upon an error between the set-point and the controlled variable. This means that once a disturbance enters a process, it must propagate through the process and force the controlled variable to deviate from the set-point before corrective action can be taken.

Feedforward control compensates for disturbances before they affect the controlled variable. In this scheme, the disturbances are measured before they enter the process and required value of the manipulated variable to maintain the controlled variable at its desired value is calculated; implementation of such a control results in undisturbed controlled variable. Design of this type of control scheme does not generally require any specialized control theory; basic system dynamics are sufficient in most cases. Success of *disturbance feedforward* control schemes depends on our ability to:

(i) measure the disturbance; and
(ii) estimate the effect of the disturbance on the controlled variable, so that we can compensate for it.

Let us consider an example of disturbance-feedforward.

Example 1.7

Heat Exchanger

The schematic diagram of a heat exchanger is shown in Fig. 1.18. The process fluid flows inside the tubes of the heat exchanger and is heated by steam condensing on the outside of the tubes. The objective is to control the outlet temperature θ of the process fluid in the presence of variations[5] in process fluid flow Q and its inlet temperature θ_i. The objective of controlling the outlet temperature in the presence of disturbances can be accomplished by setting up a feedback control loop as shown in Fig. 1.18a. The flow controller consists of an electronic amplifier and an electropneumatic transducer, which converts the voltage corresponding to the error between the controlled temperature and its set-point value to a pneumatic pressure variable (based on proportional control

5. In a typical application, the heat exchanger is a part of the overall system; disturbances in Q and θ_i are caused by other processing operations taking place in the system (in the next section, we will study a distillation system wherein the heat exchanger is a sub-system).

Copyrighted material

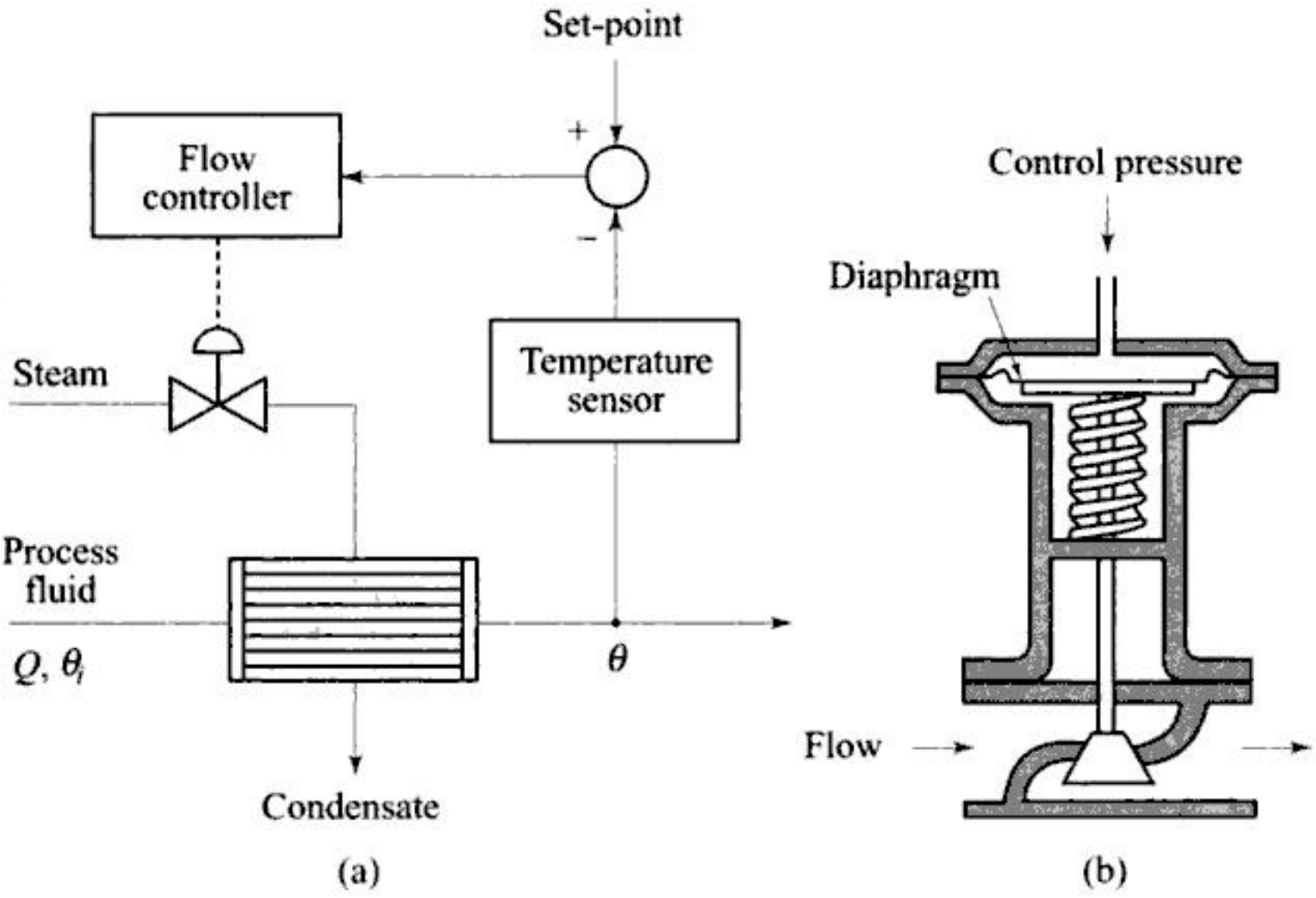


Fig. 1.18 *Feedback control loop for heat exchanger*

logic). The error voltage is derived from the output voltage of the temperature sensor (corresponding to the output temperature θ) and the set-point voltage corresponding to the desired temperature. The pneumatic pressure actuates a pneumatic valve[6], whose essential features are shown in Fig. 1.18b. The actuator section of the valve comprises a diaphragm whose position is set by the balance between the force exerted by a spring and the controller output pressure on the diaphragm.

In the control scheme of Fig. 1.18a, the feedback controller, which manipulates the heat input to the heat exchanger, will not act until an error has developed. If the system involves large time lags, it will take some time before any corrective action takes place.

If feedforward control is provided in such a system, then as soon as a change in Q and/or θ_i occurs, a corrective measure will be taken simultaneously by manipulating the heat input to the heat exchanger. Figure 1.19 shows the disturbance-feedforward control scheme.

Feedforward control can minimize the transient error. However, since it is an open-loop control, there are limitations to its functional accuracy. Feedforward control will not cancel the effects of unmeasurable disturbances.

---

6. By far, the most common form of valve used in process control is the pneumatic actuating valve which can provide large power output. Pneumatic systems use a readily available working medium—compressed air supplies, and are commonly used in process industry because of their explosion-proof characteristics, simplicity and ease of maintenance.

Copyrighted material

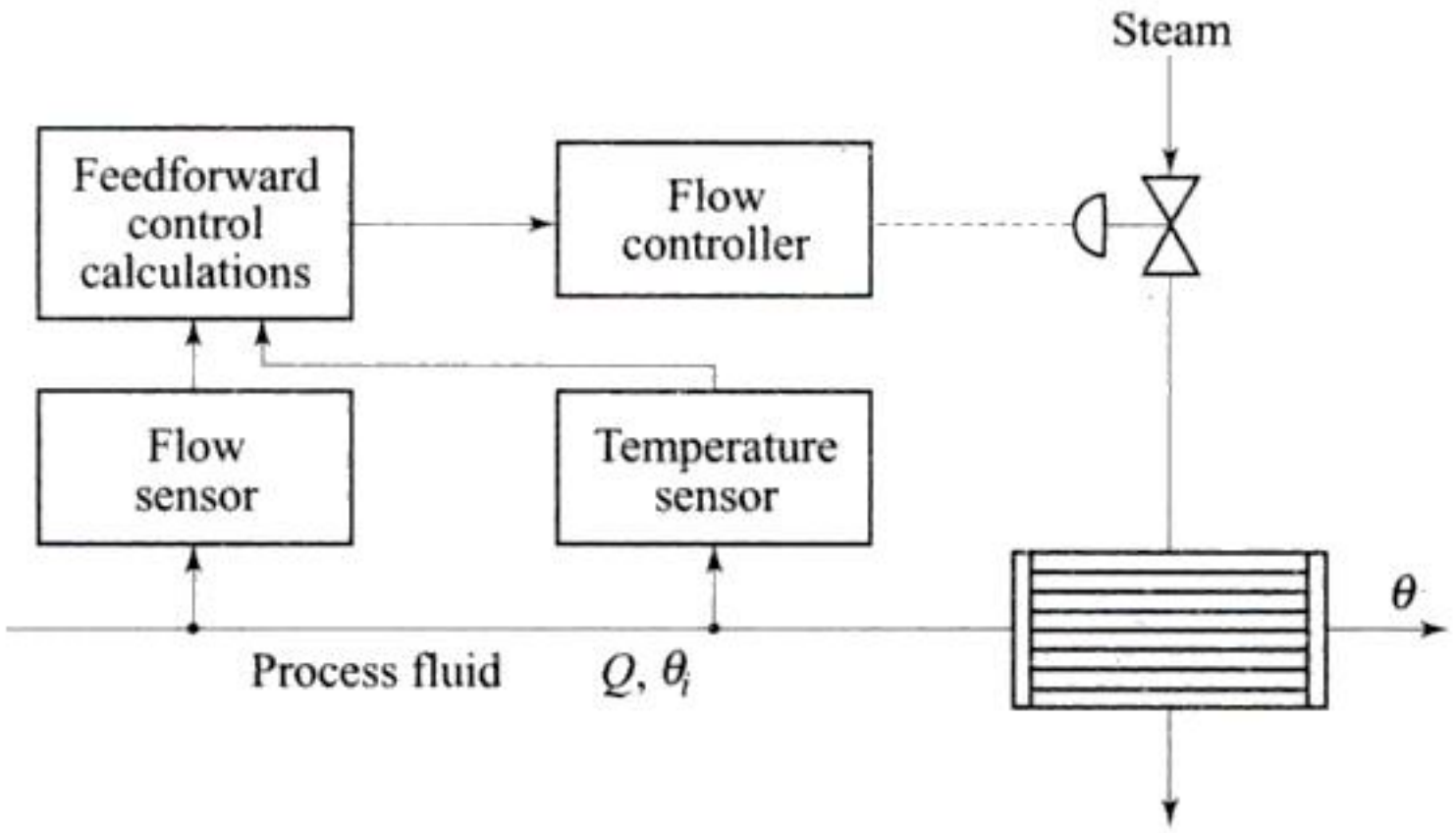


Fig. 1.19 *Disturbance compensated open-loop system*

It is therefore necessary that a feedforward control system include a feedback loop as shown in Fig. 1.20. Essentially, the feedforward control minimizes the transient error caused by measurable disturbances, while the feedback loop compensates for any imperfections in the functioning of the feedforward control and provides corrections for unmeasurable disturbances.

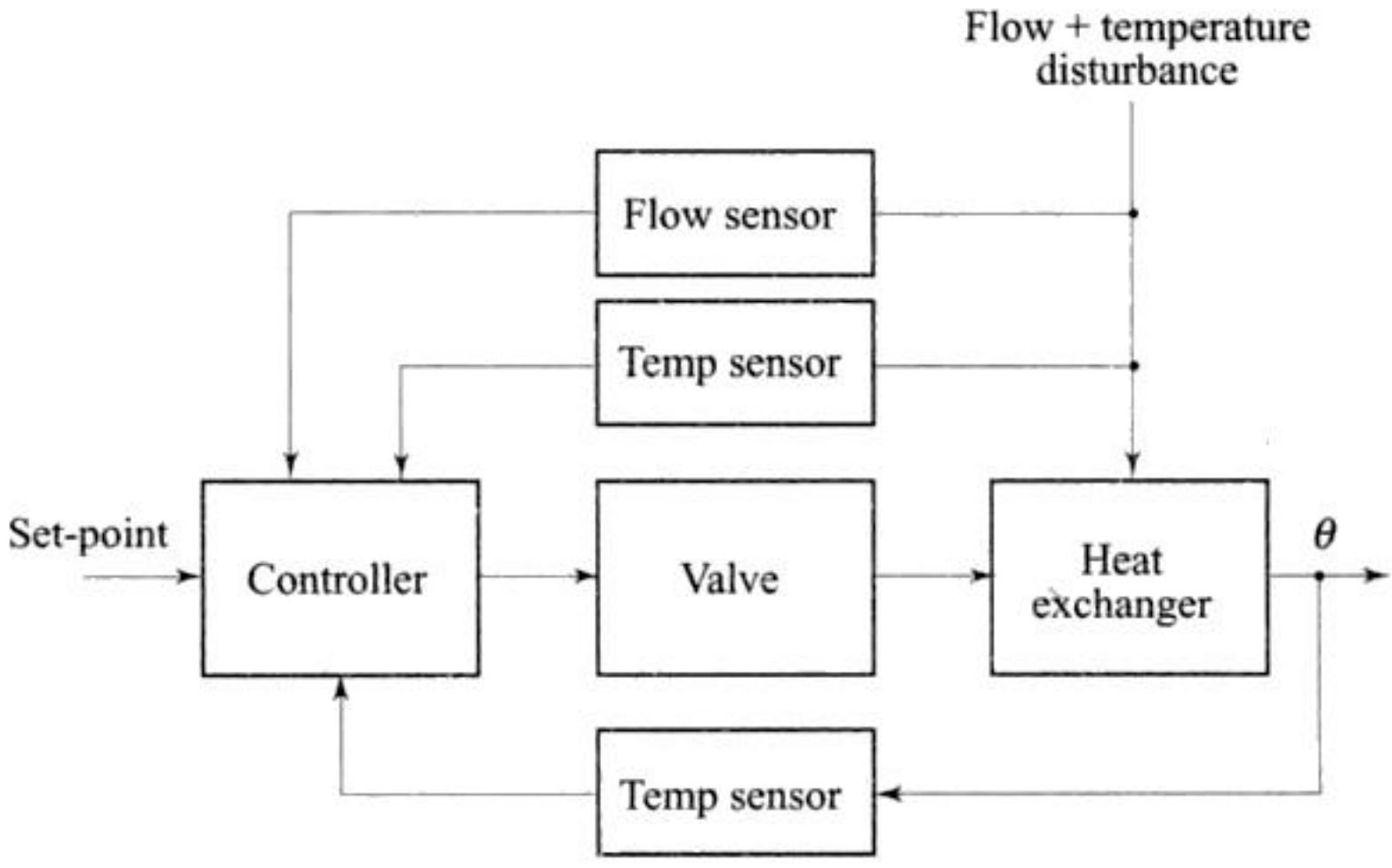


Fig. 1.20 *Feedforward–feedback control structure for the heat exchanger*

▲▲

Another control scheme using the feedforward concept is the *comimand-feedforward* in combination with feedback loop (Fig. 1.21). Here, based on the knowledge of process characteristics, the command is augmented by command-compensator to produce improved performance. Command-feedforward has been used in several ways for servo applications. In the next section, we

Copyrighted material

will give a combined feedforward-feedback scheme employing command feedforward for the angular motion control of a robot manipulator.

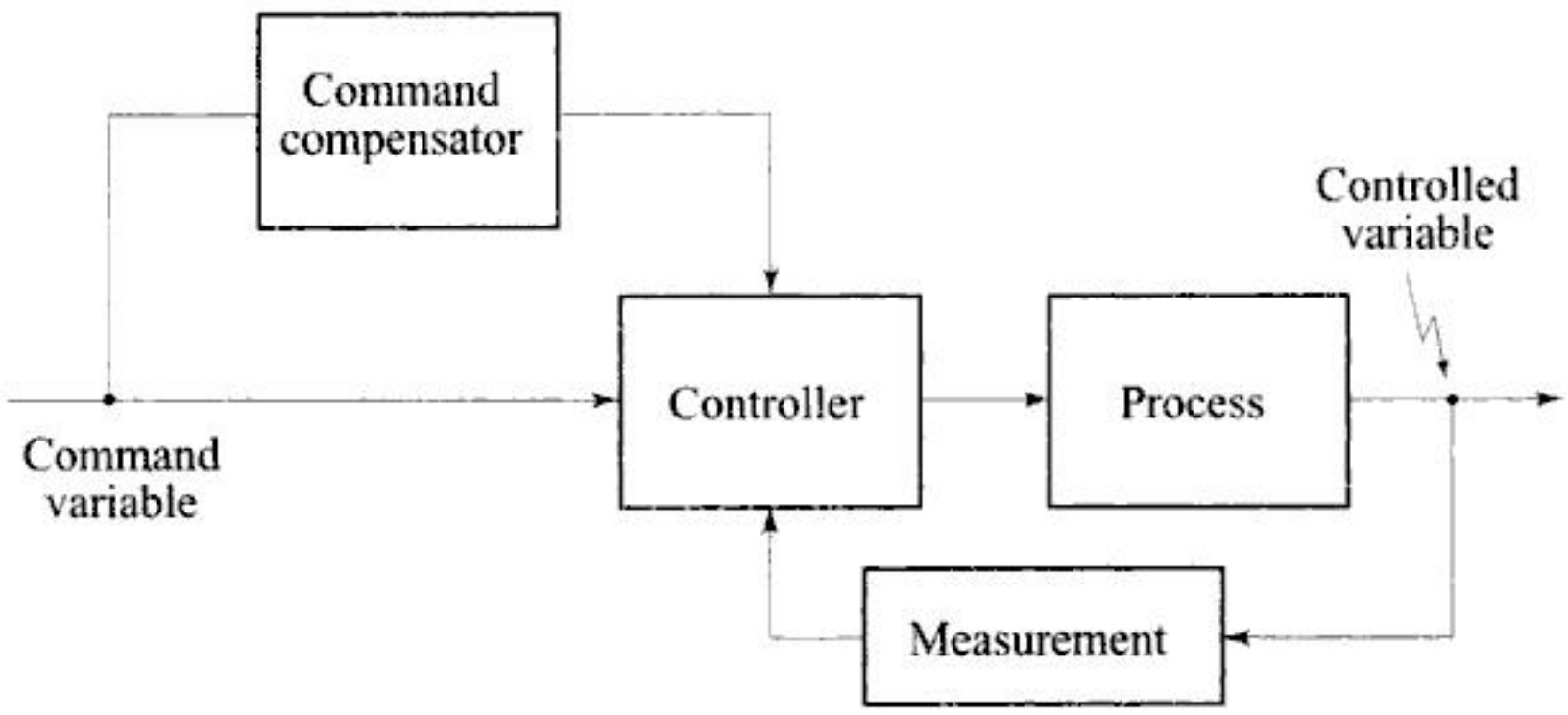


Fig. 1.21 *A control scheme employing command feedforward*

1.4 MULTIVARIABLE CONTROL SYSTEMS

Complex processes and machines often have several variables (outputs) that we wish to control, and several manipulated inputs available to provide this control. Sometimes the control situation is simple; one input affects primarily one output and has only weak effect on the other outputs. In such situations, it is possible to ignore weak *interactions* (*coupling*) and design controllers under the assumption that one input affects only one output. Input–output pairing to minimize the effect of interactions and application of SISO control schemes to obtain separate controllers for each input–output pair, results in an acceptable performance. This, in fact, amounts to considering the multivariable system as consisting of an appropriate number of separate SISO systems. Coupling effects are considered as disturbances to the separate control systems and may not cause significant degradation in their performance if the coupling is weak. We have already discussed examples of multivariable systems of this nature—the automobile driving system (Example 1.2), and the antenna stabilization system (Example 1.5).

A multivariable system is said to have strong interactions (coupling) if one input affects more than one output appreciably. There are two approaches for the design of controllers for such systems.

1. Design a *decoupling controller* to cancel the interactions inherent in the system. Consider the resulting multivariable system as consisting of an appropriate number of SISO systems, and design a controller for each system.
2. Design a single controller for the multivariable system taking interactions into account.

In this section, we give examples of multivariable systems with strong interactions. These and many other important applications are difficult to present

Copyrighted material

convincingly in an introductory text since their dynamic modelling is too complex to be accommodated. We will therefore only highlight salient features of these control systems. Selected titles for detailed study are [123–134].

Example 1.8

Distillation System

The purification of materials is a prominent operation of the chemical industry. There is scarcely any chemical process which does not require preliminary purification of raw materials or final separation of products from by-products. The towers of a modern petroleum refinery are the evidence of the important role played by these separations in a processing plant.

Figure 1.22 is a schematic diagram of a bubble-cup tray tower used for distillation [13].

Distillation is a method of separating the components of a liquid mixture by the repeated systematic application of vaporization and condensation. For example, if a liquid solution of ammonia and water is partially vaporized by heating, it is found that the newly created vapour phase and residual liquid both contain ammonia and water, but in proportions which at equilibrium are different for the two phases and different from those in the original solution. The vapour phase is richer in the more volatile component (ammonia) and the residual liquid is richer in the less volatile component (water), compared to the original solution. If the vapour and liquid are separated from each other and the vapour condensed, two solutions, one richer in ammonia and the other richer in water, are obtained. If the process of vaporization and condensation is continued over a number of stages, it eventually produces a product with a very high degree of purity in the more volatile component.

The thermal efficiency of this staged operation can be greatly improved if the energy released when the vapour is condensed in one stage is used to vaporize the liquid in an adjacent stage. If the heat required to vaporize one mole of liquid is equal to the heat that is released when one mole of vapour condenses and is independent of composition, then it is evident that a heat source and sink are needed only at the ends of the cascade.

In the distillation column, the necessary heat transfer is accomplished by the direct contact between vapour and liquid by trays (perforated plates) which are designed so that vapour stream bubbles directly through the liquid as illustrated in Fig. 1.22. The feed (multicomponent, in general) is introduced into a vertical cascade of stages close to its centre. The feed mixes with the 'downcoming' liquid. The liquid at every stage is stripped of the more volatile component by the rising vapour, originally produced at the bottom by partial vaporization of the bottom liquid in the reboiler. The liquid residue at the bottom is rich in the less volatile component and is removed. The rising vapour gets progressively enriched in the more volatile component. It is condensed and stored in the

Copyrighted material

reflux accumulator. The material returned at the top of the tower is the reflux and the material removed from the reflux accumulator is the distillate which is rich in more volatile component.

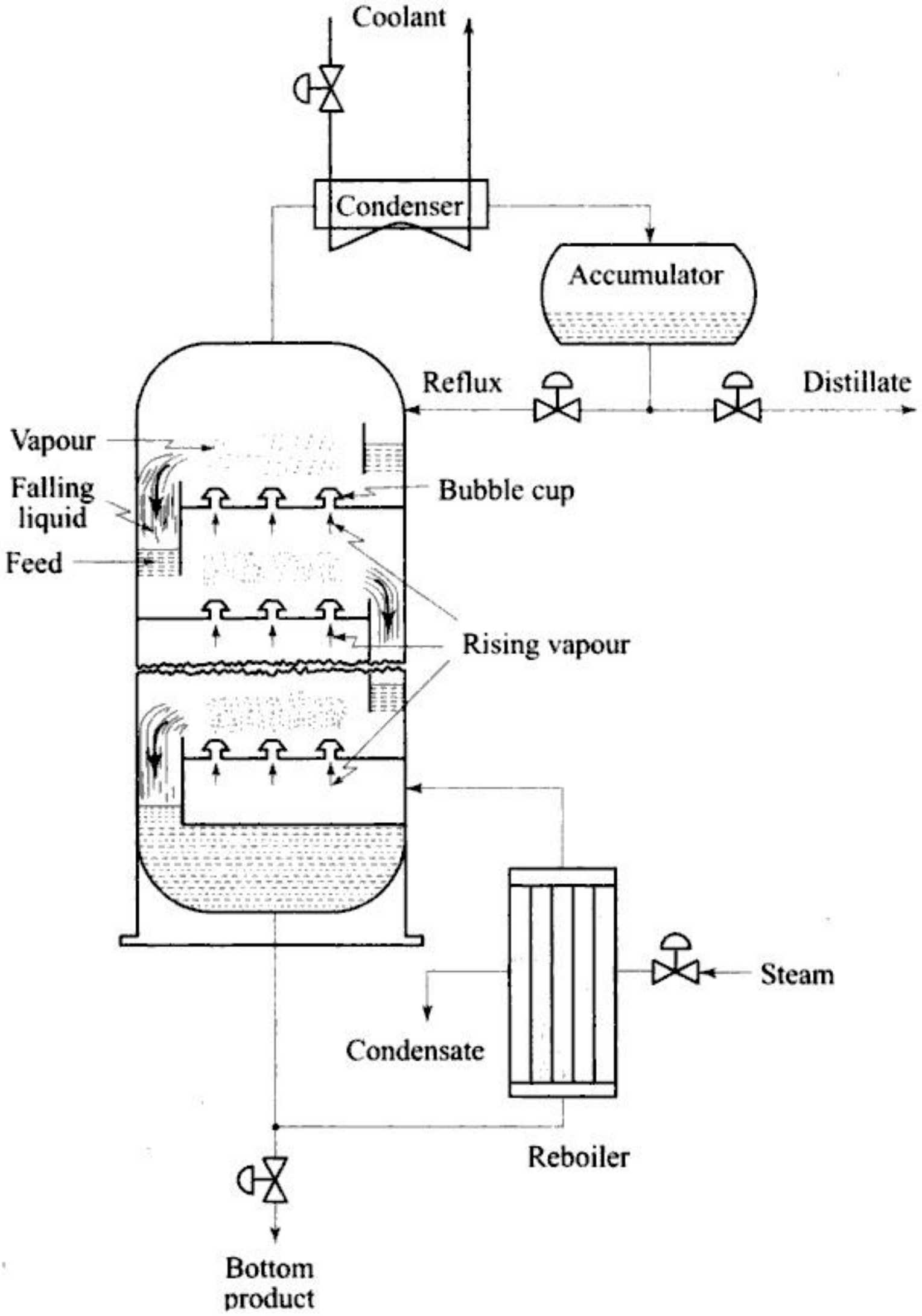


Fig. 1.22 *A distillation column with five primary controlled variables: two compositions, two levels, and pressure*

Let us now consider a simple control scheme for the distillation system. The two main objectives of the control are to maintain two product compositions, x_D (overhead (distillate) product composition) and x_B (bottom product composition), at their set points. The three secondary objectives are to maintain the

Copyrighted material

vapour balance by controlling the column pressure and the liquid balances by controlling the levels in the reflux accumulator and the column bottom.

In the control scheme shown in Figs 1.23–1.24, the distillate rate is manipulated to control the level of reflux accumulator, and the bottom rate is manipulated to control the bottom level. The two variables do not affect the operation of the column directly; the level control systems may therefore be treated as independent SISO systems.

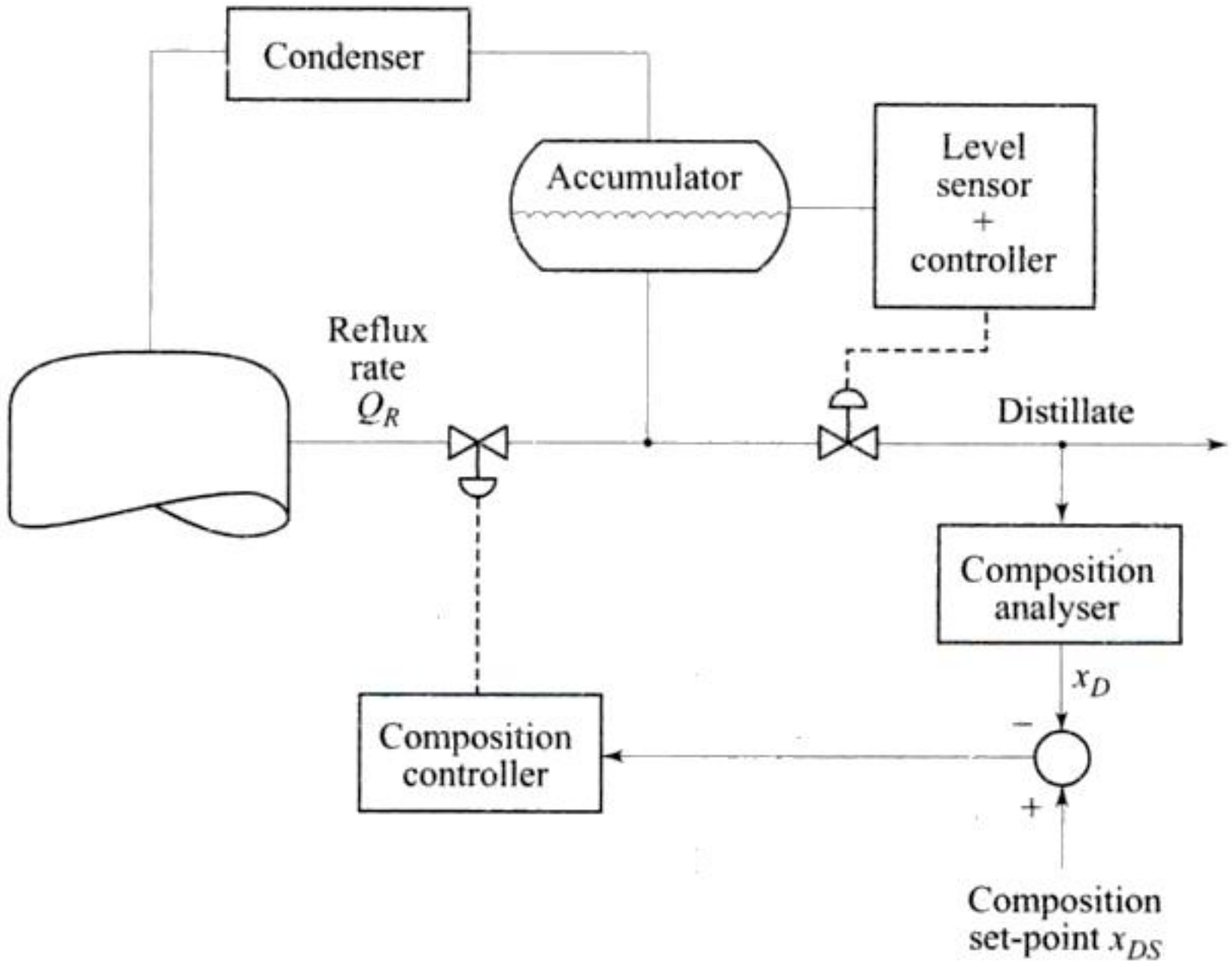


Fig. 1.23 *Distillation-column reflux*

In a column, the pressure is determined solely by the heat balance. If heat is supplied in the reboiler at a higher rate than it is removed in the condenser, the pressure in the column rises with time. Column pressure can be controlled by manipulating the reboiler heating rate or condenser cooling rate. We will assume that the pressure controller manipulates the condenser cooling rate and results in a non-interacting control loop (not shown in figures).

This reduces the problem to a two-by-two multivariable control problem: the manipulated variables are steam rate Q_S and reflux rate Q_R, and the controlled variables are the bottom product composition x_B and the distillate composition x_D. Figure 1.25 shows a block diagram representation of the resulting two-input, two-output system. Changes in the input variable Q_R cause responses in both the outputs, x_D and x_B. Similarly, input variable Q_S affects x_B as well as x_D.

In this book we will consider many examples of liquid-level, temperature, pressure, and composition control systems. SISO design techniques will provide control logic in large number of cases.

Copyrighted material

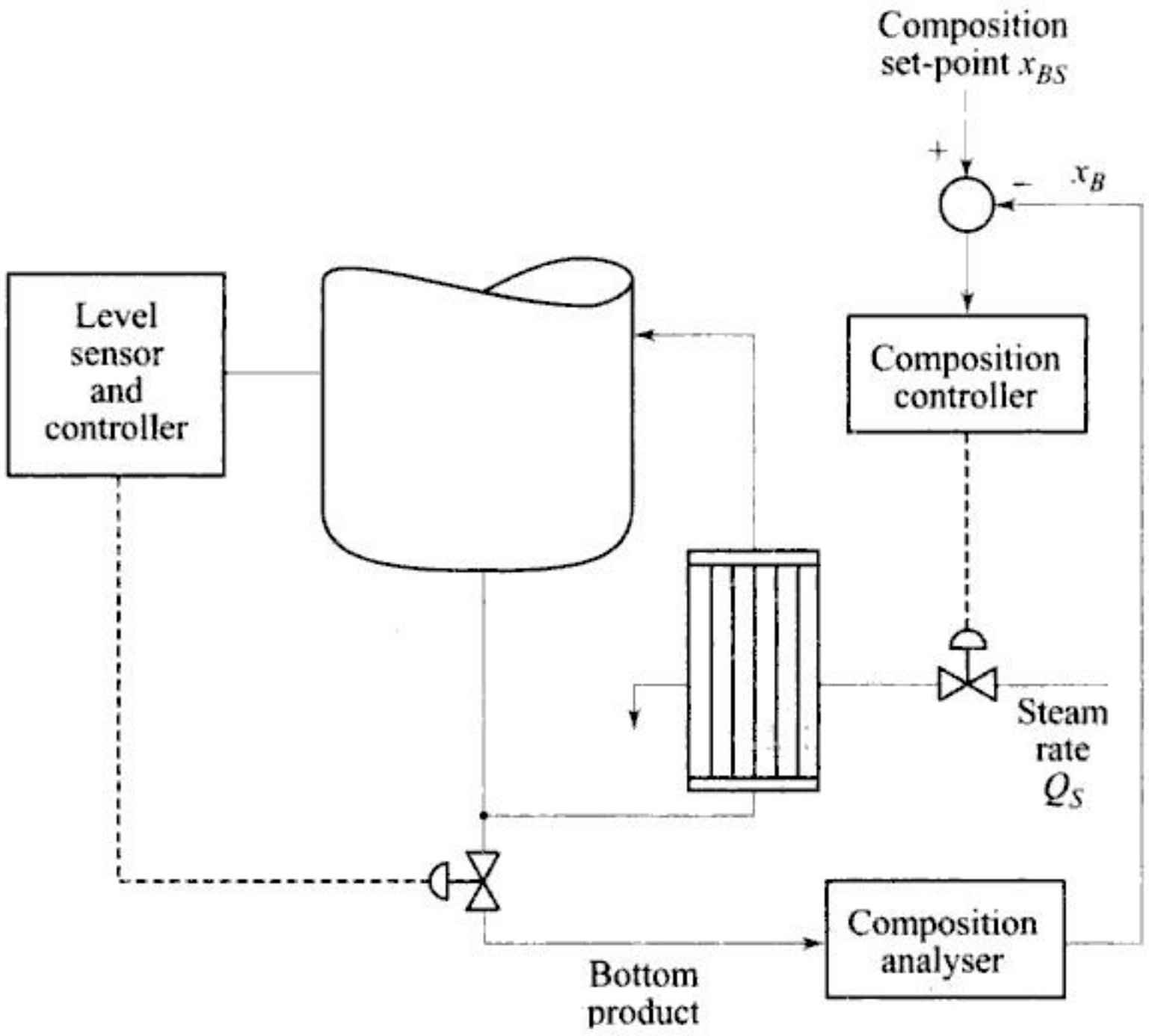


Fig. 1.24 *Distillation-column reboiler*

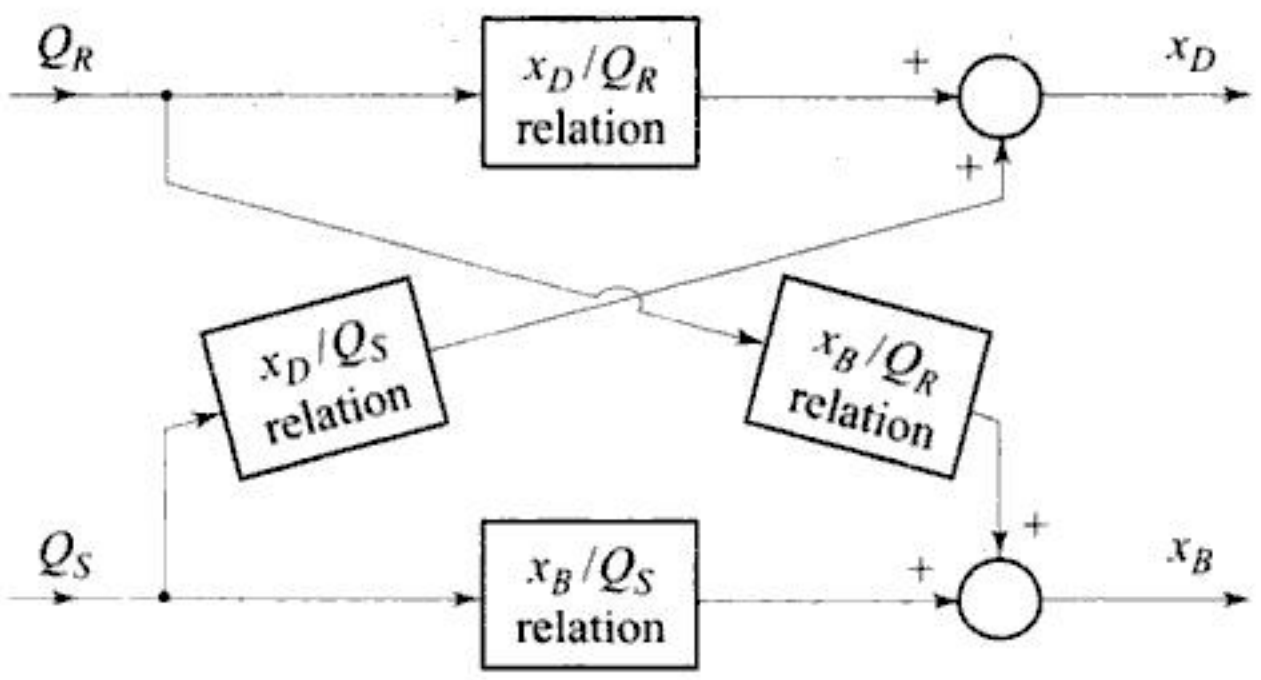


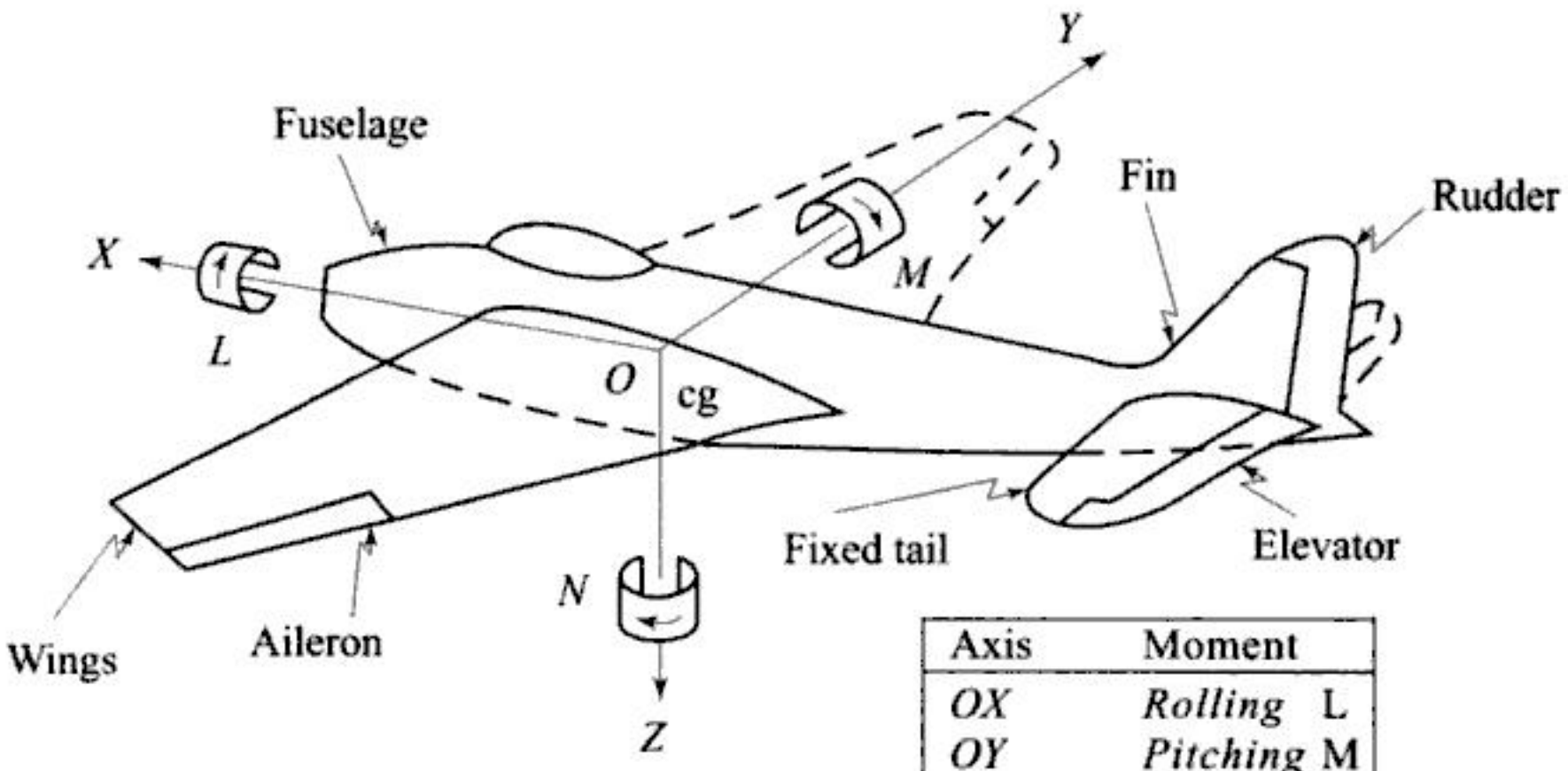
Fig. 1.25 *Block diagram representation of the multivariable control of a distillation column*

Example 1.9

Aircraft Stability and Control

Aircraft control is one of the most important applications through which control system techniques have developed. In aircraft control systems, the 'airframe' acts as a 'plant'; the behaviour of which is to be controlled. Main parts of an airframe include (Fig. 1.26):

Copyrighted material

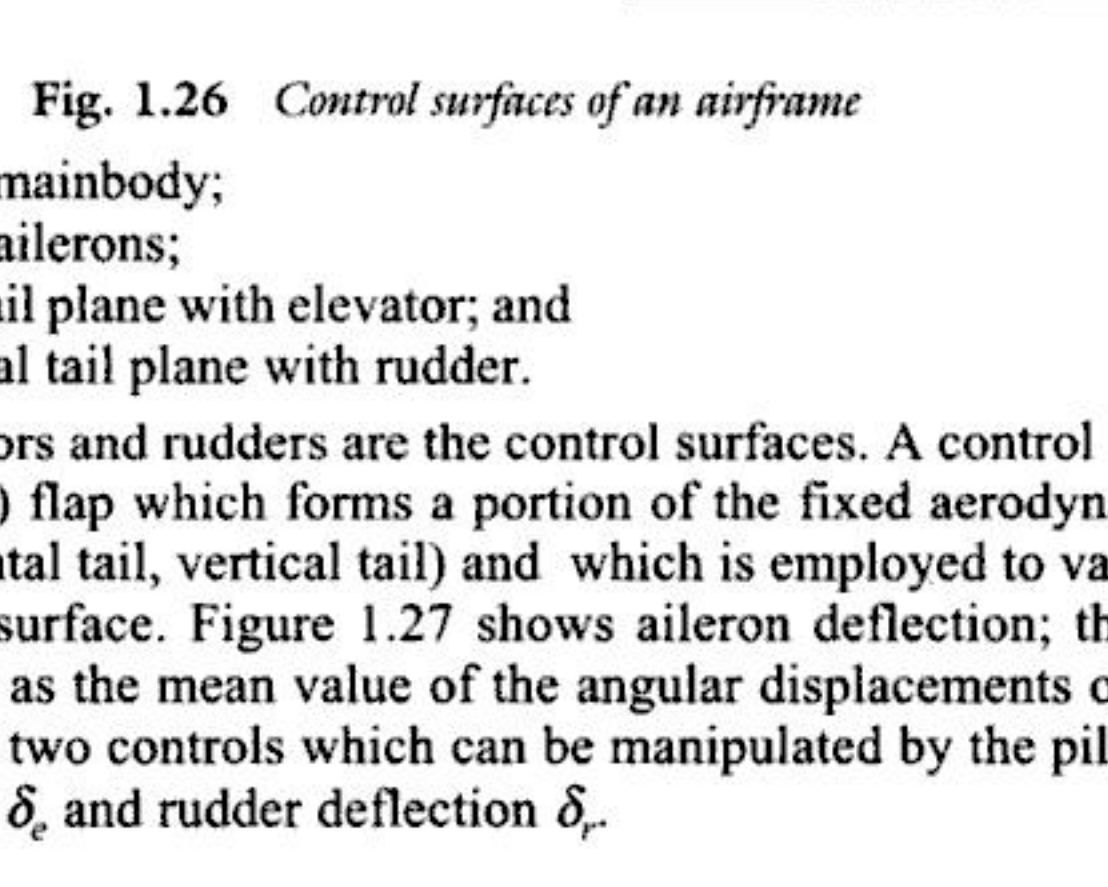


Axis	Moment	
OX	*Rolling*	L
OY	*Pitching*	M
OZ	*Yawing*	N

Fig. 1.26 *Control surfaces of an airframe*

(i) fuselage or mainbody;
(ii) wings with ailerons;
(iii) horizontal tail plane with elevator; and
(iv) fin or vertical tail plane with rudder.

Ailerons, elevators and rudders are the control surfaces. A control surface is a movable (hinged) flap which forms a portion of the fixed aerodynamic surface (wing, horizontal tail, vertical tail) and which is employed to vary the lift coefficient of the surface. Figure 1.27 shows aileron deflection; the aileron angle δ_a is defined as the mean value of the angular displacements of the two ailerons. The other two controls which can be manipulated by the pilot are the elevator deflection δ_e and rudder deflection δ_r.



$$\delta_a = \frac{1}{2}(\delta_1 + \delta_2)$$

Fig. 1.27 *Aileron deflection*

Copyrighted material

In examining the stability and control of a rigid aircraft, it is customary to separate the six degrees of freedom into two groups of three each. One group describes the longitudinal dynamics of the aircraft and comprises the translational motions along the OX- and OZ-axes, and the pitching motion. The other group describes the lateral dynamics of the aircraft and comprises the remaining three degrees of freedom, namely, the translational motion along the OY-axis, and the yawing and rolling motions. The elevator control forces and the throttle affect the longitudinal motion, whereas the aileron and rudder primarily affect the lateral motion. It has been found that for preliminary design work, the coupling of the lateral motion into longitudinal motion can be ignored.

In general, a control functions by causing a change in the pressure distribution on a surface, which results in a change in the lift coefficient of the surface. This change in the lift coefficient causes a change in the moment balance of the aeroplane and results in angular moment about one or more of the axes. The principal control actions of the three control surfaces are :

(i) the rudder controls yawing, i.e., motion about the OZ-axis;
(ii) the ailerons control rolling, i.e., motion about the OX-axis; and
(iii) the elevator controls pitching, i.e., motion about the OY-axis.

The actual positioning of control surfaces is obtained by electric or hydraulic motors which are controlled by the pilot.

Later in this book we shall analyse aircraft motions (SISO systems) under assumptions which neglect many details but preserve the essential nature of the problem. The servo problem of positioning the control surfaces in response to pilot commands will also be considered. Mathematical modelling of aircraft dynamics is beyond the scope of this book. References [14-18] give a good treatment of the subject.

Example 1.10

Robotic Control System

Machines that automatically load and unload, cut, weld or cast are used by industry in order to obtain accuracy, safety, economy, and productivity. Programmable computers integrated with machines that often substitute for human labour in specific repeated tasks, are the modern *robots*.[7] Such devices even have anthropomorphic mechanisms, including what we might recognize as mechanical arms, wrists, and hands.

A *robot manipulator* is made of several links connected usually in series by the joints to form an arm. A link is revolute or prismatic depending upon the type of motion caused by the actuator attached to its joint. When the actuator of a joint causes rotational motion, the link is *revolute*, and when the actuator produces translational motion, the link is called *prismatic*. A gripper, which is

7. The word robot seems to originate from the Czech language: robota means compulsory service.

Copyrighted material

referred to as a hand or an end-effector, is attached to the arm by means of wrist joints. The function of the wrist is to orient the end-effector properly.

The motion of a manipulator end-effector is caused by the movements of the actuators driving the joints. The joint actuators are electric or hydraulic motors, or pneumatically driven devices. The positions of the joints determine the *configuration of the arm*, which places the end-effector at a specific location in the environment. The motion of the joints produced by the actuators determines the position and orientation of the end-effector at any time. Transducers such as encoders and tachometers can be used to provide information for determining the position and orientation of the end-effector and to control the manipulator motion.

The set of all points that can be reached by the end-effector of a manipulator arm forms the *workspace* of the manipulator. A particular position of the end-effector is specified by three independent coordinates, which represent three degrees-of-freedom. Similarly, a specific orientation of the end-effector is determined by three independent variables. Thus, six independent variables are needed to describe the position and orientation of the end-effector. Commercially available robots have typically six joints giving six degrees-of-freedom. However, robots with less than six joints, designed for specific tasks, are also available. Figure 1.28 shows a picture of the PUMA (Programmable Universal Manipulator for Assembly), a revolute manipulator.

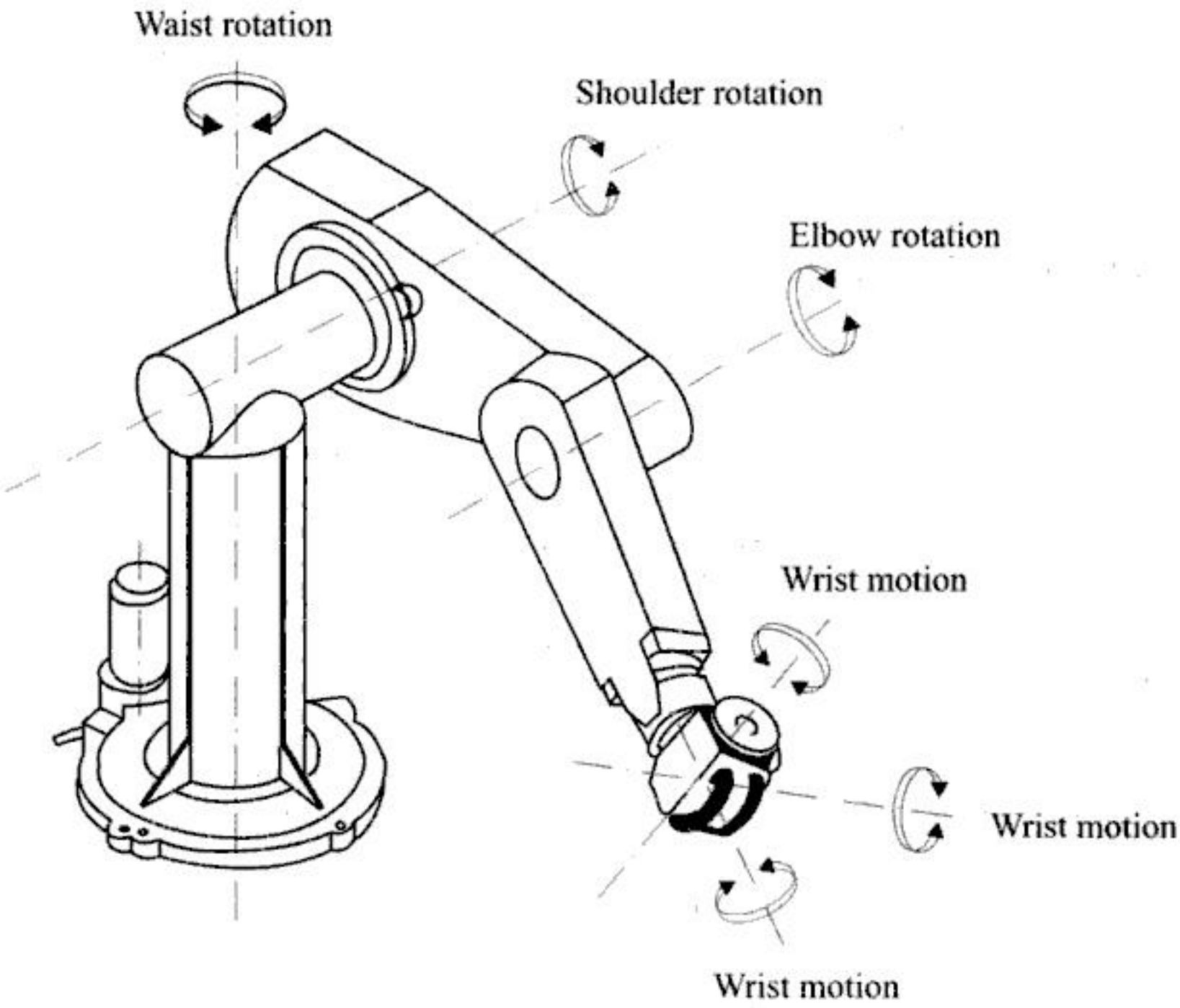


Fig. 1.28 *An industrial robot: PUMA*

Copyrighted material

The objective in providing position control for a robot manipulator is to design an appropriate controller for the robot motors so that the position and the orientation of the end-effector follow the desired trajectory with no errors even in the presence of disturbances. A multi-link manipulator is a highly complex system—each link of the robot arm has varying inertia and exerts varying torques on all the other links as the configuration of the robot arm changes. The equations of motion for a multi-link manipulator describe a MIMO system; the equations are coupled representing the effects of interactions of the joints. For a six-joint robot, joint positions θ_i, $i = 1, \ldots, 6$ (represented by the position vector $\boldsymbol{\theta}$ in Fig. 1.29) are the controlled outputs, and actuator torques u_i, $i = 1, \ldots, 6$ (represented by the input vector $\mathbf{u}$ in Fig. 1.29) are the manipulated variables. $\boldsymbol{\theta}_r$ is the position vector corresponding to the desired trajectory.

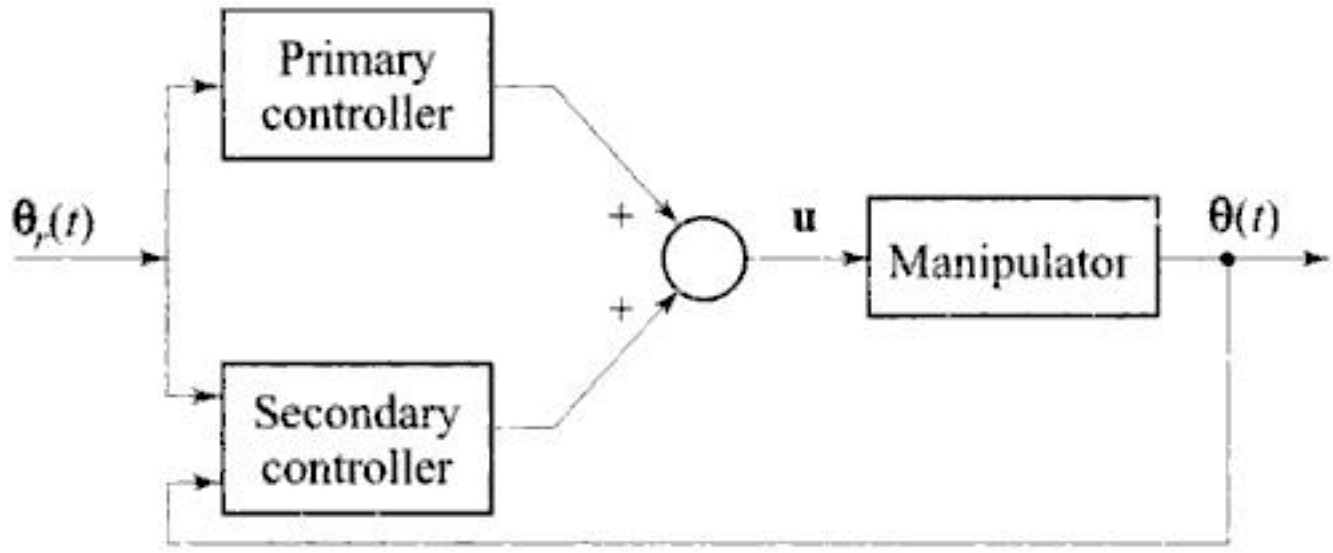


Fig. 1.29 *Manipulator system with primary and secondary controllers*

Perfect tracking can be achieved by a scheme employing command feedforward. Let $\boldsymbol{\theta}_r(t)$ be the input to a feedforward controller with dynamics which are inverse of the dynamics of the manipulator. When the manipulator is driven by the output of such a controller, we get $\boldsymbol{\theta}(t) = \boldsymbol{\theta}_r(t)$. The command-tracking based on this *inverse dynamics* concept can be perfect only if we can exactly determine the dynamic model of the manipulator.

The robotic system is too complex to allow exact identification of the dynamic model. Also, the system is subject to unmeasurable disturbances. Undesirable deviations of the actual motion of the manipulator from the desired trajectory can be corrected by means of feedback control. A block diagram showing the total control system (primary controller (feedforward) and secondary controller (feedback)) is displayed in Fig. 1.29.

The problem of control of the multi-link manipulator is too complex to be included in this introductory text. To bring robot application into our range, we will consider the problem of control of a single-link manipulator (SISO system). Selected titles for further reading are [19–24].

1.5 SCOPE AND ORGANIZATION OF THE BOOK

This text is concerned with basic concepts of feedback control theory, frequency-domain design tools, and analog/digital implementation of design. We

Copyrighted material

do not intend to solve all the control problems that can be posed under the defined category. In fact, we primarily study a special class of control systems, namely linear, time-invariant, lumped, and deterministic systems. For this class of systems, a fairly complete treatment of the control problem has been given in this book. The development of the material has been influenced by several existing books mentioned in the references given at the end of this text.

There are 11 chapters in the book in addition to this introductory chapter. In each chapter, analysis/design examples are interspersed to illustrate the concepts involved. At the end of each chapter, there are a number of review examples and questions; some of these also serve the purpose of extending the text material. The same approach is followed in unsolved problems. Answers have been given to inspire confidence in the reader.

The examples we have considered in this book are generally low-order systems. Such a selection of examples helps in conveying the fundamental concepts of feedback control without the distraction of large amounts of computations inherent in high-order systems. Many of the real-life design problems are more complex than the ones discussed in this book; high-order systems are common and, in addition, several parameters are to be varied during the design stage to investigate their effect on the system performance. Computer-Aided-Design (CAD) tools are extremely useful for complex control problems. Several software packages with computer graphics are available commercially for CAD of control systems [169–179]. Access to the CAD software is helpful, but not necessary, to solve the control problems discussed in this book. Let us now go through the organization of the chapters in sequence.

Chapter 2 combines some mathematical background with physical system modelling. Basic principles for modelling simple mechanical, electrical, hydraulic and thermal systems are treated, and transfer function and state variable models are derived. The analysis of transfer function models is also given. The analysis of state variable models, and their relationship to transfer functions is deferred to Chapter 12. References for Chapter 2 are [37–43].

Chapter 3 covers the mathematical models of different devices currently in use in industrial control practice. Models of typical industrial control systems are also included. The choice of examples is based on a desire to cover as many different application areas as possible. Devices used in computer-based control systems are covered later in Chapter 11. References for Chapter 3 are [44 – 57].

Chapter 4 introduces the basic modes of feedback control—proportional (P), integral (I), and derivative (D). A suitable combination of the three basic modes can improve all aspects of system performance. Characteristic performance features of commonly used control structures are also included in this chapter.

Copyrighted material

The material on stability has been progressively built in this book at three places. Chapter 5 introduces the two basic concepts of stability—BIBO (bounded-input, bounded-output) stability and asymptotic stability, as applied to linear time-invariant systems and presents the Routh stability criterion for stability analysis. More on stability analysis appears later in Chapters 8 and 12.

Chapter 6 gives control system performance specifications in time-domain. A number of performance measures for speed of response, relative stability, and steady-state accuracy are introduced.

Control system design has always relied heavily on graphical methods. Chapter 7 develops the root-locus method. Although computer programs are readily available for generating these plots, designers must be able to sketch them first, at least roughly, in order to use the programs efficiently and interpret the results. The material in Chapter 7 has been organized in this spirit. This chapter also uses the root-locus method for compensation; lead, and lag compensation are covered in detail.

Chapter 8 describes the Nyquist stability criterion. Robust stability measures—the gain margin and the phase margin—are introduced in this chapter.

Chapter 9 gives control system performance specifications in the frequency-domain. Correlation between time- and frequency-response is also established.

Chapter 10 uses frequency-response plots—Bode plot, and Nichols chart, for compensator design. Lead and lag compensation are covered in detail. References for the material in Chapters 4–10 are [58–77].

Chapter 11 is concerned with implementation of compensators by physical devices—passive electrical networks, op amp based networks, and digital computers. A modest investment in digital methods has been made so that the control engineer can work well in increasingly digital environment. References for digital control are [78–101].

The practice of selecting a certain class of controller (P, PI, PID) based on past experience with certain classes of processes (pressure, flow, liquid-level, temperature, etc.) and then setting controller parameters by experiment once the controller is installed, has come to be known as controller tuning. Chapter 11 also includes this 'experimental' design method for both analog and digital controllers. References for process control are [5–13].

Many computer aided design packages use state-space and matrix notation, and therefore it is helpful for control engineers to be familiar with it. Chapter 12 on state variable analysis meets this objective. It deals with the problems of state variable representation, solution, controllability, and observability. Relationship between transfer function and state variable models is also given. Although it is assumed that the reader has necessary background on vector-matrix analysis, a reasonably detailed account of vector-matrix analysis is provided in the chapter for convenient reference. References for state variable methods are [102–115].

Copyrighted material

The text presumes on the part of the reader some knowledge of basic tools like complex variables, and the Laplace transform. However, Appendix A on mathematical background has been included to make the book reasonably self-contained. Appendix B provides an introduction to the MATLAB environment for computer-aided control system design. MATLAB problems included in the appendix give the student practice with problem solving using computers. Multiple choice questions given in Appendix C serve the purpose of self-appraisal review of control theory.

Copyrighted material

chapter 2

Dynamic Models and Dynamic Response

2.1 INTRODUCTION

Modelling of physical systems is an important component of the control system design procedure. The present chapter reviews the basic laws of physics used to develop mathematical models of mechanical, electrical, hydraulic, and thermal systems that are commonly encountered in control systems as plant models or as models of control logic elements. The next chapter deals with the models of actuators, measurement sensors, and error detectors. The models of overall control systems are then developed by considering the interaction of these devices. Models of digital devices used in automatic control systems are discussed in Chapter 11.

An alternative approach of modelling is to regard the physical system as merely a 'black box', into which one can inject inputs and from which one can obtain measurements of the corresponding outputs. We then use this data to obtain a mathematical model of the system which produces the same outputs from the given inputs. This approach of modelling is known in the literature as *system identification*. Some simple identification methods will appear in later chapters.

▲▲

Different types of dynamic models used to represent control systems are classified below:

Distributed-parameter and Lumped-parameter Models

The significant variables in a system are distributed in space and they vary with the spatial coordinates and time. The resulting dynamic 1models, called *distributed-parameter models*, consist of partial differential equations with time and space coordinates as independent variables.

Copyrighted material

In *lumped-parameter models*, the matter is assumed to be lumped at some discrete points of the space, or the space is subdivided into cells and the matter is assumed to be lumped at these cells. The resulting dynamic models are ordinary differential equations with time as the only independent variable. For example, the assumption that a solid is a rigid body permits lumping all its mass at its mass centre and results in lumped-parameter models of dynamics.

Considerable simplification is achieved in mathematical models when lumped-parameter models are used. In this book, we employ lumped-parameter models for control system design.

Stochastic and Deterministic Models

In physical systems, every signal (inputs, external disturbances, measured outputs) has associated with it certain amount of randomness (usually referred to by the generic term 'noise'). These uncertainties are inconsequential in many practical cases, and we proceed as though all signals are known functions of time. This assumption gives us a *deterministic model* of the system. When signals must be treated as random functions of time, *stochastic models* are used to characterize the system behaviour. In this book, we will make the assumption of deterministic signals.

Time-varying and Time-invariant Models

When the parameters of the mathematical model are varying with time, the model is called *time-varying* or non-stationary. For example, in the guidance and control of a rocket, the mass of the rocket changes with time due to the depletion of fuel, and also the aerodynamic damping can change with time as the air density changes with altitude. The complexity of the control system design increases considerably when the parameters are time-varying.

In this book, we shall concern ourselves with those applications where the time-invariance assumption can safely be made, and therefore the models we use will have constant parameters.

Nonlinear and Linear Models

The mathematical model of a system is *linear*, if it obeys the principle of *superposition and homogeneity*. This principle implies that if a system model has responses $y_1(t)$ and $y_2(t)$ to any two inputs $r_1(t)$ and $r_2(t)$ respectively, then the system response to the linear combination of these inputs, i.e.,

$$\alpha_1\, r_1(t) + \alpha_2\, r_2(t);\ \alpha_1,\ \alpha_2 \text{ constants},$$

is given by the linear combination of the individual outputs, i.e.,

$$\alpha_1\, y_1(t) + \alpha_2\, y_2(t)$$

Powerful mathematical tools that provide general methods of analysis and design are available for *linear systems*. For *nonlinear systems*, general methods are not available and each system must be studied as one of a kind. Practically

Copyrighted material

none of the systems is completely linear, but a linear model is often appropriate over certain ranges of operation.

In control systems, nonlinearities can be classified as *incidental* and *intentional*. Incidental nonlinearities are those which are inherently present in the system and are introduced by the controlled process, sensors, actuators, controllers, etc. The designer strives to design the system so as to limit the adverse effects of these nonlinearities. The intentional nonlinearities, on the other hand, are those which are deliberately inserted in the system to modify system characteristics. The most common example is that of on-off control systems.

Linearization over desired ranges of operation is usually possible and we will mostly employ linear models for systems with incidental nonlinearities. For situations where this approximation becomes too crude to be employed and/or nonlinearities are deliberately introduced, powerful mathematical tools—the *describing function method* and the *phase-plane method*, may be employed [180].

▲▲

In this book, we will be mainly concerned with linear, time-invariant, lumped systems. Application of physical laws to such a system, as we shall see in this chapter, results in a set of ordinary differential equations which directly provide us with the rates of change of significant variables characterizing the dynamics of the system. These differential equations when rearranged in the form of a set of first-order differential equations, are called *state equations*. Laplace transformation of these differential equations with zero initial conditions gives us *transfer function* representation.

Through the examples given in this chapter, it will become clear that to obtain a transfer function model, one first writes the state equations of the system which 'naturally' arise from the application of physical laws. State variable modelling is thus a 'natural' step required for transfer function modelling.

State variable analysis and design methods use matrix theory and are, to some extent, different from those based on transfer function models. We have separated state variable methods from those based on transfer functions. State variable methods are covered in Chapter 12 while rest of the book uses the transfer function approach.

The presence of disturbances is one of the main reasons for using feedback control. Without disturbances, there is probably no need for feedback control. The character of the disturbances imposes fundamental limitations on the performance of a control system.

The disturbances may be classified as load disturbances, measurement errors, and parameter variations. *Load disturbances* are external disturbances from the process environment which influence the process variables. *Measurement errors* enter through the measuring instruments (sensors). Disturbances also enter in the form of *variations in the parameters* due to wear and tear, ageing, environmental effects, etc., or due to unmodelled dynamics. In Chapter 4, we will study the effects of these disturbances on control system performance.

Copyrighted material

In the present chapter simple, yet effective, models of load disturbances are given. Transfer functions of disturbance variables (uncontrolled inputs) on the output variables of industrial plants have been derived for commonly occurring load disturbances.

A review of the study of dynamic response of linear time-invariant systems using Laplace transforms has also been given in this chapter.

2.2 STATE VARIABLE MODELS

In this and the next two sections, three different forms of mathematical models for linear time-invariant lumped systems will be introduced. Depending upon the requirements of analysis or the design techniques used, one form of model might be preferable to another in describing the same system. Since we study only time-invariant systems, we shall assume, without loss of generality, that the initial time is zero ($t_0 = 0$) and that the time interval of interest is $[0, \infty)$, i.e., $\{0 \leq t < \infty\}$.

Consider the resistance-inductance-capacitance (RLC) network shown in Fig. 2.1. The input is a voltage source. The desired output information is usually the voltages and currents associated with various elements of the network. This information at time t can be obtained if the voltage across the capacitor and the current through the inductor of the network at that time are known, in addition to the values of the input. The voltage $e(t)$ across the capacitor and the current $i(t)$ through the inductor thus constitute a set of *characterizing variables* of the network. The selection of characterizing variables is linked with the energy concept. At time t, energy stored in the capacitor is $\frac{1}{2}Ce^2(t)$ and energy stored in the inductor is $\frac{1}{2}Li^2(t)$. Dynamical changes in characterizing variables are caused by the redistribution of energy within the network. The number of independent energy storage possibilities thus equals the number of characterizing variables of the network. The values of the characterizing variables at time t describe the *state* of the network at that time; these variables are therefore called *state variables* of the network.

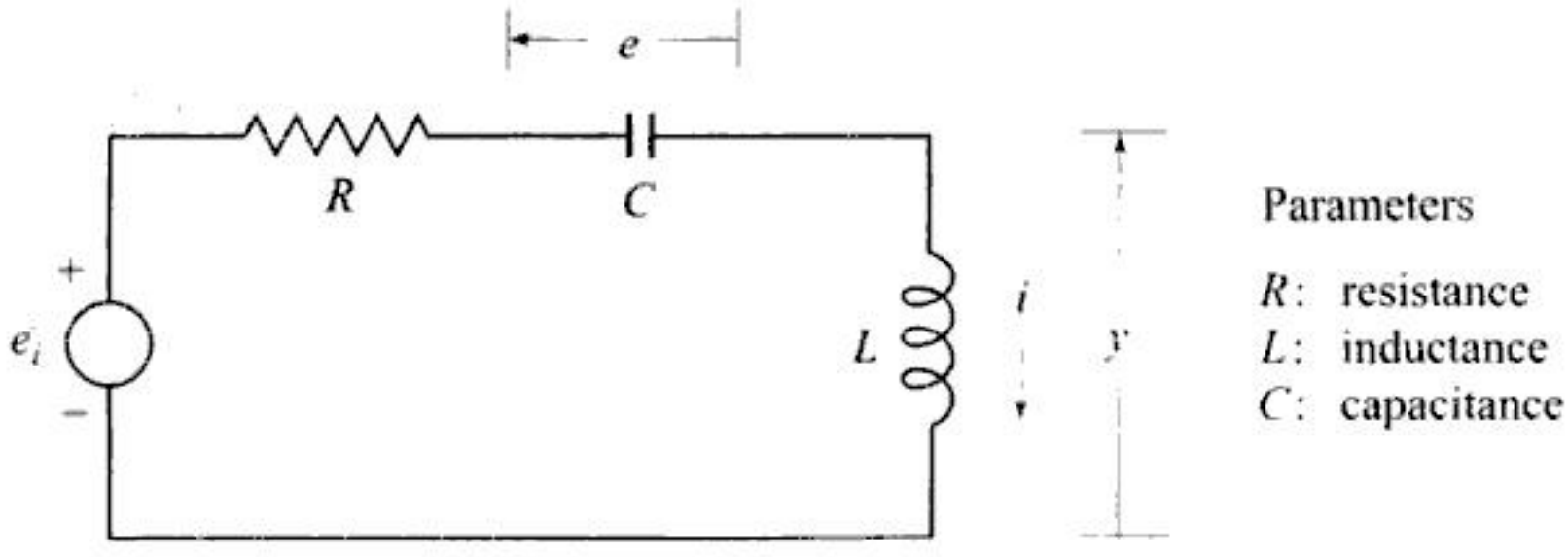


Fig. 2.1 *An RLC network*

Copyrighted material

Network analysis usually requires setting up of dynamical equations (using Kirchhoff's voltage and current laws) in terms of rates of change of capacitor voltages and inductor currents. The solution of these equations describes the state of the network at time t. Desired output information is then obtained from the state using an algebraic relation.

Let us set up dynamical equations for the RLC network of Fig. 2.1, by using Kirchhoff's voltage law. The governing equations of the system are

$$Ri(t) + e(t) + L\frac{di(t)}{dt} = e_i(t); \; C\frac{de(t)}{dt} = i(t)$$

Rearrangement of these equations gives the rates of change of capacitor voltage and inductor current.

$$\left.\begin{aligned} \frac{de(t)}{dt} &= \frac{1}{C}i(t) \\ \frac{di(t)}{dt} &= -\frac{1}{L}e(t) - \frac{R}{L}i(t) + \frac{1}{L}e_i(t) \end{aligned}\right\} \tag{2.1a}$$

The solution of these equations for given input $e_i(t)$ applied at $t = 0^+$, and given initial state $\{e(0), i(0)\}$ yields the state $\{e(t), i(t)\}$, $t > 0$. If $y(t)$ shown in Fig. 2.1 is the desired output information, we have the following algebraic relation to obtain $y(t)$:

$$y(t) = -e(t) - Ri(t) + e_i(t) \tag{2.1b}$$

Equations (2.1a) give the rates of change of state variables (capacitor voltage $e(t)$, and inductor current $i(t)$) in terms of the state variables and the input. These equations are called the *state equations*. Equation (2.1b) is an instantaneous relation, reading output $y(t)$ from the state variables $\{e(t), i(t)\}$ and the input $e_i(t)$. This equation is called the *output equation*.

It may be noted that the state of a system is not uniquely specified. For the network of Fig. 2.1, the charge $q(t)$ deposited on the capacitor is given by

$$q(t) = Ce(t)$$

Therefore, the variables $q(t)$ and $i(t)$ also qualify as state variables for this network.

In terms of these state variables, the state and output equations are given below:

$$\left.\begin{aligned} \frac{dq(t)}{dt} &= i(t) \\ \frac{di(t)}{dt} &= -\frac{1}{LC}q(t) - \frac{R}{L}i(t) + \frac{1}{L}e_i(t) \end{aligned}\right\} \tag{2.2a}$$

$$y(t) = -\frac{1}{C}q(t) - Ri(t) + e_i(t) \tag{2.2b}$$

In mass-spring-damper systems, we are usually interested in the displacements, velocities, and forces associated with various elements of the

Copyrighted material

systems. Normally, an independent set of displacements and velocities of the masses, and displacements of the springs constitutes a set of state variables of the system. The values of these variables at time t describe the status of energy storage elements at that time, and also ensure that the desired output information can be 'read' from the state variables.

For the mass-spring-damper system of Fig. 2.2a, the displacement $x(t)$ and velocity $v(t)$ are state variables. A systematic way of setting up dynamical equations for mass-spring-damper systems is to draw a free-body diagram. In a free-body diagram, each mass is isolated from the rest of the system; forces acting on each free-body are due to the rest of the system, including external forces. The free-body mass moves under the action of the resultant force. By applying Newton's law of motion to each free-body, we get the force equations describing the dynamics of the system.

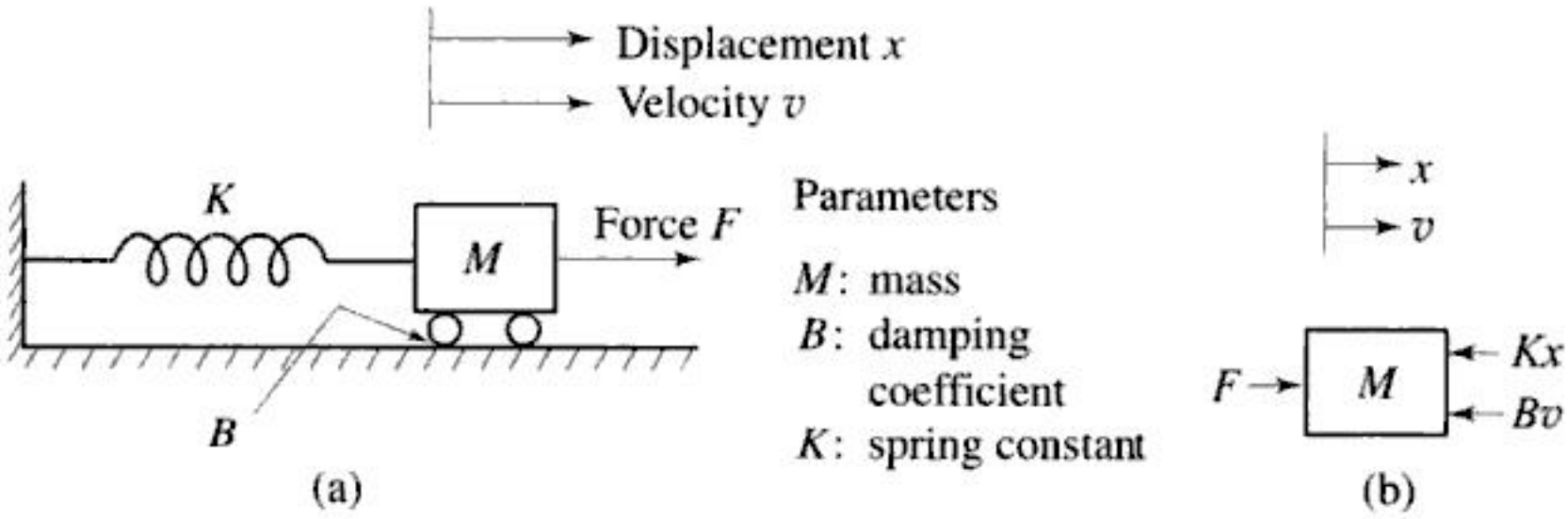


Fig. 2.2 *(a) A mass-spring-damper system (b) Free-body diagram*

Figure 2.2b shows the free-body diagram of the system of Fig. 2.2a. Applying Newton's law of motion, the force equation can be written as

$$F(t) - Bv(t) - Kx(t) = M\frac{dv(t)}{dt}$$

Since $v(t) \triangleq \frac{dx(t)}{dt}$, we have

$$M\frac{d^2x(t)}{dt^2} + B\frac{dx(t)}{dt} + Kx(t) = F(t)$$

Rearrangement of these equations gives the rates of change of displacement $x(t)$ and velocity $v(t)$:

$$\left.\begin{aligned} \frac{dx(t)}{dt} &= v(t) \\ \frac{dv(t)}{dt} &= -\frac{K}{M}x(t) - \frac{B}{M}v(t) + \frac{1}{M}F(t) \end{aligned}\right\} \qquad (2.3a)$$

Copyrighted material

The solution of these equations for given input (force $F(t)$) applied at $t = 0^+$ and given initial state $\{x(0), v(0)\}$ yields the state $\{x(t), v(t)\}$, $t > 0$. If displacement of the mass is the desired output $y(t)$, we have the output equation

$$y(t) = x(t) \tag{2.3b}$$

Examples of hydraulic and thermal systems will appear later in this chapter. ▲▲

Consider now the general SISO system shown in the block diagram of Fig. 2.3. We will denote the system *state* by *n state variables* $\{x_1(t), x_2(t), \ldots, x_n(t)\}$. In compact notation, this information may be represented by the *state vector*

$$\mathbf{x}(t) \triangleq \begin{bmatrix} x_1(t) \\ x_2(t) \\ \vdots \\ x_n(t) \end{bmatrix}$$

The dimension of the state vector defines the *order of the system*.

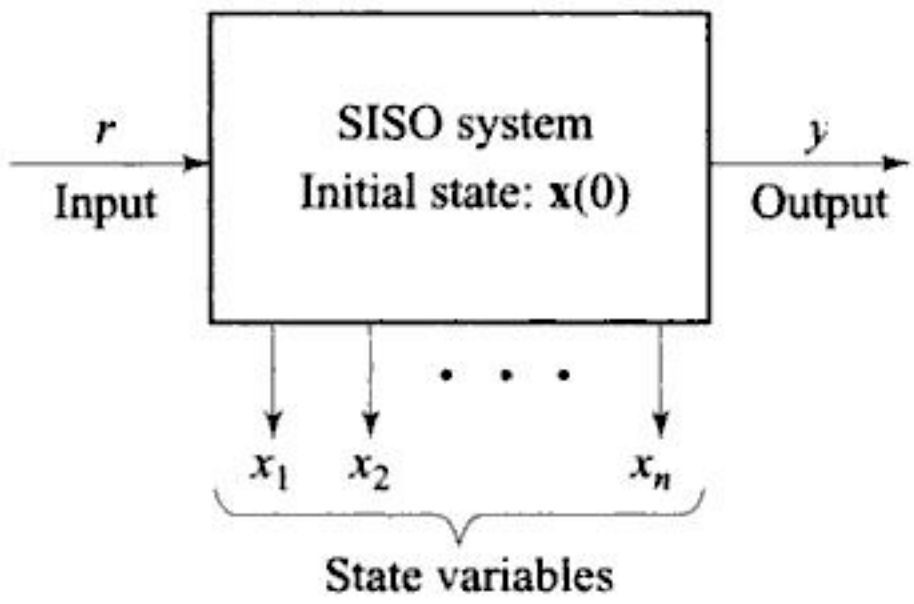


Fig. 2.3 *A SISO system*

The set of equations that describe the relationship among input, output, and the state variables, is called the *state variable model*. For *n*th order linear time-invariant system, the state variable model takes the form (refer Eqns (2.1), (2.2), (2.3)):

$$\left.\begin{aligned}
\dot{x}_1(t) \triangleq \frac{dx_1(t)}{dt} &= a_{11}x_1(t) + a_{12}x_2(t) + \cdots + a_{1n}x_n(t) + b_1 r(t) \\
\dot{x}_2(t) \triangleq \frac{dx_2(t)}{dt} &= a_{21}x_1(t) + a_{22}x_2(t) + \cdots + a_{2n}x_n(t) + b_2 r(t) \\
&\vdots \\
\dot{x}_n(t) \triangleq \frac{dx_n(t)}{dt} &= a_{n1}x_1(t) + a_{n2}x_2(t) + \cdots + a_{nn}x_n(t) + b_n r(t)
\end{aligned}\right\}$$

Copyrighted material

$$y(t) = c_1 x_1(t) + c_2 x_2(t) + \cdots + c_n x_n(t) + d\, r(t)$$

or in vector-matrix[1] form

$$\dot{\mathbf{x}}(t) = \mathbf{A}\mathbf{x}(t) + \mathbf{b}\, r(t) : \textit{state equation} \tag{2.4a}$$

$$y(t) = \mathbf{c}\mathbf{x}(t) + d\, r(t) : \textit{output equation} \tag{2.4b}$$

with

$$\mathbf{x}(t) = \begin{bmatrix} x_1(t) \\ x_2(t) \\ \vdots \\ x_n(t) \end{bmatrix}; \mathbf{A} = \begin{bmatrix} a_{11} & a_{12} & \cdots & a_{1n} \\ a_{21} & a_{22} & \cdots & a_{2n} \\ \vdots & \vdots & & \vdots \\ a_{n1} & a_{n2} & \cdots & a_{nn} \end{bmatrix}; \mathbf{b} = \begin{bmatrix} b_1 \\ b_2 \\ \vdots \\ b_n \end{bmatrix}$$

$$\mathbf{c} = \begin{bmatrix} c_1 & c_2 & \cdots & c_n \end{bmatrix}$$

where $\mathbf{x}(t)$, $r(t)$ and $y(t)$ are, respectively, the state, the input and the output of a system; $\mathbf{A}$ is $n \times n$ constant matrix; $\mathbf{b}$ is $n \times 1$ constant column vector; $\mathbf{c}$ is $1 \times n$ constant row vector; and d is a constant scalar representing direct coupling between input and output.

Equations (2.4a) are n first-order differential equations expressing time derivatives of each of the components of the state vector $\mathbf{x}(t)$ as a linear combination of system states and input. The solution of these equations for given input $r(t)$ applied at $t = 0^+$, and given initial state $\mathbf{x}(0)$ yields the system state $\mathbf{x}(t)$, $t > 0$. The output $y(t)$ (Eqn. (2.4b)) is a linear combination of system states and input.

Equations (2.4a) and (2.4b) together provide the input-output-state description of a dynamic system, represented diagrammatically in Fig. 2.4. Note that in this model structure, the dynamic evolution of system state in response to initial state $\mathbf{x}(0)$ and input $r(t)$ is obtained; desired output information $y(t)$ is then 'read' from $\mathbf{x}(t)$.

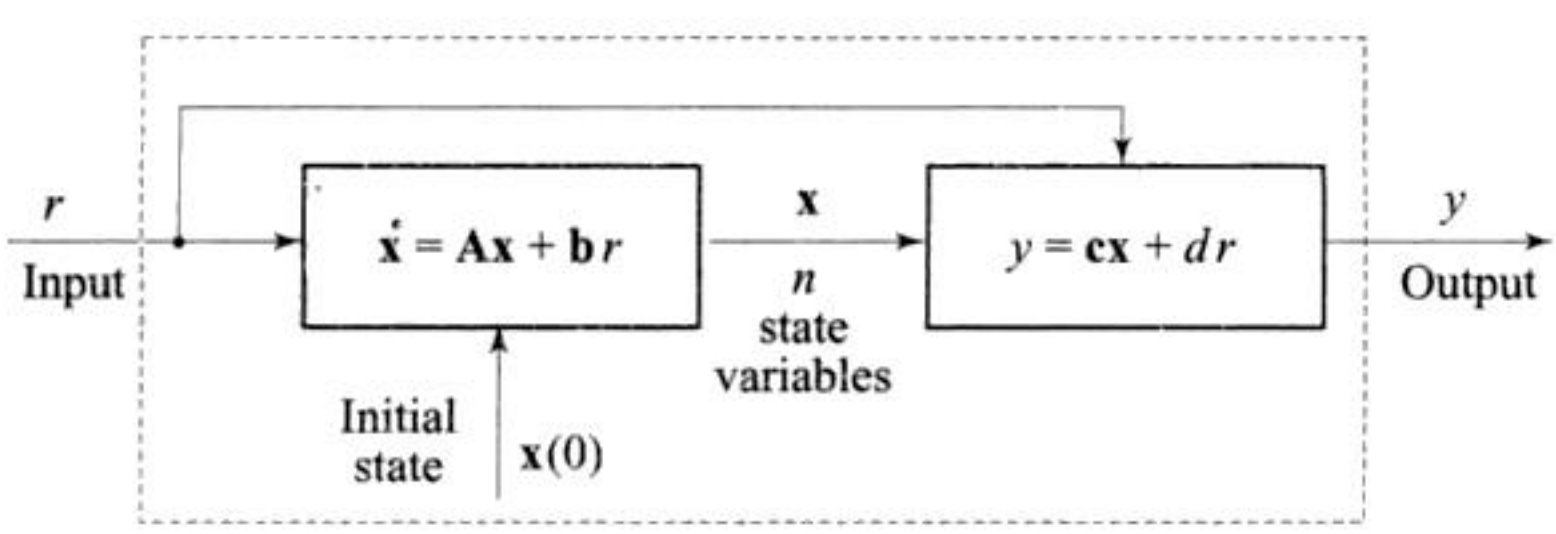


Fig. 2.4 *Input-output-state description*

The general MIMO system is shown in the block diagram of Fig. 2.5. Time functions, r_1, r_2, ..., r_p are the input variables, and y_1, y_2, ..., y_q are the output

1. We will use lower case bold letters to represent vectors, and upper case bold letters to represent matrices.

Copyrighted material

variables. The state, as in the case of SISO systems, is represented by the variables $x_1, x_2, ..., x_n$. For notational economy, the different variables may be represented by the input vector $\mathbf{r}(t)$, the output vector $\mathbf{y}(t)$, and the state vector $\mathbf{x}(t)$, where

$$\mathbf{r}(t) = \begin{bmatrix} r_1(t) \\ r_2(t) \\ \vdots \\ r_p(t) \end{bmatrix}; \mathbf{y}(t) = \begin{bmatrix} y_1(t) \\ y_2(t) \\ \vdots \\ y_q(t) \end{bmatrix}; \mathbf{x}(t) = \begin{bmatrix} x_1(t) \\ x_2(t) \\ \vdots \\ x_n(t) \end{bmatrix}$$

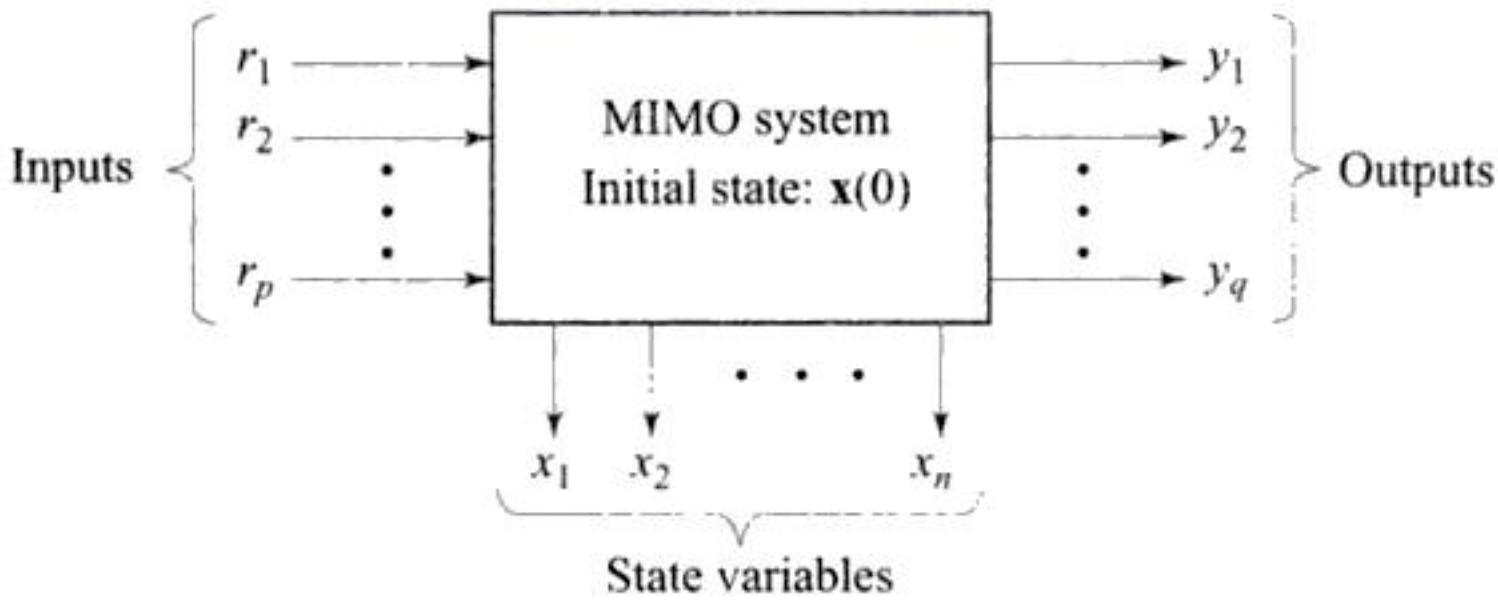


Fig. 2.5 *A MIMO system*

For MIMO systems, the derivative of each state variable becomes a linear combination of system states $x_1, x_2, \ldots, x_n$, and the inputs $r_1, r_2, \ldots, r_p$. Also, each output variable at time t is a linear combination of the states and the inputs at time t. The state variable model for MIMO systems takes the following form:

$$\dot{\mathbf{x}}(t) = \mathbf{A}\mathbf{x}(t) + \mathbf{B}\mathbf{r}(t) : \textit{state equation} \tag{2.5a}$$

$$\mathbf{y}(t) = \mathbf{C}\mathbf{x}(t) + \mathbf{D}\mathbf{r}(t) : \textit{output equation} \tag{2.5b}$$

with

$$\mathbf{A} = \begin{bmatrix} a_{11} & a_{12} & \cdots & a_{1n} \\ a_{21} & a_{22} & \cdots & a_{2n} \\ \vdots & \vdots & & \vdots \\ a_{n1} & a_{n2} & \cdots & a_{nn} \end{bmatrix}; \mathbf{B} = \begin{bmatrix} b_{11} & b_{12} & \cdots & b_{1p} \\ b_{21} & b_{22} & \cdots & b_{2p} \\ \vdots & \vdots & & \vdots \\ b_{n1} & b_{n2} & \cdots & b_{np} \end{bmatrix}$$

$$\mathbf{C} = \begin{bmatrix} c_{11} & c_{12} & \cdots & c_{1n} \\ c_{21} & c_{22} & \cdots & c_{2n} \\ \vdots & \vdots & & \vdots \\ c_{q1} & c_{q2} & \cdots & c_{qn} \end{bmatrix}; \mathbf{D} = \begin{bmatrix} d_{11} & d_{12} & \cdots & d_{1p} \\ d_{21} & d_{22} & \cdots & d_{2p} \\ \vdots & \vdots & & \vdots \\ d_{q1} & d_{q2} & \cdots & d_{qp} \end{bmatrix}$$

A, **B**, **C** and **D** are respectively. $n \times n$, $n \times p$, $q \times n$ and $q \times p$ constant matrices.

Since every real-world system has some nonlinearity, a mathematical model of the form (2.5) is always an approximation to reality. Many real-world nonlinearities involve a 'smooth' curvilinear relation between an independent variable x and a dependent variable y:

$$y = f(x) \tag{2.6a}$$

Copyrighted material

A linear approximation to the curve, accurate in the neighbourhood of selected operating point x_0, is the tangent line to the curve at that point. This approximation is given conveniently by the first two terms of the Taylor series expansion of $f(x)$:

$$y = f(x_0) + \left[\frac{df}{dx}\bigg|_{x=x_0}\right](x - x_0) + \left[\frac{d^2f}{dx^2}\bigg|_{x=x_0}\right]\frac{(x-x_0)^2}{2!} + \cdots$$

The linear approximation is

$$y \cong f(x_0) + \left[\frac{df}{dx}\bigg|_{x=x_0}\right](x - x_0) \tag{2.6b}$$

When a dependent variable y is related nonlinearly to several independent variables x_1, x_2, x_3, etc., according to

$$y = f(x_1, x_2, x_3, \ldots) \tag{2.6c}$$

we may linearize using the multivariable form of the Taylor series:

$$y \cong f(x_{10}, x_{20}, \ldots) + \left[\frac{\partial f}{\partial x_1}\bigg|_{x_{10}, x_{20}, \cdots}\right](x_1 - x_{10})$$

$$+ \left[\frac{\partial f}{\partial x_2}\bigg|_{x_{10}, x_{20}, \cdots}\right](x_2 - x_{20}) + \cdots \tag{2.6d}$$

We will use the linearizing approximations in developing linear state variable models of the form (2.5) from nonlinear relationships of the form given below:

$$\left.\begin{aligned}
\dot{x}_1(t) &= f_1(x_1(t), x_2(t), \ldots, x_n(t), r_1(t), \ldots, r_p(t)) \\
\dot{x}_2(t) &= f_2(x_1(t), x_2(t), \ldots, x_n(t), r_1(t), \ldots, r_p(t)) \\
&\vdots \\
\dot{x}_n(t) &= f_n(x_1(t), x_2(t), \ldots, x_n(t), r_1(t), \ldots, r_p(t))
\end{aligned}\right\} \tag{2.7a}$$

$$\left.\begin{aligned}
y_1(t) &= g_1(x_1(t), x_2(t), \ldots, x_n(t), r_1(t), \ldots, r_p(t)) \\
&\vdots \\
y_q(t) &= g_q(x_1(t), x_2(t), \ldots, x_n(t), r_1(t), \ldots, r_p(t))
\end{aligned}\right\} \tag{2.7b}$$

where $f_i(\cdot)$, $i = 1, 2, \ldots, n$ are nonlinear functions describing state equations, and $g_j(\cdot)$, $j = 1, 2, \ldots, q$ are nonlinear functions describing output equations.

2.3 IMPULSE RESPONSE MODELS

Consider the SISO system of Fig. 2.3. The system is excited by two types of inputs; the external input $r(t)$, and the initial state $\mathbf{x}(0)$ representing initial energy storage in the system. The response variables are the state variables $x_1(t)$, $x_2(t), \ldots, x_n(t)$, and the output variable $y(t)$.

In this section, we derive a mathematical model based on the following assumptions/requirements (Fig. 2.6):

(i) Initial state $\mathbf{x}(0) = \mathbf{0}$, i.e., the output $y(t)$ is solely and uniquely excited by the input $r(t)$ for $t \geq 0$.

Copyrighted material

A system is said to be *relaxed*[2] at $t_0 = 0$, if $\mathbf{x}(0) = \mathbf{0}$.

(ii) We are interested only in the input–output relation; dynamic evolution of the state $\mathbf{x}(t)$ is not required.

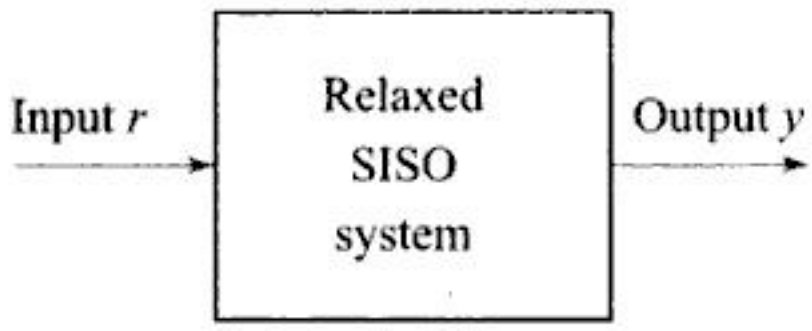


Fig. 2.6 *Input-output description*

The input $r(t)$ and the output $y(t)$ of any linear time-invariant system that is initially relaxed at $t_0 = 0$, can be described by an equation of the form

$$y(t) = \int_0^t g(t-\tau)r(\tau)d\tau = \int_0^t g(\tau)r(t-\tau)\,d\tau \tag{2.8}$$

This is called a *convolution integral*. The second integration is obtained from the first by substituting $\tau' = t - \tau$, and then changing the dummy variable τ' to τ. The function $g(t)$ is defined only for $t \geq 0$ and is called the *impulse response* of the system. In order to derive Eqn. (2.8) and give an interpretation of $g(t)$, we need the concept of impulse function.

A rectangular elementary *pulse function* is defined as

$$p_T(t) = \begin{cases} 1 & \text{for } 0 < t < T \\ 0 & \text{otherwise} \end{cases} \tag{2.9a}$$

Figure 2.7 gives the graphical representation of pulse functions. $Ap_T(t - t_0)$ is a pulse of height A and duration T occurring at $t = t_0$:

$$Ap_T(t - t_0) = \begin{cases} A & \text{for } 0 < (t - t_0) < T \\ 0 & \text{otherwise} \end{cases} \tag{2.9b}$$

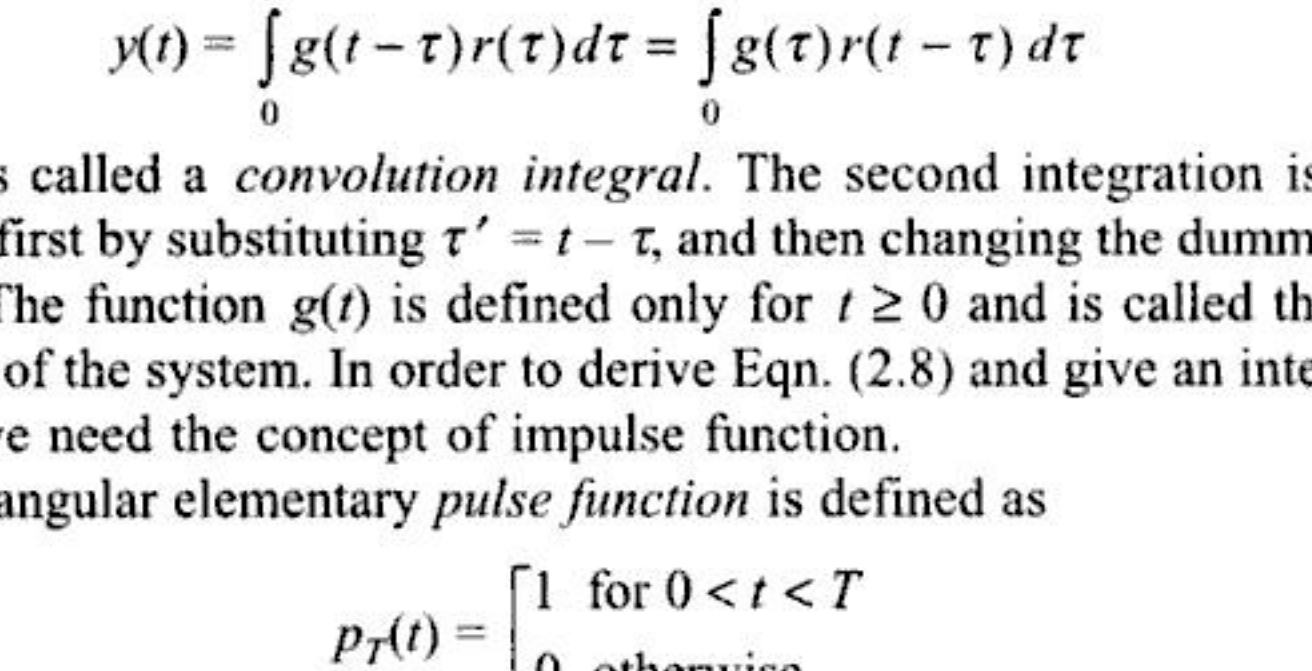


Fig. 2.7 *Pulse functions*

2. The case of zero initial conditions is common in control system design because the signals are usually defined as deviations from some initial steady-state. When this is done, the initial-value of the perturbation is, by definition, zero.

Copyrighted material

Consider the *unit pulse function*

$$\delta_\Delta(t) = \frac{1}{\Delta} p_\Delta(t) \tag{2.10}$$

It is a pulse of height $\frac{1}{\Delta}$ and duration Δ (i.e., of unit 'area') occurring at $t = 0$.

The properties of $\delta_\Delta(t)$ are such that its height increases whenever its duration decreases, but in such a way that its 'area' thereby remains constant and is equal to unity.

As $\Delta \to 0$, we obtain the limiting 'function'

$$\delta(t) \triangleq \lim_{\Delta \to 0} \delta_\Delta(t) \tag{2.11}$$

which is called the *unit impulse function* or *δ-function*.

Properties of the δ-function are:

$$\delta(t) = \lim_{\Delta \to 0} \delta_\Delta(t) = \begin{cases} 0 \text{ for } t \neq 0 \\ \infty \text{ for } t = 0 \end{cases} \tag{2.12a}$$

$$\int_{-\infty}^{\infty} \delta(t)dt = \int_{-\infty}^{\infty} \lim_{\Delta \to 0} \delta_\Delta(t)dt = 1 \tag{2.12b}$$

From these properties it follows that $\delta(t)$ is not an ordinary function as we cannot assign a value to the dependent variable for each value of the independent variable. The quantitative characteristic of $\delta(t)$ does not lie in its amplitudes but is given solely by its 'area'. Consequently, $\delta(t)$ is not defined in the ordinary sense but $\int_{-\infty}^{\infty} \delta(t)dt$ is defined; $\delta(t)f(t)$ is not defined but $\int_{-\infty}^{\infty} \delta(t)f(t)dt$ is defined:

$$\int_{-\infty}^{\infty} \delta(t)f(t)dt = \int_{-\infty}^{\infty} \lim_{\Delta \to 0} \delta_\Delta(t)f(t)dt = \lim_{\Delta \to 0} \int_{-\infty}^{\infty} \frac{1}{\Delta} p_\Delta(t)f(t)dt$$

$$= \lim_{\Delta \to 0} \frac{1}{\Delta} \int_0^\Delta f(t)dt$$

$$= f(0), \text{ assuming } f(t) \text{ is continuous at } t = 0 \tag{2.13}$$

Figure 2.8 gives the graphical representation of impulse functions. The definition of impulse $\delta(t - t_0)$ occurring at $t = t_0$ is based on the following properties.

$$\begin{aligned} &\text{(i)} \quad \int_{-\infty}^{\infty} \delta(t - t_0)dt = 1 \\ &\text{(ii)} \quad \int_{-\infty}^{\infty} f(t)\delta(t - t_0)dt = f(t_0), \text{ for any } f(t) \text{ that is continuous at } t = t_0 \end{aligned} \tag{2.14}$$

Copyrighted material

$A\delta(t - t_0)$ is an impulse of 'area' A (strength A) occurring at $t = t_0$.

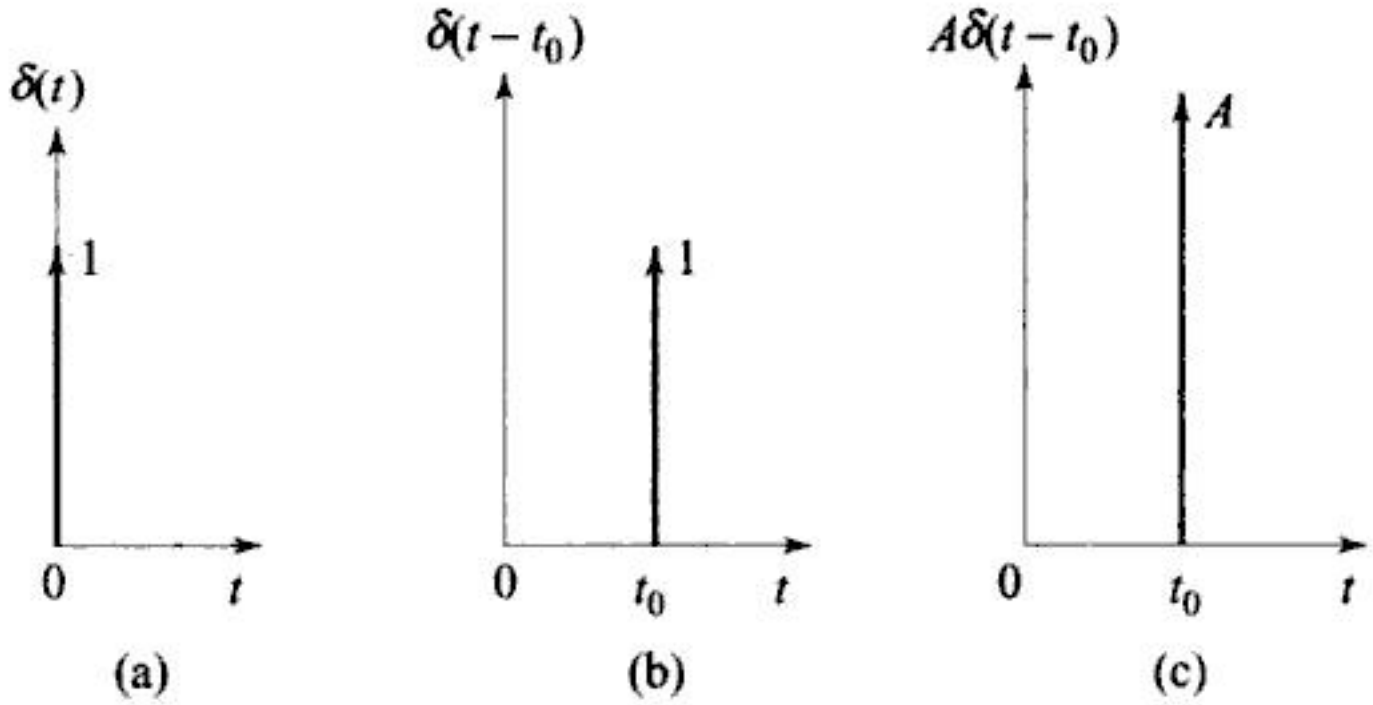


Fig. 2.8 *Impulse functions*

Example 2.1

Consider the situation shown in Fig. 2.9a where a mass M is acted upon by the force $F(t)$. The system is characterized by the second-order differential equation

$$F(t) = M\frac{d^2x(t)}{dt^2} \tag{2.15a}$$

The solution of this equation requires two initial conditions $\{x(0), \dot{x}(0) = v(0)\}$, and the input $F(t)$ applied at $t = 0^+$.

We will assume the system to be relaxed at $t = 0$, i.e.,

$$x(0) = v(0) = 0 \tag{2.15b}$$

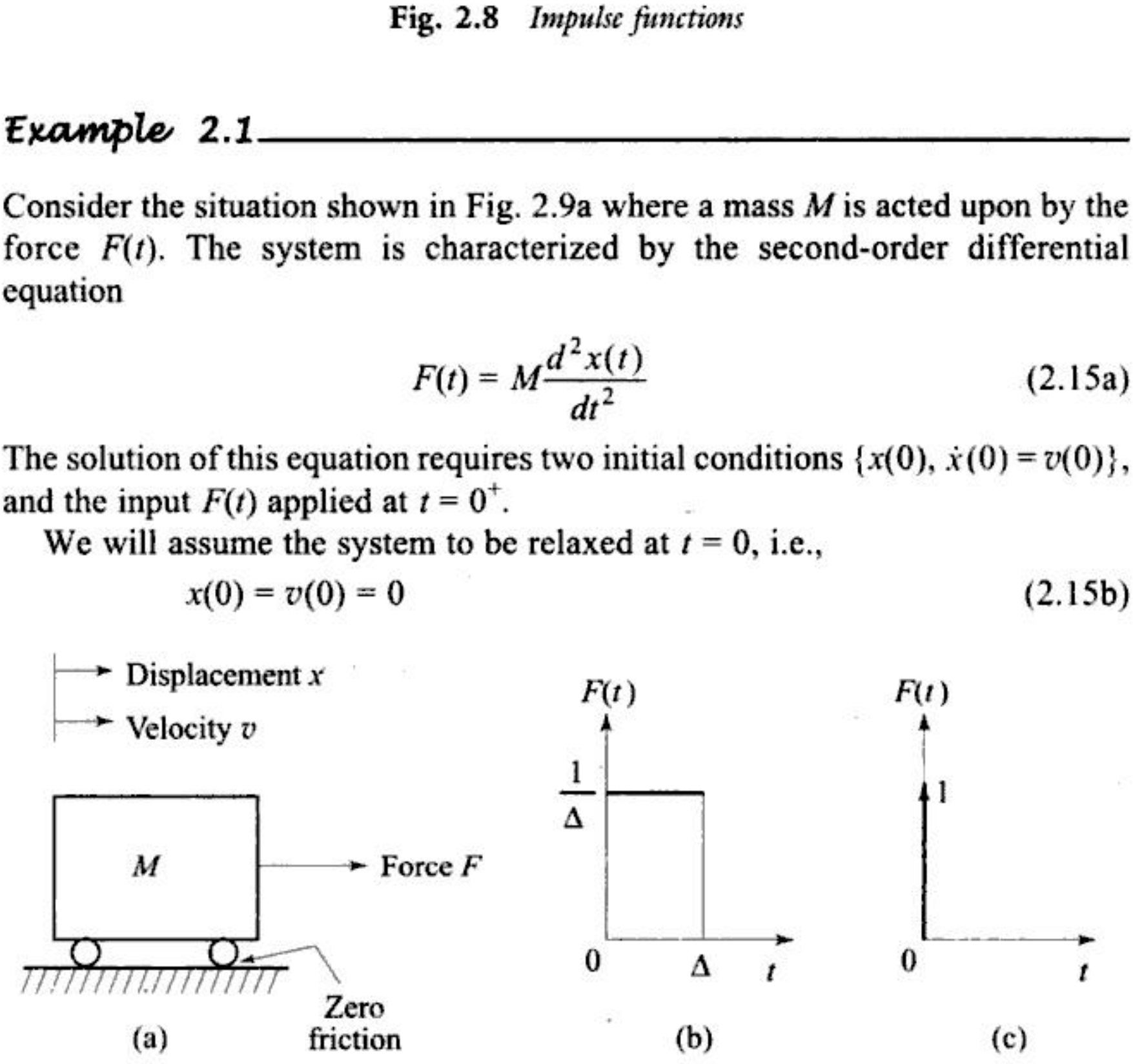


Fig. 2.9 *Approximating a pulse by an impulse*

It is intuitively obvious that the system state at time t can be described by state variables $x(t)$ and $v(t)$. The state equation for the mechanical system is given below:

Copyrighted material

$$\begin{bmatrix}\dot{x}(t)\\ \dot{v}(t)\end{bmatrix}=\begin{bmatrix}0 & 1\\ 0 & 0\end{bmatrix}\begin{bmatrix}x(t)\\ v(t)\end{bmatrix}+\begin{bmatrix}0\\ 1/M\end{bmatrix}F(t) \tag{2.16}$$

Equation (2.16) is of the form of general state equation (2.4a).

Let the force $F(t)$ be a pulse force of strength $1/\Delta$ and time duration Δ (Fig. 2.9b). For $t < \Delta$,

$$v(t) = \frac{1}{M}\int_0^t F(\tau)d\tau = \frac{t}{M\Delta};\ x(t) = \int_0^t v(\tau)d\tau = \frac{t^2}{2M\Delta}$$

The mass moves a distance

$$x(\Delta) = \frac{\Delta}{2M}$$

before acquiring a steady velocity of

$$v(\Delta) = \frac{1}{M}$$

The energy transferred from the pulse source to the mass (in time Δ) is

$$KE = \frac{1}{2}Mv^2(\Delta) = \frac{1}{2M}$$

Consider now the situatioı shown in Fig. 2.9c. The force $F(t)$ is a unit impulse $\delta(t)$ occurring at $t = 0$. The velocity of the mass is given by

$$v(t) = \frac{1}{M}\int_0^t \delta(\tau)d\tau = \frac{1}{M};\ t \geq 0$$

It is the same as the steady velocity $v(\Delta)$ for the pulse case except that it is acquired now in zero distance (and of course zero time). The energy acquired by the mass is the same in the two cases.

From Figs 2.9b and 2.9c, we see that there is practically no resemblance as far as the input function is concerned and it appears at first as if the approximation of a pulse by an impulse is in doubt. However, if our aim is to approximate the response of a linear system, the impulse approximation yields useful results provided pulse width Δ is small.

▲▲

We can now derive Eqn. (2.8). An input function $r(t)$ can easily be approximated by a train of pulses as shown in Fig. 2.10. It is convenient to take a uniform pulse width Δ for the pulse train. In the light of description of a pulse given by Eqns (2.9)–(2.10), we can express $r(t)$ as

$$r(t) \cong \sum_{i=0}^{\infty} r(i\Delta)\, p_\Delta(t - i\Delta) \cong \sum_{i=0}^{\infty} r(i\Delta)\, \delta_\Delta(t - i\Delta)\Delta \tag{2.17}$$

Copyrighted material

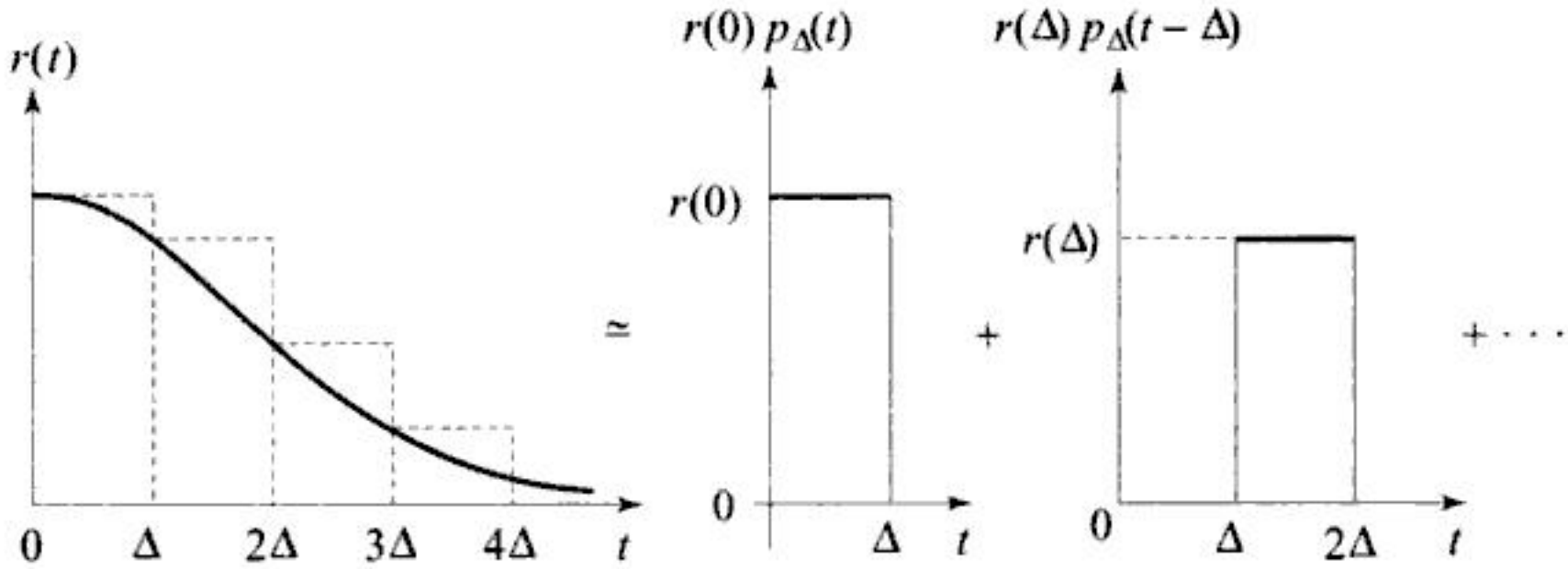


Fig. 2.10 *Resolution of a function*

Now if the output of the linear time-invariant system due to the input $\delta_\Delta(t)$ is denoted by $g_\Delta(t)$, then the properties of linearity and time-invariance imply that the output of the system due to $r(t)$ is given by

$$y(t) \cong \sum_{i=0}^{\infty} r(i\Delta) g_\Delta(t - i\Delta)\Delta \tag{2.18}$$

As we allow $\Delta \to 0$, the pulse function becomes an impulse function, number of impulses grow so that $(i\Delta)$ becomes a continuous variable τ, and the sum in Eqn. (2.18) approaches an integral. The output $y(t)$ resulting from an input $r(t)$ is thus

$$y(t) = \int_0^{\infty} r(\tau)\, g(t - \tau) d\tau \tag{2.19}$$

where
$$g(t) \triangleq \lim_{\Delta \to 0} g_\Delta(t) \tag{2.20a}$$

is the response of the system to unit impulse input applied at $t = 0$.

Hence the function $g(t)$ is called the *impulse response* of the system. Since $g(t - \tau)$ is the response due to an input applied at $t = \tau$, it is not defined for $t < \tau$;

$$g(t - \tau) = 0, \text{ for } t < \tau \tag{2.20b}$$

On the basis of this property, Eqn. (2.19) reduces to

$$y(t) = \int_0^{t} g(t - \tau) r(\tau) d\tau$$

Equation (2.8) is thus proved.

▲▲

A very important property of the impulse response model is that it can be obtained from the input and output terminals of a system even if the system's internal structure is not known. If the system is known to be linear, time-invariant, and relaxed at $t = 0$, then by applying $\delta_\Delta(t)$ function at the input terminal, the response at the output terminal gives us immediately the impulse

Copyrighted material

response (approximate one; goodness of approximation is dependent on Δ) of the system. If the impulse response is known, the output of the system due to any input can be computed from Eqn. (2.8).

▲▲

The application of Laplace transform to Eqn. (2.8) gives an extremely useful mathematical description of a linear time-invariant system. Fundamental definition for the Laplace transform[3] $F(s)$ of the time function $f(t)$ is (refer[4] Eqn. (A.28) in Appendix A)

$$\mathscr{L}[f(t)] \triangleq F(s) \triangleq \int_0^\infty f(t)e^{-st}\,dt;\ t > 0 \tag{2.21}$$

s = a complex variable = $\sigma + j\omega$

The application of Laplace transform to Eqn. (2.8) yields

$$Y(s) \triangleq \mathscr{L}[y(t)] = \int_0^\infty y(t)e^{-st}dt$$

$$= \int_0^\infty \left[\int_0^t g(t-\tau)r(\tau)d\tau\right]e^{-st}dt \tag{2.22}$$

Since $g(t-\tau) = 0$ for $\tau > t$ as implied by Eqn. (2.20b), the upper limit t of integration in Eqn. (2.22) can be set at ∞;

$$Y(s) = \int_0^\infty \left[\int_0^\infty g(t-\tau)r(\tau)d\tau\right]e^{-st}dt$$

Changing the order of integrations, gives

$$Y(s) = \int_0^\infty \left[\int_0^\infty g(t-\tau)e^{-st}dt\right]r(\tau)d\tau = \int_0^\infty \left[\int_0^\infty g(t-\tau)e^{-s(t-\tau)}dt\right]e^{-s\tau}r(\tau)d\tau$$

which, if we substitute $\theta = t - \tau$, can be expressed as

$$Y(s) = \int_0^\infty \left[\int_{-\tau}^\infty g(\theta)e^{-s\theta}d\theta\right]e^{-s\tau}\,r(\tau)d\tau$$

Using the fact that $g(\theta) = 0$ for $\theta < 0$ (refer Eqn. 2.20b)), we obtain

$$Y(s) = \int_0^\infty \left[\int_0^\infty g(\theta)e^{-s\theta}d\theta\right]e^{-s\tau}\,r(\tau)d\tau = \left[\int_0^\infty g(\theta)e^{-s\theta}d\theta\right]\left[\int_0^\infty r(\tau)e^{-s\tau}d\tau\right]$$

or
$$Y(s) = G(s)\,R(s) \tag{2.23}$$

3. It is conventional to use capital letters for s-functions and lower case for t-functions. Our notation mostly follows this convention.
4. We assume that the reader has had a previous introduction to the theory of Laplace transforms. Appendix A provides a very brief review of the Laplace transform techniques, adequate for the purposes of this text.

Copyrighted material

where $$R(s) \triangleq \mathcal{L}[r(t)]$$

and

$$G(s) \triangleq \mathcal{L}[g(t)]$$

We see that by applying the Laplace transform, a convolution integral is transformed into an algebraic equation. The function $G(s)$ is called the *transfer function* of the system. *The transfer function of a linear time-invariant system is, by definition, the Laplace transform of the impulse response of the system.*

The Laplace transform variable s in a transfer function $G(s)$, as will be seen later, can be associated with frequency. Hence the transfer function description of a system is often referred to as in *frequency-domain*, whereas the impulse response description is said to be in *time-domain*.

In this book, the major emphasis is on frequency-domain design methods. Providing more space for discussion on transfer functions will be in order here. The next section is exclusively devoted to transfer function models.

2.4 TRANSFER FUNCTION MODELS

In the last section, we have defined the transfer function of a linear time-invariant system as the Laplace transform of the impulse response of the system.

The transfer function can also be defined as (refer Eqn. (2.23)),

$$G(s) = \left.\frac{\mathcal{L}[y(t)]}{\mathcal{L}[r(t)]}\right|_{\substack{\text{system}\\ \text{relaxed}\\ \text{at } t_0 = 0}} = \left.\frac{Y(s)}{R(s)}\right|_{\substack{\text{system}\\ \text{relaxed}\\ \text{at } t_0 = 0}} \tag{2.24}$$

where $Y(s)$ = Laplace transform of the output variable $y(t)$,

$R(s)$ = Laplace transform of the input variable $r(t)$, and

$G(s)$ = transfer function of the system.

Thus the *transfer function of a time-invariant system is the ratio of the Laplace transforms of its output and input variables, assuming zero initial conditions*. Figure 2.11 gives a block diagram of a SISO system in transform domain.

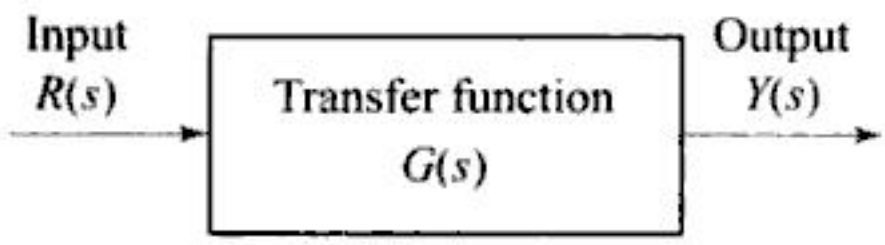


Fig. 2.11 *Description of a SISO system in transform domain*

Note that whenever a transfer function is used to describe a system, the system is always implicitly assumed to be linear, time-invariant, and relaxed at $t_0 = 0$.

Copyrighted material

There are two different ways in which transfer function models are usually obtained.

(i) For lumped linear time-invariant systems, mathematical model building based on physical laws normally results in a set of (first-order, and second-order) differential equations. Applying Laplace transform to the differential equations results in a transfer function model of the system.

We will be mostly concerned with this approach. A number of examples of mechanical, electrical, hydraulic and thermal systems will be taken to illustrate the modelling procedure. One important feature will clearly emerge from these examples—application of physical laws to a system results in a set of differential equations which directly provide us with the rates of change of state variables of the system. State variable formulation is thus a 'natural' representation of the system dynamics. We, in fact, first obtain the state variable formulation by applying physical laws and therefrom derive the transfer function model by Laplace transformation.

(ii) The transfer function model of a system can be identified from experimentally obtained input-output data. Generally the identification methods can be considered to be a type of curve-fitting, where the assumed transfer function is fitted to the available data in some optimal manner. The methods may be based on frequency response (sinusoidal input), step response (step input), impulse response (pulse input; pulse of small width approximating an impulse), or the response to more general inputs.[5]

Identification methods have not been covered in this book. Only simple methods based on step response and frequency response are given in later chapters.

Example 2.2

Consider the mass-spring-damper system shown in Fig. 2.2.

Application of Newton's law results in the following equation (refer Fig. 2.2b).

$$\left.\begin{aligned} M\frac{dv(t)}{dt} &= F(t) - Bv(t) - K\,x(t) \\ \text{with} \\ \frac{dx(t)}{dt} &= v(t) \end{aligned}\right\} \qquad (2.25)$$

$x(t)$ is the displacement of the mass, $v(t)$ is the velocity, $F(t)$ is the applied force; M, B and K are the parameters of the system.

5. In Chapter 12, methods of deriving *canonical* (special) state variable models from a given transfer function will be presented. This is called the *realization problem*.

Copyrighted material



You have either reached a page that is unavailable for viewing or reached your viewing limit for this book.



You have either reached a page that is unavailable for viewing or reached your viewing limit for this book.

We will represent the numerator polynomial of $G(s)$ by $N(s)$, and the denominator polynomial by $\Delta(s)$:

$$G(s) = \frac{N(s)}{\Delta(s)} \tag{2.32}$$

where

$$N(s) = b_0 s^m + b_1 s^{m-1} + \cdots + b_{m-1} s + b_m$$
$$\Delta(s) = s^n + a_1 s^{n-1} + \cdots + a_{n-1} s + a_n$$

Note that there is no loss in generality to assume that the coefficient of s^n in the polynomial $\Delta(s)$ is unity (i.e., the denominator polynomial $\Delta(s)$ is assumed to be *monic*[6]).

The highest power of the complex variable s in the denominator polynomial $\Delta(s)$ of the transfer function $G(s)$ determines the *order of the transfer function model*. The denominator polynomial $\Delta(s)$ is called the *characteristic polynomial*.

The roots of the equation

$$\Delta(s) = 0 \tag{2.33a}$$

are called the *poles* of the transfer function $G(s)$ and roots of the equation

$$N(s) = 0 \tag{2.33b}$$

are called the *zeros*.

Equation (2.33a) is called the *characteristic equation*; the poles are the *characteristic roots*.

The transfer function $G(s)$ given by Eqn. (2.31) can be expressed in the *pole-zero form* as

$$G(s) = \frac{K(s+z_1)(s+z_2)\cdots(s+z_m)}{(s+p_1)(s+p_2)\cdots(s+p_n)};\ m \le n \tag{2.34a}$$

where K, p_i and z_j are constants; $K = b_0$ is the *gain constant* of the transfer function, $-p_1, -p_2, \ldots, -p_n$ are the n poles (real or complex) of the transfer function (n roots of the characteristic equation (2.33a)), and $-z_1, -z_2, \ldots, -z_m$ are the m finite zeros (real or complex) of the transfer function (m roots of Eqn. (2.33b)).

In the representation of $G(s)$ in pole-zero form given by Eqn. (2.34a), it has been assumed that the poles and zeros are *distinct* (*simple*). If a pole, say at $s = -p_1$, is *multiple* (repeated) with multiplicity v, the corresponding transfer function in pole-zero form becomes

$$G(s) = \frac{K(s+z_1)(s+z_2)\cdots(s+z_m)}{(s+p_1)^v (s+p_{v+1})\cdots(s+p_n)};\ m \le n \tag{2.34b}$$

Multiple zeros may also appear in a transfer function model.

---

6. A monic polynomial has a leading coefficient equal to unity.

Copyrighted material

We have so far considered SISO systems. Consider now the two-input, two-output system shown in the block diagram of Fig. 2.12. The terms $G_{11}(s)$ and $G_{21}(s)$ are the transfer functions of the input variable $R_1(s)$ on the two output variables $Y_1(s)$ and $Y_2(s)$ respectively; the terms $G_{12}(s)$ and $G_{22}(s)$ are the corresponding transfer functions for input variable $R_2(s)$. The mathematical model of the system is, therefore, 2×2 *transfer function matrix* defined below:

$$\begin{bmatrix} Y_1(s) \\ Y_2(s) \end{bmatrix} = \underbrace{\begin{bmatrix} G_{11}(s) & G_{12}(s) \\ G_{21}(s) & G_{22}(s) \end{bmatrix}}_{\text{Transfer function matrix}} \begin{bmatrix} R_1(s) \\ R_2(s) \end{bmatrix} \tag{2.35}$$

$$G_{11}(s) = \left.\frac{Y_1(s)}{R_1(s)}\right|_{R_2(s)=0} ; \; G_{12}(s) = \left.\frac{Y_1(s)}{R_2(s)}\right|_{R_1(s)=0}$$

$$G_{21}(s) = \left.\frac{Y_2(s)}{R_1(s)}\right|_{R_2(s)=0} ; \; G_{22}(s) = \left.\frac{Y_2(s)}{R_2(s)}\right|_{R_1(s)=0}$$

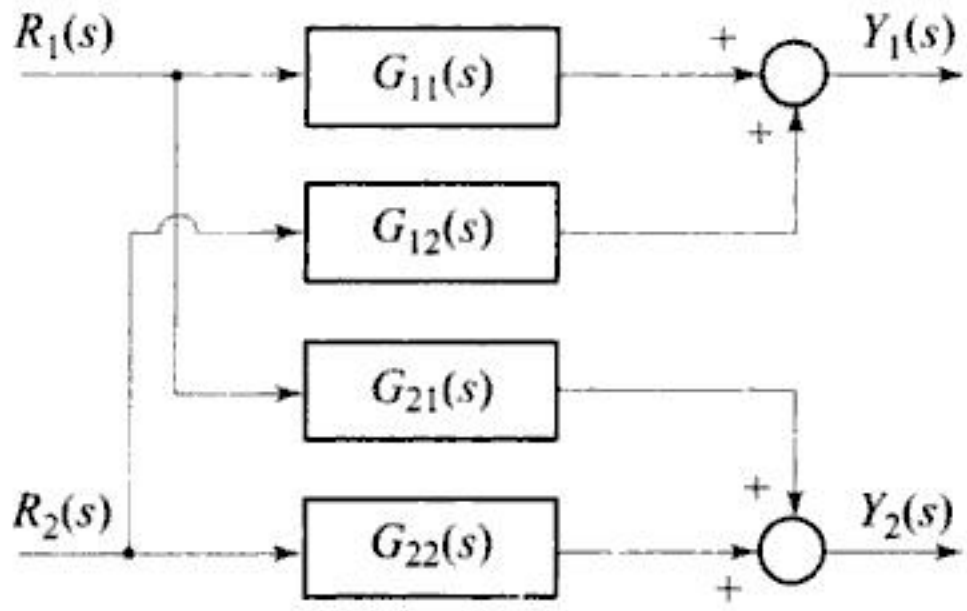


Fig. 2.12 *Description of a MIMO system in transform domain*

Extension of the model given by Eqn. (2.35) to the case of p-input, p-output system is obvious.

▲▲

In this book, the major emphasis is on frequency-domain design methods. Hence we mostly deal with transfer functions (Chapters 2–11).

The frequency-domain design methods have been greatly enhanced by the availability of low-cost computers for system analysis and simulation. The use of state variable formulation, introduced earlier in Section 2.2, has become widespread in CAD packages. In this introductory book, modest investment in state variable methods is therefore necessary. In Chapter 12, we give an adequate coverage of state variable representation and its relationship with transfer function representation.

Copyrighted material

2.5 MODELS OF DISTURBANCES AND STANDARD TEST SIGNALS

To motivate the discussion in a control systems context, we revisit the generalized functional block diagram of Fig. 1.12. There are two inputs (external excitations) applied to a control system: a command input $y_r(t)$ (or reference input $r(t)$), and a disturbance input $w(t)$. We will first talk of disturbances.

Simple Models of Disturbances

External disturbances, $w(t)$, are typically the uncontrolled variations in the load on a control system. In systems controlling mechanical motions, load disturbances may represent forces, e.g., wind gusts on a stabilized antenna (refer Example 1.5), variations in payload of a robot (refer Example 1.10), etc. In voltage regulating systems, variations in electrical load are a major source of disturbances. In thermal systems, the load disturbances may be caused by variations in surrounding temperature (refer Example 1.4). In fluidic systems, the load disturbances may result from variations in feedflow or variations in demanded flow (refer Example 1.7).

Disturbances which are erratic, uncertain signals having no distinguishing waveform properties, are commonly referred to as *noise*. The accommodation of noise in a control problem is best handled by treating the noise as a *stochastic* or *random process*. The general theory of stochastic processes is quite complex, and is beyond the scope of this book.

In this book we consider load disturbances which typically vary slowly. Such disturbances are normally well behaved uncertain signals having distinguishing waveform properties. As we shall see in Chapter 4, the errors due to load disturbances tend to be corrected by proper design of feedback control.

In the following, we consider simple, yet effective, models that characterize commonly occurring disturbances.

Pulse and Impulse Functions

The pulse and the impulse are simple idealizations of sudden disturbances of short duration.

A *pulse function* (Fig. 2.13a) is defined as (refer Eqn. (2.9a)),

$$p_T(t) = \begin{cases} 1 \text{ for } 0 < t < T \\ 0 \text{ otherwise} \end{cases} \tag{2.36a}$$

Laplace transform of pulse function is (refer Eqn. (2.21)),

Copyrighted material



You have either reached a page that is unavailable for viewing or reached your viewing limit for this book.



You have either reached a page that is unavailable for viewing or reached your viewing limit for this book.

$$f(t) = \begin{cases} \dfrac{t^2}{2} & \text{for } t > 0 \\ 0 & \text{otherwise} \end{cases} \tag{2.40a}$$

or simply

$$f(t) = \frac{t^2}{2}\,\mu(t) \tag{2.40b}$$

$$\mathcal{L}[f(t)] = \frac{1}{s^3} \tag{2.40c}$$

Sinusoidal Function

The sine wave is a prototype for a periodic disturbance—for example, waves in ship control systems.

For a sine wave of unity amplitude and frequency ω (Fig. 2.13f), i.e.,

$$f(t) = \sin \omega t\ \mu(t), \tag{2.41a}$$

the Laplace transformation gives

$$\mathcal{L}[f(t)] = \frac{\omega}{s^2 + \omega^2} \tag{2.41b}$$

Standard Test Signals

In addition to disturbance input, the other excitation signal to a control system is the command input (Fig. 1.12). The command (or reference) signals of some control systems are known to the designer. The command signal of a residential heating system (Example 1.4) is a step function, whose magnitude is the desired temperature. If an antenna is used to track a communication satellite (refer Example 1.5), then the command signal is very close to a ramp function.

In many control systems, however, the command signals are not known fully ahead of time. For instance, in a radar tracking system for military applications (refer Example 1.5), the position and speed of the target to be tracked vary in an unpredictable manner; it is thus difficult to express the actual input signals mathematically by simple functions. The characteristics of actual signals which severely strain a control system are

(i) a sudden shock (modelled by impulse function),
(ii) a sudden change (modelled by step function),
(iii) a linear change with time (modelled by ramp function), and
(iv) faster changes with time (a parabolic function is one degree faster than a ramp function).

System dynamic behaviour can be adequately judged and compared under the application of standard test signals—an impulse input, a step input, a ramp input, and a parabolic input.

Another standard test signal of great importance is the sinusoidal signal. When the response of a linear time-invariant system is analysed in frequency

Copyrighted material

domain, a sinusoidal function with variable frequency is used as input function. Input frequency is swept from zero to beyond the significant range of system characteristics; curves in terms of amplitude ratio and phase between input and output are drawn as functions of frequency. It is possible to predict the time-domain behaviour of the system from its frequency-domain characteristics. We will take up this aspect of control system analysis in Chapters 8 and 9.

2.6 DYNAMIC RESPONSE

This section is concerned with the dynamic response of linear time-invariant systems to disturbance signals and standard test signals. We will study the response of a system from its transfer function model; therefore the system is implicitly assumed to be initially relaxed.

Basically four steps are involved in the computation of $y(t)$ from

$$Y(s) = G(s)\,R(s)$$

1. Find the Laplace transform of $r(t)$ using results of Section 2.5 or Table of transform pairs given in Appendix A.
2. Compute the poles of $G(s)\,R(s)$.
3. Expand $Y(s)$ into partial fractions (Eqns (A.3)–(A.14) of Appendix A give the required procedure).
4. Obtain $y(t)$ by taking inverse Laplace transform of $Y(s)$ using transform pairs listed in the Table of Appendix A.

In the following, we give examples to illustrate the procedure.

Example 2.4

Given the transfer function

$$G(s) = \frac{Y(s)}{R(s)} = \frac{1}{s^2 + 3s + 2};$$

find the response $y(t)$ to the input

(i) $r(t) = 5\ \mu(t)$, (ii) $r(t) = 5t\ \mu(t)$

Solution

(i) For the given step input, $R(s) = \dfrac{5}{s}$

Therefore,

$$Y(s) = \frac{1}{s^2 + 3s + 2} R(s) = \frac{1}{(s+1)(s+2)}\left(\frac{5}{s}\right)$$

Expanding $Y(s)$ into partial fractions, gives

$$Y(s) = \frac{5}{s(s+1)(s+2)} = \frac{A_1}{s} + \frac{A_2}{s+1} + \frac{A_3}{s+2}$$

Copyrighted material

$$A_1 = \lim_{s\to 0}\left[(s)\frac{5}{s(s+1)(s+2)}\right] = \frac{5}{2}$$

$$A_2 = \lim_{s\to -1}\left[(s+1)\frac{5}{s(s+1)(s+2)}\right] = -5$$

$$A_3 = \lim_{s\to -2}\left[(s+2)\frac{5}{s(s+1)(s+2)}\right] = \frac{5}{2}$$

or
$$Y(s) = \underbrace{\frac{5/2}{s}}_{\text{Excitation pole}} \underbrace{-\frac{5}{s+1}+\frac{5/2}{s+2}}_{\text{System poles}}$$

Inverting $Y(s)$, we obtain the time response

$$y(t) = \underbrace{\left[\frac{5}{2}\right.}_{\text{Steady-state response}} \underbrace{\left.-5e^{-t}+\frac{5}{2}e^{-2t}\right]}_{\text{Transient response}} \mu(t)$$

The transient response terms correspond to system poles excited by the input. These terms vanish as $t \to \infty$.

The second response term arises due to the excitation pole, and has the same nature as the input itself except for a modification in magnitude caused by the system's behaviour to the specified input. Since the input exists as $t \to \infty$, the second response term does not vanish and is called the *steady-state response* of the system. Figure 2.14a shows the response to the given step input.

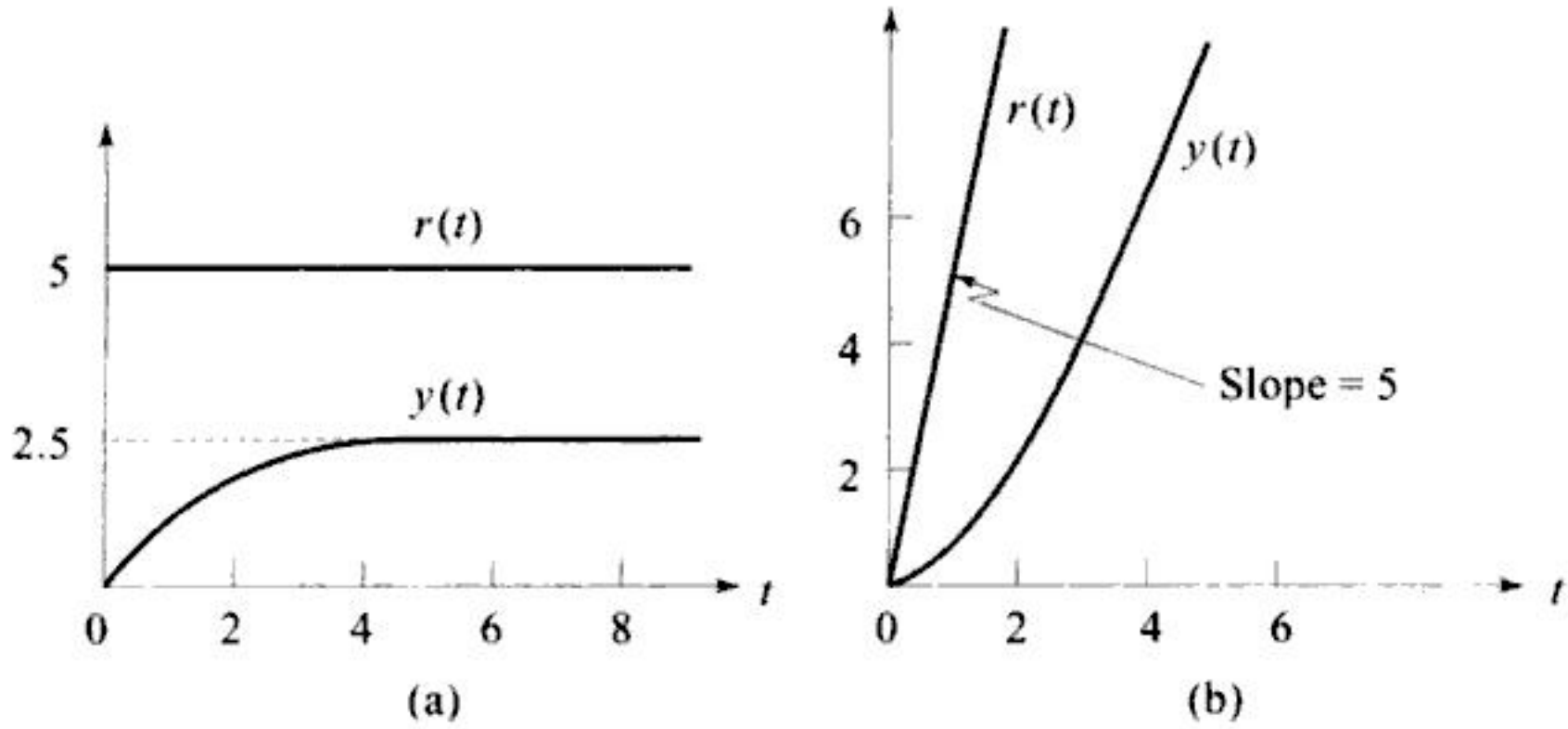


Fig. 2.14 *(a) Step response; (b) Ramp response*

The steady-state response can be quickly obtained without doing the complete inverse Laplace transform, by use of the *final value theorem* (Eqn. (A.35) of Appendix A):

$$\lim_{t\to\infty} y(t) = \lim_{s\to 0} sY(s) \tag{2.42}$$

Copyrighted material

if $s\,Y(s)$ has no poles on the imaginary axis and in the right half s-plane.

(ii) For the given ramp input, $R(s) = \dfrac{5}{s^2}$

Therefore, $$Y(s) = \frac{5}{s^2(s+1)(s+2)}$$

Expanding $Y(s)$ in partial fractions, gives

$$Y(s) = \frac{A_1}{s^2} + \frac{A_2}{s} + \frac{A_3}{s+1} + \frac{A_4}{s+2}$$

$$A_1 = \lim_{s\to 0}\left[(s^2)\frac{5}{s^2(s+1)(s+2)}\right] = \frac{5}{2}$$

$$A_2 = \lim_{s\to 0}\frac{d}{ds}\left[(s^2)\frac{5}{s^2(s+1)(s+2)}\right]$$

$$= \lim_{s\to 0}\left[\frac{-5(2s+3)}{(s^2+3s+2)^2}\right] = \frac{-15}{4}$$

$$A_3 = \lim_{s\to -1}\left[(s+1)\frac{5}{s^2(s+1)(s+2)}\right] = 5$$

$$A_4 = \lim_{s\to -2}\left[(s+2)\frac{5}{s^2(s+1)(s+2)}\right] = \frac{-5}{4}$$

or $$Y(s) = \frac{5/2}{s^2} - \frac{15/4}{s} + \frac{5}{s+1} - \frac{5/4}{s+2}$$

Inverting $Y(s)$, we obtain the time response

$$y(t) = \left(\frac{-15}{4} + \frac{5}{2}t + 5e^{-t} - \frac{5}{4}e^{-2t}\right)\mu(t)$$

The ramp response is composed of three types of terms—constant, ramp, and exponentials. The exponentials (transient component) decay leaving behind the steady-state response

$$y_{ss}(t) = \frac{5}{2}t - \frac{15}{4}$$

Figure 2.14b shows the response to given ramp input.

Example 2.5

Given the transfer function

$$G(s) = \frac{Y(s)}{R(s)} = \frac{K}{s+a};$$

Copyrighted material

find the response $y(t)$ to the input $r(t) = R_0 \sin \omega t$; K, a and R_0 are constants, and ω is sinusoidal frequency.

Solution

For the given sinusoidal input, $R(s) = \dfrac{R_0\,\omega}{s^2 + \omega^2}$

Therefore,

$$Y(s) = \frac{KR_0\,\omega}{(s+a)(s^2+\omega^2)}$$

$$= \frac{KR_0\,\omega}{(s+a)(s-j\omega)(s+j\omega)}; \; j \triangleq \sqrt{-1}$$

Expanding $Y(s)$ in partial fractions, gives

$$Y(s) = \frac{A_1}{s+a} + \frac{A_2}{s-j\omega} + \frac{A_3}{s+j\omega}$$

$$A_1 = \lim_{s \to -a}\left[(s+a)\frac{KR_0\omega}{(s+a)(s^2+\omega^2)}\right] = \frac{KR_0\omega}{\omega^2+a^2}$$

$$A_2 = \lim_{s \to j\omega}\left[(s-j\omega)\frac{KR_0\omega}{(s+a)(s-j\omega)(s+j\omega)}\right]$$

$$= \frac{KR_0\omega}{j2\omega(a+j\omega)} = \frac{-KR_0(\omega+ja)}{2(\omega^2+a^2)}$$

$A_3 =$ complex conjugate of A_2

$$= \frac{-KR_0(\omega-ja)}{2(\omega^2+a^2)}$$

or

$$Y(s) = \frac{KR_0\,\omega}{\omega^2+a^2}\left(\frac{1}{s+a}\right) - \frac{KR_0}{2(\omega^2+a^2)}\left[\frac{\omega+ja}{s-j\omega} + \frac{\omega-ja}{s+j\omega}\right]$$

$$= \frac{KR_0\,\omega}{\omega^2+a^2}\left(\frac{1}{s+a}\right) - \frac{KR_0\,\omega}{\omega^2+a^2}\left(\frac{s-a}{s^2+\omega^2}\right)$$

Inverting $Y(s)$, we obtain the time response

$$y(t) = \frac{KR_0\,\omega}{\omega^2+a^2}e^{-at} + \frac{KR_0\,\omega}{\omega^2+a^2}\left(\frac{a}{\omega}\sin\omega t - \cos\omega t\right)$$

$$= \frac{KR_0\,\omega}{\omega^2+a^2}e^{-at} + \frac{KR_0\,a}{\omega^2+a^2}\left(\sin\omega t - \frac{\omega}{a}\cos\omega t\right)$$

Using the identity

$A \cos at + B \sin at = R \sin(at + \theta)$

Copyrighted material

where $$R = \sqrt{A^2 + B^2}, \quad \theta = \tan^{-1}\left(\frac{A}{B}\right),$$

the $y(t)$ expression can be changed to

$$y(t) = \frac{KR_0\omega}{\omega^2 + a^2}e^{-at} + \frac{KR_0}{\sqrt{\omega^2 + a^2}}\sin\left[\omega t - \tan^{-1}\left(\frac{\omega}{a}\right)\right] \tag{2.43}$$

Equation (2.43) shows that as time increases, the exponential term goes to zero; this is the transient term that dies out. When this happens, the output expression becomes

$$y(t)\Big|_{t \text{ very large}} = y_{ss}(t) = \frac{KR_0}{\sqrt{\omega^2 + a^2}}\sin\left[\omega t - \tan^{-1}\left(\frac{\omega}{a}\right)\right] \tag{2.44}$$

which displays the sinusoidal behaviour of the output signal. The amplitude of this output is

$$Y_0 = \frac{KR_0}{\sqrt{\omega^2 + a^2}}$$

The output 'lags' the input signal by an amount $\theta = \tan^{-1}\left(\frac{\omega}{a}\right)$. All of this information is shown graphically in Fig. 2.15.

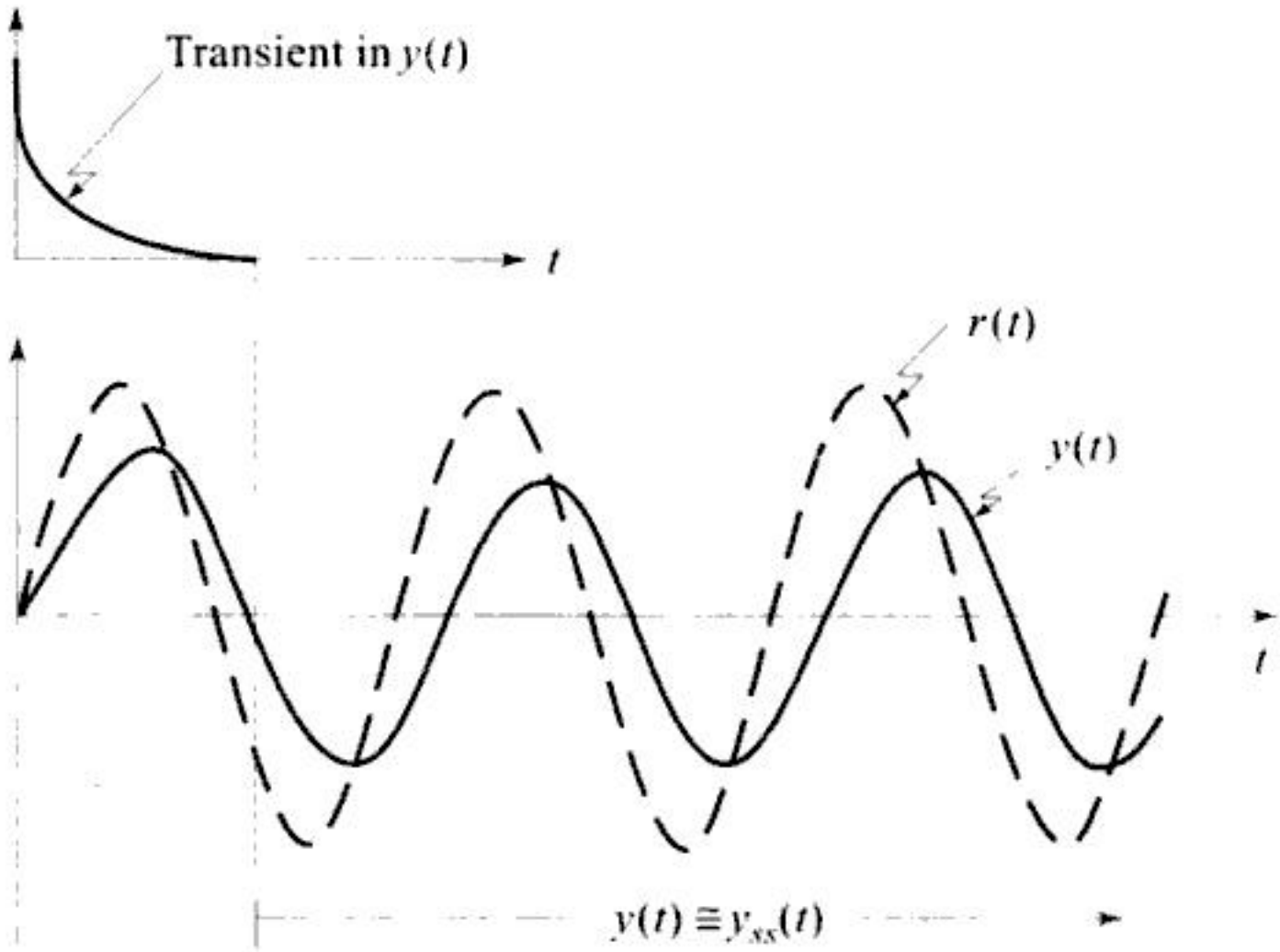


Fig. 2.15 *Sinusoidal response*

Copyrighted material



You have either reached a page that is unavailable for viewing or reached your viewing limit for this book.

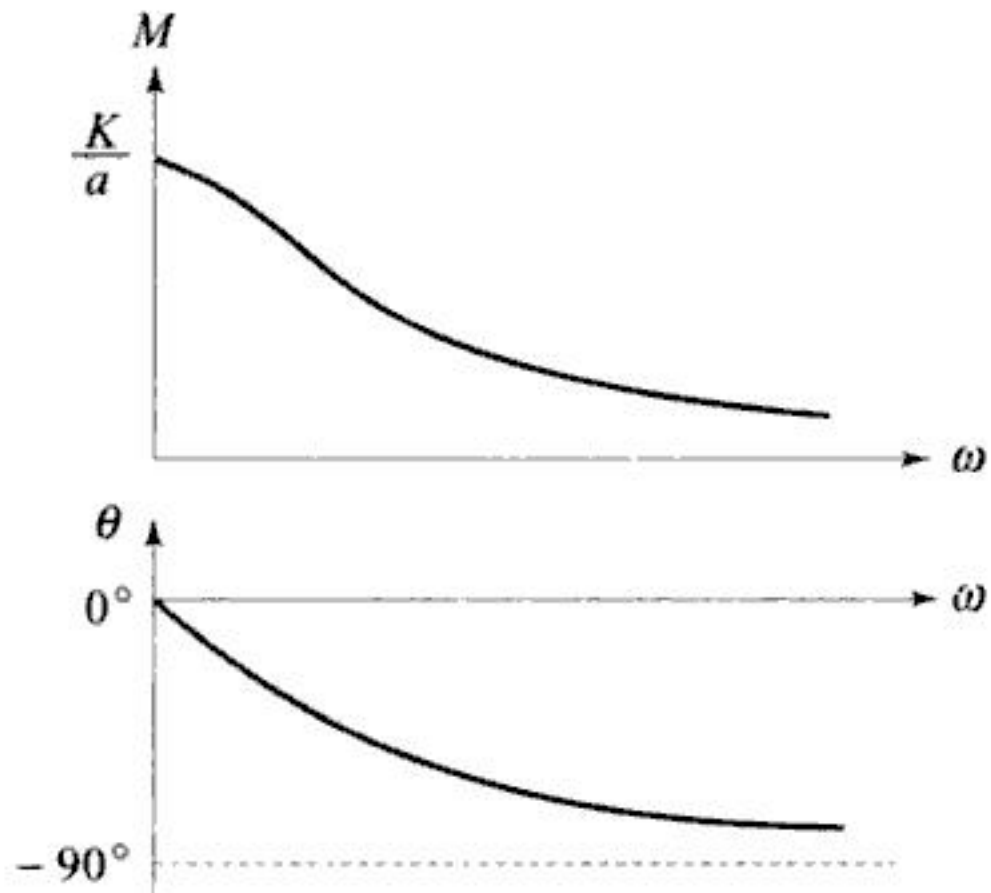


Fig. 2.16 *Frequency-response curves*

variable y is given by a mathematical expression in terms of independent variable t. The method works well if the system model is relatively of low-order, with relatively simple input functions[8]. If the model does not have these characteristics, we have to resort to numerical solution methods (*digital simulation*). The disadvantage of this type of solution is that generality is lost; the numerical values of the input functions, coefficients of the model, etc., must be specified [173-175, 177-178]. However, often there is no alternative.[9]

2.7 CHARACTERISTIC PARAMETERS OF FIRST- AND SECOND-ORDER MODELS

In this book, we will frequently come across first- and second-order transfer function models. Special emphasis on the characteristics of these models is justified.

First-Order Models

As an example of a dynamic system represented by a first-order model, we consider here mechanical system of Fig. 2.17a involving fixed-axis rotation.

8. Most of the models used in the following chapters are of first-, second-, and third-order with simple input functions. Computer simulation is therefore not essential. However CAD facility, if available, can provide a better feel of how control system design is done in practice.
9. The analog computer simulation provides another way of investigating system dynamics. This method is rarely used now because of the advantages of digital simulation. However, it still provides an excellent means of developing control system prototypes (Section 2.9).

Copyrighted material

The free-body diagram is shown in Fig. 2.17b. It is assumed that the torque $T(t)$ is the input and angular velocity $\omega(t)$ is the output.

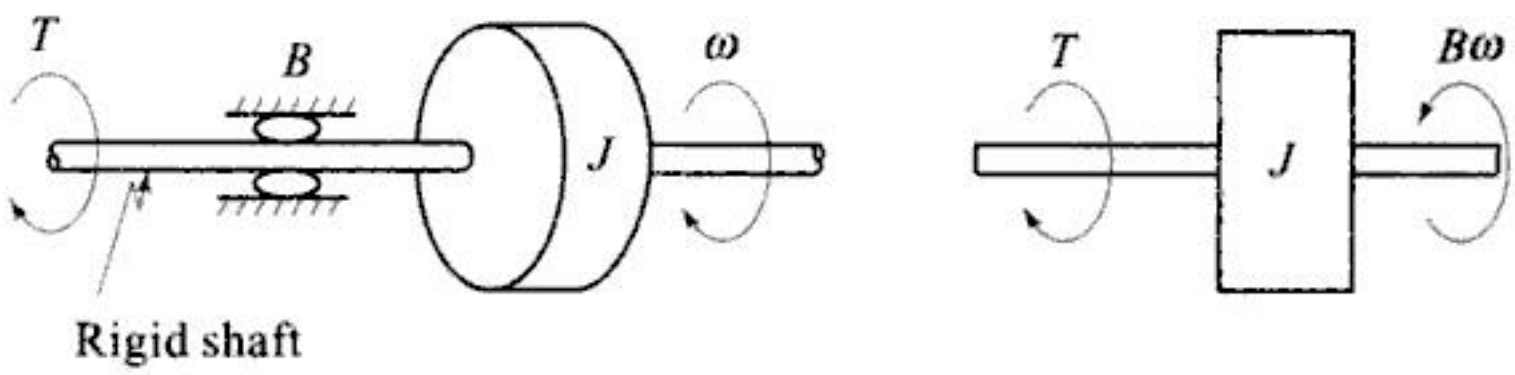


Fig. 2.17 *(a) An inertia-damper system (b) Free-body diagram*

The torque equation obtained from the free-body diagram is

$$T(t) - B\omega(t) = J\frac{d\omega(t)}{dt}$$

or
$$J\frac{d\omega(t)}{dt} + B\omega(t) = T(t) \tag{2.47}$$

This is a linear constant-coefficient differential equation of first order.

Taking the Laplace transform of each term of this equation (assuming zero initial conditions), we obtain

$$Js\omega(s) + B\omega(s) = T(s)$$

where

$$\omega(s) \triangleq \mathscr{L}[\omega(t)];\ T(s) \triangleq \mathscr{L}[T(t)]$$

Therefore, the transfer function of the system is

$$G(s) = \frac{\omega(s)}{T(s)} = \frac{1}{Js + B} = \frac{1/J}{s + B/J} \tag{2.48}$$

J = moment of inertia, Newton-m/(rad/sec^2)

B = damping coefficient, Newton-m/(rad/sec)

Equation (2.48) gives a first-order transfer function of the mechanical system in pole-zero form; with pole at $s = -B/J$, no finite zero and gain constant = $1/J$.

A more common notation for first-order transfer functions is

$$G(s) = \frac{K}{\tau s + 1},$$

since the physical meaning can be given to both K and τ.

For the mechanical system under consideration,

$$\tau = J/B, \text{ and } K = 1/B \tag{2.49a}$$

$$\frac{\omega(s)}{T(s)} = \frac{K}{\tau s + 1} \tag{2.49b}$$

Copyrighted material

In the following, we obtain the time response from Eqns (2.49) to a step signal. From the characteristics of the time response, the physical meaning of the parameters K and τ will become clear,
For a unit-step input $T(t) = \mu(t)$, we have $T(s) = 1/s$.
Therefore,

$$\omega(s) = \frac{K}{s(s\tau + 1)} = K\left[\frac{1}{s} - \frac{\tau}{s\tau + 1}\right]$$

$$\omega(t) = K(1 - e^{-t/\tau});\ t \geq 0 \qquad (2.50)$$

This solution is now investigated in detail. The step response as given by Eqn. (2.50) is plotted in Fig. 2.18; the two components of the response are plotted separately along with the complete response. Note that the exponentially decaying term has an initial slope of K/τ, i.e.,

$$\left.\frac{d}{dt}(-Ke^{-t/\tau})\right|_{t=0} = \left.\frac{K}{\tau}e^{-t/\tau}\right|_{t=0} = \frac{K}{\tau}$$

Mathematically, the exponential term does not decay to zero in a finite length of time. However, if the term continued to decay at its initial rate, the term would reach a value of zero in time $t = \tau$. The parameter τ is called the system *time-constant*.

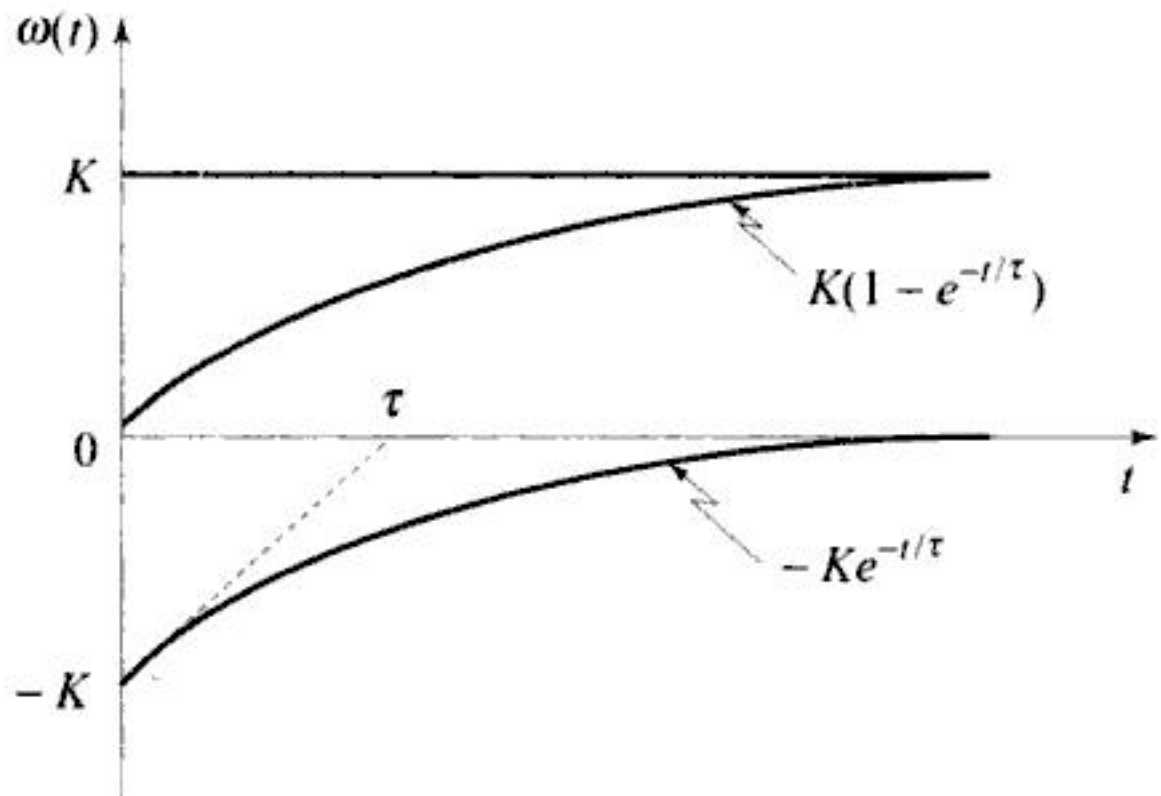


Fig. 2.18 *Step-response of a first-order system*

The decay of the exponential term is illustrated in Table 2.1 as a function of time-constant τ.

Table 2.1

t	$e^{-t/\tau}$
τ	$e^{-1} = 0.3679$
2τ	$e^{-2} = 0.1353$
3τ	$e^{-3} = 0.0498$
4τ	$e^{-4} = 0.0183$
5τ	$e^{-5} = 0.0067$

Copyrighted material

We observe that the exponential function has decayed to less than two per-cent of its initial value in four time-constants and to less than one per cent of its initial value in five time-constants. In a practical sense, we consider an exponential term to have decayed to zero in four to five time-constants.

Therefore, the time-constant is related to the speed of response of the system. The slower the system responds to an input, the larger the value of τ. The faster the system responds to an input, the smaller the value of τ. The unit of τ is seconds (this can be verified from Eqns (2.49a) using the units of the physical parameters given in Eqn. (2.48)).

Another important parameter encountered in Eqns (2.49) – (2.50) is K. Note that

$$\lim_{t \to \infty} \omega(t) = K$$

The parameter K is the *system gain*, which tells us how much the output variable will change at steady-state in response to a unit change in the input variable.

The gain K and time-constant τ are the two parameters which describe the 'personality' of the first-order system. These parameters may be obtained from the physical parameters of the system or experimentally by conducting the step-response test/sinusoidal-response test.

The transfer function

$$G(s) = \frac{K}{\tau s + 1} \tag{2.51}$$

is called the time-constant form for first-order transfer functions and will be encountered in all types of systems—electrical, mechanical, thermal, hydraulic, etc. A process described by this form of transfer function is called a *first-order lag* or a *simple lag*.

Second-Order Models

The study of second-order systems may be generalized by the introduction of certain parameters just as the study of first-order systems was facilitated by the use of time-constant.

As an example of a dynamic system represented by a second-order model, we consider here the mechanical system of Fig. 2.19(a) involving fixed-axis rotation. The shaft is assumed to behave like a torsional spring. The free-body diagram is shown in Fig. 2.19(b). It is assumed that the torque $T(t)$ is the input and angular displacement $\theta(t)$ is the output.

The torque equation obtained from the free-body diagram is

$$T(t) - B\frac{d\theta(t)}{dt} - k\theta(t) = J\frac{d^2\theta(t)}{dt^2}$$

or

$$J\frac{d^2\theta(t)}{dt^2} + B\frac{d\theta(t)}{dt} + k\theta(t) = T(t) \tag{2.52}$$

Copyrighted material

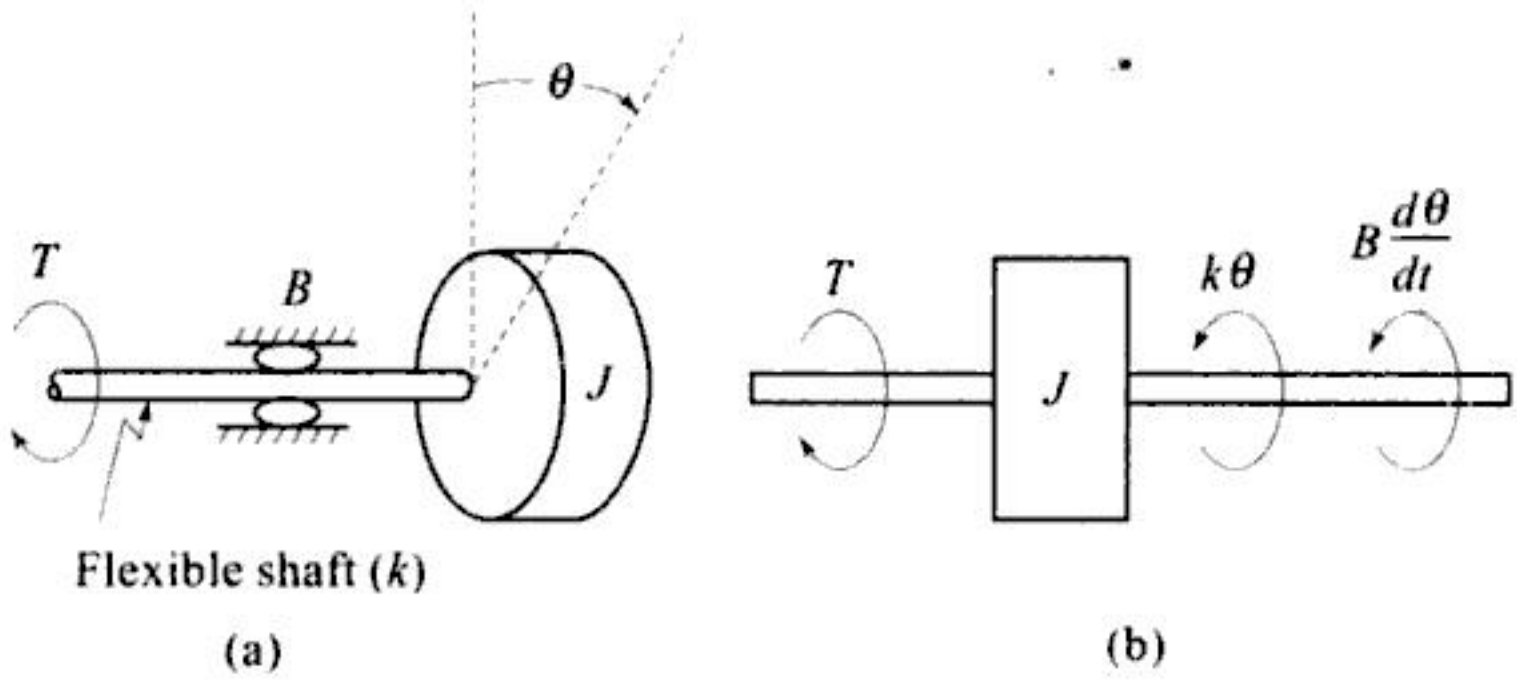


Fig. 2.19 *(a) An inertia-spring-damper system (b) A free-body diagram*

This is a linear constant-coefficient differential equation of second-order.

Taking the Laplace transform of each term of this equation (assuming zero initial conditions), we obtain

$$Js^2\,\theta(s) + Bs\theta(s) + k\theta(s) = T(s)$$

where $\theta(s) \triangleq \mathcal{L}[\theta(t)];\ T(s) \triangleq \mathcal{L}[T(t)]$

Therefore, the transfer function of the system is

$$G(s) = \frac{\theta(s)}{T(s)} = \frac{1}{Js^2 + Bs + k} = \frac{1/J}{s^2 + \frac{B}{J}s + \frac{k}{J}} \tag{2.53}$$

J = moment of inertia, Newton-m/(rad/sec^2)
B = damping coefficient, Newton-m/(rad/sec)
k = torsional spring constant, Newton-m/rad

Equation (2.53) gives a second-order transfer function of the mechanical system; the system has two poles—the roots of second-order characteristic polynomial with coefficients B/J and k/J, no finite zeros, and gain constant = $1/J$.

A more common notation for second-order transfer function is

$$G(s) = \frac{K}{\frac{1}{\omega_n^2}s^2 + \frac{2\zeta}{\omega_n}s + 1}$$

As we shall see shortly, physical meaning can be given to the three parameters K, ζ, and ω_n.

For the mechanical system under consideration,

$$K = \frac{1}{k},\ \omega_n = \sqrt{\frac{k}{J}},\ \zeta = \frac{1}{2}\frac{B}{\sqrt{kJ}} \tag{2.54a}$$

$$\frac{\theta(s)}{T(s)} = \frac{K\omega_n^2}{s^2 + 2\zeta\omega_n s + \omega_n^2} \tag{2.54b}$$

Copyrighted material

In the following, we investigate the time response to a step signal. From the characteristics of the time response, the physical meaning of the parameters K, ω_n, and ζ will become clear.

Physical parameters of the mechanical system—J, B, and k, can lead to the following four situations.

1. *Undamped systems* $(\zeta = 0)$

For $B = 0$ (no damping), we have

$$\frac{\theta(s)}{T(s)} = \frac{1/J}{s^2 + k/J} = \frac{K\omega_n^2}{s^2 + \omega_n^2} \tag{2.55}$$

where K and ω_n are given by Eqns (2.54a). Note that this case corresponds to $\zeta = 0$.

For $T(t) = \mu(t)$ or $T(s) = 1/s$, we have

$$\theta(s) = \frac{K\omega_n^2}{s(s^2 + \omega_n^2)} = K\left[\frac{1}{s} - \frac{s}{s^2 + \omega_n^2}\right]$$

$$\theta(t) = K(1 - \cos\omega_n t);\ t \geq 0 \tag{2.56}$$

The curve corresponding to $\zeta = 0$ in Fig. 2.20 follows Eqn. (2.56). This curve provides the physical significance of the parameter ω_n, called the *undamped natural frequency* of the system. It is the frequency at which the system would oscillate if the damping were reduced to zero. It has the dimension of reciprocal time (this can be verified from Eqns (2.54a) using the units of the physical parameters given in Eqn. (2.53)), and its unit is rad/sec.

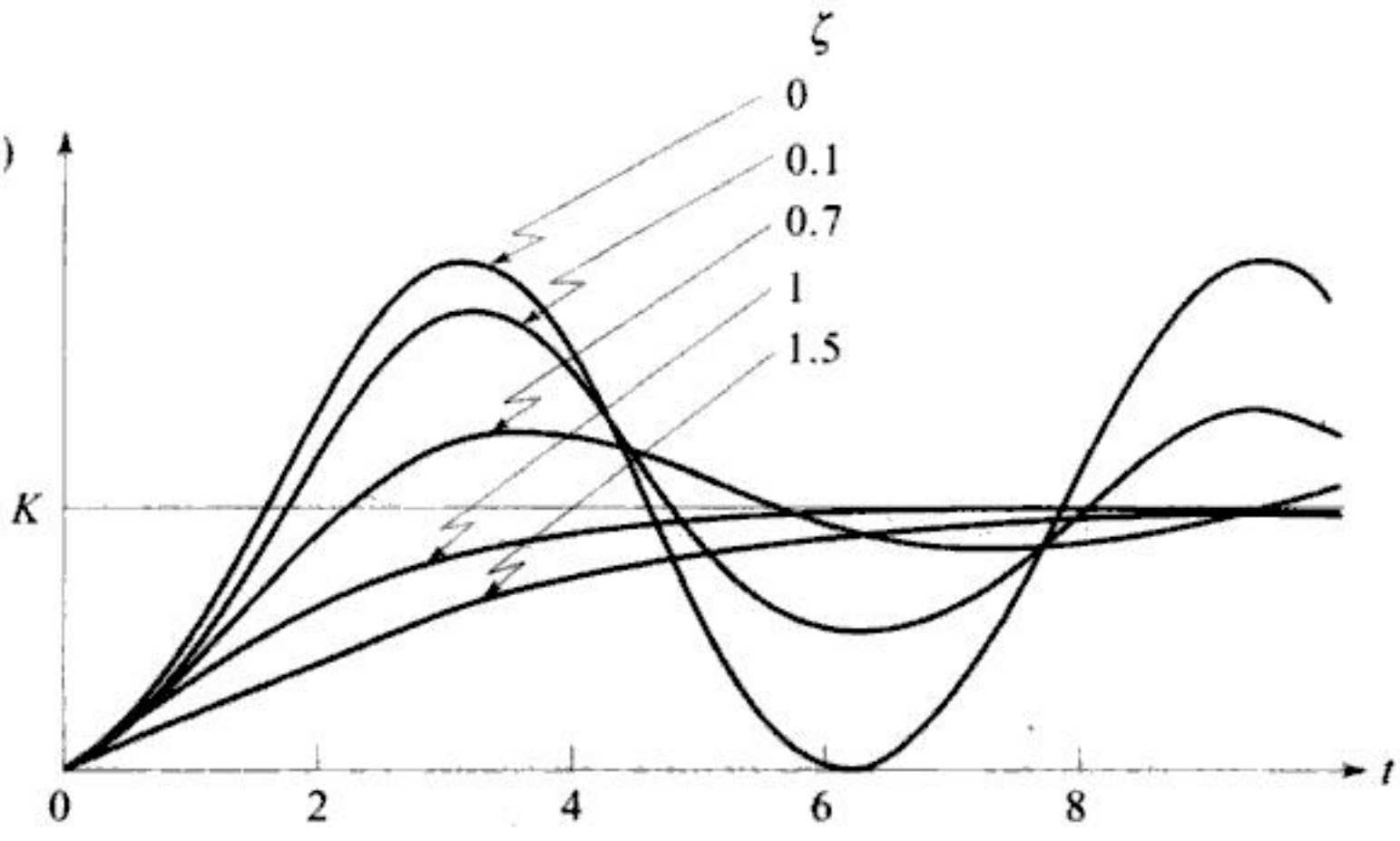


Fig. 2.20 *Step-response curves of a second-order system ($\omega_n = 1$)*

2. *Underdamped systems* $(0 < \zeta < 1)$

Let us now consider the damped case $(B \neq 0)$ under the condition,

Copyrighted material

$$\frac{k}{J} > \left(\frac{B}{2J}\right)^2$$

In terms of the parameter ζ given in Eqns (2.54a), this condition corresponds to $0 < \zeta < 1$. The parameter ζ, called the *damping ratio*, is a dimensionless quantity (this can be verified from Eqns (2.54a) using the units of the physical parameters given in Eqn. (2.53)).

For $T(t) = \mu(t)$ or $T(s) = 1/s$, we have

$$\theta(s) = \frac{K\omega_n^2}{s(s^2 + 2\zeta\omega_n s + \omega_n^2)}$$

$$= K\left[\frac{1}{s} - \frac{s + \zeta\omega_n}{(s + \zeta\omega_n)^2 + \omega_d^2} - \frac{\zeta\omega_n}{(s + \zeta\omega_n)^2 + \omega_d^2}\right] \qquad (2.57a)$$

where $$\omega_d = \omega_n\sqrt{1 - \zeta^2} \qquad (2.57b)$$

Using the Table of transform pairs given in Appendix A, we get

$$\theta(t) = K\left[1 - e^{-\zeta\omega_n t}\left(\cos\omega_d t + \frac{\zeta}{\sqrt{1-\zeta^2}}\sin\omega_d t\right)\right]$$

$$= K\left[1 - \frac{e^{-\zeta\omega_n t}}{\sqrt{1-\zeta^2}}\sin\left(\omega_d t + \tan^{-1}\frac{\sqrt{1-\zeta^2}}{\zeta}\right)\right]; \; t \geq 0 \qquad (2.58)$$

The step response as given by Eqn. (2.58) is plotted in Fig. 2.20 for various values of ζ ($0 < \zeta < 1$), and fixed ω_n. These plots provide the physical significance of the parameter ζ. For $0 < \zeta < 1$, the system response exhibits decaying oscillations of frequency $\omega_d = \omega_n\sqrt{1 - \zeta^2}$. ω_d is called the *damped natural frequency*. With ζ approaching zero, ω_d approaches ω_n, and the system response exhibits continuous oscillations. With ζ approaching one, the system response approaches the final value without overshooting it and consequently there are no oscillations (this will be proved shortly). Systems with $0 < \zeta < 1$ are called underdamped systems.

The curves

$$K\left[1 \pm \frac{e^{-\zeta\omega_n t}}{\sqrt{1-\zeta^2}}\right] \qquad (2.59a)$$

are the envelope curves for the step response. The response curve $\theta(t)$ always remains within this pair of envelope curves as shown in Fig. 2.21. The time-constant of these envelope curves is $1/\zeta\omega_n$. The speed of decay of the transient response depends on the value of the time-constant

$$\tau = \frac{1}{\zeta\omega_n} \qquad (2.59b)$$

Copyrighted material



You have either reached a page that is unavailable for viewing or reached your viewing limit for this book.

$$\theta(s) = \frac{K\omega_n^2}{s(s^2 + 2\zeta\omega_n s + \omega_n^2)}$$

$$= \frac{K\omega_n^2}{s\left(s + \zeta\omega_n + \omega_n\sqrt{\zeta^2 - 1}\right)\left(s + \zeta\omega_n - \omega_n\sqrt{\zeta^2 - 1}\right)}$$

$$= K\left[\frac{1}{s} + \frac{1}{2\sqrt{\zeta^2 - 1}\left(\zeta + \sqrt{\zeta^2 - 1}\right)}\left(\frac{1}{s + \zeta\omega_n + \omega_n\sqrt{\zeta^2 - 1}}\right)\right.$$

$$\left. - \frac{1}{2\sqrt{\zeta^2 - 1}\left(\zeta - \sqrt{\zeta^2 - 1}\right)}\left(\frac{1}{s + \zeta\omega_n - \omega_n\sqrt{\zeta^2 - 1}}\right)\right]$$

$$\theta(t) = K\left[1 + \frac{1}{2\sqrt{\zeta^2 - 1}\left(\zeta + \sqrt{\zeta^2 - 1}\right)}e^{-\left(\zeta + \sqrt{\zeta^2 - 1}\right)\omega_n t}\right.$$

$$\left. - \frac{1}{2\sqrt{\zeta^2 - 1}\left(\zeta - \sqrt{\zeta^2 - 1}\right)}e^{-\left(\zeta - \sqrt{\zeta^2 - 1}\right)\omega_n t}\right]; t \geq 0 \qquad (2.61)$$

Representative response curve for $\zeta > 1$ is shown in Fig. 2.20. The effect of increasing damping beyond its critical value is to make the response sluggish. Systems with $\zeta > 1$ are called overdamped systems.

▲▲

The parameters K, ζ, and ω_n describe the 'personality' of a second-order system. These parameters may be obtained from the physical parameters of a system or experimentally by conducting the sinusoidal response test.

The transfer function

$$G(s) = \frac{K}{\frac{1}{\omega_n^2}s^2 + \frac{2\zeta}{\omega_n}s + 1} \qquad (2.62)$$

is the standard form for second-order transfer functions, and will be encountered in all types of systems—electrical, mechanical, thermal, hydraulic, etc. It is called a *second-order lag* or *quadratic lag*. For $\zeta > 1$, the system no longer has a quadratic lag; it is then a cascade of two simple lags.

2.8 MODELS OF MECHANICAL SYSTEMS

The present and the next four sections are concerned with the modelling of simple physical systems. In these sections, the presentation of the basic mate-

Copyrighted material

rial from the system dynamics area is, for reasons of space, limited to essentials. The reader interested in more detail is referred to other literature [37–43].

In the analysis of mechanical systems, it is convenient to make use of three idealized elements—the mass, the spring and the dashpot. These elements represent three essential phenomena which occur in various ways in mechanical systems.

Mechanics of Translation

The ideal mass element represents a particle of mass which is the lumped approximation of the mass of a body concentrated at the centre of the mass.

The concept of the elastic deformation of a body is symbolized by the ideal element shown as a helical spring.

Friction exists in physical systems whenever mechanical surfaces are operated in sliding contact. Friction encountered in physical systems may be of many types.

1. *Coulomb friction force*: It is the force of sliding friction between dry surfaces. This force is substantially constant.
2. *Viscous friction force*: It is the force of friction between moving surfaces separated by viscous fluid, or the force between a solid body and a fluid medium. This force is approximately linearly proportional to velocity over a certain limited velocity range.
3. *Stiction*: It is the force required to initiate motion between two contacting surfaces (which is obviously more than the force required to maintain them in relative motion).

In many situations of interest, viscous friction predominates. Our models of mechanical systems are based on this assumption. Refer [180] for situations where this approximation is not valid.

Sometimes it may even be necessary to introduce viscous friction intentionally to improve the dynamic response of a system. A *dashpot* is a device that provides viscous friction or damping. It consists of a piston and an oil-filled cylinder with a narrow annular passage between the piston and the cylinder (Fig. 2.22). Any relative motion between the piston and the cylinder is resisted by oil.

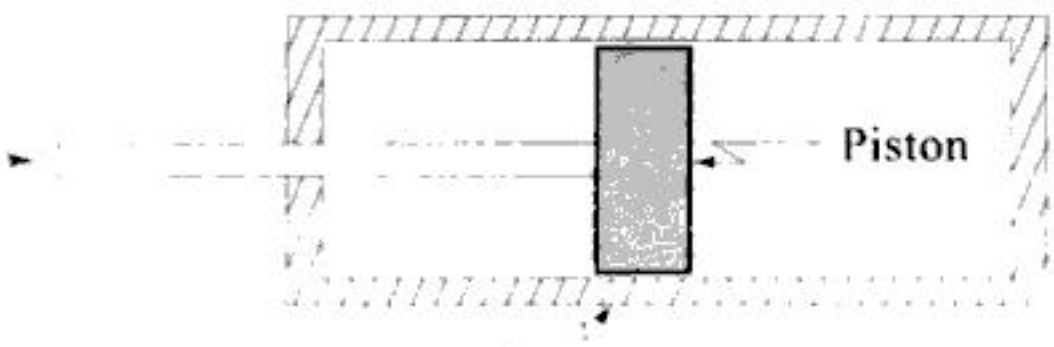


Fig. 2.22 *Dashpot*

Copyrighted material

Mechanical translational systems consisting of the three parameters M, B, and K are components of many control systems. To cite an example, we revisit the hydraulic power steering mechanism for automobiles shown in Fig. 1.8. In this system, the rotation of the steering wheel is the command signal. This signal is amplified by the hydraulic power amplifier; the force signal $F(t)$ so generated causes the power ram to move which then rotates the wheels through a proper drive linkage.

The load on the power ram is the mass M of the power piston, wheels, and the drive linkage; tyre stiffness represented by spring constant K; and friction with coefficient B because of the motion of the power piston, drive linkage, etc., in the viscous medium. Constant sliding friction also exists at the tyre–road interface. This force depends on road conditions and is therefore an uncontrolled disturbance input to the system.

As another example, consider the system for machining a work piece on a lathe. Tool movement of such a system is shown in Fig 2.23a. The carriage is moved at a constant speed and the control of the tool position is in the direction of the cross slide. The load on the hydraulic actuator consists of mass M, and viscous friction with coefficient B. The disturbance acting on the actuator is the thrust force on the tool required to machine the work piece.

Yet another example of mass-spring-damper systems is shown in Fig. 2.23b. The system controls the thickness of the rolled steel in a steel mill. The rolls are driven at a constant speed by drive motors. The translational motion of the movable roll is controlled by the hydraulic actuator. The load on the hydraulic actuator consists of mass M, and viscous friction with coefficient B. The disturbance acting on the actuator is the upward force on the roll which is quite significant when the slabs enter the rolls or leave the rolls.

Feedback control schemes for the applications referred above will be discussed in the next chapter.

The mass-spring-damper system shown in Fig. 2.24a is thus a useful model of the load on a linear actuator in industrial control systems. The viscous friction has been indicated by a stylized dashpot and F_w represents the load disturbance. Let us obtain the transfer function model of this system. In order to obtain a linear model, we will assume that the friction force of the dashpot is proportional to $\dot{y}$ (true for small velocities). Also the spring is considered a linear device; the spring force is proportional to y (true for small displacements).

Figure 2.24b shows the free-body diagram of the system. Applying Newton's law of motion, the force equation can be written as

$$F(t) - F_w(t) - B\frac{dy(t)}{dt} - Ky(t) = M\frac{d^2y(t)}{dt^2}$$

or

$$M\frac{d^2y(t)}{dt^2} + B\frac{dy(t)}{dt} + Ky(t) = F(t) - F_w(t) \qquad (2.63)$$

Copyrighted material

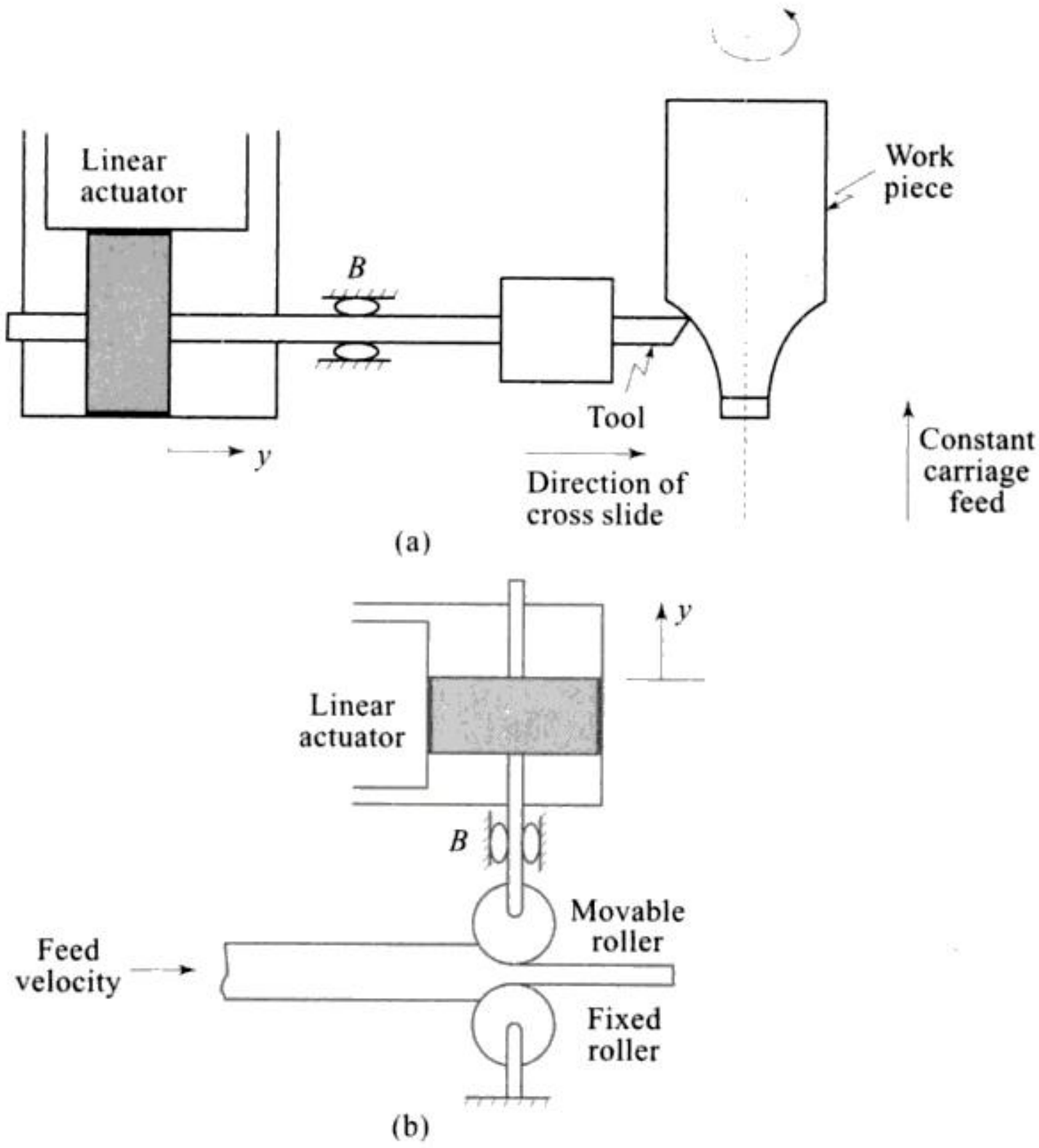


Fig. 2.23 *(a) Machining control system; (b) System for controlling the thickness of rolled steel*

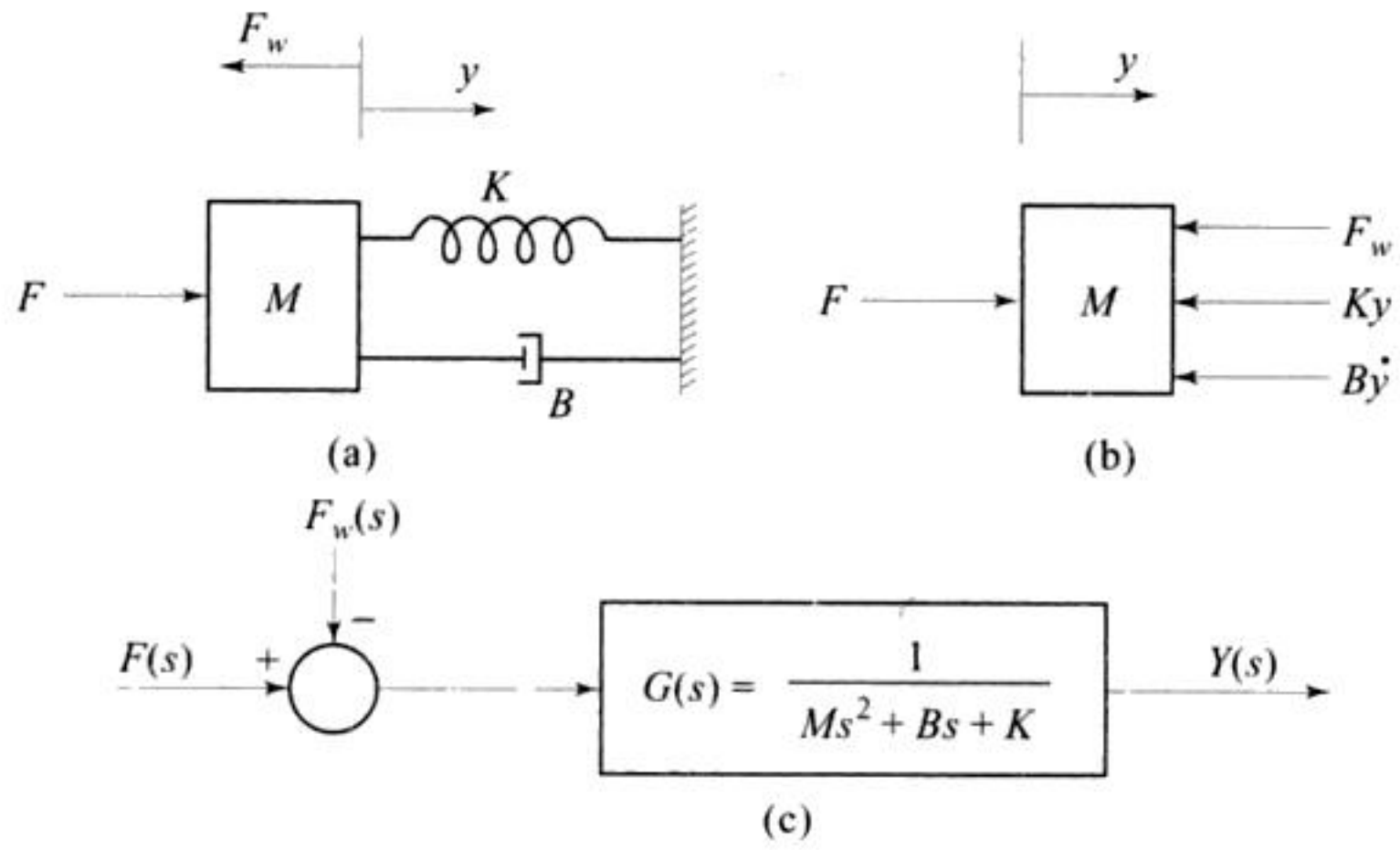


Fig. 2.24 *A mass-spring-damper system*

Copyrighted material

This is a linear, constant-coefficient differential equation of the second-order.

Taking the Laplace transform of each term of this equation (assuming zero initial conditions), we obtain

$$Ms^2Y(s) + BsY(s) + KY(s) = F(s) - F_w(s)$$

where

$$Y(s) \triangleq \mathcal{L}[y(t)]; F(s) \triangleq \mathcal{L}[F(t)]; F_w(s) \triangleq \mathcal{L}[F_w(t)]$$

Therefore,

$$Y(s) = \frac{1}{Ms^2 + Bs + K} F(s) - \frac{1}{Ms^2 + Bs + K} F_w(s) \qquad (2.64a)$$

Figure 2.24c gives the block diagram representation of the system.

$$G(s) = \frac{1}{Ms^2 + Bs + K} = \frac{1/K}{\frac{M}{K}s^2 + \frac{B}{K}s + 1} = \frac{1/K}{\frac{1}{\omega_n^2}s^2 + \frac{2\zeta}{\omega_n}s + 1} \qquad (2.64b)$$

is a quadratic lag; the parameters of the standard form (2.62) of a quadratic lag can easily be obtained from the physical parameters M, B, and K.

The metric system of units for mechanical translational systems is given in Table 2.2.

Fixed-Axis Rotation

Mechanical systems involving fixed-axis rotation occur in the study of machinery of many types and are very important. The modelling procedure is very close to that used in translation. In these systems, the variables of interest are the torque and the angular velocity (or angular displacement). The three basic components for the rotational systems are moment of inertia, torsional spring, and viscous friction.

In low-power servos, the driving and driven shafts can be treated as having negligible elasticity; these rotational systems can therefore be modelled using two components: the moment of inertia J, and the viscous friction with coefficient B. High-power servos, however, may require three components: moment of inertia J, viscous friction with coefficient B, and torsional spring with spring constant K.

To cite an example of rotational load, we revisit the servomechanism for steering of the antenna, shown in Fig. 1.16a. A simple model of the load (antenna) is the moment of inertia–damper system shown in Fig. 1.16b. This model is resketched in Fig. 2.25a; J is the moment of inertia of the antenna, and B represents the viscous friction introduced by bearings and other sources. Torque $T(t)$ is the controlled input generated by the motor, angular displacement $\theta(t)$ of the antenna is the output, and $T_w(t)$ represents the uncontrolled load disturbance torque (due to wind, for example).

The free-body diagram is shown in Fig. 2.25b. The torque equation is

Copyrighted material

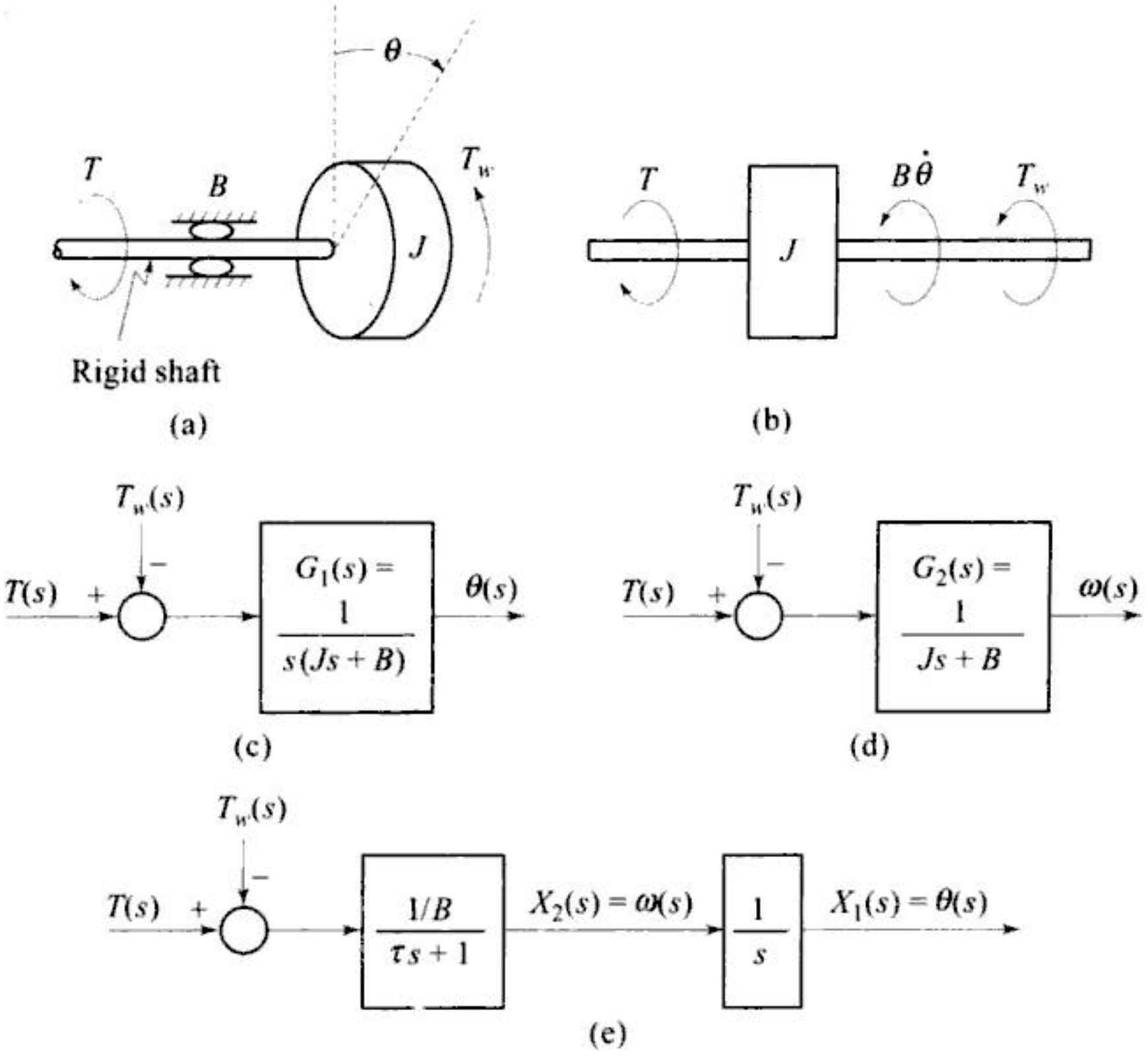


Fig. 2.25 *An inertia-damper system*

$$T(t) - B\frac{d\theta(t)}{dt} - T_w(t) = J\frac{d^2\theta(t)}{dt^2}$$

or
$$J\frac{d^2\theta(t)}{dt^2} + B\frac{d\theta(t)}{dt} = T(t) - T_w(t) \tag{2.65}$$

This is a linear, constant-coefficient differential equation of second-order.

Taking the Laplace transform of each term of this equation (assuming zero initial conditions), we obtain

$$Js^2\theta(s) + Bs\theta(s) = T(s) - T_w(s)$$

where $\theta(s) \triangleq \mathcal{L}[\theta(t)]$; $T(s) \triangleq \mathcal{L}[T(t)]$; $T_w(s) \triangleq \mathcal{L}[T_w(t)]$

Therefore,
$$\theta(s) = \frac{1}{Js^2 + Bs}T(s) - \frac{1}{Js^2 + Bs}T_w(s) \tag{2.66a}$$

Figure 2.25c gives the block diagram representation of the system.

$$G_1(s) = \frac{1}{s(Js+B)} = \frac{1/B}{s\left(\frac{J}{B}s+1\right)} = \frac{1/B}{s(\tau s+1)} \tag{2.66b}$$

Copyrighted material

where $\tau = J/B$.

If we assume that angular velocity $\omega(t) = \dfrac{d\theta(t)}{dt}$ is the output, then the differential equation of the system becomes

$$J\frac{d\omega(t)}{dt} + B\omega(t) = T(t) - T_w(t) \tag{2.67}$$

This is a linear constant-coefficient differential equation of the first-order.

The Laplace transformation of Eqn. (2.67) under the assumption of zero initial conditions, gives

$$(Js + B)\omega(s) = T(s) - T_w(s)$$

where

$$\omega(s) \triangleq \mathcal{L}[\omega(t)].$$

Therefore, $$\omega(s) = \frac{1}{Js + B}T(s) - \frac{1}{Js + B}T_w(s) \tag{2.68a}$$

Figure 2.25d shows the corresponding block diagram.

$$G_2(s) = \frac{1}{Js + B} = \frac{1/B}{\frac{J}{B}s + 1} = \frac{1/B}{\tau s + 1} \tag{2.68b}$$

where τ is the time-constant of the simple lag.

The differential equations obtained by applying physical laws to mechanical rotational systems are, in fact, the state equations[10] of the system. Only some rearrangement of these equations is required to obtain state variable model in the standard format given in Eqns (2.4).

A selection of the state variables and corresponding state equations are given below.

$$x_1(t) = \theta(t);\ x_2(t) = \omega(t) = \dot{\theta}(t)$$

$$\dot{x}_1(t) = x_2(t)$$

$$\dot{x}_2(t) = -\frac{B}{J}x_2(t) + \frac{1}{J}(T(t) - T_w(t))$$

Taking the Laplace transform on both sides of the state equations (assuming zero initial conditions), we obtain

$$sX_1(s) = X_2(s)$$

$$sX_2(s) = -\frac{B}{J}X_2(s) + \frac{1}{J}[T(s) - T_w(s)]$$

$$X_1(s) \triangleq \mathcal{L}[x_1(t)];\ X_2(s) \triangleq \mathcal{L}[x_2(t)]$$

---

10. In mechanical rotational systems with inertia, torsional spring, and damper elements, normally an independent set of angular velocities and displacements associated with inertia elements, and angular displacements associated with torsional spring elements constitutes a state vector.

Copyrighted material

The corresponding block diagram representation is shown in Fig. 2.25e. It consists of two blocks; the first block is a simple lag with speed $\omega(s)$ as the output, and the second block is an integrator whose output is displacement $\theta(s)$.

The metric system of units for mechanical rotational systems is summarized in Table 2.2.

Table 2.2 *Mechanical symbols and units*

Quantity	*Metric units*	*Quantity*	*Metric units*
Force (F)	Newton or kg-m/sec^2	Torque (T)	Newton-m
Displacement (y)	Metres (m)	Angle (θ)	Radians (rad)
Velocity (v)	m/sec	Angular velocity (ω)	rad/sec
Acceleration ($\dot{v}$)	m/sec^2	Angular acceleration ($\dot{\omega}$)	rad/sec^2
Mass (M)	kg	Moment of inertia(J)	Newton-m/(rad/sec^2) or kg-m^2
Spring constant(K)	Newtons/m	Torsional spring constant (K)	Newton-m/rad
Damping coefficient (B)	Newtons/(m/sec)	Damping coefficient (B)	Newton-m/(rad/sec)

Example 2.6

Consider the mechanical system shown in Fig. 2.26a. This system is a simplified 'one-wheeled' model of an automobile suspension system with M_1: the mass of the automobile, B: the shock absorbers, K_1: the springs, M_2: the mass of the wheels, and K_2: the elastance of the tyres. The system objective is to reduce vibrations $y_1(t)$ due to disturbance force $F_w(t)$.

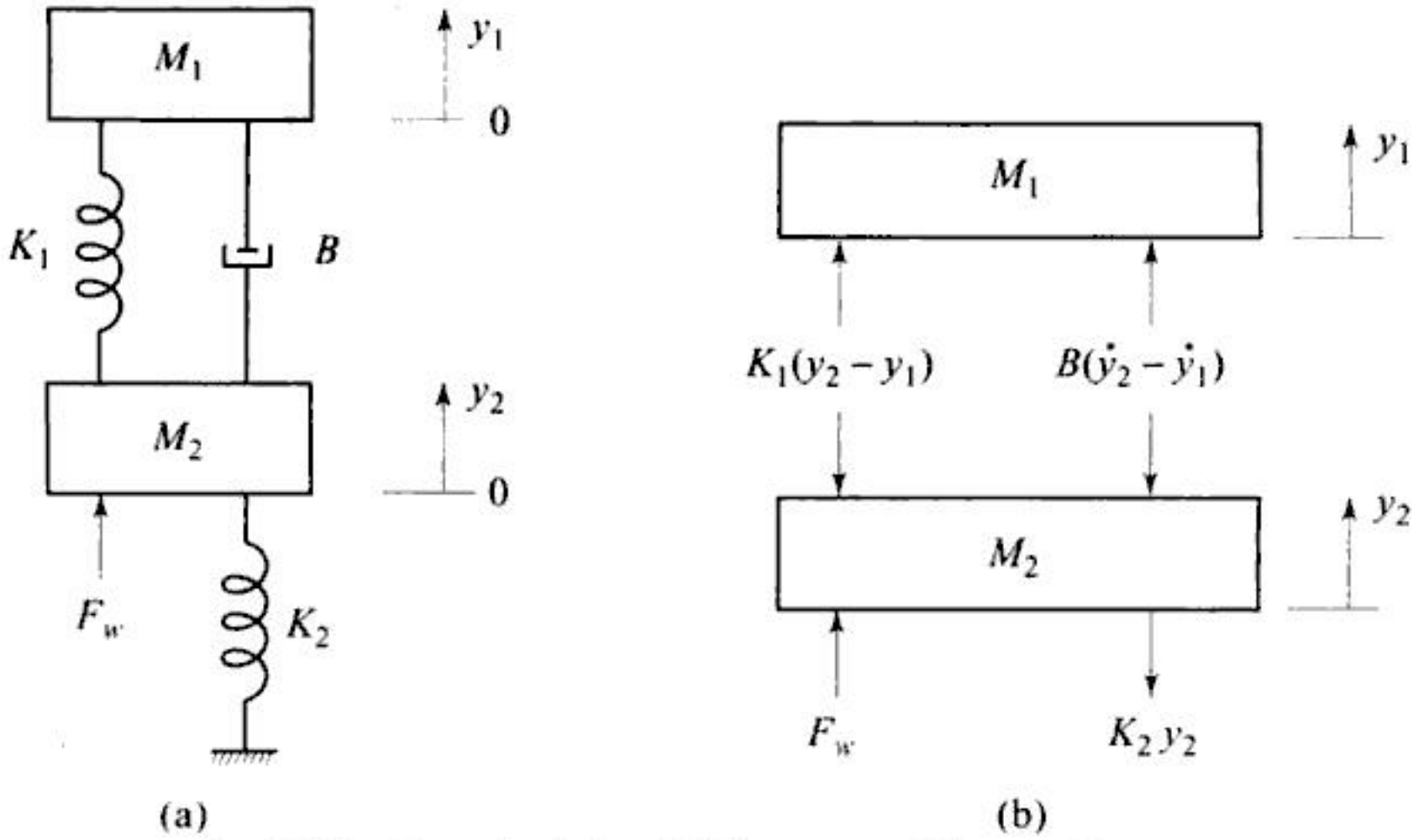


Fig. 2.26 *One-wheeled model of an automobile suspension system*

Copyrighted material

The displacements $y_1(t)$ and $y_2(t)$ are considered with respect to positions of the vehicle and the wheels on a level road under the loaded condition. The gravitational forces, therefore, do not appear in the model being formulated.

Figure 2.26b shows the free-body diagram for the system. From this figure, we have the following differential equations describing the dynamics of the system.

$$M_1\ddot{y}_1(t) = K_1(y_2(t) - y_1(t)) + B(\dot{y}_2(t) - \dot{y}_1(t)) \tag{2.69a}$$

$$M_2\ddot{y}_2(t) = F_w(t) - K_1(y_2(t) - y_1(t)) - B(\dot{y}_2(t) - \dot{y}_1(t)) - K_2\, y_2(t) \tag{2.69b}$$

Taking the Laplace transform of these equations, assuming zero initial conditions, we obtain

$$M_1s^2Y_1(s) + B(sY_1(s) - sY_2(s)) + K_1(Y_1(s) - Y_2(s)) = 0 \tag{2.70a}$$

$$M_2s^2Y_2(s) + B(sY_2(s) - sY_1(s)) + K_1(Y_2(s) - Y_1(s)) + K_2Y_2(s) = F_w(s) \tag{2.70b}$$

Suppose that a transfer function is desired between $F_w(s)$ and $Y_1(s)$, i.e., between the disturbance force applied to the wheels and the resulting displacement of the automobile. This transfer function can be found by eliminating $Y_2(s)$ in Eqns (2.70). Solving Eqn. (2.70a) for $Y_1(s)$, we obtain

$$Y_1(s) = \frac{Bs + K_1}{M_1s^2 + Bs + K_1}\, Y_2(s)$$

Now Eqn. (2.70b) can be solved for $Y_2(s)$:

$$Y_2(s) = \frac{1}{M_2s^2 + Bs + K_1 + K_2} F_w(s) + \frac{Bs + K_1}{M_2s^2 + Bs + K_1 + K_2} Y_1(s)$$

Eliminating $Y_2(s)$ from these equations, gives

$$G(s) = \frac{Y_1(s)}{F_w(s)}$$

$$= \frac{Bs + K_1}{\left[M_1M_2s^4 + B(M_1 + M_2)s^3 + (K_1M_2 + K_1M_1 + K_2M_1)s^2 + K_2Bs + K_1K_2\right]}$$

The dynamics of the mechanical system are completely described by the transfer function. Given the mass of the automobile, the mass of the wheels, and the elastance of the tyres, the smoothness of the ride is determined by the parameters of the shock absorber and the springs. These parameters are used to tune the system to give a good response. As a physical shock absorber deteriorates, the value of the parameter B changes, which changes the transfer function and the quality of the ride.

Rearrangement of Eqns (2.69) in the standard form given by Eqns (2.4) directly gives us the state variable formulation of the mechanical system.

Independent set of displacements and velocities of masses, and displacements of springs constitutes a state vector for the mass-spring-damper systems. In accordance with this choice, state variables for the system of Fig. 2.26 are

Copyrighted material

$$x_1(t) = y_1(t); \quad x_2(t) = y_2(t);$$
$$x_3(t) = \dot{y}_1(t); \quad x_4(t) = \dot{y}_2(t)$$

With these definitions of state variables, the two second-order differential equations (2.69a) and (2.69b) can be written in the form of state equations (first-order equations):

$$\dot{x}_1(t) = x_3(t)$$
$$\dot{x}_2(t) = x_4(t)$$
$$\dot{x}_3(t) = -\frac{K_1}{M_1}x_1(t) + \frac{K_1}{M_1}x_2(t) - \frac{B}{M_1}x_3(t) + \frac{B}{M_1}x_4(t)$$
$$\dot{x}_4(t) = \frac{K_1}{M_2}x_1(t) - \frac{(K_1 + K_2)}{M_2}x_2(t) + \frac{B}{M_2}x_3(t) - \frac{B}{M_2}x_4(t) + \frac{1}{M_2}F_w(t)$$

In the vector-matrix notation, these equations are written as

$$\begin{bmatrix} \dot{x}_1(t) \\ \dot{x}_2(t) \\ \dot{x}_3(t) \\ \dot{x}_4(t) \end{bmatrix} = \begin{bmatrix} 0 & 0 & 1 & 0 \\ 0 & 0 & 0 & 1 \\ -\frac{K_1}{M_1} & \frac{K_1}{M_1} & -\frac{B}{M_1} & \frac{B}{M_1} \\ \frac{K_1}{M_2} & -\frac{(K_1 + K_2)}{M_2} & \frac{B}{M_2} & -\frac{B}{M_2} \end{bmatrix} \begin{bmatrix} x_1(t) \\ x_2(t) \\ x_3(t) \\ x_4(t) \end{bmatrix} + \begin{bmatrix} 0 \\ 0 \\ 0 \\ 1/M_2 \end{bmatrix} F_w(t)$$

Since $y_1(t)$ is the desired output, the output equation is

$$y(t) = y_1(t) = \begin{bmatrix} 1 & 0 & 0 & 0 \end{bmatrix} \begin{bmatrix} x_1(t) \\ x_2(t) \\ x_3(t) \\ x_4(t) \end{bmatrix}$$

Example 2.7

Many servomechanisms involve mechanical systems that can be modelled as in Fig. 2.27a. The inertia J_1 represents the rotating member of a motor that applies the torque T; whereas J_2 is the driven load. Twisting of the long shaft due to the application of the torque is represented by the torsional spring constant K. Damping B represents frictional losses in the shaft.

Figure 2.27b shows the free-body diagram for the system. From this figure, we have the following differential equations describing the dynamics of the system.

$$J_1\ddot{\theta}_1(t) = T(t) - B(\dot{\theta}_1(t) - \dot{\theta}_2(t)) - K(\theta_1(t) - \theta_2(t))$$
$$J_2\ddot{\theta}_2(t) = B(\dot{\theta}_1(t) - \dot{\theta}_2(t)) + K(\theta_1(t) - \theta_2(t))$$

Laplace transformation of these equations under the assumption of zero initial conditions, gives

Copyrighted material

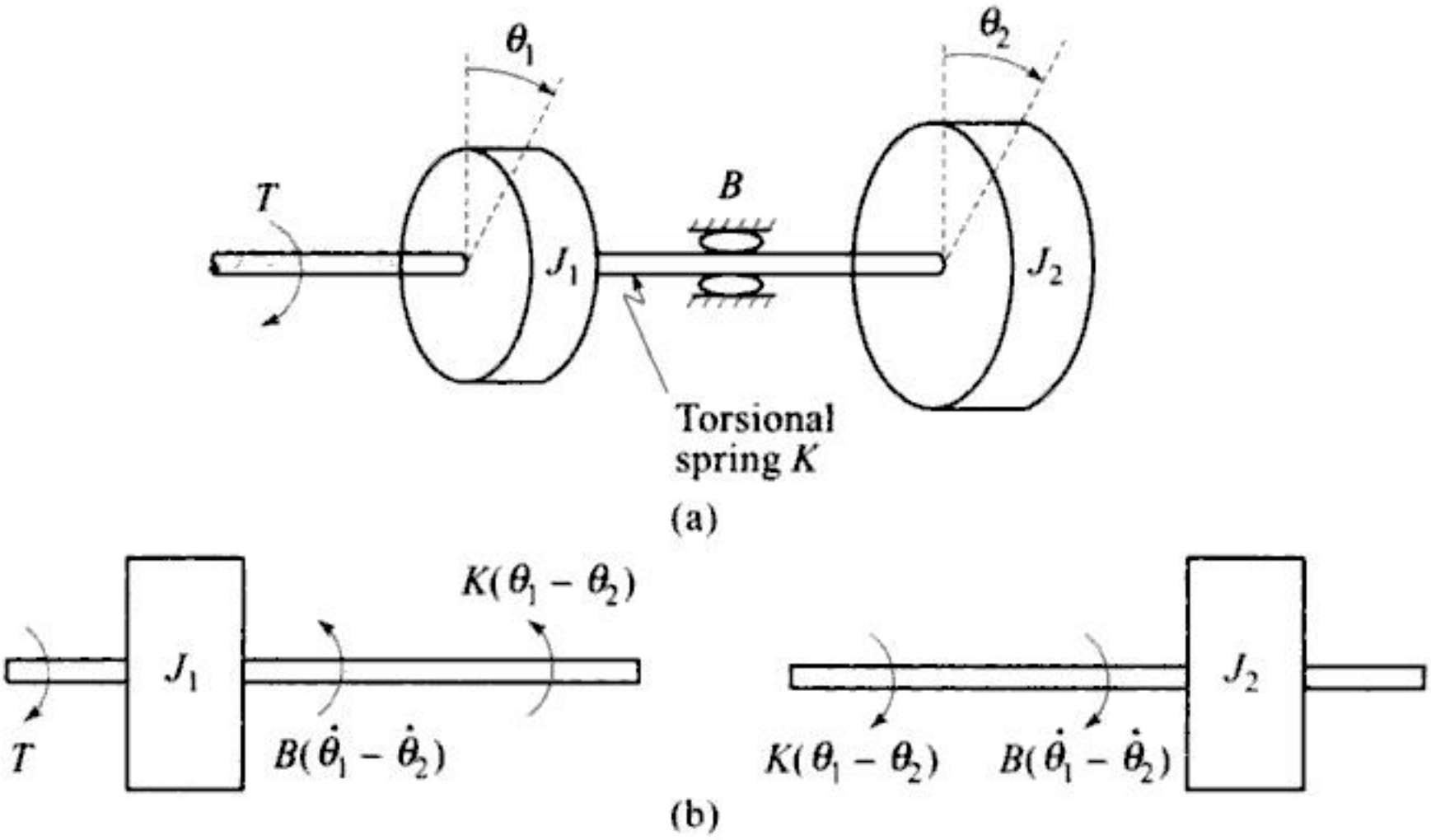


Fig. 2.27 *A motor-load system*

$$(J_1 s^2 + Bs + K)\theta_1(s) = (Bs + K)\theta_2(s) + T(s)$$
$$(J_2 s^2 + Bs + K)\theta_2(s) = (Bs + K)\theta_1(s)$$

Manipulation leads to

$$\frac{\theta_2(s)}{T(s)} = G(s) = \frac{\left[\dfrac{1}{J_1 + J_2}\right](\tau s + 1)}{s^2\left[\dfrac{1}{\omega_n^2}s^2 + \dfrac{2\zeta}{\omega_n}s + 1\right]} \tag{2.71}$$

where $\tau = \dfrac{B}{K}$; $\omega_n = \sqrt{\dfrac{K(J_1 + J_2)}{J_1 J_2}}$; $\zeta = \dfrac{B}{2\sqrt{KJ_1J_2/(J_1 + J_2)}}$

2.9 MODELS OF ELECTRICAL CIRCUITS

In later chapters of this book, we will frequently use electric circuits to meet the functional requirements of the amplification of weak control/sensor signals, filtering of high frequency 'noise' (such as measurement noise), and to improve the performance of feedback control systems. Here the objective is to develop mathematical models of commonly used electric circuits.

Passive Circuits

The resistor, the inductor, and the capacitor are the three basic elements of passive (no internal power source) electric circuits. These circuits are analysed by the application of Kirchhoff's voltage and current laws.

Let us analyse the RLC circuit of Fig. 2.28 by using Kirchhoff's current law.

Copyrighted material

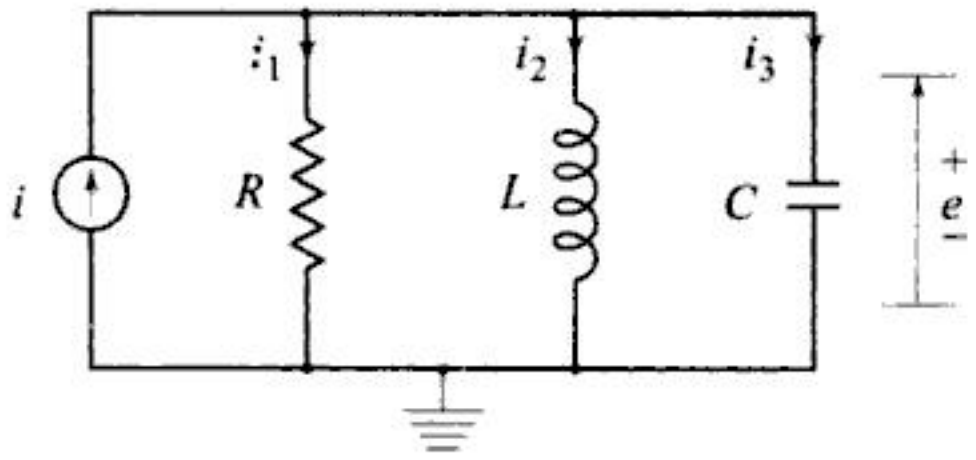


Fig. 2.28 *An RLC circuit*

The governing equations of the system are

$$i(t) = i_1(t) + i_2(t) + i_3(t) = \frac{e(t)}{R} + i_2(t) + C\frac{de(t)}{dt}$$

$$e(t) = L\frac{di_2(t)}{dt}$$

These equations may be rearranged to give state equations for the circuit:

$$\left.\begin{aligned} \frac{de(t)}{dt} &= -\frac{1}{RC}e(t) - \frac{1}{C}i_2(t) + \frac{1}{C}i(t) \\ \frac{di_2(t)}{dt} &= \frac{1}{L}e(t) \end{aligned}\right\} \tag{2.72}$$

$e(t)$ and $i_2(t)$ are the state variables and $i(t)$ is the current source (input variable).

Analogous Systems

If two systems are described by dynamical equations of identical form, these are said to be *analogs* of each other. For example, the electric analog of the mechanical system of Fig. 2.2 is the RLC circuit shown in Fig. 2.28. This can be established as follows.

The mechanical system of Fig. 2.2 is governed by the differential equation (refer Eqn. (2.26))

$$M\frac{d^2x(t)}{dt^2} + B\frac{dx(t)}{dt} + Kx(t) = F(t)$$

Rewriting this equation in terms of velocity variable $v(t) = \dot{x}(t)$ results in the following integro-differential equation.

$$M\frac{dv(t)}{dt} + Bv(t) + K\int_{-\infty}^{t} v(\tau)d\tau = F(t) \tag{2.73}$$

The electric circuit of Fig. 2.28 is governed by the state equations (2.72). Rewriting these equations in terms of voltage $e(t)$, results in the following integro-differential equation.

Copyrighted material

$$C\frac{de(t)}{dt}+\frac{1}{R}e(t)+\frac{1}{L}\int_{-\infty}^{t}e(\tau)d\tau=i(t)$$

Comparing this equation with Eqn. (2.73), we at once observe their mathematical similarity with respect to the following analogous pairs:

$$\begin{gathered}F(t)\leftrightarrow i(t);\ v(t)\leftrightarrow e(t)\\ M\leftrightarrow C;\ K\leftrightarrow 1/L;B\leftrightarrow 1/R\end{gathered}\qquad(2.74)$$

The commonly-used characterizing variables in an electrical system—the voltage and the current—are respectively called *across* and *through* variables of the system. By analogy, velocity and force are, respectively, the across and through variables of mechanical systems. The analogous variables and element pairs in (2.74) are appropriately called the *force-current analogy*.[11]

The variables and basic elements of mechanical rotational systems with their electrical analogs (*torque-current analogy*) are listed below.

$$\begin{gathered}T(t)\leftrightarrow i(t);\quad \omega(t)\leftrightarrow e(t)\\ J\leftrightarrow C;\quad K\leftrightarrow 1/L;\ B\leftrightarrow 1/R\end{gathered}\qquad(2.75)$$

▲▲

The concept of analogous systems is a useful technique for the study of various systems such as electrical, mechanical, thermal, liquid level, etc. Generally it is convenient to study a non-electrical system in terms of its electrical analog as electrical systems are more easily amenable to experimental study.

The principle of analogy is the basic principle behind the use of analog computers for investigating system behaviour—an analog to the physical system can be developed, as will be seen shortly, from the components of an analog computer.

The metric system of units for electrical systems is summarized in Table 2.3.

Table 2.3 *Electrical symbols and units*

Quantity	*Metric units*
Voltage (e)	Volts
Current (i)	Amperes
Inductance, (L)	Henrys
Capacitance (C)	Farads
Resistance (R)	Ohms

Example 2.8

Figure 2.29 shows five passive (no internal power source) circuits. In the following, we write describing equations (using Kirchhoff's voltage and cur-

11. Another possible analogy between mechanical and electrical systems is the *force-voltage analogy*. The corresponding analogous electrical system for the mechanical system of Fig. 2.2 will be an RLC series circuit excited by a voltage source.

Copyrighted material

rent laws) for each circuit. Transfer function models are then obtained by Laplace transformation.

For each circuit given in Fig. 2.29, capacitor voltages are the state variables. State equations can directly be 'read' from the describing equations given here.

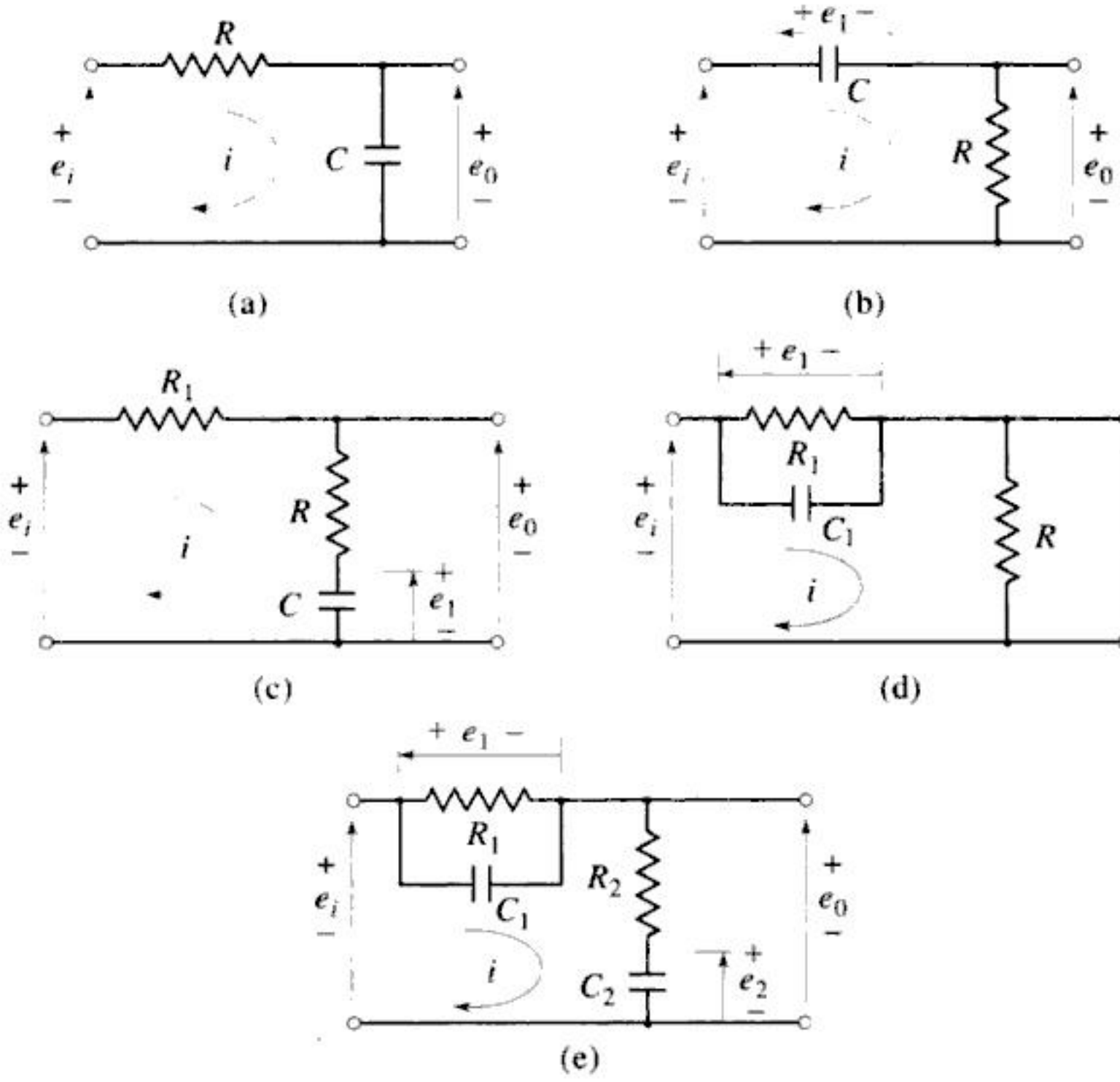


Fig. 2.29 *Commonly-used passive circuits*

Figure 2.29a

$$i(t) = C\,\frac{de_0(t)}{dt}\,;\; R\,i(t) + e_0(t) = e_i(t)$$

$$G(s) = \frac{E_0(s)}{E_i(s)} = \frac{1}{\tau s + 1};\; \tau = RC \tag{2.76}$$

Figure 2.29b

$$e_1(t) = e_i(t) - e_0(t);\quad i(t) = C\,\frac{de_1(t)}{dt};\; e_0(t) = Ri(t)$$

$$G(s) = \frac{E_0(s)}{E_i(s)} = \frac{\tau s}{\tau s + 1}\;;\; \tau = RC \tag{2.77}$$

Figure 2.29c

$$e_1(t) = e_0(t) - Ri(t);\quad i(t) = C\,\frac{de_1(t)}{dt};\quad (R + R_1)\,i(t) + e_1(t) = e_i(t)$$

Copyrighted material

$$G(s) = \frac{E_0(s)}{E_i(s)} = \frac{\tau s + 1}{(\tau / \alpha)s + 1} \; ; \; \tau = RC, \; \alpha = \frac{R}{R_1 + R} \tag{2.78}$$

Figure 2.29d

$$e_1(t) = e_i(t) - e_0(t); \quad i(t) = \frac{e_1(t)}{R_1} + C_1 \frac{de_1(t)}{dt}; \; e_0(t) = R\, i(t)$$

$$G(s) = \frac{E_0(s)}{E_i(s)} = \alpha \frac{\tau s + 1}{\alpha \tau s + 1}; \; \tau = R_1 C_1, \; \alpha = \frac{R}{R_1 + R} \tag{2.79}$$

Figure 2.29e

$$e_1(t) = e_i(t) - e_0(t); \quad e_2(t) = e_0(t) - R_2\, i(t);$$

$$i(t) = \frac{e_1(t)}{R_1} + C_1 \frac{de_1(t)}{dt} = C_2 \frac{de_2(t)}{dt}$$

$$G(s) = \frac{E_0(s)}{E_i(s)} = \frac{(\tau_1 s + 1)(\tau_2 s + 1)}{\tau_1 \tau_2 s^2 + (\tau_1 + \tau_2 + \tau_{12})s + 1}; \tag{2.80}$$

$$\tau_1 = R_1 C_1, \; \tau_2 = R_2 C_2, \; \tau_{12} = R_1 C_2$$

▲▲

As a final point on circuit analysis, we cover the technique that is called the *impedance approach*. This approach is useful for developing transfer function models of electric circuits.

Impedance $Z(s)$ of a passive circuit is the ratio of the Laplace transform of the voltage across the circuit to the Laplace transform of the current through the circuit under the assumption of zero initial conditions. For impedances in series, the equivalent impedence is equal to the sum of the individual impedances. For impedances in parallel, the reciprocal of the equivalent impedance is equal to the sum of the reciprocals of the individual impedances.

Figure 2.30a shows an RLC-series circuit.

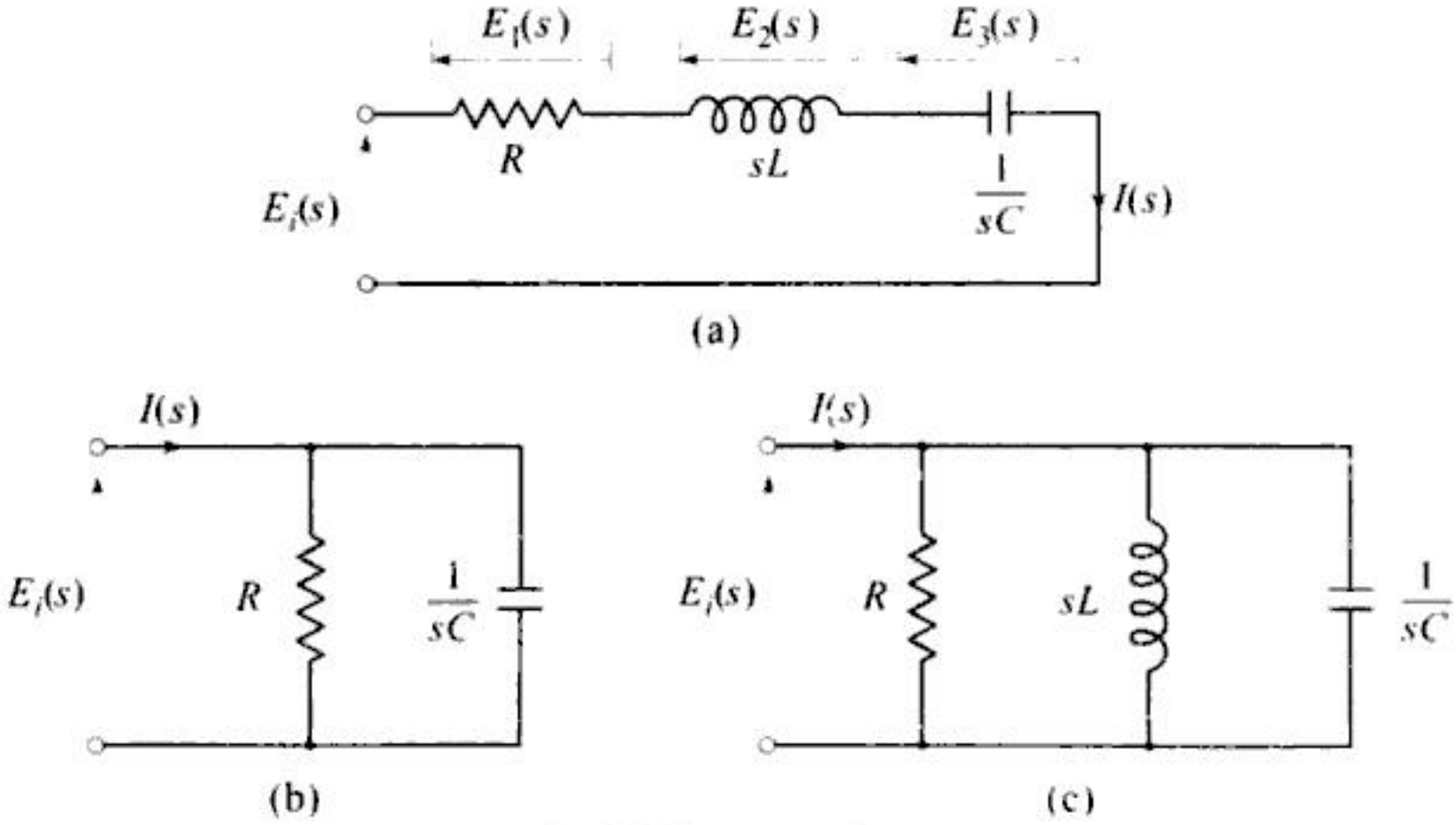


Fig. 2.30 *RLC circuits*

Copyrighted material



You have either reached a page that is unavailable for viewing or reached your viewing limit for this book.

Figure 2.29c

$$E_0(s) = \left(R + \frac{1}{sC}\right) I(s) = \left(R + \frac{1}{sC}\right)\left[\frac{E_i(s)}{R + R_1 + 1/sC}\right]$$

Manipulation of this equation gives Eqn. (2.78).

Figure 2.29d

$$E_0(s) = RI(s) = R\left[\frac{E_i(s)}{R + \dfrac{R_1(1/sC_1)}{R_1 + 1/sC_1}}\right]$$

Manipulation of this equation gives Eqn. (2.79).

Figure 2.29e

$$E_0(s) = \left(R_2 + \frac{1}{sC_2}\right) I(s) = \left(R_2 + \frac{1}{sC_2}\right)\left[\frac{E_i(s)}{R_2 + 1/sC_2 + \dfrac{R_1(1/sC_1)}{R_1 + 1/sC_1}}\right]$$

Manipulation of this equation gives Eqn. (2.80).

Op Amp Circuits

With the development of operational amplifiers (op amps), and the ever-increasing reliability of integrated circuits, electronic controllers are commonly used in industrial applications. In the process industry, electronic controllers have gradually replaced pneumatic controllers. The development is fast moving towards microprocessor-based controllers.

In the following, we give some simple and useful op amp circuit models. In later chapters, these circuits will be used as control logic elements.

The circuit symbol for an op amp is shown in Fig. 2.31a. Two input terminals marked '+' and '–' are shown. These polarity signs refer to the phase relationship between the individual input signals and the output signal; the output signal is in phase with the signal applied to the input pin marked '+', known as the *non-inverting input*, and is in antiphase to the signal applied to the pin marked '–', known as the *inverting input*. The power supply connections are labelled V^+ for the positive voltage and V^- for the negative voltage. The op amp is usually shown as in Fig. 2.31b, without the power supply connections.

Characteristics of an *ideal amplifier* are listed below.

1. Infinite input impedance; an ideal amplifier can be connected to any signal source with no loading effects.
2. Infinite gain.
3. Zero output impedance; an ideal amplifier is capable of driving any load

Copyrighted material

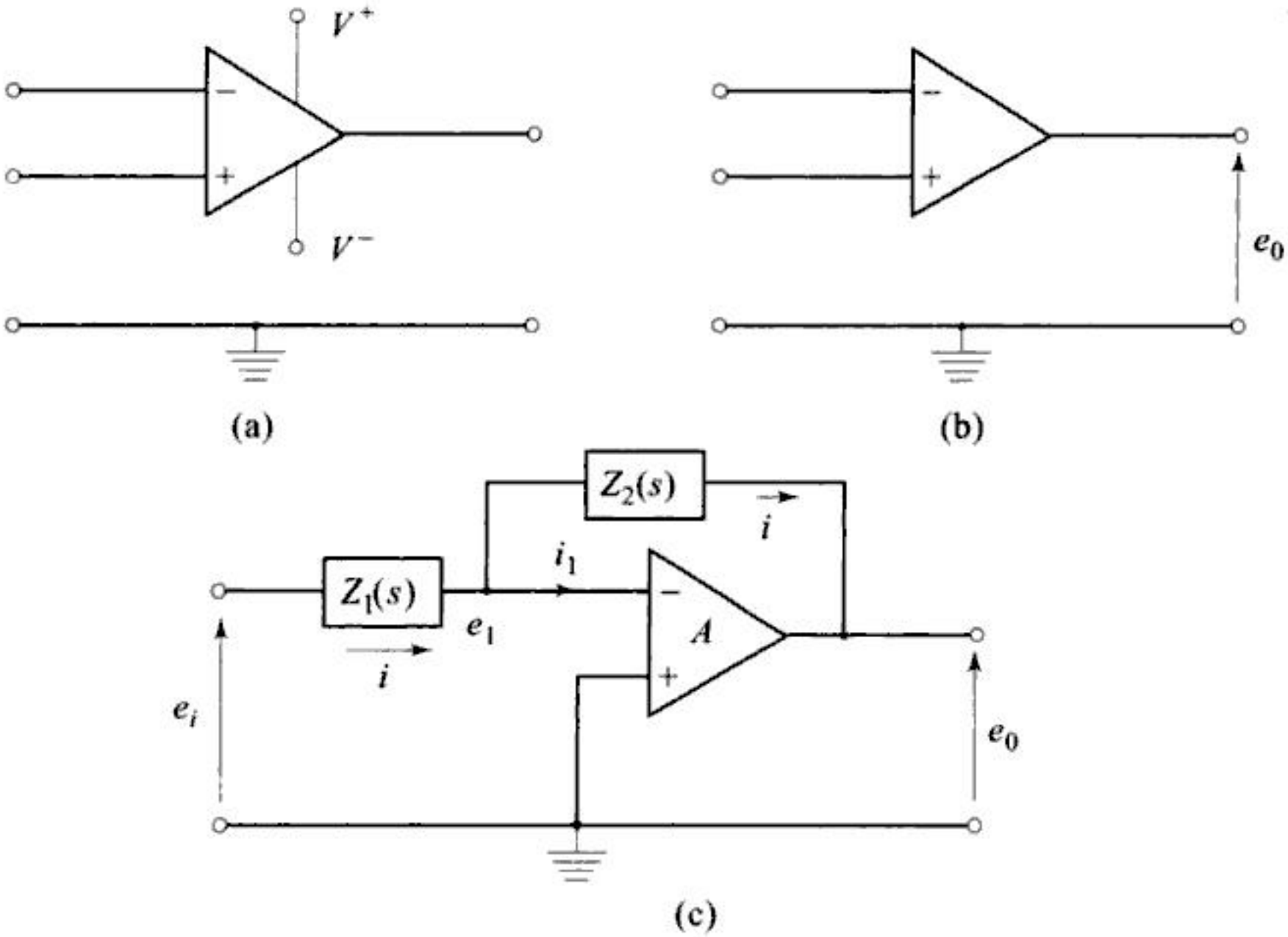


Fig. 2.31 *(a) Circuit symbol of op amp*
(b) Simplified symbol
(c) Op amp circuit building block

4. Infinite bandwidth; an ideal amplifier can amplify any signal frequency.

Op amps approach the first three characteristics closely. The 741 op amp has an input impedance of 6 MΩ, gain of the order of 10^5, and can supply at least 5 mA to a load of 2000 Ω.

The gain of 741 op amp is 10^5 at frequencies between zero (dc) and 10 Hz. Beyond this value of frequency, the gain reduces considerably. Therefore, the op amps approach the ideal amplifier for dc and low frequency signals.

Analysis of op amp circuits becomes simple under the assumption of ideal characteristics. Consider, for example, the circuit of Fig. 2.31c.

1. Since gain A is infinite and output e_0 is finite, the voltage e_1 is virtually zero.
2. Input impedance is infinite, therefore $i_1 = 0$.

For the circuit of Fig. 2.31c (under the second assumption),

$$I(s) = \frac{E_i(s) - E_1(s)}{Z_1(s)} = \frac{E_1(s) - E_0(s)}{Z_2(s)}$$

Since $E_1(s) = 0$ as per first assumption, we get

$$I(s) = \frac{E_i(s)}{Z_1(s)} = -\frac{E_0(s)}{Z_2(s)}$$

Copyrighted material

or
$$\frac{E_0(s)}{E_i(s)} = -\frac{Z_2(s)}{Z_1(s)} \tag{2.81}$$

where

$Z_1(s)$ = impedance connected to the input of the amplifier,

$Z_2(s)$ = impedance connected between output and input of the amplifier.

By choosing proper values of $Z_1(s)$ and $Z_2(s)$, operational amplifiers can be used for various purposes.

Example 2.10

Figure 2.32 shows seven simple op amp circuits. In the following, we derive transfer function for each circuit. From the transfer function models, it will become obvious that these circuits are used for amplification, integration, and differentiation of a given signal.

Figure 2.32a

$$\frac{E_0(s)}{E_i(s)} = \frac{-R_2}{R_1} \tag{2.82a}$$

The circuit is thus a constant gain amplifier. The gain can be made adjustable by using a potentiometer for one of the resistances.

Note the phase relationship between input and output; the circuit of Fig. 2.32a is called an *inverting amplifier*.

Figure 2.32b

A circuit with $R_1 = R_2$ is an *inverter*; it simply inverts the sign of the input voltage without changing its magnitude. It can be used in cascade with other elements to maintain proper sign relations, as shown in Fig. 2.32b. For this circuit,

$$\frac{E_0(s)}{E_i(s)} = \frac{R_2}{R_1} \tag{2.82b}$$

Figure 2.32c

$$\frac{E_0(s)}{E_i(s)} = -\frac{1/sC}{R} = -\frac{1}{RCs} \tag{2.83a}$$

The circuit is thus an integrator.

Equation (2.83a) is true if the initial voltage on the capacitor is zero. Inverse Laplace transformation of this equation gives

$$e_0(t) = -\frac{1}{RC}\int_0^t e_i(\tau)d\tau \tag{2.83b}$$

Figure 2.32d

$$\frac{E_0(s)}{E_i(s)} = -\frac{R_2 + 1/sC}{R_1} = -\frac{R_2}{R_1} - \frac{1}{R_1Cs} \tag{2.84a}$$

Copyrighted material



You have either reached a page that is unavailable for viewing or reached your viewing limit for this book.

$$e_0(t) = -\frac{R_2}{R_1}e_i(t) - \frac{1}{R_1 C}\int_0^t e_i(\tau)d\tau \qquad (2.84b)$$

The circuit thus processes the input signal by 'proportional + integral' action.

Figure 2.32e

$$\frac{E_0(s)}{E_i(s)} = -\frac{R}{1/sC} = -RCs \qquad (2.85a)$$

$$e_0(t) = -RC\frac{de_i(t)}{dt} \qquad (2.85b)$$

The circuit is thus a differentiator.

Figure 2.32f

$$\frac{E_0(s)}{E_i(s)} = -\frac{R_2}{\dfrac{R_1(1/sC)}{R_1 + 1/sC}} = -\frac{R_2}{R_1}(R_1Cs + 1) \qquad (2.86a)$$

$$e_0(t) = -\frac{R_2}{R_1}e_i(t) - R_2C\frac{de_i(t)}{dt} \qquad (2.86b)$$

The circuit thus processes the input signal by 'proportional + derivative' action.

Figure 2.32g

$$\frac{E_0(s)}{E_i(s)} = -\frac{R_2 + 1/sC_2}{\dfrac{R_1(1/sC_1)}{R_1 + 1/sC_1}} = -\frac{(R_2C_2s + 1)(R_1C_1s + 1)}{R_1C_2s}$$

$$= -\left[\frac{R_2C_2R_1C_1s^2 + R_2C_2s + R_1C_1s + 1}{R_1C_2s}\right]$$

$$= -\left[\frac{R_1C_1 + R_2C_2}{R_1C_2} + \frac{1}{R_1C_2s} + R_2C_1s\right] \qquad (2.87a)$$

$$e_0(t) = -\frac{R_1C_1 + R_2C_2}{R_1C_2}e_i(t) - \frac{1}{R_1C_2}\int_0^t e_i(\tau)d\tau - R_2C_1\frac{de_i(t)}{dt} \qquad (2.87b)$$

The circuit thus processes the input signal by 'proportional + integral + derivative' action.

Simulation with an Analog Computer

Operational amplifiers can be used to solve the dynamic model of a physical system. The essence of the technique is to construct an op amp circuit whose governing equations are the same as those of the system under study except for

Copyrighted material

magnitude and time-scale factors. The resulting circuit is said to be an *analog computer*.

Analog computation has lost some of its importance because of the increasing availability of digital computers. However, it still provides an excellent means of developing control system prototypes.

2.10 MODELS OF THERMAL SYSTEMS

The basic requirement for the representation of thermal systems by lumped-parameter models is that the temperature of the medium be considered uniform. When the medium is small, this approximation is valid. Also when the medium consists of a body of air or liquid, the temperature can be considered uniform if there is perfect mixing of the fluid. When a single temperature does not accurately represent the thermal state of the entire medium, i.e., there is complex temperature distribution throughout the medium, the problem becomes one of the distributed parameters, requiring the use of partial differential equations. Here, however, in order to simplify the analysis, uniformity of temperature is assumed and thereby the systems are represented by lumped-parameter models.

Heat flow rate h (through variable; analogous to current), and temperature θ (across variable; analogous to voltage) are the commonly used characterizing variables of thermal systems for the purpose of modelling. Thermal resistance and capacitance are the two basic elements. The resistance that we have encountered so far has been an element that dissipates energy and converts it into heat (damper in mechanical systems, and resistor in electrical systems). Thermal resistance is not an element that dissipates energy; it is a consequence of the fact that a temperature difference is required to cause heat to flow. Thermal capacitance is an energy storage element; a parameter representing internal thermal energy (determined by molecular activity) of the substance.

Heat-Transfer Systems without Carrier Fluids

The flow of heat through a solid material occurs by conduction. The basic equation for one-dimensional heat conduction through a plane wall of surface area $A(\text{m}^2)$ and thickness $l(\text{m})$ is

$$h = \sigma A\left(\frac{\theta_1 - \theta_2}{l}\right) \tag{2.88}$$

where h = heat flow rate, Joules/sec;

$\Delta\theta = \theta_1 - \theta_2$ = temperature drop along the direction of heat flow, °C; and

σ = thermal conductivity of the material, Joules/(°C) (m) (sec).

Many solids interface with fluids. A simple model for convective heat transfer mechanism at solid–fluid interface is given by the relation

$$h = UA(\theta_S - \theta_F) \tag{2.89}$$

where h = heat flow rate, Joules/sec (negative sign of h will indicate flow of heat from fluid to solid);

Copyrighted material

A = area of the surface (solid–fluid interface), m^2;
θ_S = temperature of the solid, °C;
θ_F = temperature of the fluid, °C; and
U = film coefficient of the solid–fluid interface, Joules/(m^2) (°C) (sec).

Using Eqns (2.88)–(2.89), we define *thermal resistance* as follows:

$$R_{CD} = \text{conductive thermal resistance} = \frac{l}{\sigma A}, \text{ °C/(Joules/sec)} \qquad (2.90a)$$

$$R_{CV} = \text{convective thermal resistance} = \frac{1}{UA}, \text{ °C/(Joules/sec)} \qquad (2.90b)$$

The rate of heat storage (in the form of internal energy) in a substance is governed by the relation

$$h_1 - h_2 = Mc\frac{d\theta}{dt} \qquad (2.91)$$

where h_1 = heat-input rate, Joules/sec;
h_2 = heat-output rate, Joules/sec;
M = mass of the substance, kg;
c = specific heat of the substance, Joules/(kg) (°C); and
θ = temperature of the substance, °C.

Using Eqn. (2.91), we define *thermal capacitance* as follows:

$$C = Mc, \text{ Joules/°C} \qquad (2.92)$$

Heat-Transfer Systems with Carrier Fluids

When large quantities of heat are to be transported over considerable distances, it can be best done by the flowing fluid as a carrier of thermal energy. In such systems, there exist many energy storage effects, in addition to storage of energy in the form of internal thermal energy—storage in a gravity field, storage due to compressibility of the fluid, storage due to change in the volume of the container, storage due to inertia of the fluid flowing through a pipe, etc.

We first consider the case where the changes in internal thermal energies outweigh the changes in the mechanical energies associated with the fluid. The extreme opposite case will be taken up in the next section where it will be assumed that the changes in mechanical energies outweigh the changes in internal thermal energy. There are many important practical examples where none of these two approximations is sufficiently accurate for dynamic modelling. These are characterized by strong mechanical–thermal interactions. Fuel flow in turbines and rockets are specific examples. These areas are somewhat specialized; we shall give examples from only the two simple categories mentioned above.

In the following we define important parameters of heat-transfer systems with carrier fluids, under the assumption that the changes in the internal thermal energy outweigh the changes in mechanical energies.

Copyrighted material

Thermal capacitance of the carrier fluid is defined as follows:

$$C = V\rho c, \text{ Joules/°C} \tag{2.93}$$

where

V = volume of the fluid chamber, m^3;
ρ = fluid density, kg/m^3; and
c = specific heat of the fluid, Joules/(kg) (°C).

Carrier fluid-flow into a chamber is a source of thermal-energy input. Also, the outflowing fluid takes away thermal energy from the chamber. Carrier flow heat-input rate and heat-output rate depend upon the temperatures of the inflowing and outflowing fluids, respectively.

Let θ_i (°C) be the temperature of the inflowing fluid into a chamber and θ_0(°C) be the temperature of the outflowing fluid. Flow rate $Q(m^3/sec)$ and density ρ (kg/m^3) are assumed constant.

Heat-input rate, $h_1 = Q\rho c\theta_i$, Joules/sec

Heat-output rate, $h_2 = Q\rho c\theta_0$, Joules/sec

Net change in transportation of heat is given by

$$h_1 - h_2 = Q\rho c(\theta_i - \theta_0) \tag{2.94}$$

From this equation, we define the *thermal resistance* due to carrier fluid-flow as

$$R = \frac{1}{Q\rho c}, \text{ °C/(Joules/sec)} \tag{2.95}$$

Table 2.4 summarizes the metric system of units for thermal systems.

Table 2.4 *Thermal symbols and units*

Quantity	*Metric units*
Rate of heat flow (h)	Joules/sec
Temperature (θ)	°C
Thermal capacitance (C)	Joules/°C
Thermal resistance (R)	°C/(Joules/sec)

Example 2.11

As an illustration of a heat-transfer system without carrier fluids, consider the room-heating system shown in Fig. 2.33. The heat released for heating the room is the latent heat of condensation.

To obtain a lumped-parameter model for the system, assume that the state of air in the room can be described by a single temperature. Definitions of system parameters and variables are as follows:

Copyrighted material

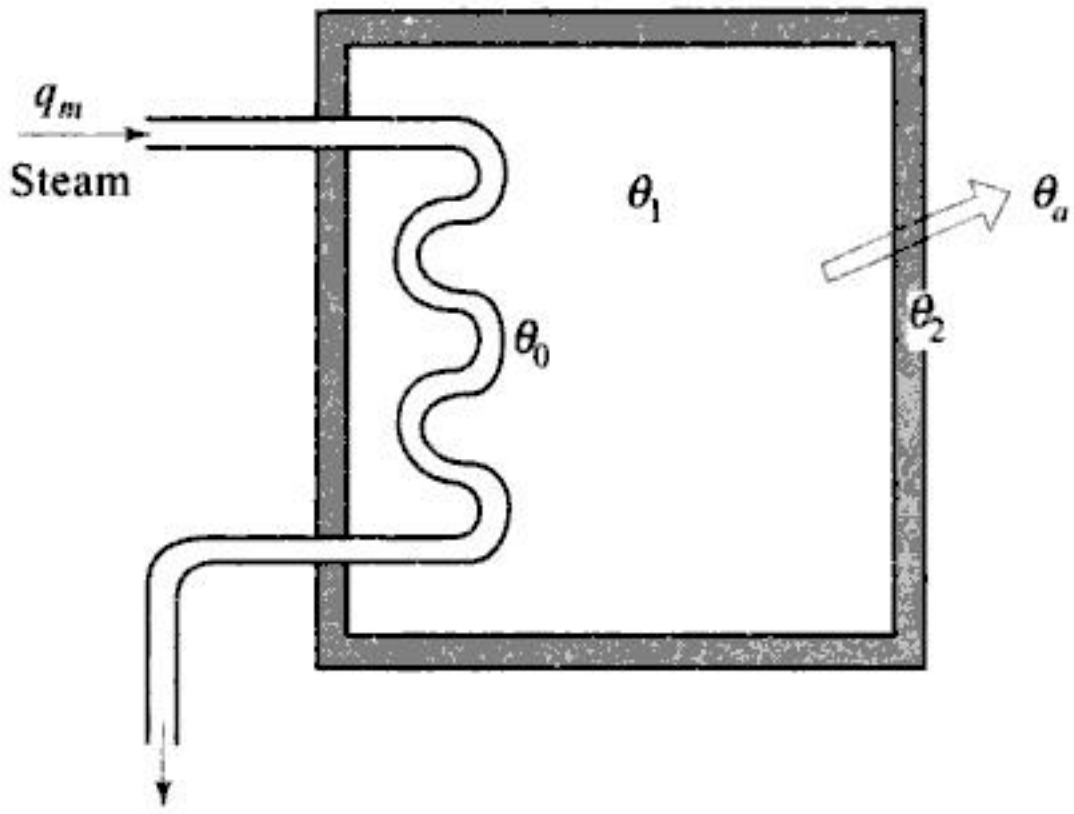


Fig. 2.33 *A room-heating system*

$\overline{Q}_m$ = steady-state steam flow rate, kg/sec

λ = latent heat of condensation, Joules/kg

C_0 = thermal capacitance of the radiator, Joules/°C

C_1 = thermal capacitance of air in the room, Joules/°C

C_2 = thermal capacitance of the room walls, Joules/°C

R_0 = convective thermal resistance for heat transfer at the solid–fluid interface bet *v*een the radiator and the room-air, °C/(Joules/sec)

R_1 = $R_{CV} + R_{CD}$; R_{CV} is convective thermal resistance for heat transfer at the fluid–solid interface between the fluid and inside of the room walls; R_{CD} is conductive thermal resistance for conduction through the room walls, °C/(Joules/sec).

R_2 = convective thermal resistance for heat transfer between the outside of room walls and its surroundings, °C/(Joules/sec).

$\theta_0, \theta_1, \theta_2$: perturbations in temperatures of the radiator, the room-air, and the room-walls respectively from the nominal point of operation $\{\overline{\theta}_0, \overline{\theta}_1, \overline{\theta}_2, \}$, in response to perturbation $q_m(t)$ in the steam flow rate.

θ_a: perturbation in ambient temperature; it is uncontrolled and hence is the disturbance input for the process.

Heat-balance equation for the radiator is

$$\underbrace{C_0 \frac{d\theta_0(t)}{dt}}_{\text{Rate of heat storage}} = \underbrace{q_m(t)\lambda}_{\text{Rate of heat input}} - \underbrace{\frac{\theta_0(t) - \theta_1(t)}{R_0}}_{\text{Rate of heat output}} \tag{2.96a}$$

Heat-balance equation for the room-air is

$$C_1 \frac{d\theta_1(t)}{dt} = \frac{\theta_0(t) - \theta_1(t)}{R_0} - \frac{\theta_1(t) - \theta_2(t)}{R_1} \tag{2.96b}$$

Copyrighted material



You have either reached a page that is unavailable for viewing or reached your viewing limit for this book.



You have either reached a page that is unavailable for viewing or reached your viewing limit for this book.

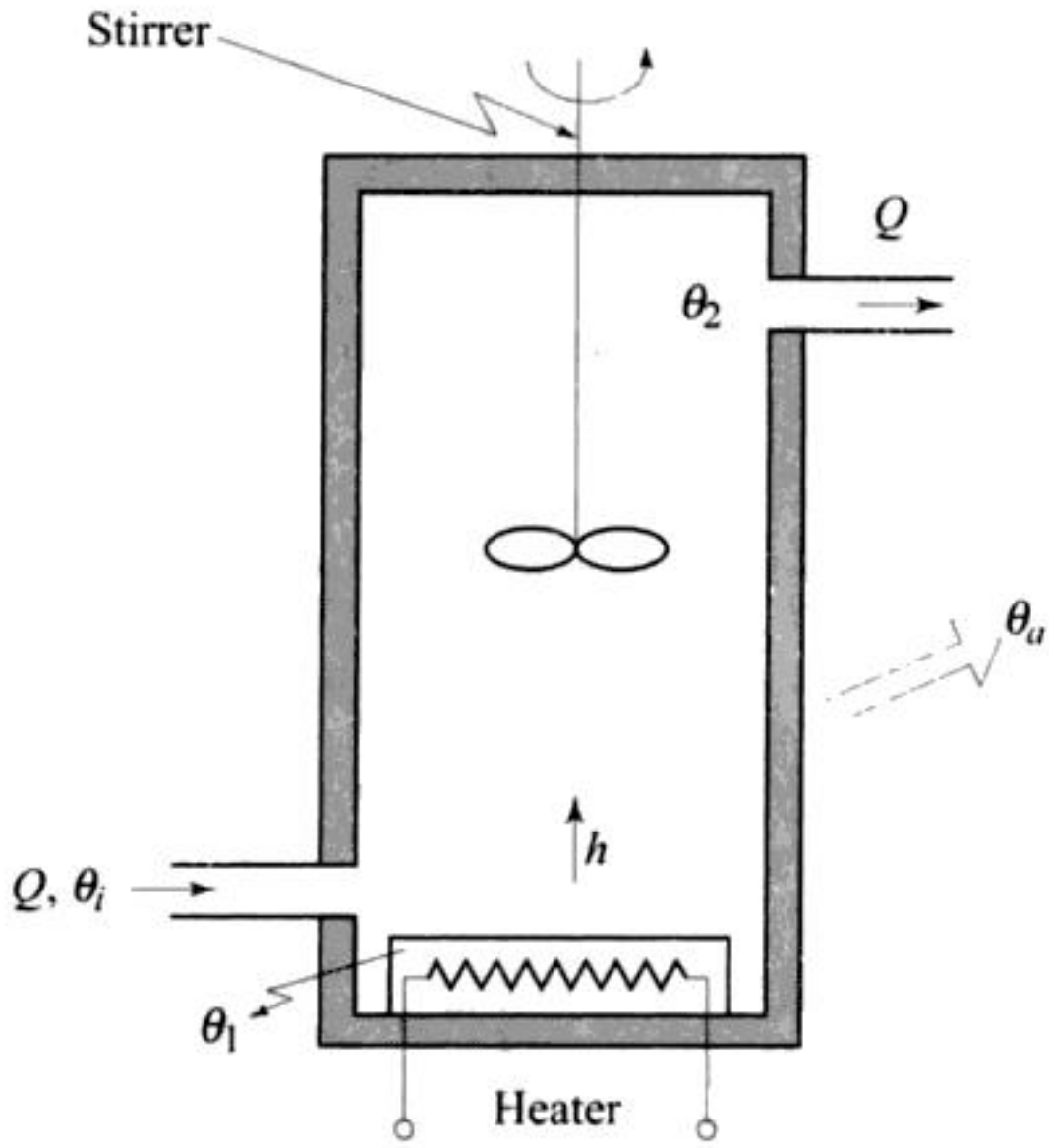


Fig. 2.35 *Continuously stirred tank heater*

R_2 = thermal resistance of the carrier fluid, °C/(Joules/sec)
R_3 = convective thermal resistance for heat transfer at the tank wall–air interface, °C/(Joules/sec)
Q = flow rate of liquid (constant), m^3/sec
θ_1, θ_2 : perturbations in temperatures of heater-mass, and liquid in the tank respectively from the nominal point of operation, in response to perturbation h (Joules/sec) in the heat flow rate.
θ_i, θ_a : perturbations in inflowing liquid and ambient temperatures respectively. These perturbations are uncontrolled and hence are disturbance inputs for the process.

The following assumptions are made for simplified analysis.

1. The liquid inflow and outflow rates for the tank are equal so that the liquid level in the tank is maintained constant during the operation.
2. The tank is kept at a uniform temperature by perfect mixing with the help of a stirrer. Thus, a single temperature is used to describe the thermal state of the entire liquid. The temperature inside the tank = temperature of the outflowing liquid.
3. The heat storage capacity of the tank walls is negligible.

The heat balance equation for the heater:

$$C_1 \frac{d\theta_1(t)}{dt} = h(t) - \frac{\theta_1(t) - \theta_2(t)}{R_1} \qquad (2.100a)$$

The heat balance equation for the tank liquid:

Copyrighted material



You have either reached a page that is unavailable for viewing or reached your viewing limit for this book.



You have either reached a page that is unavailable for viewing or reached your viewing limit for this book.



You have either reached a page that is unavailable for viewing or reached your viewing limit for this book.

$$\overline{Q}_i = \overline{Q}\,;\ \overline{H} = \text{constant}$$

The hydrostatic pressure due to height $\overline{H}$ is

$$\overline{P} = \rho g \overline{H}\,,\ \text{Newtons/m}^2$$

where ρ = density of the liquid, kg/m^3; and
g = acceleration due to gravity, m/sec^2.

The standard unit of pressure is *pascal* (Pa): 1 Pa of pressure is defined as the force of 1 Newton applied over an area of 1 m^2. Industrial pressures are often measured in pounds per square inch (psi). Pascals can be obtained by multiplying psi by 6.8948×10^3.

The atmospheric pressure is 14.70 psi (101 kPa) at sea level. *Gauge pressure* is referenced to atmospheric pressure, and *absolute pressure* is referenced to perfect vacuum. Gauge pressure can be obtained by subtracting the ambient atmospheric value from the absolute value. Likewise, absolute pressure can be found by adding the ambient pressure to the gauge pressure. Letters g or a may be suffixed to the pressure units to clearly denote gauge pressure or absolute pressure (e.g., psig, psia). The pressure variables in our discussion represent gauge pressures. The atmospheric pressure has been taken as zero gauge pressure.

In the system of Fig. 2.37, the disturbance $q_i(t)$ in the inflow rate will change the height of the liquid in the tank by $h(t)$, the pressure across the pipe by $p(t)$ and the outflow rate by $q(t)$. The volume-balance equation becomes

$$\overline{Q}_i + q_i(t) = A\frac{d}{dt}(\overline{H} + h(t)) + \overline{Q} + q(t)$$

Perturbation from steady-state is described by the equation

$$q_i(t) = A\frac{dh(t)}{dt} + q(t) \tag{2.103}$$

Since

$$p(t) = \rho g h(t), \tag{2.104}$$

it follows that

$$q_i(t) - q(t) = \frac{A}{\rho g}\frac{dp(t)}{dt} \tag{2.105}$$

The *hydraulic capacitance* due to storage in gravity field is defined as

$$C = \frac{A}{\rho g},\ \text{cub-m/(Newtons/m}^2) \tag{2.106}$$

In terms of hydraulic capacitance, Eqn. (2.105) may be written as

$$q_i(t) - q(t) = C\frac{dp(t)}{dt} \tag{2.107}$$

With reference to Fig. 2.37, the outflow $q(t)$ should obviously depend on $p(t)$ somehow. The greater the pressure $p(t)$, the greater the outflow rate. The

Copyrighted material

concept of hydraulic resistance introduced below will help in establishing a relationship between $q(t)$ and $p(t)$.

Liquid trying to flow out of a container, as in Fig. 2.37, can meet with resistance in several ways. If the outlet is simply a hole, the liquid meets resistance merely because it cannot easily flow through the hole. This is known as *orifice flow*. If the outlet is a pipe, the friction between the liquid and the pipe walls produces resistance to flow. The presence of a component such as valve in the pipe increases the resistance. Components such as elbow bends, couplings of pipes of different diameters, etc., also resist the flow.

Symbolic representation of an obstruction to flow is shown in Fig. 2.38a. A controllable obstruction, such as a hydraulic valve with an adjustable opening, may be represented as in Fig. 2.38b. The upstream pressure is P_1 and the back pressure achieved downstream is P_2. The flow rate Q depends on the pressure difference $\Delta P = (P_1 - P_2)$. This relationship is usually nonlinear; it can be obtained either experimentally or analytically.

Suppose that an experimental curve relating the flow rate Q to the pressure drop ΔP is available for an obstruction. A typical curve is shown in Fig. 2.38c.

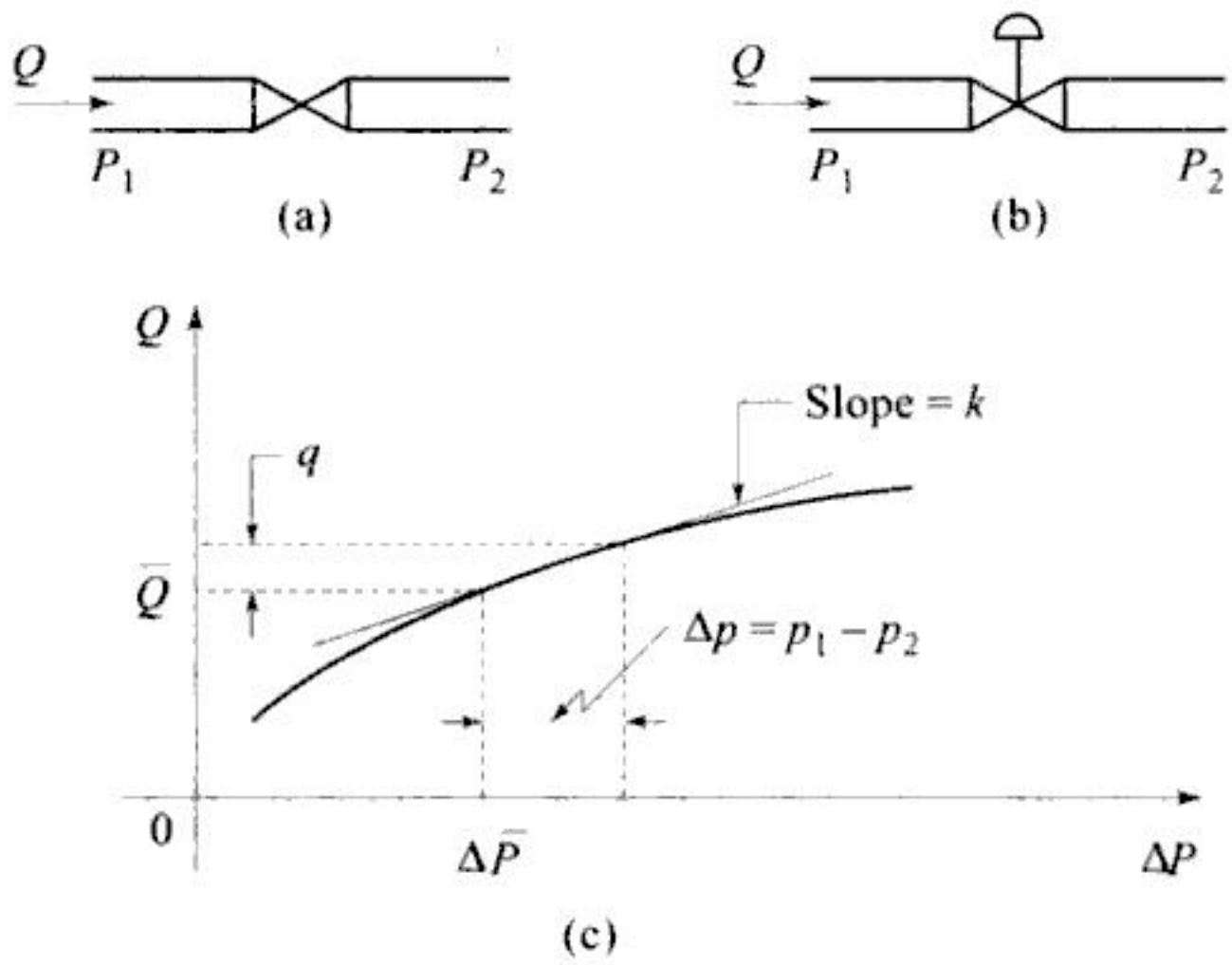


Fig. 2.38 *(a) Flow obstruction; (b) Adjustable obstruction; (c) Steady-state operating point*

Let the slope of the curve at the equilibrium point $(\bar{Q}, \Delta\bar{P})$ be denoted by k. Then, for a small deviation from equilibrium, we obtain

$$q(t) = k\Delta p(t) \tag{2.108}$$

From this equation, *hydraulic resistance* is defined as

$$R = \frac{1}{k}, \left(\frac{\text{Newton/m}^2}{\text{m}^3/\text{sec}} \right) \tag{2.109}$$

Copyrighted material

The value of R depends on the steady-state condition chosen for linearization.

When an equation relating the flow to the pressure drop is available, the resistance can be obtained analytically. The following flow-pressure relationship models the orifice flow.

$$Q = C_0 A_0 \sqrt{\frac{2(P_1 - P_2)}{\rho}} \tag{2.110}$$

where

A_0 = orifice area;
C_0 = the experimentally determined number, called the orifice coefficient;
ρ = density of the fluid;
$P_1 - P_2 = \Delta P$ = pressure difference across the orifice.

The orifice coefficient is dependent on the geometric configuration of the orifice and to some extent upon the flow velocity. For sharp-edged orifices, it normally ranges from 0.6 to 0.8.

For incompressible fluids, ρ is constant and therefore Q is a function of pressure difference ΔP:

$$Q = f(\Delta P) \tag{2.111a}$$

This equation may be linearized about an equilibrium point using Taylor series expansion (refer Eqns (2.6)).

The flow rate through a valve with adjustable opening is a function of both the pressure difference ΔP across the valve and the adjustable area A_0, or equivalently the adjustable valve opening x_v:

$$Q = f(x_v, \Delta P) \tag{2.111b}$$

Table 2.5 summarizes the metric system of units for hydraulic systems.

Table 2.5 *Hydraulic symbols and units*

Quantity	*Metric units*
Volume flow rate(q)	m^3/sec
Pressure (p)	Newtons/m^2
Hydraulic capacitance (C)	m^3/(Newtons/m^2)
Hydraulic resistance (R)	$\frac{\text{Newtons}/\text{m}^2}{\text{m}^3/\text{sec}}$

▲▲

The concepts of hydraulic capacitance and hydraulic resistance will now be used to develop models of hydraulic systems. In the following, we develop a complete model for a liquid-level system. Models of hydraulic devices for controlling forces and motions will be developed in the next chapter.

Copyrighted material



You have either reached a page that is unavailable for viewing or reached your viewing limit for this book.



You have either reached a page that is unavailable for viewing or reached your viewing limit for this book.



You have either reached a page that is unavailable for viewing or reached your viewing limit for this book.



You have either reached a page that is unavailable for viewing or reached your viewing limit for this book.



You have either reached a page that is unavailable for viewing or reached your viewing limit for this book.

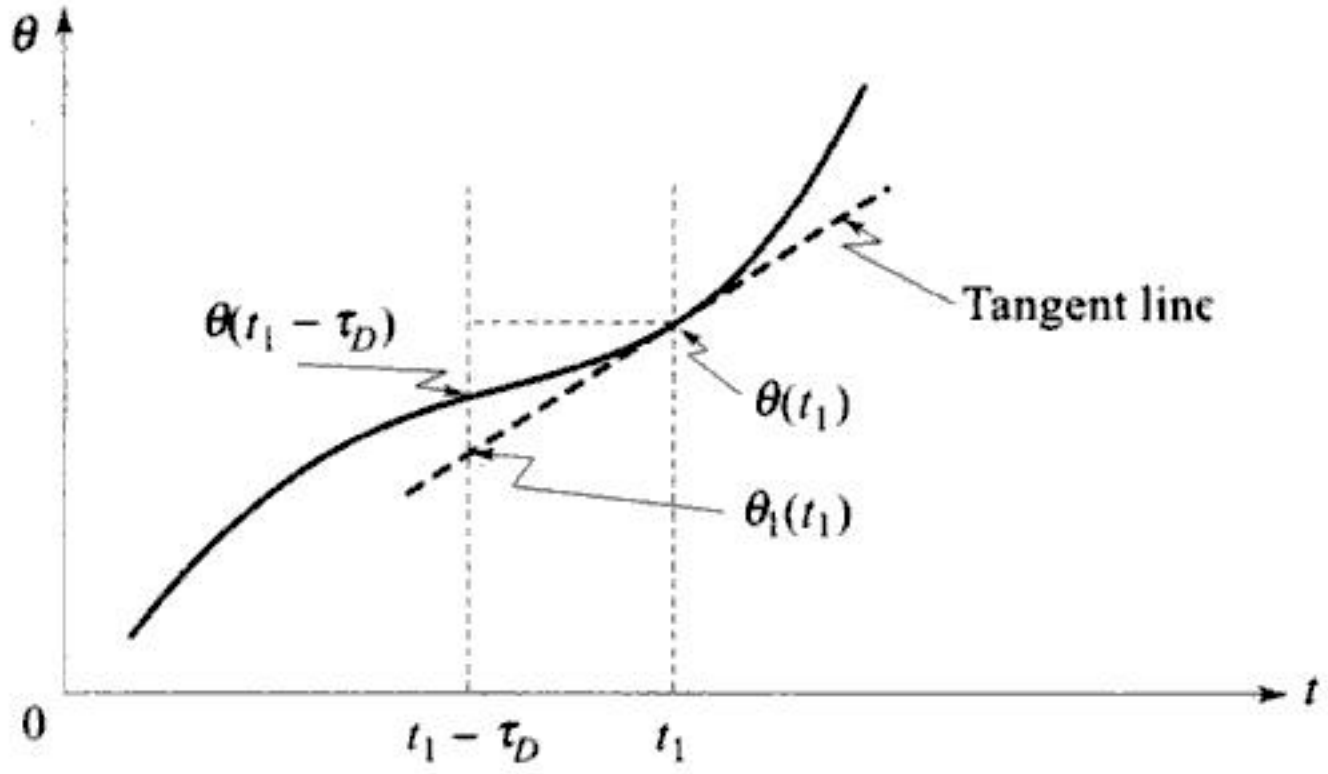


Fig. 2.43 *Dead-time approximation*

$$\theta_1(t) \equiv \theta(t) - \tau_D \frac{d\theta(t)}{dt}$$

or
$$\theta_1(s) \equiv (1 - \tau_D s)\theta(s)$$

With this approximation, the transfer function of dead-time element becomes

$$\frac{\theta_1(s)}{\theta(s)} = (1 - \tau_D s) \tag{2.117}$$

The accuracy of this approximation depends on the dead-time being sufficiently small relative to the rate of change of the slope of θ. If θ were a ramp function (constant slope), the approximation would be perfect for any value of τ_D. When the slope of θ varies rapidly, only small τ_D will give a good approximation.

The Pade approximants [77] provide a family of approximations of increasing accuracy and complexity. These approximations are based on frequency-response comparisons; the simpiest one being

$$\frac{\theta_1(s)}{\theta(s)} = \frac{1 - \frac{\tau_D}{2} s}{1 + \frac{\tau_D}{2} s} \tag{2.118}$$

▲▲

In control systems, we frequently come across situations where there is unavoidable time delay in the signal flow between sub-systems or components. The delay usually results from the physical separation of the components and typically occurs as a delay between the change in the manipulated variable and its effect on the plant, or a delay in the measurement of the output. Dead-time elements are needed for accurate modelling of such systems. Digital computers in control systems also introduce the necessity of dead-time elements to model the computational delay inherent in these systems.

Copyrighted material



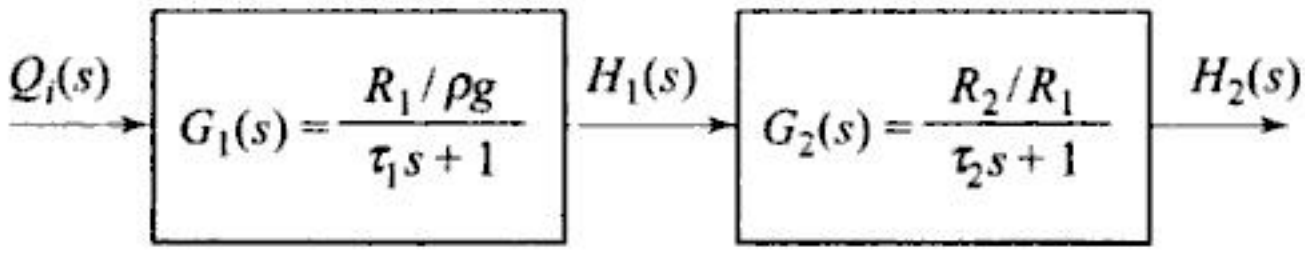
You have either reached a page that is unavailable for viewing or reached your viewing limit for this book.



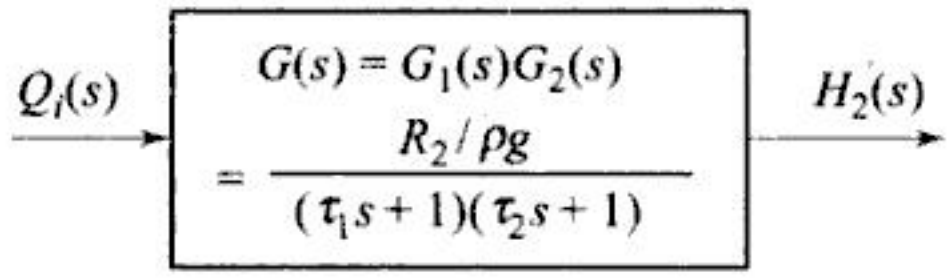
You have either reached a page that is unavailable for viewing or reached your viewing limit for this book.

by multiplying together the individual transfer functions. The block diagram of Fig. 2.45a can be reduced to that of Fig. 2.45b. The overall transfer function of the two-tank system of Fig. 2.44 is given by

$$\frac{H_2(s)}{Q_i(s)} = \frac{R_2/\rho g}{\tau_1\tau_2 s^2 + (\tau_1 + \tau_2)s + 1} \tag{2.124}$$



(a)



(b)

Fig. 2.45 *Block diagram models of the system of Fig. 2.44*

We now connect the two tanks as shown in Fig. 2.46. Loading is now present and Eqn. (2.124) is not a valid transfer function model for this system as explained below.

The flow-balance equation for tank 1 is

$$q_i(t) = C_1\frac{dp_1(t)}{dt} + q_1(t)$$

Similarly, for tank 2

$$q_1(t) = C_2\frac{dp_2(t)}{dt} + q(t)$$

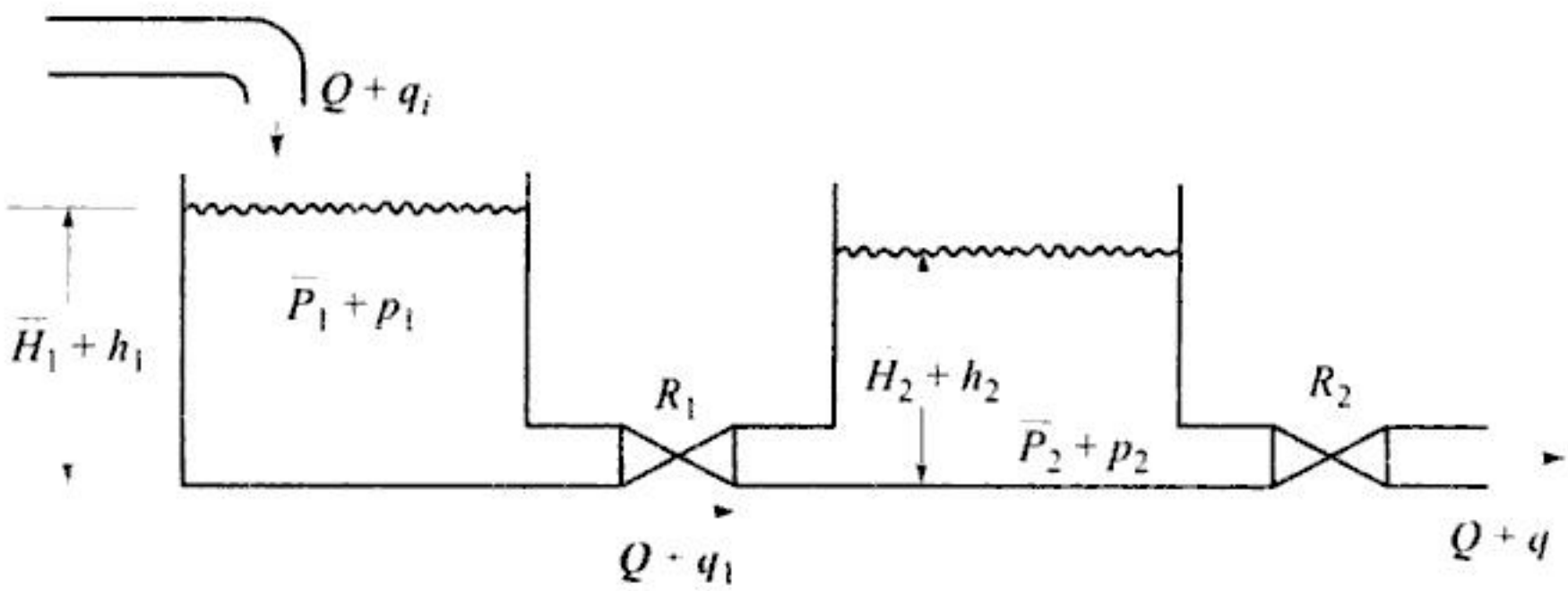


Fig. 2.46 *Loading effect in a two-tank system*

Copyrighted material

The flow $q_1(t)$ through resistance R_1 is governed by the equation

$$q_1(t) = \frac{p_1(t) - p_2(t)}{R_1}$$

and the flow $q(t)$ through resistance R_2 is given by

$$q(t) = \frac{p_2(t)}{R_2}$$

If $h_2(t)$ is considered the output and $q_i(t)$ the input, the transfer function of the system becomes

$$\frac{H_2(s)}{Q_i(s)} = \frac{R_2/\rho g}{\tau_1\tau_2 s^2 + \left(\tau_1 + \tau_2 + \frac{R_2}{R_1}\tau_1\right)s + 1} \tag{2.125}$$

Note that the transfer function is not equal to that given by Eqn. (2.124). The difference is due to the presence of the loading effect; the level $h_2(t)$ of tank 2 now affects the level $h_1(t)$ of tank 1. The degree to which the overall transfer function is modified from the product of the individual transfer functions depends upon the amount of loading.

▲▲

In general, loading effects occur because while analysing an isolated sub-system, we assume that no power is being withdrawn at its output location. When we later decide to attach another sub-system to the output of the first, this second sub-system does withdraw some power violating our earlier assumption and thereby invalidating the analysis based on this assumption.

One way to reduce loading effects to negligible proportions is to interpose *buffer amplifiers* between the sub-systems. These devices, which may be electrical, hydraulic, pneumatic, or the like, to suit the physical nature of the connected sub-systems, have their own internal power supplies and can thus supply power to a 'downstream' sub-system without withdrawing their power from the 'upstream' sub-system. That is, such amplifiers have high input impedance and low output impedance (op amp is one example).

When we model chains of sub-systems by simple multiplication of their individual transfer functions later in the text, the assumption will always be that the interconnection of various sub-systems is non-loading; loading effects are either not present, have been proven negligible, or have been made negligible by use of buffer amplifiers.

Review Examples

Review Example 2.1

Consider a first-order system described by the transfer function

$$\frac{Y(s)}{R(s)} = \frac{K}{\tau s + 1}$$

Copyrighted material

where τ is the time-constant of the system.

For a unit ramp input $r(t) = t\mu(t)$, we have

$$R(s) = \frac{1}{s^2}$$

Therefore, the unit ramp response is

$$Y(s) = \frac{K}{s^2(\tau s + 1)} = K\left[\frac{1}{s^2} - \frac{\tau}{s} + \frac{\tau^2}{\tau s + 1}\right]$$

$$y(t) = K(t - \tau + \tau e^{-t/\tau})$$

The term $K\tau e^{-t/\tau}$ is the transient response term which decays to zero with increasing time. Its rate of decay is dictated by the time-constant τ. The steady-state component of the response to unit ramp input $r(t) = t$ is

$$y_{ss} = K(t - \tau),$$

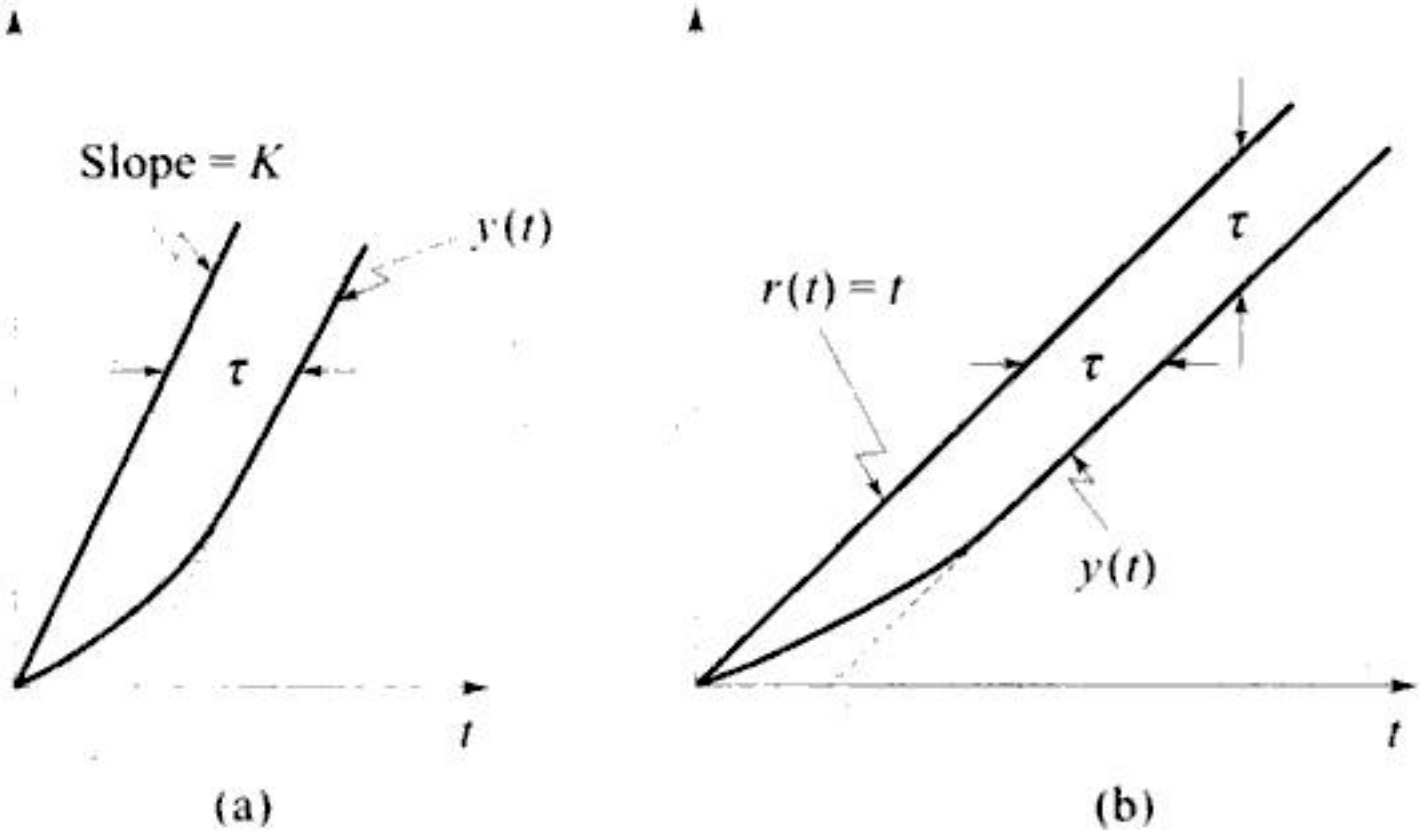
which is also a ramp function.

Note that the steady-state ramp output is nothing but Kt delayed by τ as shown in Fig. 2.47a. This phenomenon of steady-state lag in ramp response gives another interpretation of the time-constant of first-order system.

For $K = 1$, the steady-state error (Fig. 2.47b)

$$e_{ss} = r(t) - y_{ss} = \tau$$

If K does not equal 1, the response diverges from the unit ramp input as t increases.



(a) (b)

Fig. 2.47 *Ramp response of first-order systems*

Review Example 2.2

Consider a second-order system described by the transfer function

$$\frac{Y(s)}{R(s)} = \frac{K}{\frac{1}{\omega_n^2}s^2 + \frac{2\zeta}{\omega_n}s + 1}$$

Copyrighted material

where ω_n = undamped natural frequency
ζ = damping ratio

For an underdamped system, $0 < \zeta < 1$.

Assume that this system is excited by a unit ramp input

$$R(s) = \frac{1}{s^2}$$

This gives

$$Y(s) = \frac{K\omega_n^2}{s^2\left(s^2 + 2\zeta\omega_n s + \omega_n^2\right)}$$

$$= K\left[\frac{1}{s^2} - \frac{2\zeta/\omega_n}{s} + \frac{2\zeta}{\omega_n}\frac{s + \zeta\omega_n}{(s + \zeta\omega_n)^2 + \omega_d^2} + \frac{2\zeta^2 - 1}{(s + \zeta\omega_n)^2 + \omega_d^2}\right]$$

where $\omega_d = \omega_n\sqrt{1 - \zeta^2}$

Using the table of transform pairs given in Appendix A, we get

$$y(t) = K\left[t - \frac{2\zeta}{\omega_n} + \frac{2\zeta}{\omega_n}e^{-\zeta\omega_n t}\cos\omega_d t + \frac{(2\zeta^2 - 1)}{\omega_d}e^{-\zeta\omega_n t}\sin\omega_d t\right]$$

$$= K\left[t - \frac{2\zeta}{\omega_n} + \frac{e^{-\zeta\omega_n t}}{\omega_d}\left\{2\zeta\sqrt{1 - \zeta^2}\cos\omega_d t + (2\zeta^2 - 1)\sin\omega_d t\right\}\right]$$

$$= Kt - \frac{2\zeta}{\omega_n}K + \frac{Ke^{-\zeta\omega_n t}}{\omega_n\sqrt{1 - \zeta^2}}\sin\left(\omega_d t + 2\tan^{-1}\frac{\sqrt{1 - \zeta^2}}{\zeta}\right) \qquad (2.126)$$

The last term in this expression is the transient response term, which decays to zero with increasing time. Its rate of decay is dictated by the time-constant $1/\zeta\omega_n$. The steady-state component of the response to unit ramp input $r(t) = t$ is

$$y_{ss} = K\left(t - \frac{2\zeta}{\omega_n}\right) \qquad (2.127)$$

which is also a ramp function.

Note that the steady-state ramp output is nothing but Kt delayed by $2\zeta/\omega_n$ as shown in Fig. 2.48a. The damped oscillations contributed by the transient component of the response are centred on the ramp.

For $K = 1$, the steady-state error (Fig. 2.48b)

$$e_{ss} = r(t) - y_{ss} = \frac{2\zeta}{\omega_n} \qquad (2.128)$$

If K does not equal 1, the response diverges from the unit ramp input as t increases.

Copyrighted material

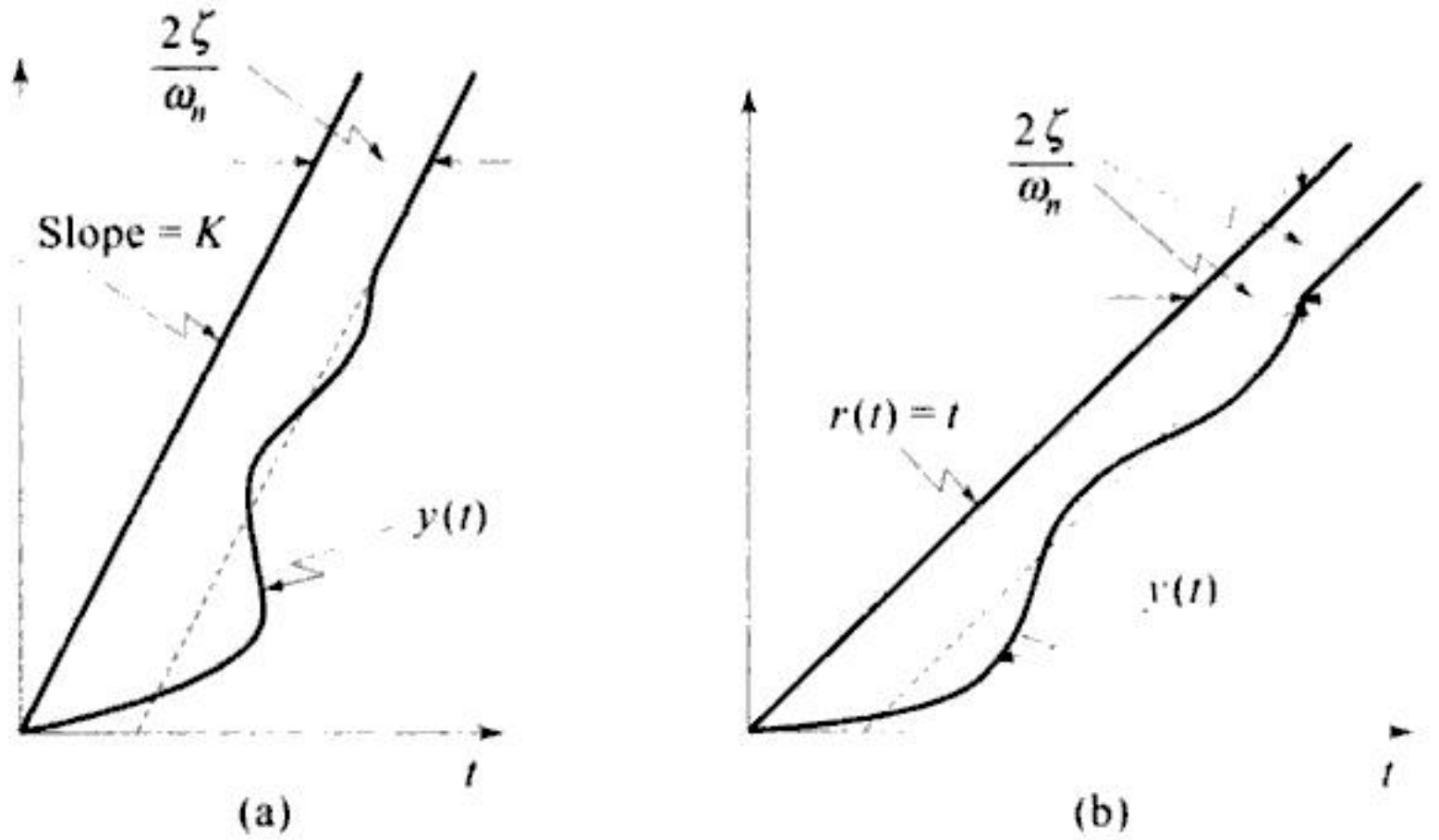


Fig. 2.48 *Ramp response of second-order underdamped systems*

By similar analysis, it can easily be established that the critically damped and overdamped responses ($\zeta \geq 1$) are characterized by the exponential rise toward the steady-state ramp output $K\left(t - \frac{2\zeta}{\omega_n}\right)$.

Review Example 2.3

A common cause of sinusoidal forcing in machines is the imbalance that exists to some extent in every rotating machine. The imbalance is caused by the fact that the centre of mass of the rotating part does not coincide with the centre of rotation. Figure 2.49 shows a situation where the main mass of a machine is constrained to have only vertical motion. The rotating mass m is lumped at its

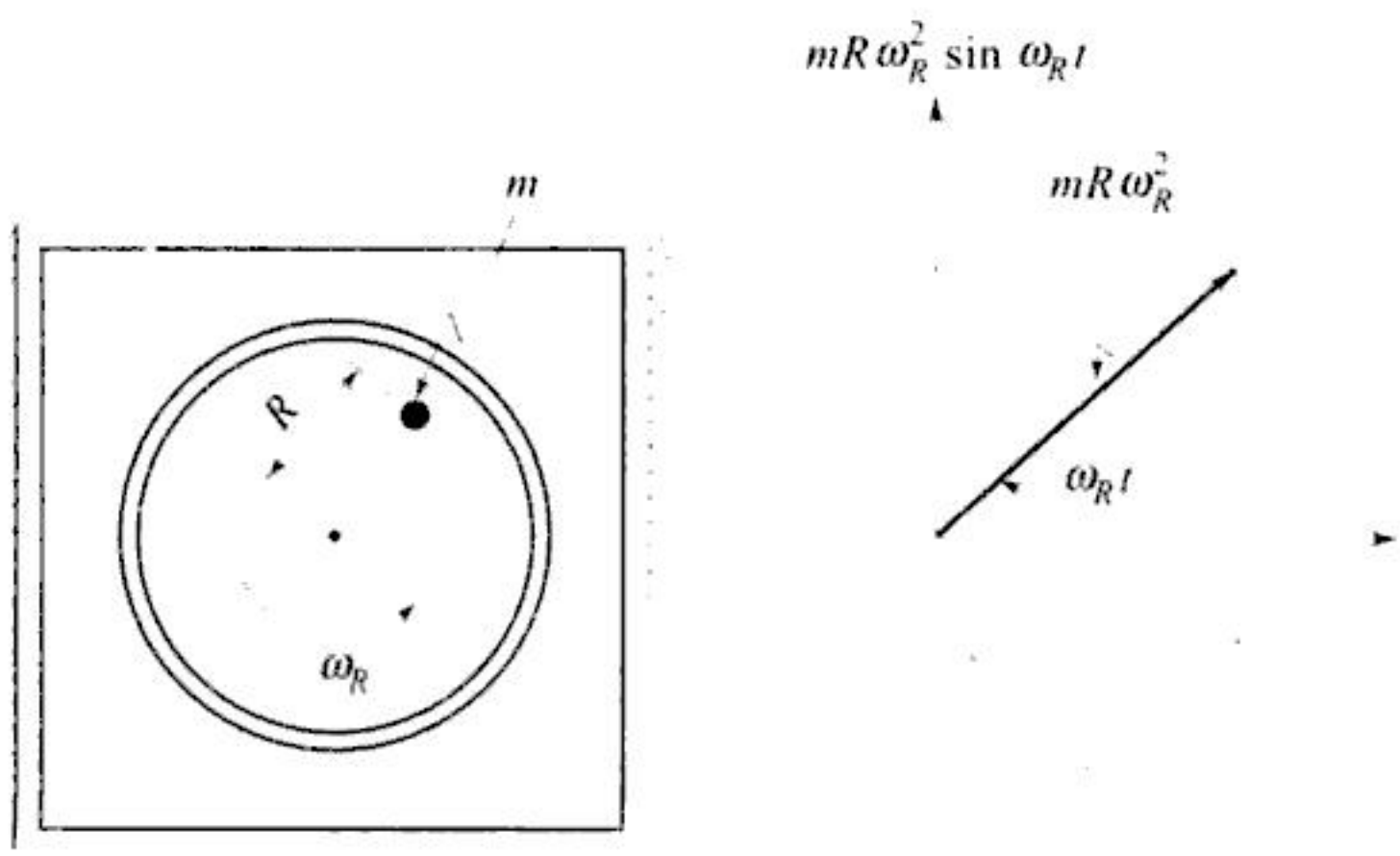


Fig. 2.49 *Machine with rotating imbalance*

Copyrighted material

centre of mass, a distance R from the centre of rotation. For a constant speed of rotation ω_R, a radial acceleration of m equal to $R\omega_R^2$ is produced. This causes a force to be exerted on the bearings at the centre of rotation. This force has a magnitude of $mR\omega_R^2$, and is directed radially outward. The vertical component of this imbalance force is $mR\omega_R^2 \sin \omega_R t$.

Consider the system of Fig. 2.50a, where an ac motor designed to run at a constant speed is mounted on a steel cantilever beam. The rotating part of the motor has an eccentricity; this gives rise to an exciting force of frequency, say ω_F: $F(t) = A \sin \omega_F t$.

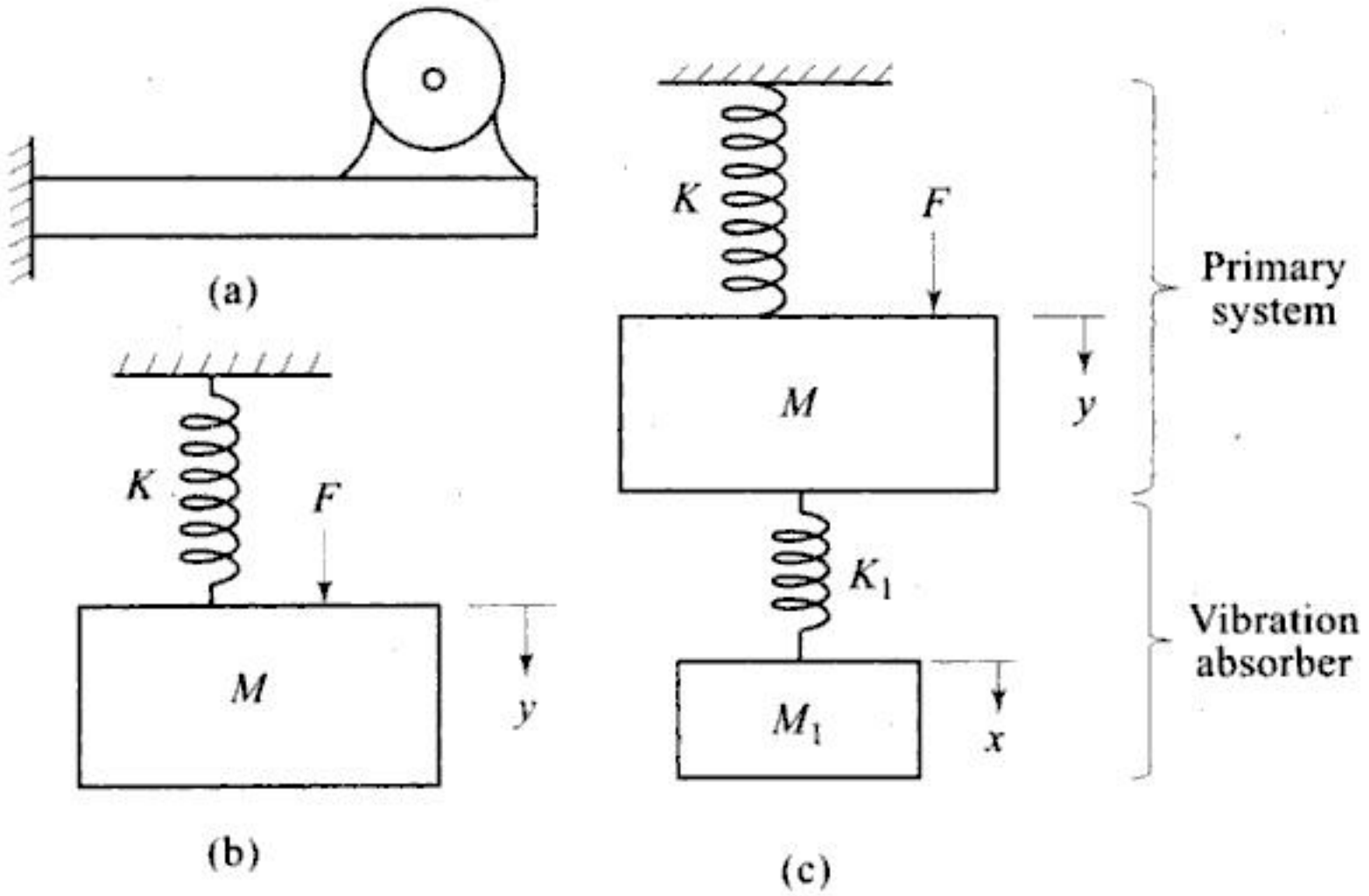


Fig. 2.50 *Motor vibration problem*

A lumped-parameter model for the system of Fig. 2.50a is of the form shown in Fig. 2.50b [31]. For this model, the governing equation is

$$F(t) - K y(t) = M\ddot{y}(t)$$

or
$$M\ddot{y}(t) + K y(t) = F(t) \qquad (2.129)$$

The zero position of y is taken to be at the point where the spring and the mass are in static equilibrium. The gravitational effect is eliminated by this choice of the zero position.

From Eqn. (2.129), we obtain

$$G(s) = \frac{Y(s)}{F(s)} = \frac{1}{Ms^2 + K} = \frac{1/K}{\frac{M}{K}s^2 + 1}$$

The sinusoidal transfer function

$$G(j\omega) = \frac{1/K}{1 - \left(\frac{\omega}{\omega_n}\right)^2}; \omega_n = \sqrt{\frac{K}{M}}$$

Copyrighted material



You have either reached a page that is unavailable for viewing or reached your viewing limit for this book.



You have either reached a page that is unavailable for viewing or reached your viewing limit for this book.

of the free terminal is measured. As an example, the mechanical system of Fig. 2.52a is redrawn in Fig. 2.52c which may be referred to as the *mechanical network.*

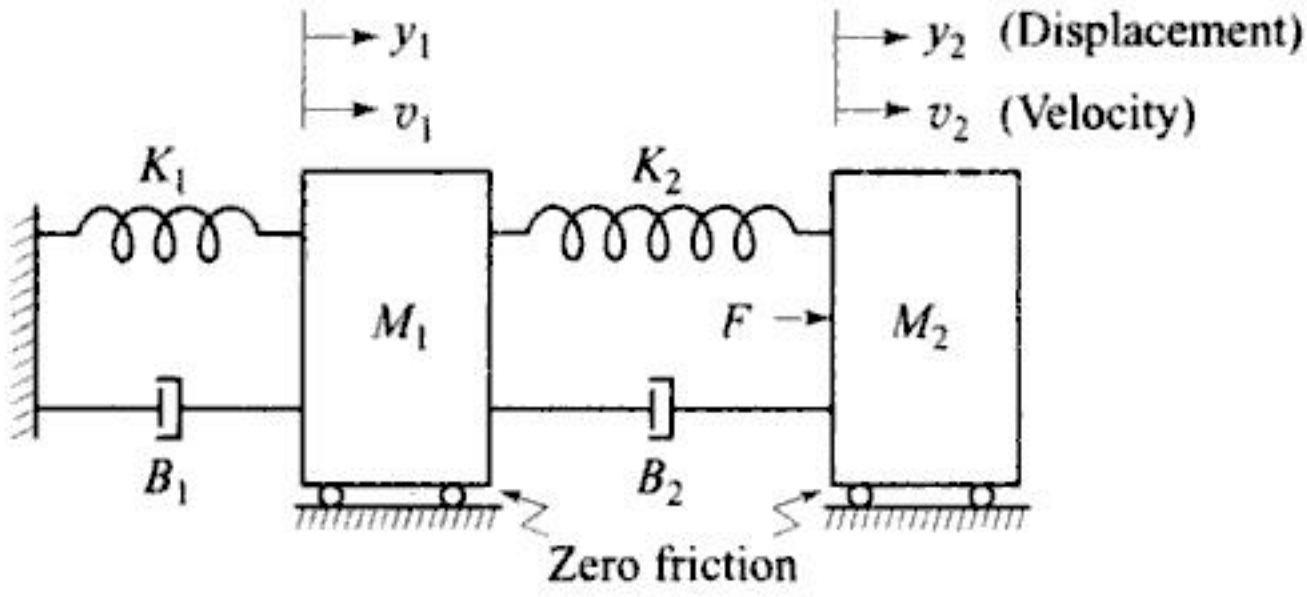


Fig. 2.52 *(a) A mechanical system*
(b) Free-body diagram
(c) Mechanical network

The dynamical equations of the system of Fig. 2.52a could also be obtained by writing nodal equations for the mechanical network of Fig. 2.52c (with force and velocity analogous to current and voltage, respectively; the algebraic sum of all the forces at a node is zero). The result is

$$B_1 v_1 + K_1 \int_{-\infty}^{t} v_1 dt + M_1 \dot{v}_1 + K_2 \int_{-\infty}^{t} (v_1 - v_2) dt + B_2 (v_1 - v_2) = 0$$

$$M_2 \dot{v}_2 + K_2 \int_{-\infty}^{t} (v_2 - v_1) dt + B_2 (v_2 - v_1) = F(t)$$

Copyrighted material

Since $\int_{-\infty}^{t} v dt = y$, we can write these equations as

$$B_1 v_1 + K_1 y_1 + M_1 \dot{v}_1 + K_2(y_1 - y_2) + B_2(v_1 - v_2) = 0$$

$$M_2 \dot{v}_2 + K_2(y_2 - y_1) + B_2(v_2 - v_1) = F(t)$$

The result is same as obtained earlier using the free-body diagram approach.

Review Example 2.5

A large number of process systems, used to control temperature, liquid level, composition and the like, use some sort of valve as the control actuator. The flow rate through a valve with adjustable opening is a function of both the pressure difference ΔP across the valve and the valve opening x_v:

$$Q = f(x_v, \Delta P) \tag{2.130a}$$

In many applications, there is a fairly constant pressure drop across the control valves; therefore the flow through a control valve is directly related to valve opening. If all components (including the process) in a feedback control system are essentially linear, then the valve characteristic—relation between the valve flow rate and valve opening when valve pressure drop is kept constant—is designed to be *linear*, since then the system performance (stability, response speed, etc.) will be uniform over all operating conditions. The linear characteristic of a valve is described by the relation

$$q(t) = K_v\, x_v(t) \tag{2.130b}$$

where K_v is the *valve gain*.

Let us consider a simple *composition control process* using a valve with linear characteristic as control actuator. In the scheme of Fig. 2.53a, a concentrated solution of salt is continuously mixed with pure water in a mixing valve. The valve characteristic is such that the total flow rate Q through it is maintained constant. When the inflow of the salt solution is varied by q_i from its initial equilibrium value $\overline{Q}_i$, the water inflow is automatically adjusted to the value $(Q - \overline{Q}_i - q_i)$. The inflow q_i may be linearly varied by controlling valve stem position x_v. The outflow rate from the salt-mixing tank is the same as the flow rate into it from the mixing valve, such that the level of the dilute salt solution in the tank is maintained constant. We assume that $\overline{C}_i$ (moles[12] of salt/m^3 of solution) is the concentration of the salt in the inflow stream at the initial equilibrium operating point; $c_i(t)$ represents the uncontrolled disturbance in the inlet concentration. The outlet stream has a concentration $\overline{C}$ at the equilibrium operating point; $c(t)$ represents perturbations in concentration due to $q_i(t)$ and/or $c_i(t)$.

12. A mole of a substance is defined as the amount of substance whose mass numerically equals its molecular weight. For example, a gram-mole of helium would have mass of 4.003 g (molecular weight of helium = 4.003).

Copyrighted material

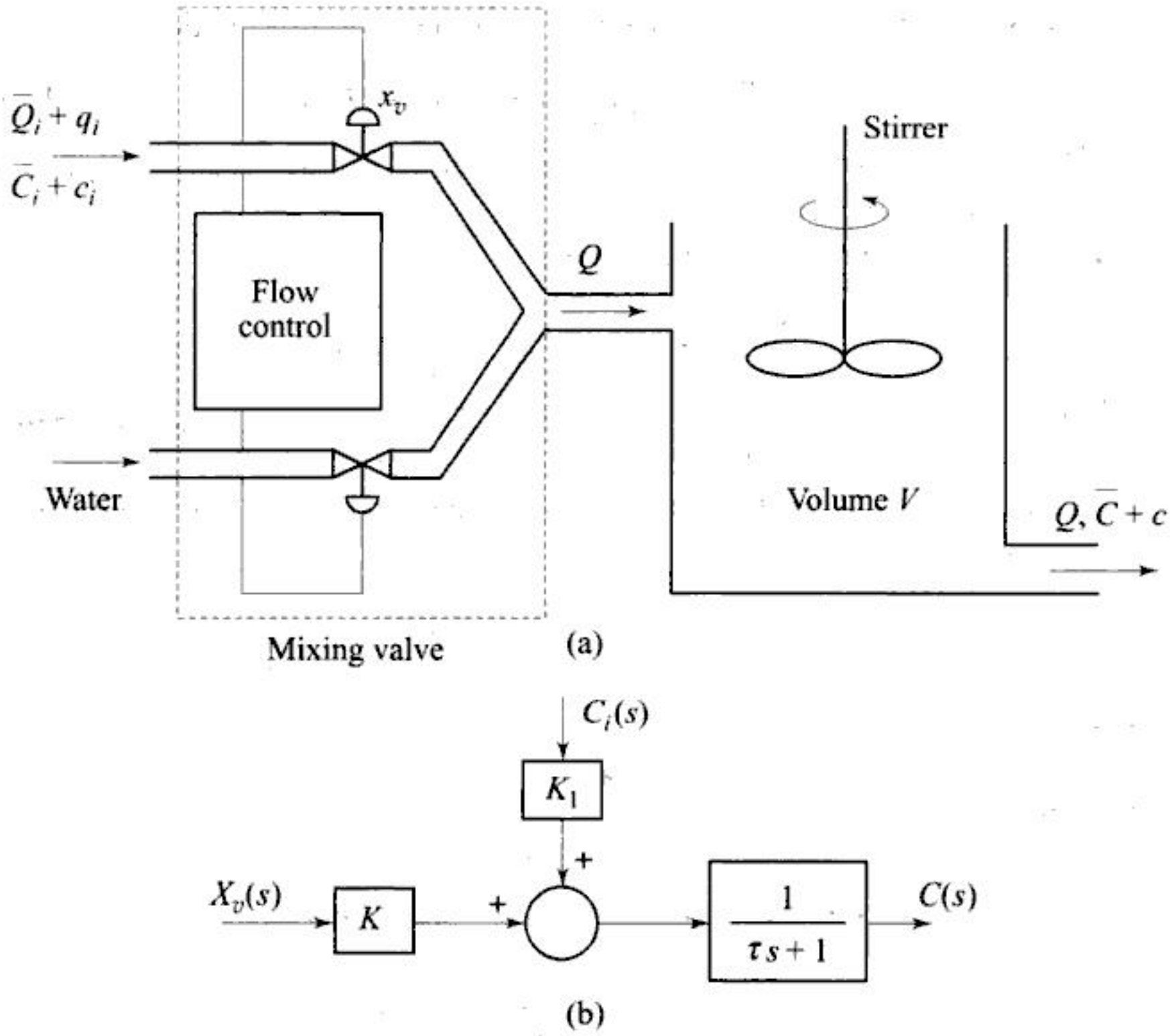


Fig. 2.53 *A salt-mixing tank*

We assume that stirring causes perfect mixing so that composition of the liquid in the tank is uniform throughout.

The rate of salt inflow in the tank

$$= [\bar{Q}_i + q_i(t)][\bar{C}_i + c_i(t)] \left(\frac{\text{m}^3}{\text{sec}} \frac{\text{moles}}{\text{m}^3} = \text{moles / sec} \right)$$

The rate of salt outflow from the tank

$$= Q(\bar{C} + c(t)) \text{ moles/sec}$$

The rate of salt accumulation in the tank

$$= \frac{d}{dt}[V(\bar{C} + c(t))] = V \frac{dc(t)}{dt}$$

From the law of conservation of mass, we have

$$V \frac{dc(t)}{dt} = [\bar{Q}_i + q_i(t)][\bar{C}_i + c_i(t)] - Q(\bar{C} + c(t))$$

Under steady-state,

$$0 = \bar{Q}_i \bar{C}_i - Q\bar{C}$$

Copyrighted material



You have either reached a page that is unavailable for viewing or reached your viewing limit for this book.



You have either reached a page that is unavailable for viewing or reached your viewing limit for this book.



You have either reached a page that is unavailable for viewing or reached your viewing limit for this book.



You have either reached a page that is unavailable for viewing or reached your viewing limit for this book.



You have either reached a page that is unavailable for viewing or reached your viewing limit for this book.

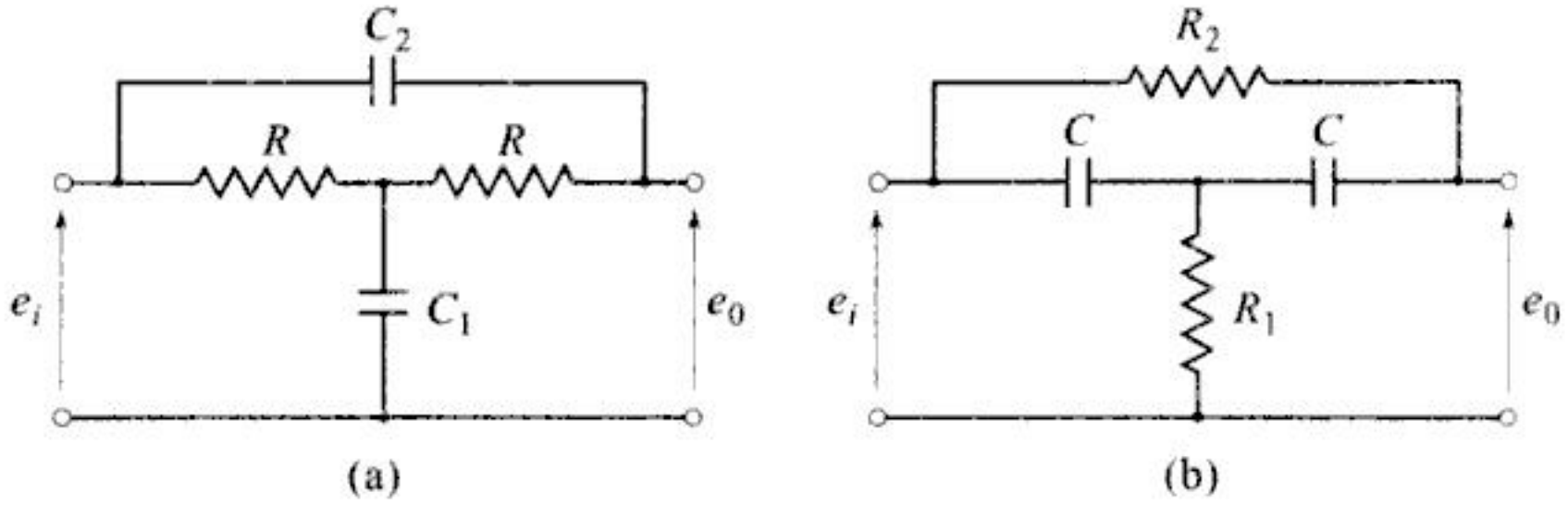


Fig. P2.12

2.13 Consider the op amp circuit shown in Fig. P2.13; $r(t)$ and $y(t)$ are the inputs and $e(t)$ is the output. Neglecting the loading effect on the potentiometer R_2, prove that

$$E(s) = \frac{R_2}{R_2'}\left(1 + \frac{1}{R_3 C s}\right)[R(s) - Y(s)]$$

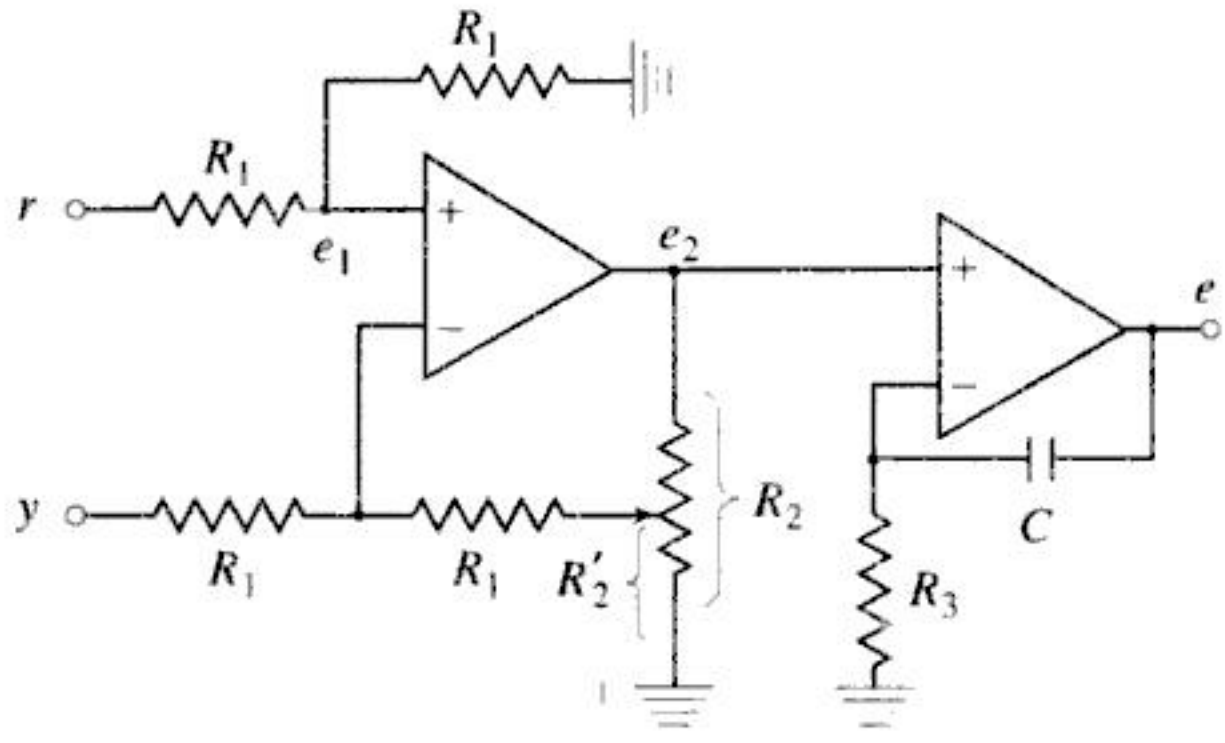


Fig. P2.13

2.14 Consider the op amp circuit shown in Fig. P2.14, $r(t)$ and $y(t)$ are the inputs and $e(t)$ is the output. Prove that

$$E(s) = R_2 C s\,[R(s) - Y(s)]$$

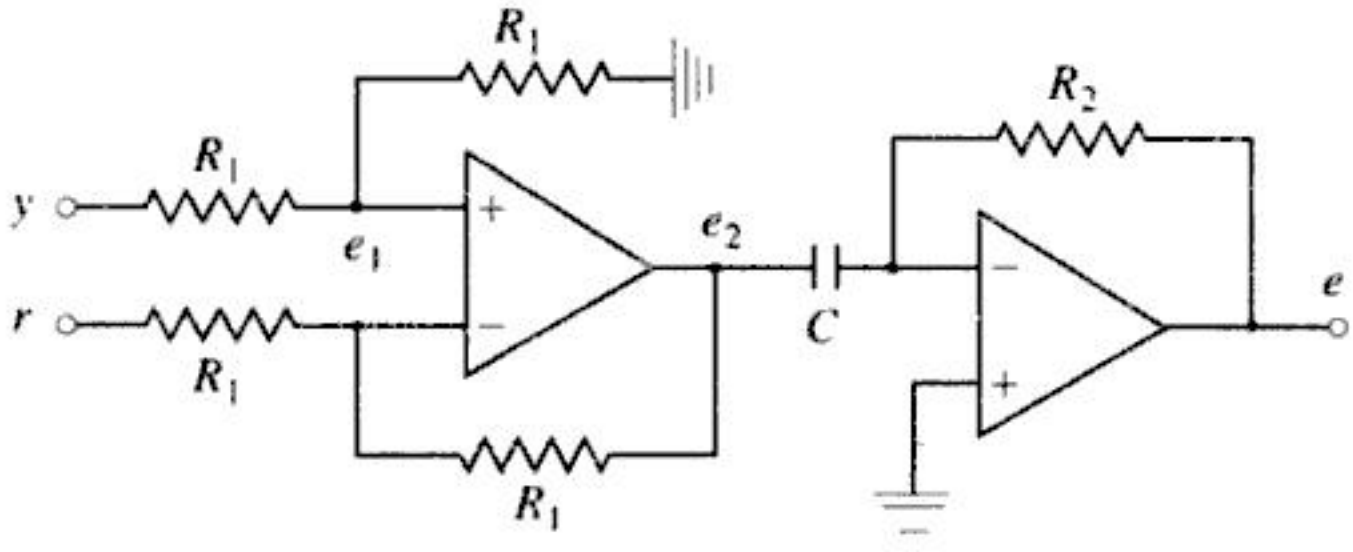


Fig. P2.14

Copyrighted material



You have either reached a page that is unavailable for viewing or reached your viewing limit for this book.



You have either reached a page that is unavailable for viewing or reached your viewing limit for this book.



You have either reached a page that is unavailable for viewing or reached your viewing limit for this book.



You have either reached a page that is unavailable for viewing or reached your viewing limit for this book.



You have either reached a page that is unavailable for viewing or reached your viewing limit for this book.



You have either reached a page that is unavailable for viewing or reached your viewing limit for this book.



You have either reached a page that is unavailable for viewing or reached your viewing limit for this book.



You have either reached a page that is unavailable for viewing or reached your viewing limit for this book.

indirectly controlled variable $q(t)$ to the controlled variable $y(t)$. Note that $Z(s)$ is outside the feedback loop.

The dashed-line portion of Fig. 3.2 shows the *system error* $e(t) = y_r(t) - y(t)$. Note that the actuating error signal $\hat{e}(t)$ and the system error $e(t)$ are two different variables.

Figure 3.2 defines the basic types of signals and components necessary for description of any feedback control system; however it must be adopted to the needs of each specific design. A large number of motion and process control examples given later in this chapter will (surely) help in better appreciation of what has been said in this section.

3.3 BLOCK DIAGRAM MANIPULATIONS

The basic feedback system block diagram of Fig. 3.2 is shown in abridged form in Fig. 3.3. The output $Y(s)$ is influenced by the control signal $U(s)$ and the disturbance signal $W(s)$ as per the following relation:

$$Y(s) = G_P(s)G_A(s)U(s) + G_P(s)W(s) \tag{3.1a}$$

$$= G(s)U(s) + N(s)W(s) \tag{3.1b}$$

where $G(s)$ is the transfer function from the control signal $U(s)$ to the output $Y(s)$, and $N(s)$ is the transfer function from the disturbance input $W(s)$ to the output $Y(s)$. Using Eqns (3.1), we can modify the block diagram of Fig. 3.3 to the form shown in Fig. 3.4. Note that in the block diagram model of Fig. 3.4, the plant includes the actuator elements.

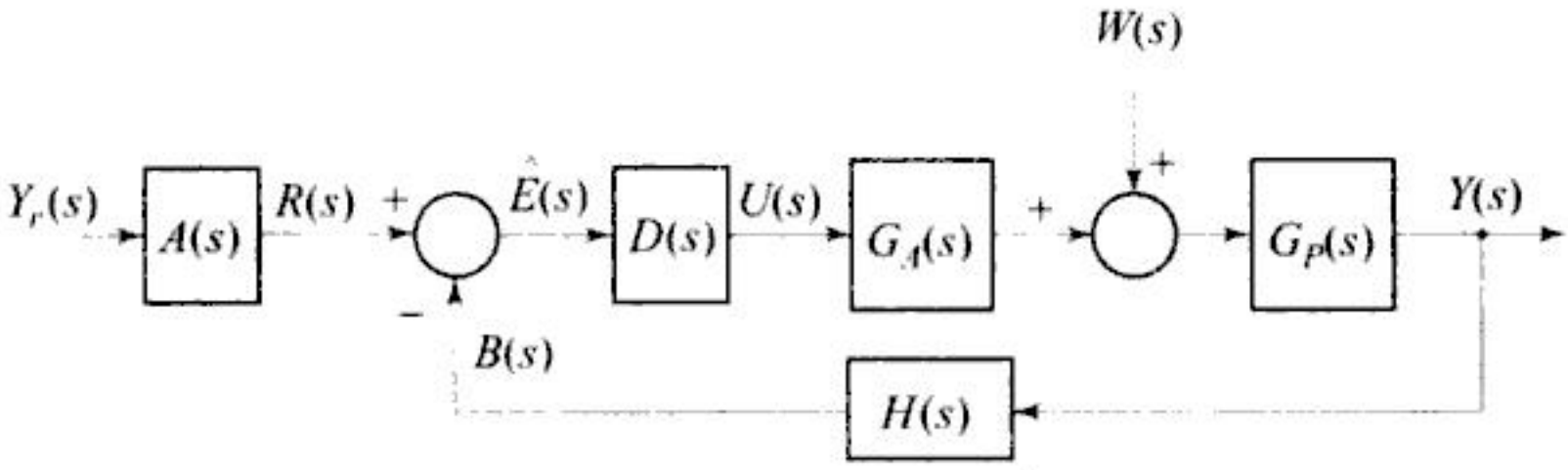


Fig. 3.3 *A general linear feedback system*

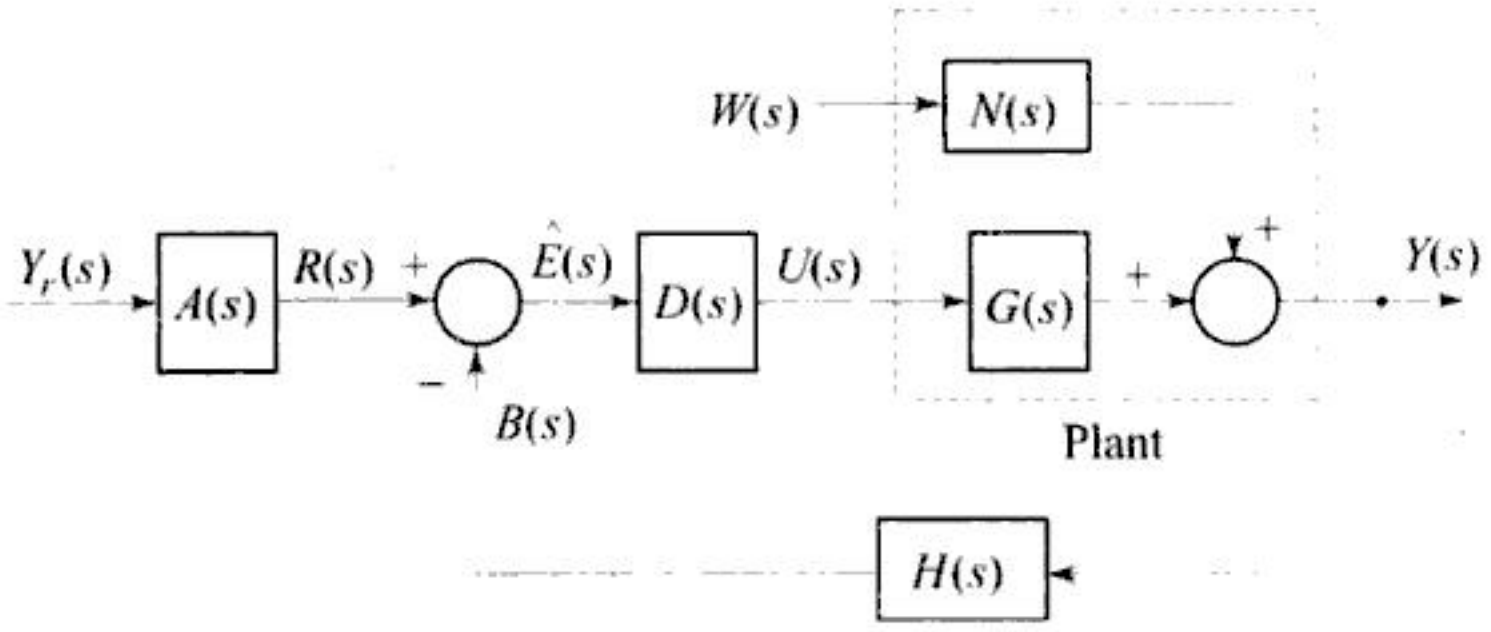


Fig. 3.4 *Equivalent representation of the block diagram of Fig. 3.3*

Copyrighted material

The actuating error signal

$$\hat{E}(s) = R(s) - B(s) = A(s)\,Y_r(s) - H(s)Y(s)$$

The control signal

$$U(s) = D(s)A(s)Y_r(s) - D(s)H(s)Y(s) \tag{3.2a}$$

$$= D(s)H(s)\left[\frac{A(s)}{H(s)}\,Y_r(s) - Y(s)\right] \tag{3.2b}$$

Using Eqns (3.2), we can simplify Fig. 3.4 to obtain the structure shown in Fig. 3.5.

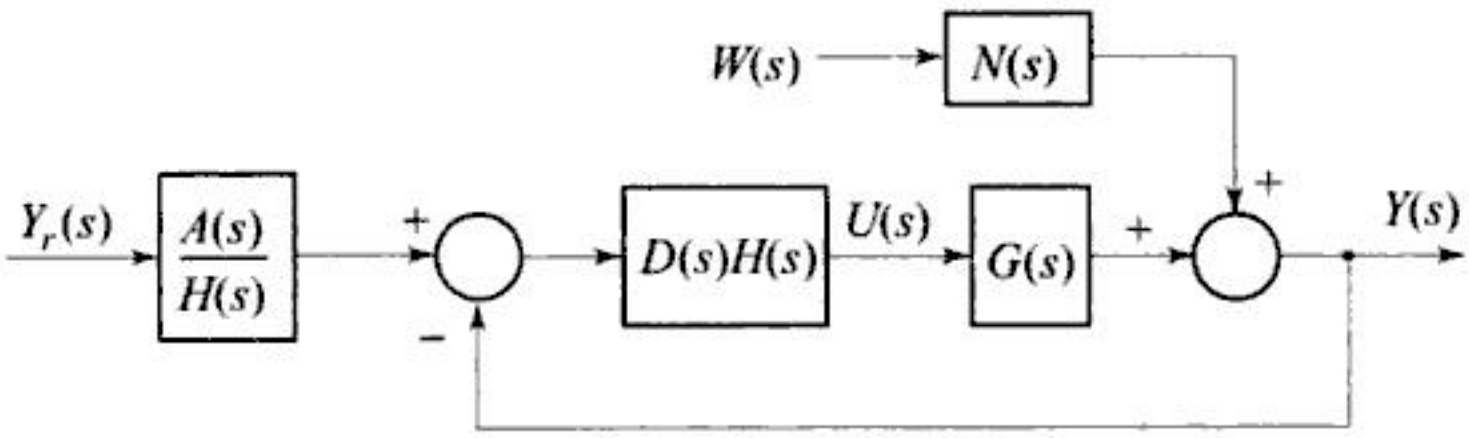


Fig. 3.5 *Simplification of the block diagram of Fig. 3.4*

A further simplification of Fig. 3.5 is possible if $H = A$. In this case, which is quite common, we can model the system as the *unity feedback system* as shown in Fig. 3.6, and take advantage of the fact that now the actuating signal is the system error $e(t)$.

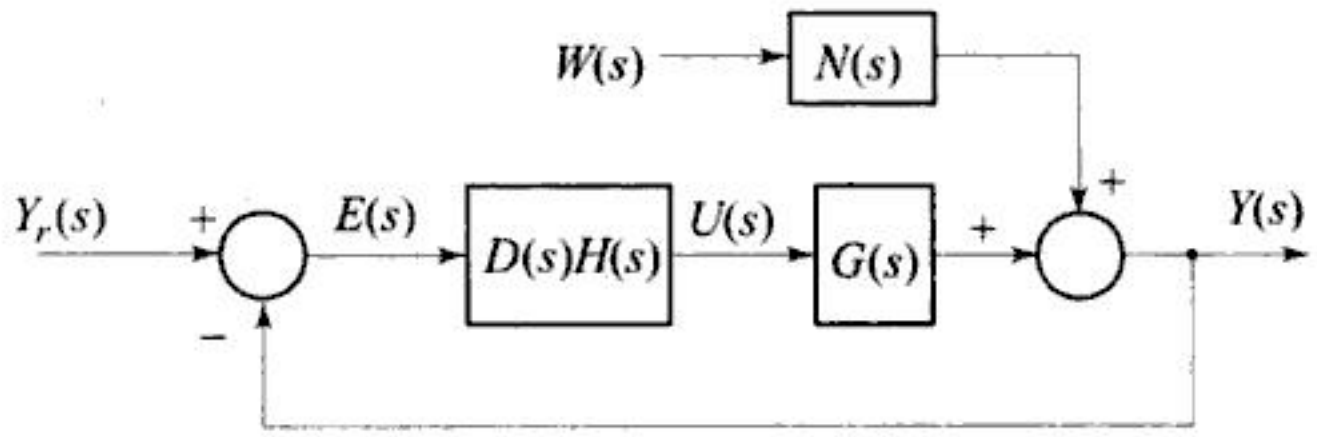


Fig. 3.6 *Unity feedback system*

The block diagrams in Figs 3.4–3.6, as we shall see later, are very useful for the purpose of system design. However, it should be clear that these block diagrams have lost the physical significance. For example, the block in Fig. 3.5 with transfer function $A(s)/H(s)$, does not refer to any physical portion of the original system. Rather, it represents the result of manipulating Eqn. (3.2a) into the form given by Eqn. (3.2b).

Thus the reader is advised to think in terms of the *equations* that the block diagrams represent, rather than to attach any special significance to block diagrams themselves. The only role played by a block diagram is that it is a convenient means of representing the various system equations, rather than writing

Copyrighted material



You have either reached a page that is unavailable for viewing or reached your viewing limit for this book.

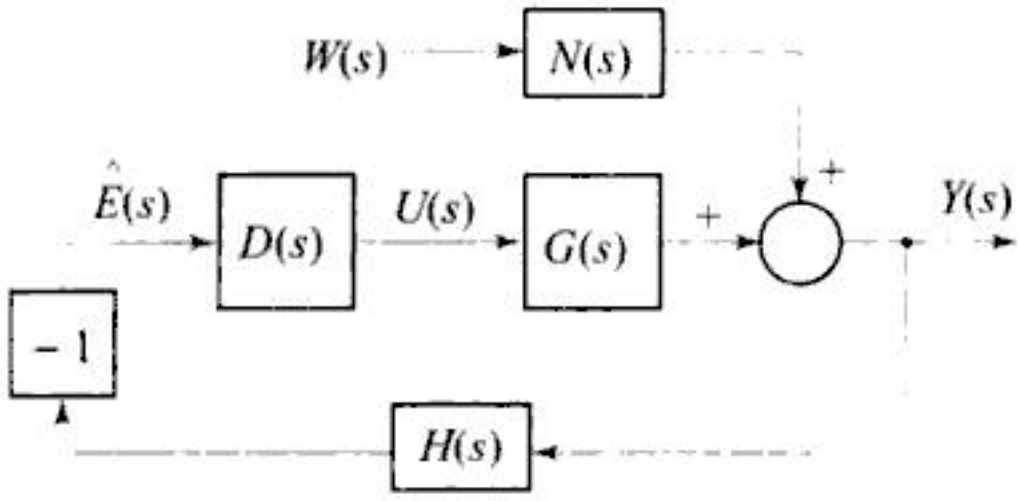


Fig. 3.9 *Block diagram without reference input*

$$\hat{E}(s) = -H(s)Y(s)$$

$$Y(s) = G(s)D(s)\hat{E}(s) + N(s)W(s)$$

from which $\hat{E}(s)$ can be eliminated to give

$$M_w(s) = \left.\frac{Y(s)}{W(s)}\right|_{R(s)=0} = \frac{N(s)}{1 + D(s)G(s)H(s)} \tag{3.4}$$

The response to the simultaneous application of $R(s)$ and $W(s)$ is given by

$$Y(s) = M(s)R(s) + M_w(s)W(s) \tag{3.5}$$

Figure 3.10 shows the reduced block diagram model of the given feedback system.

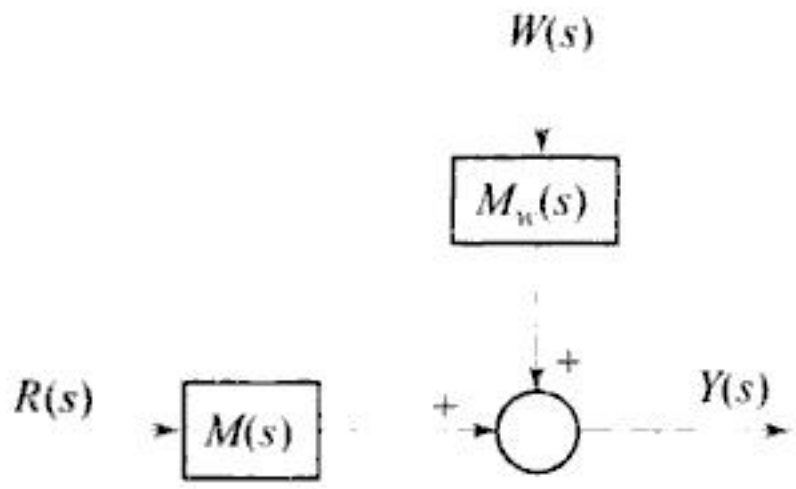


Fig. 3.10 *Reduced block diagram model for system of Fig. 3.7*

The transfer functions given by Eqns (3.3) and (3.4) are referred to as *closed-loop* transfer functions. Looking at Eqn. (3.3), we notice that the numerator is the multiplication of the transfer functions in the *forward path* between the two variables $R(s)$ and $Y(s)$. The denominator of this equation has the term $D(s)G(s)H(s)$ which is the multiplication of all the transfer functions in the *feedback loop*. An inspection of Eqn. (3.4) shows that the numerator is again the multiplication of the transfer functions in the forward path between $W(s)$ and $Y(s)$. The denominator is the same as in the case of Eqn. (3.3).

▲▲

From the examples of block diagram manipulations given above, we observe that there are two different objectives which may motivate one to manipulate a block diagram. The most obvious is to obtain the overall transfer function for the purpose of analysis (the block diagram of Fig. 3.7 was manipulated to obtain the one given in Fig. 3.10). The other objective is to manipulate a block diagram into a simpler form which is more convenient in the design process (the block diagram of Fig. 3.3 was manipulated to obtain the one given in Fig. 3.6).

Copyrighted material



You have either reached a page that is unavailable for viewing or reached your viewing limit for this book.



You have either reached a page that is unavailable for viewing or reached your viewing limit for this book.



You have either reached a page that is unavailable for viewing or reached your viewing limit for this book.



You have either reached a page that is unavailable for viewing or reached your viewing limit for this book.



You have either reached a page that is unavailable for viewing or reached your viewing limit for this book.



You have either reached a page that is unavailable for viewing or reached your viewing limit for this book.

$$X_5 = X_5$$

in the set (3.6).

However, we cannot convert a non-input node into an input node by a similar operation.

(v) *Path*: It is the traversal of connected branches in the direction of the branch arrows such that no node is traversed more than once.

(vi) *Forward path*: It is a path from the input node to the output node.

For the signal flow graph of Fig. 3.15g, there are two forward paths shown in Figs 3.16a and 3.16b.

(vii) *Loop*: It is a path which originates and terminates at the same node. The flow graph of Fig. 3.15g has five loops shown in Figs 3.16c to 3.16g.

(viii) *Nontouching loops*: Loops are said to be nontouching if they do not possess any common node.

The flow graph of Fig. 3.15g has two possible combinations of two nontouching loops. These are shown in Figs 3.16h and 3.16i. This flow graph does not have combinations of more than two nontouching loops.

(ix) *Forward path gain*: It is the product of the branch gain encountered in traversing a forward path.

The two forward paths of Figs 3.16a and 3.16b have the path gains $(G_{12}G_{23}G_{34}G_{45})$ and $(G_{12}G_{23}G_{35})$ respectively.

(x) *Loop gain*: It is the product of the branch gains encountered in traversing a loop.

The five individual loops of Figs 3.16c to 3.16g have loop gains $(G_{23}G_{32})$, $(G_{23}G_{34}G_{42})$, G_{44}, $(G_{23}G_{34}G_{45}G_{52})$; and $(G_{23}G_{35}G_{52})$ respectively.

The Mason's Gain Rule

The relationship between an input variable and an output variable of a signal flow graph is given by the net gain between the input and the output nodes and is known as the overall gain of the system. Mason's gain rule[1] for the determination of the overall system gain is given below.

$$M = \frac{1}{\Delta}\sum_{k=1}^{N} P_k \Delta_k = \frac{X_{\text{out}}}{X_{\text{in}}} \tag{3.7a}$$

where M = gain between X_{in} and X_{out}
X_{out} = output node variable
X_{in} = input node variable
N = total number of forward paths
P_k = path gain of the kth forward path
Δ = 1–(sum of loop gains of all individual loops) + (sum of gain products of all possible combinations of two nontouching loops)–(sum of gain products of all possible combinations of three nontouching loops) + ⋯

1. For the derivation, based on Cramer's rule for solving linear equations by determinants, the papers of Mason [44, 45] should be consulted.

Copyrighted material

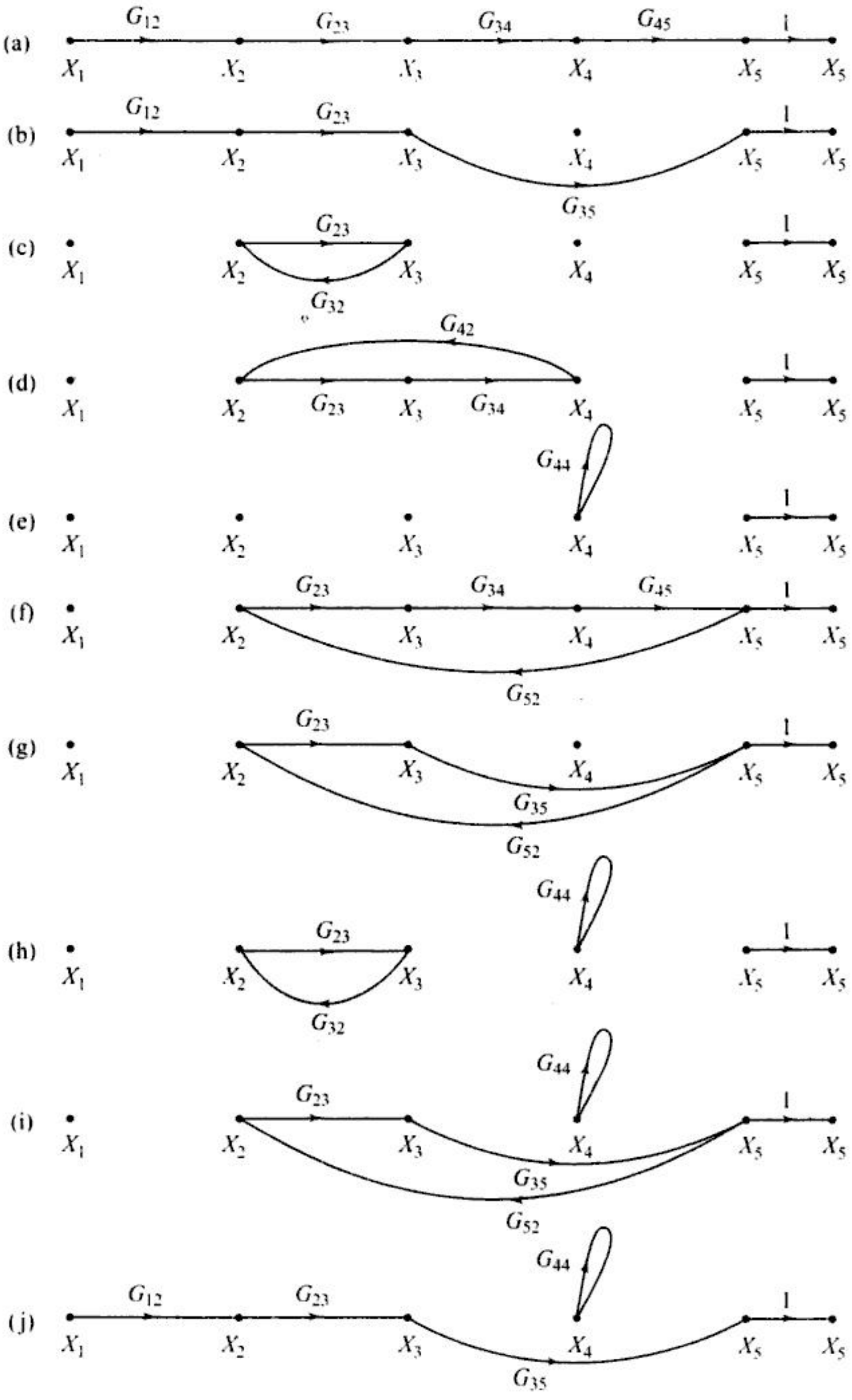


Fig. 3.16 *Application of Mason's gain rule to the signal flow graph of Fig. 3.15a*

Copyrighted material

$$= 1 - \sum_m P_{m1} + \sum_m P_{m2} - \sum_m P_{m3} + \cdots \qquad (3.7b)$$

P_{mr} = gain product of the mth possible combination of r nontouching loops.
Δ_k = the value of Δ for that part of the graph not touching the kth forward path.

▲▲

Let us illustrate the use of Mason's gain rule by finding the overall gain of the signal flow graph shown in Fig. 3.15g. The following conclusions are drawn by inspection of this signal flow graph.

(i) There are two forward paths with path gains

$$P_1 = G_{12}G_{23}G_{34}G_{45} \qquad \text{(Fig. 3.16a)}$$
$$P_2 = G_{12}G_{23}G_{35} \qquad \text{(Fig. 3.16b)}$$

(ii) There are five individual loops with loop gains

$$P_{11} = G_{23}G_{32} \qquad \text{(Fig. 3.16c)}$$
$$P_{21} = G_{23}G_{34}G_{42} \qquad \text{(Fig. 3.16d)}$$
$$P_{31} = G_{44} \qquad \text{(Fig. 3.16e)}$$
$$P_{41} = G_{23}G_{34}G_{45}G_{52} \qquad \text{(Fig. 3.16f)}$$
$$P_{51} = G_{23}G_{35}G_{52} \qquad \text{(Fig. 3.16g)}$$

(iii) There are two possible combinations of two nontouching loops with loop gain products

$$P_{12} = G_{23}G_{32}G_{44} \qquad \text{(Fig. 3.16h)}$$
$$P_{22} = G_{23}G_{35}G_{52}G_{44} \qquad \text{(Fig. 3.16i)}$$

(iv) There are no combinations of three nontouching loops, four nontouching loops, etc. Therefore

$$P_{m3} = P_{m4} = \cdots = 0$$

Hence from Eqn. (3.7b),

$$\Delta = 1 - (G_{23}G_{32} + G_{23}G_{34}G_{42} + G_{44} + G_{23}G_{34}G_{45}G_{52} + G_{23}G_{35}G_{52}) + (G_{23}G_{32}G_{44} + G_{23}G_{35}G_{52}G_{44})$$

(v) The first forward path is in touch with all the loops. Therefore $\Delta_1 = 1$. The second forward path is not in touch with one loop (Fig. 3.16j). Therefore, $\Delta_2 = 1 - G_{44}$.

From Eqn. (3.7a), the overall gain is

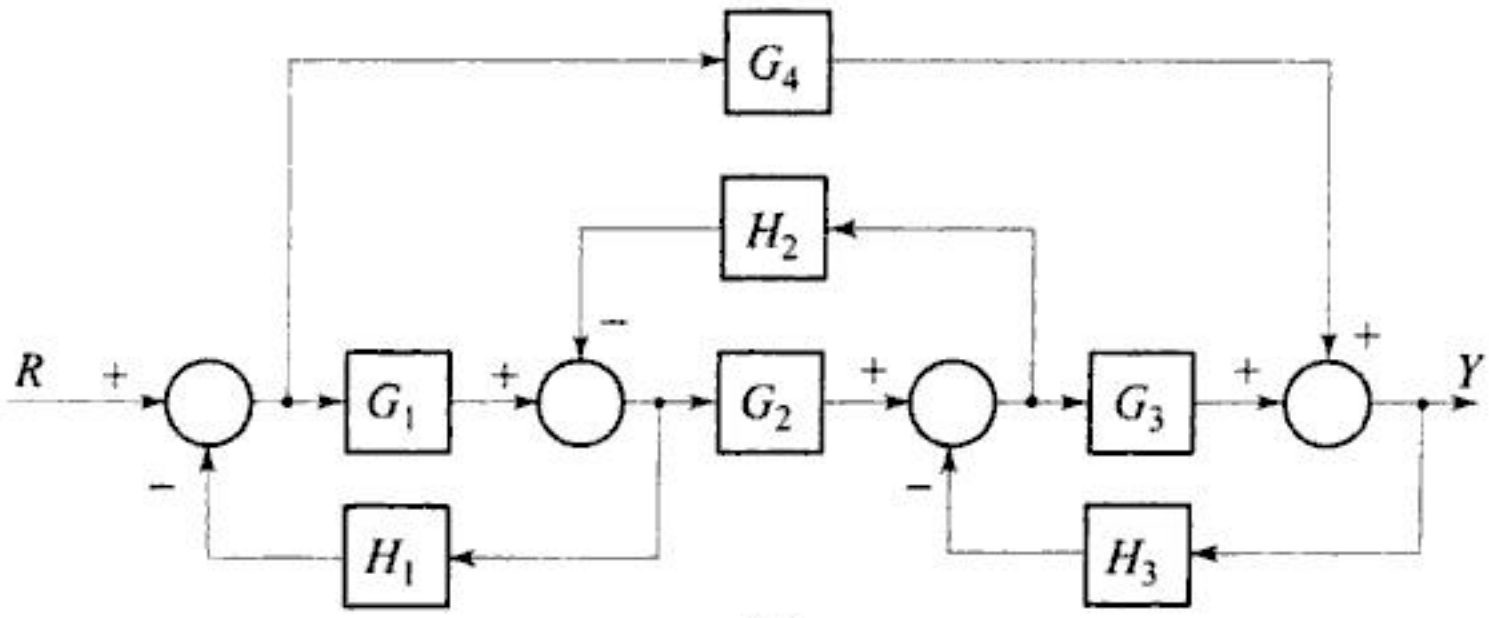
$$M = \frac{X_5}{X_1} = \frac{P_1\Delta_1 + P_2\Delta_2}{\Delta}$$

$$= \frac{G_{12}G_{23}G_{34}G_{45} + G_{12}G_{23}G_{35}(1 - G_{44})}{\left[1 - (G_{23}G_{32} + G_{23}G_{34}G_{42} + G_{44} + G_{23}G_{34}G_{45}G_{52} + G_{23}G_{35}G_{52}) + G_{23}G_{32}G_{44} + G_{23}G_{35}G_{52}G_{44}\right]}$$

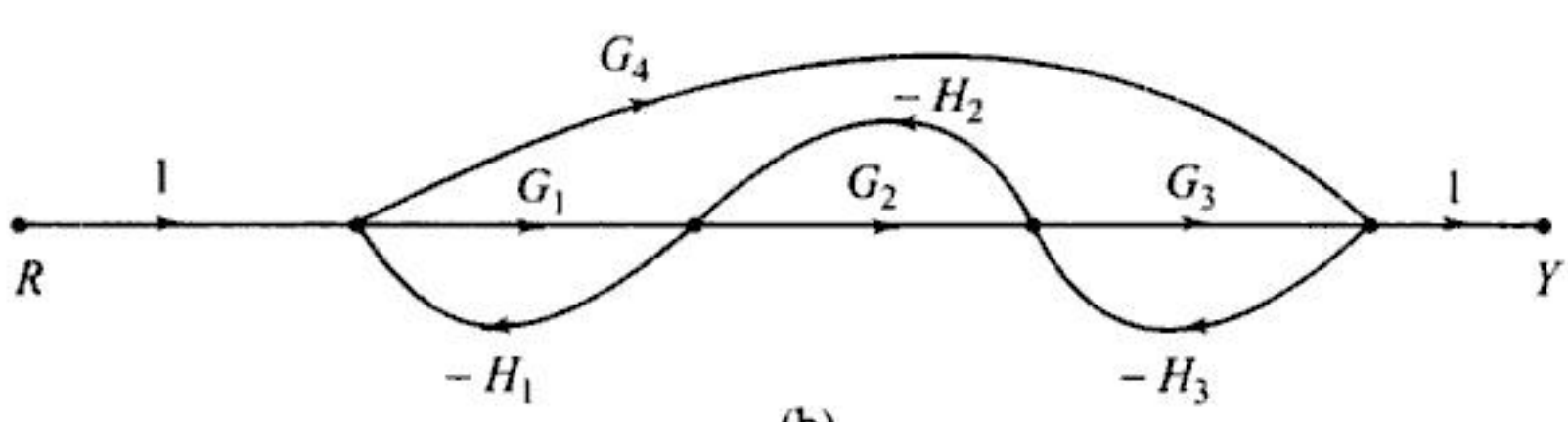
Copyrighted material



You have either reached a page that is unavailable for viewing or reached your viewing limit for this book.



(a)



(b)

Fig. 3.17 *(a) Block diagram of a control system*
(b) Equivalent signal flow graph

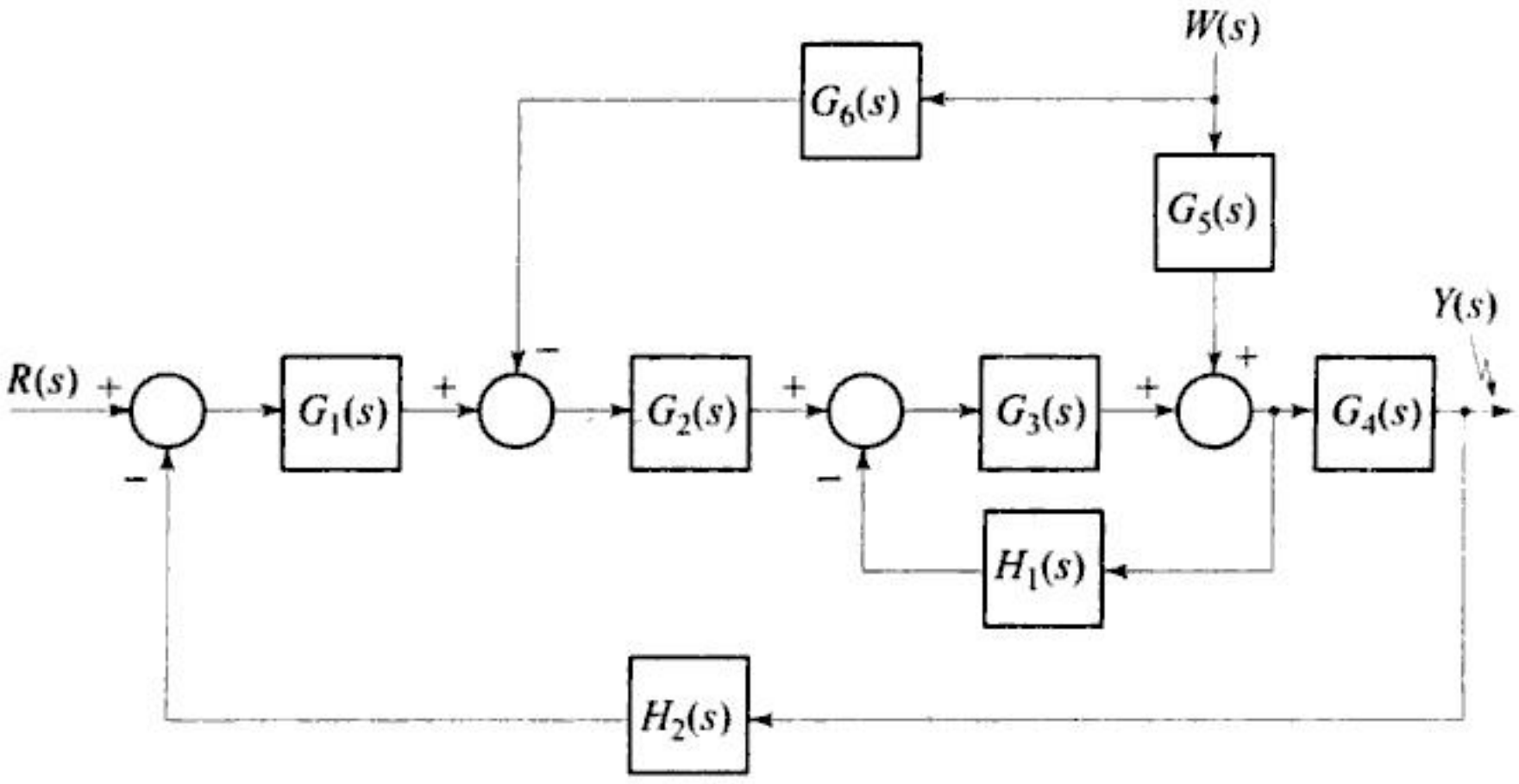


Fig. 3.18 *Block diagram of a control system*

$$M(s) = \frac{Y(s)}{R(s)}\bigg|_{W(s)=0} = \frac{G_1(s)G_2(s)G_3(s)G_4(s)}{1 + G_3(s)H_1(s) + G_1(s)G_2(s)G_3(s)G_4(s)H_2(s)}$$

With $R(s) = 0$, the block diagram has two forward paths and two loops. The two loops touch each other and both the forward paths touch both the loops. By Mason's gain rule,

Copyrighted material



You have either reached a page that is unavailable for viewing or reached your viewing limit for this book.



You have either reached a page that is unavailable for viewing or reached your viewing limit for this book.

As the armature rotates in the magnetic field, a voltage is induced into the armature winding. This voltage is 180° out of phase with the applied armature voltage and is therefore called back emf. The relationship among the back emf e_b (volts), rotor velocity ω (rad/sec) and flux ϕ (webers) is

$$e_b = K_{m1}\,\phi\,\omega \tag{3.9a}$$

where K_{m1} is a constant

For the wound-field motor,

$$e_b = K_{m2}\,i_f\,\omega \tag{3.9b}$$

where K_{m2} is a constant.

Equations (3.8) and (3.9) form the basis of dc motor operation.

In a permanent-magnet (PM) motor, the flux ϕ is constant; the torque T_M exerted on the motor rotor can therefore be controlled by varying the armature current (refer Eqn. (3.8a)). If the direction of the armature current is reversed, the direction of the torque is reversed.

In a wound-field motor, the torque may be controlled by varying the armature current and/or the field current (refer Eqn. (3.8b)). Generally, one of these is varied to control the torque while the other is held constant. In the *armature control* mode of operation, the field current is held constant and armature current is varied to control the torque. In the *field-control* mode, the armature current is maintained constant and field current controls the torque; a reversal in the direction of field current reverses the direction of the torque.

In servo applications, a dc motor is required to produce rapid accelerations from standstill. Therefore, the physical requirements of such a motor are low inertia and high starting torque. Low inertia is attained with reduced armature diameter, with a consequent increase in armature length such that the desired power output is achieved. Thus, except for minor differences in constructional features, a dc servomotor is essentially an ordinary dc motor.

Armature-Controlled dc Motor

The symbolic representation of armature-controlled dc motor as a control system component is shown in Fig. 3.20. Under consideration is a wound-field motor. An external dc source supplies a constant current i_f to the field winding. The armature circuit consists of the armature resistance R_a and the armature

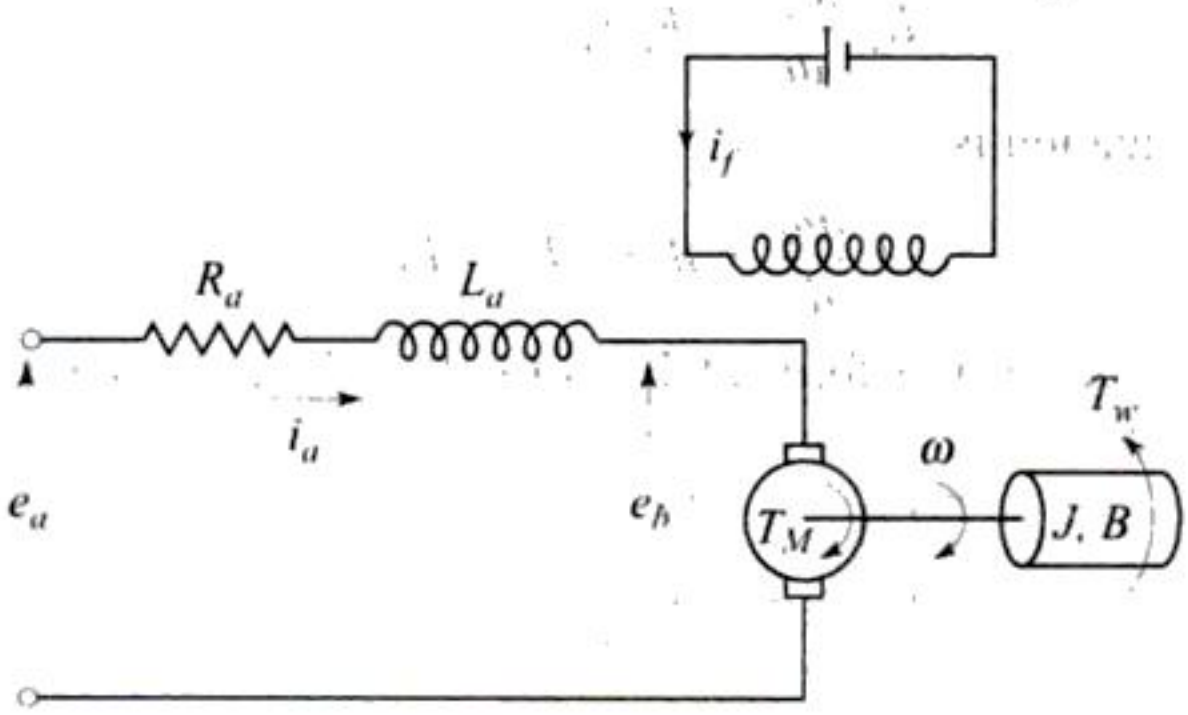


Fig. 3.20 *Armature-controlled dc motor with load*

Copyrighted material

inductance L_a; both are due to the total armature winding which makes an electrical contact with the brushes of the commutator, e_a is the applied armature voltage which controls the motor operation, and e_b is the back emf.

On the mechanical side, the motor rotor and the attached load can be treated as inertia and viscous friction; J and B are the corresponding parameters. T_w is the disturbance load torque. The torque T_M developed by the motor drives the load with angular velocity ω.

Let us summarize the variables and parameters in the dc motor model of Fig. 3.20:

R_a = armature winding resistance (ohms);
L_a = armature winding inductance (henrys);
i_a = armature current (amps);
i_f = field current (amps) = a constant;
e_a = applied armature voltage (volts);
e_b = back emf (volts);
ω = angular velocity of the motor rotor (rad/sec);
θ = angular displacement of the motor rotor (rad);
T_M = torque developed by the motor (newton-m);
J = moment of inertia of the motor rotor with attached mechanical load (kg-m^2 or (newton-m)/(rad/sec^2));
B = viscous-friction coefficient of the motor rotor with attached mechanical load ((newton-m)/(rad/sec)); and
T_w = disturbance load torque (newton-m).

Since the field current is kept constant in the armature-control mode of operation, Eqns (3.8b) and (3.9b) become

$$T_M = K_T\, i_a \tag{3.10a}$$

$$e_b = K_b \omega \tag{3.10b}$$

where

$K_T \triangleq$ torque constant; $K_b \triangleq$ back emf constant

The differential equation of the armature circuit is

$$L_a \frac{di_a}{dt} + R_a\, i_a + e_b = e_a \tag{3.11}$$

The torque equation is

$$J \frac{d\omega}{dt} + B\omega + T_w = T_M \tag{3.12}$$

Taking the Laplace transform of Eqns (3.10)–(3.12), assuming zero initial conditions, we get

$$T_M(s) = K_T\, I_a(s) \tag{3.13a}$$

$$E_b(s) = K_b \omega(s) \tag{3.13b}$$

$$(L_a s + R_a)\, I_a(s) = E_a(s) - E_b(s) \tag{3.13c}$$

Copyrighted material

$$(Js + B)\,\omega(s) = T_M(s) - T_w(s) \tag{3.13d}$$

Figure 3.21 shows a block diagram representation of the dc motor system. The block diagram gives a clear picture of the cause and effect relationships in the physical system of Fig. 3.20. The voltage applied to the armature circuit is $E_a(s)$ which is opposed by the back emf $E_b(s)$. The net voltage $(E_a(s)-E_b(s))$ acts on a linear circuit comprised of resistance and inductance in series, having the transfer function $1/(sL_a + R_a)$. The result is an armature current $I_a(s)$. For the fixed field, the torque developed by the motor is $K_T I_a(s)$. The torque rotates the load at a speed $\omega(s)$ against the disturbance $T_w(s)$; the load having moment of inertia J and viscous friction with coefficient B has the transfer function $1/(Js + B)$. The back emf signal $E_b(s) = K_b\omega(s)$ is taken off from the shaft speed and fedback negatively to the summing point. Note that although a dc motor by itself is basically an open-loop system, it has a 'built in' feedback loop caused by the back emf.

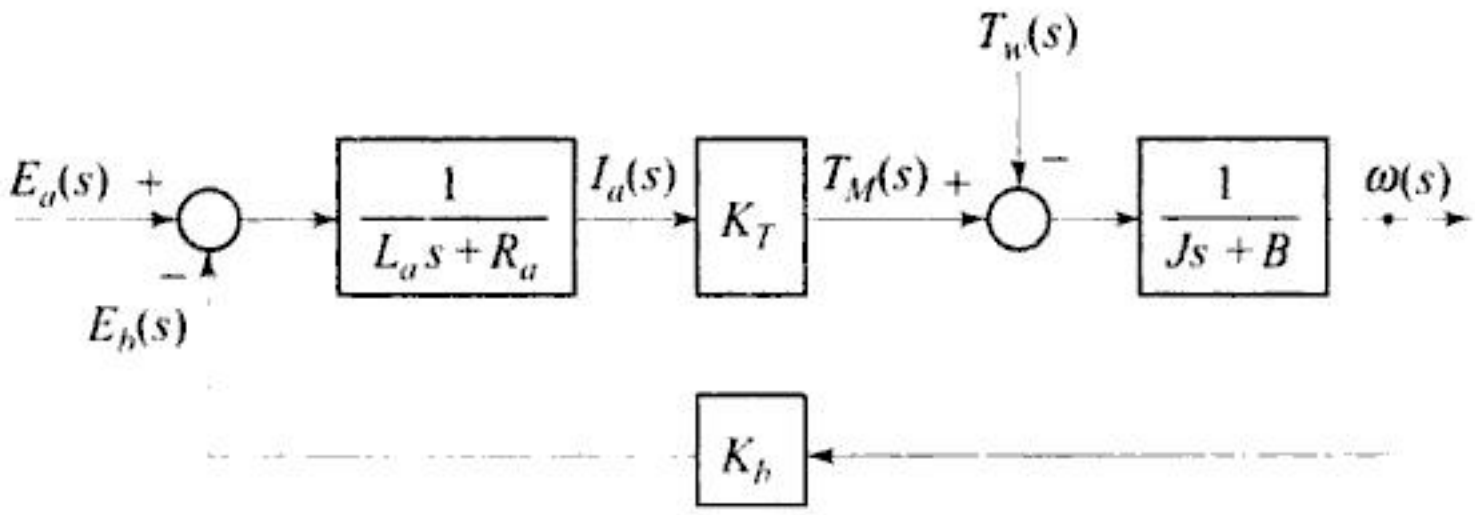


Fig. 3.21 *Block diagram of a dc motor (armature-controlled) system*

The transfer function between the motor velocity $\omega(s)$ and the input voltage $E_a(s)$, obtained from the block diagram, is

$$\frac{\omega(s)}{E_a(s)} = \frac{K_T}{(L_a s + R_a)(Js + B) + K_T K_b} \tag{3.14}$$

The inductance L_a in the armature circuit is usually small and may be neglected. If L_a is neglected, then the transfer function given by Eqn. (3.14) reduces to

$$\frac{\omega(s)}{E_a(s)} = \frac{K_T/R_a}{Js + B + K_T K_b/R_a} \tag{3.15}$$

The back emf constant K_b represents an added term to the viscous friction coefficient B. Therefore, the back emf effect is equivalent to an 'electric friction' which tends to improve the stability of the dc motor system.

The transfer function given by Eqn. (3.15) may be written in the form given below.

$$\frac{\omega(s)}{E_a(s)} = \frac{K_m}{\tau_m s + 1} \tag{3.16}$$

where $$K_m = \frac{K_T}{R_a B + K_T K_b}$$ = motor gain constant

Copyrighted material

and $$\tau_m = \frac{R_a J}{R_a B + K_T K_b} = \text{motor time-constant}$$

When the motor is used to control shaft position θ, rather than the speed ω, we get the block diagram model shown in Fig. 3.22. The transfer function between the shaft position $\theta(s)$ and the input voltage $E_a(s)$ becomes

$$\frac{\theta(s)}{E_a(s)} = \frac{K_m}{s(\tau_m s + 1)} \tag{3.17}$$

The significance of this transfer function is that the dc motor is essentially an integrating device between the input voltage and the shaft position. This is expected since if e_a is a constant input, the motor displacement will behave as the output of an integrator; that is, it will increase linearly with time. We shall see later that the integrating effect $1/s$ in Eqn. (3.17) gives a feedback position control system better steady-state behaviour than the corresponding speed control system.

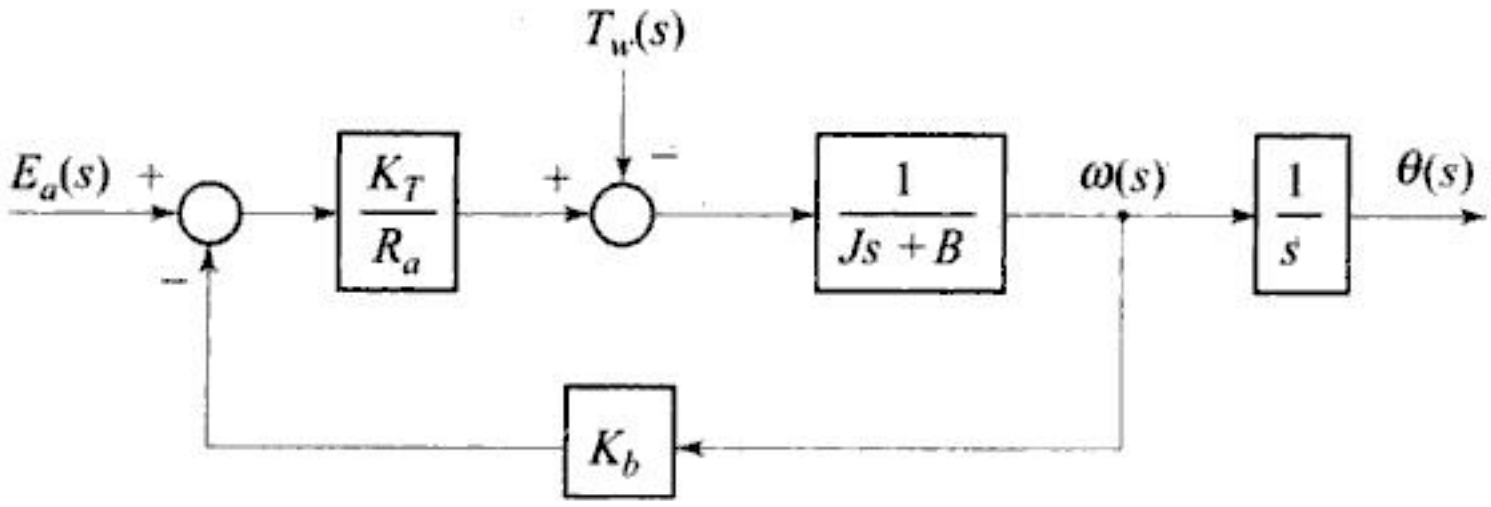


Fig. 3.22 *The dc motor (armature-controlled) model with displacement as output*

The motor torque and back emf constants are inter-related. Their relationship is deduced below.

Power developed in the armature is

$$P = e_b(t)\, i_a(t) \text{ [(volts) (amps) = watts]}$$

$$= K_b\, \omega(t)\, i_a(t) \left[\left(\frac{\text{volts}}{\text{rad/sec}}\right)(\text{rad/sec})(\text{amp})\right]$$

In terms of torque and angular velocity,

$$P = T_M(t)\omega(t) \text{ [(newton-m) (rad/sec) = watts]}$$

$$= K_T\, i_a(t)\omega(t) \left[\left(\frac{\text{(newton-m)}}{\text{amp}}\right)(\text{amp})(\text{rad/sec})\right]$$

Therefore,

$$K_b(\text{volts/(rad/sec)}) = K_T\ (\text{newton-m/amp}) \tag{3.18}$$

This result can be used to advantage in practice as K_b can be measured more easily and with greater accuracy than K_T.

In a PM motor, the field winding is absent and a constant magnetic flux is provided by the permanent magnet. Since in the preceding development, the magnetic flux is a constant, Eqns (3.14)–(3.18) are also valid for a PM motor.

Copyrighted material

Torque Speed Curves

The torque-speed curves of a dc motor describe the static torque-producing capability of the motor with respect to the applied voltage and motor speed. With reference to Fig. 3.21, in the steady-state the effect of the inductance is zero, and the torque equation of the motor is

$$T_M = \frac{K_T}{R_a}(E_a - K_b\omega) = -\frac{K_T K_b}{R_a}\omega + \frac{K_T}{R_a}E_a$$

where T_M, E_a, and ω represent the steady-state values of the motor torque, applied voltage and speed, respectively.

Figure 3.23 shows a typical set of torque-speed curves (experimentally obtained/supplied by the manufacturer) of a dc motor for various constant armature voltages.

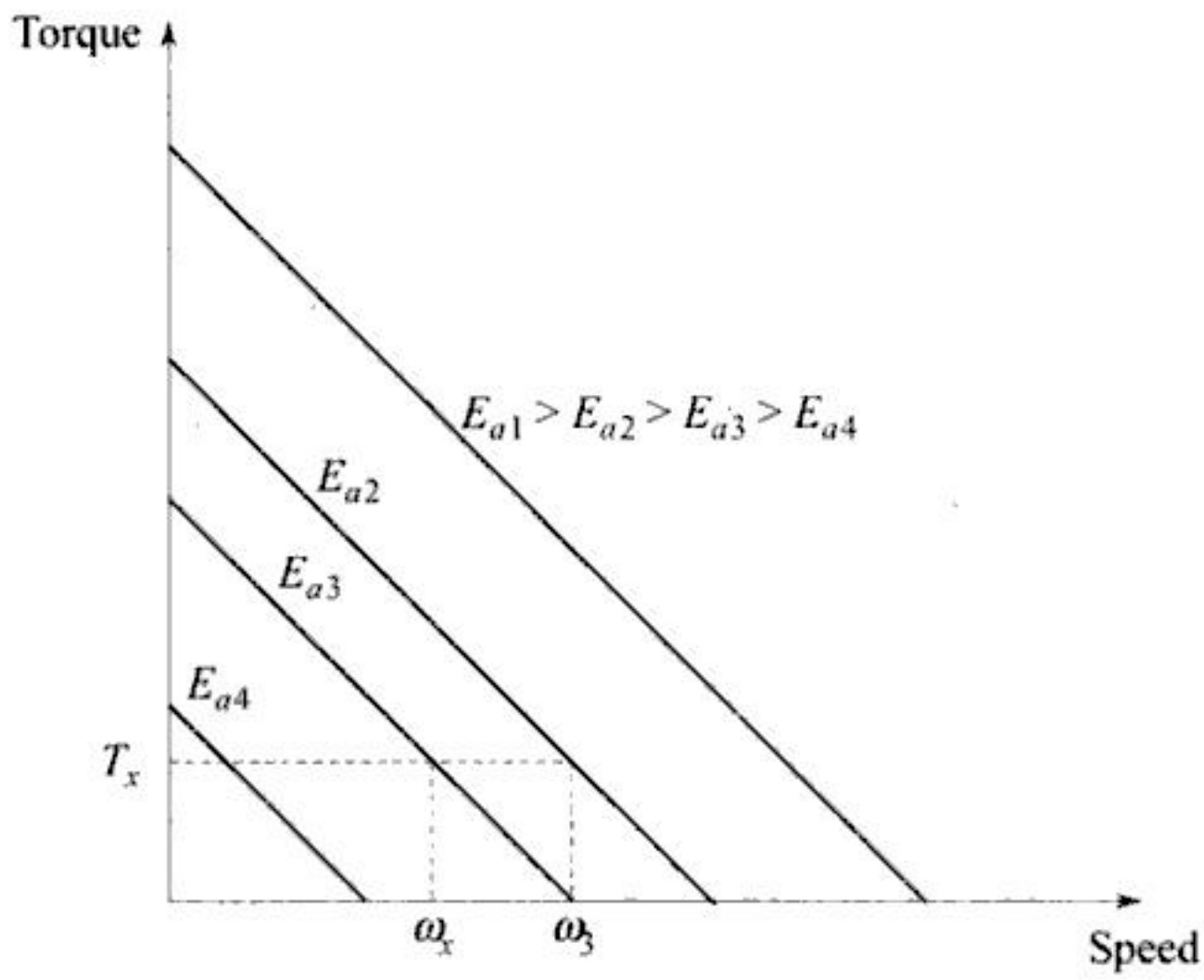


Fig. 3.23 *Typical torque-speed curves of an armature-controlled dc motor*

The no-load point on the torque-speed characteristic corresponding to armature voltage E_{a3} is defined by the coordinates $(\omega_3, 0)$ in Fig. 3.23. If a load T_x is applied to the motor shaft, the operating point of the motor shifts from the point $(\omega_3, 0)$ to the point (ω_x, T_x) as shown in the figure.

Thus, the applied torque reduces the motor speed. The reduction in speed results in a lower back emf and, for a constant armature voltage E_{a3}, reduction in back emf causes an increase in armature current. The increase in armature current is responsible for an increase in motor-generated torque to accommodate the applied load T_x. If the new steady-state speed ω_x is too low and the original speed ω_3 must be restored, the armature voltage must be increased. This is illustrated in Fig. 3.23; the increase in armature voltage from E_{a3} to E_{a2} restores the original no-load speed ω_3 with the load T_x applied.

▲▲

Copyrighted material

In a dc motor system, there may be a significant nonlinear friction due to the rubbing contact between the brushes and the commutator. Also, torque saturation may occur because of limitation of the maximum current that the motor can handle due to the heat-dissipation rating of the motor. Refer [180] for methods for analysis of control systems with nonlinearities in the closed loop.

Field-Controlled dc Motor

The schematic diagram of a field-controlled dc motor is shown in Fig. 3.24. In this system,

R_f = field winding resistance (ohms);
L_f = field winding inductance (henrys);
i_f = field current (amps);
i_a = armature current (amps) = a constant;
e_f = applied field voltage (volts);
ω = angular velocity of the motor rotor (rad/sec);
θ = angular displacement of the motor rotor (rad);
T_M = torque developed by the motor (newton-m);
J = moment of inertia of the motor rotor with attached mechanical load (kg-m^2 or (newton-m)/(rad/sec^2));
B = viscous-friction coefficient of the motor rotor with attached mechanical load ((newton-m)/(rad/sec)); and
T_w = disturbance load torque (newton-m).

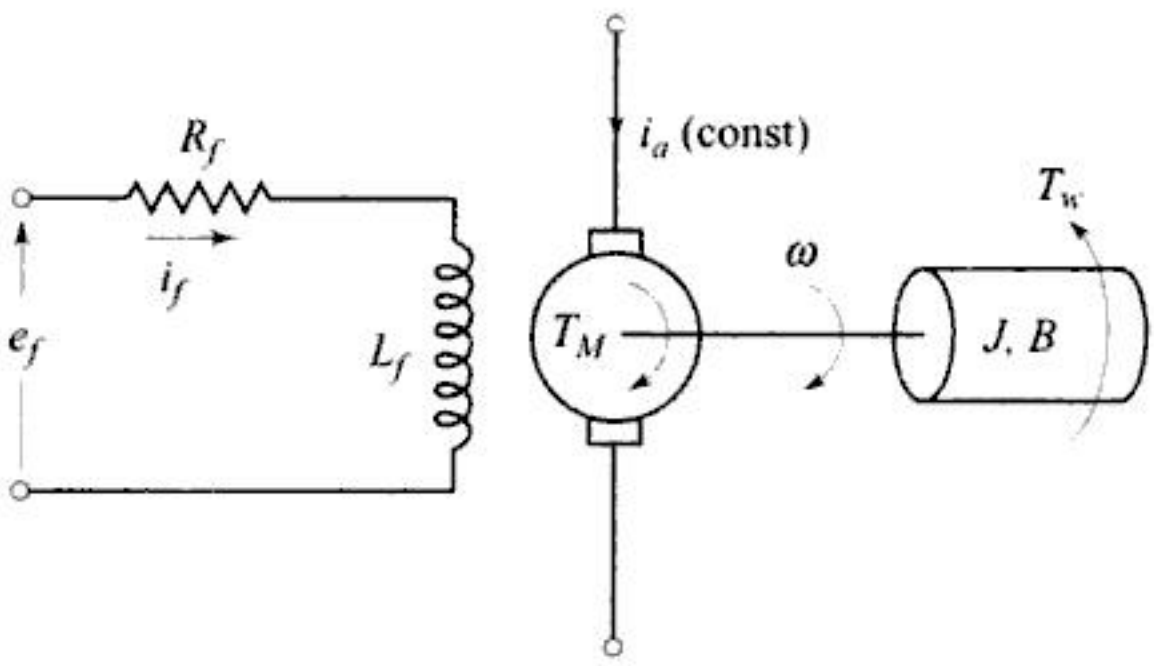


Fig. 3.24 *Field-controlled dc motor with load*

The following assumptions are made in the derivation of the transfer function of field-controlled motor:

(a) a constant current i_a is fed into the armature;
(b) the air gap flux ϕ is proportional to field current i_f; and
(c) the torque developed by the motor is proportional to field current;

$$T_M = K_T' i_f;\ K_T' \triangleq \text{torque constant.}$$

The voltage applied to the field circuit is $E_f(s)$ which acts on a linear circuit comprising of resistance and inductance in series, having the transfer function $1/(L_f s + R_f)$. The result is a field current $I_f(s)$. For fixed armature current, the torque developed by the motor is $K_T' I_f(s)$. This torque rotates the load at a

Copyrighted material

speed $\omega(s)$ against the disturbance $T_w(s)$; the load having moment of inertia J and viscous-friction coefficient B has the transfer function $1/(Js + B)$. These cause and effect relationships are described by the block diagram of Fig. 3.25. The transfer function between the motor displacement $\theta(s)$ and the input voltage $E_f(s)$, obtained from the block diagram, is

$$\frac{\theta(s)}{E_f(s)} = \frac{K'_T}{s(L_f s + R_f)(Js + B)} = \frac{K'_m}{s(\tau_f s + 1)(\tau_m s + 1)} \tag{3.19}$$

where

$K'_m = K'_T/(R_f B)$ = motor gain constant;
$\tau_f = L_f/R_f$ = time-constant of the field circuit; and
$\tau_m = J/B$ = mechanical time-constant.

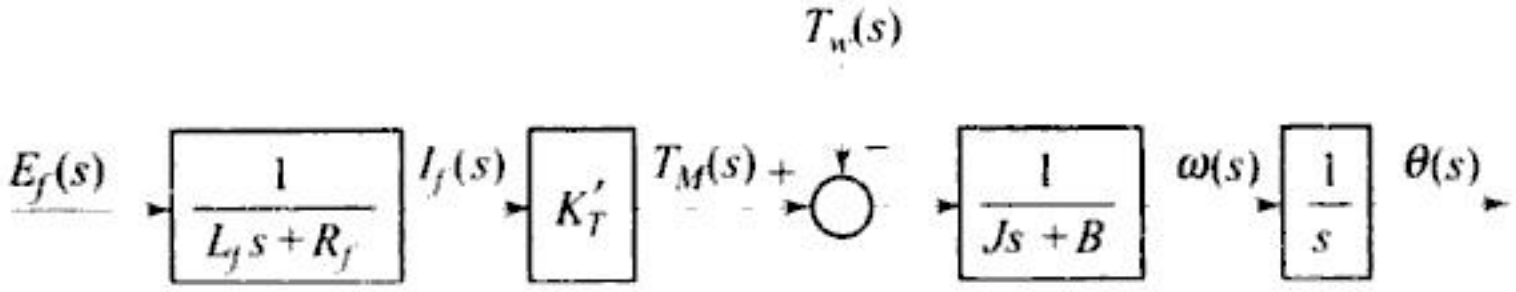


Fig. 3.25 *Block diagram of a field-controlled dc motor*

▲▲

Split-field motors are used to provide a smooth control of motor speed (or position) in low-power systems. The general arrangement is shown in Fig. 3.26, the armature current being kept substantially constant by using a high voltage E and a high value of resistance R. Providing that the back emf of the motor at its maximum speed is small compared with E, the armature current is approximately E/R. The field is energized by a balanced amplifier which has the input e_f. When this input is zero, the currents i_1 and i_2 are equal. Since they flow in opposite directions, the net flux is zero; thus the torque is zero and the motor is stationary. If e_f is not zero, one of the currents increases and the other decreases in proportion to the magnitude of e_f. The resulting flux is proportional to the magnitude of e_f, and its direction depends on the polarity of e_f. The size and direction of the generated torque and the resulting speed therefore respond to the magnitude and polarity of the input e_f.

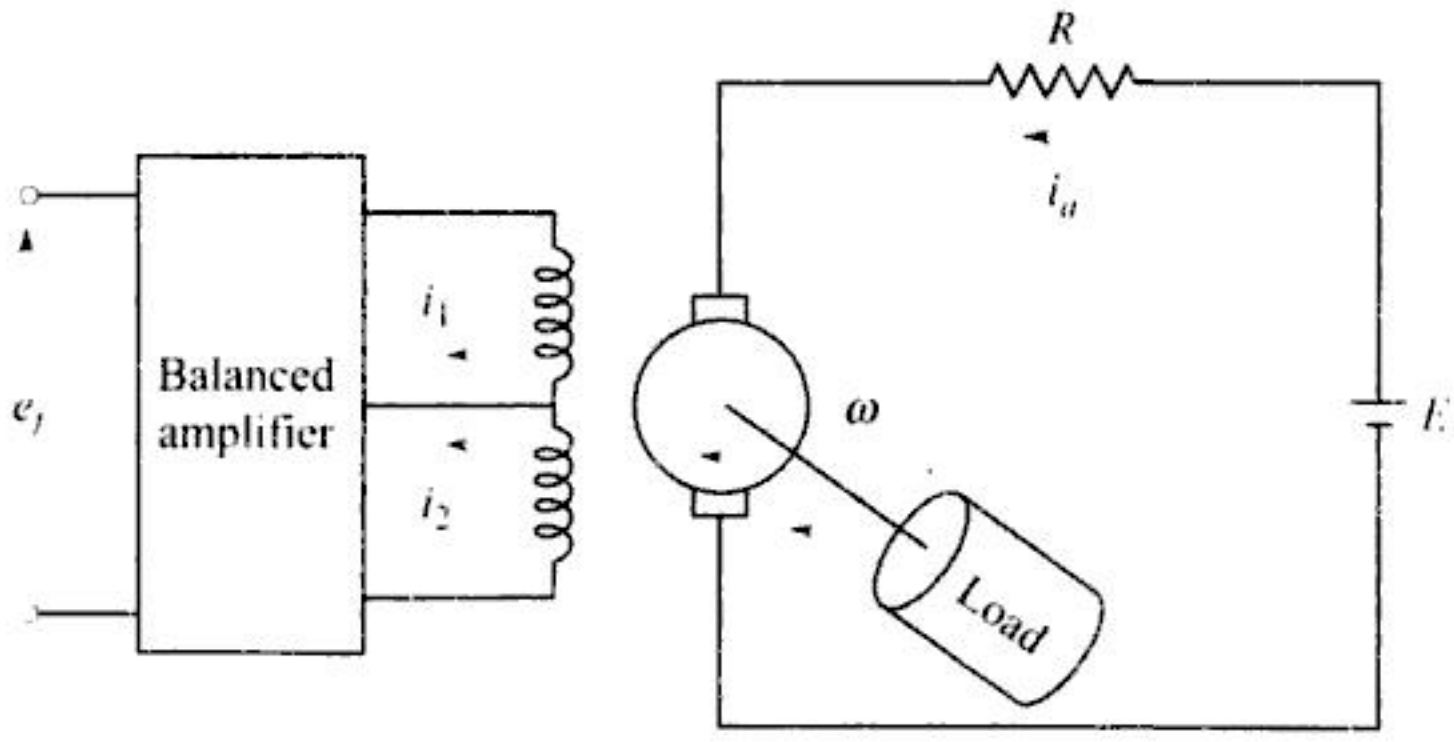


Fig. 3.26 *A split-field dc motor*

Copyrighted material

For small-size motors, field control is advantageous because only a low power servo amplifier is required while the constant armature current, which is not large, can be supplied from an inexpensive constant voltage source. This control scheme poses great practical difficulties in medium- and large-size motors; because of large back emf of the motor, the armature current cannot be kept constant by supplying a constant voltage to the armature. The assumption of constant armature current leads to the linear equations representing the operation of the motor. However, if instead, a constant voltage source is applied to the armature, the equation of the motor becomes nonlinear and cannot be handled by linear analysis methods. For this reason, it is normal practice to have a fixed excitation and control the armature current.

AC Servomotors

An ac servomotor is basically a two-phase induction motor except for certain special design features. A brief description of constructional and operational features of induction motors will be helpful in developing a mathematical model of an ac servomotor.

The two inputs required for motor action are a magnetic field and current-carrying conductors. In the dc motor, current for the conductors is supplied conductively by connection to a voltage source. In the ac induction motor, current for the conductors is supplied inductively by the change in the flux linkages of the conductors with the alternating magnetic field, supplied by an electromagnetic field structure excited by alternating current. The field windings are on the stationary part of the motor (stator) and the current carrying conductors are on the rotating part (rotor).

Figure 3.27a shows the physical arrangement of a two-phase field. This consists of two identical pole pairs A–B and C–D oriented 90° away from each other in space (space quadrature). The two currents used to excite the two pole pairs are 90° out of phase (time quadrature).

The simplest form of rotor construction is shown in Fig. 3.27b, comprising copper or aluminium conductors connected by stout end-rings formed into a cylindrical cage-like structure (squirrel-cage construction). The conductors pass through the laminated iron rotor core. Since no external connections are made to the rotor circuit, the motor can be made very robust and requires little maintenance. The machine characteristics can be modified by altering the rotor conductor resistance, and by having two or three sets of rotor bars set at different depths in the rotor.

The principle of operation of the induction motor is as follows. Voltages of equal rms magnitude and 90° phase difference are applied to the two field windings. This results in field currents i_1 and i_2 that are phase displaced by 90° and have equal rms values. These currents give rise to a rotating magnetic field of constant magnitude. The direction of rotation depends on the phase relationship of the two currents (or voltages). Assuming that the two currents shown in Fig. 3.27a result in CW rotation, then a phase shift of 180° in i_1 will cause rotation in CCW direction.

Copyrighted material

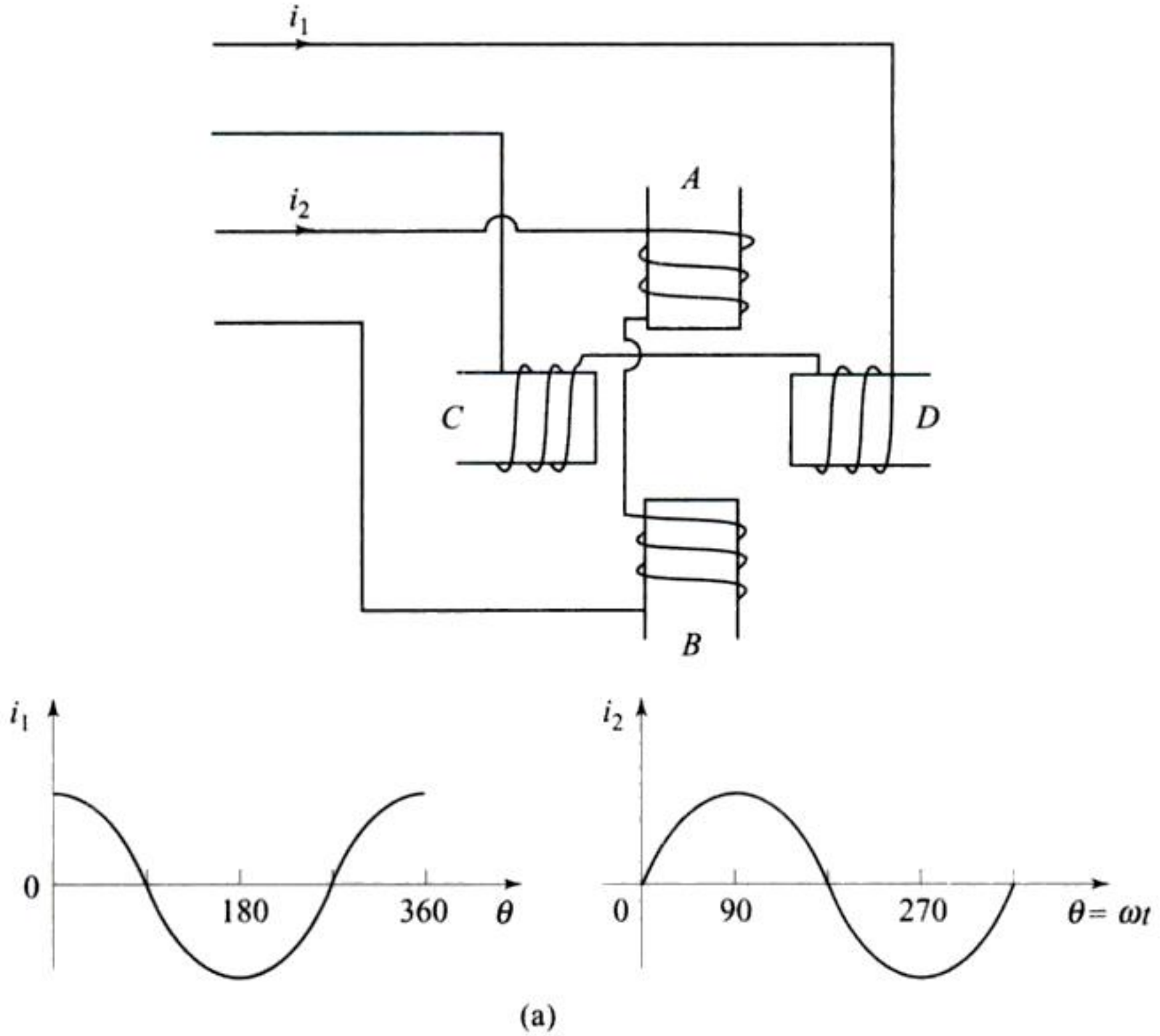


Fig. 3.27 *Constructional features of induction motor*

As the moving field sweeps over the rotor, voltages are induced in the rotor conductors, producing currents in the short-circuited paths. The rotating field interacts with these currents producing a torque on the rotor in the direction of field rotation. This torque causes the rotor to turn so that it chases the rotating magnetic field.

Elementary analysis of the ac motor is more complex than is that of the dc motor. So, rather than give the details of production of rotating magnetic field, and derivation of motor-torque equation, we present the experimental facts in the form of set of curves of speed versus torque. A typical set appears in

Copyrighted material

Fig. 3.28. For an induction motor used in power applications, the rotor resistance is low in order to obtain high maximum torque (Curve *A*, Fig. 3.28). However, this type of characteristic is not suitable for feedback control systems, mainly because of the positive slope on part of the curve. We will shortly see that a negative slope on the torque-speed curve is essential for stability (The dc motors inherently exhibit the desired torque-speed characteristic, Fig. 3.23). In order to obtain the desired type of characteristic, induction motors for servo applications are designed to have high rotor resistance (Curve *B*, Fig. 3.28). It should be noted that the required characteristic is purchased at a price of power which is dissipated as heat in the high rotor resistance. This decreases the efficiency of the motor and also limits its maximum power rating since the temperature rise in the motor becomes excessive for motors with high power rating.

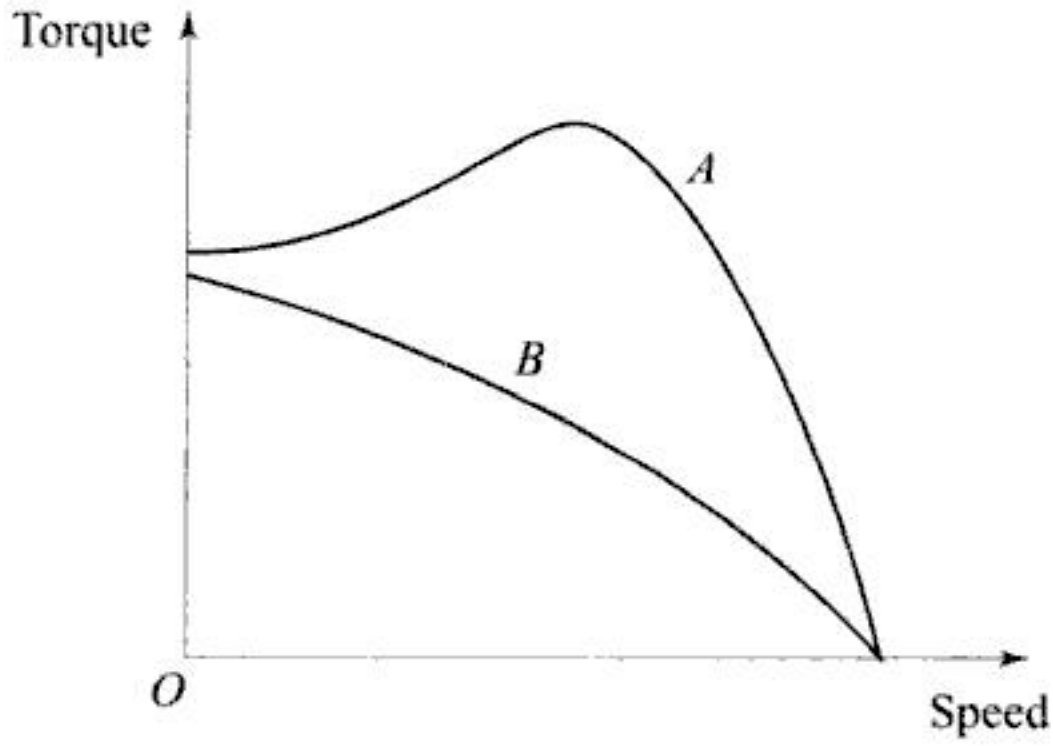


Fig. 3.28 *Torque-speed characteristics of ac motors*

In servo applications, an induction motor is required to produce rapid accelerations from standstill. Therefore, low inertia is a physical requirement of a servomotor. In a squirrel-cage construction, low inertia is attained with reduced rotor diameter (drag-cup construction is used for very low inertia applications [57]). Thus, except for minor differences in constructional features (rotor has high resistance and low inertia), an ac servomotor is essentially a two-phase induction motor.

The symbolic representation of an ac servomotor as a control system component is shown in Fig. 3.29. One phase, designated as the *reference phase*, is excited by a constant voltage source, the frequency of which is usually 50/60, 400, or 1000 Hz. By using frequencies of 400 Hz or higher, the system can be made less susceptible to low-frequency noise. Due to this feature, ac devices are extensively used in aircraft and missile control systems in which noise and disturbance often create problems.

The second phase of the servomotor, designated as the *control phase*, is excited by a voltage of variable magnitude and polarity. The control signal of the servo loop dictates the magnitude and polarity of this voltage.

Copyrighted material

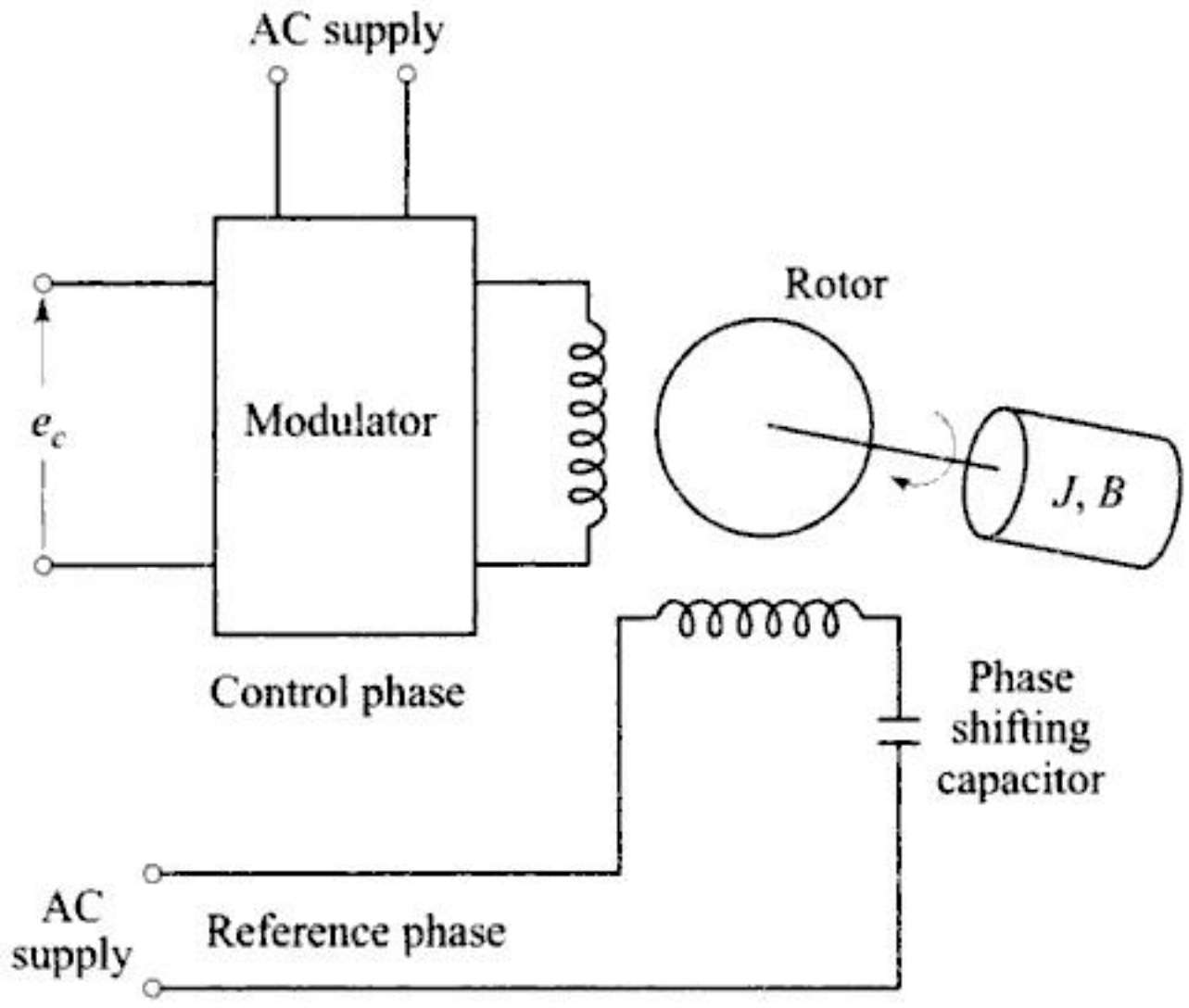


Fig. 3.29 *Symbolic representation of an ac servomotor*

The control signals in a servo loop are usually of low frequency, in the range of 0 to 20 Hz. For production of rotating magnetic field, the control-phase voltage must be of the same frequency as the reference-phase voltage, and in addition, the two voltages must be in time quadrature. The arrangement shown in Fig. 3.29 meets these requirements. The input signal $e_c(t)$ is applied to the control phase after modulation; the carrier frequency of the modulation process is equal to the frequency of the reference-phase supply. The 90° phase difference between the control-phase and reference-phase voltages is obtained by the insertion of a capacitor. (Note that a single-phase power supply is required to run the motor).

Figure 3.30 shows the waveforms of a typical input signal $e_c(t)$, the carrier signal $\cos \omega_c t$ and the *suppressed-carrier modulated signal* $e_{cm}(t) = e_c(t) \cos \omega_c t$. Note that the envelope of the modulated signal e_{cm} is identical to the low-frequency signal e_c. The polarity of e_c dictates the phase of e_{cm} with respect to that of $\cos \omega_c t$. If e_c is positive, then e_{cm} and $\cos \omega_c t$ have the same phase; otherwise they have 180° phase difference:

$$\begin{aligned} e_{cm}(t) &= |e_c(t)| \cos \omega_c t && \text{for } e_c(t) > 0 \\ &= |e_c(t)| \cos(\omega_c t + \pi) && \text{for } e_c(t) < 0 \end{aligned} \tag{3.20}$$

This means that a reversal in phase of e_{cm} occurs whenever the signal e_c crosses the zero-magnitude axis. This reversal in phase causes a reversal in the direction of rotation of the magnetic field and hence a reversal in the direction of rotation of the motor shaft.

The modulator in Fig. 3.29 transforms the signal e_c into the signal e_{cm}. If we consider e_c as the input and e_{cm} in Eqn. (3.20) as the output, then the math-

Copyrighted material

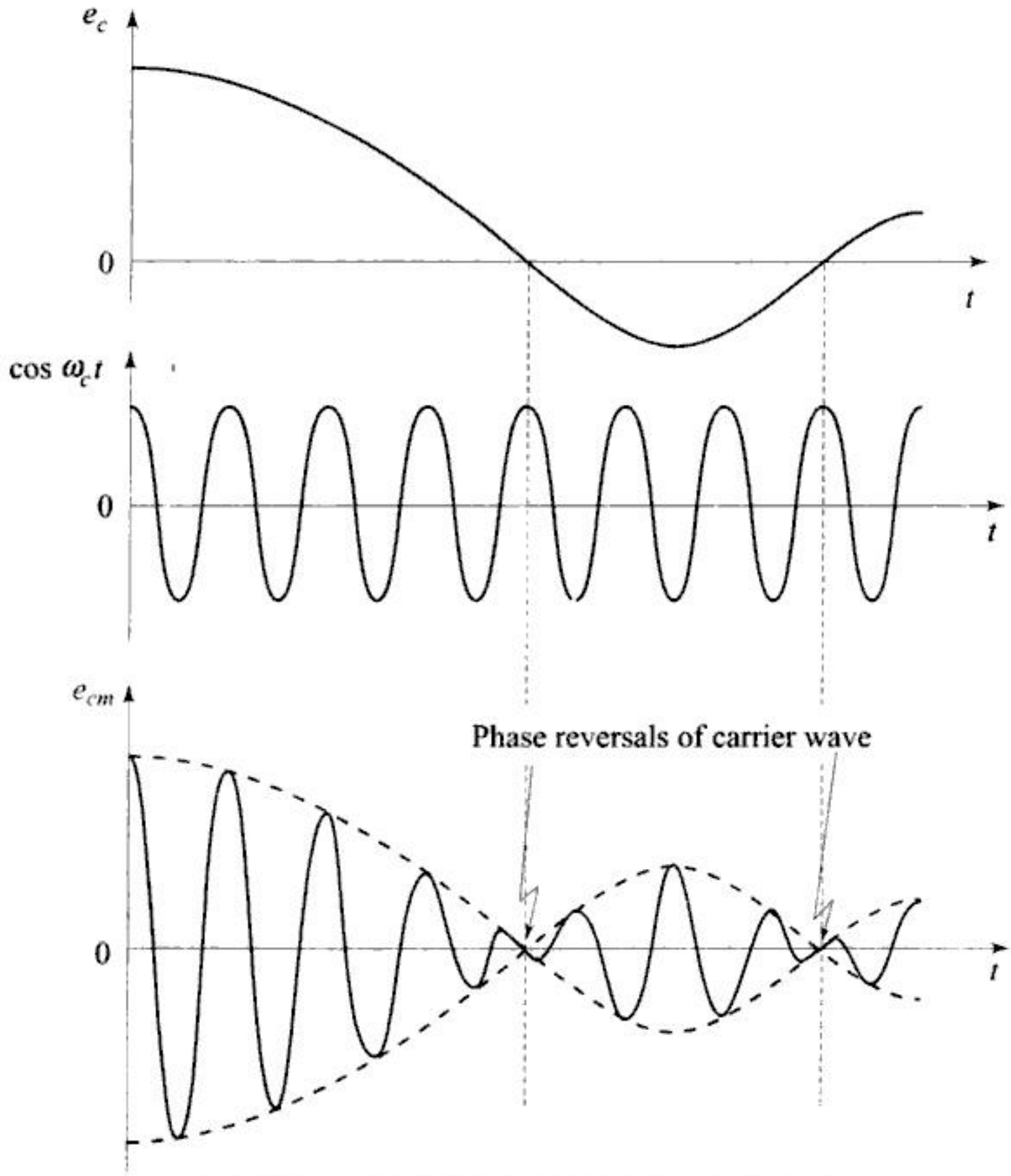


Fig. 3.30 *Input–output waveforms of a modulator*

ematical description of the modulator will be rather complicated. Recall that the reason for the introduction of e_{cm} is to match the operational frequency ranges; therefore the information is not stored in e_{cm}, but rather in its envelope. Hence, we should consider e_c as the input and the envelope of e_{cm} as the output of the modulator. Therefore, the transfer function of the modulator is just equal to 1, for the envelope of e_{cm} is identical to e_c.

The torque-speed curves of typical ac servomotor plotted for fixed reference-phase voltage $E_r \cos \omega_c t$ and different values of constant input voltages $e_c \leq E_r$ are shown in Fig. 3.31. All these curves have negative slope. Note that the curve for $e_c = 0$ goes through the origin; this means that when the control-phase voltage becomes zero, the motor develops a decelerating torque, causing it to stop. The curves show a large torque at zero speed. This is a requirement for a servomotor in order to provide rapid acceleration.

It is seen that the torque-speed curves of ac servomotor are nonlinear except in the low-speed region. In order to derive a transfer function for the motor, some linearizing approximations are necessary. A servomotor seldom operates

Copyrighted material



You have either reached a page that is unavailable for viewing or reached your viewing limit for this book.

$$T_M = K_1 e_c - K_2 \dot{\theta} \tag{3.21}$$

where K_1 and K_2 are the slopes defined in Figs 3.31 and 3.32. Note that both K_1 and K_2 are positive numbers.

If we consider that the moment of inertia of the motor rotor with attached mechanical load is J, the viscous-friction coefficient of the motor rotor with attached mechanical load is B, and the disturbance load torque is T_w, then we have

$$T_M = K_1 e_c - K_2 \dot{\theta} = J\ddot{\theta} + B\dot{\theta} + T_w \tag{3.22}$$

Figure 3.33 shows a block diagram representation of the ac motor system. The transfer function between the shaft position $\theta(s)$ and the input voltage $E_c(s)$, obtained from the block diagram, is

$$\frac{\theta(s)}{E_c(s)} = \frac{K_1}{s(Js + B + K_2)} = \frac{K_m}{s(\tau_m s + 1)} \tag{3.23}$$

where $K_m = \dfrac{K_1}{B + K_2}$ = motor gain constant

$\tau_m = \dfrac{J}{B + K_2}$ = motor time-constant

Since K_2 is a positive number, the above equations show that the effect of the slope of the torque-speed curve is to add more friction to the motor, which does improve the damping of the motor. However, if K_2 is a negative number, for $|K_2| > B$, negative damping occurs and the motor becomes unstable. This verifies the statement made previously that the conventional induction motors are not suitable for servo applications.

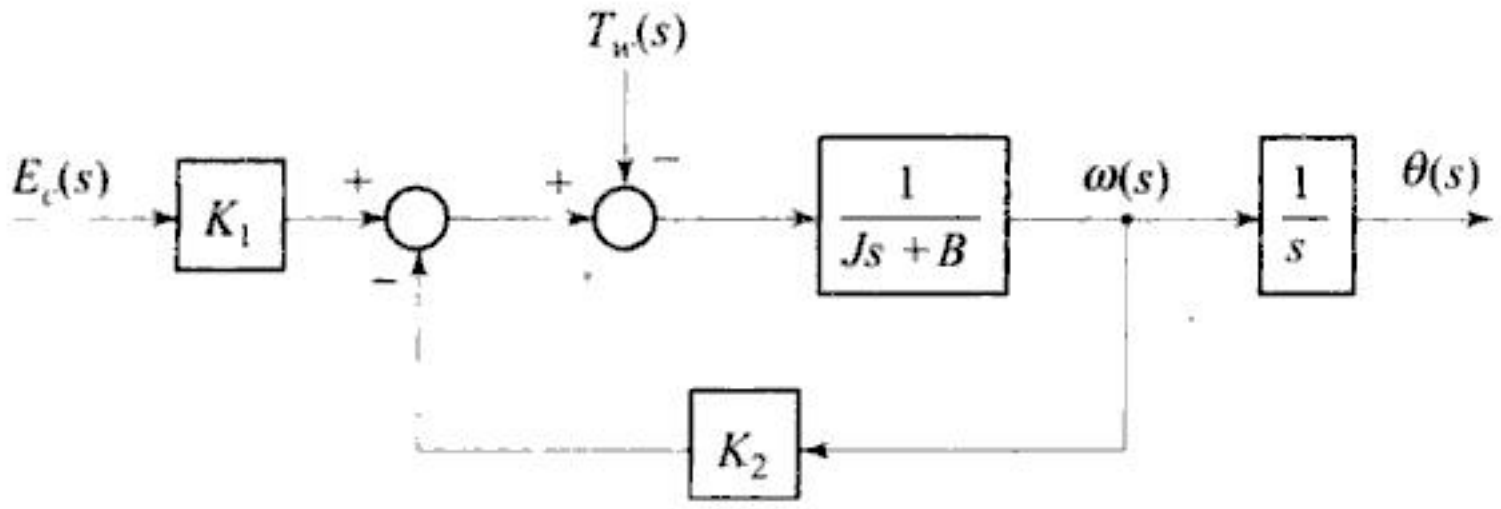


Fig. 3.33 *Block diagram of an ac motor system*

It must be noted that the modulation process for running the ac servomotor is not necessary if the control signal in the servo loop is an ac signal of frequency equal to that of reference phase supply. The transfer function model given by Eqn. (3.23) is applicable in these situations also, with the only difference that the input variable for the model is not the control-phase voltage itself but rather its envelope. This is in order as the information about the required control action is stored in the envelope of the control-phase voltage; the frequency of the voltage is governed only by the operational frequency range of the servomotor.

Copyrighted material

3.6 MOTION CONTROL SYSTEMS

This section is concerned with speed and position control systems, and the components that make up these systems. We begin with the discussion of the commonly used components. Here, our discussion is restricted to devices used in analog control systems. The devices commonly used in digital control systems are covered later in Chapter 11.

Geared Drives

Electrical motors generally produce their maximum power at high speed. In other words, generally electrical motors exert rather small torques while rotating at high speeds (power = torque × angular velocity). In consequence, appropriate gearing is necessary for the electrical motors in order for these systems to drive large loads (requiring large torques) at low speeds. For example, robot arms are usually moved at low speeds, less than 1 revolution/sec, while required maximum torques range from a few newton-m to several hundred newton-m. A large gear reduction is typically required for standard servomotors.

Figure 3.34 shows a motor driving a load through a gear train which consists of two gears coupled together. The gear with N_1 teeth is called the primary gear and the gear with N_2 teeth is called the secondary gear. Angular displacements of shafts 1 and 2 are denoted by θ_1 and θ_2 respectively with their positive directions as indicated in the figure. The moment of inertia and viscous friction of motor and gear 1 are denoted by J_1 and B_1 respectively, and those of gear 2 and load are denoted by J_2 and B_2 respectively. T_M is the torque developed by the motor and T_w is the disturbance torque on the load. Elasticity of the gear teeth and shafts is assumed negligible.

A free-body diagram is shown in Fig. 3.35. T_{12} is the torque exerted on gear 1 by gear 2, and T_{21} is the torque transmitted to gear 2 through gear 1. For the motor shaft, the differential equation is

$$J_1\ddot{\theta}_1 + B_1\dot{\theta}_1 + T_{12} = T_M \tag{3.24}$$

For the load shaft,

$$J_2\ddot{\theta}_2 + B_2\dot{\theta}_2 + T_w = T_{21} \tag{3.25}$$

Idealized characteristic of the gear train is given by the relationship $\theta_2 = (N_1/N_2)\ \theta_1$. In reality, there is always a certain amount of backlash (free play) between coupled gears. Keeping the backlash small will inevitably increase the friction between the teeth, and wear out the teeth faster. On the other hand, an excessive amount of backlash may cause sustained oscillations or chattering phenomenon in control systems (refer [180]). The assumption of zero backlash is reasonable for high quality, well-adjusted gear boxes.

Copyrighted material

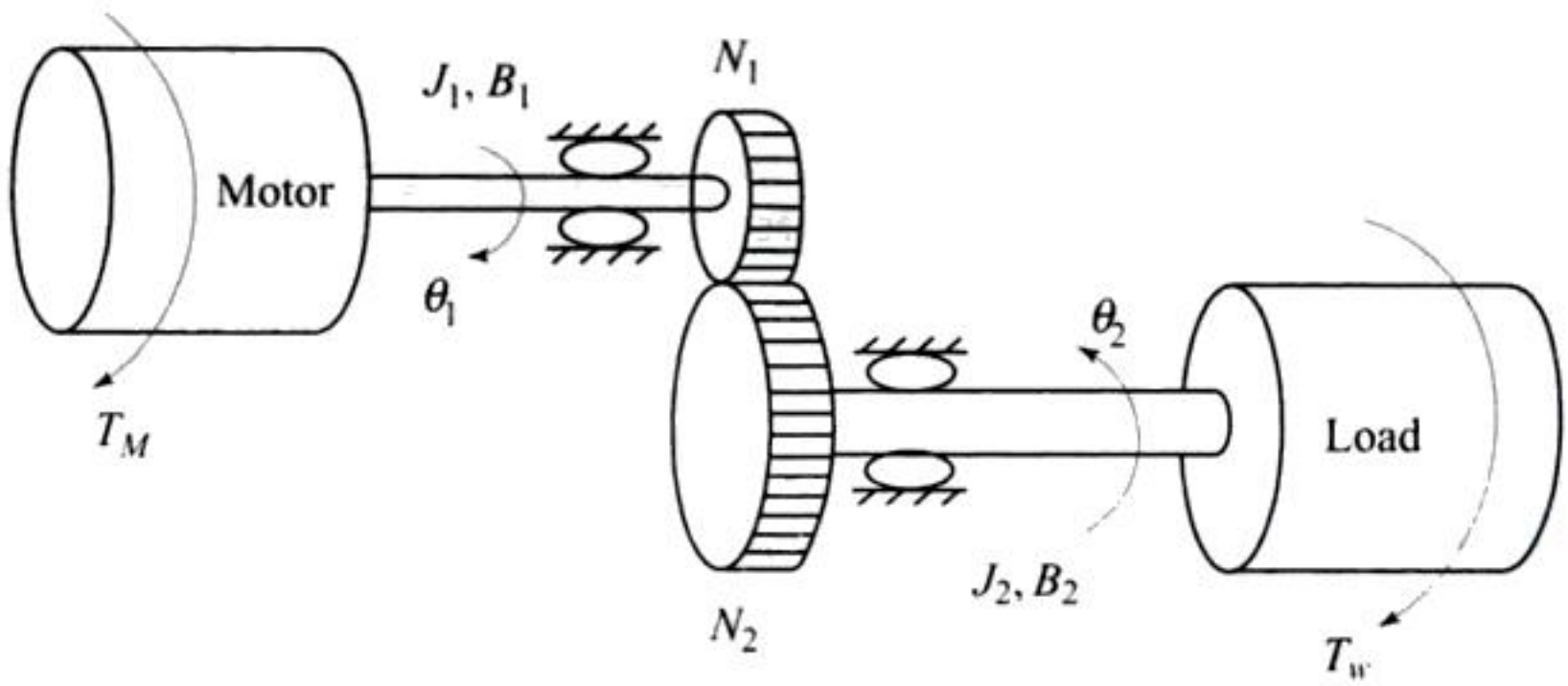


Fig. 3.34 *Motor driving a load through gearing*

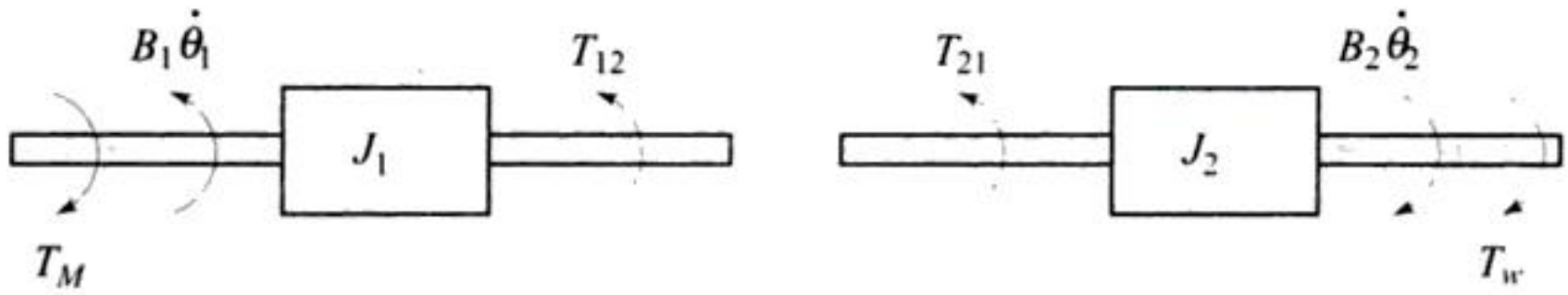


Fig. 3.35 *Free-body diagram for system of Fig. 3.34*

Let r_1 be the radius of gear 1 and r_2 be the radius of gear 2. Since the linear distance travelled along the surface of each gear is the same, $\theta_1 r_1 = \theta_2 r_2$. The number of teeth on a gear surface being proportional to gear radius, we have $(N_1 / r_1) = (N_2 / r_2)$. The linear forces developed at the contact point of both the gears are equal, hence $(T_{12} / r_1) = (T_{21} / r_2)$. By combining these equalities, we obtain

$$\frac{T_{12}}{T_{21}} = \frac{N_1}{N_2} = \frac{\theta_2}{\theta_1} \tag{3.26}$$

Differentiating this equation twice, we have the following relation for speed and acceleration:

$$\frac{\ddot{\theta}_2}{\ddot{\theta}_1} = \frac{\dot{\theta}_2}{\dot{\theta}_1} = \frac{N_1}{N_2} \tag{3.27}$$

From Eqns (3.26) and (3.27), it is observed that with $(N_1 / N_2) < 1$, the gear train provides torque magnification and speed reduction. By proper selection of N_1 / N_2, gear trains can be used to attain mechanical matching of motor to load: a servomotor operating at high speed and generating low torque is matched to a load to be moved at low speed but requiring high torque.

Eliminating T_{12} and T_{21} from Eqns (3.24) and (3.25) with the help of Eqn. (3.26), we obtain

$$J_1\ddot{\theta}_1 + B_1\dot{\theta}_1 + \frac{N_1}{N_2}(J_2\ddot{\theta}_2 + B_2\dot{\theta}_2 + T_w) = T_M \tag{3.28}$$

Copyrighted material

Elimination of θ_2 from Eqn. (3.28) with the help of Eqn. (3.27), yields

$$\left[J_1 + \left(\frac{N_1}{N_2}\right)^2 J_2\right]\ddot{\theta}_1 + \left[B_1 + \left(\frac{N_1}{N_2}\right)^2 B_2\right]\dot{\theta}_1 + \frac{N_1}{N_2} T_w = T_M \qquad (3.29)$$

Note that the load inertia J_2 is reflected on the motor shaft as $(N_1/N_2)^2 J_2$, load viscous-friction B_2 is reflected on the motor shaft as $(N_1/N_2)^2 B_2$, and the load disturbance T_w is reflected on the motor shaft as $(N_1/N_2)\, T_w$.

Equation (3.29) suggests that the geared system of Fig. 3.34 is equivalent to non-geared (direct drive) system of Fig. 3.36 with equivalent moment of inertia

$$J_{1eq} = J_1 + \left(\frac{N_1}{N_2}\right)^2 J_2, \qquad (3.30a)$$

equivalent friction

$$B_{1eq} = B_1 + \left(\frac{N_1}{N_2}\right)^2 B_2 \qquad (3.30b)$$

and equivalent disturbance torque

$$T_{weq} = \left(\frac{N_1}{N_2}\right) T_w \qquad (3.30c)$$

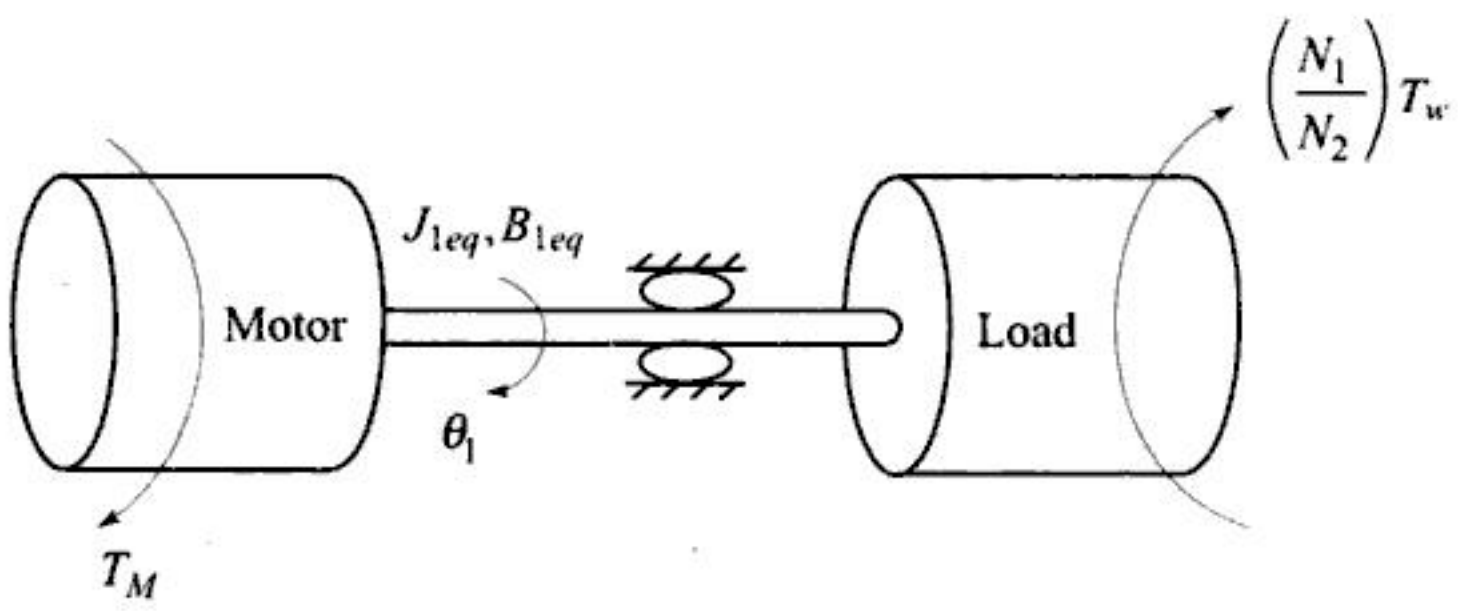


Fig. 3.36 *Equivalent direct-drive system for the geared system of Fig. 3.34*

▲▲

The problems that the mechanical gearing unavoidably possesses (backlash, friction, etc.), can be solved completely using the *direct-drive technology*. An order of magnitude larger torque must be generated by direct-drive motors in a compact and light-weight body. The dc torque motors are capable of exerting much larger torque compared with regular dc motors. These motors are designed in such a way that the output torque rather than power is maximized (refer [22] for details).

Copyrighted material

Electronic Amplifiers

Broadly speaking, there are two types of electronic amplifiers used in control systems:

(a) A *small signal amplifier* is one which linearly amplifies a small signal (usually voltage) and is suitable for sensor circuits to amplify weak measured signals. The operational amplifier (usually called the op amp) is in common use.

From the block diagram of Fig. 3.2, we see that a control signal in a feedback loop is a function of the error signal. The functional dependence is given by the controller transfer function $D(s)$. Mechanization of $D(s)$, as we shall see in the next chapter, usually requires amplification of the error signal, and generation of the derivative and the integral of the error signal. Op amp circuits are now commonly used for mechanization of the controller transfer function $D(s)$.

(b) A *power amplifier* is one which controls a large amount of power, and is therefore suitable for actuating devices.

Power amplifiers are available in three major types: the smooth transistor, the switching transistor (pulse-width modulated (PWM)), and the silicon control rectifier (SCR). Smooth transistor amplifiers use the transistors in a smooth modulating fashion and produce an output voltage that is high-power copy of the input. These amplifiers are used mainly below 1 kW applications. Switching (PWM) amplifiers use the transistors as on–off switches; the output voltage is a constant-frequency, fixed-amplitude waveform whose duty cycle is smoothly varied with input voltage. Switching amplifiers are economical in the 25 W to 5 kW range. In SCR amplifiers, the input voltage smoothly modulates the point in each power-line cycle at which the SCR (this term arises from the device as controlled rectifier constructed from silicon), also known as the *thyristor*, is made to conduct. These amplifiers are often used in high power applications.

To be precise, the transfer function of an electronic amplifier is of the form

$$G(s) = \frac{K_A}{\tau_A s + 1} \tag{3.31}$$

However, usually the time constant τ_A is negligibly small compared to the dynamics of the plant; the transfer function can therefore be approximated as

$$G(s) = K_A \tag{3.32}$$

where K_A is the proportional gain of the amplifier.

In addition to neglecting 'fast' dynamics, the model (3.32) of the amplifier further differs from reality because of its perfect linearity which assumes no limit on the magnitude of the input signal. Actually the amplifier, like other devices, exhibits saturation, limiting its output when input becomes too large (refer [180]).

Copyrighted material



You have either reached a page that is unavailable for viewing or reached your viewing limit for this book.



You have either reached a page that is unavailable for viewing or reached your viewing limit for this book.



You have either reached a page that is unavailable for viewing or reached your viewing limit for this book.



You have either reached a page that is unavailable for viewing or reached your viewing limit for this book.

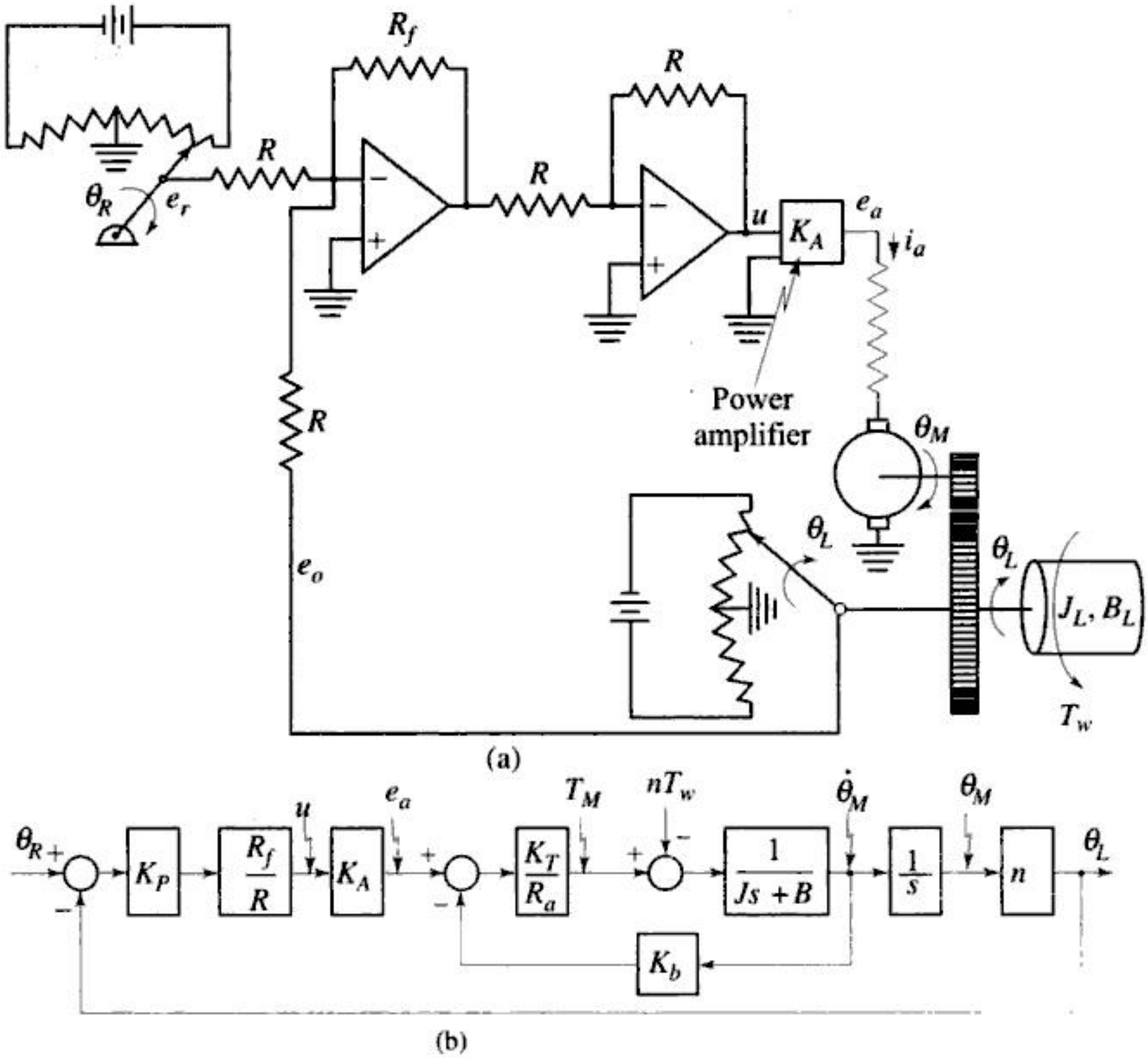


Fig. 3.40 *Closed-loop position control system (a) Schematic diagram (b) block diagram*

for the position control of arms. Usually each degree of freedom employs its own actuator and this example has relevance to the control of a single axis (see Fig. 1.28).

The operation of the system is as follows. The load with an inertia J_L and viscous friction with coefficient B_L is to be positioned at some desired angle θ_R (T_w represents the load torque disturbance). The desired angle θ_R may be set, as shown in Fig. 3.40a, on an input potentiometer which provides the reference voltage e_r. The feedback potentiometer, whose wiper arm is mechanically coupled to the load shaft, produces a voltage e_o which represents the actual load position θ_L. The error voltage $(e_r - e_o)$ is amplified by an op amp circuit that supplies a voltage u to a power amplifier. The output e_a of the power amplifier drives the armature-controlled dc motor (reversal in the polarity of e_r reverses the direction of rotation of the motor). The torque developed by the motor is transmitted to the load shaft through a gear train. The transmitted torque rotates the load shaft in the direction to reduce the error $(e_r - e_o)$ as a consequence of the negative feedback. When $e_r = e_o$, the motor stops, as its drive is

Copyrighted material

cut off. This must necessarily occur when $\theta_R = \theta_L$ because both the potentiometers have the same sensitivity K_P:

$$e = K_P\theta \tag{3.35}$$

where K_P = sensitivity of the potentiometer is volts/deg.

A change in the load position caused by disturbances in the system (internal or external) causes the error signal $(e_r - e_o)$ to reappear, which after amplification acts on the motor; the motor torque transmitted to the load shaft forces the load to return to its original position.

A block diagram of the system is shown in Fig. 3.40b (refer Eqns (3.10)–(3.13), (3.30), and Fig. 3.22). Here K_b is the back emf constant of the motor, R_a is the armature resistance (armature inductance is assumed negligible), K_T is the torque constant of the motor, n is the gear ratio (n = load shaft speed $\dot{\theta}_L$/ motor shaft speed $\dot{\theta}_M$), J and B are, respectively, equivalent moment of inertia and viscous-friction coefficient on motor shaft, and nT_w is the equivalent disturbance torque on motor shaft.

It will be seen in the next chapter that the performance of position control system of Fig. 3.40 can be improved by introducing minor-loop feedback (refer Figs 1.15 and 1.16). A signal proportional to motor/load angular velocity, generated by a tachometer, is fedback. Since tachometers tend to be noisy at low speeds, in a geared system one usually puts the tacho on the motor, rather than the load.

Potentiometers, LVDT and Synchros

Potentiometers

For conversion of a linear or an angular displacement into voltage, a potentiometer (refer Figs 3.39a and 3.40a) is probably the simplest device. Potentiometric transducers are relatively inexpensive and easy to apply. However, they have some limitations. The resolution (minimum change in output voltage obtained by moving the wiper, expressed as a percentage of the total applied voltage) of precision wire-wound potentiometers (constructed by winding resistance wire on a form) ranges from 0.001 to 0.5 percent. This discontinuous output voltage contributes to servo inaccuracy. Potentiometers are temperature-sensitive, a characteristic that affects their accuracy. The wiper contact is another limiting factor, being subject to wear and dirt and potentially producing electrical noise.

In a large number of control systems, the low-amplitude high-frequency noise generated by the potentiometer does not create problems. This is because the plant usually acts as a low-pass filter. However, if the potentiometer output is differentiated to obtain a measure of velocity, the resulting signal will be completely useless.[3]

3. Differentiation of the signal $\sin t$ contaminated by low-magnitude high-frequency noise $0.01 \sin 10^3 t$ gives $(\cos t + 10 \cos 10^3 t)$; noise becomes the dominant term after differentiation.

Copyrighted material

A non-wire potentiometer (constructed by depositing conductive plastic resistance material on a form) is stepless and therefore resolution is better. However, values less than 1000 Ω are hard to obtain with non-wire type of potentiometers, while wire-wound potentiometers can be made with very low values.

The applied voltage of a potentiometer can be either a dc or an ac source. In case of an ac source, the information is transmitted in the envelope of the output voltage signal.

In addition to the potentiometer, displacement can also be measured electrically with a *linear variable differential transformer* (LVDT) or a *synchro*. An LVDT measures a linear displacement, and a synchro measures an angular displacement. These devices are more costly but outperform the potentiometric transducers.

Linear Variable Differential Transformer

The schematic diagram of an LVDT is shown in Fig. 3.41. A primary coil is wound between two secondary coils on a hollow cylindrical form. A movable core is positioned inside the coil form. The primary is excited by an ac source. When the core is in its exact centre position ($y = 0$), the two secondaries are linked by an equal number of flux lines; the emf induced in secondary 1 will be the same as the emf induced in secondary 2. The two secondaries are so connected that their induced voltages oppose each other, and the output voltage

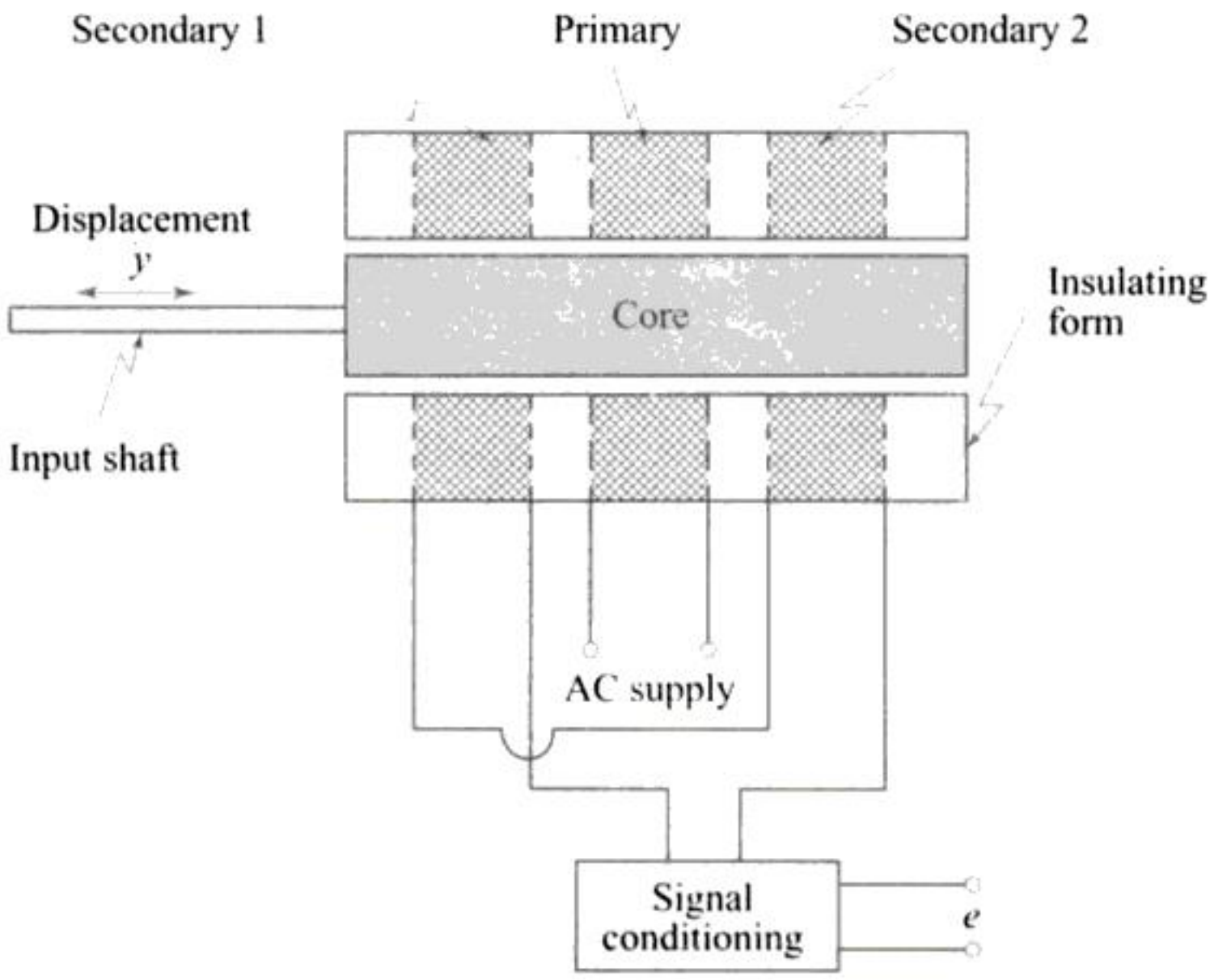


Fig. 3.41 *Linear variable differential transformer (LVDT)*

Copyrighted material

will be zero corresponding to $y = 0$. When the core is moved to the right, fewer lines of flux link secondary 1 than secondary 2. Thus a greater emf is induced in secondary 2 than in secondary 1 and a net voltage appears at the output. When the core is moved to the left, a net voltage will again appear at the output, but it is in anti-phase to that for an equivalent displacement to the right.

The output voltage of LVDT is in a modulated form, i.e.,

$$e_m(t) = K y(t) \sin \omega_c t$$

where ω_c, the carrier frequency, is the same as the frequency of ac supply. The magnitude of the modulated carrier wave is proportional to the core displacement $y(t)$ with K as the constant of proportionality, and the phase reversals of the modulated carrier wave depend on the sign of $y(t)$ (refer Fig. 3.38).

Signal conditioning by a demodulator and an amplifier gives an output voltage

$$e(t) = K_s y(t) \tag{3.36}$$

where K_s = sensitivity of the displacement transducer in volts/mm.

Synchros

The term *synchro* is a generic name for a family of inductive devices which can be connected in various ways to form shaft angle measurements. All of these devices work on essentially the same principle, which is that of a rotating transformer.

A synchro system formed by interconnection of the devices called the *synchro transmitter* and the *synchro control transformer*, is perhaps the most widely used error detector in feedback control systems. It measures and compares two angular displacements and its output voltage is approximately linear with angular difference. Our discussion on synchro devices will be limited to the basic features of the synchro transmitter and the synchro control transformer.

The constructional features, electrical circuit, and a schematic symbol of a synchro transmitter are shown in Fig. 3.42. The stationary part of the machine (stator) is of laminated silicon steel and is slotted to accommodate three Y connected coils wound with their axes 120° apart. The stator windings are not directly connected to the ac power source. Their excitation is supplied by the ac magnetic field produced by the rotating part of the machine (rotor).

The rotor is of dumb-bell construction with a single winding. A single-phase excitation voltage is applied to the rotor through two slip rings. The resultant current produces a magnetic field and by transformer action induces voltages

Copyrighted material



You have either reached a page that is unavailable for viewing or reached your viewing limit for this book.



You have either reached a page that is unavailable for viewing or reached your viewing limit for this book.



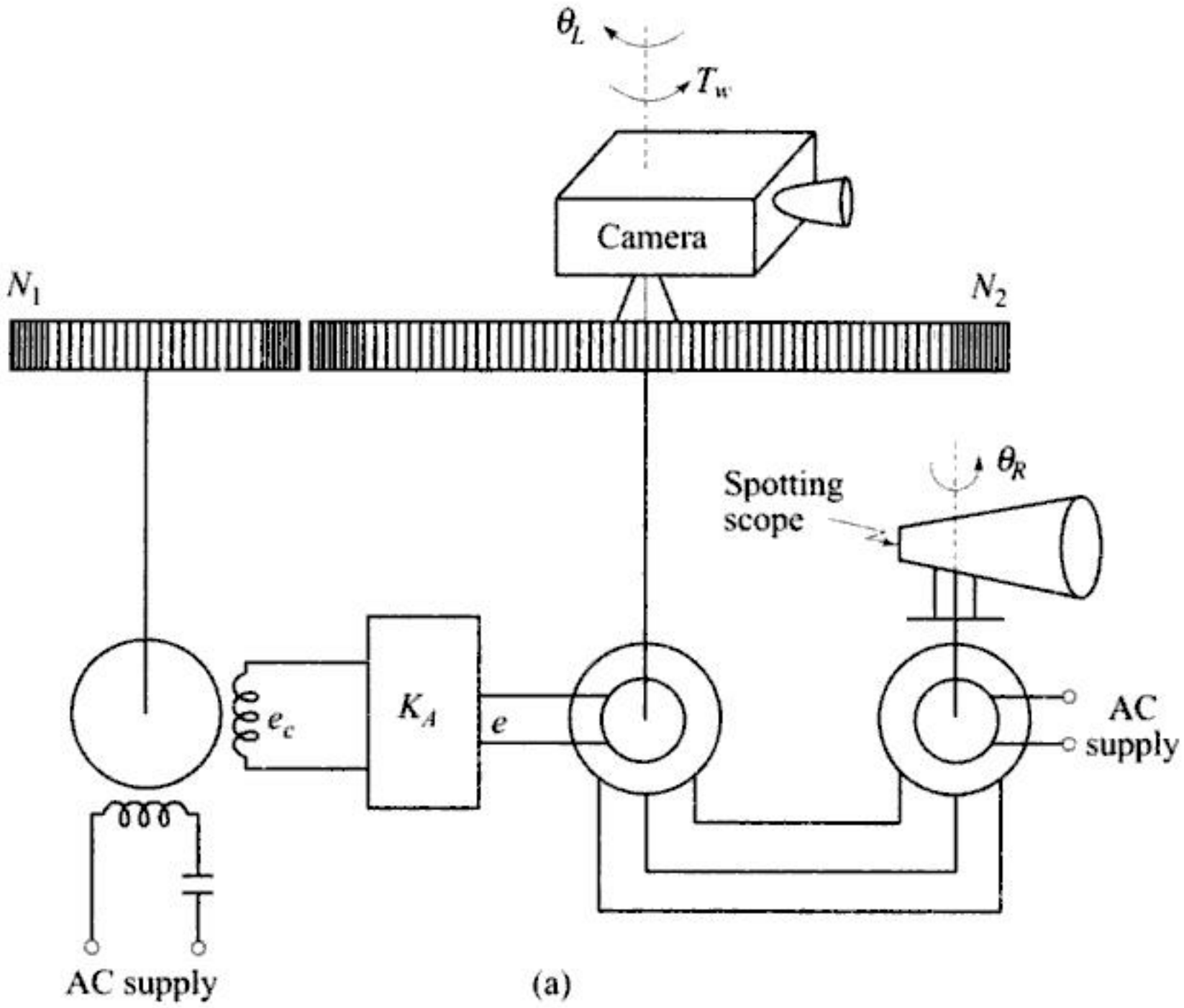
You have either reached a page that is unavailable for viewing or reached your viewing limit for this book.



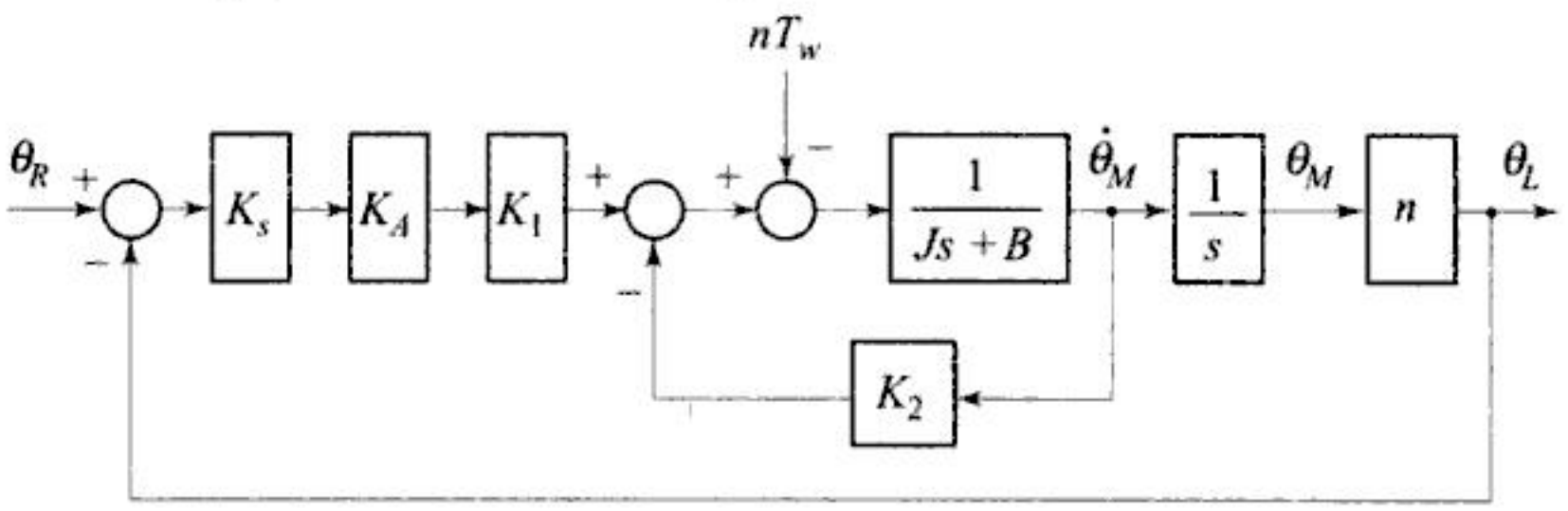
You have either reached a page that is unavailable for viewing or reached your viewing limit for this book.



You have either reached a page that is unavailable for viewing or reached your viewing limit for this book.



(a)



(b)

Fig. 3.45 *An ac (carrier) control system (a) schematic diagram (b) block diagram*

and the equivalent viscous-friction coefficient

$$B = B_M + n^2 B_L$$

nT_w is the equivalent disturbance torque on the motor shaft.

In terms of these parameters, the torque equation of the system becomes

$$T_M = J\ddot{\theta}_M + B\dot{\theta}_M + nT_w$$

A block diagram of the system is shown in Fig. 3.45b.

Copyrighted material

In the electromechanical servo of Fig. 3.40, angle measurement and comparison is by means of a synchro pair. Compared with potentiometers, the synchros offer higher sensitivity, longer life, ruggedness, and continuous rotation capability.

The output of the synchro error detector is a carrier-modulated signal. The information about the misalignment of the two shaft positions is carried by the envelope of this signal. As we shall see in the next chapter, generation of the control signal requires processing on the information signal, i.e., the envelope of the synchro-output signal. For example, we may require derivative and/or integration of the information signals in addition to amplification. A demodulator provides the necessary interface between the synchro error detector and the op amp circuit for generating the control signal. The low-frequency control signal can drive a dc motor after power amplification. Alternatively, the control signal may be modulated to drive an ac motor.

3.7 HYDRAULIC DEVICES FOR MOTION CONTROL

Hydraulically operated devices are frequently used in control systems. In these devices, power is transmitted through fluid flow under pressure. The fluid used is relatively incompressible such as petroleum-based oils or certain non-inflammable synthetic oils.

There are certain advantages and disadvantages in using hydraulic systems. The important ones are listed below.

1. A comparatively small-size hydraulic actuator using high-pressure fluid can develop very large forces or torques to provide rapid acceleration or deceleration of heavy loads. Hence, for the same horse power, hydraulic actuators are lighter than electric motors and considerable reduction in size and weight can be achieved.
2. Hydraulic components are more rugged and more resistant to vibrations and shocks than electrical components.
3. Availability of both the hydraulic linear actuators and rotary motors makes the design versatile.
4. Electrical power is readily available; for hydraulic systems, a source of pressurized hydraulic fluid with supply and return lines is required.
5. It has to be ensured that dirt does not contaminate the hydraulic fluid; this may lead to the failure of the components.
6. Leaks can be a problem and cause fire hazards unless fire-resistant hydraulic fluids are used.
7. The cost of a hydraulic system may be higher than a comparable electrical system performing a similar function.

When both high speed and high power are required, hydraulic systems may be mandatory or desirable. Common hydraulic control applications are power steering and brakes in automobiles, steering mechanism of ships, aircraft con-

Copyrighted material

trol surface actuators, control of large machine tools, servo systems for cranes and hoists, robots, and rolling mills, etc.

Some of the important hydraulic devices are discussed in this section.

Hydraulic Actuators

The hydraulic output devices used in control systems are generally of two types—those intended to produce rotary motion and those whose output is translational. The first type is known as the hydraulic motors and the second ones known as the hydraulic linear actuators.

The hydraulic linear actuator shown in Fig. 3.46 consists of a pilot valve and a power cylinder. The piston inside the power cylinder divides the cylinder into two chambers. The pilot valve—known as *spool valve* because of its shape—controls the flow rate of the hydraulic fluid to the power cylinder. It is a four-port valve: one port is connected to the hydraulic fluid supply at constant pressure, two control ports are connected to each chamber of the cylinder, and the drain port (the two drain ports are joined) is connected to the reservoir. The valve spool has two lands.

When the spool is in the neutral position ($x = 0$), the fluid flow in the power cylinder is blocked completely and the position of the piston, which moves the load, is $y = 0$. As the spool is moved to the right (x positive), the right-chamber port of the power cylinder is opened to the supply pressure P_s whereas the left-

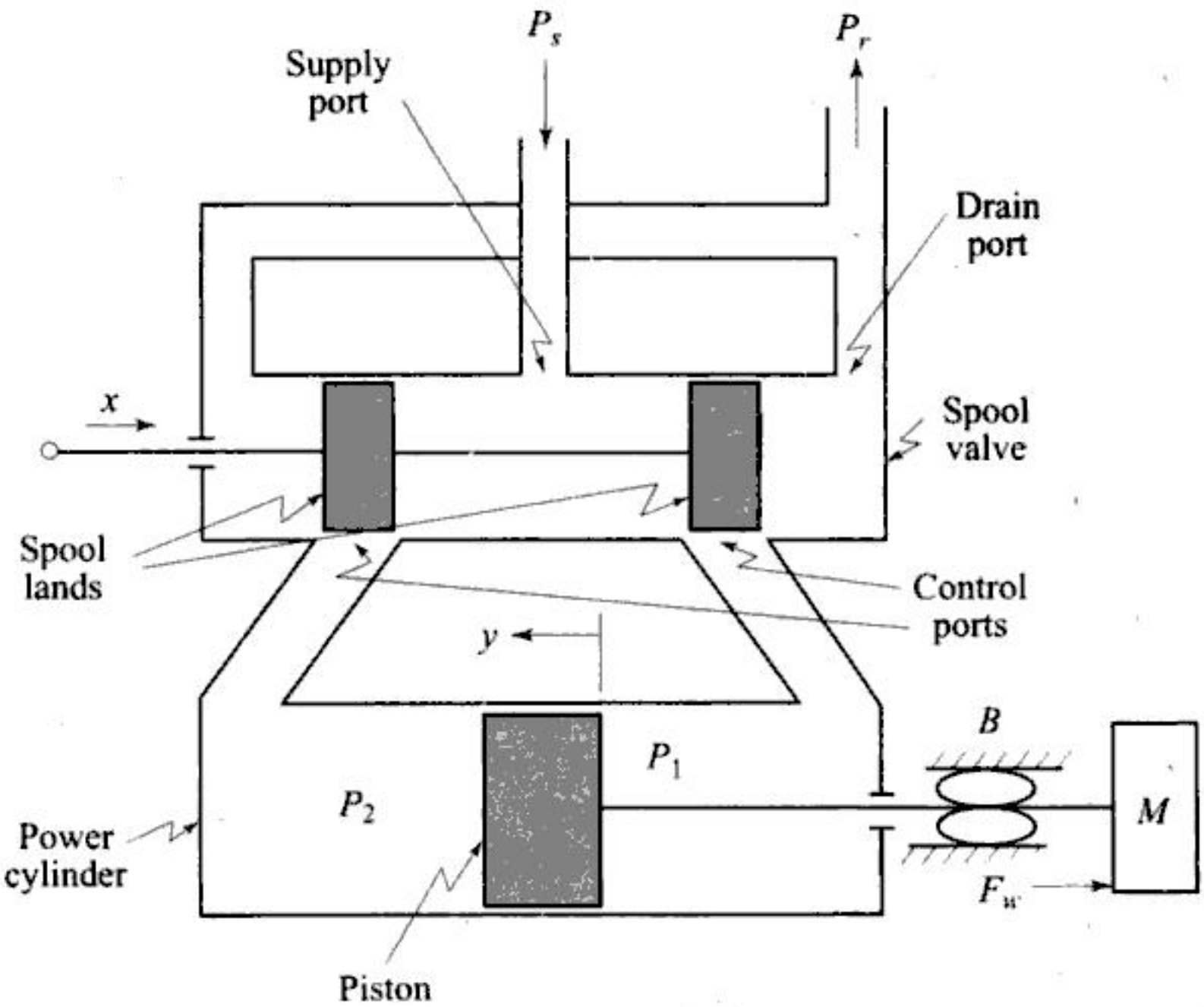


Fig. 3.46 *Hydraulic linear actuator with a load*

Copyrighted material

chamber port is opened to pressure P_r, which is slightly above the atmospheric pressure but we approximate it as zero gauge pressure in our model. Right-chamber pressure P_1 thus rises (while left-chamber pressure P_2 falls), producing an accelerating force on the load that moves to the left (y positive). If the spool is moved to the left (x negative), the left-chamber port of the power cylinder is opened to the supply pressure P_s, whereas the right-chamber port is opened to P_r. The direction of the fluid flow in the cylinder and hence the direction of displacement y of the load is reversed. This hydromechanical system acts as a power amplifier since the power (force × velocity) applied to position the valve is much smaller than that developed at the load.

Note that when the valve spool is in its neutral position, the flow area of the control ports is not in general zero. This is because spool lands and ports cannot be manufactured with perfectly sharp edges. Thus, a real valve will either be underlapped or overlapped (Fig. 3.47). Since an overlapped valve causes a dead zone for small spool motions (which is undesirable in control systems [180]), underlapped valves are often preferred.

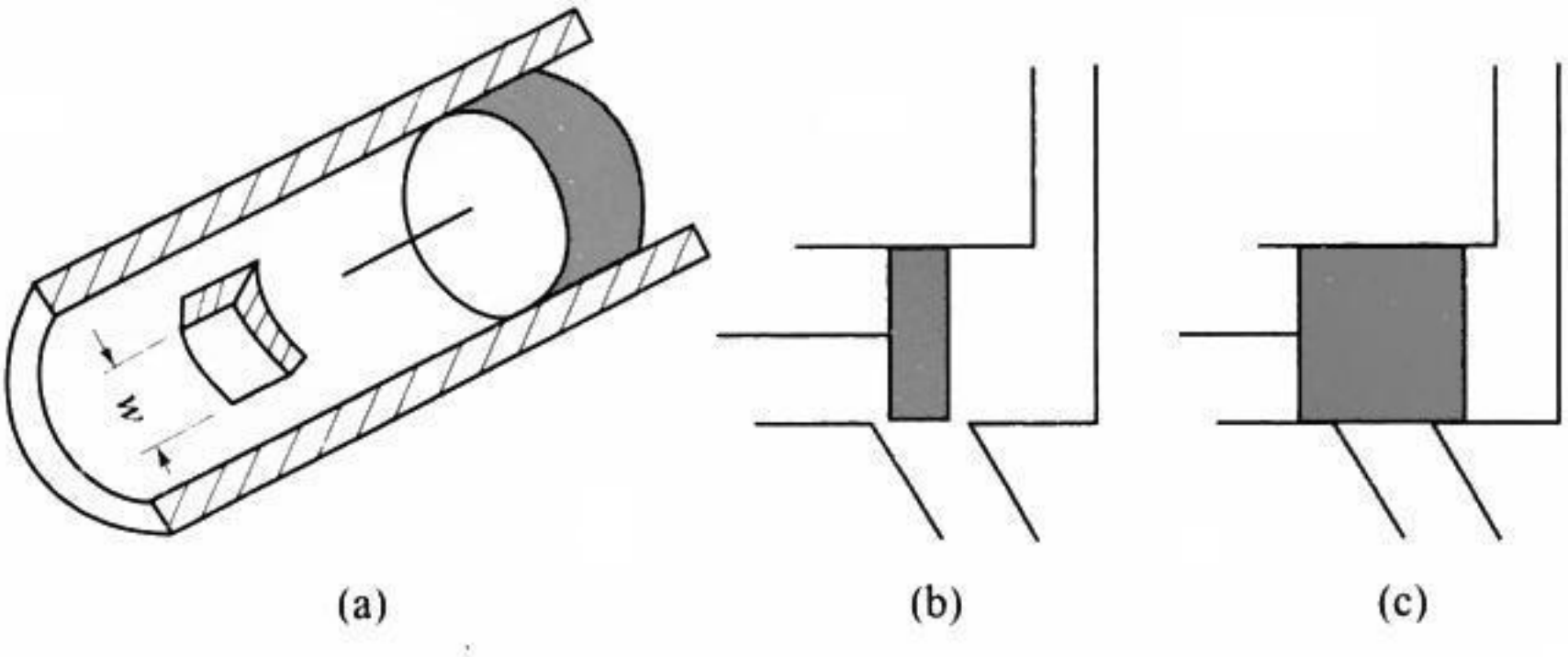


Fig. 3.47 *(a) Spool valve construction (b) underlapped valve (c) overlapped valve*

With an underlapped valve in the neutral position, the cylinder pressures P_1 and P_2 will approach one half the supply pressure P_s. This can be explained as follows.

The fluid flow through the valve ports is similar to the flow through an orifice; the orifice flow relation (2.110) can therefore be applied. Let ΔP_v be the pressure drop across a valve port. Then

$$q = C_o A_o \sqrt{\frac{2(\Delta P_v)}{\rho}} \tag{3.41}$$

where

q = volume flow rate through the port;
A_o = uncovered area of the port;
C_o = discharge coefficient; and
ρ = density of the fluid.

Copyrighted material

The area A_o is equal to $w \times x$, where w is the width of the port (refer Fig. 3.47a). Since C_o, ρ (compressibility assumed negligible), and w are constant, the flow q is a function of x and ΔP_v.

Let us now examine the neutral position of the spool valve. In this position, the fluid leakage into the right chamber of the cylinder is at the rate proportional to $(P_s - P_1)^{1/2}$, and the leakage out of the right chamber is at the rate proportional to $(P_1 - P_r)^{1/2}$. Equilibrium of leakage in and out of the right chamber of the cylinder will be achieved when $P_1 = P_s/2$. Similarly, equilibrium of leakage in and out of the left chamber will be achieved when $P_2 = P_s/2$. This situation will be taken as the equilibrium point.

The movement of the spool from its neutral position and the load-induced pressure on the power piston will disturb the system from its equilibrium position. Assume that the load changes the right-chamber pressure to $P_1 = (P_s/2) + p_1$, and the left-chamber pressure to $P_2 = (P_s/2) + p_2$; the load-induced pressure

$$\Delta p = P_1 - P_2 = p_1 - p_2$$

The pressure drop from the supply to the reservoir, $P_s - P_r$, must equal the sum of the drops across both the control ports and the power piston. That is

$$P_s - P_r = 2\Delta P_v + \Delta p$$

where the drop across a control port is $\Delta P_v = P_s - P_1 = P_2 - P_r$ and the drop across the piston is

$$\Delta p = P_1 - P_2$$

Therefore,

$$\Delta P_v = \frac{1}{2}[P_s - P_r - \Delta p]$$

Since P_s = constant and $P_r = 0$, we see that ΔP_v varies only if Δp changes. Thus the variables x and Δp determine the volume flow rate:

$$q = f(x, \Delta p) \tag{3.42}$$

This relation is nonlinear. Linearization about the equilibrium point ($x = 0$, $\Delta p = 0$, $q = 0$) gives

$$q = K_1 x - K_2 \Delta p \tag{3.43}$$

where $K_1 \triangleq \left.\dfrac{\partial f}{\partial x}\right|_{x = \Delta p = 0} > 0$ is the flow gain; and

$K_2 \triangleq \left.\dfrac{\partial f}{\partial \Delta P}\right|_{x = \Delta p = 0} > 0$ is the pressure coefficient.

Figure 3.48 shows this linearized relationship among q, x, and Δp. The straight lines shown are the linearized characteristic curves of hydraulic actuator. Note that the region near the origin is most important because system operation usually occurs near this point. The flow gain K_1 and the pressure coefficient K_2 can be estimated theoretically from Eqn. (3.41), or more accurately from the experimental tests once the valve has been built.

Copyrighted material

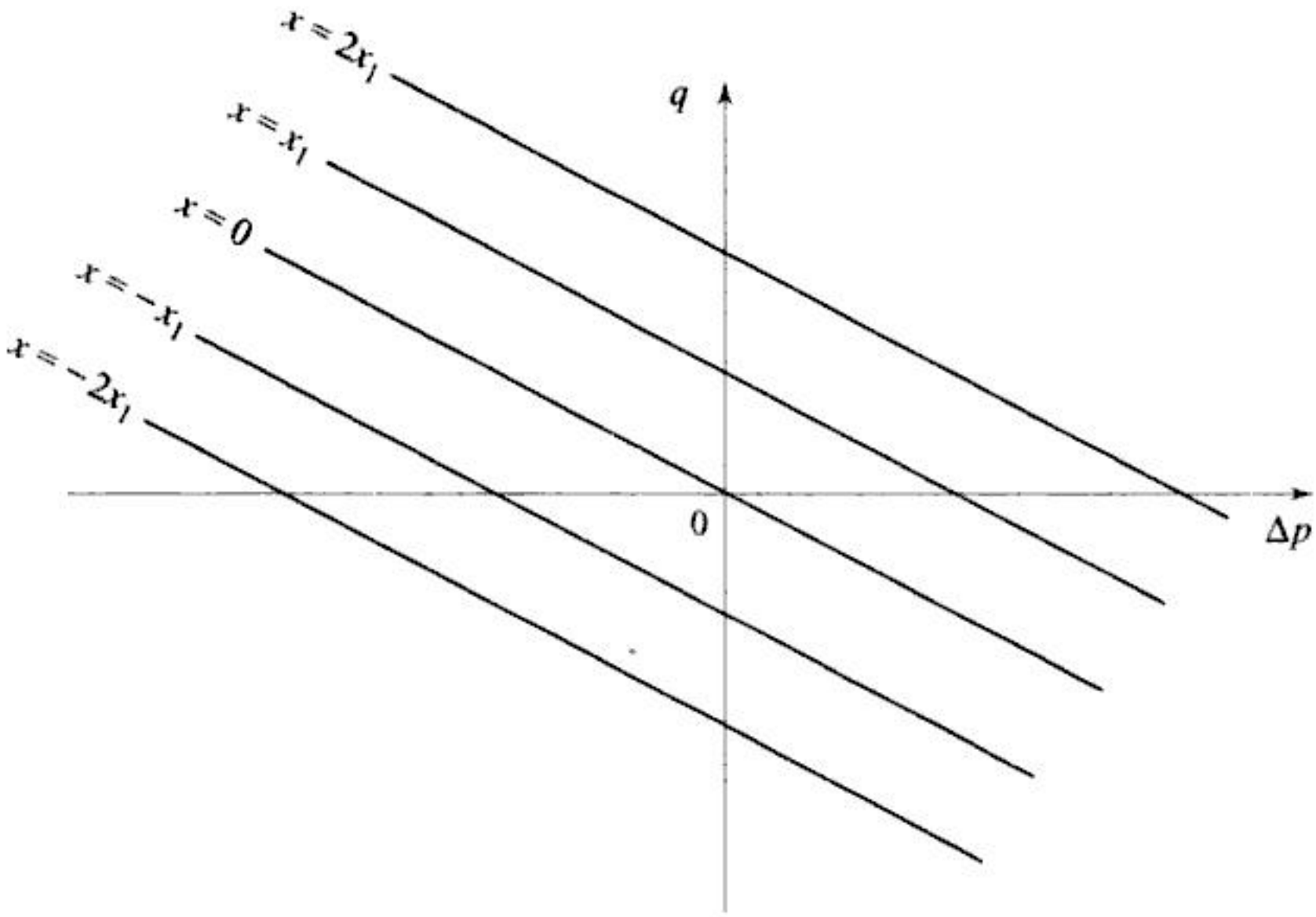


Fig. 3.48 *Linearized characteristic curves of a hydraulic*

Referring to Fig. 3.46 we see that the rate of fluid flow into the power cylinder is proportional to the rate at which the piston moves, i.e.,

$$K_1 x - K_2 \Delta p = A \dot{y} \tag{3.44}$$

where A is the area of the piston.

Notice that because of high force levels and pressure differentials, there may be leakage from one chamber of the power cylinder to the other. However, translational actuators usually have piston rings that are essentially leak free. Equation (3.44) is true under the assumption of zero leakage around the piston.

The force developed by the power piston is equal to the pressure difference Δp times the piston area A. Assume that the power piston moves a load consisting of a mass M, and viscous friction with coefficient B. Then

$$A \Delta p = M \ddot{y} + B \dot{y} + F_w \tag{3.45}$$

where F_w represents the load disturbance.

Figure 3.49 shows a block diagram representation of the hydraulic system. The transfer function between the load displacement y and the spool displacement x, obtained from the block diagram,

$$\text{is} \frac{Y(s)}{X(s)} = \frac{K}{s(\tau s + 1)} \tag{3.46}$$

where $K = \dfrac{AK_1}{BK_2 + A^2}$ = gain constant of the actuator,

$\tau = \dfrac{MK_2}{BK_2 + A^2}$ = time-constant of the actuator.

▲▲

Copyrighted material

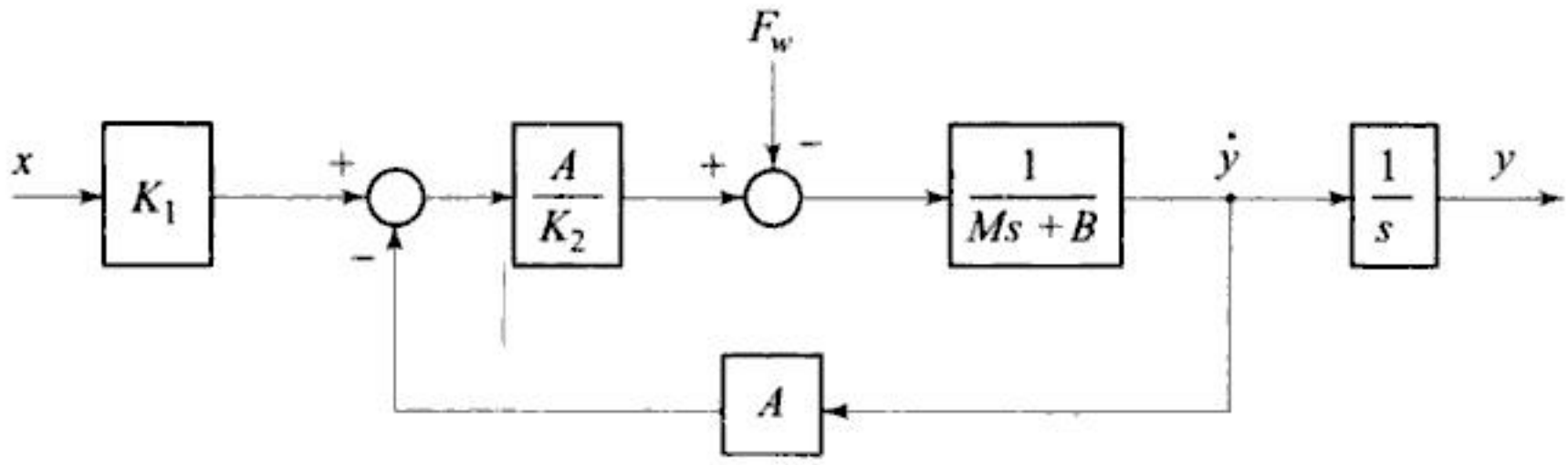


Fig. 3.49 *Block diagram of the hydraulic system of Fig. 3.46*

The controlled fluid power from a spool valve can be converted into rotating mechanical power by a hydrualic motor (refer [48, 57]).

Electrohydraulic Servovalves

The key to harnessing the power developed by hydraulic actuators and controlling them with analog electronic devices/digital computers, is the electrohydraulic servovalve. In its simplest form, an electrohydrualic servovalve is a spool valve with a spool positioned by solenoid-type magnetic actuators. These valves are called *single-stage valves.*

For a large flow rating, the forces required to rapidly and accurately position the spool are beyond the capabilities of solenoid-type electromagnetic positioners. Miniature hydromechanical actuators, internal to the servovalve perform this function. Large electrohydraulic servovalves will thus have an electromechanical first stage and a hydromechanical second stage.

Electrohydraulic valves of different sizes and constructional features are commercially available. The basic principle of operation of these valves is illustrated by the schematic diagram in Fig. 3.50. A magnetic torque motor activates this *two-stage valve*. The armature of the torque motor, which acts as a flapper, extends into the airgaps of the magnetic flux provided by a permanent magnet. The armature (flapper) is pivoted and its one end is positioned between two nozzles.

The armature winding is energized by a balanced amplifier which has the input e. When the input is zero, the currents i_1 and i_2 are equal. Since they flow in opposite directions, the net flux is zero, thus the torque is zero and the flapper is stationary at its central position between the two nozzles. If e is not zero, one of the currents increases and the other decreases in proportion to the magnitude of e. The resulting flux is proportional to the magnitude of e and its direction depends on the polarity of e. The size and direction of the generated torque therefore respond to the magnitude and polarity of e.

The developed torque, balanced by the torsional spring at the pivot, moves the flapper to the right or left. If the flapper moves to the right, the back pressure of the right-hand nozzle rises while that of the left-hand nozzle falls. A differential pressure between the nozzles is created which produces a force on

Copyrighted material



You have either reached a page that is unavailable for viewing or reached your viewing limit for this book.

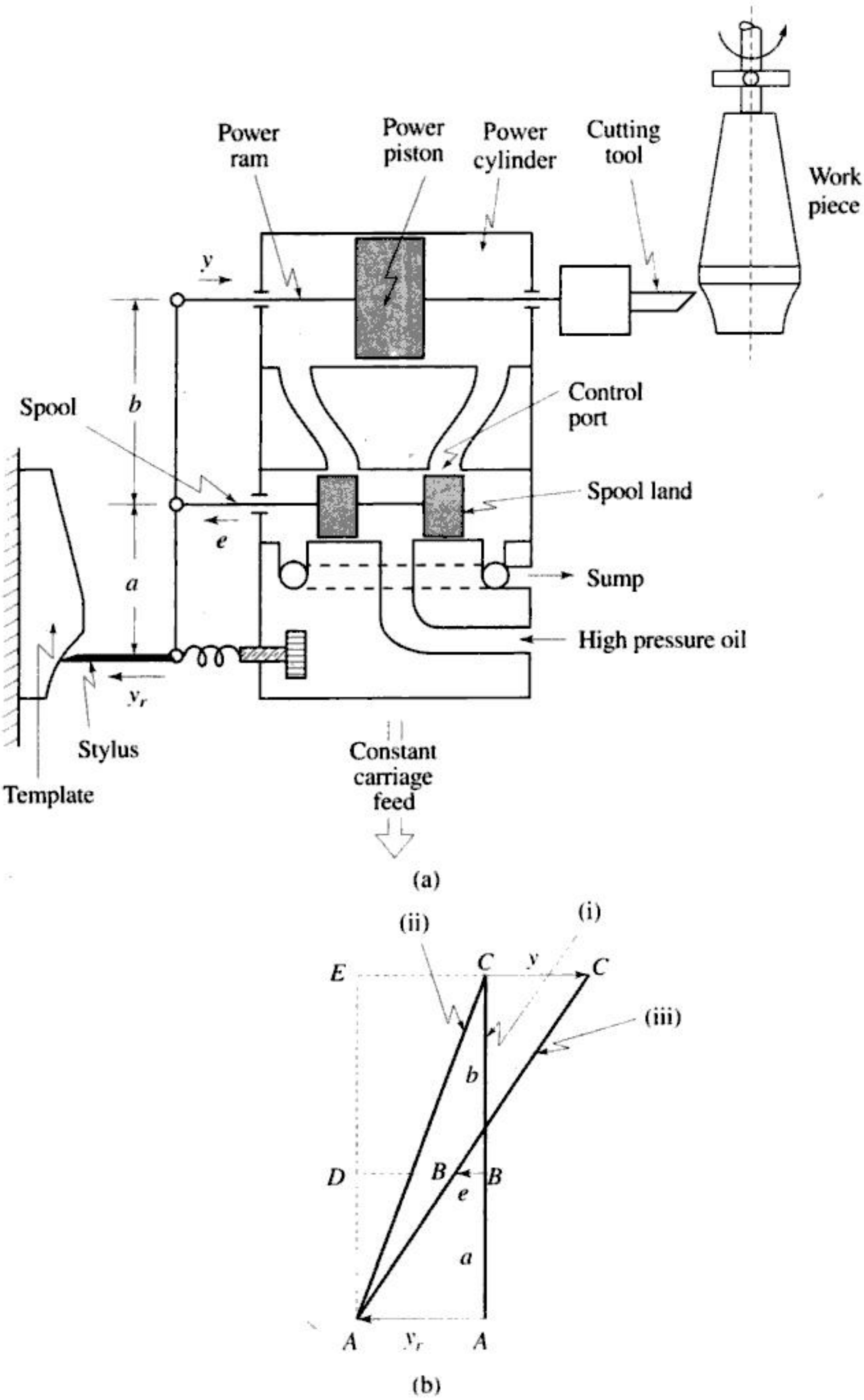


Fig. 3.51 *(a) A simple position control system using mechanical feedback (b) Geometry of feedback linkage for small values of* y_r

Copyrighted material

The operation of the system is as follows. Assume that the displacements y_r, y, and e are measured from an equilibrium position corresponding to some rest position of the load (the spool lands completely cover the control ports). This is shown in Fig. 3.51b as lever position (i). For a reference displacement y_r to the left from the equilibrium position, the upper end of the lever acts as a pivot, because the inertia and friction of the power piston are greater than those of the spool (lever position (ii) in Fig. 3.51b). This motion moves the spool to the left, admitting high pressure fluid to the left chamber of the power cylinder and thereby causing the power piston to move to the right. The lever now pivots about the lower end, which is held fixed by the mechanism that produces the reference displacement (lever position (iii) in Fig. 3.51b). This motion moves the spool to the right until the flow is shut off and the load comes to rest at a new position.

For small movements, y_r, y, and e can be regarded as linear. From the link geometry in Fig. 3.51b,

$$\frac{C'E}{A'E} = \frac{B'D}{A'D}$$

or
$$\frac{y + y_r}{a + b} = \frac{y_r - e}{a}$$

or
$$e = \frac{b}{a+b} y_r - \frac{a}{a+b} y \tag{3.48}$$

In the system of Fig. 3.51a, the servomechanism has been used as a hydraulic shaper. A spring-loaded stylus traces over the template; the cutting tool is powerfully positioned by the hydraulic cylinder fed by the spool valve. The load on the power piston may be assumed to consist of mass M and viscous friction with coefficient B. The disturbance acting on the power piston is the thrust force F_w on the tool.

A block diagram of the system is shown in Fig. 3.52 (refer Eqns (3.42)—(3.46), and Fig. 3.49). Here K_1 and K_2 are given by the linearized characteristic curves of the hydraulic actuator, and A is the area of the power piston.

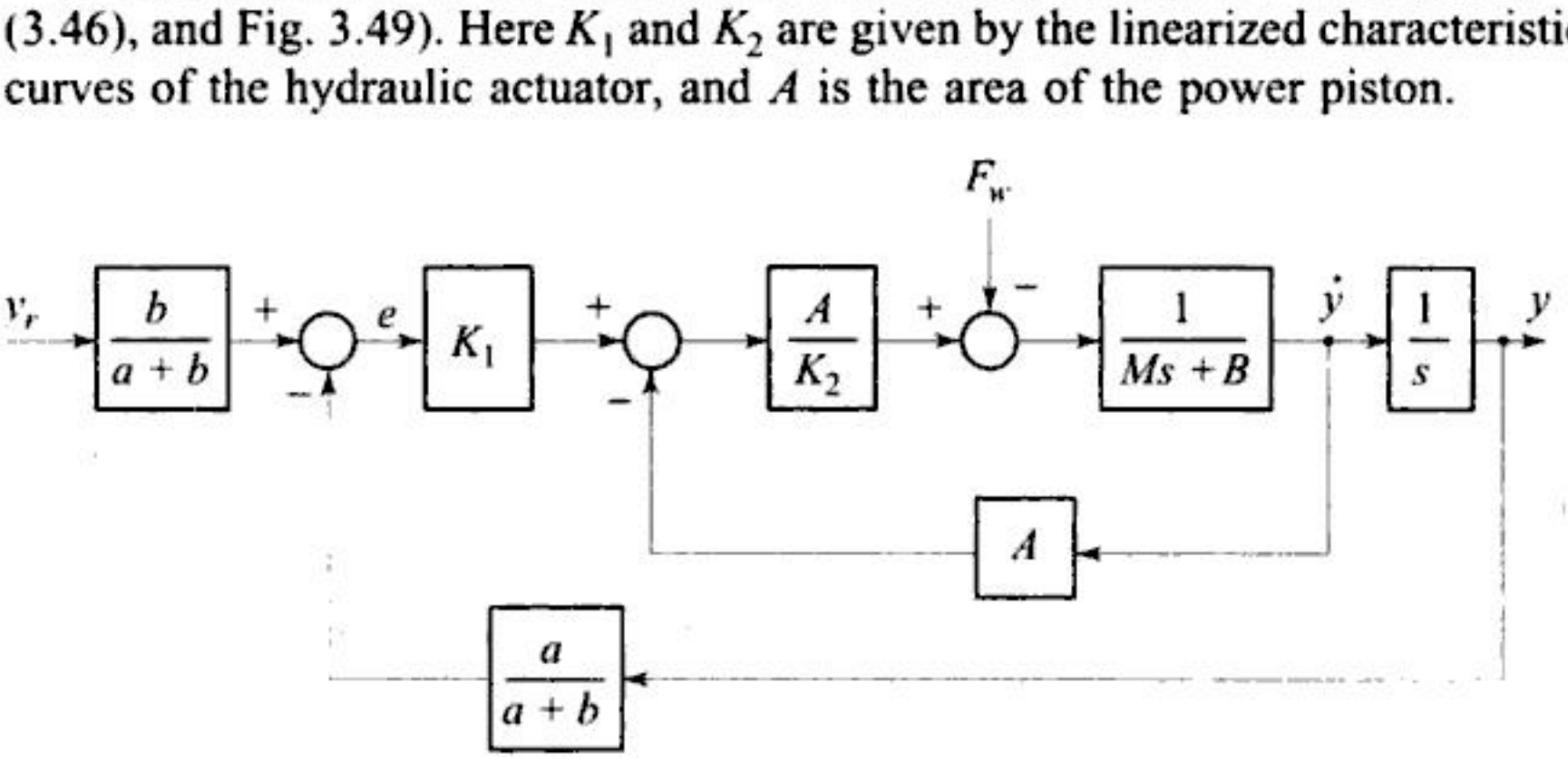


Fig. 3.52 *Block diagram of the hydraulic shaper shown in Fig. 3.51*

Copyrighted material

Example 3.8

Figure 3.53 shows the conceptual design of an electrohydraulic servomechanism used to position an aerodynamic control surface, such as aileron (refer Fig. 1.26), to the commands of the control stick. Very little power should be required to move the control stick so that it can be moved quickly and accurately by the pilot. However, large forces are required to move the control surface against the wind pressure. The servomechanism shown provides the necessary power boost.

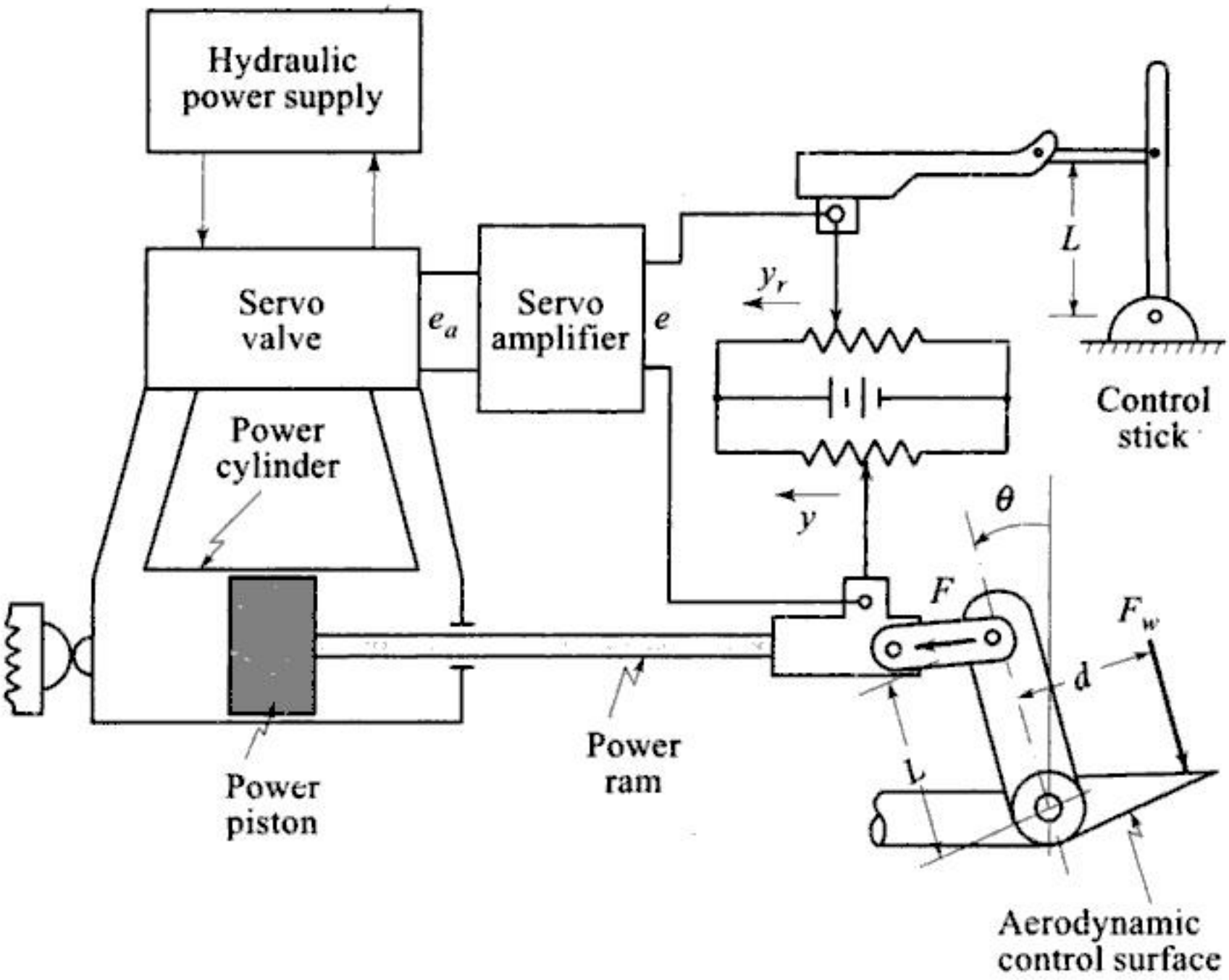


Fig. 3.53 *Electrohydraulic servomechanism*

The operation of the system is as follows. The command θ_r from the pilot moves the wiper on the input potentiometer by $y_r = L\theta_r$. The controlled position θ is sensed by the output potentiometer; the movement y of the wiper of the output potentiometer is related to θ as $y = L\theta$. The servo amplifier amplifies the error voltage $e = K_P(y_r - y)$ and generates a signal $e_a = K_A e$. The polarity of this voltage depends on the direction the stick is moved, and the magnitude of the voltage is proportional to the difference in commanded position θ_r and actual position θ of the control surface. The servovalve admits hydrualic fluid to one of the chambers of the power cylinder, depending on the polarity of e_a. The power piston positions the load; power piston displacement y follows the reference y_r.

Copyrighted material

A linear mathematical model of this control system is now obtained in the following. Spool displacement x of the servovalve is related to the voltage e_a as (refer Eqn. (3.47))

$$x = K_v e_a$$

where K_v = valve gain.
Rate of fluid flow into the power cylinder is given by (refer Eqn. (3.43))

$$q = K_1 x - K_2 \Delta p$$

where Δp is the pressure drop across the piston, and K_1 and K_2 are constants obtained from linearized characteristic curves of the hydrualic actuator.
The rate of fluid flow into the power cylinder is proportional to the rate at which the piston moves (refer Eqn. (3.44)), i.e.,

$$K_1 x - K_2 \Delta p = A\dot{y}$$

where A = area of the piston.

The force balance on the power piston yields,

$$A\Delta p - F = M\ddot{y}$$

where M is the mass of the power piston and power ram, and F is the force applied by the power ram to the control surface attachment point. Furthermore, the control surface moment balance yields

$$J\ddot{\theta} = FL - F_w d$$

where J is the moment of inertia of the control surface and attachment about the hinge, and F_w is the applied aerodynamic load.

Compared to the inertial force $J\ddot{\theta}$, the inertial force $M\ddot{y}$ may be neglected. The block diagram of Fig. 3.54 is based on this assumption.

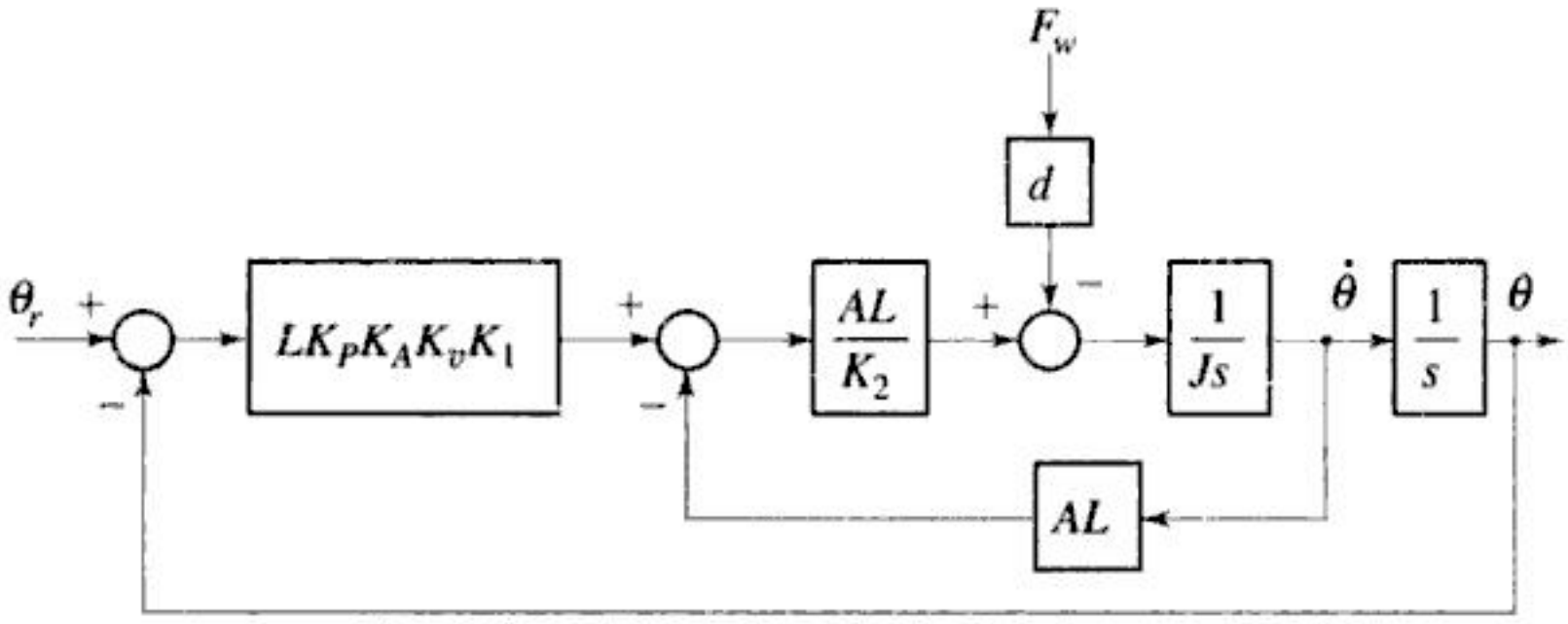


Fig. 3.54 *A block diagram for the system of Fig. 3.53*

3.8 PNEUMATIC DEVICES FOR PROCESS CONTROL

While hydraulic devices use an incompressible fluid (oil), the working medium in a pneumatic device is a compressible fluid, generally air. It is primarily the

Copyrighted material

different properties of the fluids involved that characterize the differences between the two types of devices. These differences can be listed as follows.

1. The air as a working medium is an advantage for pneumatic devices because it may be exhausted to the atmosphere at the end of the device's work cycle, thus eliminating the need for return lines.
2. The air medium has the advantage of being non-inflammable.
3. Air has almost negligible viscosity compared to the high viscosity of oils, which varies considerably with temperature. Pneumatic systems are thus insensitive to temperature changes in contrast to hydraulic systems where fluid friction due to viscosity depends greatly on temperature.
4. High incompressibility of the hydraulic fluid causes the force wave to travel faster and therefore hydraulic systems have shorter response time; while in pneumatic systems there is a considerable amount of compressibility flow so that such systems are characterized by longer time delays.
5. Air lacks lubricating property and always contains water vapour. Oil functions as a hydraulic fluid as well as a lubricator.
6. The normal operating pressure of pneumatic systems is much less than that of hydraulic systems, and consequently the output power is also less for the same size.

Many additional factors bear on the electric/hydraulic/pneumatic decision for those applications where all are technically feasible. Some of these factors are initial cost, maintenance, the nonlinear and other complex characteristics involved, etc.

Pneumatic devices are widely used in process systems used to control temperature, pressure, flow rate, liquid level, and the like. These systems have long time-constants; the response time of pneumatic devices is adequate for their control. Some of the important devices used in process control systems are discussed in this section.

Flow Control Valve

In a large number of process control systems, the final actuator controls the flow of some fluid—liquid, gas, or steam—using flow control valves. All control valves operate by inserting a variable restriction in the flow path. The plug valve (Fig. 3.55) operates by moving a tapered plug, thereby varying the gap between the plug and the valve seat. The flow is controlled by the linear movement of the valve stem.

Pneumatic actuation of the control valves is most common in the process industries. When a valve is supplied by a manufacturer; the pneumatic actuator and the valve are usually attached to each other to form one unit. Figure 3.55 shows a unit where the pneumatic device controls the reciprocating stem of the

Copyrighted material

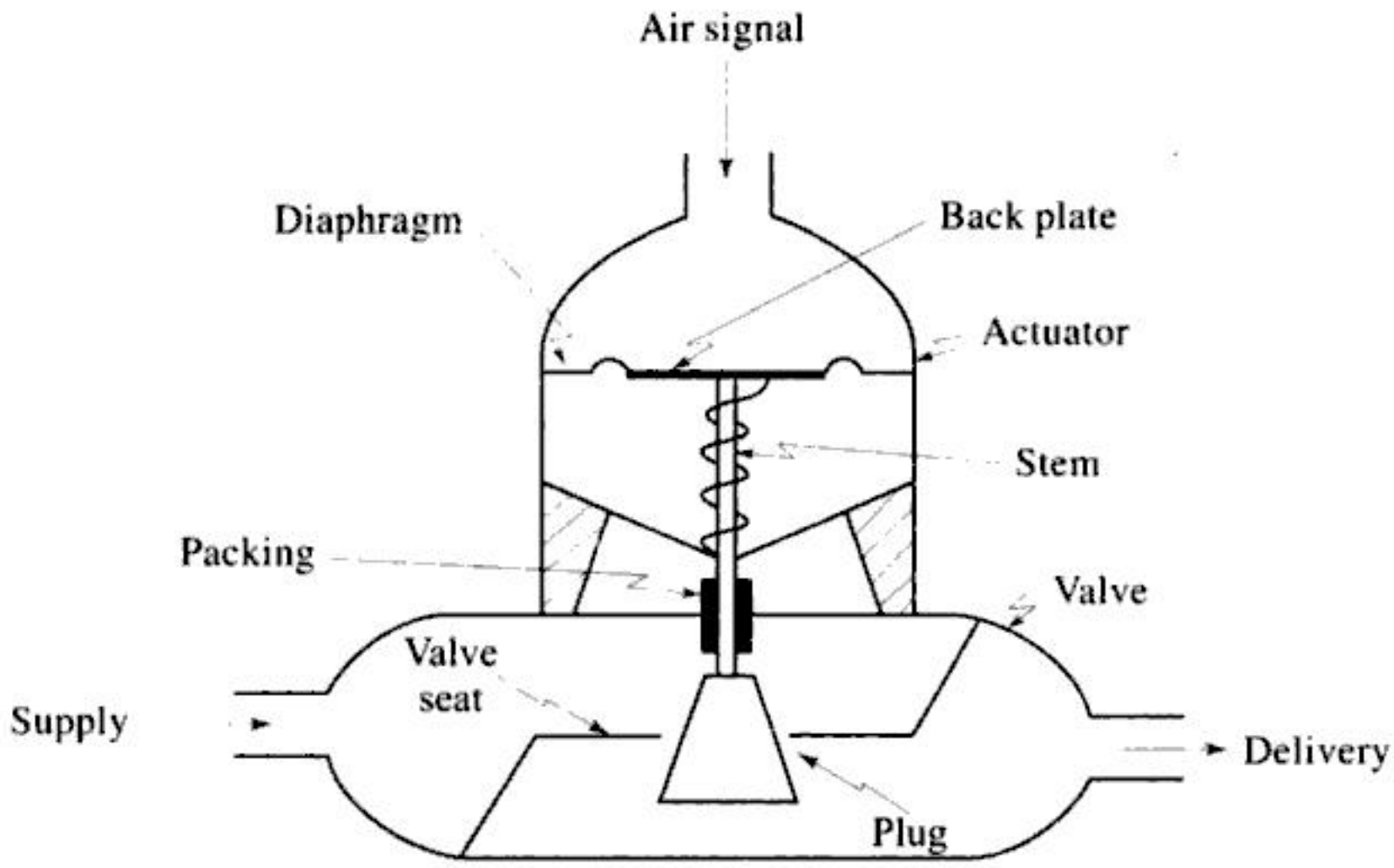


Fig. 3.55 *A pneumatic control valve*

valve as the pressure on the spring-loaded diaphragm changes[5]. The stem positions a plug in the orifice of the valve body.

An increase in the signal pressure above the diaphragm exerts a force on the diaphragm and the back plate which causes the stem to move down 'until the force from the now more compressed spring balances the force on the stem. This results in an increase in the cross-sectional area for flow between the plug and the seat, thereby increasing the flow.[6]

In general, the flow rate of fluid through the valve depends upon the upstream and downstream fluid pressures and the size of the opening through the valve. If all components (including the process) in a feedback control system are essentially linear, then the control valve flow characteristic (relationship between flow through the valve and valve stem position) should also be linear, since then system performance (stability, speed of response, etc.) will be uniform over all system operating conditions. If other system components (usually the process) exhibit significant nonlinearities, then we can choose a valve characteristic that is the inverse of the process nonlinearity, thereby linearizing the overall system and gaining the benefits of uniform performance [48].

---

5. Electromechanical actuation of a control valve having rotating stem is another popular choice. A dc motor is configured as the position control actuator. The shaft of the motor is coupled to the rotating stem of the valve through gearing. The motor and the reduction gears provide an incremental control of fluid flow.
6. The reverse action—reduction in flow with increase in the signal pressure—can be accomplished by inverting the plug on the valve stem. Refer Chapter 11 for details.

Copyrighted material

Control valves with linear flow characteristics are commonly used in processes where the pressure drop across the valve is fairly constant. In our process control examples, we will use control valves with the following characteristics:

(i) the flow through the valve is proportional to valve stem position; and
(ii) the valve stem position is proportional to input signal pressure.

Electropneumatic Transducer

The key to harnessing the power developed by pneumatic actuators and controlling them with analog electronic devices/digital computers, is the electropneumatic transducer. It receives an electrical signal and transmits a proportional output pressure.

Electropneumatic transducers of different sizes and constructional features are commercially available. The basic principle of operation of these devices is illustrated by the schematic diagram in Fig. 3.56. A magnetic torque motor

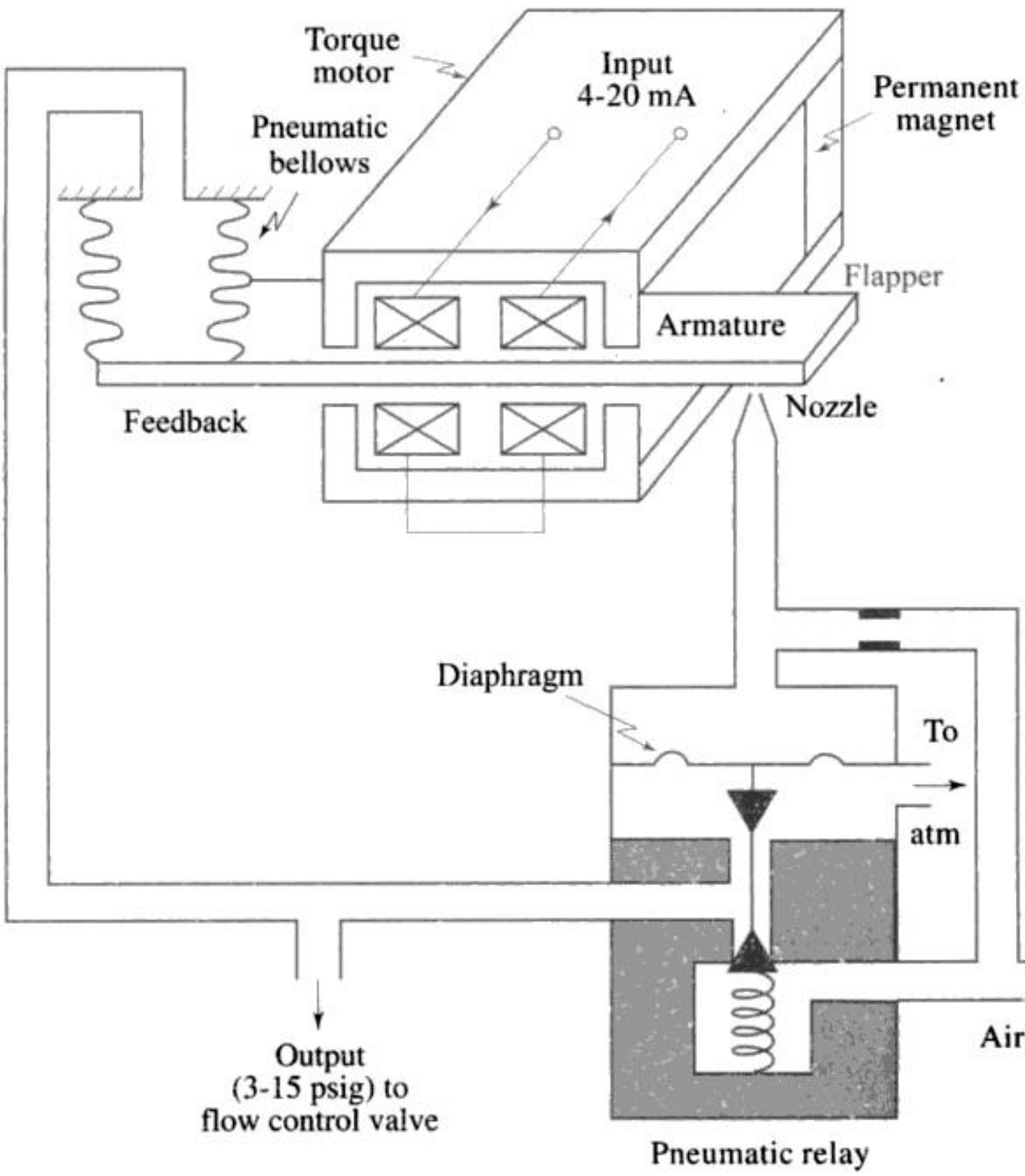


Fig. 3.56 *Current to pressure converter*

Copyrighted material

activates the transducer. The armature of the torque motor, which acts as a flapper, extends into the airgaps of magnetic flux provided by a permanent magnet. The signal current is passed through four coils, wired as shown, and causes a rotary torque on the armature (flapper arm). The torque is proportional to the signal current and causes a change in the flapper/nozzle gap.

Assume that an increase in signal current develops a torque that moves the flapper downwards at the nozzle end. The resulting restriction produces an increased pressure in the nozzle and in the upper chamber of the pneumatic relay. The relay responds to the increase in pressure by closing the exhaust port and opening the supply port, thereby increasing the output pressure to the control valve.

When a decreasing signal current is received, the armature rotates to uncover the nozzle, resulting in a decrease in the pressure in the nozzle and the relay. The relay diaphragm moves upward and the exhaust port opens to bleed the output pressure to atmosphere, thereby reducing the pressure applied to the control valve.

Figure 3.56 shows that the electropneumatic transducer is also itself a complete feedback system; thus it must be properly designed for stability and accuracy. If we are users (rather than designers) of such a device, we are concerned only with its overall dynamics from input current i to output pressure p. The dynamics relating p to i is generally quite fast compared to other time-constants in the process control loop; so we model the electropneumatic transducer as a zero-order system with p proportional to i.

Example 3.9

The stirred tank in Fig. 3.57 is used to heat a process stream so that its premixed components achieve a uniform composition. Temperature control is important because a high temperature tends to decompose the product while a low temperature results in incomplete mixing. The tank is heated by the steam condensing inside a coil. The temperature in the tank is controlled by manipulating the steam valve position.

The control hardware required to control the temperature of a process stream leaving a continuously stirred tank reactor (CSTR) is shown in Fig. 3.57. This hardware, available from manufacturers of process-control equipment, consists of the components listed below along with their respective conversions:

- sensor (temperature to current);
- controller (current to current);
- transducer (current to pressure); and
- control valve (pressure to flow rate).

A thermocouple is used to measure the temperature; the signal from the thermocouple is sent to the signal-conditioning circuit, which produces an output in the range of 4-20 mA, which is a linear function of the input. The output

Copyrighted material

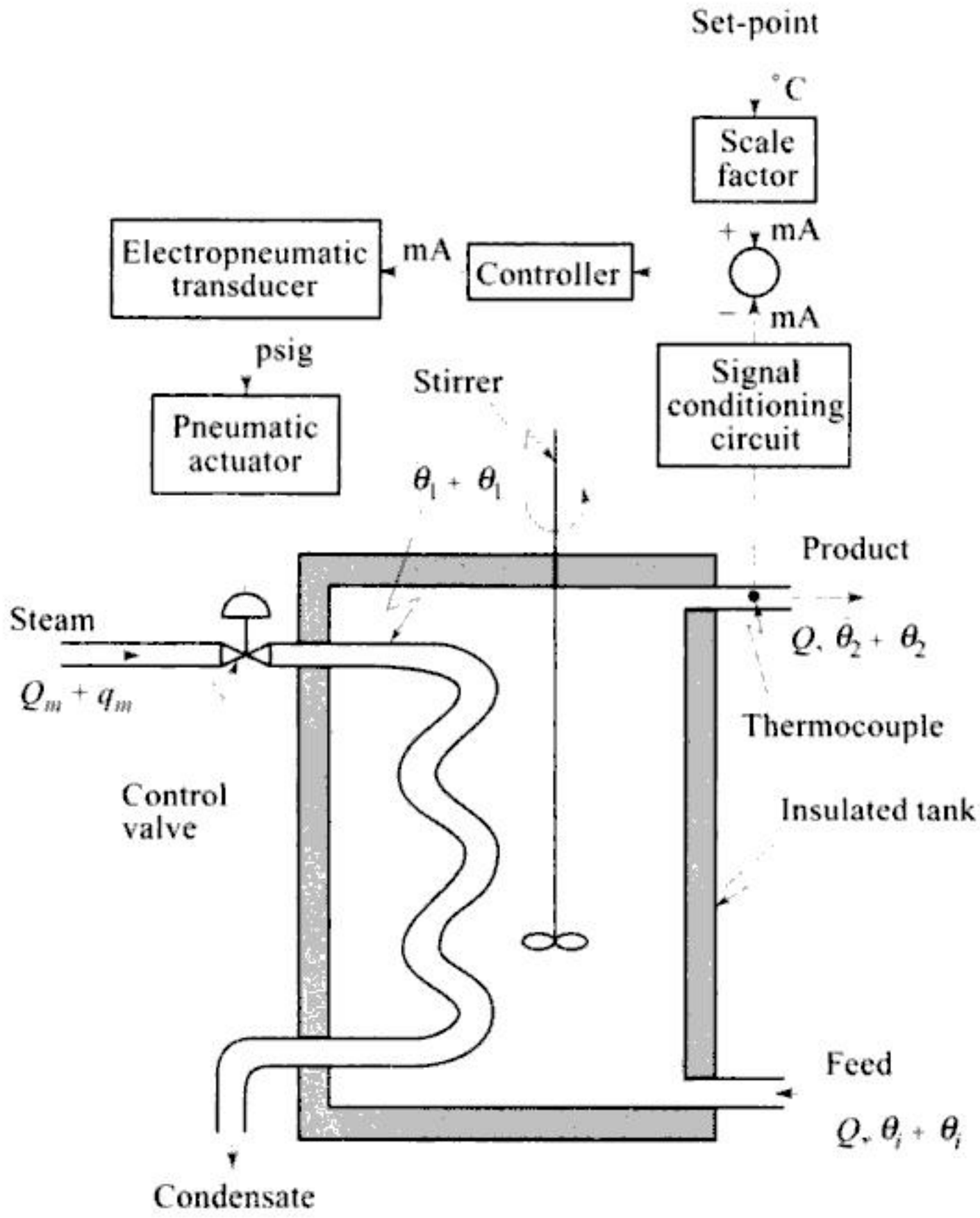


Fig. 3.57 *Temperature control of a continuously stirred tank reactor*

of the sensor is compared with the set-point to produce an error signal. The controller converts the error to an output in the range of 4-20 mA according to the control law. The only control law we have considered so far has been proportional. In the next chapter, other control laws will be described. The output of the controller enters the electropneumatic transducer, which produces an output in the range of 3-15 psig, which is a linear function of the input. Finally, the output of the electropneumatic transducer is sent to the top of the pneumatic control valve, which adjusts the flow of the steam to the coil in the stirred tank. We will assume that the valve is linear.

Simplifying assumptions:

1. The liquid inflow and outflow rates for the tank are equal so that the liquid level in the tank is maintained constant during the operation.
2. The liquid in the tank is well-stirred so that its state can be described by the temperature of the outflowing liquid.
3. The tank is well-insulated so that the heat loss through its walls is negligible. Also, the heat storage capacity of the tank walls is negligible.

Copyrighted material

We consider here a CSTR where the process feed has a density ρ of 1090 kg/m^3 and a heat capacity c of 3350 Joules/kg-°C. The volume V of the liquid in the reactor is maintained constant at 3.4 m^3 by a constant feed rate Q of 0.425 m^3/min. Thermal capacitance C_1 of the coil mass is 503×10^3 Joules/°C. The heat transfer area A is 22.57 m^2 and the heat transfer coefficient U is 42.97×10^3 Joules/min-m^2-°C. The steam available is saturated; it can be assumed that its latent heat of condensation λ is constant at 2247×10^3 Joules/kg.

At steady state, the temperature of the feed $\bar{\theta}_i$ is 55 °C. Assume that the design requirement is to maintain the tank liquid at a temperature $\bar{\theta}_2$ of 80 °C. Possible perturbations from the steady state are caused by the desired change θ_r in the temperature of the tank liquid, and the change θ_i in the feed temperature (a disturbance). These perturbation signals give rise to perturbations θ_1 and θ_2 in the temperatures of the coil mass and the tank liquid, respectively, from their steady-state values $\bar{\theta}_1$ and $\bar{\theta}_2$.

The heat balance for the coil mass:

$$C_1 \frac{d}{dt}(\bar{\theta}_1 + \theta_1) = (\bar{Q}_m + q_m)\lambda - UA\,[\bar{\theta}_1 + \theta_1 - (\bar{\theta}_2 + \theta_2)] \tag{3.49}$$

where

$\bar{Q}_m$ = steam flow rate (kg/min) at steady state, and
q_m = manipulation of the steam flow rate.

The heat balance for the tank liquid:

$$V\rho c \frac{d}{dt}(\bar{\theta}_2 + \theta_2) = Q\rho c\,[\bar{\theta}_i + \theta_i] + UA\,[\bar{\theta}_1 + \theta_1 - (\bar{\theta}_2 + \theta_2)] - Q\rho c\,[\bar{\theta}_2 + \theta_2] \tag{3.50}$$

The process steady state is described by the following equations:

$$\bar{Q}_m\,\lambda - UA(\bar{\theta}_1 - \bar{\theta}_2) = 0$$

$$Q\rho c\bar{\theta}_i + UA(\bar{\theta}_1 - \bar{\theta}_2) - Q\rho c\,\bar{\theta}_2 = 0$$

This gives $$Q\rho c(\bar{\theta}_i - \bar{\theta}_2) + \bar{Q}_m\,\lambda = 0$$

Since $\bar{\theta}_i$ = 55 °C and $\bar{\theta}_2$ = 80 °C, the steady-state mass flow rate of steam through the coil is

$$\bar{Q}_m = \frac{0.425 \times 1090 \times 3350 \times (80 - 55)}{2247 \times 10^3}$$

$$= 17.27 \text{ kg/min}$$

At steady state, the error signal in the control configuration of Fig. 3.57 is zero. The necessary steam flow rate $\bar{Q}_m$ can be achieved with the zero error signal because the electropneumatic transducer has a zero adjustment which allows pressure to be at the middle (9 psig) of its 3–15 psig range when the input to the transducer is zero, and the valve actuator has a zero adjustment which allows the valve opening to be put anywhere desired with its input pressure at 9 psig.

Copyrighted material



You have either reached a page that is unavailable for viewing or reached your viewing limit for this book.

$$\theta_2(s) = G_p(s)\, Q_m(s) + N(s)\theta_i(s)$$

where

$$G_p(s) = \frac{0.35}{s^2 + 2.13s + 0.24};\ N(s) = \frac{0.24(0.52s + 1)}{s^2 + 2.13s + 0.24}$$

The dynamics of the other components of the feedback system—the temperature sensor, the controller (amplifier), the electropneumatic transducer and the pneumatic control valve—are negligible relative to the process time-constants. All these components are fast enough to be treated as zero-order systems. Fig. 3.58b shows a block-diagram representation of the temperature control loop.

Review Examples

Review Example 3.1

Consider the temperature control system of Fig. 3.59 which is set up to produce a steady process stream at a controlled temperature. The temperature θ(°C) of the outflowing liquid is measured by a thermocouple which produces an output voltage e_t(volts) proportional to $\theta(e_t = K_t\theta)$. This voltage is subtracted from the reference voltage e_r to generate the error signal $e = (e_r - e_t)$ which in turn regulates the heating rate h by means of an SCR amplifier [3]. Basically a solid state switch, the SCR amplifier controls the heating rate by varying the point in the ac power cycle at which the heater is connected to (or disconnected from) the power line (see Fig. 3.60). As the line frequency (50 Hz) is very high relative to the thermal system frequency response, we take h to

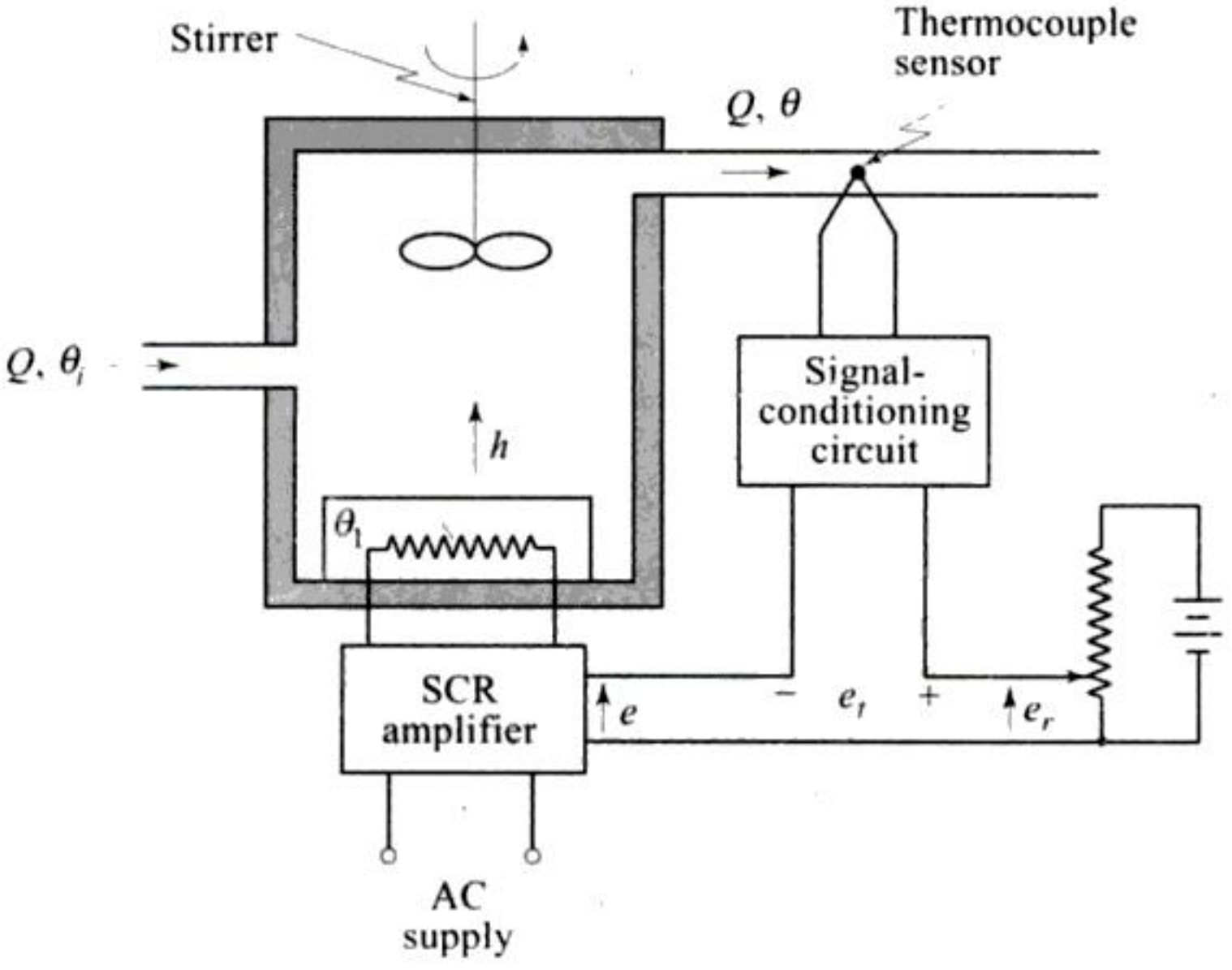


Fig. 3.59 *A temperature control system*

Copyrighted material

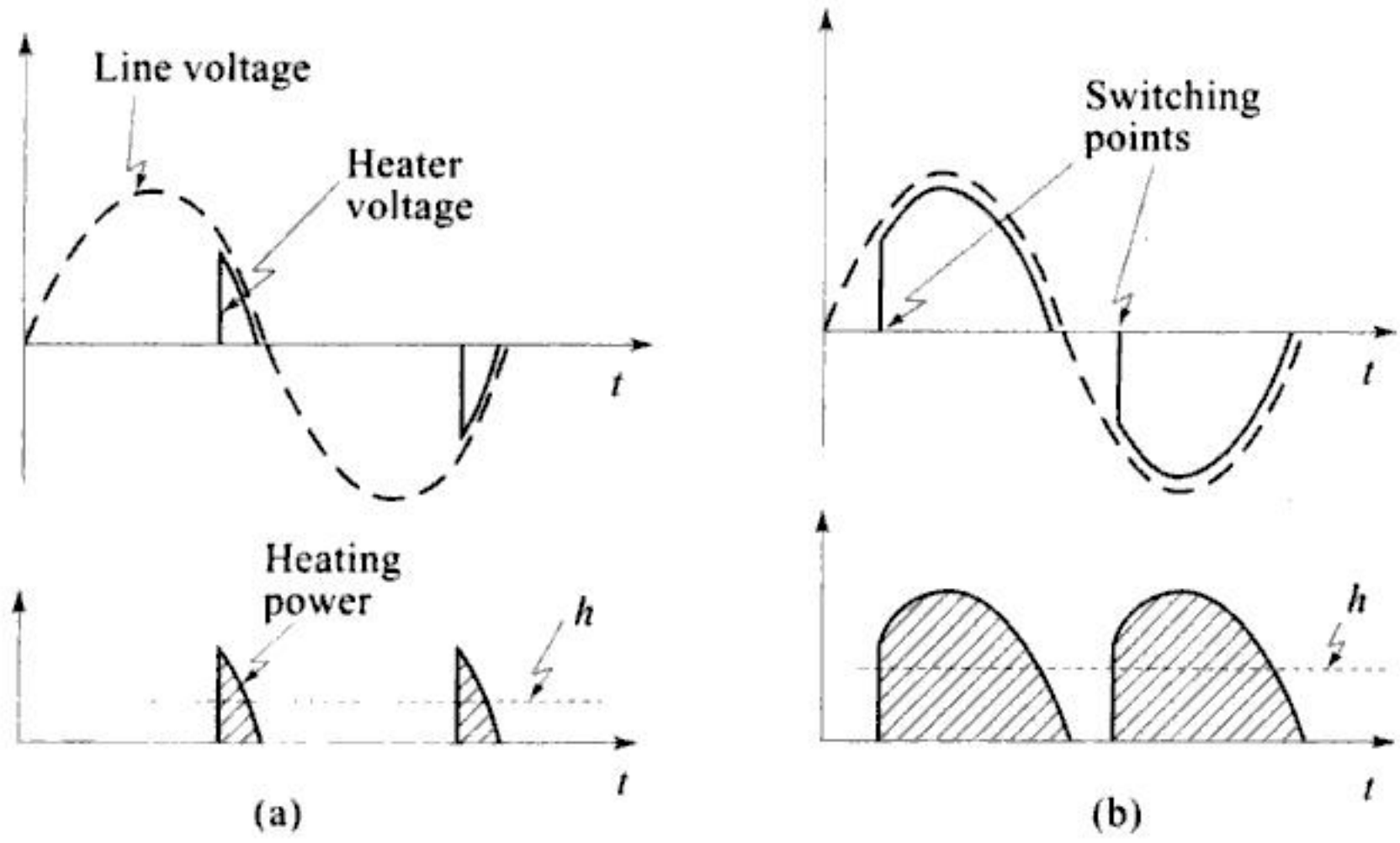


Fig. 3.60 *SCR control of heating rate; (a) low heating rate (b) high heating rate*

mean the *average* power over the cycle, rather than the instantaneous electrical power and assume that h follows the amplifier input voltage e instantly. The nonlinear steady-state relation (static calibration curve) between e and h can be linearized at any chosen operating point, giving heater gain K_h; $h = K_h e$ watts. Simplifying assumptions:

1. The liquid inflow and outflow rates for the tank are equal (Q m^3/sec) so that the liquid level in the tank is maintained constant (volume V m^3 of the liquid in the tank is therefore constant).
2. The liquid in the tank is well stirred so that its state can be described by the temperature θ of the outflowing liquid.
3. The tank is well insulated so that the heat loss through its walls is negligible. Also the heat storage capacity of the tank walls is negligible.
4. The heat storage capacity of the heater mass is negligible.

Assuming an initial equilibrium point and taking all the variables as perturbations, we obtain the following heat-balance equation.

$$V\rho c\frac{d\theta}{dt} = h + Q\rho c\ \theta_i - Q\rho c\,\theta \tag{3.51}$$

where ρ = density of the liquid;
c = specific heat of the liquid; and
θ_i = perturbation in the temperature of the inflowing stream; this will be treated as a disturbance in our model.

Taking the Laplace transform of Eqn. (3.51) and reorganizing, we get

$$(s\tau + 1)\,\theta(s) = \frac{1}{Q\rho c}H(s) + \theta_i(s) \tag{3.52}$$

where $\tau = \dfrac{V}{Q}$ = process time-constant.

Copyrighted material

Although we generally prefer to measure the controlled variable as directly as possible, location of the thermocouple (which has an output of a few millivolts) in the tank encounters problems of electrical noise due to high-power SCR switching, and vibration caused by the tank stirrer. Thus, we locate it in the pipeline downstream of the tank causing a deadtime τ_D between θ and its measurement θ_m:

$$\frac{\theta_m(s)}{\theta(s)} = e^{-s\tau_D} \tag{3.53}$$

Using Eqns (3.52) and (3.53), we can draw the block diagram of the system as shown in Fig. 3.61.

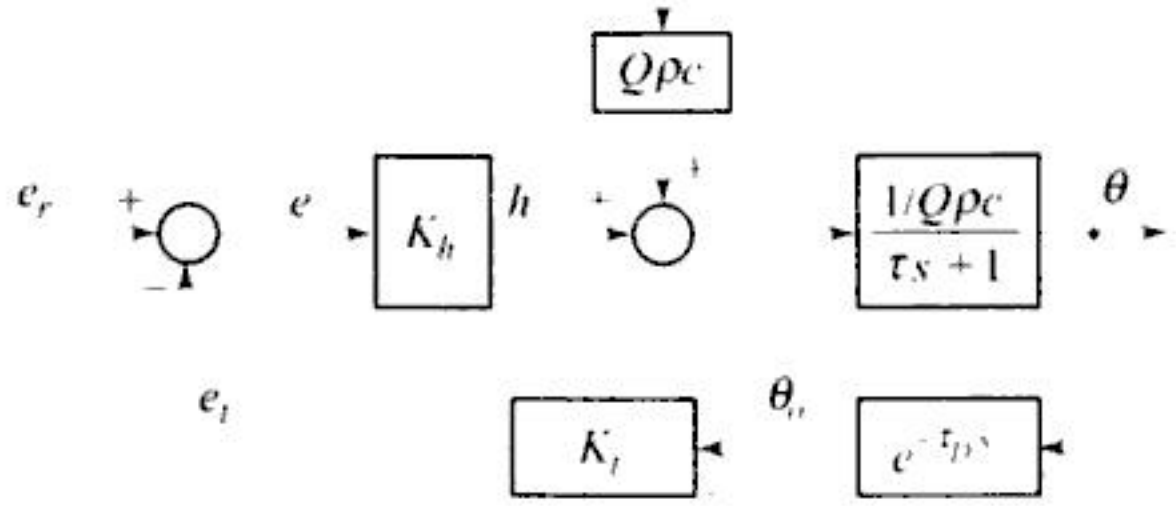


Fig. 3.61 *A block diagram for the system of Fig. 3.59*

Review Example 3.2

Let us reconsider the toilet-tank control system of Fig. 1.5. A change in the liquid level is sensed by a float which is connected by a mechanical lever to a control valve. At steady state, the upward-acting buoyant force due to the liquid displaced by the float is just balanced by its weight. The control valve is closed in this state. Assume now that due to disturbance flow q_w, the liquid level goes down by h. This will decrease the buoyant force, and the float will start moving down. We denote the downward movement of the float by x.

Due to unavoidable friction effects, x and h will be related by

$$X(s) = \frac{1}{\tau_f s + 1} H(s)$$

where τ_f is the time-constant of the float dynamics. However τ_f is normally quite small compared to the process dynamics and an be neglected.

The downward movement of the float by x will cause a downward movement of the control valve stem by z:

$$z = \frac{l_1}{l_1 + l_2} x$$

This will give rise to liquid inflow at the rate $q_i(t)$: $q_i(t) = K_v z(t)$; K_v = valve gain.

Copyrighted material



You have either reached a page that is unavailable for viewing or reached your viewing limit for this book.



You have either reached a page that is unavailable for viewing or reached your viewing limit for this book.

inserted in the armature circuit to generate a voltage proportional to the armature current. An isolating amplifier is used to take care of the loading effect.

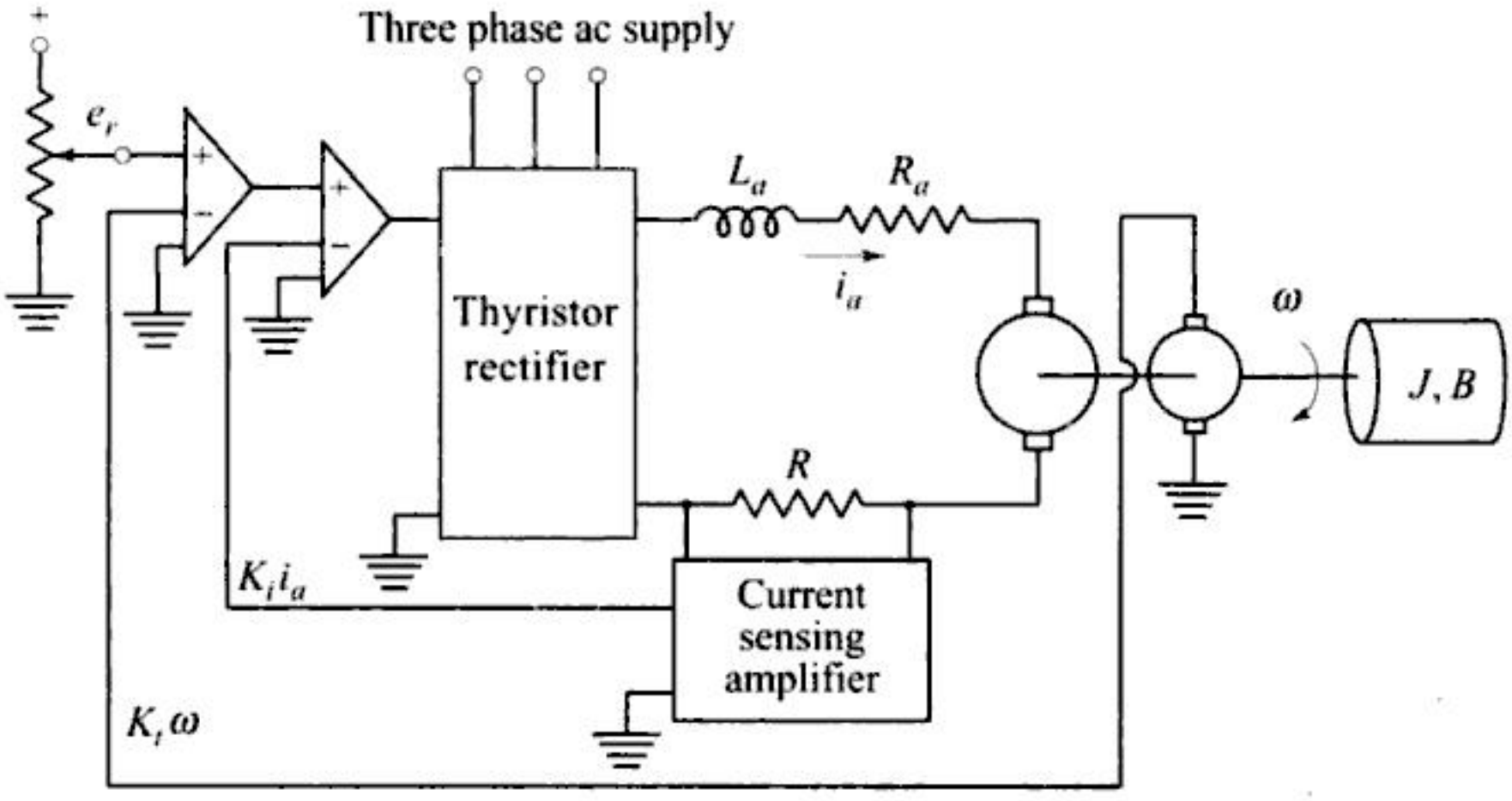


Fig. 3.64 *Speed control system with inner current-control loop*

Review Example 3.4

Let us reconsider the hydraulic power steering mechanism discussed earlier in Example 1.3. A simplified schematic diagram of the system is shown in Fig. 1.8. The input to the system is rotation (θ_r) of the steering wheel by the driver, and the output is position (θ) of the tyre wheels of the vehicle.

When the steering wheel is in the zero position, i.e., the cross bar is horizontal, the tyre wheels are directed parallel to the longitudinal axis of the vehicle. For this condition, the spool is in the neutral position ($x = 0$) and the oil supply to the power cylinder is cut-off. When the steering wheel is turned anticlockwise through an angle θ_r, the spool is made to move towards right by an amount x with the help of the gear mechanism. The high-pressure oil enters on the left-hand side of the power cylinder causing the power piston and hence the power ram to move towards right by an amount y. Through a proper drive linkage, a torque is applied to the wheels causing a displacement θ of wheels.

A rigid linkage bar connects the power ram and the movable housing. Movement y of the power ram towards right causes a movement z of the valve housing in such a direction as to seal off the high pressure line.

The geometry of the linkage is shown in Fig. 3.65, from which we obtain for small movements.

$$\frac{AA'}{AC} = \frac{AA'}{AB + BC} = \frac{BB'}{BC}$$

or

$$\frac{y}{a + b} = \frac{z}{a}$$

Copyrighted material

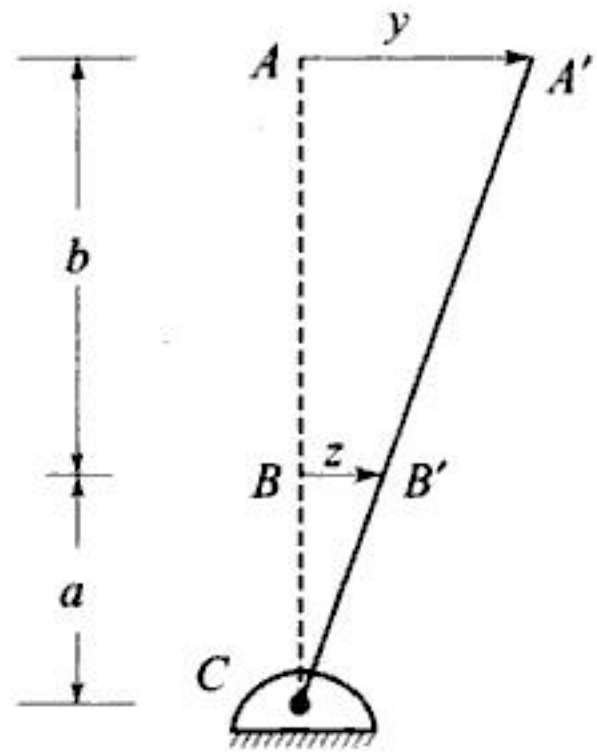


Fig. 3.65 *Geometry of the feedback linkage in the system in Fig. 1.8*

Therefore
$$z = \frac{a}{a+b} y \tag{3.55}$$

The flow rate of the oil into power cylinder due to spool movement is given by (refer Eqn. (3.43))

$$q = K_1 e - K_2 \Delta p, \quad K_1 \text{ and } K_2 \text{ are constants;}$$

where $e = (x - z)$ is the net displacement of the spool relative to the valve housing, and Δp is the differential pressure across the piston.

The flow rate of the oil into the power cylinder is proportional to the rate at which the piston moves (refer Eqn. (3.44)), i.e.,

$$K_1 e - K_2 \Delta p = A \dot{y} \tag{3.56}$$

where A is the area of the piston.

Assuming the load on the power piston to consist of mass M, tyre stiffness K and viscous friction coefficient B, the force equation is given by (refer Eqn. (3.45))

$$A \Delta p = M \ddot{y} + B \dot{y} + K y \tag{3.57}$$

A block diagram of the power steering mechanism obtained from Eqns (3.55) – (3.57) is shown in Fig. 3.66.

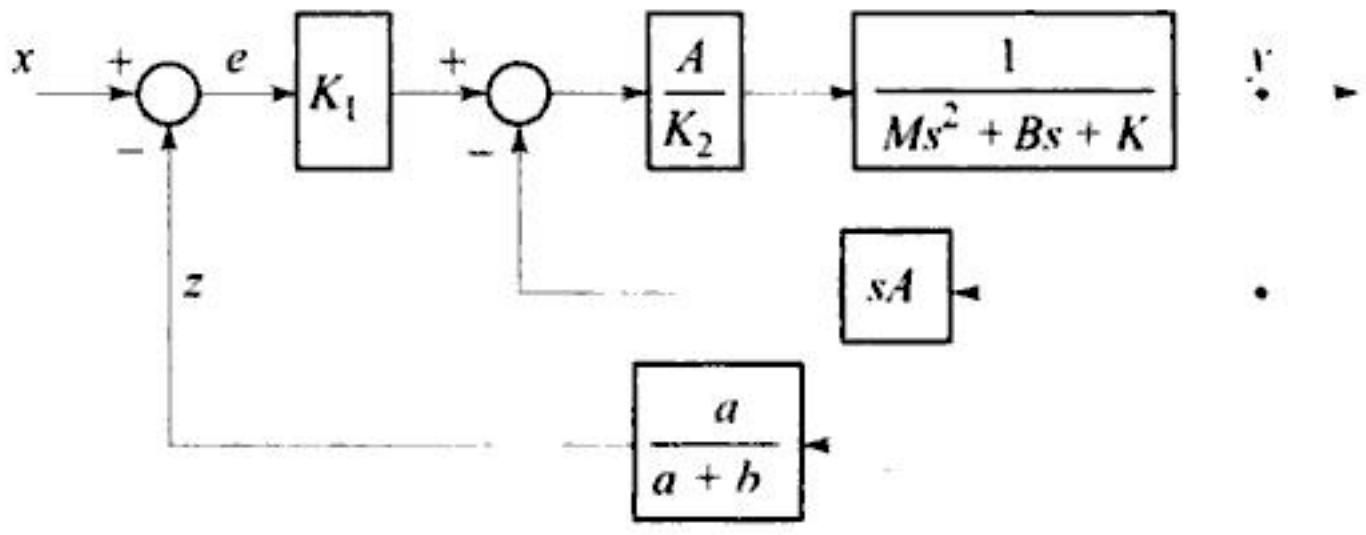


Fig. 3.66 *A block diagram of the system in Fig. 1.8*

Copyrighted material

Review Example 3.5

The dynamic behaviour of certain processes deviates drastically from what we have seen so far. Consider the simple drum boiler shown in Fig. 3.67a. Feedwater enters the boiler with a mass flow rate $\overline{Q}_{mf} + q_{mf}$, at a constant temperature. It is heated by a constant amount of heat supplied by burned fuel. The generated steam flows out from the top of the boiler with a mass flow rate $\overline{Q}_{ms} + q_{ms}$, at a constant pressure. A simple feedback control system has been installed to keep the level of the water in the drum boiler constant by manipulating the flow rate q_{mf} of the feedwater stream. Variations in steam flow q_{ms} are the main disturbances affecting the system.

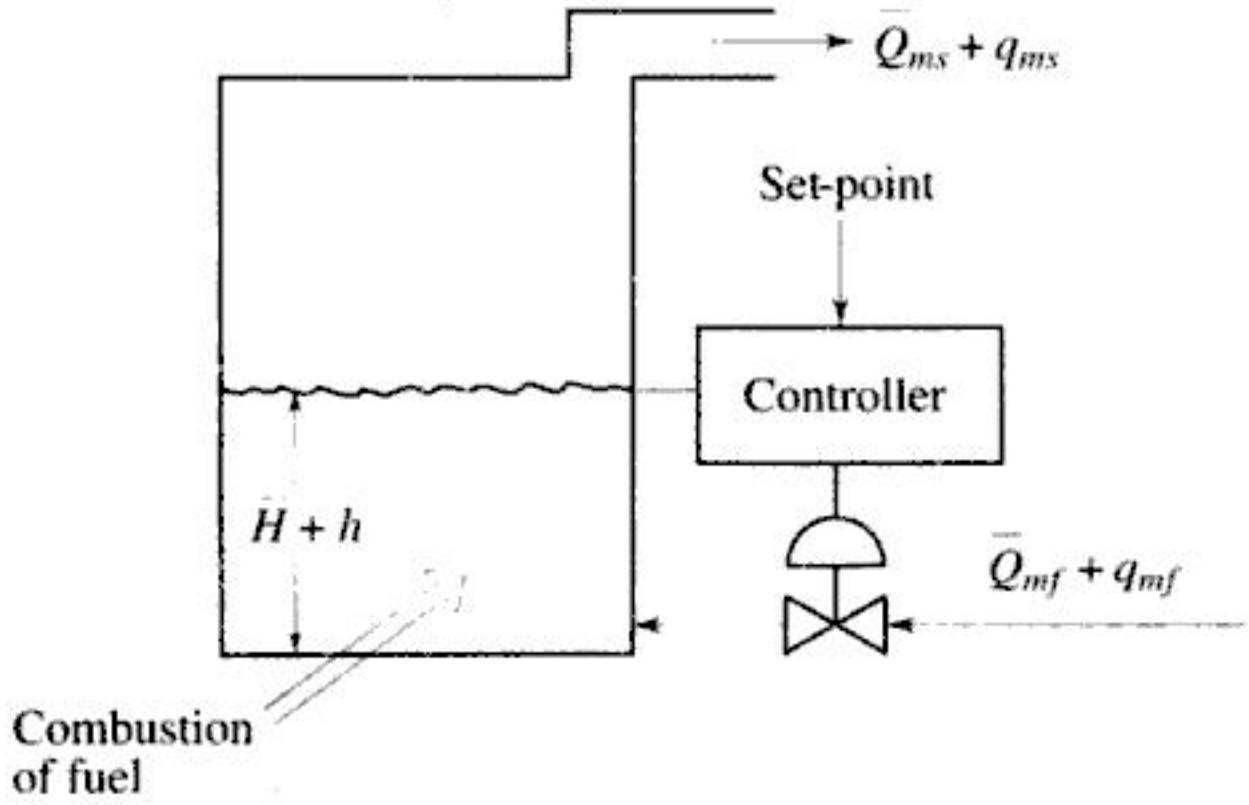


Fig. 3.67 *Liquid-level control in a boiler system*

Copyrighted material



You have either reached a page that is unavailable for viewing or reached your viewing limit for this book.



You have either reached a page that is unavailable for viewing or reached your viewing limit for this book.

3.7 Explain with the aid of a sketch, the construction and operation of a linear variable differential transformer (LVDT). Describe briefly using appropriate diagrams, an application of LVDT in motion control systems. (Help: Fig. P3.15)

3.8 (a) Explain with the aid of appropriate diagrams, the construction and operation of
(i) synchro transmitter; and
(ii) synchro control transformer
Give a schematic diagram showing how the synchro pair (transmitter and control transformer) would be embodied in an ac position control system. (Help: Fig. 3.45)

(b) Rotor of synchro transmitter is of dumb-bell type while that of control transformer is cylindrical. Why? (Help: p189)

(c) Is synchro a three phase machine? Justify your answer. (Help: p188)

3.9 (a) Compare the advantages and disadvantages of the following transducers when used as error-forming devices in servosystems:
(a) a pair of rotary potentiometers; and
(b) a synchro pair.
Give a schematic diagram showing how each would be embodied in a position control system. (Help: p184, p186, Fig. 3.40; Fig. 3.45)

(b) Why are ac devices (servomotor, synchro) normally operated at higher frequencies (400 Hz, for example) and not at 50 Hz? (Help: p170)

3.10 Draw an electromechanical schematic diagram of a dc position control servosystem incorporating tachogenerator damping. Describe the operation of the main components used, explaining clearly how the error signal is formed. (Help: Figs 1.15 and 1.16)
Why do we put tacho on the motor shaft rather than the load shaft? (Help: Problem 3.9)

3.11 (a) Armature control of a dc motor is used in a closed-loop speed control system. Draw a schematic layout for the system. Describe the operation of main components used, explaining clearly how the error signal is formed. (Help: Review Example 3.3)

(b) The classical approach of variable speed drives was motor-generator set; generator used as a power amplifier. What is the modern approach? (Help: p 214)

3.12 (a) Sketch an op amp circuit capable of providing an output which approximates to proportional plus integral plus derivative of the input.
Explain using a block diagram how this unit can be connected into a position control system which has been constructed using synchro error detector, ac servomotor, gear box, and other relevant components. (Help: Example 2.10; p193)

(b) Modify the block diagram to include an ac tachogenerator to provide damping, with the op amp circuit providing proportional plus integral plus derivative actions.

3.13 Hydraulically operated devices are frequently used in control systems. List the advantages and disadvantages in using hydraulic systems. (Help: p193)
Using appropriate diagrams, give the constructional and operational features of a hydraulic linear actuator. Derive the transfer function model of the actuator. Use appropriate symbols for variables and parameters. Clearly state the assumptions made.

Copyrighted material

3.14 Draw a schematic diagram of position control system for controlling the linear displacement of a load mass. Use potentiometers for formation of error and hydraulic linear actuator for moving the mass. Give a brief description of the equipment used in the system. (Help: Fig. 3.53)

3.15 Pneumatic devices are widely used in process control systems. In a thermal system, the following hardware has been used to control the temperature of the process stream leaving a CSTR (Continuously Stirred Tank Reactor):
Sensor (temperature to current)
Controller (current to current)
Transducer (current to pressure)
Control valve (pressure to flow rate)
Select appropriate control hardware and draw a schematic diagram describing the complete temperature control system. Explain the constructional and operational features of the selected hardware. (Help: Fig. 3.57)

3.16 Give an example of a feedback system with closed-loop transfer function of the form

$$\frac{Y(s)}{R(s)} = \frac{K}{\tau s + 1}$$

Find the response of the system to unit-step input and discuss the effects of variations in parameters K and τ on transient behaviour. What is the effect of variations in these parameters on steady-state response to step and ramp inputs? (Help: Fig. 3.39, pp 69-71, Review Example 2.1)

3.17 Give an example of a feedback system into closed-loop transfer function of the form

$$\frac{Y(s)}{R(s)} = \frac{K\omega_n^2}{s^2 + 2\zeta\omega_n s + \omega_n^2}$$

Find the response of the system to unit-step input and discuss the effects of variations in parameters K, ζ, and ω_n, on transient behaviour. What are the effects of variations in these parameters on steady-state response to step and ramp inputs? (Help: Fig. 3.40, pp 72-77, Review Example 2.2)

Problems

3.1 A linear feedback control system has the block diagram shown in Fig. P3.1. Using block diagram reduction rules, obtain the closed-loop transfer function $Y(s)/R(s)$.

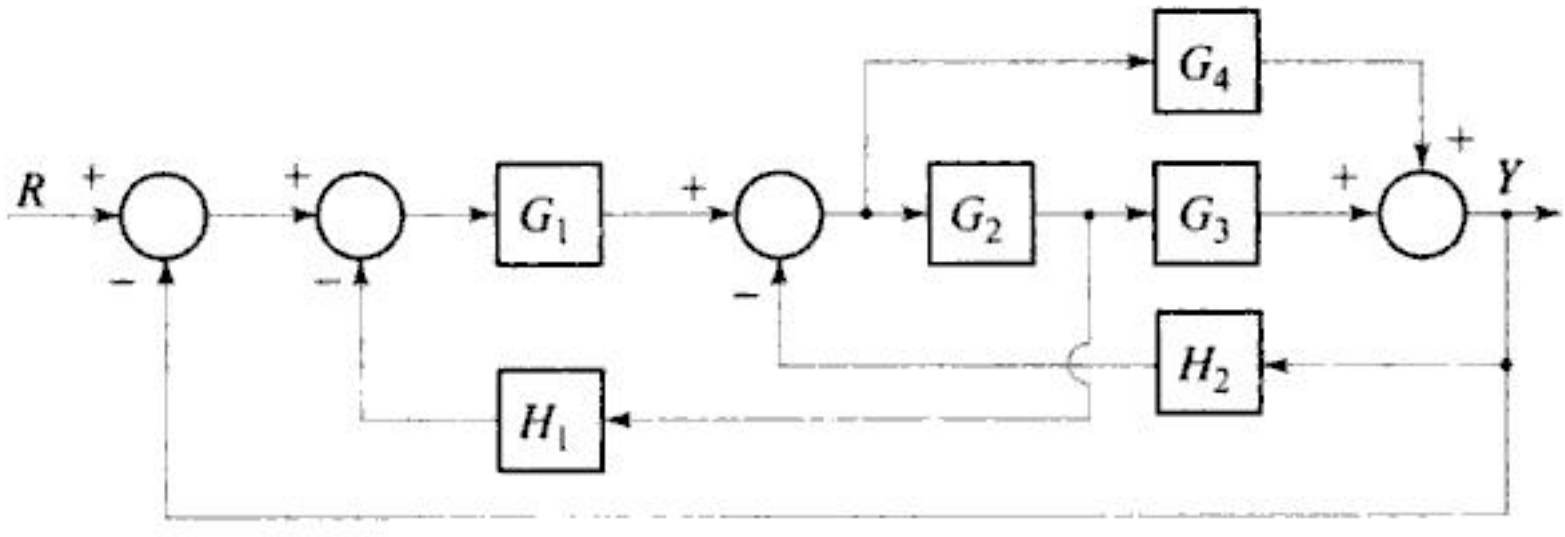


Fig. P3.1

Copyrighted material

3.2 Using block diagram reduction rules, convert the block diagram of Fig. P3.2 to a simple loop.

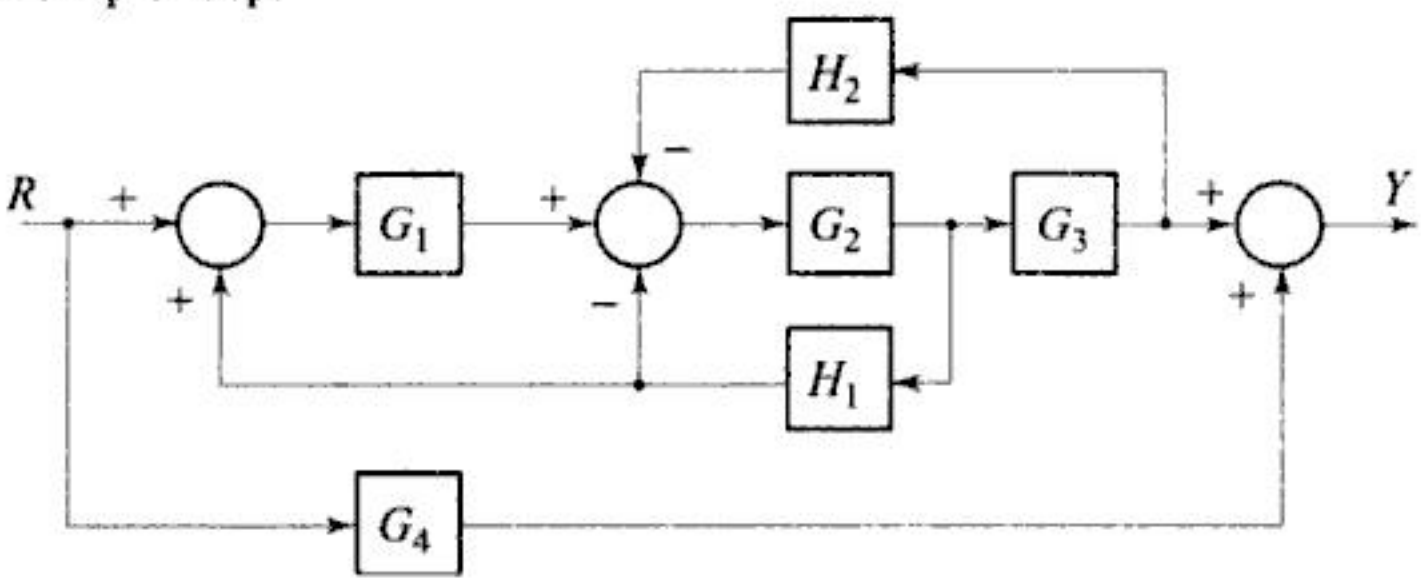


Fig. P3.2

3.3 Convert the block diagram of Fig. P3.3 to a signal flow graph, and therefrom obtain the input–output transfer function using Mason's gain rule.

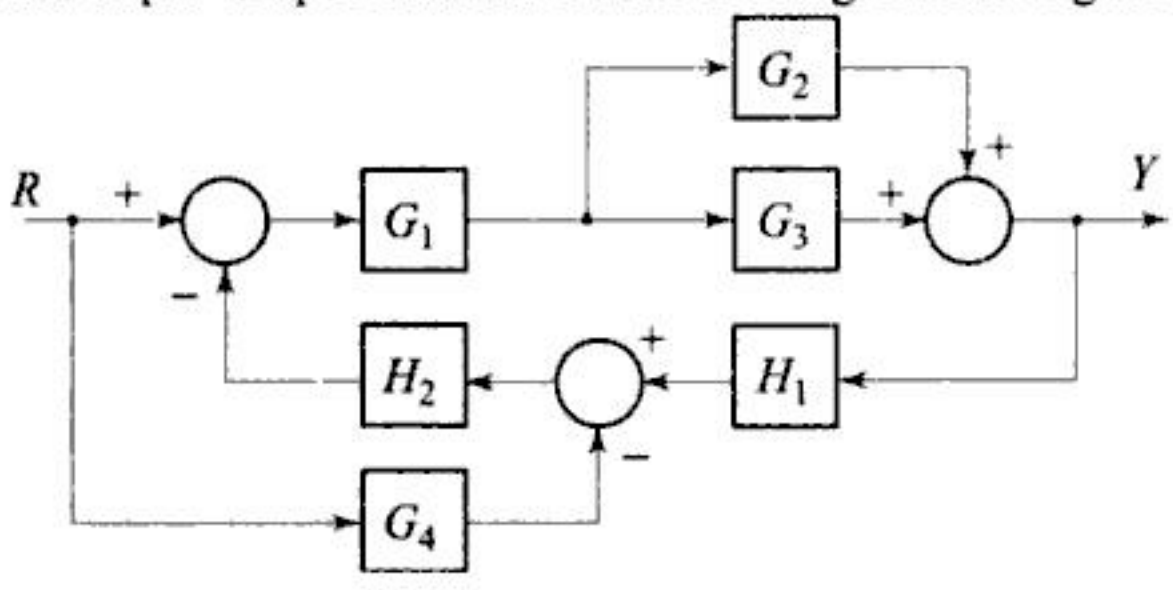


Fig. P3.3

3.4 The block diagram of a feedback control system is shown in Fig. P3.4. The output

$$Y(s) = M(s)R(s) + M_w(s)W(s)$$

Find the transfer functions $M(s)$ and $M_w(s)$.

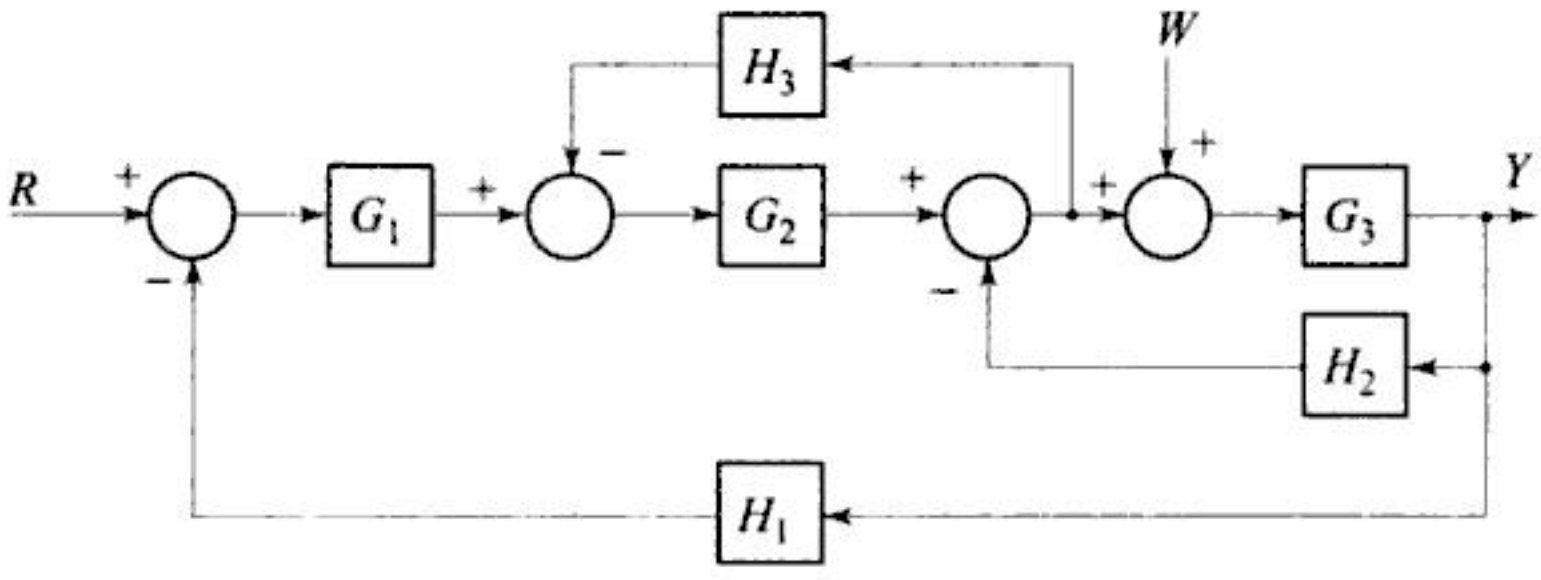


Fig. P3.4

Copyrighted material



You have either reached a page that is unavailable for viewing or reached your viewing limit for this book.

Determine how the load speed will change with time.

Given: $K_A = 4$ amps/volts; $K_T = 1.5$ N-m/amp;
$K_g = 50$ volts/amp; $K_t = 0.2$ volts/(rad/sec);
$R_a = 1\Omega$; $J = 6$ kg-m^2

3.7 Consider the positional servomechanism shown in Fig. P3.7. Assume that the input to the system is reference shaft position θ_R and the system output is the load shaft position θ_L. Draw a block diagram of the system indicating the transfer function of each block. Simplify the block diagram to obtain $\theta_L(s)/\theta_R(s)$. The parameters of the system are given below.

Sensitivity of error detector	$K_P = 10$ volts/rad
Amplifier gain	$K_A = 50$ volts/volt
Motor field resistance	$R_f = 100$ ohms
Motor field inductance	$L_f = 20$ henrys
Motor torque constant	$K_T = 10$ Newton-m/amp
Moment of inertia of load	$J_L = 250$ kg-m^2
Coefficient of viscous friction of load	$B_L = 2500$ Newton-m/(rad/sec)
Motor to load gear ratio	$\dot{\theta}_L/\dot{\theta}_M = 1/50$
Load to potentiometer gear ratio	$\dot{\theta}_P/\dot{\theta}_L = 1$

Motor inertia and friction are negligible.

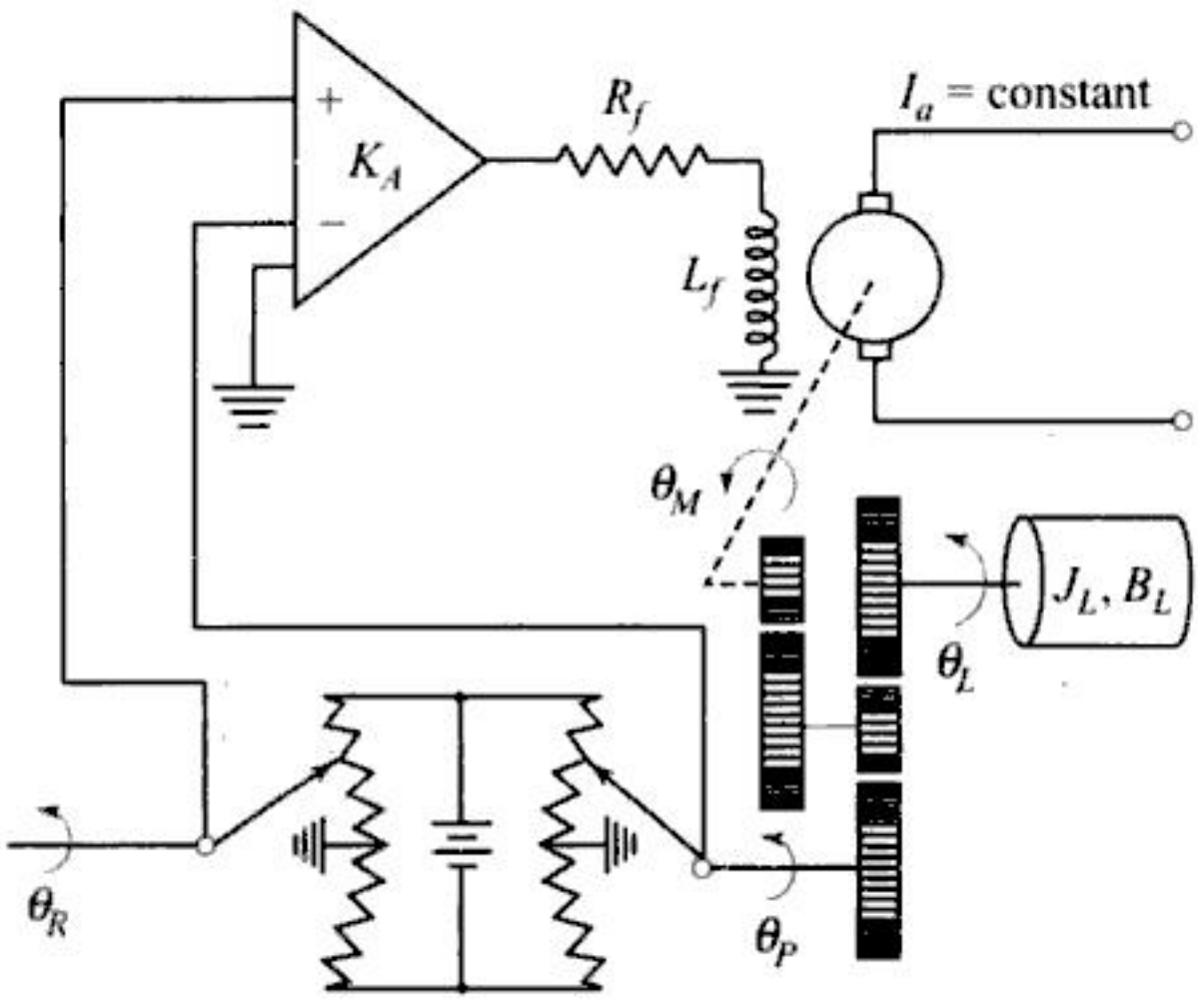
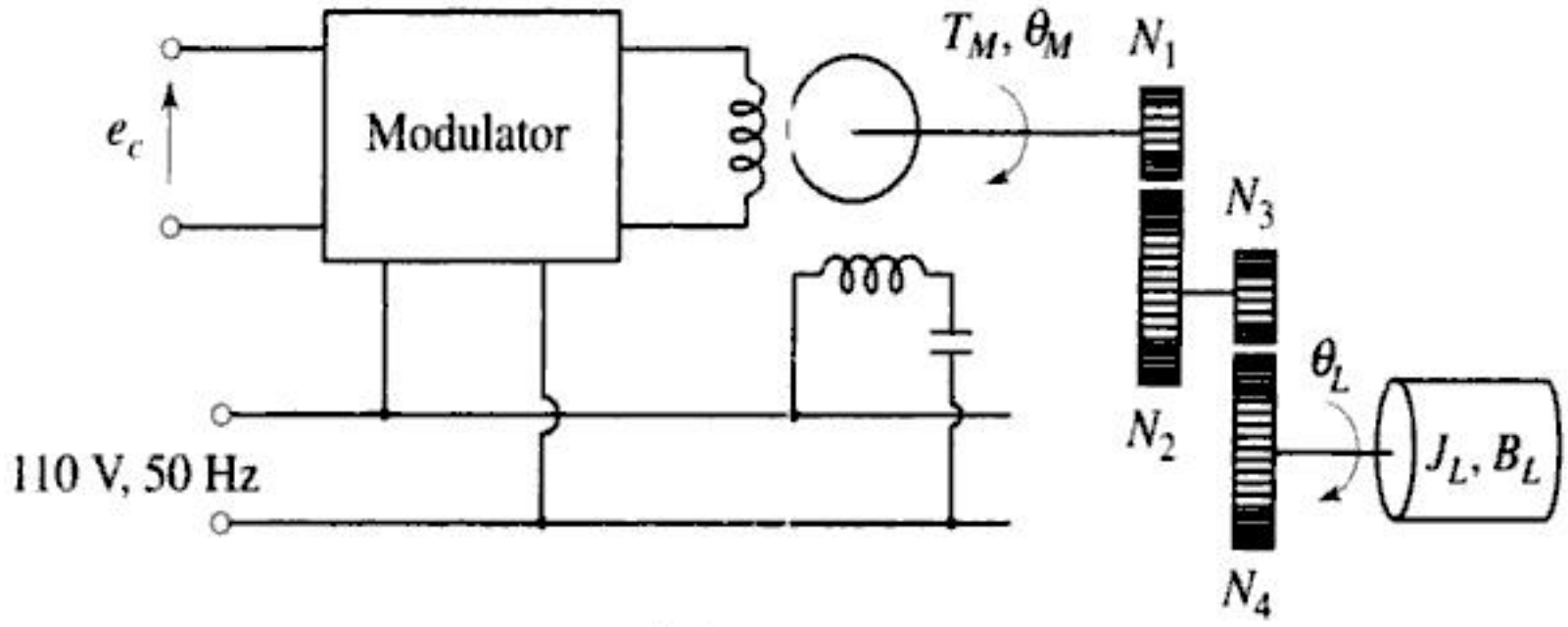


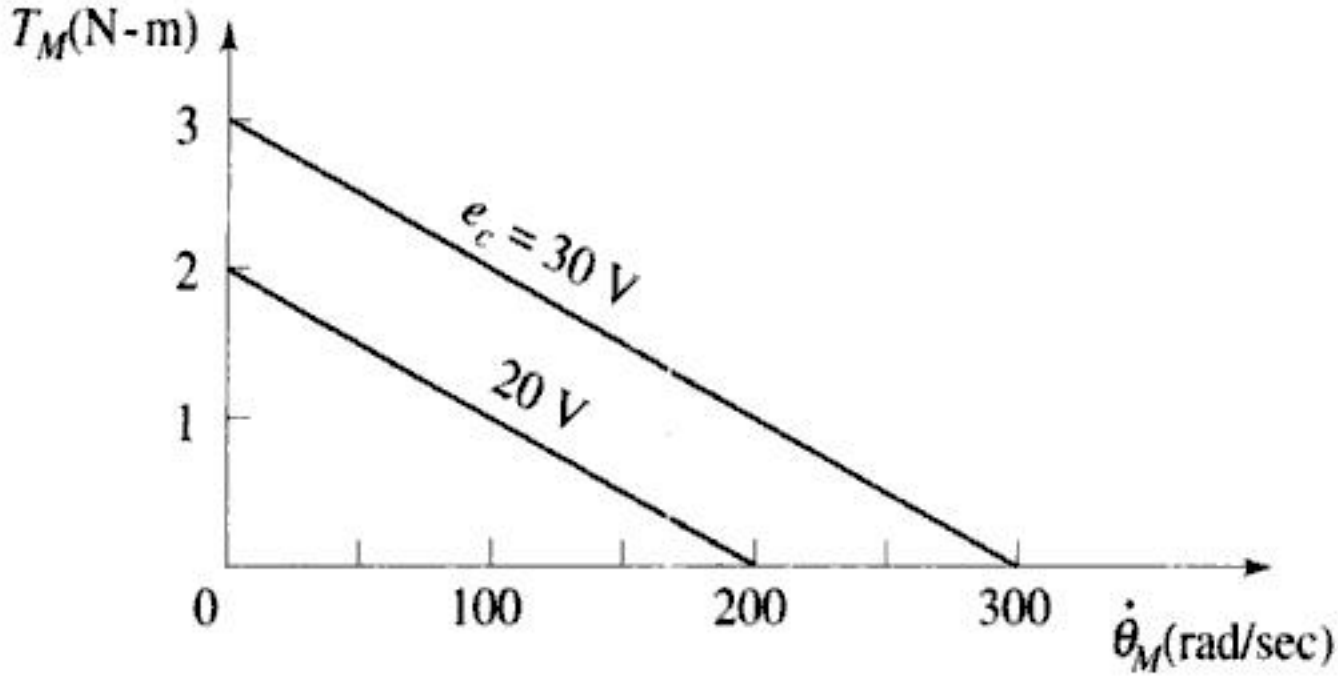
Fig. P3.7

3.8 Consider the system shown in Fig. P3.8a. The characteristic of ac motor is shown in Fig. P3.8b. The moment of inertia of the motor is $J_M = 0.003$ N-m/(rad/sec^2). The motor drives a load through a gear train. N_1, N_2, N_3, and N_4 are the number of teeth with $N_1/N_2 = 1/2$ and $N_3/N_4 = 1/5$. The moment of inertia of the load is $J_L = 0.02$ N-m/(rad/sec^2), and coefficient of viscous friction of the load is $B_L = 0.001$ N-m/(rad/sec). Find the transfer function $\theta_L(s)/E_e(s)$.

Copyrighted material



(a)



(b)

Fig. P3.8

3.9 Consider the system shown in Fig. P3.9 with $R_a = 10\ \Omega$, $L_a = 0.1$H, $K_b = 1$ volt/(rad/sec), $\dot{\theta}_L/\dot{\theta}_M = 1/2$, $K_t = 0.8$ volt/(rad/sec), $K_P = 1.5$ volt/rad.
Moment of inertia of load, $J_L = 2$ N-m/(rad/sec^2).
Moment of inertia of motor shaft, $J_M = 0.1$ N-m/(rad/sec^2).
Coefficient of viscous friction of load, $B_L = 0.02$ N-m/(rad/sec).
Coefficient of viscous friction on motor shaft, $B_M = 0.01$ N-m/(rad/sec)

(i) Find the transfer function $\theta_M(s)/E_a(s)$

(ii) A multi-loop (consisting of a speed-feedback loop and a position-feedback loop) feedback control system built around the system of Fig. P3.9 with suitable additional hardware drives the load to the commanded position θ_R inspite of load torque disturbances.
Make a sketch of the feedback control system showing how the hardware is connected.

(iii) What will be the effect of opening the position feedback loop on the performance of the control system?

(iv) What will be the effect of opening the speed feedback loop on the performance of the control system?

Copyrighted material

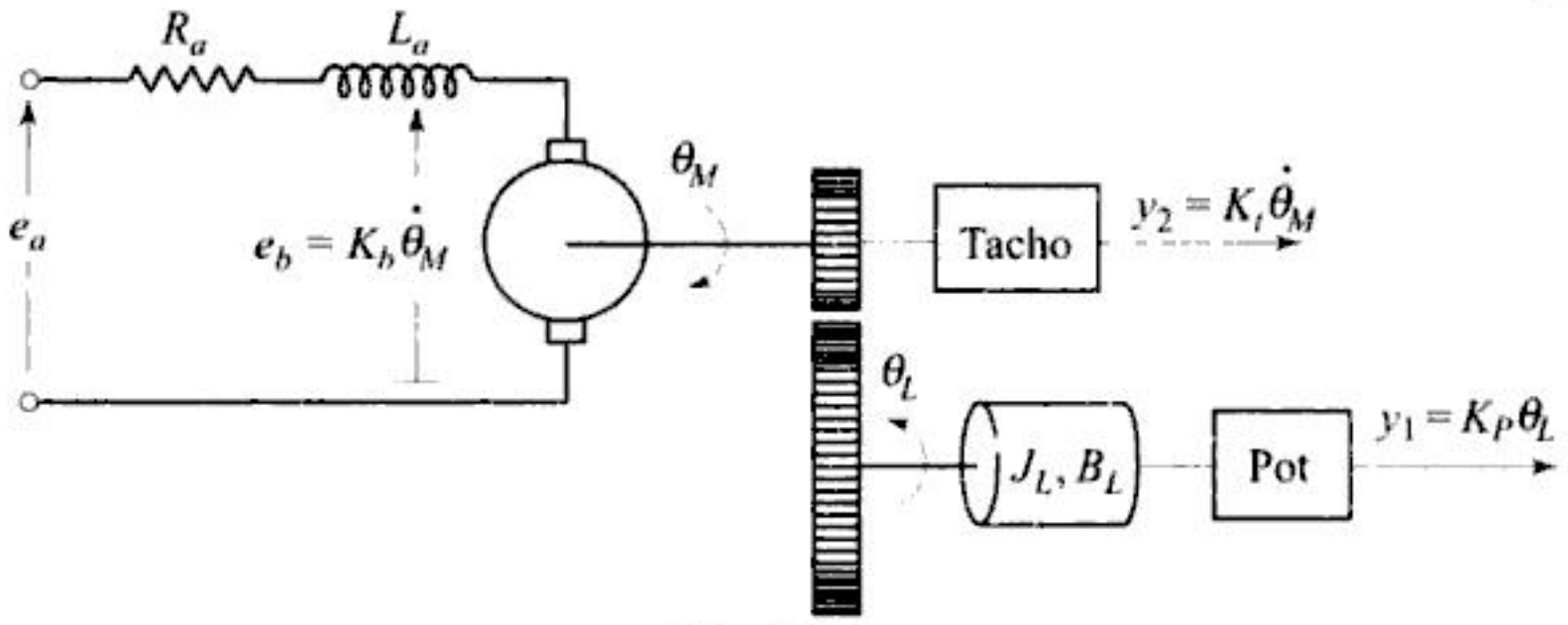


Fig. P3.9

(Since tachometers tend to be noisy at low speeds, in a geared system one usually puts the tacho on the motor, rather than the load)

3.10 The schematic diagram of a servo system is shown in Fig. P3.10. The two-phase servomotor develops a torque in accordance with the equation

$$T_M = K_1 e_c - K_2\dot{\theta}_M$$

where

$$K_1 = 1 \times 10^{-5} \text{ N-m/volt};\ K_2 = 0.25 \times 10^{-5} \text{ N-m/(rad/sec)}$$

The other parameters of the system are:

Synchro sensitivity	$K_s = 1$ volt/rad
Amplifier gain	$K_A = 20$ volt/volt
Tachometer constant	$K_t = 0.2$ volt/(rad/sec)
Load inertia	$J_L = 1.5 \times 10^{-5}$ kg-m^2
Viscous friction	$B_L = 1 \times 10^{-5}$ N-m/(rad/sec)

$$\dot{\theta}_M/\dot{\theta}_S = 1;\ \dot{\theta}_M/\dot{\theta}_T = 1$$

Motor inertia and friction are negligible.

Draw the block diagram of the system and therefrom obtain the transfer function $\theta_M(s)/\theta_R(s)$.

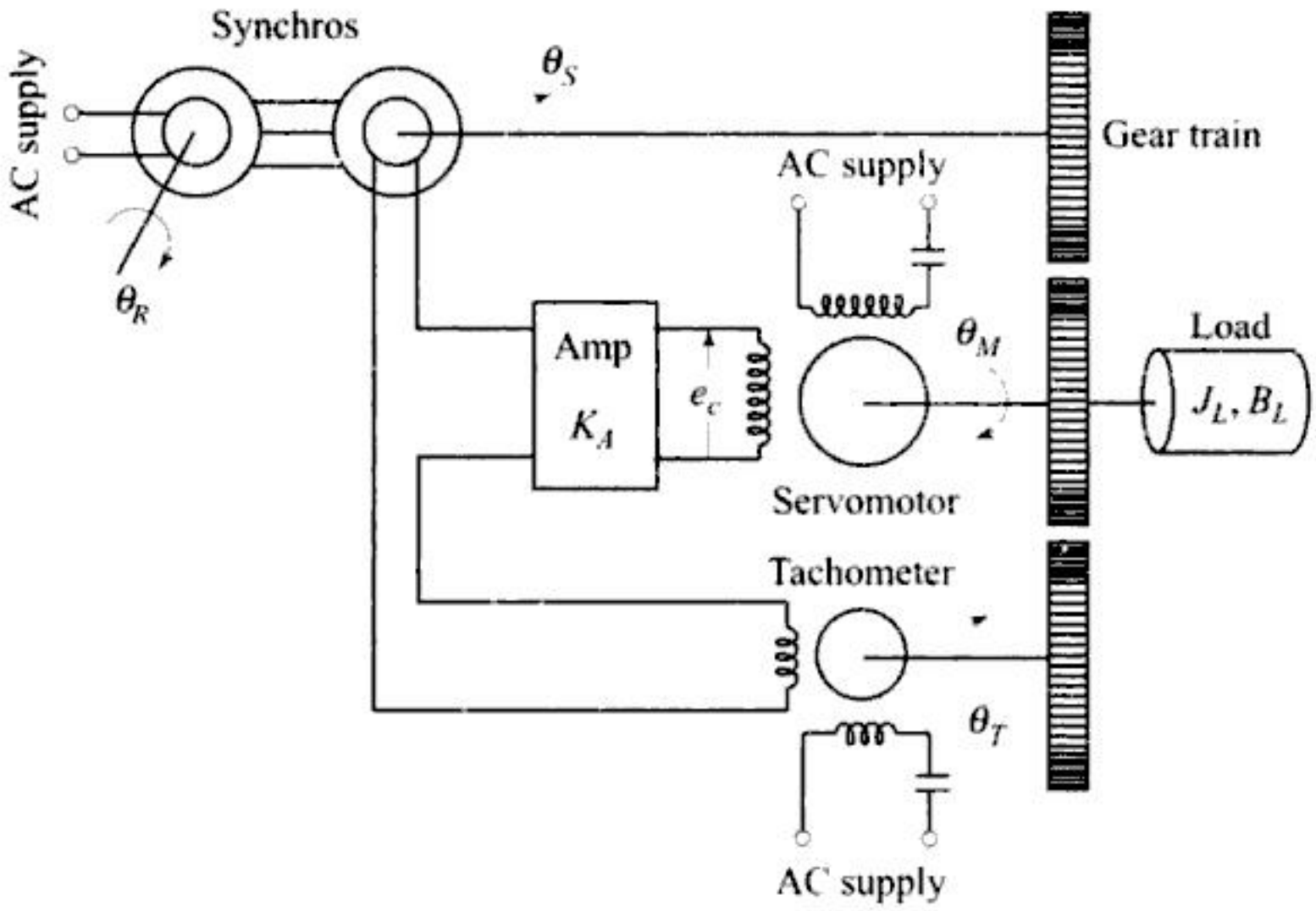


Fig. P3.10

Copyrighted material

3.11 An ac-dc servo system is shown in Fig. P3.11. The sensitivity of the synchro error detector is K_s volt/rad, and the gain of the generator is K_g volts/field amp. The dc motor is separately excited and has a back emf of K_b volts/(rad/sec) and a torque constant of K_T N-m/amp. Motor inertia and friction are negligible. Draw the block diagram of the system indicating the transfer function of each block. Obtain $\theta_L(s)/\theta_R(s)$.

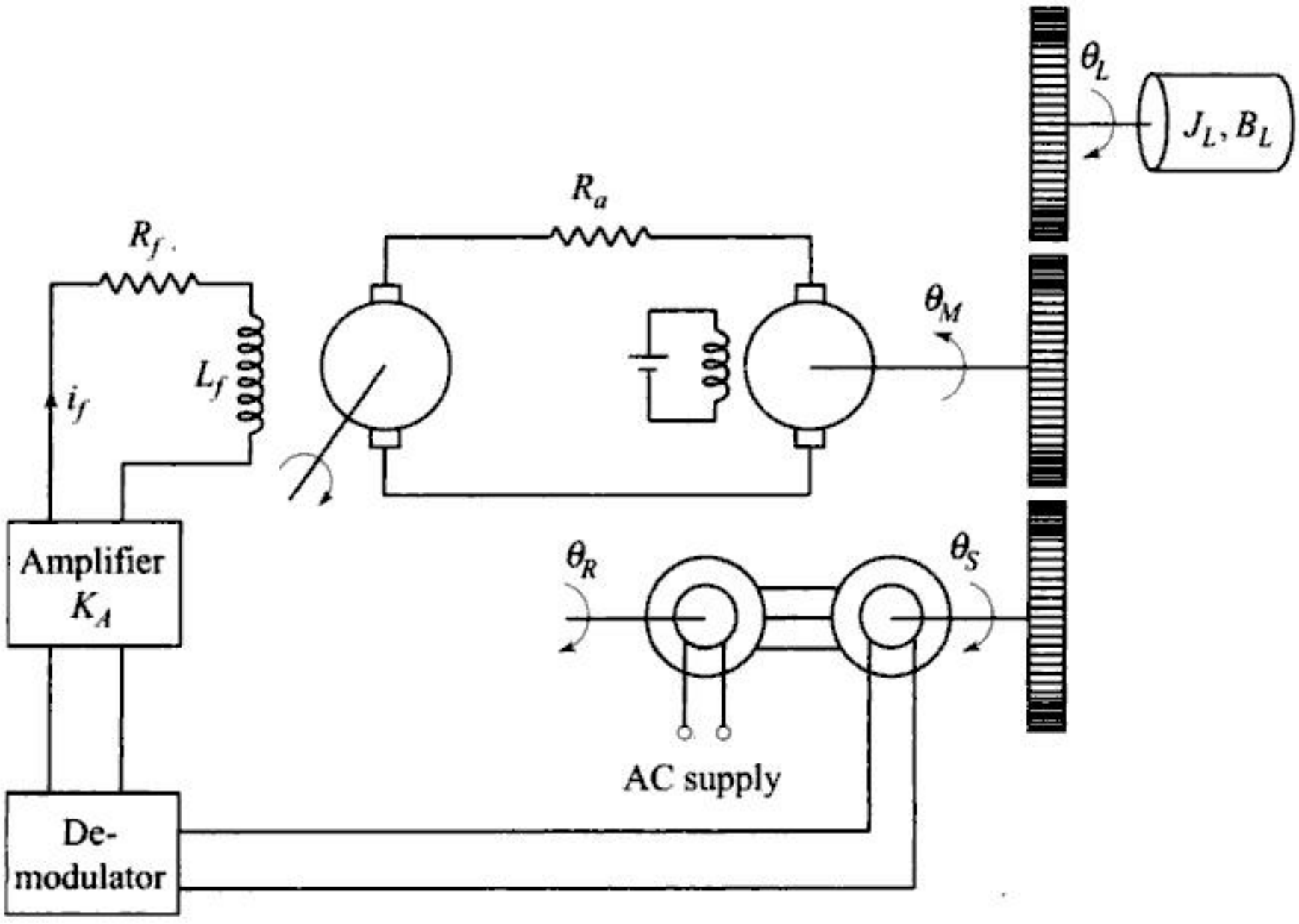


Fig. P3.11

The system parameters are given below:

$K_s = 30$ volts/rad; $K_A = 5$ volts/volt; $R_f = 100$ ohms;
$L_f = 2$ henrys; $K_g = 100$ volts/field amp; $R_a = 1$ ohm;
$K_b = 1$ volt/(rad/sec); $J_L = 0.5$ kg-m^2 $B_L = 1$ N-m/(rad/sec);
$\dot{\theta}_L/\dot{\theta}_M = \dot{\theta}_S/\dot{\theta}_M = 1$

3.12 Figure P3.12 shows a closed-loop drive system. The desired speed ω_r is set on a potentiometer which provides the reference voltage e_r. The parameters describing the system are given below:

$R_a = 6\,\Omega$,	$L_a = 46$ mH
$J = 0.093$ kg-m^2,	$B = 0.008$ N-m/(rad/sec)
Motor torque constant	$K_T = 0.55$ N-m/amp
Thyristor rectifier gain constant	$K_r = 25$
Amplifier gain	$K_A = 20$
Tachometer sensitivity	$K_t = 0.057$ volts/(rad/sec)

(a) Draw a block diagram of the system that includes transfer functions of all the sub-systems, and therefrom obtain $\omega(s)/E_r(s)$.

Copyrighted material

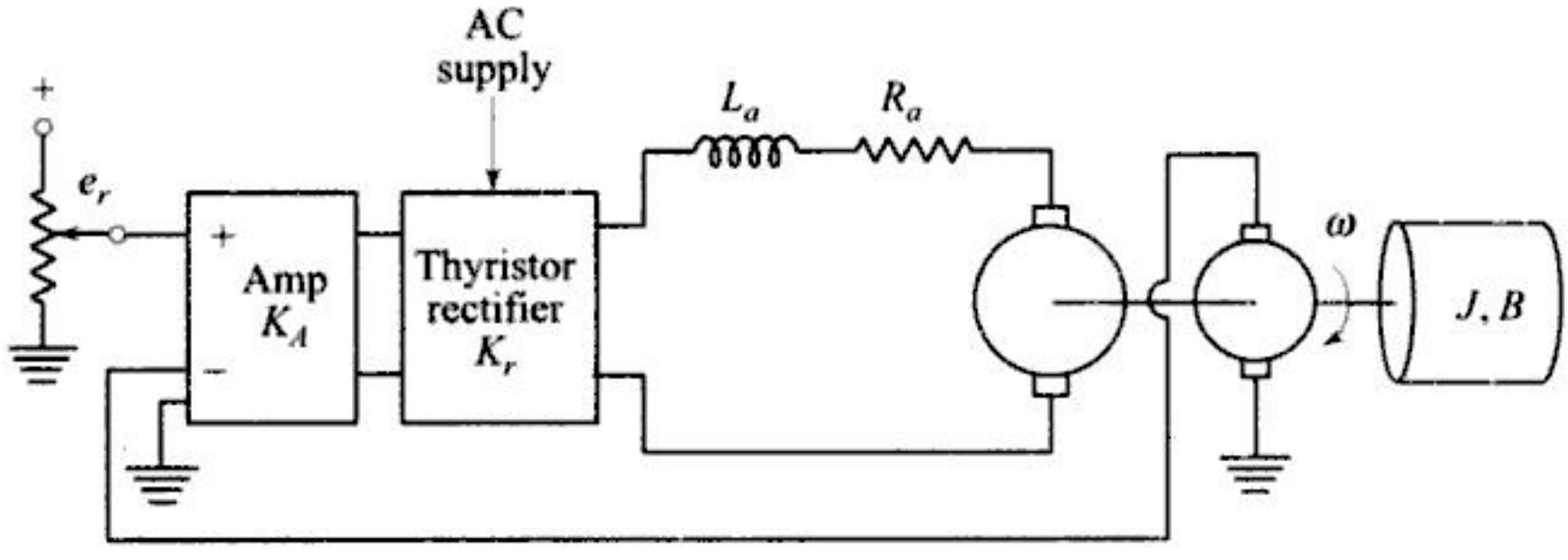


Fig. P3.12

(b) The thyristorized drives are usually provided with a current-limiting feature to prevent damage to the thyristors. Modify the drive system of Fig. P3.12 to implement the current limit. Draw a block diagram of the proposed system.

3.13 A dc position control servomechanism comprises of a split-field dc servomotor with constant armature current, potentiometer error detector with sensitivity K_P volts/rad, and a dc amplifier of gain K_A amps/volts. The motor produces a torque of K_T N-m/amp. Separate motor and load inertias J_M (kg-m^2) and J_L (kg-m^2) are identified, and the connecting structure is modelled by a shaft with spring constant K (N-m/rad) and damping coefficient B (N-m per rad/sec). A load disturbance T_w (N-m) acts on J_L opposite the developed motor torque T_M (N-m). T_M accelerates J_M and supplies the torque transmitted by the shaft. This shaft torque, in turn, accelerates J_L and supplies T_w.

Motor field time-constant is assumed to be negligible.

(a) Make a sketch of the system showing how the hardware is connected.

(b) Determine the transfer functions $\theta_L(s)/\theta_R(s)$ and $\theta_L(s)/T_w(s)$, where θ_L (rad) and θ_R (rad) are, respectively, the actual and commanded load positions.

3.14 The electrohydraulic position control system shown in Fig. P3.14 positions a mass M with negligible friction. Assume that rate of oil flow in the power cylinder is $q = K_1 x - K_2 \Delta p$ where x is the displacement of the spool and Δp is the differential pressure across the power piston. Draw a block diagram of the system and obtain therefrom the transfer function $Y(s)/R(s)$.

The system constants are given below.

Mass $M = 1000$ kg

Constants of the hydraulic actuator:

$K_1 = 200$ cm^2/sec per cm of spool displacement

$K_2 = 0.5$ cm^2/sec per gm-wt/cm^2

Potentiometer sensitivity $K_P = 1$ volt/cm

Power amplifier gain $K_A = 500$ mA/volt

Linear transducer constant $K = 0.1$ cm/mA

Piston area $A = 100$ cm^2

Copyrighted material

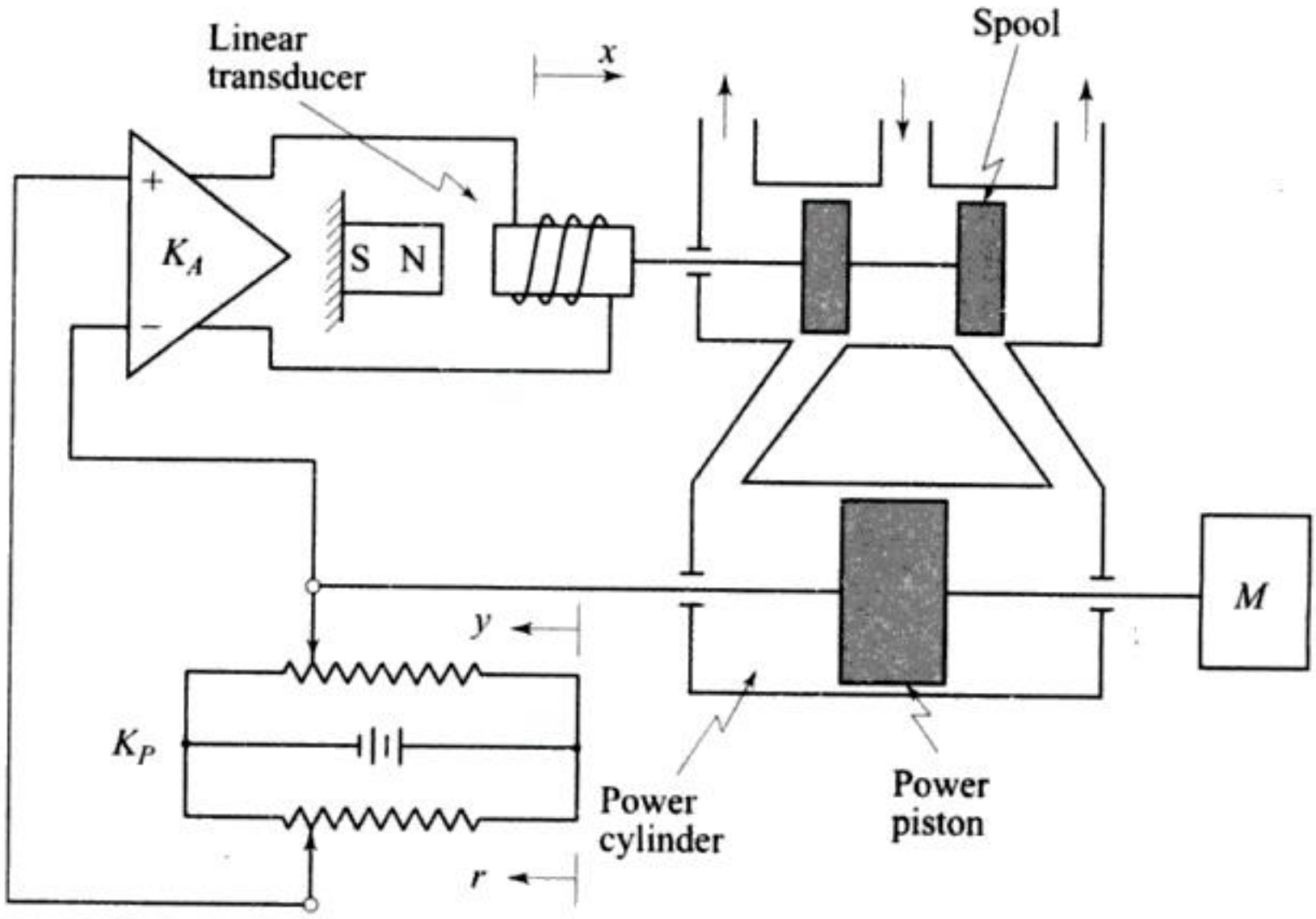


Fig. P3.14

3.15 The conceptual design of a hydraulic control system for machining a workpiece on a lathe is shown in the schematic diagram of Fig. P3.15. The control system is a servomechanism, where the actual tool position $y(t)$ is required to follow a time-varying command input position $y_r(t)$. The command input $y_r(t)$ may be generated by a punched-tape reader. The input device produces a voltage $e_r = K_r y_r$. The carriage is moved at a constant speed and the control of the tool position is in the direction of the cross slide.

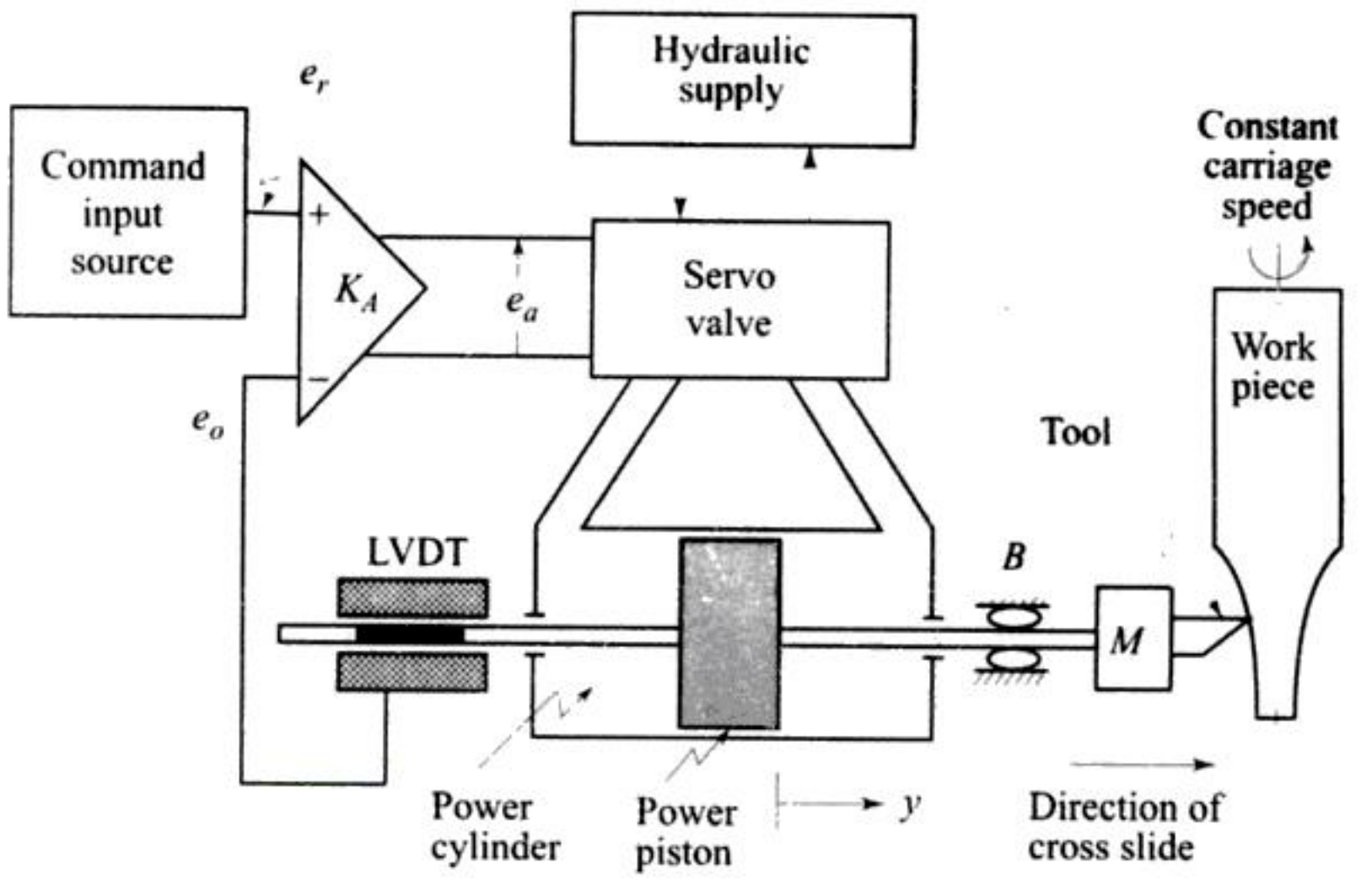


Fig. P3.15

Copyrighted material

The LVDT provides a feedback voltage $e_o(t)$ proportional to the actual tool position ($e_o(t) = K_s y(t)$, K_s is a constant). The error ($e_r - e_o$) is amplified by an amplifier of gain K_A volts/volt. The servovalve regulates the spool displacement and hence controls port opening x; $x = K_v e_a$, where K_v is the valve gain. The rate of oil flow in the power cylinder is $q = K_1 x - K_2 \Delta p$, where Δp is the differential pressure across the piston of area A, and K_1 and K_2 are constants.

The load on the piston consists of mass M and viscous friction with coefficient B. Treat the reactive force F_r of the cutting tool as a disturbance. Assuming all the variables to be deviations from an equilibrium position, draw a functional block diagram that describes perturbation dynamics of the system. Derive the transfer function $Y(s)/E_r(s)$.

3.16 A hydraulic servo system used to control the transverse feed of a machine tool is shown in Fig. P3.16. Each angular position of the cam corresponds to a desired reference position y_r such that $x = K_r y_r$. The load on the piston is that due to tool reactive force and may be assumed to consist of mass M, friction B and spring with constant K. Draw a block diagram and obtain therefrom the transfer function $Y(s)/Y_r(s)$, assuming that rate of oil flow in the power cylinder is $q = K_1 e - K_2 \Delta p$, where K_1 and K_2 are constants and Δp is the differential pressure across the power piston of area A.

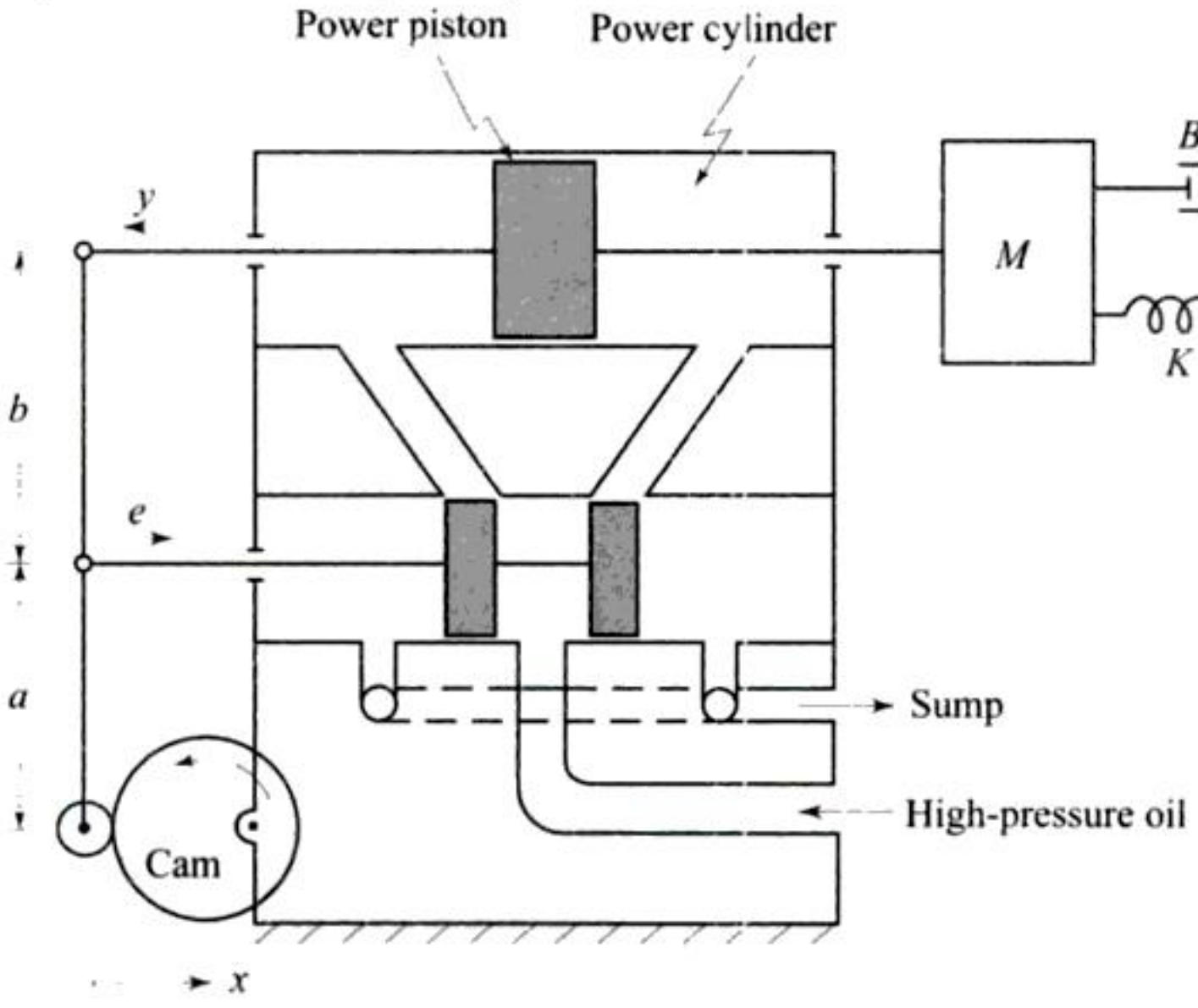


Fig. P3.16

3.17 The schematic diagram of a steel-rolling process is shown in Fig. P3.17. The steel plate is fed through rollers at a constant speed of v cm/sec. The distance between the rollers and the point where the thickness is measured is d cm. The thickness gauge provides a feedback voltage $e_o(t)$ proportional to the actual

Copyrighted material

thickness $y(t)$ of the plate ($e_o(t) = K_s\, y(t)$; K_s is a constant). A voltage e_r corresponding to the desired thickness is the reference input to the system. The error $(e_r - e_o)$ is amplified by an amplifier of gain K_A amps/volt. The servo valve regulates the spool displacement and hence controls port opening x; $x = K_v i$, where K_v is the valve gain. The rate of oil flow in the power cylinder is $q = K_1 x - K_2 \Delta p$ where Δp is the differential pressure across the piston of area A, and K_1 and K_2 are constants.

The load on the piston is that of the roller mass M and viscous friction with coefficient B. Normal force F_w on the roller is a load disturbance.

Assuming all the variables to be deviations from an equilibrium position, draw a functional block diagram that describes perturbation dynamics of the system. Derive the transfer function $Y(s)/E_r(s)$.

3.18 Consider the two-tank system shown in Fig. P3.18. The height h_2 in the second tank is to be controlled by adjusting the flow rate q_1 into the first tank. The system disturbance is the flow rate q_w drawn off from the first tank (to be used elsewhere in the processing operation) by a variable displacement pump.

The command signal h_r for the desired height in tank 2 is set on a pot whose output is $e_r = K_s h_r$. The sensor output is $e_o = K_s h_2$. The differential amplifier has a gain K_a, the electropneumatic transducer has a gain K_e, and the pneumatic control valve (pneumatic actuator + flow control valve) has a gain K_v. At the initial equilibrium point, the inflow rate exactly matches the outflow rates, and the heights in the two tanks are $\overline{H}_1$ and $\overline{H}_2$ with $h_2 = h_r = 0$. A_1 is the surface area of tank 1, and R_1 is the resistance to flow offered by the valve in the outflow path (R = incremental change in pressure across the valve/ incremental change in flow through the valve). A_2 and R_2 are the corresponding values for tank 2.

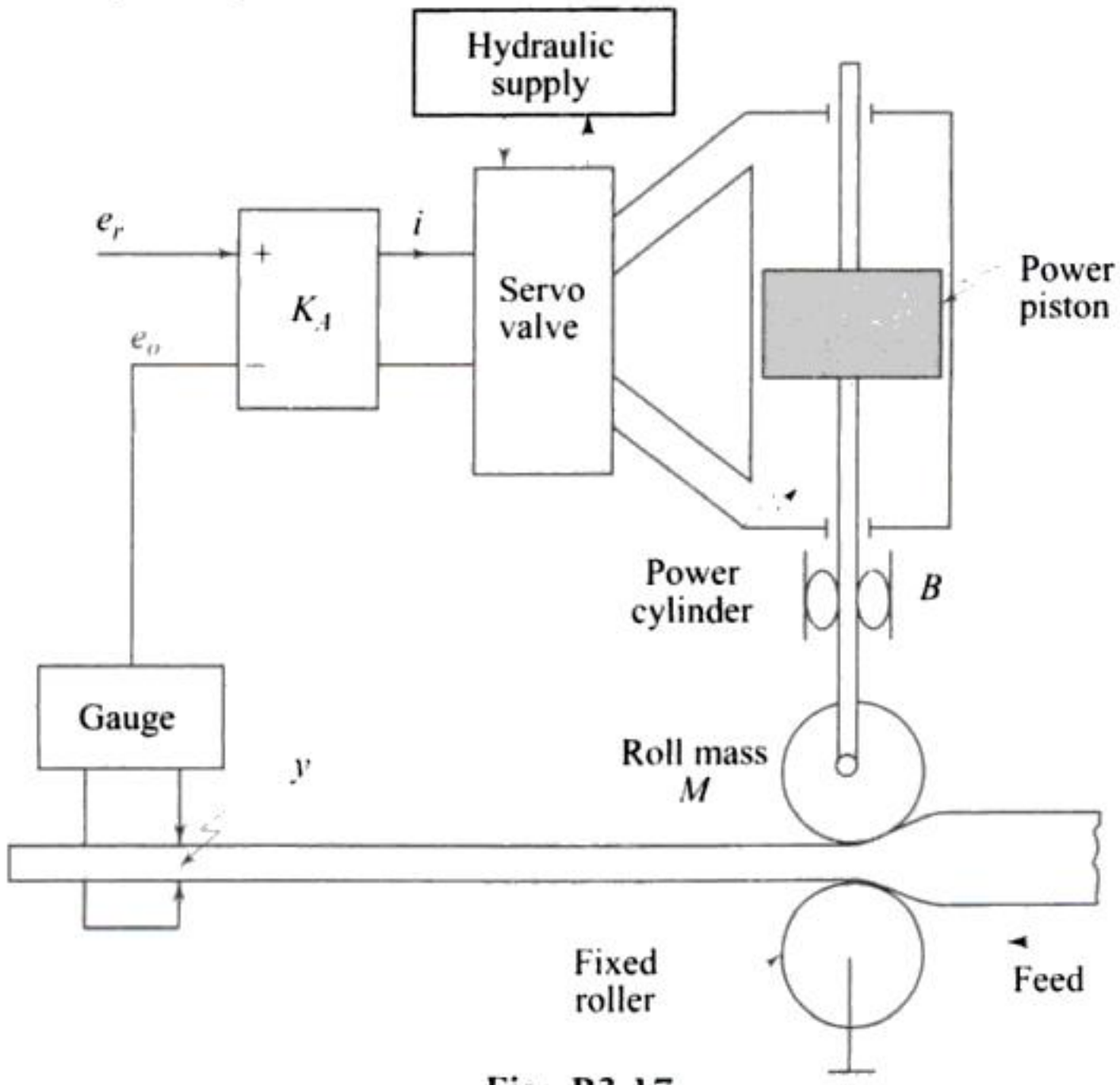


Fig. P3.17

Copyrighted material

Draw a functional block diagram of the system and therefrom derive the transfer function between h_2 and h_r.

3.19 A system to control the temperature of an oven chamber is shown in Fig. P3.19. The temperature θ is sensed by a thermocouple whose output is $K_t\theta_2$. The desired temperature θ_r is set on a pot whose output is e_r. The differential amplifier generates a signal e_A which controls the electrical resistance heater through an SCR amplifier and gives rise to heat flow at the rate $h = K_h e_A$ to the oven chamber. Heat also flows out of the oven due to imperfect insulation of its walls. The temperature of the ambient air is θ_a. Thermal capacitance of the medium inside the chamber is C_t and thermal resistance of the wall material is R_t. Thermal capacitances of the heater and wall are negligible.

Assuming all the variables are deviations from the equilibrium, obtain a block diagram model of the system that includes the transfer functions of all the sub-systems. Derive the transfer function $\theta(s)/E_r(s)$.

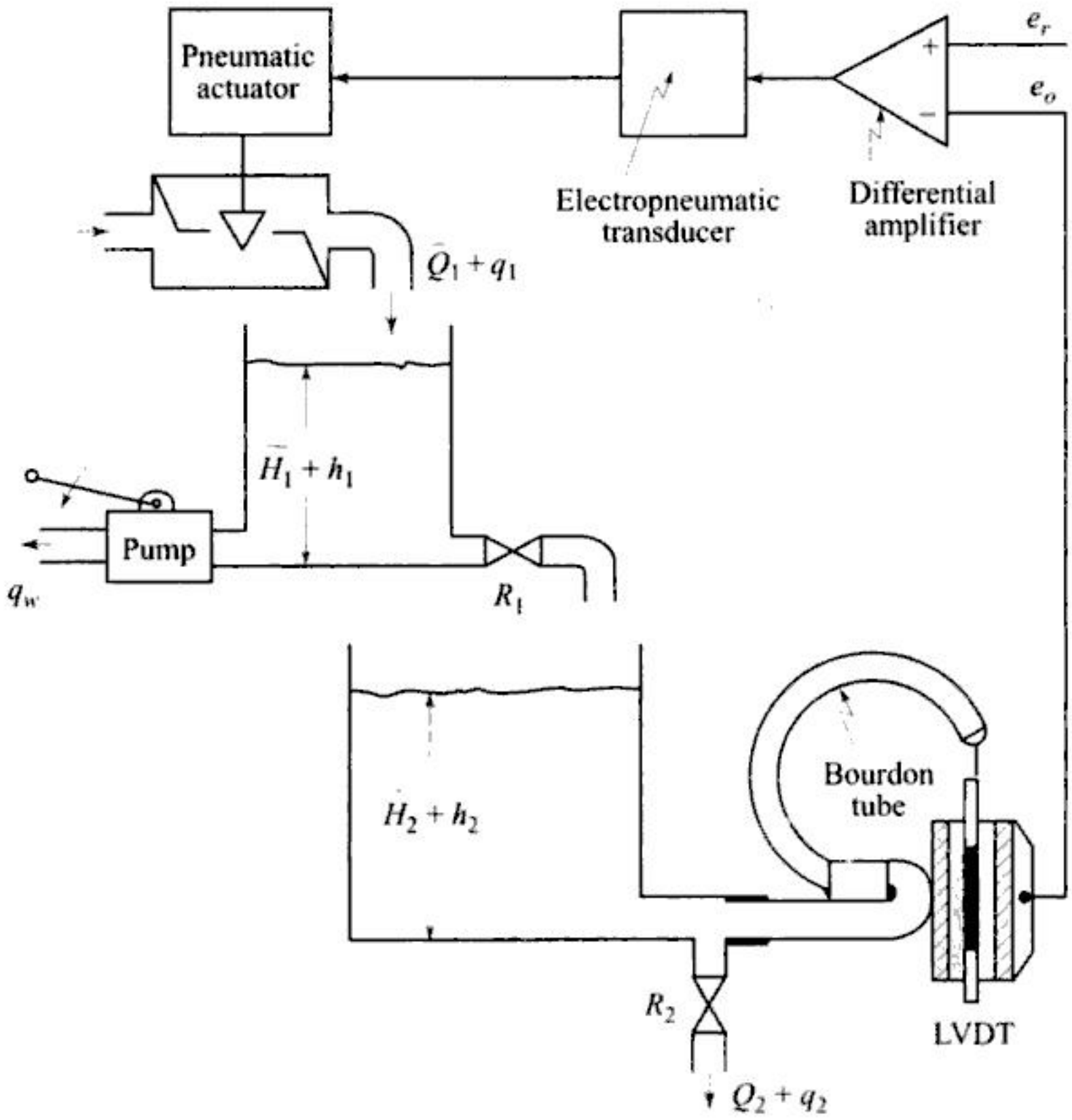


Fig. P3.18

Copyrighted material

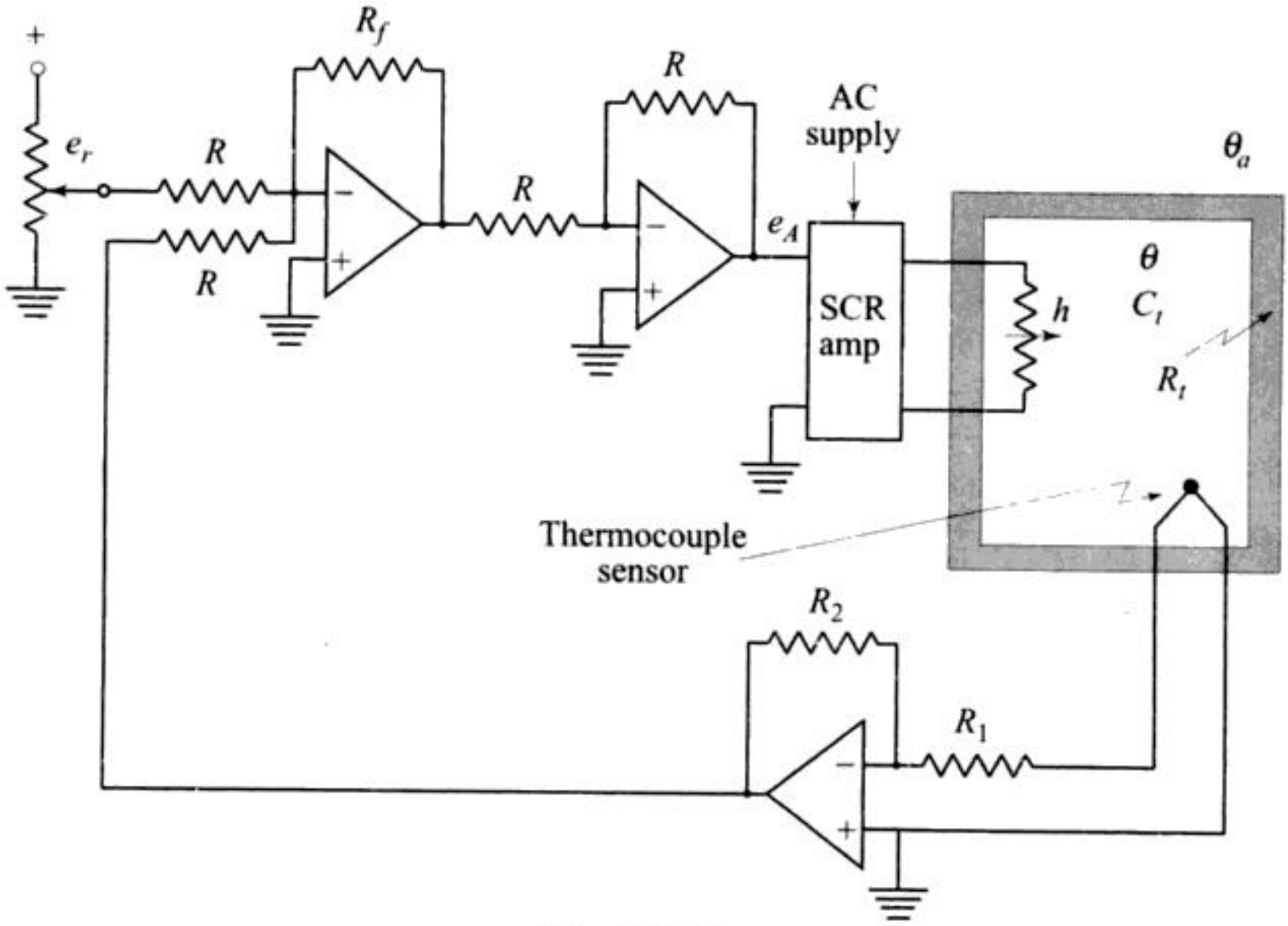


Fig. P3.19

3.20 In a heating system, air flows at constant volumetric flow rate Q into and out of a chamber of volume V. The density of the inflowing air is ρ, specific heat c, and temperature θ_i.

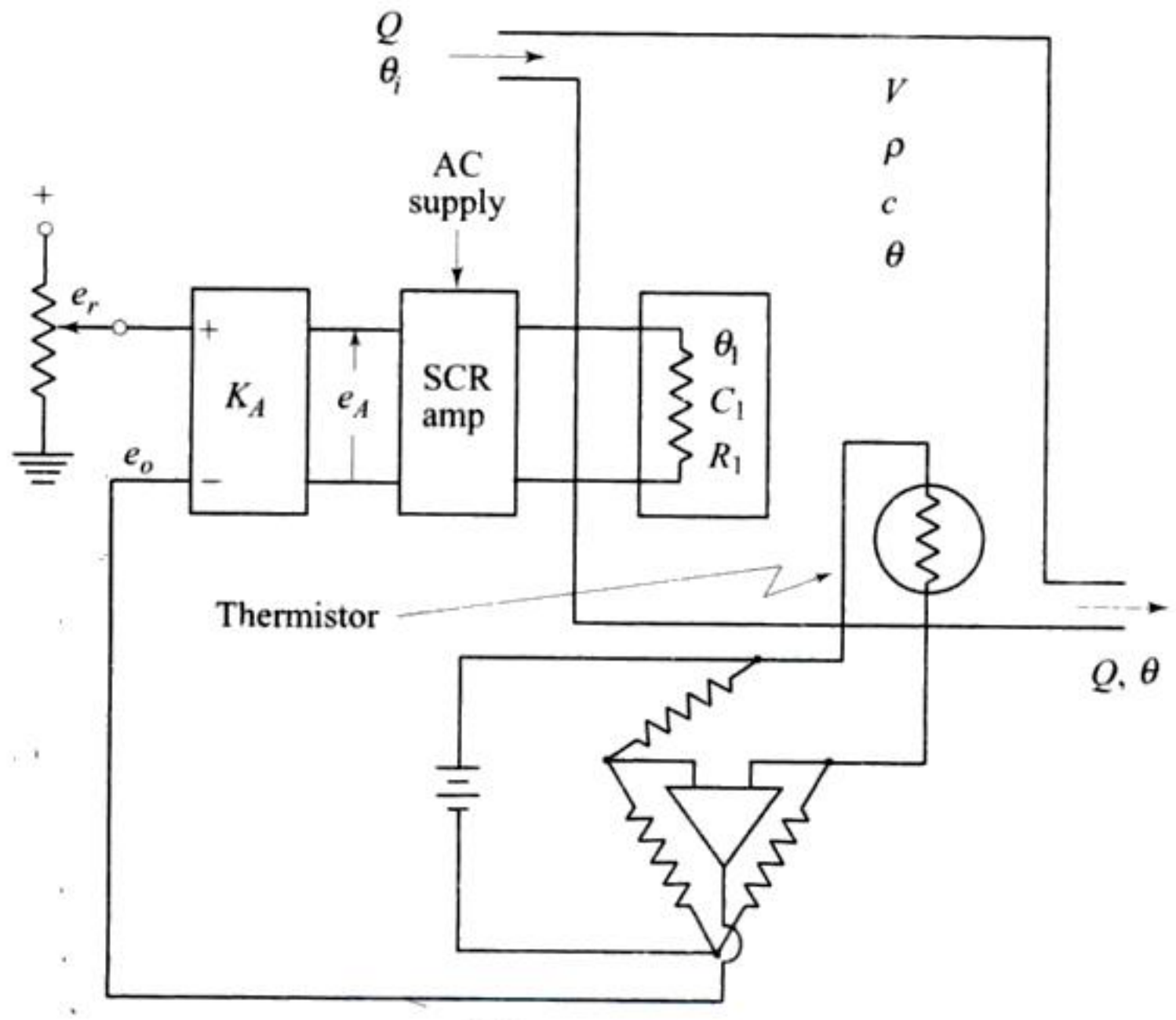


Fig. P3.20

Copyrighted material

A system to control the outflow temperature is shown in Fig. P3.20. The temperature θ is sensed by a thermistor with a Wheatstone bridge whose output $e_o = K_2\theta$. The desired temperature θ_r is set on a pot whose output $e_r = K_P\theta_r$. The differential amplifier generates a signal e_A which controls electrical resistance heater through an SCR amplifier and gives rise to heat flow at the rate $h = K_h e_A$. The heater has temperature θ_1, thermal capacitance C_1, and thermal resistance R_1. The walls of the chamber are perfectly insulated and have negligible thermal capacitance.

Assume that the variables $\{\theta_r, \theta, \theta_1, \theta_i\}$ are deviations from the equilibrium position. Considering θ_i as the disturbance, draw a functional block diagram of the system that includes the transfer functions of all the sub-systems. Derive the transfer functions $\theta(s)/\theta_r(s)$, and $\theta(s)/\theta_i(s)$.

3.21 Consider the unit shown in Fig. P3.21. The objective of this unit is to cool a hot process fluid of density ρ_2 and heat capacity c_2, flowing at a rate Q_2; the temperature of the inflowing process fluid is $\bar{\theta}_{i2} + \theta_{i2}$

The cooling medium (water) having density ρ_1 and heat capacity c_1 is circulated through the jacket at the rate $(\bar{Q}_1 + q_1)$, the temperature of the inflowing cooling water is $\bar{\theta}_{i1} + \theta_{i1}$. It is assumed that the jacketed tank is well-insulated.

Write the unsteady-state energy balance equations on the process fluid with temperature $(\bar{\theta}_2 + \theta_2)$, and on the cooling water with temperature $(\bar{\theta}_1 + \theta_1)$. Linearize these equations about the operating point $\{\bar{Q}_2, \bar{\theta}_{i2}, \bar{\theta}_{i1}, \bar{Q}_1, \bar{\theta}_1, \bar{\theta}_2\}$.

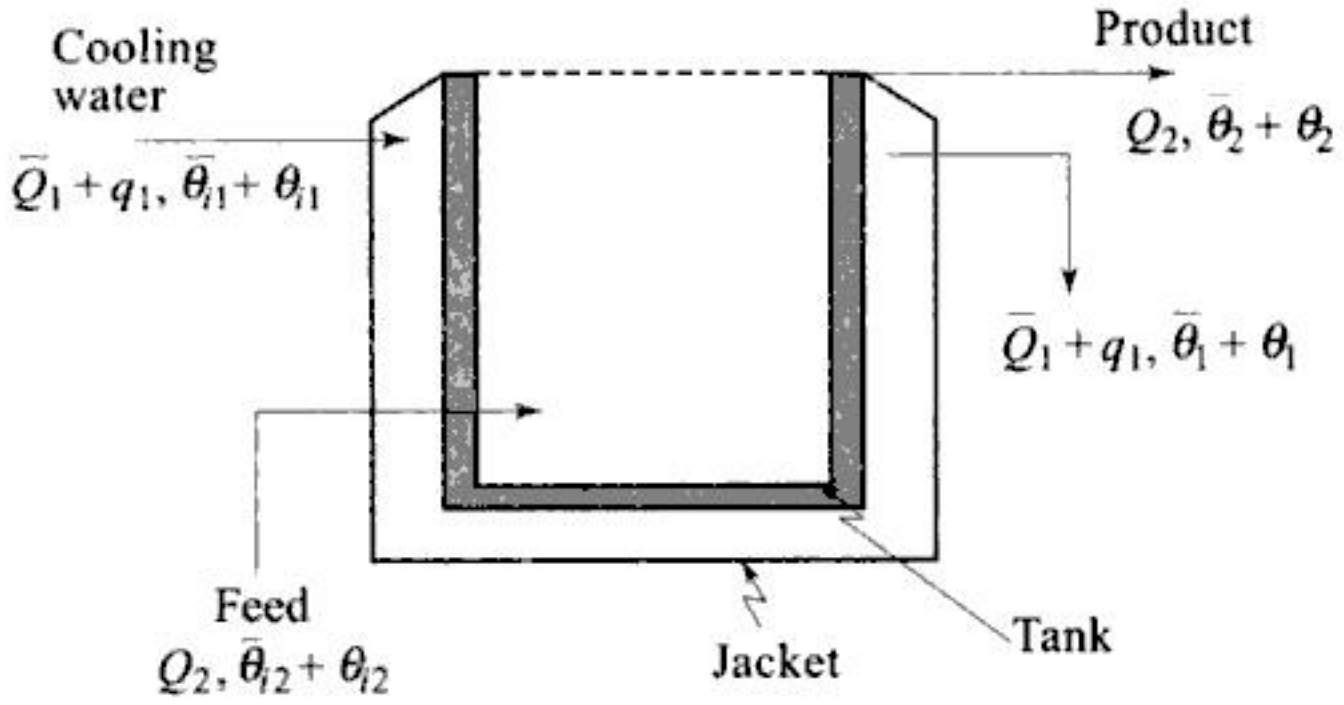


Fig. P3.21

The control hardware required to control the temperature of the process stream consists of the following components:

Sensor (temperature to voltage): gain K_1
Reference signal generator (temperature to voltage): gain K_1
Amplifier (voltage to voltage): gain K_2
Converter (voltage to pressure): gain K_3
Control valve (pressure to flow rate): gain K_4

q_1 is the manipulated variable, θ_{i1} and θ_{i2} are the disturbance variables, θ_2 is

Copyrighted material

the output variable, and θ_r represents the desired change in the initial setting of the output variable.

(i) Suggest suitable hardware and make a sketch of the system showing how the hardware is connected.

(ii) Draw a functional block diagram of the system that includes the transfer functions of all the sub-systems.

(iii) Derive the transfer function $\theta_2(s)/\theta_r(s)$.

Given: $\rho_2 = 19.2$ kg-mole/m^3; $c_2 = 1.815 \times 10^5$ J/kg-moles-°C;
$\rho_1 = 1000$ kg/m^3; $c_1 = 4184$ J/kg-°C
$V_2 =$ volume of the tank $= 7.08$ m^3
$A =$ heat transfer area $= 5.4$ m^2
$U =$ average convective heat transfer coefficient
$= 3550$ J/sec-m^2-°C
$V_1 =$ volume of the jacket $= 1.82$ m^3

Design conditions:

$Q_2 = 7.5 \times 10^{-3}$ m^3/sec;
$\bar{\theta}_{i2} = 66$ °C; $\bar{\theta}_2 = 55$ °C;
$\bar{\theta}_{i1} = 27$ °C

3.22 Reconsider the system of Fig. P3.21. The simplest control strategy to handle disturbances satisfactorily is to measure the tank temperature, compare it with the reference value and adjust the control valve on the cooling water inlet stream to eliminate the error.

For fast control action, a feedback controller for the jacket temperature with its set-point determined by the feedback controller for the tank temperature could be added to provide cascade control. The two feedback control loops are nested, with the jacket-temperature control loop (secondary control loop) located inside the tank-temperature control loop (primary control loop). Suggest suitable hardware and make a sketch showing how the hardware is connected to implement the cascade control scheme.

Copyrighted material

chapter 4

Basic Principles of Feedback Control

4.1 INTRODUCTION

Although a detailed exploration of the possibilities and problems of feedback control will mostly occupy the rest of this text, some essential characteristics can be illustrated quite easily to give a helpful preview of the forthcoming developments.

Recall the basic feedback system block diagram defined in Chapter 3 and shown in abridged form as Fig. 4.1a. When we speak of a controller $D(s)$, our concern is mainly with the *information handling devices*; the sources of information are the reference input $r(t)$ which is derived from the command $y_r(t)$, and the feedback signal $b(t)$ which is produced by the feedback path elements $H(s)$ from the controlled output $y(t)$. The *power handling devices*—actuators and the controlled process itself—are represented by $G(s)$ in the block diagram of Fig. 4.1a. $N(s)$ is the plant transfer function from the disturbance input $w(t)$ to the output $y(t)$.

The controller $D(s)$ is designed to act on the actuating error signal $\hat{e}(t) = r(t) - b(t)$ to produce the control signal $u(t)$. The control logic that is physically implemented for this purpose is the *control law* or *control action*.

A non-zero system error $e(t) = y_r(t) - y(t)$ results from either a change in command or a disturbance. The general function of the controller is to keep the controlled variable near its desired value. Since we never know the numerical values of the parameters of the controlled process with true certainty, and some controller designs can be more sensitive to such parameter variations than others, a parameter sensitivity specification might also be included. In this chapter, we will demonstrate that by using feedback control configuration of the form shown in Fig. 4.1a, we can meet these control requirements.

Copyrighted material

A special case of feedback systems which is of particular interest arises when $H(s) = 1$ (Fig. 4.1b) and is often referred to as a *unity-feedback system*. The reference input $r(t)$, in this case, is equal to the commanded value of the controlled output. It may be noted that a system's block diagram may not appear to be of unity-feedback form when initially derived. It is often possible and convenient to manipulate the block diagram into a unity-feedback model where the system error appears explicitly as the actuating signal.

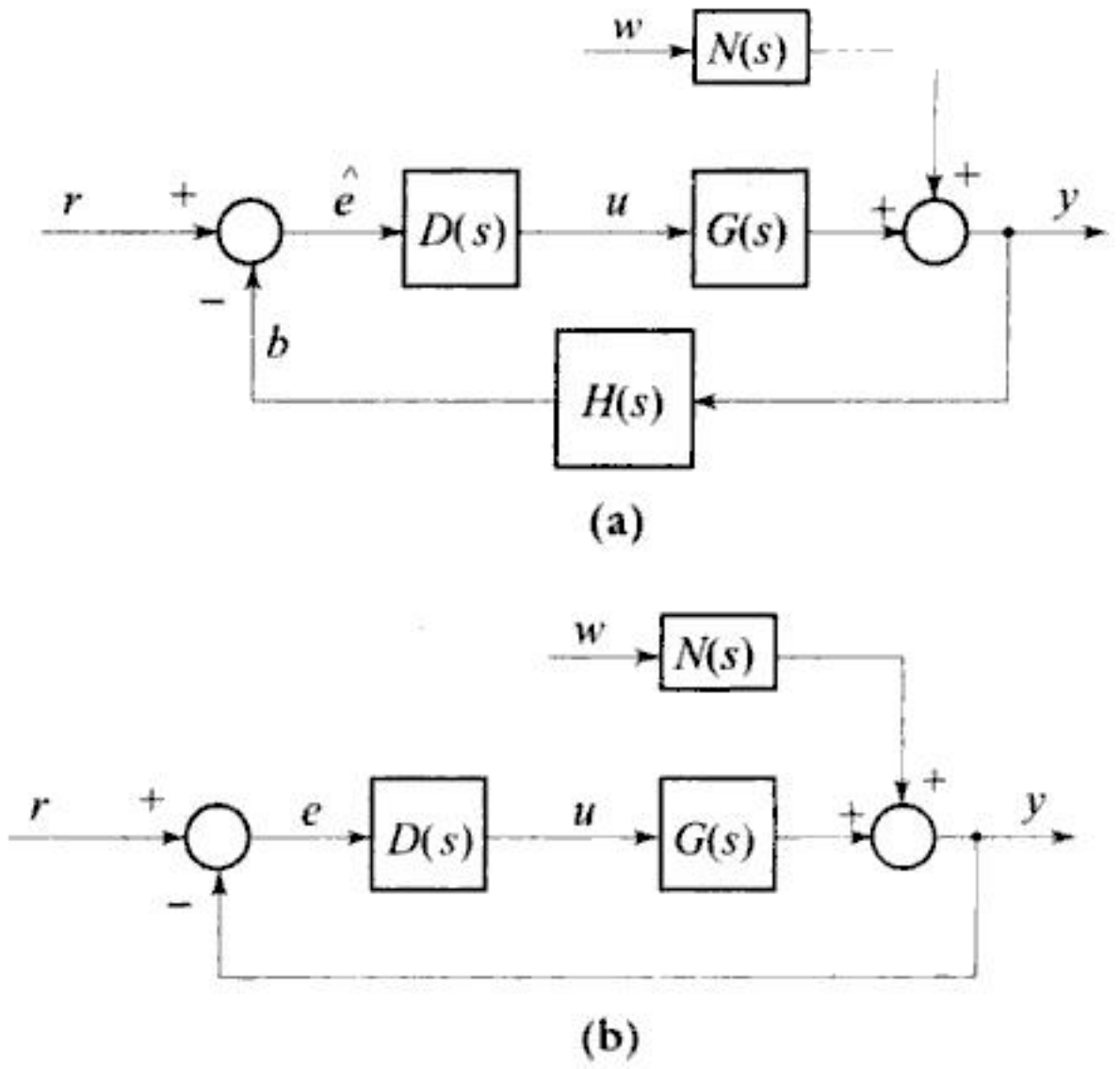


Fig. 4.1 *(a) A nonunity feedback system (b) A unity feedback system*

An important aspect of feedback control covered in this chapter is the characteristics of various commonly used modes of control. By *mode of control* we mean the nature of behaviour of the controller $D(s)$ in the general system diagrams of Fig. 4.1. The basic modes of control are:

(i) on-off control;
(ii) proportional control;
(iii) integral control; and
(iv) derivative control.

In the control system field, on–off controls are generally the simplest possible from a hardware point of view. This class of controllers have only two fixed states rather than a continuous output; the fixed states are, in many cases, simply on and off. In its wider application, the states of an on-off controller may not be simply on and off however, but could represent any two values of a control variable. Figure 4.2 shows a unity-feedback system with an on-off controller (refer Example 1.4). Oscillatory behaviour is a typical response characteristic of a system under two-portion control. Refer [180] for details.

Copyrighted material

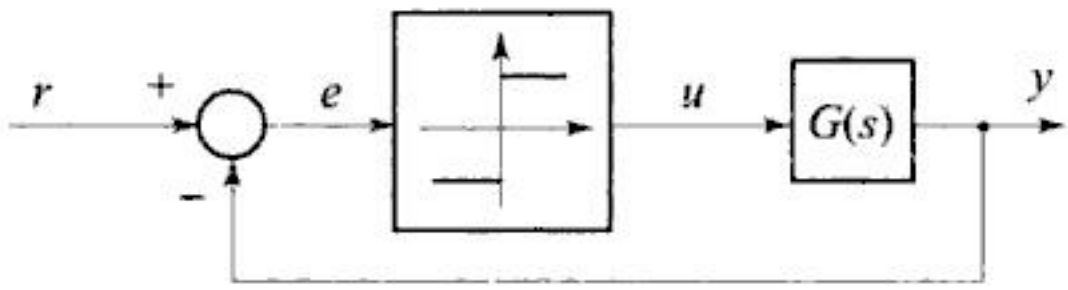


Fig. 4.2 *An on-off controller in a control loop*

For a controller with proportional control mode, the relationship between the control variable $u(t)$ and the error signal $e(t)$ is

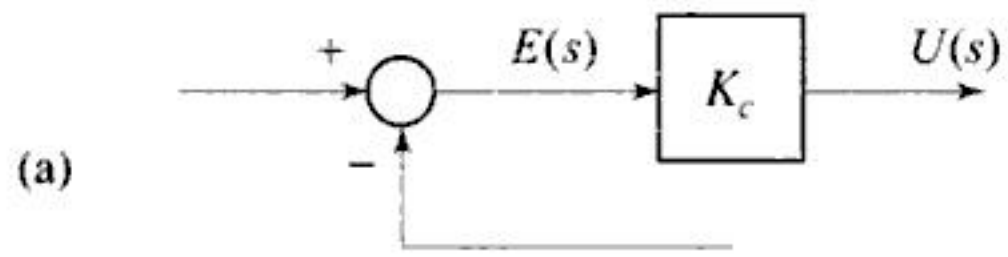
$$u(t) = K_c\, e(t) \tag{4.1a}$$

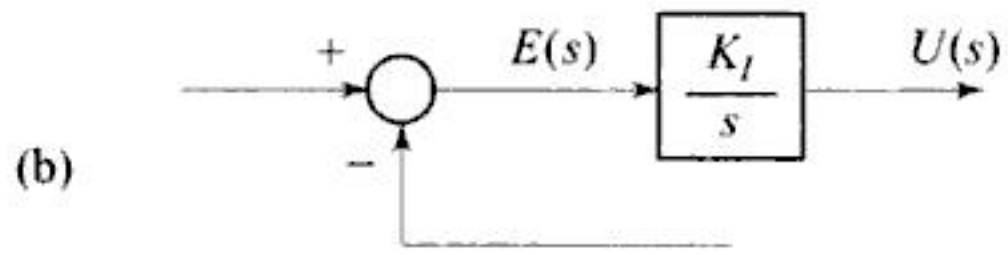
or

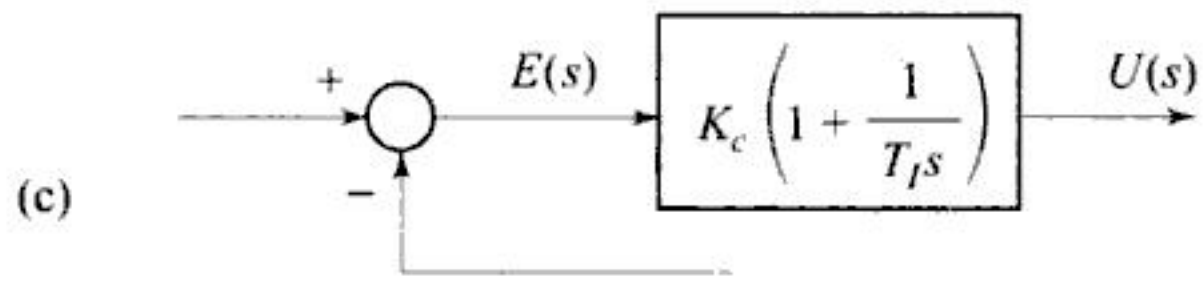
$$U(s) = K_c\, E(s) \tag{4.1b}$$

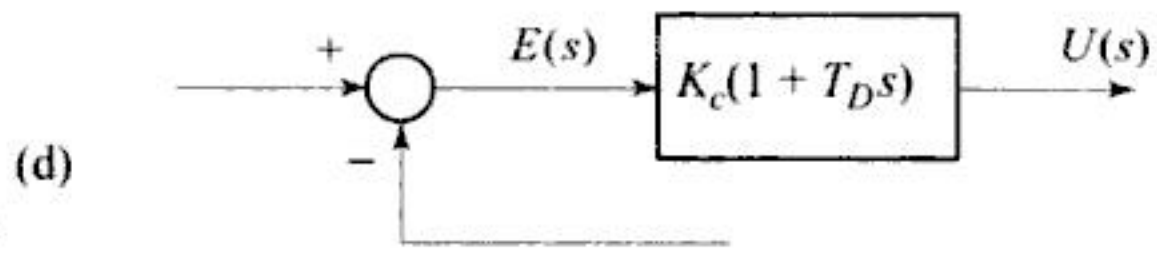
where K_c is the *controller gain*.

Whatever the actual mechanism may be and whatever the form of operating power, the proportional controller is essentially an amplifier with an adjustable gain. A block diagram of such a controller is shown in Fig. 4.3a.









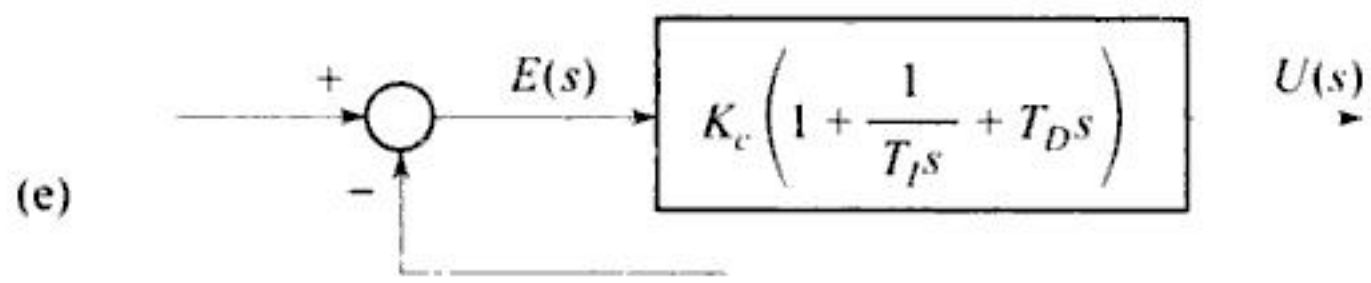


Fig. 4.3 *(a) Proportional control (b) Integral control (c) PI control (d) PD control (e) PID control*

Copyrighted material

In the integral control mode, also called the *reset control*, the change in the control signal is proportional to the integral of the error:

$$u(t) = K_I \int_0^t e(t)dt \tag{4.2a}$$

or

$$U(s) = \frac{K_I}{s} E(s) \tag{4.2b}$$

where K_I is the *integral gain*.

Figure 4.3b shows the block diagram of such a controller.

Integral control can be used by itself or in combination with other control modes; indeed *proportional plus integral* (PI) control is the most common mode. The control action of a PI controller is defined by the following equations:

$$U(s) = K_c E(s) + \frac{K_I}{s} E(s)$$

$$= K_c \left(1 + \frac{1}{T_I s}\right) E(s) \tag{4.3a}$$

$$u(t) = K_c \left[e(t) + \frac{1}{T_I} \int_0^t e(t)dt \right] \tag{4.3b}$$

where T_I is the *integral* or *reset time*.

Figure 4.3c shows the block diagram of a PI controller.

The derivative control mode, also called the *rate control*, is described by the following equations:

$$u(t) = K_D \frac{d}{dt} e(t) \tag{4.4a}$$

or

$$U(s) = K_D s E(s) \tag{4.4b}$$

where K_D is the *derivative gain*.

Derivative control mode is normally not used alone; this is because the control produces no corrective effort for any constant error and would therefore allow uncontrolled steady-state errors. A combination of proportional and derivative controls is a practical mode of control for industrial processes. The control action of a *proportional plus derivative* (PD) controller is defined by the following equations:

$$U(s) = K_c E(s) + K_D s E(s)$$

$$= K_c (1 + T_D s) E(s) \tag{4.5a}$$

$$u(t) = K_c \left[e(t) + T_D \frac{de(t)}{dt} \right] \tag{4.5b}$$

where T_D is the *derivative* or *rate time*.

Figure 4.3d shows the block diagram of a PD controller.

Copyrighted material

A combination of the three basic modes—proportional, integral and derivative—results in a *proportional plus integral plus derivative* (PID) controller described by the following equations:

$$U(s) = K_c\left(1 + \frac{1}{T_I s} + T_D s\right)E(s) \tag{4.6a}$$

$$u(t) = K_c\left[e(t) + \frac{1}{T_I}\int_0^t e(t)dt + T_D\frac{de(t)}{dt}\right] \tag{4.6b}$$

Figure 4.3e shows the block diagram of such a controller.

In the block diagrams of Fig. 4.3, the controller is in the forward path and therefore the control actions are based on the error signal. This, however, is not a restriction. The PID control actions may be taken on controlled output variable/state variables; many a times to advantage , as we shall see in this chapter. The resulting *multiloop* (loop within a loop) *control configuration* is known in the literature as *cascade control/state variable feedback control.*

In this chapter, we will also study the basic characteristics of feedforward-feedback control configurations, and the control of multivariable systems.

4.2 THE CONTROL OBJECTIVES

In this section, we describe a control problem in general terms. Given a plant, which cannot be altered by the designer, with the following variables associated with it (Fig. 4.4):

1. A controlled variable $y(t)$, which is the variable we wish to control.
2. A command variable $y_r(t)$ which represents the prescribed value of the controlled variable.
3. An observed variable $y_s(t)$ which is measured by means of a sensor and which is used to obtain information about the plant during operation; the observed variable is usually contaminated with observation noise $v(t)$.
4. A disturbance variable $w(t)$ which influences the plant but which cannot be manipulated.
5. A control variable $u(t)$ which influences the plant and which can be manipulated.

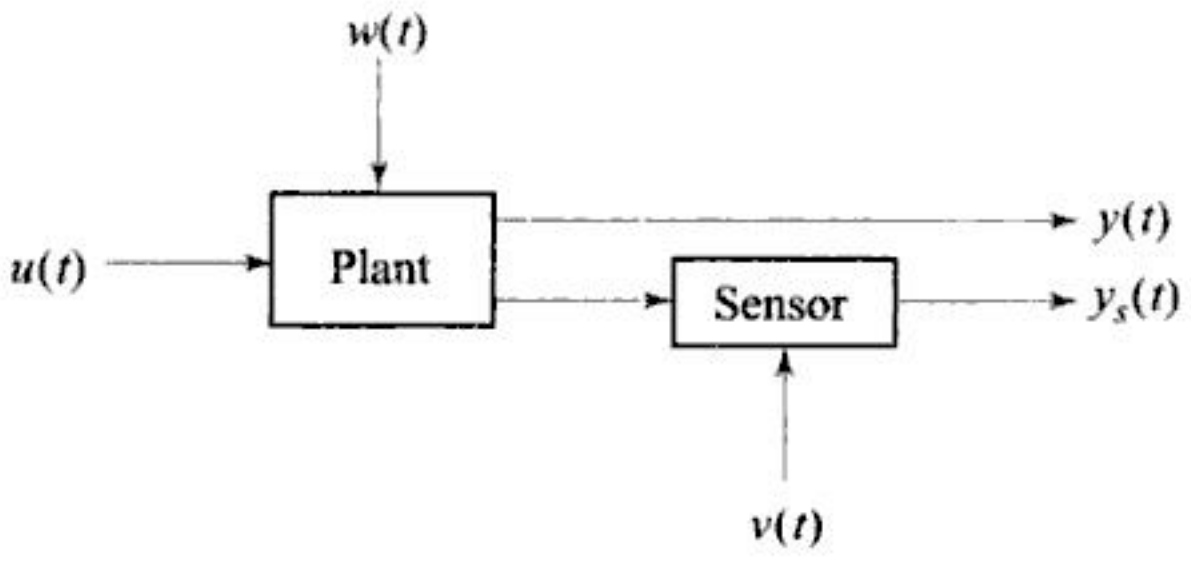


Fig. 4.4 *The plant of a control system*

Copyrighted material

The *control problem* is roughly described below.

For a given command variable, find an appropriate input $u(t)$ so that the controlled variable follows the command variable:

$$y(t) \cong y_r(t);\ t \geq t_0$$

where t_0 is the time at which the control starts.

An important class of control problems consists of those problems where the command variable is constant over long periods of time; the control objective is to force the controlled variable to reach the commanded value quickly and to maintain the controlled variable at that value thereafter. The duration of the transient period of control, which starts at the beginning of the control process and terminates when the controlled variable approximately reaches its prescribed value, will be referred to as the *settling time*. The lower the settling time, the higher the *speed of response* of the process. The *steady-state accuracy* (negligible error between the controlled output and command input during steady-state period of control) is of critical importance in control systems.

In designing control systems, the following aspects must be taken into account.

1. Stability Roughly speaking, stability in a system implies that small changes in reference inputs, disturbance inputs, and/or initial conditions do not result in large changes in the system output. Stability is a very important property of control systems. Almost every working system is designed to be stable; we seek to improve the speed of response, steady-state accuracy, and other aspects of system performance within the constraints imposed by stability considerations. Analytical study of stability will be taken up in Chapter 5.

Feedback control systems are prone to instability. For a stable plant, the closed-loop system may not be always stable. Feedback control system design may therefore demand a trade off between the accuracy in realizing control objectives and the stability.

2. Input Amplitude Constraints For a control system designed according to linear theory and methods, it is essential that the devices used in the system operate in linear fashion under various operating conditions. If under certain circumstances, the devices are driven into the region of nonlinear characteristics, linear design theory may describe only approximately, or quite often may give a completely erroneous prediction of the system performance. Excessive large magnitudes of signals at various levels in a control system can drive the devices into the nonlinear region of operation. Some examples are: torque-speed curves of motors, synchro error detectors, process control valves, hydraulic servovalves, amplifiers, gears, dampers, etc. The requirement of linear operation of devices under various operating conditions imposes a constraint on the range of values over which the plant input $u(t)$ is allowed to vary. As will be seen, this constraint is of major importance and prevents us from obtaining perfect command-following systems.

Copyrighted material

3. Disturbance Rejection External disturbances $w(t)$ influence the plant in an unpredictable way. They are typically the uncontrolled variations in the load on a system. In systems controlling mechanical motions, load disturbances may represent forces, e.g., wind gusts on a stabilized antenna, waves on a ship, variations in payload of a robot manipulator, etc. In voltage regulating systems, variations in electrical load is a major source of disturbances. In thermal systems, the load disturbances may be caused by variations in surrounding temperature. In fluid systems, the load disturbances may result from variations in feed flow or variations in demanded flow.

Load disturbances typically vary slowly. As we shall see later in this chapter, the errors due to load disturbances tend to be corrected by proper design of feedback control.

4. Noise Filtering Excitation of the plant by high-frequency measurement-error signals (observation noise) $v(t)$, entering through the sensors of the controlled variable, influences the plant in an unpredictable way. In systems controlling mechanical motions, mechanical vibrations may lead to high-frequency components in the output signals of position and speed sensors. Continuous stirring of fluid in tank reactors gives rise to noise in output signals of thermocouple or other temperature sensors.

Feedback control depends virtually on accurate measurement of controlled variables, because the feedback action has little correcting effect for the wrong information given by the sensors. The character of the measurement errors often depends on filtering in the instruments. Effects of measurement errors on control system performance can therefore be reduced by examining the instrument and modifying the filtering so that it satisfies the requirements of the particular control problem.

5. Sensitivity and Robustness Robustness is an important concern in control system design. We will briefly discuss two aspects of the robustness problem.

The first aspect arises because every control system is designed on the basis of necessarily approximate model of the plant. Since the success of the analytical approach of design is heavily dependent on the simplicity of the mathematical model, many idealizing assumptions are usually made which lead to uncertainties not only in the parameters of the model but also in the model structure—using a linear model for an intrinsically nonlinear process is an example of deviation in model structure; omitting certain time lags in order to obtain a reduced-order model is another example. The question arises: will the physical system have a performance that is sufficiently close to the performance predicted by the idealized model? For example, if the linear model is stable, will the physical system, which in fact is a small perturbation (possibly nonlinear) from the linear model, still be stable?

The second aspect of the robustness appears in the following manner: the design is based on the (idealized) model which characterizes a number of nominal properties of the plant. Once the controller is implemented and the control-

Copyrighted material

led plant is operating in the field, the properties of the physical system differ from the nominal properties because of environment effects, wear, aging, and other natural factors. So the question is: what is the effect of all such time dependent deviations from nominal values on the performance of the physical system in the field? Such questions can be studied by calculating the effect on the system performance due to changes in design parameters and exogenous disturbances. It is a fact that some designs, which perform nominally perfectly, are totally inadequate in the field because they are too sensitive to small perturbations in some of their parameters.

In the course of this text, we will discuss from time to time these questions of *robustness*.

The effect of differentially small deviations in the parameters of a model of known structure can be studied using *sensitivity* analysis. The motivation for sensitivity analysis is given by the practical experience that parameters often drift during the operation of the system in the field, but they typically remain in the vicinity of their nominal values. It is interesting to know whether such parameter variations cause severe changes of the system behaviour or have merely a minor influence on the important system properties.

For the analysis, the system behaviour is characterized by some specific measure, e.g., speed of response; or even by some characteristic function such as the frequency response of the closed-loop system. For the sake of simplicity of representation, we take J as the performance measure characterizing the system behaviour, which depends on parameter θ in addition to other parameters. Consider perturbation only in the parameter θ. For the nominal parameter θ_n, we get the nominal value of the performance measure as $J_n = J(\theta_n)$.

Parameter changes $\Delta\theta$ induce changes ΔJ in the performance measure. Hence, instead of J_n, we get the new value $J_n + \Delta J = J(\theta_n + \Delta\theta)$.

Taylor's series expansion of $J(\theta)$ about the nominal point θ_n yields (assuming that the function is differentiable):

$$J(\theta_n + \Delta\theta) = J(\theta_n) + \left.\frac{\partial J(\theta)}{\partial \theta}\right|_{\theta=\theta_n} \Delta\theta + \cdots$$

If we restrict our attention to terms of atmost first order, we get

$$\Delta J = \left.\frac{\partial J(\theta)}{\partial \theta}\right|_{\theta=\theta_n} \Delta\theta$$

Expressing deviations in terms of relative changes, we obtain

$$\frac{\Delta J}{J_n} = \frac{\Delta\theta}{\theta_n}\left[\left(\left.\frac{\partial J(\theta)}{\partial \theta}\right|_{\theta=\theta_n}\right)\frac{\theta_n}{J_n}\right]$$

System sensitivity to parameter θ is defined as the ratio of the percentage change in the system performance measure J from its nominal value to the percentage change in the parameter. S_θ^J denotes the sensitivity of J with respect to θ and is given by

Copyrighted material

$$S_\theta^J = \frac{\Delta J/J_n}{\Delta\theta/\theta_n} = \left[\left.\frac{\partial J(\theta)}{\partial\theta}\right|_{\theta=\theta_n}\right]\frac{\theta_n}{J_n} \tag{4.7}$$

If $S_\theta^J = 0$, then the measure J is insensitive to the parameter θ at the nominal point θ_n. If $S_\theta^J \neq 0$, then J is sensitive and the value of S_θ^J is a measure of the degree of dependence of J on θ.

A plausible interpretation of the sensitivity function is shown in Fig. 4.5. Here we treat the relative change in the parameter θ, $\Delta\theta/\theta_n$, as an input to the process modelled by the sensitivity function with the output being the relative change in the system performance measure, $\Delta J/J_n$.

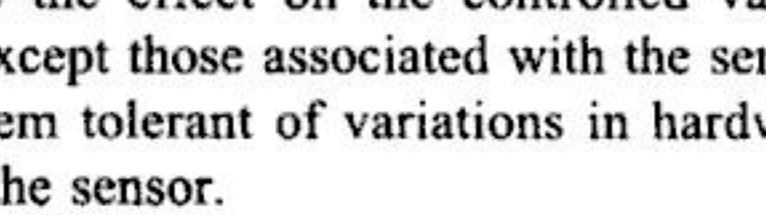


Fig. 4.5 *Interpretation of sensitivity function as a gain function*

Note that sensitivity function deals with infinitesimally small parameter perturbations near a given nominal parameter value and does not refer to the amount of perturbation. Experience on use of such functions, however, shows that sensitivity function is a reasonable characteristic of the effects of small rather than infinitesimally small perturbations.

As we shall see later in this chapter, the errors due to parameter variations tend to be corrected by the proper design of feedback control. ▲▲

The next section will demonstrate that feedback control can

(i) force the controlled variable to accurately follow its prescribed value in steady-state;
(ii) shape the dynamics of the controlled variable;
(iii) greatly reduce the effect on the controlled variable of all external disturbances except those associated with the sensor; and
(iv) make the system tolerant of variations in hardware parameters other than those of the sensor.

The use of feedback is motivated by the presence of external disturbances and model uncertainties. More strictly, the use of feedback can be regarded as unreasonable if there is no uncertainty in the system because, for the unperturbed system, open-loop control may produce the same or probably better result.

Example 4.1

In the following, we review the control objectives of heat-exchanger control system discussed in Chapter 1 (Fig. 1.18). A sketch of the exchanger is given in Fig. 4.6a.

The objective is to maintain the outlet temperature of the process fluid, $\theta(t)$ °C, at its desired value or set point, θ_r°C, in the presence of disturbances in

Copyrighted material

the process fluid flow, $q_m(t)$ kg/sec (= $Q\rho$; Q m^3/sec is the volumetric fluid flow and ρ kg/m^3 is the fluid density), flowing inside the tubes of the heat exchanger, and inlet temperature $\theta_i(t)$°C. The steam flow, $q_{ms}(t)$ kg/sec, con-

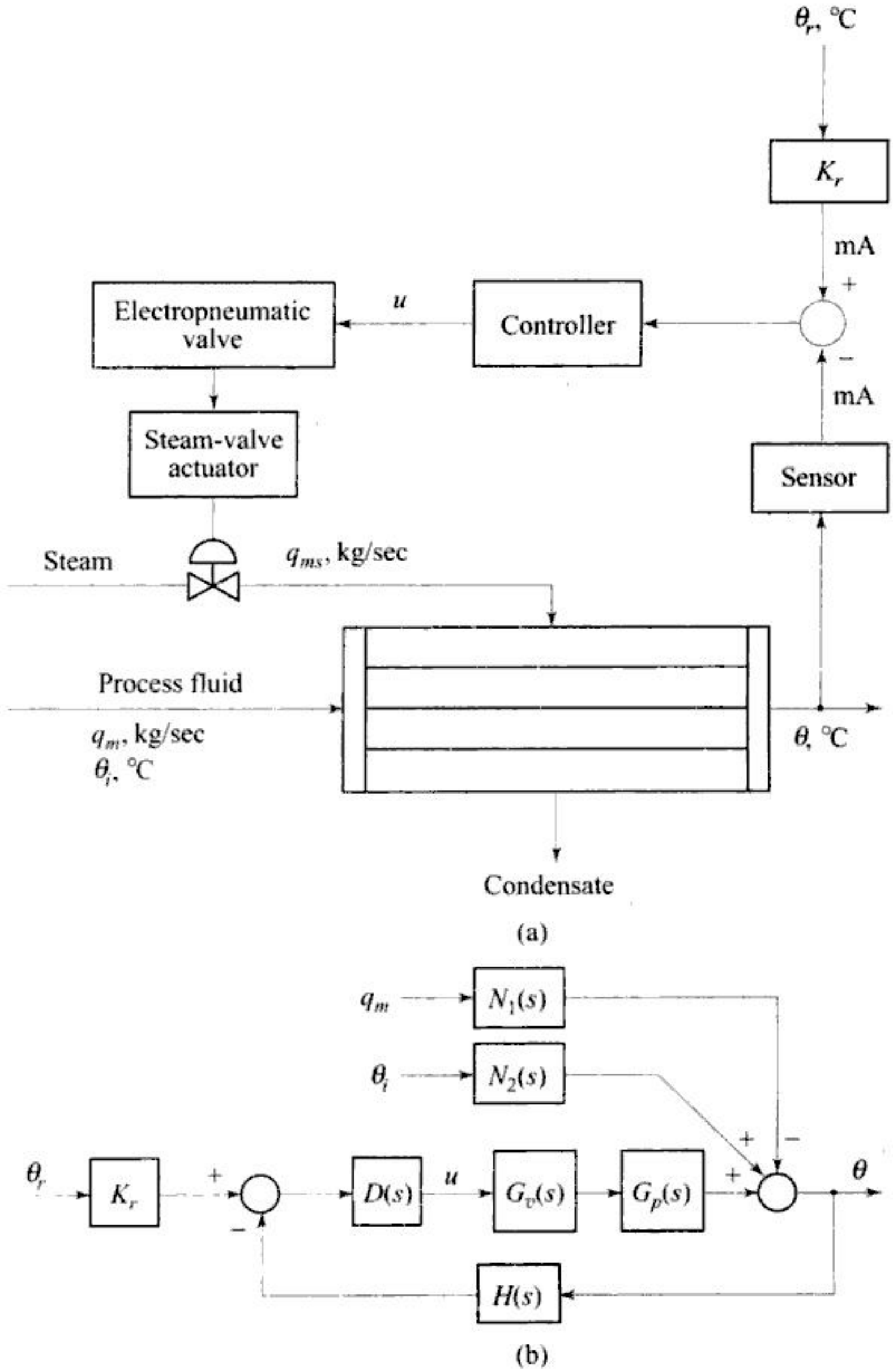


Fig. 4.6 *Heat exchanger control loop*

Copyrighted material

densing on the outside of the tubes, is the variable that can be adjusted to control the outlet temperature as it determines the amount of energy supplied to the process fluid. In addition to counteracting the effects of disturbances, the control system will be called upon to follow the commands for change in the outlet temperature of the process fluid.

The first step in the design is the selection of the temperature sensor and steam-valve actuator. For temperature measurement, we select an intelligent sensor which has, in addition to the basic device such as thermocouple, a signal processing circuit which takes the output from the thermocouple and converts it to a current signal that is proportional to the temperature. The signal processing circuit includes an amplifier and a filter. For steam valve adjustments, we select a pneumatic actuator which can provide large output power. Since the valve actuator must be operated by air pressure and the sensor generates electric current signals, a current to pressure transducer is also required in the feedback loop.

The feedback control scheme works as follows: the measured controlled variable is compared with the set-point; K_r in Fig. 4.6a represents the conversion of set-point scale. The controller generates a control signal, $u(t)$, on the basis of the difference between the measurement and set-point. The control signal is then connected to the pneumatic actuator of the steam valve through an electropneumatic device—a current to pressure transducer. The function of the valve actuator is to position the valve in proportion to the control signal. The steam flow is then a function of the valve position.

Once the hardware is chosen, the remainder of the design is concerned with trying to make the best use of the process. If the design is to be carried out analytically, a transfer function description of the feedback system must be found. Figure 4.6b shows the block diagram of the entire feedback loop. We now find the transfer function model of each block. Let us start with the heat exchanger.

As shown in Fig. 4.6b, the heat exchanger consists of three blocks, one for each of its three inputs. $G_p(s)$ is the process transfer function relating the outlet temperature to the steam flow, $N_1(s)$ is the process transfer function relating the outlet temperature to disturbance in process fluid flow and $N_2(s)$ is the process transfer function to disturbance in inlet temperature.

The following experimentally obtained parameters will be used in developing a model of the feedback system.

The exchanger response to the steam flow has a gain of 50 °C/(kg/sec), and a time-constant of 30 sec. The exchanger response to the process fluid flow has a gain of 3 °C/(kg/sec), and to inlet temperature the gain is 1°C/ °C. Therefore

$$G_p(s) = \frac{50}{30s+1}; N_1(s) = \frac{3}{30s+1}; N_2(s) = \frac{1}{30s+1}$$

The time-constant of the process depends on the residence time (tube volume/volumetric flow rate) of the fluid in the tubes. As a consequence, the time-

Copyrighted material

constant may vary because of flow rate fluctuations and fouling. Therefore, we should ascertain how sensitive the performance of the final system design will be to changes in the time-constant of the process.

The control valve has a maximum capacity of 1.6 kg/sec of steam, linear characteristics, and a time-constant of 3 sec. The nominal pressure range of the valve is 3 to 15 psig.

$$\text{Valve gain} = \frac{1.6(\text{kg/sec})}{(15-3)\text{psi}} = \frac{1.6}{12}(\text{kg/sec})/\text{psi}$$

The electropneumatic valve has a constant gain

$$\frac{\Delta P}{\Delta I} = \frac{(15-3)\text{psi}}{(20-4)\text{mA}} = \frac{12}{16}\text{psi/mA}$$

Including the constant gain of the current-to-pressure transducer in the control-valve transfer function, $G_v(s)$, we obtain

$$G_v(s) = \frac{0.1}{3s+1}$$

The sensor has a calibrated range of 50 to 150°C and a time-constant of 10 sec.

$$\text{Sensor gain} = \frac{16\,\text{mA}}{(150-50)^\circ\text{C}} = 0.16\,\text{mA/°C}$$

The transfer function of the sensor is given by

$$H(s) = \frac{0.16}{10s+1}$$

The set-point scale factor

$$K_r = 0.16\ \text{mA/°C}$$

The block diagram of the temperature control loop, as initially proposed, is shown in Fig. 4.7. θ_r is the change in the set-point value from the initial setting

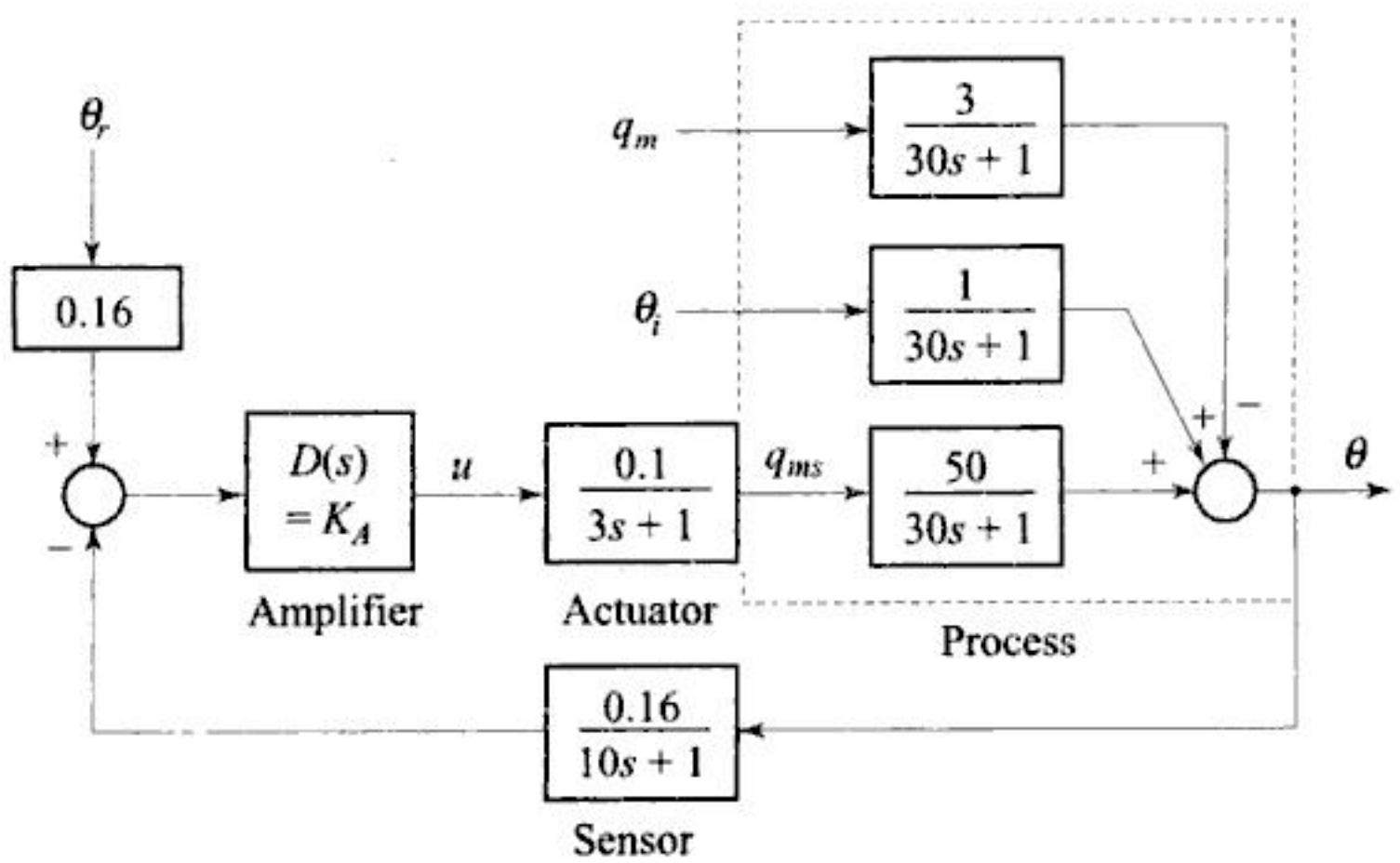


Fig. 4.7 *A model of a heat exachanger control loop*

Copyrighted material

$\bar{\theta}_r$, θ_i is the deviation in the process fluid temperature from the nominal value $\bar{\theta}_i$, q_m is the deviation in the process fluid flow from the nominal value $\bar{Q}_m$. θ is the deviation in the outlet temperature from the nominal value $\bar{\theta}$, and q_{ms} is the deviation in the steam flow rate from the nominal value $\bar{Q}_{ms}$ (refer Review Example 4.2).

Example 4.2

Consider the problem of design of an attitude control system for a rigid satellite. Satellites usually require attitude control so that antennas, sensors, and solar panels are properly oriented. For example, antennas are usually pointed toward a particular location on earth, while solar panels need to be oriented toward the sun for maximum power generation.

The satellite will be subjected to a variety of disturbance torques from such sources as aerodynamic drag, solar pressure, gravity gradient torques, and the rotation of various satellite components, e.g., pumps, motors and antennas. It will be assumed that the vehicle has initially been aligned to the desired attitude. Due to the above mentioned disturbance torques, it will be necessary to provide a feedback control system in order to maintain the satellite very close to the desired attitude. In addition to counteracting the effects of the disturbance torques acting on the vehicle, the control system will be called upon to change the attitude, subject to commands received from ground stations.

In this example, we shall highlight the important physical aspects of the system, taking a number of liberties with the practical aspects so as to avoid undue complication which should tend to obscure our main objectives.

So long as the angular velocity and the error angles of the vehicle are small, angular motions about the three axes are essentially *uncoupled* and may be controlled independently. Thus, we may design each of the three attitude-control loops independently, which is an important simplification. Figure 4.8 depicts single-axis attitude control schematic, where motion is only allowed about the axis perpendicular to the page. The angle θ that describes the satellite orientation must be measured with respect to an 'inertial' reference, that is, a reference that has no angular acceleration. The control signal comes from the gas jets that produce a torque $T(t)(= F \times d)$ about the mass centre.

A block diagram of the control system, as initially proposed, is given in Fig. 4.9. The command signal θ_r rad, transmitted from earth, is converted to electrical form ($e_r = K_P\theta_r(t)$ volts) in the satellite. A sensor on the satellite measures the deviation θ rad; its output is a voltage equal to $K_P\theta(t)$. A difference amplifier provides the voltage $u(t)$ proportional to $\hat{e}(t)$: the difference of the voltages corresponding to the command signal and measured signal. The amplifier must provide sufficient power to actuate the gas jets. The gas jets exert a torque $T(t) = K_T\, u(t)$ about the mass centre. We have neglected the dynamics of the gas jets, assuming that the opening time is short compared to the important time-constants of the system.

Copyrighted material

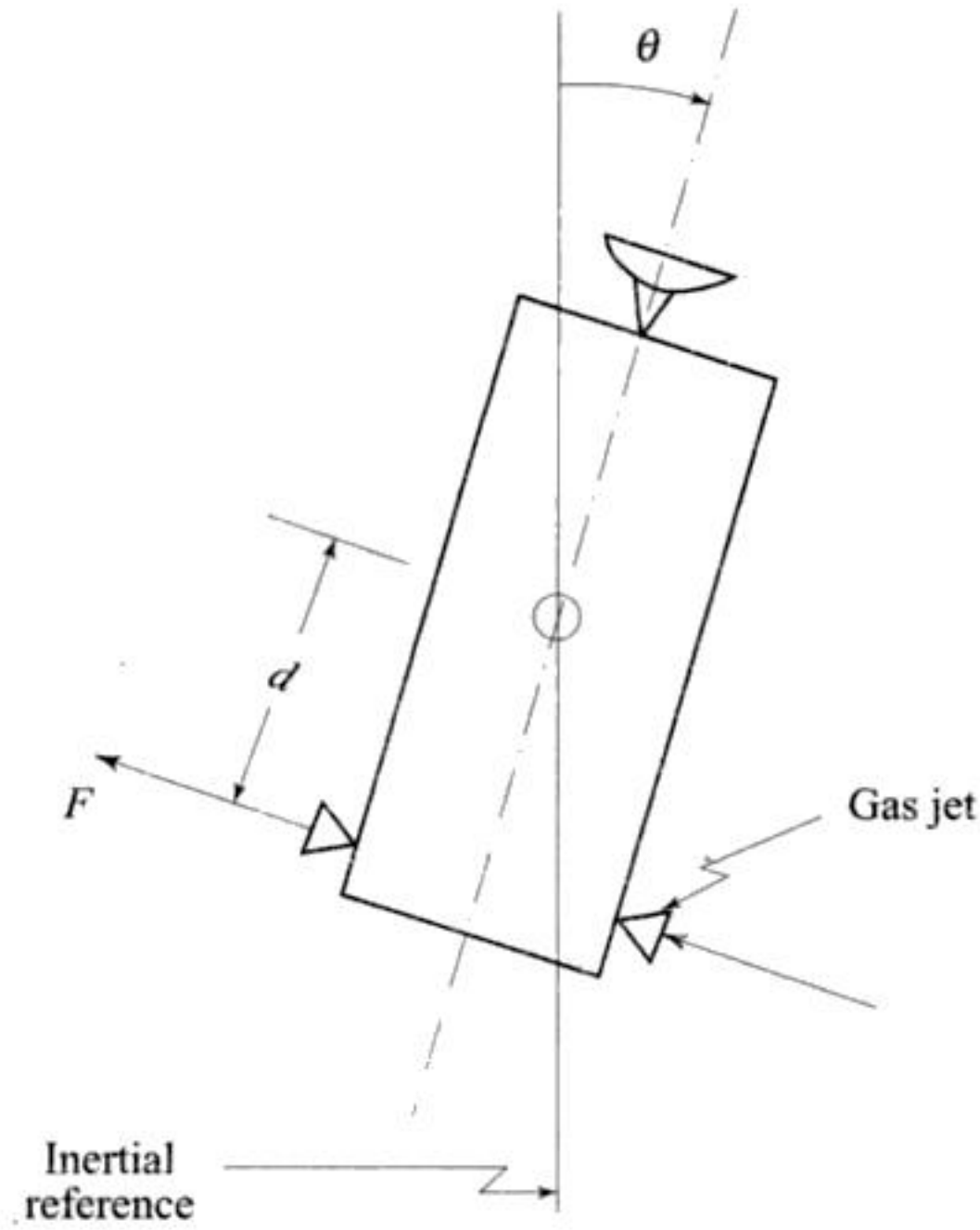


Fig. 4.8 *Satellite control schematic*

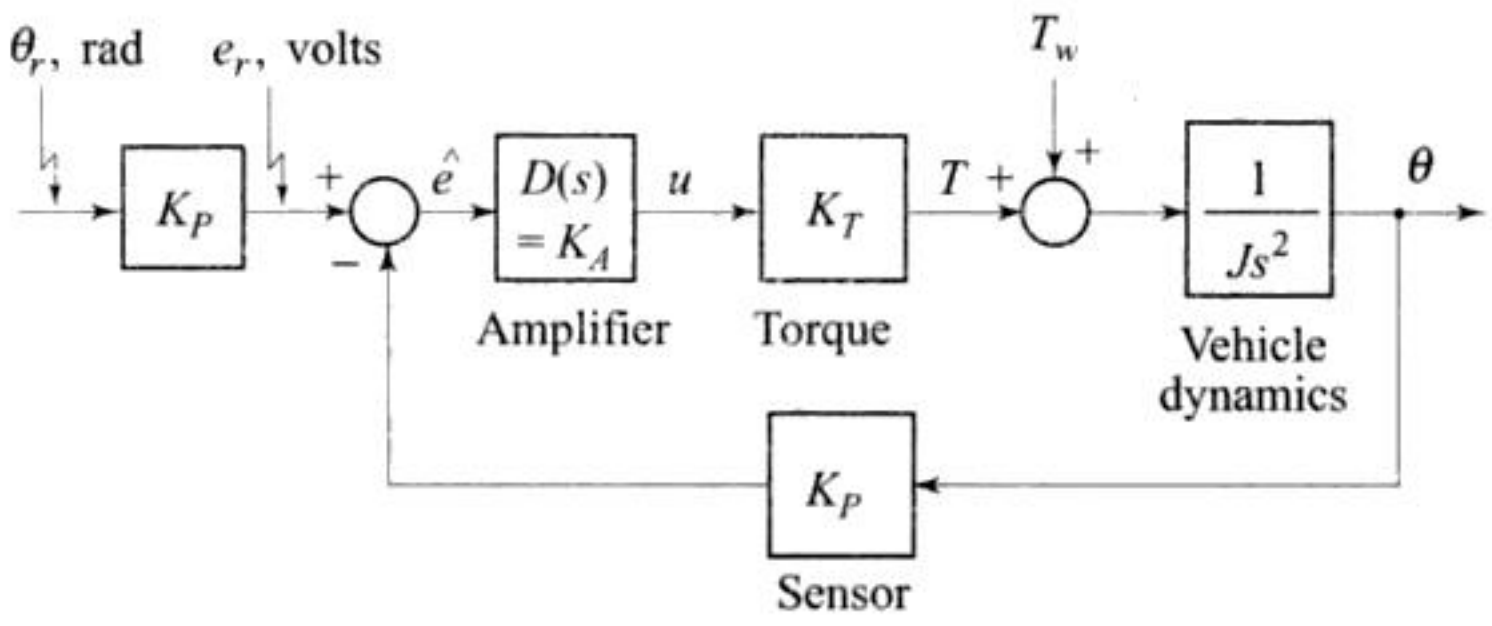


Fig. 4.9 *A model of a satellite attitude control system*

The vehicle dynamics are governed by the differential equation (assuming frictionless environment)

$$J\ddot{\theta} = T(t) + T_w(t)$$

where J is the moment of inertia about the axis of rotation, and the total torque is the sum of control torque and the disturbance torque. Although the moment of inertia will vary over the life of the satellite because of the consumption of fuel, it presumably changes very slowly compared with the response of the

Copyrighted material

vehicle. Thus, we are justified in treating it as a constant but should ascertain how sensitive the performance of the final system design is to anticipated changes in J.

4.3 FEEDBACK CONTROL SYSTEM CHARACTERISTICS

Feedback systems play an important role in control engineering practice because the use of feedback can accomplish certain desirable results that would not be readily possible with an open-loop system. Some of the potential benefits (and liabilities) of feedback will be discussed in this section. Generally, the material presented here is applicable to any system whose mathematical model takes the form of a fixed linear feedback configuration. These occur not only in automatic control systems and electronic circuits, where the feedback is introduced by design, but also in much diverse fields as physiology, economics, ecology, etc., where feedback is inherent in the natural laws governing the process. However, consistent with the major thrust of this book, our terminology, convention, and illustrations will be taken in the context of control engineering.

System Sensitivity

A process represented by the transfer function $G(s)$, whatever its nature, is subject to modelling errors, changing environment, aging, and other natural factors that affect the control system performance. Consider the open-loop control system of Fig. 4.10. Assume that the controller $D_o(s)$ has been designed using a given transfer function model of the process, and it meets the specifications on the system output $y(t)$. Obviously, the output will approach the desired value only if the dynamical behaviour of the real process approaches that of its model. The modelling approximations and the process-behaviour changes with time during operation result in an inaccurate output. There is no provision within the system for supervision of the output and no mechanism is provided to correct the output. Consider now the closed-loop control system of Fig. 4.11. This system senses the change in the output through the feedback signal and attempts to correct the output. The feedback signal gives this system the capability to act as a self-correcting mechanism.

For simplicity, we assume that the structure and order of the process model are chosen exactly and they do not change with time. Then the differences

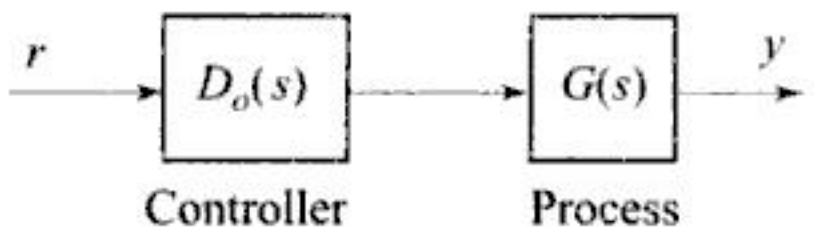


Fig. 4.10 *An open-loop control system*

Copyrighted material

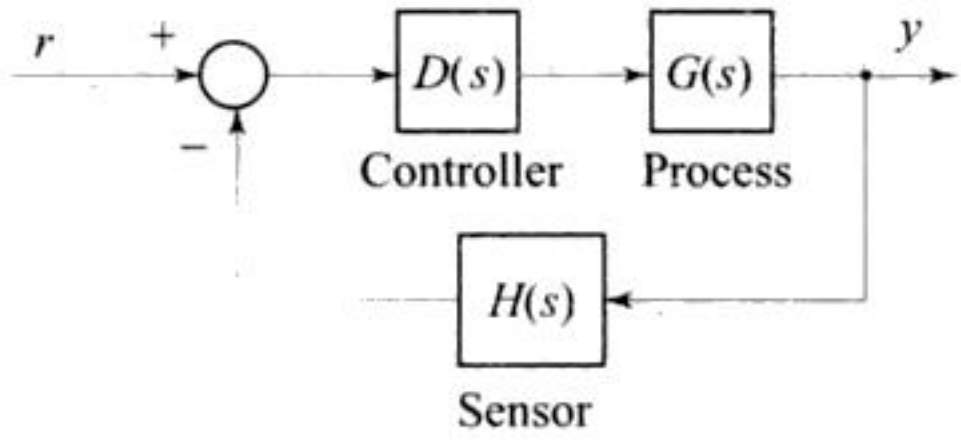


Fig. 4.11 *A closed-loop control system*

between the process model and the real process behaviour are manifested as *parameter errors*. Let $\theta_1, \theta_2, \ldots$ be the parameters of the process model $G(s)$ which are subject to change. If $\theta_{n1}, \theta_{n2}, \ldots$ are the nominal values of the parameters, then the process model corresponding to the nominal working point may be expressed as $G(\boldsymbol{\theta}_n, s)$, where $\boldsymbol{\theta}_n$ is the nominal parameter vector. We assume that $H(s)$ is not subject to parameter variations.

The closed-loop input/output behaviour corresponding to the nominal working point is described by (Fig. 4.11)

$$M(\boldsymbol{\theta}_n, s) = \frac{Y(s)}{R(s)} = \frac{D(s)G(\boldsymbol{\theta}_n, s)}{1 + D(s)G(\boldsymbol{\theta}_n, s)H(s)} \tag{4.8}$$

The process parameter vector now changes by an infinitesimal value $d\boldsymbol{\theta}$. For the closed loop, it follows that

$$\left.\frac{\partial M(\boldsymbol{\theta}, s)}{\partial \boldsymbol{\theta}}\right|_{\boldsymbol{\theta}=\boldsymbol{\theta}_n} = \frac{D(s)}{[1 + D(s)G(\boldsymbol{\theta}_n, s)H(s)]^2}\left.\left(\frac{\partial G(\boldsymbol{\theta}, s)}{\partial \boldsymbol{\theta}}\right)\right|_{\boldsymbol{\theta}=\boldsymbol{\theta}_n} \tag{4.9}$$

From Eqns (4.7)–(4.9), it follows that

$$\frac{dM(\boldsymbol{\theta}_n, s)}{M(\boldsymbol{\theta}_n, s)} = S(\boldsymbol{\theta}_n, s)\frac{dG(\boldsymbol{\theta}_n, s)}{G(\boldsymbol{\theta}_n, s)} \tag{4.10a}$$

with the *sensitivity function* of the feedback control given as

$$S_G^M = S(\boldsymbol{\theta}_n, s) = \frac{1}{1 + D(s)G(\boldsymbol{\theta}_n, s)H(s)} \tag{4.10b}$$

Consider perturbation only in θ_i. Sensitivity of M with respect to θ_i is given by

$$S_{\theta_i}^M = \frac{dM(\boldsymbol{\theta}_n, s)/M(\boldsymbol{\theta}_n, s)}{d\theta_{in}/\theta_{in}} \tag{4.11a}$$

$$= \frac{dM/M}{dG/G}\left(\frac{dG/G}{d\theta_{in}/\theta_{in}}\right)$$

$$= S(\boldsymbol{\theta}_n, s)\left[\frac{\theta_{in}}{G(\boldsymbol{\theta}_n, s)}\right]\left[\frac{\partial G(\boldsymbol{\theta}_n, s)}{\partial \theta_i}\right]\Bigg|_{\theta_i = \theta_{in}} \tag{4.11b}$$

Copyrighted material

The sensitivity function given by Eqns (4.10) shows how relative changes in the input/output behaviour of the closed-loop depend on the changes in the process transfer function. In general, the sensitivity function is a function of the Laplace transform variable s, which makes sensitivity very difficult to interpret. However, if we replace s in Eqn. (4.10b) by $j\omega$, we get the sensitivity as a frequency response. Then we can assign meaning to the sensitivity for frequencies within the bandwidth[1] of the system. Since the system will not transmit frequencies outside its bandwidth (an approximation), the sensitivity for frequencies much greater than the system bandwidth is of little interest.

Evaluating the sensitivity in Eqn. (4.10b) as a function of frequency, yields

$$S_G^M = S(\boldsymbol{\theta}_n, j\omega) = \frac{1}{1 + D(j\omega)G(\boldsymbol{\theta}_n, j\omega)H(j\omega)} \tag{4.12}$$

The term DGH evaluated at a specific frequency is called the *loop gain* at that frequency. At frequencies within the system bandwidth, we would like the loop gain to be as large as possible to reduce the sensitivity of the closed-loop behaviour to the process parameters. Generally, one of the purposes of the controller $D(s)$ is to allow the loop gain to be increased without destabilizing the system.

Assume now that we are dealing with an open-loop system such as the one depicted in Fig. 4.10. It is clear that for this system we can apply the result given by Eqns (4.10) with $H(s) = 0$. Thus

$$S_G^M = 1, \text{ where } M(\boldsymbol{\theta}_n, \text{s}) = D_o(s)G(\boldsymbol{\theta}_n, s) \tag{4.13}$$

It can readily be seen that feedback reduces the system sensitivity to changes in process parameters.

Next we derive the sensitivity of the closed-loop transfer function to parameter changes in the sensor $H(s)$. Assume that the parameter vector $\boldsymbol{\theta}_n$ is a part of $H(s)$, and the process transfer function $G(s)$ is not subject to parameter variations. For this case, the closed-loop transfer function becomes

$$M(\boldsymbol{\theta}_n, s) = \frac{Y(s)}{R(s)} = \frac{D(s)G(s)}{1 + D(s)G(s)H(\boldsymbol{\theta}_n, s)} \tag{4.14}$$

For an infinitesimal change $d\boldsymbol{\theta}$ in the nominal parameter vector, $\boldsymbol{\theta}_n$, we obtain

$$\left.\frac{\partial M(\boldsymbol{\theta}, s)}{\partial \boldsymbol{\theta}}\right|_{\boldsymbol{\theta} = \boldsymbol{\theta}_n} = -\left[\frac{D(s)G(s)}{1 + D(s)G(s)H(\boldsymbol{\theta}_n, s)}\right]^2 \left.\frac{\partial H(\boldsymbol{\theta}, s)}{\partial \boldsymbol{\theta}}\right|_{\boldsymbol{\theta} = \boldsymbol{\theta}_n} \tag{4.15}$$

From Eqns (4.14) and (4.15), it follows that

$$\frac{dM(\boldsymbol{\theta}_n, s)}{M(\boldsymbol{\theta}_n, s)} = S_H^M \frac{dH(\boldsymbol{\theta}_n, s)}{H(\boldsymbol{\theta}_n, s)} \tag{4.16a}$$

---

1. It gives the significant frequency range of the closed-loop system. Chapter 9 on frequency response analysis will describe this important parameter of control system performance.

Copyrighted material

where
$$S_H^M = \frac{-D(s)G(s)H(\boldsymbol{\theta}_n, s)}{1 + D(s)G(s)H(\boldsymbol{\theta}_n, s)} \tag{4.16b}$$

This equation shows that for large values of loop gain DGH, sensitivity of the feedback system with respect to H approaches unity. Thus, we see that the changes in H directly affect the system output. To solve this problem, we generally can use high-quality stable components for the sensor.

The use of feedback in reducing sensitivity to parameter variations is an important advantage of the feedback control systems. To have a highly accurate open-loop system, the components of the process plant must be carefully selected so that the parameters of the physical system are close to that of $G(s)$—the model used in design, under all operating conditions. On the other hand, a closed-loop system allows $G(s)$ to be less accurately specified, since the effects of parameter variations are mitigated by the use of feedback. However, a closed-loop system requires careful selection of the components of the feedback sensor. Since the plant is made up of power elements and the sensor is made up of measuring elements which operate at low power levels, the selection of accurate $H(s)$ is far less costly than that of $G(s)$ to meet the exact specifications.

Many plants, by their very nature, have parameters that vary extensively during operation. An example is an aircraft whose parameters vary over very wide ranges with speed, altitude, and so on. Hence, aircraft autopilot design must satisfy a rigorous specification on sensitivity to plant parameter variations. Feedback control is the only solution.

The price for improvement in sensitivity by use of feedback is paid in terms of *loss of system gain*. The gain of the closed-loop system shown in Fig. 4.11 is $D(s)G(s)/[1 + D(s)G(s)H(s)]$ while with $H(s) = 0$, the gain becomes $D(s)G(s)$. Hence, by use of feedback, the system gain is reduced by the same factor as by which the sensitivity of the system to parameter variations is reduced. Sufficient open-loop gain can, however, be built into a system so that we can afford to lose some gain to achieve improvement in sensitivity. We should not place a gain outside the feedback loop; the overall system will be quite sensitive to elements outside the loop.

Example 4.3

Several important speed control systems are used in steel mills for rolling the steel sheets and moving the steel through the mill (Fig. 4.12). We consider here a speed control system employing an armature-controlled dc motor with negligible armature inductance, as the actuator. Figure 4.13 gives the schematic of the speed control system and Fig. 4.14 gives the operational block diagram:

$e_a(t)$ = armature applied voltage
R_a = armature resistance
K_b = motor back-emf constant
K_T = motor torque constant

Copyrighted material

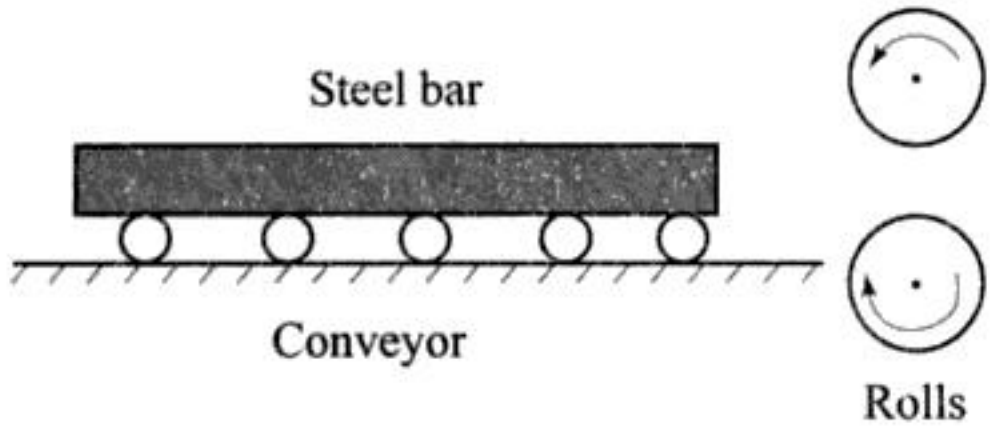


Fig. 4.12

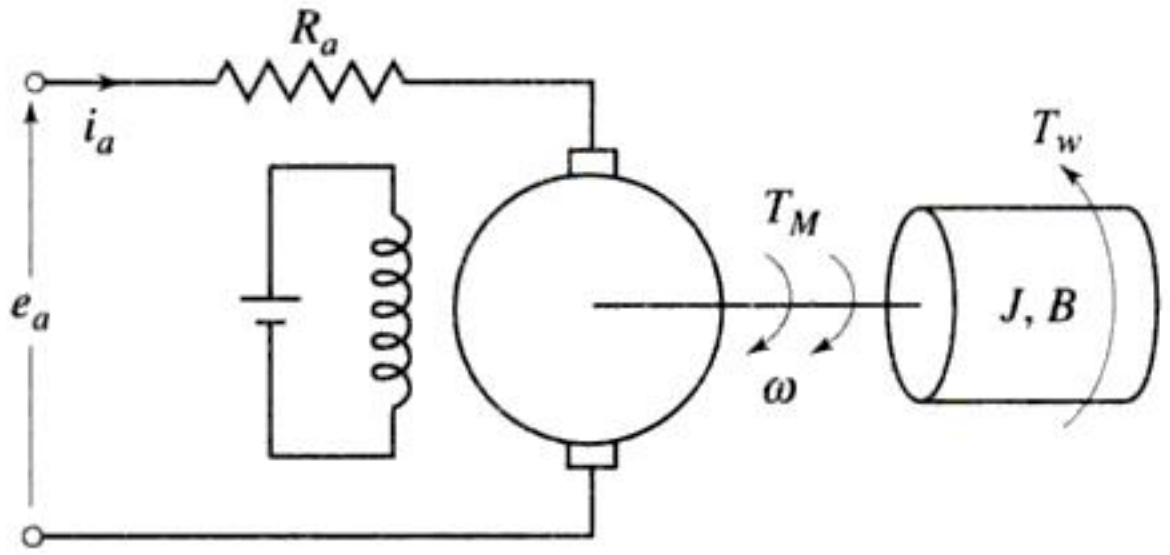


Fig. 4.13

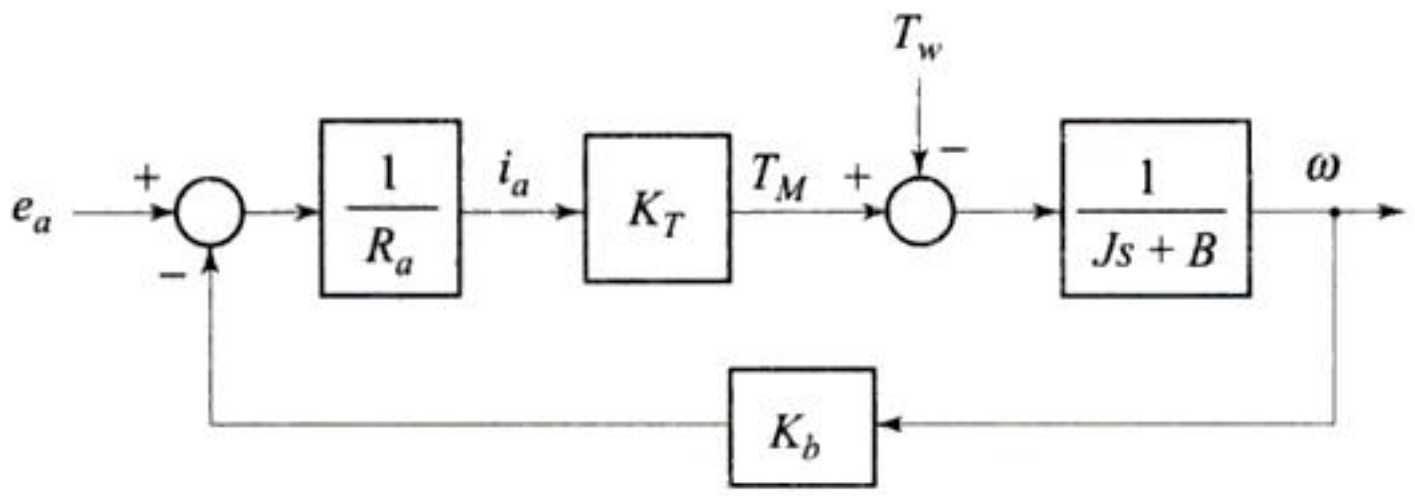


Fig. 4.14 *Open-loop speed control system*

J = moment of inertia of motor and load

B = viscous-friction coefficient of motor and load

$T_w(t)$ = disturbance torque representing loading effect on the rolls when the steel bar engages in the rolls

$\omega(t)$ = motor velocity

The transfer function of the open-loop speed control system obtained from Fig. 4.14, is

$$M_o(s) = \frac{\omega(s)}{E_a(s)} = \frac{K}{\tau s + 1} \tag{4.17}$$

where $$K = \frac{K_T}{BR_a + K_T K_b} ; \tau = \frac{J R_a}{BR_a + K_T K_b}$$

The sensitivity of the open-loop mode of operation to variation in the constant K is

Copyrighted material



You have either reached a page that is unavailable for viewing or reached your viewing limit for this book.



You have either reached a page that is unavailable for viewing or reached your viewing limit for this book.



You have either reached a page that is unavailable for viewing or reached your viewing limit for this book.



You have either reached a page that is unavailable for viewing or reached your viewing limit for this book.

and
$$\frac{H_1(s)}{H_2(s)} \triangleq H(s) \tag{4.25c}$$

Substituting $D(s)$, $G(s)$ and $H(s)$ from Eqns (4.25) into Eqns (4.24), we obtain

$$M(s) = \frac{D_1(s)\,G_1(s)/D_2(s)\,G_2(s)}{1 + D_1(s)\,G_1(s)H_1(s)/D_2(s)\,G_2(s)H_2(s)}$$

which reduces to
$$M(s) = \frac{D_1(s)G_1(s)H_2(s)}{D_2(s)G_2(s)H_2(s) + D_1(s)G_1(s)H_1(s)} \tag{4.26}$$

Having obtained the closed-loop transfer function in rational form, we are ready to make two rather important observations.

First, the finite *zeros* of $M(s)$ are given by the zeros of the plant transfer function $G(s)$, the poles of the feedback block $H(s)$, and the zeros of the controller transfer function $D(s)$. Second, the *poles* of $M(s)$ are the roots of the equation

$$D_2(s)G_2(s)H_2(s) + D_1(s)G_1(s)H_1(s) = 0 \tag{4.27}$$

which, because its left-hand side is the denominator polynomial of the transfer function, must be the *characteristic equation* of the closed-loop system.

We will see in the next chapter that the poles of $M(s)$ determine the modes of closed-loop system's response; poles in the left-half of the complex plane give rise to decaying modes (a requirement for system stability) and the poles in the right-half of the complex plane give rise to growing modes (making the system unstable). The zeros of $M(s)$ control the magnitude of each mode and, hence, the contribution of each mode in the total response. Thus, we can shape the dynamic response of the closed-loop system by controlling the locations of poles and zeros of $M(s)$ through the controller $D(s)$.

We see from Eqn. (4.26) that the poles of a feedback system do not have a direct relationship to the open-loop poles and zeros; this tends to complicate the analysis. However, it does mean that the designer has the capability of making the closed-loop system behave quite differently from the open-loop system. In order to make effective use of this ability, it is necessary to have methods for analyzing the effects of changes in parameters of the controller $D(s)$ without having to solve Eqn. (4.26) for $M(s)$ or Eqn. (4.27) for the closed-loop poles each time a parameter is changed. Much of our subsequent work will be directed toward developing analytical tools that will allow us to take advantage of this unusual property of feedback systems.

Consider now the total response of the closed-loop system of Fig. 4.1a to both the reference and the disturbance inputs (refer Eqn. (4.21)):

$$\begin{aligned} Y(s) &= \frac{D(s)G(s)}{1 + D(s)G(s)H(s)} R(s) + \frac{N(s)}{1 + D(s)G(s)H(s)} W(s) \\ &= M(s)R(s) + M_w(s)W(s) \end{aligned}$$

Copyrighted material

The denominators of $M(s)$ and $M_w(s)$ are identical, implying that both the transfer functions have precisely the same poles. This situation is a consequence of the fact that the characteristic equation is a property of the closed-loop configuration and not of the particular variables that happen to be designated as the input and output.

The zeros of $M(s)$ and $M_w(s)$ are different. In fact, it would be rather unfortunate if this difference did not exist because we certainly do not want the output to respond to disturbance inputs in the same way that it responds to reference inputs—generally we would prefer $M(s)$ to be unity, so that the output follows the reference input exactly, and $M_w(s)$ to be zero, so that the output would be unaffected by disturbances.

Upon examination of Fig. 4.10, one notes that the open-loop control system can easily shape the dynamics of the controlled output: the output y follows the input r exactly if

$$D_o(s) = \frac{1}{G(s)}$$

If $D_o(s)$ is realizable (i.e., a physical system with transfer function $D_o(s)$ can be constructed), it can cancel the process dynamics completely since it has the reciprocal transfer function behaviour. Therefore, one may logically ask, what is the advantage of the closed-loop system in this case? Again, we return to the concepts of the sensitivity of the system to parameter changes and effects of disturbances as our answer to this question. In the open-loop control configuration of Fig. 4.10, one may implement $D_o(s)$ so that it is equal to the inverse of the nominal transfer function $G(s)$, but $G(s)$ is usually an approximate model of the process, and during the operation of the system it is inevitable that the parameters of $G(s)$ will change due to environmental changes and $D_o(s)G(s)$ will no longer be equal to unity. Also, because of the disturbances acting on the process $G(s)$ but not on the controller $D_o(s)$, the output $y(t)$ will deviate from the input $r(t)$. By contrast, a closed-loop system continually monitors the output $y(t)$, and provides an actuating signal in order to reduce the effects of parameter variations and disturbances. Thus, we find that the properties of insensitivity to model uncertainties, parameter variations, and disturbance rejection encourage the introduction of feedback.

Example 4.5

Figure 4.7 gives the block diagram description of a heat-exchanger control system (refer Example 4.1). Assume that the actuator and the sensor devices have zero dynamic lags, i.e., the transfer function of the actuator is 0.1, and that of the sensor is 0.16. Under this assumption,

$$\frac{\theta(s)}{\theta_r(s)} = \frac{D(s)G(s)}{1 + D(s)G(s)}$$

where

$$G(s) = \frac{0.8}{30s + 1}.$$

Copyrighted material

If the controller $D(s)$ is an amplifier of gain K_A with negligible dynamic lag, we get

$$\frac{\theta(s)}{\theta_r(s)} = \frac{0.8\,K_A}{30s + 1 + 0.8\,K_A}$$

For positive values of K_A, the effect of the feedback is to shift the pole negatively from the open-loop location $s = -1/30$ to the location $s = -(1+0.8K_A)/30$; the time-constant reduces from 30 to $30/(1 + 0.8K_A)$. This implies that as K_A (and hence the loop gain) increases, the system dynamics continuously becomes faster, i.e., the transient response decays more quickly. Thus, the *relative stability* (which is a quantitative measure of how fast the transients die out in the system) improves with an increase in loop gain.

Consider now the situation which is more closer to the real world: the actuator and the sensor devices in heat-exchanger control system have dynamic lags as shown in Fig. 4.7. Excessive loop gain may result in the instability of the feedback system. The instability phenomenon may be qualitatively described as follows (quantitative discussion will appear in the next chapter).

Consider the feedback system of Fig. 4.7 with a fixed desired value θ_r and in equilibrium with the controlled variable θ at the desired value. If a process disturbance occurs, the ensuing deviation of the controlled variable will cause a correction to be applied but it will be delayed by the cumulative lags of the sensor, actuator, and process. Eventually, however, the trend of the controlled variable caused by the disturbance will be reversed by the opposition of the process manipulated input q_{ms}, returning the controlled variable toward the desired value. Now if the loop gain is high, a *strong* correction is applied and the controlled variable overshoots the desired value, causing a reversal in the algebraic sign of the system error (difference between desired value and controlled variable). Unfortunately, because of the system lags, a reversal of the correction does not occur immediately, and the process manipulated input (acting on 'old' information) is now actually driving the controlled variable in the same direction as it was already going, rather than opposing its excursions, leading to a larger deviation. If the loop gain is not too large and/or system lag is not too large, it may be possible to bring the controlled variable back to its desired value. The combination of excessive loop gain with excessive lags always results in feedback system instability.

Steady-State Accuracy

A feedback control system is valuable because the sensitivity of the system to parameter variations, and effect of disturbances can be reduced significantly. In addition, as we have seen, it provides us with the ability to adjust the transient response. However, as a further requirement, one must examine and compare the final steady-state error for an open-loop and a closed-loop system.

The error of the closed-loop system shown in Fig. 4.1b with $W(s) = 0$ is given by

Copyrighted material



You have either reached a page that is unavailable for viewing or reached your viewing limit for this book.



You have either reached a page that is unavailable for viewing or reached your viewing limit for this book.

of its 3-to-15 psig range when $e_A = 0$, and the valve positioner has a zero adjustment which allows the valve opening to be put anywhere desired, with the pressure $\overline{P}$ at 9 psig. With these initial 'trimming' adjustments made, all the variables named in Fig. 4.18 are considered as small perturbations away from the initial steady state.

The thermocouple output is $e_t = K_t\theta$. This simple model is justifiable if the dynamics of the sensor are negligible relative to the process time-constant τ_p. The electronic amplifier is obviously fast enough to be treated as zero-order system. The dynamics of the electropneumatic transducer and valve positioner have been neglected in the block diagram of Fig. 4.18, assuming their response to be very fast relative to τ_p. Also the relation between q_m and x is assumed statically linear and dynamically instantaneous.

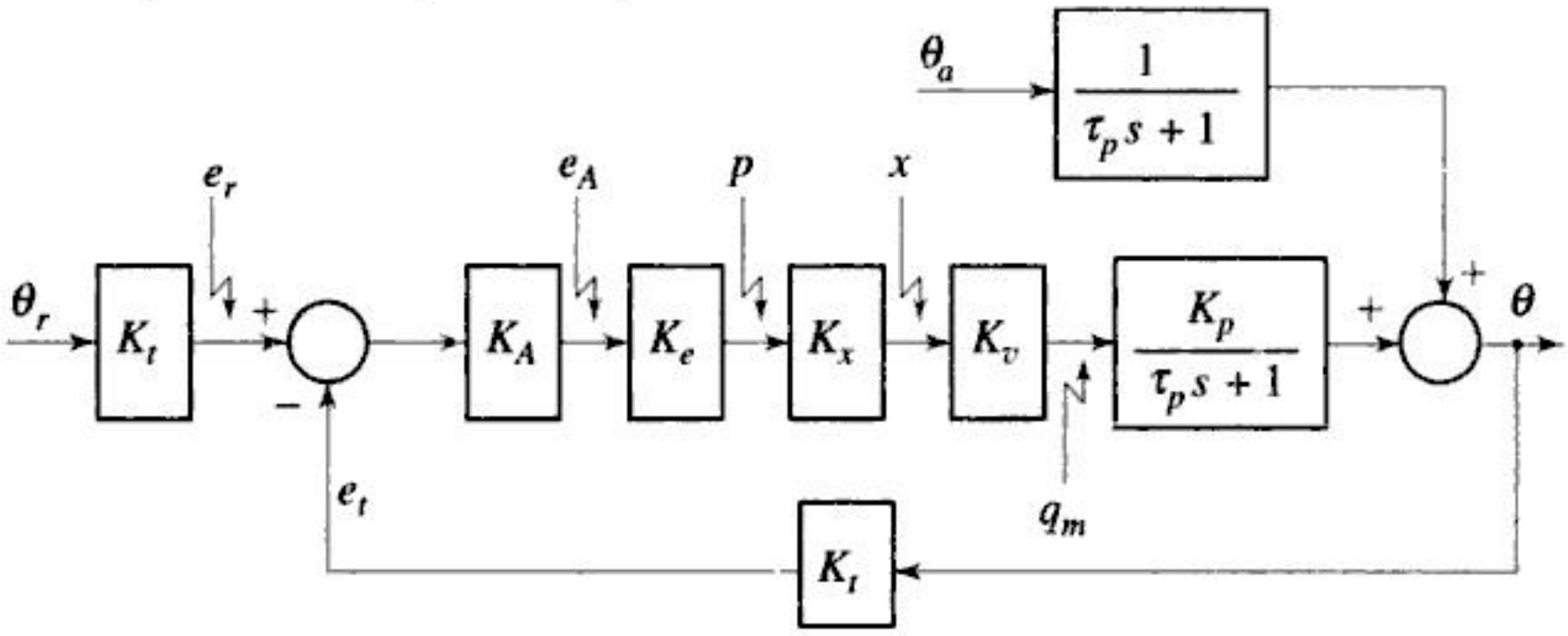


Fig. 4.18 *A block diagram for the system of Fig. 4.17*

Having justified the block diagram of Fig. 4.18, we now use it directly to obtain the transfer function of the closed-loop system, relating θ to θ_r and θ_a:

$$[(K_t\theta_r(s) - K_t\theta(s))K_AK_eK_xK_v]\frac{K_p}{\tau_p s+1} + \left(\frac{1}{\tau_p s+1}\right)\theta_a(s) = \theta(s)$$

$$\text{or} \quad (\tau_p s+1)\theta(s) + K_tK_AK_eK_xK_vK_p\theta(s) = K_tK_AK_eK_xK_vK_p\theta_r(s) + \theta_a(s)$$

$$\text{or} \qquad (\tau s+1)\theta(s) = \frac{K}{1+K}\theta_r(s) + \frac{1}{1+K}\theta_a(s) \qquad (4.30)$$

where $\tau \triangleq$ closed-loop system time-constant $= \dfrac{\tau_p}{1+K}$;

$K \triangleq$ system loop gain $= K_tK_AK_eK_xK_vK_p$

For the linear model of Eqn. (4.30), superposition holds and we can investigate the effects of command θ_r and disturbance θ_a separately. For θ_r, a step input of size unity (perturbation θ_a is held at zero), we get

$$\theta(t) = \frac{K}{1+K}(1 - e^{-t/\tau}) \qquad (4.31)$$

Figure 4.19 shows the first-order system response with speed determined by τ and the steady-state error given by

Copyrighted material

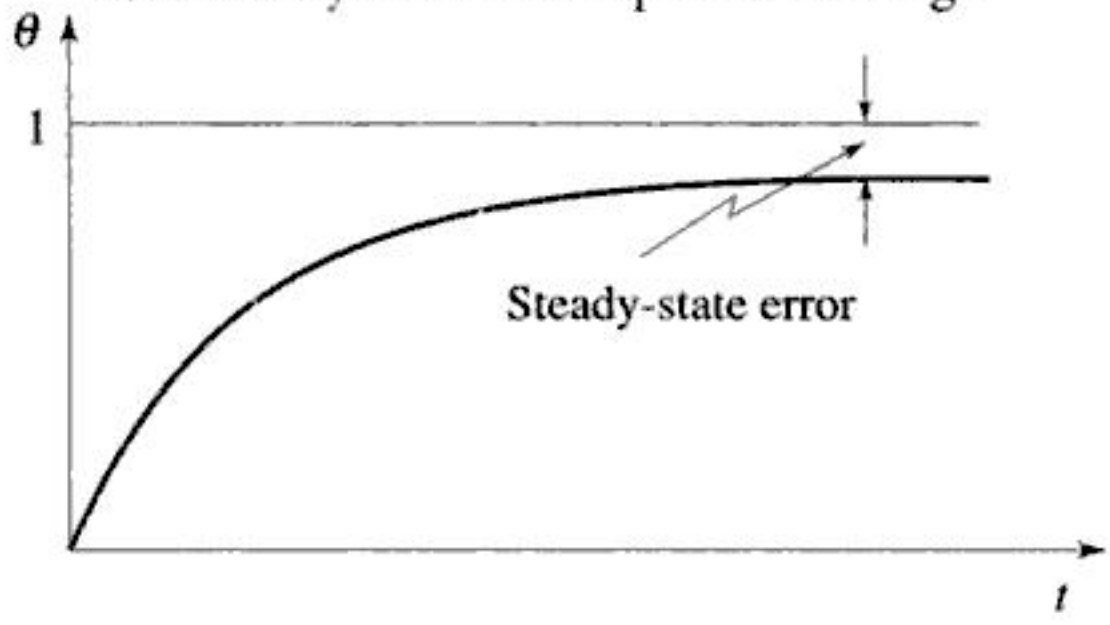


Fig. 4.19 *System response to step command*

$$e_{ss} = 1 - \theta_{ss} = \frac{100}{K+1}\%$$

Since $\tau = \tau_p/(K+1)$, we see that both the speed of response and the steady-state error are improved if we increase loop gain K. For step disturbance input $\theta_a(s) = 1/s$ ($\theta_r = 0$), we get

$$\theta(t) = \frac{1}{(K+1)}(1 - e^{-t/\tau}) \tag{4.32}$$

and again increasing K improves both the speed of response and the steady-state error.

The steady-state errors discovered in the present example are in fact characteristic of the proportional control in general. The basic reason for this behaviour can be explained as follows. For the initial equilibrium point assumed, we are able to get zero steady-state error because the zero adjustments on various devices allow us to open the valve exactly the right amount to supply the steam with $e = \theta_r - \theta = 0$. When we then ask θ_r to change by a unit step, a different valve opening is required to reach equilibrium at the new θ_r because the required rate of steam flow will be larger than that for the initial equilibrium state. When flow rate q_m is proportional to e, a new q_m can only be achieved if e is different from zero; thus there must be a steady-state error. Similar reasoning holds for step changes in disturbances. Thus for any initial equilibrium condition, we can 'trim' the system for zero error but subsequent steady commands and/or disturbances must cause steady-state errors.

The steady-state error due to step commands can theoretically be eliminated from proportional control systems by intentionally 'misadjusting' θ_r. For example, for a step input θ_r of size $(1 + K)/K$ with $\theta_a = 0$, we get from Eqn. (4.30):

$$\theta(t) = 1 - e^{-t/\tau}\ ;\ \theta_{ss} = \text{steady-state value of } \theta(t) = 1$$

Thus, if we want θ to change by a unit step, we ask for a step input of size $(1 + K)/K$.

This trick does in fact work, but depends upon our knowledge about K. If K is not accurately known or varies, then the trick is not 100% effective. Also the trick does not help in reducing steady-state errors caused by disturbances. In the next section we will see that the *integral mode* of feedback control removes

Copyrighted material

steady-state errors due to both commands and disturbances and does not depend on the knowledge of specific numerical values for system parameters.

Equations (4.30)–(4.32) indicate that the following aspects of systems behaviour are improved by increasing loop gain:

(i) steady-state tracking accuracy;
(ii) disturbance signal rejection; and
(iii) relative stability, i.e., rate of decay of the transients.

In addition, it can easily be established that increase in loop gain decreases the sensitivity of the system to parameter variations. Thus all aspects of system behaviour are improved by high-gain proportional control. This is, however, true up to a point but connot be carried to extremes because the system will go unstable. Note that the model of Fig. 4.18 gives no warning of instability[2]. This defect in our model is caused by our neglect of dynamics in some of the system components. We originally neglected these dynamics relative to τ_p, but in the closed-loop system, response speed is determined by τ and not τ_p. Equation (4.30) shows that τ decreases as K is increased and therefore at some point the initially neglected dynamics are no longer negligible. Thus, the model of Fig. 4.18 correctly predicts system behaviour, as long as loop gain is not made 'too large'; it is not valid for stability predictions. If we want to make valid stability predictions, we must include enough dynamics in our system model. The next chapter will show that instability will occur for large values of loop gain when the closed-loop system is of order 3 or more.

In addition to neglecting some 'fast' dynamics, the model of Fig. 4.18 further differs from reality because of its perfect linearity, which assumes no limit on the magnitude of corrective control action that can be applied by the system. Actually the amplifier, the electropneumatic transducer, and valve positioner all exhibit saturation, limiting their output when input becomes too large. All aspects of closed-loop system behaviour suffer from saturation.

4.5 INTEGRAL MODE OF FEEDBACK CONTROL

Consider the closed-loop system of Fig. 4.20a. Assume that initial 'trimming' (zero adjustments) of the control system has been done to obtain $y = r$, with $e = u = 0$. In response to a change in the set-point, the controller must change the flow of energy and/or material to the process in order to achieve equilibrium at the new operating conditions. If the controller is based on proportional logic, then in the new steady-state, a non-zero error e_{ss} must exist to get a non-zero value of control signal u_{ss} (Fig. 4.20b). The new set-point is, say, 10. It will result in a response y_{ss} of less value, say 9.9. The steady-state error is 0.1 and the steady value of the control signal is $0.1K_c$ where K_c is controller gain. The operator must then 'reset' the set-point to bring the output to the desired value of 10.

---

2. The characteristic equation of the system is (refer Eqn. (4.30))

$$\tau_p s + 1 + K = 0$$

The characteristic root (closed-loop pole) is always in the left half of complex plane.

Copyrighted material

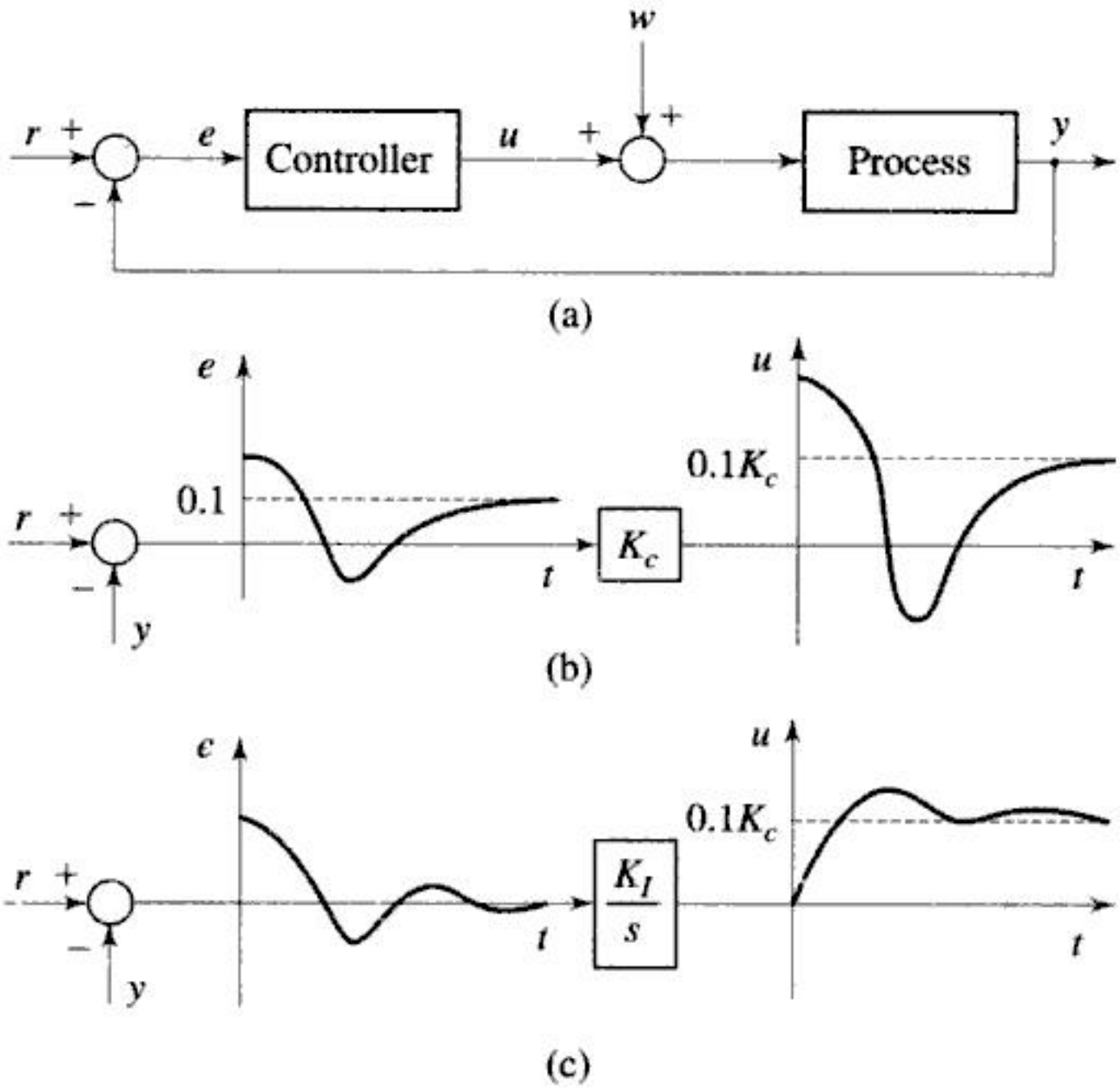


Fig. 4.20 *Comparison of proportional and integral control*

We need a controller that automatically brings the output to 10 with a set-point of 10, i.e., it gives a steady control signal of value $0.1K_c$ with system error $e_{ss} = 0$. An integrator is capable of exactly this type of behaviour (Fig. 4.20c). Integral control is thus a means of removing steady-state errors without the need for manual reset and, in fact, it is sometimes called *automatic reset*. We shall see that integral control can be used by itself or in combination with other control modes; indeed, PI control is the most common mode (refer Eqns (4.3)):

$$u(t) = K_c\left[e(t) + \frac{1}{T_I}\int_0^t e(t)dt\right] \tag{4.33a}$$

or

$$U(s) = K_c\left(1 + \frac{1}{T_I s}\right)E(s) \tag{4.33b}$$

where T_I is the integral or reset time.

Although integral control is very useful for removing or reducing steady-state errors, it has the undesirable side-effects of degrading stability. Conversion of the proportional control system of Fig. 4.18 to integral control will bring out some general results about integral mode. Suppose we replace the amplifier block K_A by K_I/s. The closed-loop system is then described by the equation

Copyrighted material

$$\left[(K_t\theta_r(s) - K_t\theta(s))\frac{K_I}{s}K_eK_xK_v\right]\frac{K_p}{\tau_p s+1} + \frac{1}{\tau_p s+1}\theta_a(s) = \theta(s)$$

$$\text{or } (\tau_p s+1)\theta(s) + \frac{K_tK_IK_eK_xK_vK_p}{s}\theta(s) = \frac{K_tK_IK_eK_xK_vK_p}{s}\theta_r(s) + \theta_a(s)$$

$$\text{or} \qquad (\tau_p s^2 + s + K)\theta(s) = K\theta_r(s) + s\theta_a(s) \tag{4.34}$$

where $K \triangleq$ loop gain $= K_tK_IK_eK_xK_vK_p$

For θ_r, step input of size unity (perturbation θ_a held at zero), we get

$$\theta(s) = \left(\frac{K}{\tau_p s^2 + s + K}\right)\frac{1}{s}$$

By final-value theorem, the steady-value of the output is unity, and therefore steady-state error is zero. For step disturbance input $\theta_a(s) = 1/s$ ($\theta_r = 0$), we get

$$\theta(s) = \left(\frac{s}{\tau_p s^2 + s + K}\right)\frac{1}{s};\ \theta_{ss} = \text{ steady-state value of output} = 0$$

Thus, step changes of θ_r and θ_a give zero steady-state errors regardless of the value of loop gain K. The steady-state performance of the system with constant inputs is thus insensitive to parameter variations.

We need to consider what integral control does to the dynamic response. For this we need to look at the characteristic equation corresponding to Eqn. (4.34), which is

$$\tau_p s^2 + s + K = 0.$$

The roots of this equation,which are readily computed, vary as gain K is varied. In fact, it is informative to compute these and plot them as a function of K. By quadratic formula of algebra, the roots are

$$s = \frac{-1 \pm \sqrt{1 - 4K\tau_p}}{2\tau_p}$$

and are plotted in Fig. 4.21b for changing values of the gain K. When the gain is zero, the roots are at $-1/\tau_p$ and at 0. As the gain is raised, the roots move closer until there is a double root at $-1/2\tau_p$, and then for higher gains, the roots become complex conjugate.

Recall the case of proportional control; from Eqn. (4.30), we obtain the following characteristic equation:

$$\frac{\tau_p}{1+K}s + 1 = 0$$

The root of this equation, $s = -\dfrac{1+K}{\tau_p}$, moves increasingly to the left in the complex plane for increasing values of K (Fig. 4.21a) which implies a decreas-

Copyrighted material

ing time-constant for the closed-loop system; the larger the loop gain, faster is the rate of decay of transients. With integral control, the rate of decay of transients is dictated by the real root closer to the imaginary axis or real part of the pair of complex conjugate roots. There is obviously a limit on the speed of response; also the response will be oscillatory for large values of K rather than exponential as with proportional control. Due to our too-simple dynamic modelling, instability for large values of loop gain is not predicted.

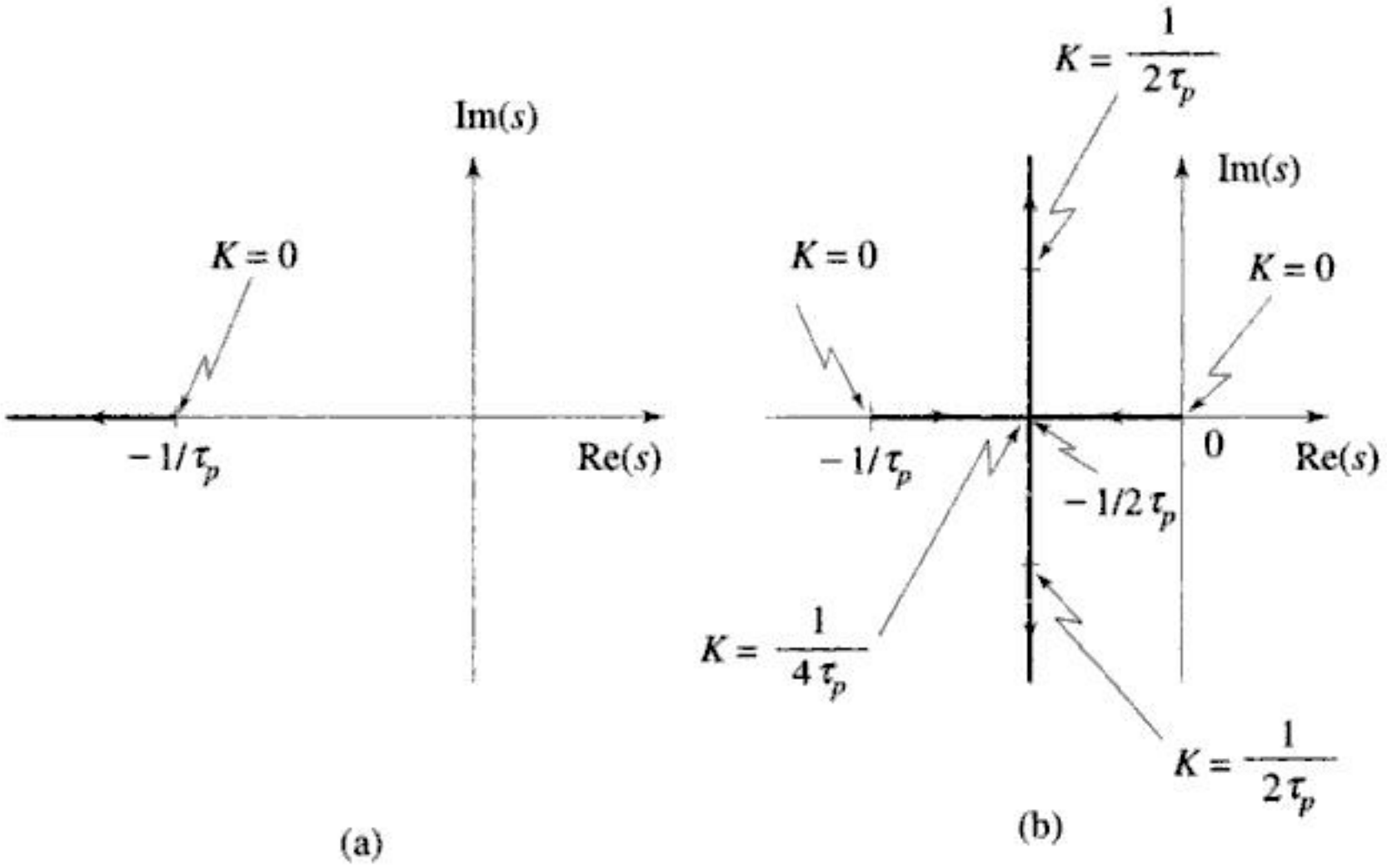


Fig. 4.21 *Destabilizing effect of integral control*

Example 4.6

Figure 4.22 shows an electromechanical servo wherein motor torque T_M controls position θ of inertia J which is subject to torque disturbance T_w. The field

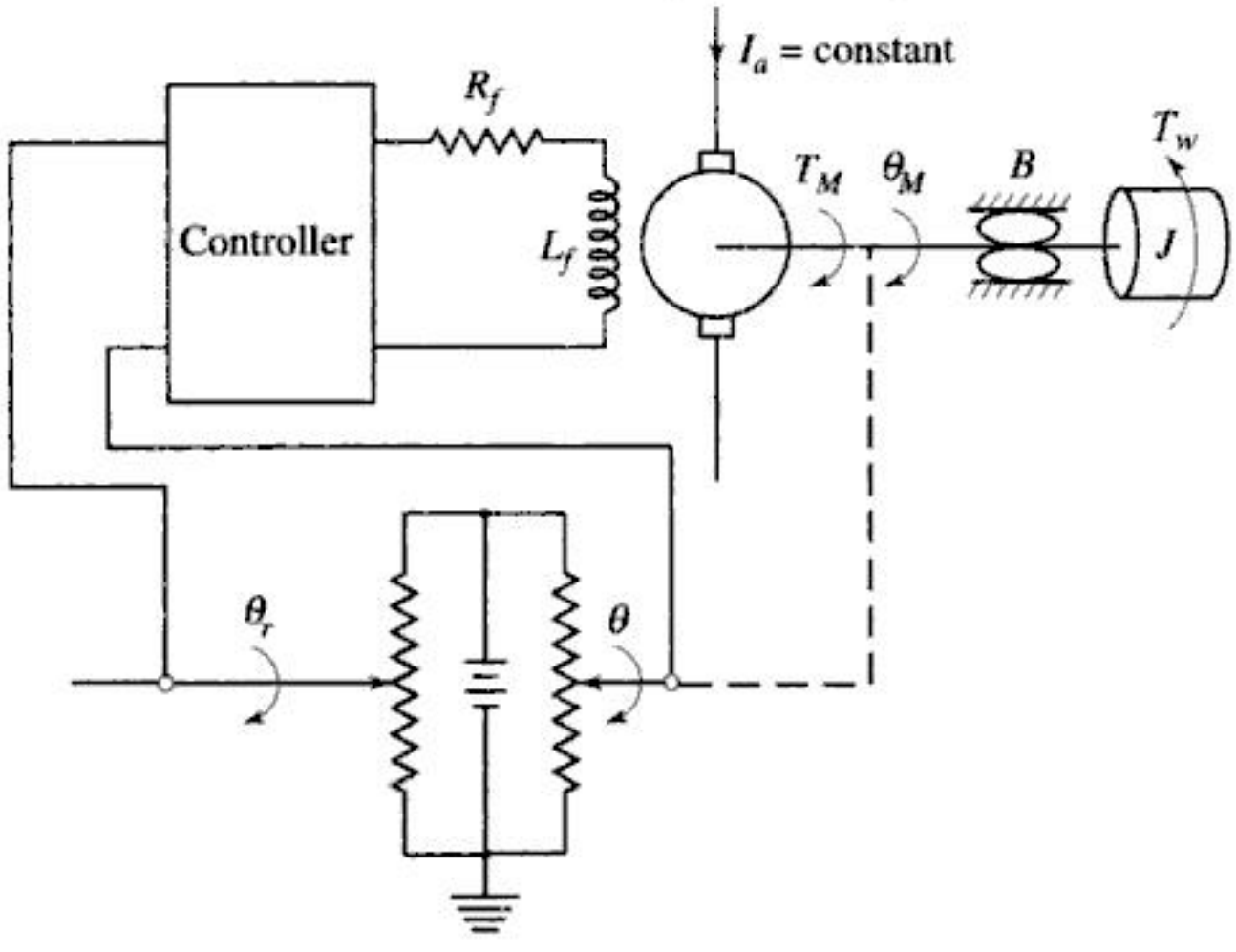


Fig. 4.22 *An electromechanical servo*

Copyrighted material

time-constant $\tau_f = L_f/R_f$ is negligibly small; K_T is the motor torque constant and K_P is the potentiometer sensitivity.

Notice that integrating effect naturally appears in the system plant. Let us examine whether we need integral control for such a plant. The block diagram in Fig. 4.23 shows the integrating plant with proportional control. The following equation easily follows from this block diagram:

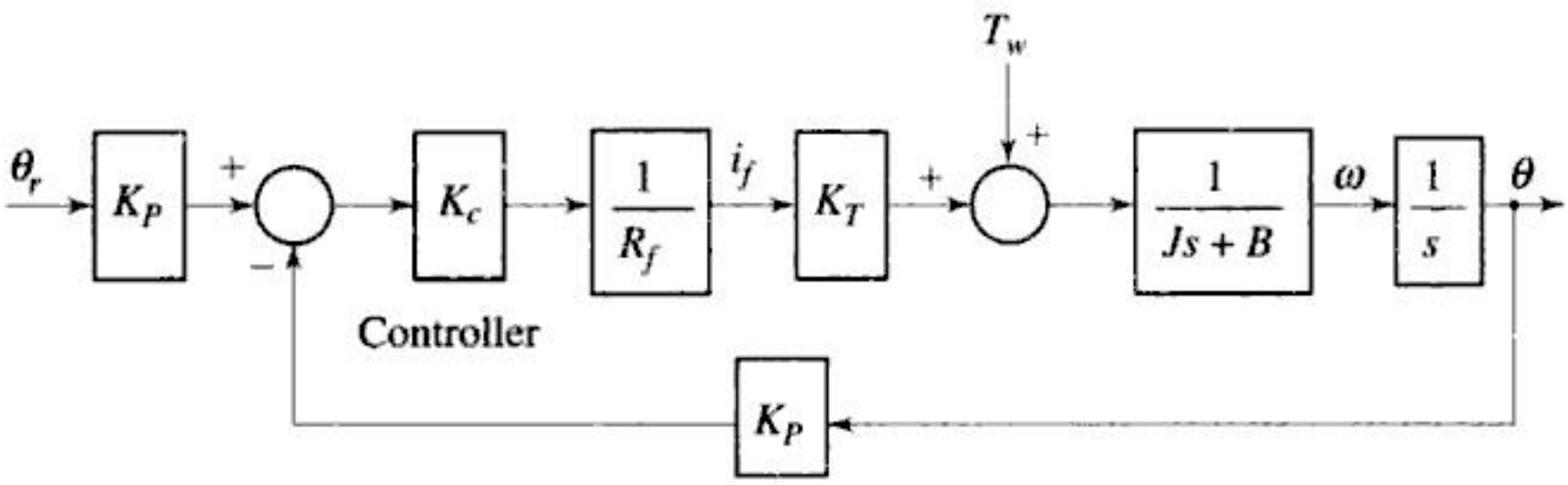


Fig. 4.23 *A block diagram of the system in Fig. 4.22*

$$[(\theta_r(s)K_P - \theta(s)K_P)K_c(K_T/R_f) + T_w(s)]\frac{1}{Js^2 + Bs} = \theta(s)$$

or
$$(Js^2 + Bs + K)\theta(s) = K\theta_r(s) + T_w(s) \tag{4.35}$$

where

$$K \triangleq \frac{K_P K_c K_T}{R_f} = \text{loop gain}$$

For a unit step command input with $T_w = 0$, we have

$$\theta(s) = \left(\frac{K}{Js^2 + Bs + K}\right)\frac{1}{s}$$

By final-value theorem, the steady-state value of the output is given by

$$\theta_{ss} = \lim_{s\to 0} s\left(\frac{K}{Js^2 + Bs + K}\right)\frac{1}{s} = 1$$

and therefore, the steady-state error, $e_{ss} = \theta_r - \theta_{ss}$, is zero.

For a unit step disturbance with $\theta_r = 0$, have

$$\theta(s) = \left(\frac{1}{Js^2 + Bs + K}\right)\frac{1}{s}$$

and the steady-state value of the output is $\theta_{ss} = \frac{1}{K}$.

The plant integrator, thus, gives zero steady-state error for a step command but not for a step disturbance. If we replace the controller gain K_c by

Copyrighted material

$K_c\left(1+\frac{1}{T_I s}\right)$, and examine the system for steady-state accuracy, we find that the steady-state errors to step commands as well as to step disturbances are zero. Therefore, the location of the integrator relative to disturbance injection points determines its effectiveness in removing steady-state errors. The integrator must be located before the disturbance enters the system if it is to be effective in removing steady-state error due to disturbance; however, location is not significant for steady-state errors caused by commands.

Let us study the effect of the integrator on the stability of the system of Fig. 4.23. With proportional control, the characteristic equation of the system is (refer Eqn. (4.35))

$$Js^2 + Bs + K = 0$$

which has roots in the left-half of the complex plane for all values of K; hence the system is stable for all values of loop gain.

Replacing K_c by $K_c\left(1+\frac{1}{T_I s}\right)$, we get the following characteristic equation:

$$Js^3 + Bs^2 + Ks + K/T_I = 0$$

It is a third-order characteristic equation and, as we shall see in the next chapter, large values of loop gain K lead to instability.

▲▲

A controller with integral action can exhibit the phenomenon called *integral windup* (*reset windup*) when overdriven, if it is not properly designed. Chapter 11 gives the details.

Although controllers with a single integrator are most common, double (and occasionally triple)integrators are useful for the more difficult steady-state error problems; however they require careful stability augmentation. Conventionally, the number of integrators in the forward path has been called the system *type number*; type 0 systems have no integrators, type 1 have one, and so forth. In addition to the number of integrators, their location (relative to disturbance injection points) determines their effectiveness in removing steady-state errors. Detailed treatment of steady-state error analysis will appear in Chapter 6.

4.6 DERIVATIVE MODE OF FEEDBACK CONTROL

Consider the closed-loop system shown in Fig. 4.24. The controller is given the information on system error $e(t)$ and has the task of changing control variable $u(t)$ so as to keep $e(t)$ close to zero. If the control logic is a proportional control action, then the value of u at time t_1 will be same as that at t_2. However, a stronger corrective effort seems appropriate at t_1 and lesser one at t_2, since at t_1 the error is e_{12} and *increasing*, whereas at t_2 it is again e_{12} but *decreasing*. That

Copyrighted material

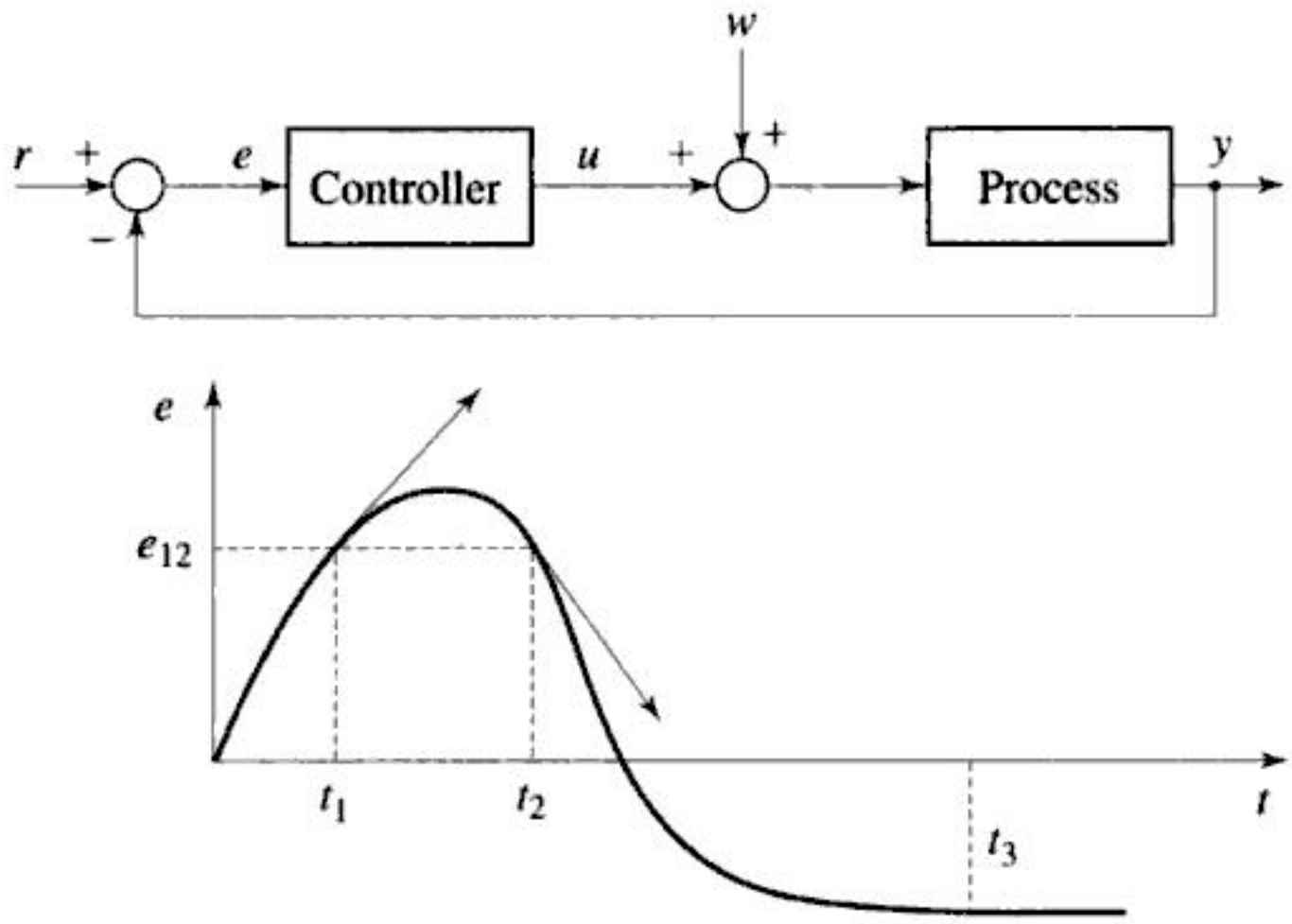


Fig. 4.24 *Genesis of derivative control*

is, the controller must sense not only the ordinate of the error curve but also its trend or slope. Slope is clearly *de/dt*; so to mechanize this desirable control logic, we need a controller sensitive to error derivative. Such a controller can, however, not be used alone since it acts as open circuit for *steady* errors of any size, as at t_3; thus a combination of proportional plus derivative (PD), for example, makes sense (refer Eqns (4.5)):

$$u(t) = K_c \left[e(t) + T_D \frac{de(t)}{dt} \right] \tag{4.36a}$$

or

$$U(s) = K_c (1 + T_D s) E(s) \tag{4.36b}$$

where K_c is the controller gain and T_D is the derivative or rate time.

The noise-accentuating characteristics of derivative operations may often require use of approximate (low-pass filtered) derivative signals. This prevents realization of ideal performance but significant system improvement is still often possible. Here we will explore idealized versions of derivative controls in order to make clear their basic characteristics. Later chapters will develop their practical implementation in a more comprehensive way.

Figure 4.22 shows an electromechanical servo where motor torque T_M controls position θ of inertia J which is subject to torque disturbance T_w. The damper torque on J, due to viscous friction with coefficient B, behaves exactly like a derivative control mode in that it always opposes velocity $d\theta/dt$ with a strength proportional to $d\theta/dt$, making motion less oscillatory. We can therefore, by careful mechanical design, reduce the real friction B to nearly zero and obtain desired damping electronically by introducing derivative control as shown in Fig. 4.25a. The field time-constant $\tau_f = L_f / R_f$ has been assumed to be negligibly small; K_T is the motor torque constant and K_P is the potentiometer sensitivity. The closed-loop system is described by the following equation:

Copyrighted material

$$[(\theta_r(s)K_P - \theta(s)K_P)K_c(1 + T_D s)(K_T/R_f) + T_w(s)]\frac{1}{Js^2} = \theta(s)$$

or $$\left(s^2 + \frac{KT_D}{J}s + \frac{K}{J}\right)\theta(s) = \frac{K}{J}(1 + T_D s)\theta_r(s) + \frac{1}{J}T_w(s) \quad (4.37)$$

where $K \triangleq \dfrac{K_P\, K_c\, K_T}{R_f}$ = loop gain.

The second-order characteristic equation is

$$s^2 + 2\zeta\omega_n s + \omega_n^2 = s^2 + \frac{KT_D}{J}s + \frac{K}{J} = 0$$

Therefore

$$\omega_n = \sqrt{\frac{K}{J}}\ ;\ \zeta = \frac{T_D}{2}\sqrt{\frac{K}{J}}$$

If T_D is positive, motor torque is felt by the load in exactly the same way as a mechanical viscous damping torque; the load cannot distinguish between them. The derivative control may therefore be interpreted as pseudo-friction effect.

We now change the system of Fig. 4.25a by using a proportional controller in the forward path and adding derivative mode at the controlled variable θ (Fig. 4.25b). Derivative modes of angular position are extremely common in all kinds of servomechanisms and are usually implemented using a tachogenerator to get a voltage proportional to shaft speed (Fig. 4.25c).

From the block diagram of Fig. 4.25b, we obtain

$$\left[[(\theta_r(s) - \theta(s))K_P\, K_1 - K_2 s\theta(s)]\frac{K_T}{R_f} + T_w(s)\right]\frac{1}{Js^2} = \theta(s)$$

or $$\left(s^2 + \frac{K_2 K_T}{JR_f}\,s + \frac{K_P K_1 K_T}{JR_f}\right)\theta(s) = \frac{K_P\, K_1 K_T}{JR_f}\theta_r(s) + \frac{1}{J}T_w(s) \quad (4.38)$$

In comparing derivative control applied to system error with that applied to the controlled variable, we see that the effects on the characteristic equation are identical. Error-derivative control, however, has a more violent response to sudden command changes (such as steps) because of the presence of derivative term of θ_r (refer Eqn. (4.37)).

Let us now study the effect of derivative control on steady-state errors. For a unit step disturbance with $\theta_r = 0$, the steady-state value of the output, obtained from Eqn. (4.38), is given below.

$$\theta_{ss} = \lim_{s\to 0} s\left[\frac{1/J}{s^2 + (K_2\, K_T/JR_f)s + K_P\, K_1 K_T/JR_f}\right]\frac{1}{s} = \frac{R_f}{K_P\, K_1 K_T}$$

This constant steady-state error for a step disturbance does not depend on K_2; so this feature of performance is unaffected by the derivative control mode. However, there is an indirect method for possibly gaining some improvement in

Copyrighted material



You have either reached a page that is unavailable for viewing or reached your viewing limit for this book.



You have either reached a page that is unavailable for viewing or reached your viewing limit for this book.



You have either reached a page that is unavailable for viewing or reached your viewing limit for this book.



You have either reached a page that is unavailable for viewing or reached your viewing limit for this book.



You have either reached a page that is unavailable for viewing or reached your viewing limit for this book.



You have either reached a page that is unavailable for viewing or reached your viewing limit for this book.



You have either reached a page that is unavailable for viewing or reached your viewing limit for this book.



You have either reached a page that is unavailable for viewing or reached your viewing limit for this book.



You have either reached a page that is unavailable for viewing or reached your viewing limit for this book.



You have either reached a page that is unavailable for viewing or reached your viewing limit for this book.



You have either reached a page that is unavailable for viewing or reached your viewing limit for this book.



You have either reached a page that is unavailable for viewing or reached your viewing limit for this book.



You have either reached a page that is unavailable for viewing or reached your viewing limit for this book.



You have either reached a page that is unavailable for viewing or reached your viewing limit for this book.



You have either reached a page that is unavailable for viewing or reached your viewing limit for this book.



You have either reached a page that is unavailable for viewing or reached your viewing limit for this book.



You have either reached a page that is unavailable for viewing or reached your viewing limit for this book.



You have either reached a page that is unavailable for viewing or reached your viewing limit for this book.



You have either reached a page that is unavailable for viewing or reached your viewing limit for this book.

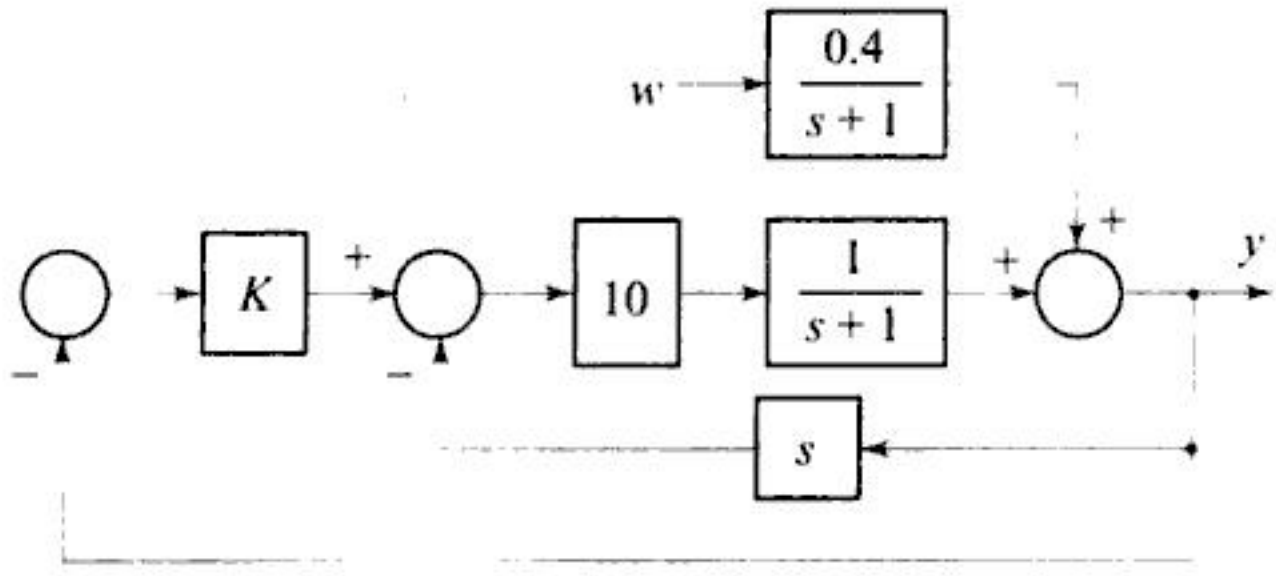


Fig. P4.6

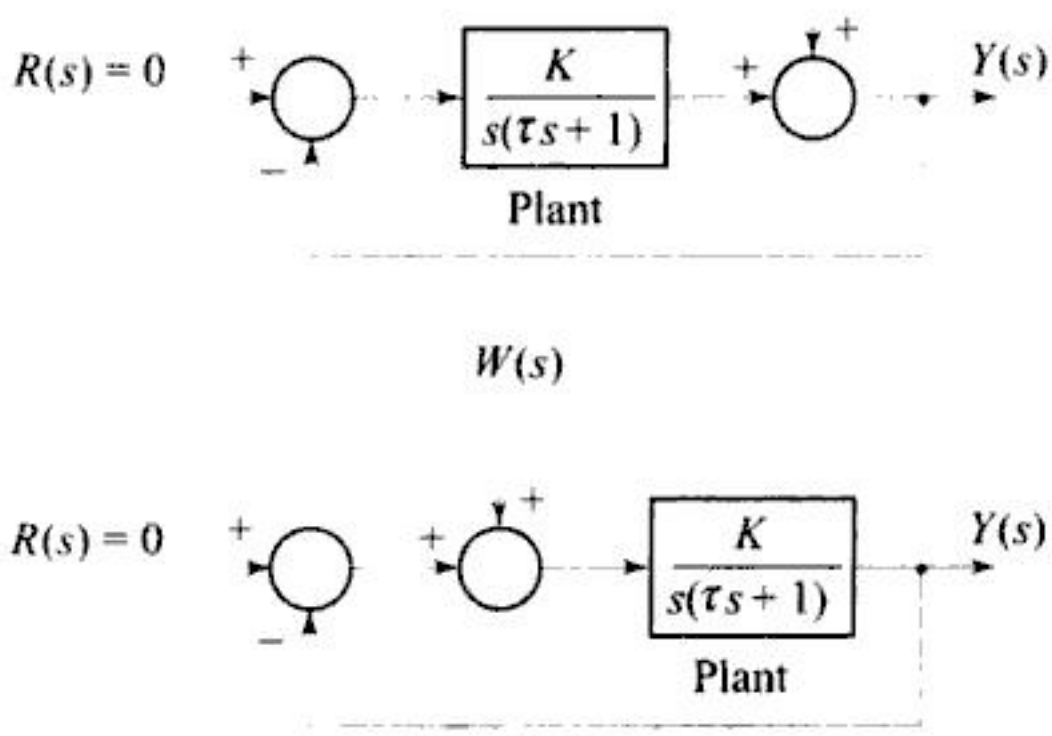


Fig. P4.7

4.8 A temperature control system has the block diagram given in Fig. P4.8. The input signal is a voltage and represents the desired temperature θ_r. Find the steady-state error of the system when θ_r is a unit step function and (i) $D(s) = 1$, (ii) $D(s) = 1 + \frac{0.1}{s}$, (iii) $D(s) = 1 + 0.3s$. What is the effect of the integral term in the PI controller, and derivative term in the PD controller on the steady-state error ?

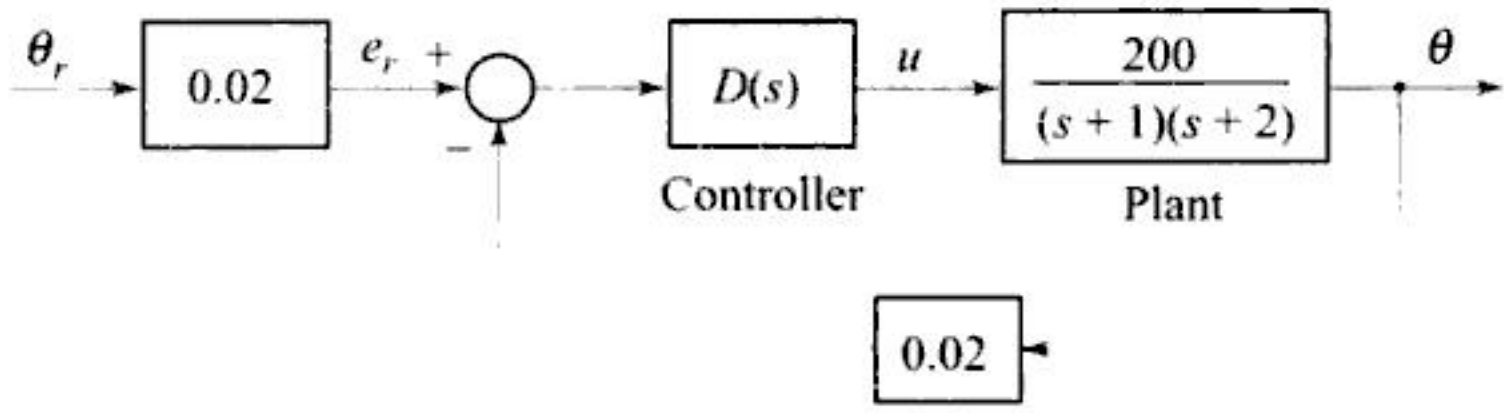


Fig. P4.8

4.9 Consider the closed-loop system of Fig. P4.9. Compute the characteristic equation and therefrom determine the stability of the system when

Copyrighted material



You have either reached a page that is unavailable for viewing or reached your viewing limit for this book.



You have either reached a page that is unavailable for viewing or reached your viewing limit for this book.



You have either reached a page that is unavailable for viewing or reached your viewing limit for this book.

$$\dot{\theta}_L / \dot{\theta}_M = \dot{\theta}_L / \dot{\theta}_C = 1/2$$
$$R_f = 20\ \Omega,\ L_f = 5\text{H},\ R_a = 1\Omega$$

Load friction, and motor inertia and friction are negligible.

The antenna is subject to wind gust torque T_w. Experiments on the antenna show that wind exerts a maximum disturbance of 100 N-m at the antenna.

(a) Draw a block diagram of the system showing the variables θ_R, θ_C, θ_M, θ_L, and T_w. Give the transfer function of each block.

(b) Determine the sensitivity of $\theta_L(s)/\theta_R(s)$ to changes in generator gain K_g for $s = j\omega = j0.1$.

(c) Determine the steady-state error in θ_L when the antenna is subjected to a constant wind gust torque of 100 N-m, with the reference position $\theta_R = 0$.

(d) The antenna is required to have steady-state error of less than 0.2°. Propose a control scheme to meet this objective.

4.14 Aircraft transfer function relating pitch angle θ to the elevator angle δ is of the form

$$\frac{\theta(s)}{\delta(s)} = \frac{K(\tau s + 1)}{s\left(\frac{s^2}{\omega_n^2} + \frac{2\zeta}{\omega_n} s + 1\right)}$$

For a given vehicle, the numerical values of the parameters K, τ, ζ and ω_n vary with altitude and Mach number. For a vehicle flying at four times the speed of sound (Mach 4) at an altitude of 30,000 m, the parameters are

$$\tau = 25,\ K = 0.02,\ \omega_n = 2,\ \zeta = 0.02$$

A basic pitch-command control system is shown in Fig. P4.14. θ_r is the pilot's control stick rotation. The elevator is controlled by an electrohydraulic servo. The transfer function of the servo compared with the dynamics of the aircraft, may be simplified as a constant K_e.

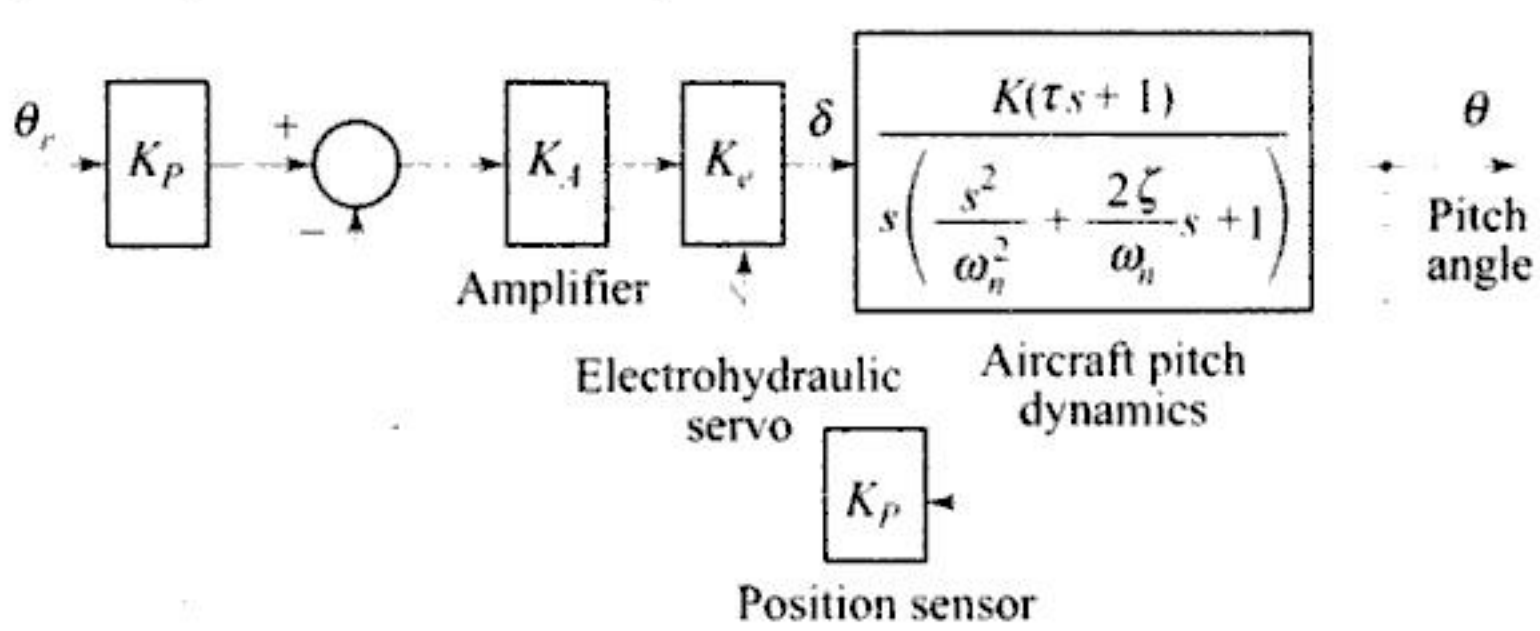


Fig. P4.14

(a) Compare the open-loop and closed-loop systems for sensitivity to changes in the parameter K.

(b) Assume that both the pitch angle θ and its rate of change $\dot{\theta}$ are available for feedback. Suggest a feedback control scheme for increasing the aircraft damping.

Copyrighted material



You have either reached a page that is unavailable for viewing or reached your viewing limit for this book.



You have either reached a page that is unavailable for viewing or reached your viewing limit for this book.



You have either reached a page that is unavailable for viewing or reached your viewing limit for this book.



You have either reached a page that is unavailable for viewing or reached your viewing limit for this book.

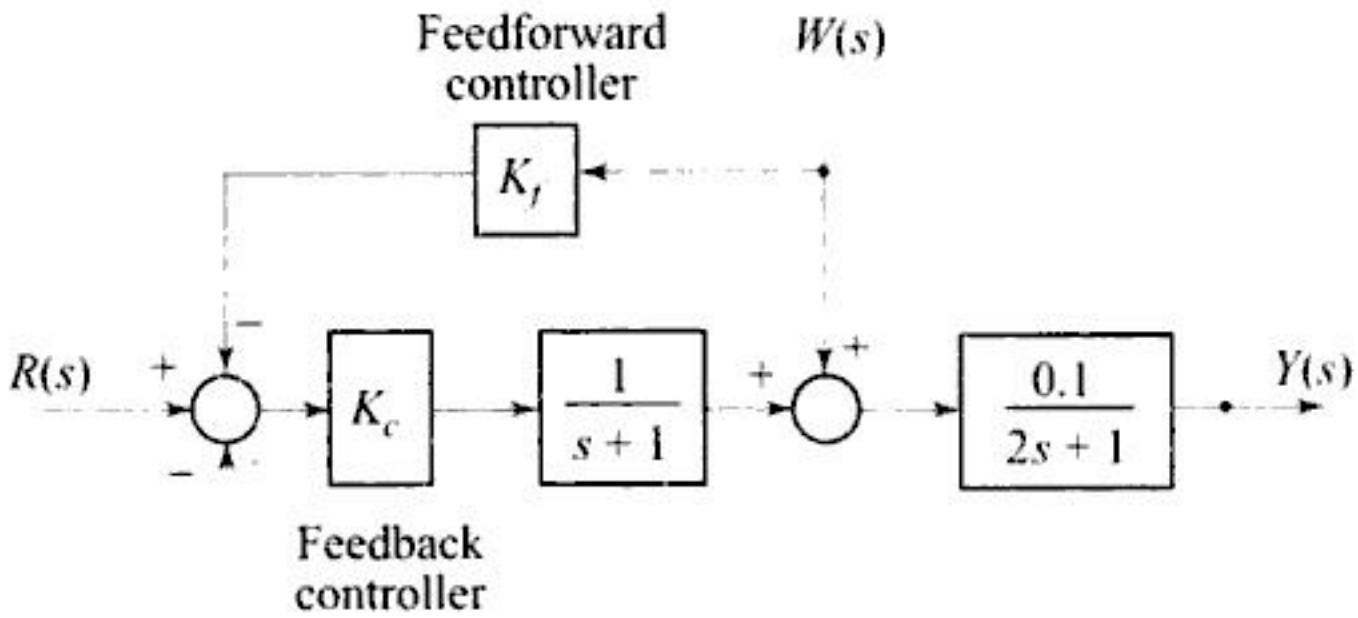


Fig. P4.19

4.20 Figure P4.20 shows a field controlled dc motor with a dc amplifier. The parameters of the system are given below:

Amplifier gain	$K_A = 50$ volt/volt
Motor field resistance	$R_f = 99\ \Omega$
Motor field inductance	$L_f = 20$ H
Motor torque constant	$K_T = 10$ N-m/amp

Moment of inertia of load, $J = 0.5$ N-m/(rad/sec^2)
Coefficient of viscous friction of load, $B = 0.5$ N-m/(rad/sec)
Motor inertia and friction are negligible.

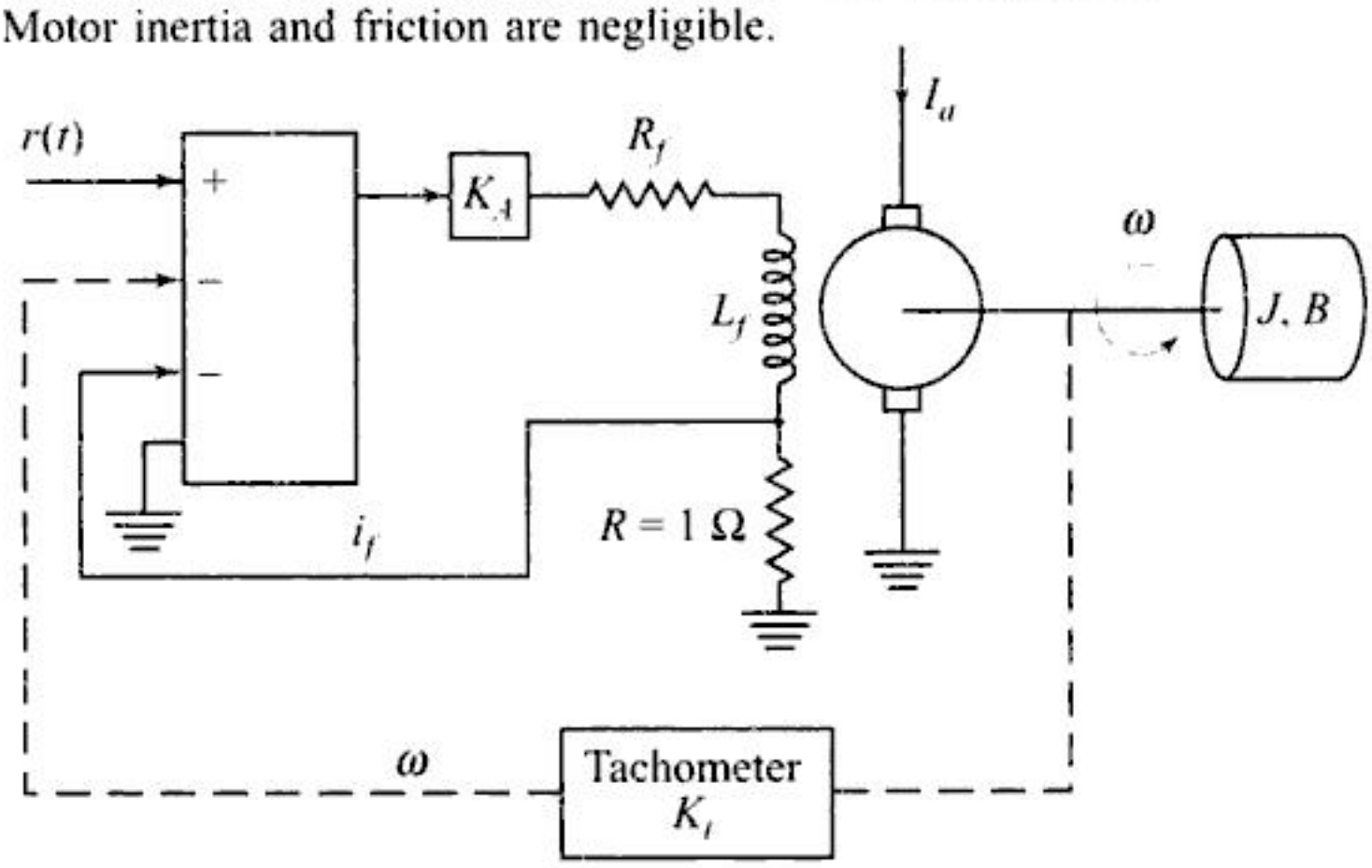


Fig. P4.20

(a) The time-constant of devices with high inductance, such as the field-controlled dc motor, is too long for design requirements. Current feedback may be used to decrease the time-constant. For the system of Fig. P4.20, determine the time-constant of the field circuit with and without current feedback.

(b) Now add a speed-feedback loop (shown dotted in Fig. P4.20) around the current-feedback loop and obtain the closed-loop transfer function of the system.

Copyrighted material



You have either reached a page that is unavailable for viewing or reached your viewing limit for this book.



You have either reached a page that is unavailable for viewing or reached your viewing limit for this book.



You have either reached a page that is unavailable for viewing or reached your viewing limit for this book.

may be different from that for large deviations. Also because of possible existence of multiple equilibrium states in nonlinear systems, the system may move away from one equilibrium state to the other as time progresses.

Another important point to be kept in mind is that when oscillations occur in free linear time-invariant systems, the amplitude of the oscillations is not fixed; it changes with the size of the initial conditions. Slight changes in system parameters will destroy the oscillations. In nonlinear systems, on the other hand, there can be oscillations that are independent of the size of initial conditions and these oscillations (*limit cycles*) are usually much less sensitive to parameter variations. Limit cycles of fixed amplitude and period can be sustained over a finite range of system parameters.

Treatment of nonlinear systems is beyond the scope of this book. Reference [180] highlights the problems associated with nonlinear control systems, and presents commonly used analysis tools. In this chapter, we concern ourselves exclusively with the stability of linear time-invariant systems.

5.2 BOUNDED-INPUT BOUNDED-OUTPUT STABILITY

A linear relaxed system (initial conditions zero) is said to have BIBO stability if every bounded input results in a bounded[1] output. A test for this property is readily found using convolution (refer Section 2.3). If the system has input $r(t)$, output $y(t)$, and impulse response $g(t)$, then

$$y(t) = \int_0^\infty g(\tau) r(t - \tau) d\tau \tag{5.2}$$

If $r(t)$ is bounded, there exists a constant M such that $|r(t)| \leq M < \infty$, and the output is bounded by

$$|y(t)| = \left| \int_0^\infty g(\tau) r(t - \tau) d\tau \right| \tag{5.3}$$

Since the absolute value of an integral is not greater than the integral of the absolute value of the integrand, Eqn. (5.3) may be written as

$$|y(t)| \leq \int_0^\infty |g(\tau) r(t - \tau)| d\tau \leq \int_0^\infty |g(\tau)| |r(t - \tau)| d\tau \leq M \int_0^\infty |g(\tau)| d\tau$$

Therefore, the output will be bounded if

$$\int_0^\infty |g(\tau)| d\tau < \infty \tag{5.4}$$

The condition given by (5.4) is *sufficient* to guarantee BIBO stability. This condition is also *necessary*, for if we consider the bounded input

1. A function $f(t)$ is said to be bounded if its magnitude does not go to infinity in the time interval $[0, \infty)$, or equivalently there exists a real constant M such that $|f(t)| \leq M < \infty$ for all t in $[0, \infty)$.

Copyrighted material



You have either reached a page that is unavailable for viewing or reached your viewing limit for this book.



You have either reached a page that is unavailable for viewing or reached your viewing limit for this book.



You have either reached a page that is unavailable for viewing or reached your viewing limit for this book.

table. All the roots which have non-zero real parts [cases (i), (ii), (iii), and iv)] contribute response terms with a multiplying factor of $e^{\sigma t}$. If $\sigma < 0$ (i.e., the roots have negative real parts), the response terms vanish as $t \to \infty$, and if $\sigma > 0$ (i.e., the roots have positive real parts), the response terms increase without bound. Roots on the $j\omega$-axis with multiplicity two or higher [cases (vi) and (viii)] also contribute terms which increase without bound as $t \to \infty$. Single root at the origin [case (v)] or non-multiple root pairs on the $j\omega$-axis [case (vii)] contribute terms which are constant amplitude or constant amplitude oscillation. These observations lead us to the following general conclusions on BIBO stability.

1. If all the roots of the characteristic equation lie in the left half of the s-plane, then the impulse response is bounded and eventually decays to zero. Therefore $\int_0^\infty |g(\tau)|\, d\tau$ is finite and the system is BIBO stable.

Table 5.1 *Response terms contributed by various types of roots*

Type of roots	*Nature of response terms*
(i) Single root at $s = \sigma$	$Ae^{\sigma t}$
(ii) Roots of multiplicity m at $s = \sigma$	$\left[A_1 + A_2 t + \frac{A_3}{2!}t^2 + \cdots + \frac{A_m}{(m-1)!}t^{m-1}\right]e^{\sigma t}$
(iii) Complex-conjugate root pair at $s = \sigma \pm j\omega$	$A\cos(\omega t + \phi)\, e^{\sigma t}$
(iv) Complex-conjugate root pairs of multiplicity m at $s = \sigma \pm j\omega$	$[A_1\cos(\omega t + \phi_1) + A_2 t\cos(\omega t + \phi_2) + \cdots + \frac{A_m}{(m-1)!}t^{m-1}\cos(\omega t + \phi_m)]e^{\sigma t}$
(v) Single root at the origin, i.e., $s = 0$	A
(vi) Roots of multiplicity m at the origin	$\left[A_1 + A_2 t + \cdots + \frac{A_m}{(m-1)!}t^{m-1}\right]$
(vii) Single complex-conjugate root pair on the $j\omega$-axis, i.e., $s = \pm j\omega$	$A\cos(\omega t + \phi)$
(viii) Complex-conjugate root pair of multiplicity m on the $j\omega$-axis	$[A_1\cos(\omega t + \phi_1) + A_2 t\cos(\omega t + \phi_2) + \cdots + \frac{A_m}{(m-1)!}t^{m-1}\cos(\omega t + \phi_m)]$

Copyrighted material



You have either reached a page that is unavailable for viewing or reached your viewing limit for this book.



You have either reached a page that is unavailable for viewing or reached your viewing limit for this book.



You have either reached a page that is unavailable for viewing or reached your viewing limit for this book.



You have either reached a page that is unavailable for viewing or reached your viewing limit for this book.

We therefore conclude that the absence or negativeness of any of the coefficients of a characteristic polynomial indicates that the system is either unstable or at most marginally stable. Thus, it is necessary for a stable system that all the coefficients of its characteristic polynomial be positive. If any coefficient is zero/negative, we immediately know that the system is not stable. The converse is, however, not true: when all the coefficients are positive, the system is not necessarily stable; there may still be roots in the right half plane and/or on the imaginary axis. In order for all the roots to have negative real parts, it is *necessary but not sufficient* that all of the coefficients of the characteristic equation be positive. For example, when the characteristic equation is

$$\Delta(s) = (s+2)\left(s - \frac{1}{2} - j\frac{\sqrt{15}}{2}\right)\left(s - \frac{1}{2} + j\frac{\sqrt{15}}{2}\right) = s^3 + s^2 + 2s + 8 = 0,$$

the system is unstable, and yet the polynomial possesses all positive coefficients.

The first step in analysing the stability of a system is to examine its characteristic equation. If some of the coefficients are zero or negative, it can be concluded that the system is not stable. On the other hand, if all the coefficients of the characteristic equation are positive, the possibility of the stability of the system exists and one should proceed further to examine the sufficient conditions of stability.

A. Hurwitz and E. J. Routh independently published the method of investigating the sufficient conditions of stability of a system. The Hurwitz criterion is in terms of determinants and the Routh criterion is in terms of array formulation, which is more convenient to handle. We present here the Routh stability criterion[3].

The Routh stability criterion is based on ordering the coefficients of the characteristic equation

$$\Delta(s) = a_0 s^n + a_1 s^{n-1} + a_2 s^{n-2} + \cdots + a_{n-1} s + a_n = 0;\ a_0 > 0 \qquad (5.13)$$

into a schedule, called the *Routh array*.

A necessary and sufficient condition for stability is that all of the elements in the first column of the Routh array be positive. If this condition is not met, the system is unstable, and the number of sign changes in the elements of the first column of the Routh array corresponds to the number of roots of the characteristic equation in the right half of the s-plane.

To determine the Routh array, coefficients of the characteristic equation are arranged in two rows, beginning with the coefficients of s^n and s^{n-1}, respectively, and followed by even-numbered and odd-numbered coefficients as follows:

$$\begin{array}{lcccc} s^n & : & a_0 & a_2 & a_4 \ \cdots \\ s^{n-1} & : & a_1 & a_3 & a_5 \ \cdots \end{array}$$

3. Proof of the Routh stability criterion involves delicate algebra and is omitted here. This algebraic criterion is derived in textbooks, such as Schwarz and Friedland [43], on linear systems.

Copyrighted material



You have either reached a page that is unavailable for viewing or reached your viewing limit for this book.



You have either reached a page that is unavailable for viewing or reached your viewing limit for this book.



You have either reached a page that is unavailable for viewing or reached your viewing limit for this book.



You have either reached a page that is unavailable for viewing or reached your viewing limit for this book.



You have either reached a page that is unavailable for viewing or reached your viewing limit for this book.



You have either reached a page that is unavailable for viewing or reached your viewing limit for this book.



You have either reached a page that is unavailable for viewing or reached your viewing limit for this book.



You have either reached a page that is unavailable for viewing or reached your viewing limit for this book.

s^4	1	2	1	
s^3	1	2		
s^2	~~0~~	~~1~~		← replace 0 by ε
	ε	1		
s^1	$\frac{2\varepsilon - 1}{\varepsilon}$			
s^0	1			

As $\varepsilon \to 0$, there are two sign changes in the first column of the array. This indicates that there are two roots in the right half s-plane. The original polynomial $\Delta(s)$, therefore, has two roots in the right-half plane and two roots on the imaginary axis.

Relative Stability (Shifting the Origin)

The Routh stability criterion ascertains *absolute stability* of a system by determining if all the roots of the characteristic equation lie in the left half of s-plane. Once a system is found to be absolutely stable (all characteristic roots in left half of s-plane), it is desirable to determine its *relative stability,* which is concerned with the attributes of transient behaviour of the system. We shall see in the next chapter that parameters such as overshoot, settling time, etc., are used to capture important attributes of transient response of a stable system; these parameters are therefore quantitative measures of relative stability. Stability margins (gain margin, phase margin) are commonly used as frequency-domain measures of relative stability. Frequency-domain analysis will appear in Chapter 8.

In the following, we show that the Routh stability criterion can be extended for a preliminary relative-stability analysis. We know that for a real root or a complex-conjugate pair of roots on the vertical line in the s-plane defined by $s = -\sigma$, $\sigma > 0$ (refer Fig. 5.3), the time-constant $\tau = 1/\sigma$. The transient response modes corresponding to smaller time-constants decay faster, and therefore the dynamic behaviour of a system is dominated by the roots with larger time-constants. The largest time-constant associated with a system can be obtained by determining the minimum distance of the characteristic roots from the imaginary axis.

We substitute

$$s = \hat{s} - \sigma \tag{5.17}$$

into the characteristic equation, write a polynomial in terms of $\hat{s}$, and apply Routh stability criterion to the new polynomial in $\hat{s}$. If there are no changes of sign in the first column of the array developed for the polynomial in $\hat{s}$, it implies that all the roots of the original characteristic equation are more negative than $-\sigma$. Shifting the vertical axis on a trial-and-error basis, we can find the mini-

Copyrighted material



You have either reached a page that is unavailable for viewing or reached your viewing limit for this book.



You have either reached a page that is unavailable for viewing or reached your viewing limit for this book.



You have either reached a page that is unavailable for viewing or reached your viewing limit for this book.

satisfy Re $(s) < -2$. Thus, we require that K_c satisfy all the following conditions:

$$K_c > 4;\ K_c > 4.3892 \quad \text{or} \quad K_c < -1.1392;\ K_c > \frac{4}{3}$$

The requirement $K_c < -1.1392$ is disregarded since K_c cannot be negative. Therefore, we have Re$(s) < -2$ for all closed-loop poles provided that $K_c > 4.3892$.

Review Examples

Review Example 5.1

Consider the polynomial

$$\Delta(s) = s^5 + 2s^4 + 2s^3 + 4s^2 + 11s + 10$$

The Routh array is calculated as

s^5	1	2	11	
s^4	~~2~~	~~4~~	~~10~~	← divide by 2
	1	2	5	
s^3	~~0~~	~~6~~		← replace 0 by ε
	ε	6		
s^2	$-\frac{6}{\varepsilon}$	5		
s^1	6			
s^0	5			

In array formation, the limits were taken as $\varepsilon \to 0$ at convenient points in the calculations rather than waiting until the array was complete. This procedure simplifies the calculations and the final form of the array.

From the array we see that there are two sign changes in the first column; the polynomial $\Delta(s)$, by Routh stability criterion, has two roots in the right half s-plane.

Review Example 5.2

A feedback control system is shown in Fig. 5.6. The process transfer function is

$$G(s) = \frac{K(s + 40)}{s(s + 10)}$$

Copyrighted material



You have either reached a page that is unavailable for viewing or reached your viewing limit for this book.



You have either reached a page that is unavailable for viewing or reached your viewing limit for this book.



You have either reached a page that is unavailable for viewing or reached your viewing limit for this book.

5.3 Stability of a linear time-invariant system can easily be determined by finding roots of its characteristic polynomial using commercially available CAD software tools. What, then, is the use of Routh stability criterion? (Help: p 314) Demonstrate, through an example, the application of the criterion in control systems field. (Help: Review Example 5.3)

Problems

5.1 Use the Routh stability criterion to determine the number of roots in the left-half plane, the right-half plane, and on the imaginary axis for the given characteristic equation:

(a) $s^4 + 2s^3 + 8s^2 + 4s + 3 = 0$

(b) $s^6 + 3s^5 + 2s^4 + 9s^3 + 5s^2 + 12s + 20 = 0$

(c) $s^5 + s^4 + 2s^3 + 2s^2 + 3s + 5 = 0$

(d) $s^5 + 4s^4 + 8s^3 + 8s^2 + 7s + 4 = 0$

(e) $s^4 + 9s^3 + 4s^2 - 36s - 32 = 0$

(f) $s^7 + 5s^6 + 9s^5 + 9s^4 + 4s^3 + 20s^2 + 36s + 36 = 0$

5.2 Obtain the roots of the given characteristic polynomial on the basis of the Routh array:

(a) $s^4 + 2s^3 + 11s^2 + 18s + 18 = 0$

(b) $s^5 + 2s^4 + 24s^3 + 48s^2 - 25s - 50 = 0$

(c) $s^6 + 3s^5 + 5s^4 + 9s^3 + 8s^2 + 6s + 4 = 0$

5.3 Determine whether the largest time-constant of the roots of the characteristic equation given below is greater than, less than or equal to 1.0 sec.

$$s^3 + 4s^2 + 6s + 4 = 0$$

5.4 The characteristic equations for certain feedback control systems are given below. In each case, determine the range of values of K ($K > 0$) for which the system is stable.

(a) $s^4 + s^3 + s^2 + s + K = 0$

(b) $s^4 + Ks^3 + s^2 + s + 1 = 0$

(c) $s^4 + 3s^3 + 3s^2 + 2s + K = 0$

(d) $s^3 + 3Ks^2 + (K + 2)s + 4 = 0$

5.5 Determine the range of values of K ($K > 0$) such that the characteristic equation

$$s^3 + 3(K + 1)s^2 + (7K + 5)s + (4K + 7) = 0$$

has roots more negative than $s = -1$.

5.6 The block diagram of a feedback control system is shown in Fig. P5.6. Determine the values of K ($K > 0$) that result in a stable closed-loop system.

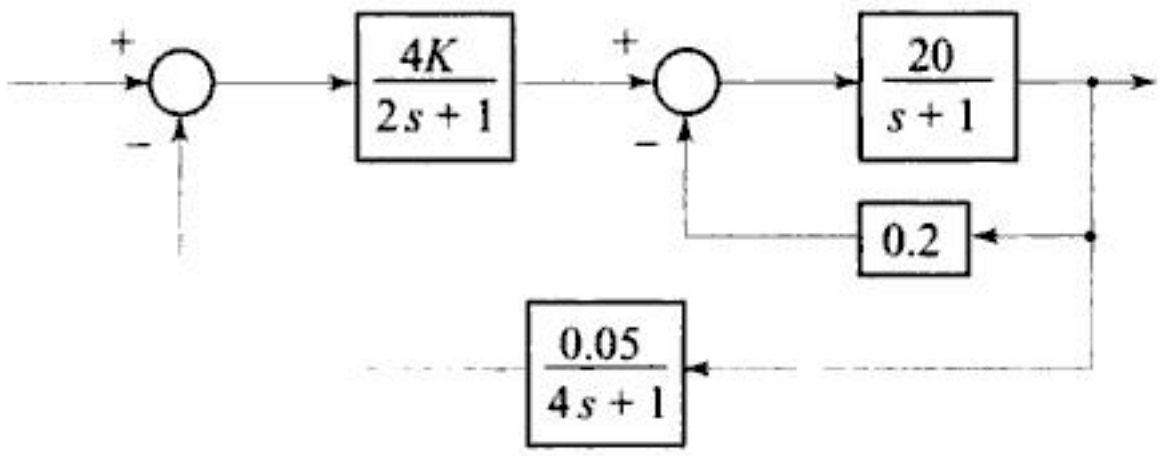


Fig. P5.6

Copyrighted material



You have either reached a page that is unavailable for viewing or reached your viewing limit for this book.



You have either reached a page that is unavailable for viewing or reached your viewing limit for this book.



You have either reached a page that is unavailable for viewing or reached your viewing limit for this book.



You have either reached a page that is unavailable for viewing or reached your viewing limit for this book.

system, difficult. It is common to base performance evaluation on system response to simple 'standard' test signals such as impulse, pulse, step, ramp, parabola, and sine wave (refer Section 2.2). This approach has been successful for a number of reasons.

1. The characteristics of actual signals which severely strain a control system are a sudden shock (impulse), a sudden change (step), constant velocity (ramp), and constant acceleration (parabola). Experience with the actual performance of various classes of control systems has established a good correlation between the response of systems to standard inputs and the capability of the systems to accomplish their required tasks.
2. Design is much concerned with the comparison of competitive systems. This comparison can often be made nearly as well in terms of standard inputs as for real inputs.
3. The simplicity of the form of standard inputs facilitates mathematical analysis and experimental verification.
4. For linear time-invariant systems, frequency-response curves (Chapter 9) are a complete description of the system's dynamic behaviour and allow one to compute the response to any input, not just sine waves.

The standard performance criteria in common use may be classified as falling into the *time domain* or the *frequency domain*. Time-domain specifications have to do with the response to steps, ramps, parabolas, and the like; while frequency-domain specifications are concerned with certain characteristics of the system's frequency response. Both types of specifications are often applied for the same system to ensure that certain behaviour characteristics will be obtained. It may be noted that all performance specifications are meaningless unless the system is absolutely stable.

The majority of analysis and design tools for feedback systems presuppose that a sufficiently accurate model of the process to be controlled has been set up. Using this model, the design is carried out to meet the time-domain and/or frequency-domain performance specifications. The analysis tools that verify the design also use the same model. This design is bound to be a disappointing one when the control system is put to real-life use. This is because in a reasonably complex system, there are always discrepancies between the model and the real process. Design methods that enable us to explicitly consider these discrepancies, i.e., designing a controller without having a precise mathematical model at hand, have yet to mature [158–168]. We need the design that is not only valid for the approximate model but does hold with certainty for a class of plant models and hence for the real process. Good robustness against modelling errors and against variations in parameters of the model due to environmental and other effects, is an important design requirement.

We will not include the robustness/insensitivity requirements in our performance specifications for design. Our design is based on the assumption that the

Copyrighted material



You have either reached a page that is unavailable for viewing or reached your viewing limit for this book.



You have either reached a page that is unavailable for viewing or reached your viewing limit for this book.



You have either reached a page that is unavailable for viewing or reached your viewing limit for this book.

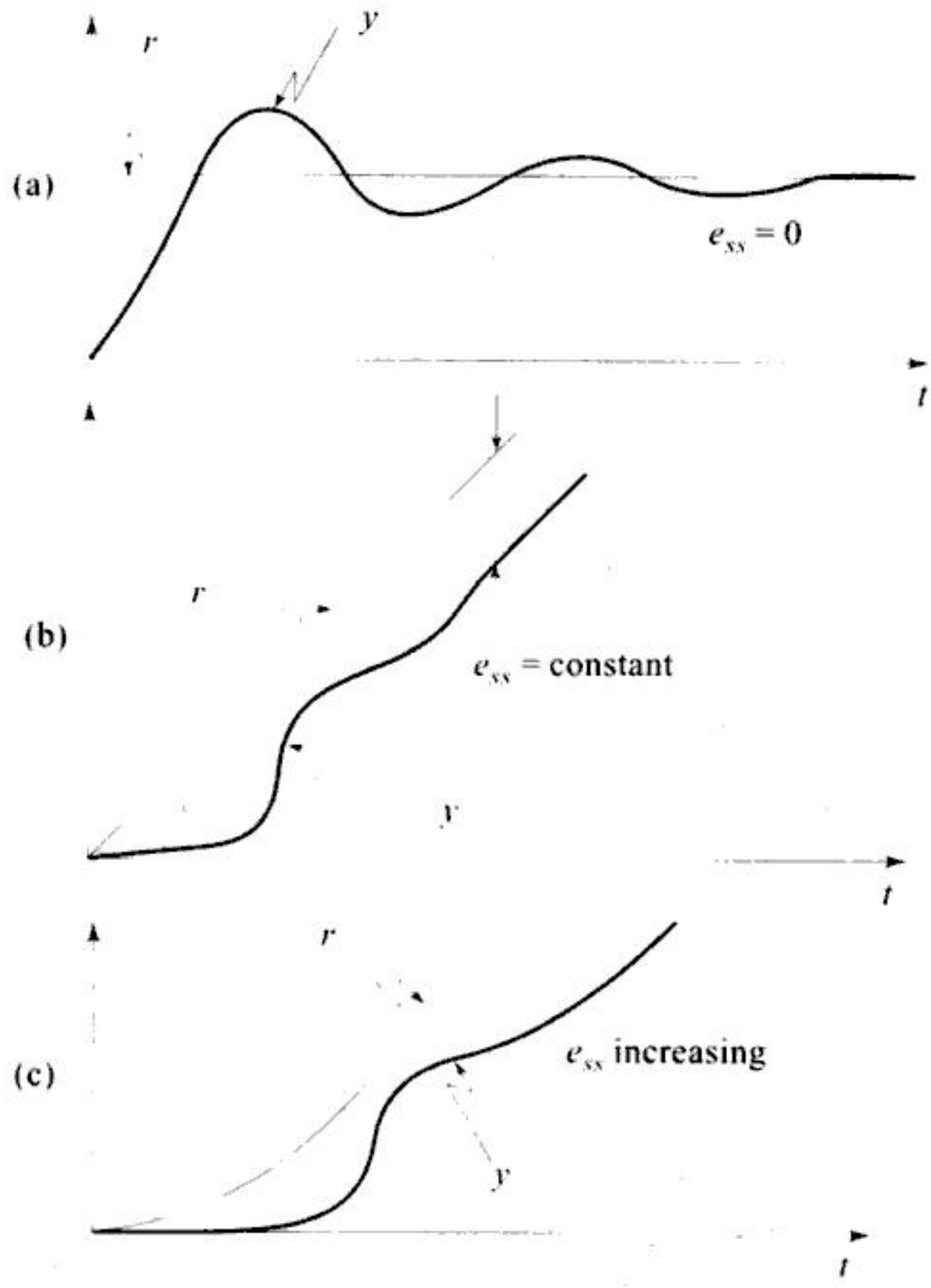


Fig. 6.4 *Effect of input severity on steady-state error*

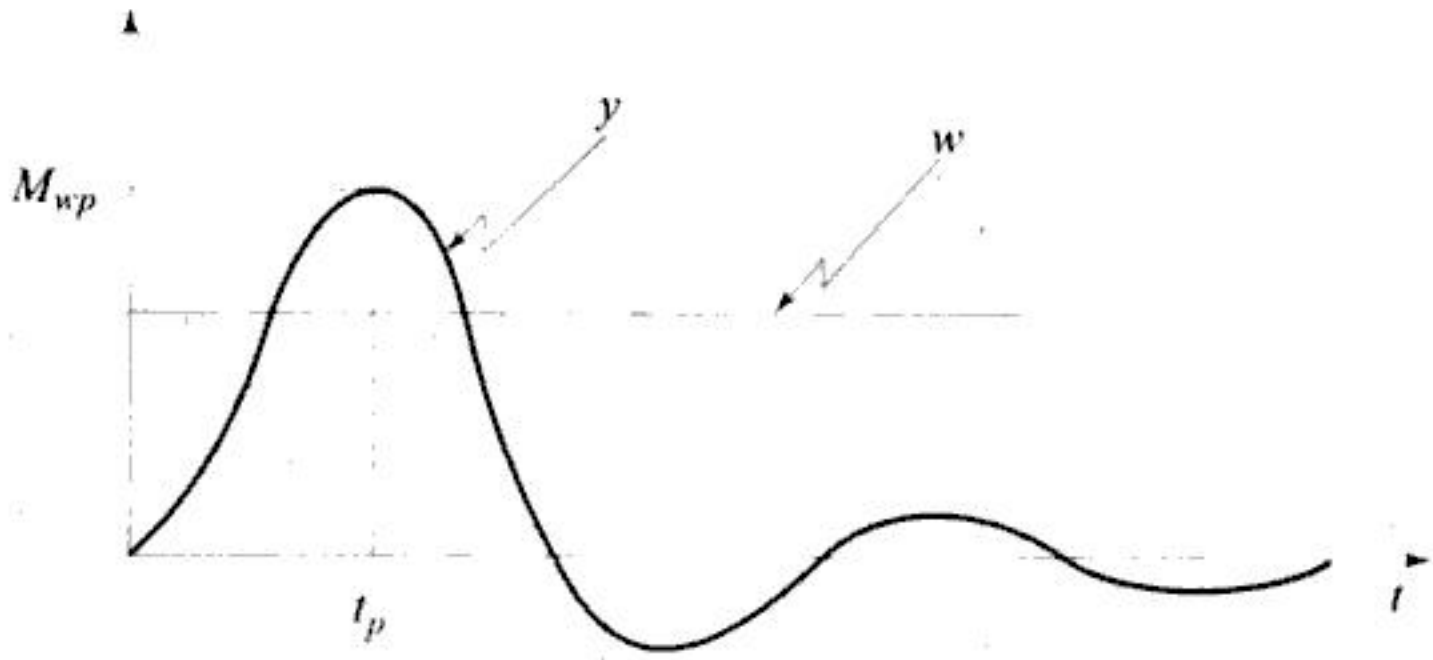


Fig. 6.5 *Time-domain specifications for disturbance input*

Copyrighted material



You have either reached a page that is unavailable for viewing or reached your viewing limit for this book.



You have either reached a page that is unavailable for viewing or reached your viewing limit for this book.



You have either reached a page that is unavailable for viewing or reached your viewing limit for this book.



You have either reached a page that is unavailable for viewing or reached your viewing limit for this book.



You have either reached a page that is unavailable for viewing or reached your viewing limit for this book.



You have either reached a page that is unavailable for viewing or reached your viewing limit for this book.



You have either reached a page that is unavailable for viewing or reached your viewing limit for this book.



You have either reached a page that is unavailable for viewing or reached your viewing limit for this book.



You have either reached a page that is unavailable for viewing or reached your viewing limit for this book.



You have either reached a page that is unavailable for viewing or reached your viewing limit for this book.



You have either reached a page that is unavailable for viewing or reached your viewing limit for this book.

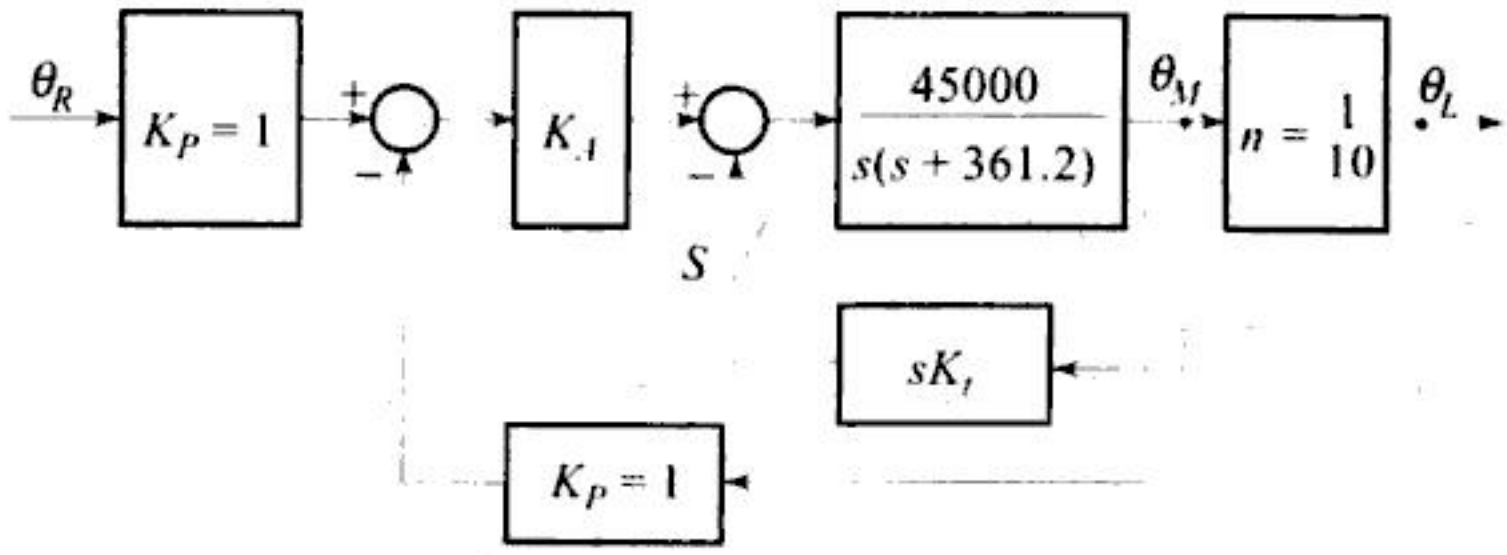


Fig. 6.15 *Block diagram of a position control system*

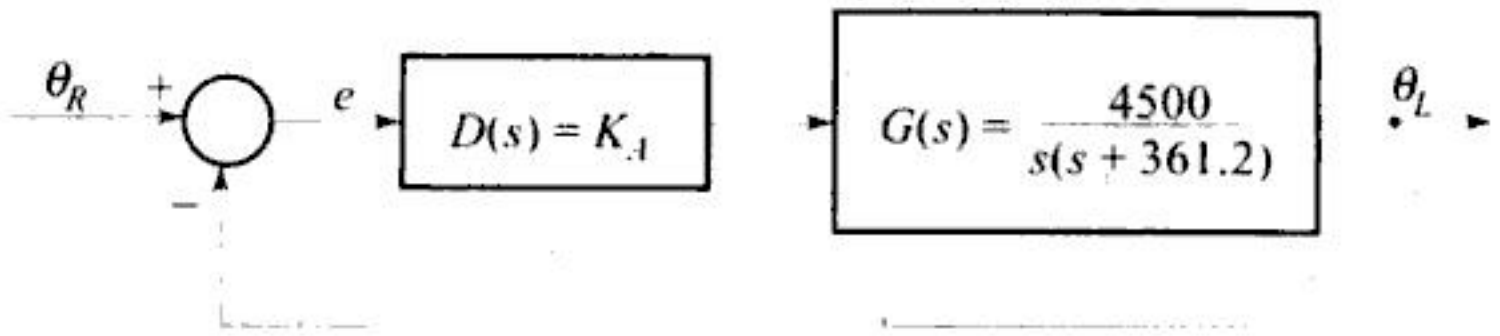


Fig. 6.16 *Simplified block diagram of the system in Fig. 6.15 with $K_t = 0$*

$$s^2 + 361.2\,s + 4500K_A = s^2 + 2\zeta\omega_n\,s + \omega_n^2 = 0 \tag{6.27a}$$

Natural frequency $$\omega_n = \sqrt{4500K_A} \tag{6.27b}$$

Damping ratio $$\zeta = \frac{361.2}{2\sqrt{4500K_A}} = \frac{2.692}{\sqrt{K_A}} \tag{6.27c}$$

The closed-loop poles are

$$s_{1,2} = -180.6 \pm \sqrt{32,616.36 - 4500K_A} \tag{6.28}$$

From the block diagram of Fig. 6.16, we obtain

$$\frac{E(s)}{R(s)} = \frac{1}{1 + D(s)G(s)} = \frac{1}{1 + \dfrac{4500K_A}{s(s + 361.2)}} = \frac{s(s + 361.2)}{s(s + 361.2) + 4500K_A}$$

The steady-state error of the system due to a ramp input $R(s) = 1/s^2$ is given by

$$e_{ss}|_{\text{unit ramp}} = \lim_{s \to 0} s\,E(s) = \frac{361.2}{4500K_A} = \frac{0.0803}{K_A} \tag{6.29}$$

(i) *System with critical damping*

For $K_A = 7.247$, the damping ratio $\zeta = 1$, the natural frequency $\omega_n = 180.6$, and both the closed-loop poles are located at -180.6. From Fig. 6.13a, we observe that normalized settling time (five per cent tolerance) corresponding to $\zeta = 1$ is 4.7. Therefore

$$t_s\ (5\%\ \text{tolerance}) = \frac{4.7}{180.6} = 0.026\ \text{sec}$$

The steady-state error (Eqn. (6.29))

Copyrighted material



You have either reached a page that is unavailable for viewing or reached your viewing limit for this book.



You have either reached a page that is unavailable for viewing or reached your viewing limit for this book.



You have either reached a page that is unavailable for viewing or reached your viewing limit for this book.



You have either reached a page that is unavailable for viewing or reached your viewing limit for this book.



You have either reached a page that is unavailable for viewing or reached your viewing limit for this book.



You have either reached a page that is unavailable for viewing or reached your viewing limit for this book.



You have either reached a page that is unavailable for viewing or reached your viewing limit for this book.



You have either reached a page that is unavailable for viewing or reached your viewing limit for this book.



You have either reached a page that is unavailable for viewing or reached your viewing limit for this book.



You have either reached a page that is unavailable for viewing or reached your viewing limit for this book.



You have either reached a page that is unavailable for viewing or reached your viewing limit for this book.



You have either reached a page that is unavailable for viewing or reached your viewing limit for this book.



You have either reached a page that is unavailable for viewing or reached your viewing limit for this book.



You have either reached a page that is unavailable for viewing or reached your viewing limit for this book.



You have either reached a page that is unavailable for viewing or reached your viewing limit for this book.



You have either reached a page that is unavailable for viewing or reached your viewing limit for this book.



You have either reached a page that is unavailable for viewing or reached your viewing limit for this book.



You have either reached a page that is unavailable for viewing or reached your viewing limit for this book.



You have either reached a page that is unavailable for viewing or reached your viewing limit for this book.



You have either reached a page that is unavailable for viewing or reached your viewing limit for this book.



You have either reached a page that is unavailable for viewing or reached your viewing limit for this book.



You have either reached a page that is unavailable for viewing or reached your viewing limit for this book.

The velocity error constant

$$K_v = \lim_{s \to 0} sG(s) = \frac{K K_1}{1 + K K_2} \tag{6.63}$$

The closed-loop transfer function is given by

$$\frac{Y(s)}{R(s)} = \frac{K K_1}{\tau s^2 + (1 + K K_2)s + K K_1} \tag{6.64}$$

and the characteristic equation is

$$s^2 + \frac{(1 + K K_2)}{\tau} s + \frac{K K_1}{\tau} = 0 \tag{6.65}$$

The natural frequency and damping of the compensated system are given by

$$\omega_n = \sqrt{\frac{K K_1}{\tau}} \tag{6.66a}$$

$$\zeta = \frac{1}{2}\left[\frac{1 + K K_2}{\sqrt{K K_1 \tau}}\right] \tag{6.66b}$$

For a specified K_v and ζ, we can write from Eqns (6.63) and (6.66b),

$$\zeta K_v = \frac{1}{2}\left[\sqrt{\frac{K K_1}{\tau}}\right] \tag{6.67}$$

from which K_1 can be determined. Using this value of K_1, K_2 is obtained from Eqn. (6.63). Thus, we notice that by a suitable choice of K_1 and K_2, we can simultaneously meet the specifications on K_v and ζ. We will have to resort to trial and error methods of compensator design if the resulting speed of response is not acceptable.

Example 6.3

Consider the position control system of Fig. 6.15. When switch 'S' is open (tachogenerator disconnected), the forward-path transfer function of the system becomes

$$G(s) = \frac{4500\, K_A}{s(s + 361.2)}$$

Assume that the steady-state error to unit-ramp input is required to be less than 0.025 deg (0.000436 rad).

$$\text{Required } K_v = \frac{1}{0.000436} = 2293.6$$

This requirement is satisfied if

$$K_A = \frac{2293.6 \times 361.2}{4500} = 184.1$$

Copyrighted material



You have either reached a page that is unavailable for viewing or reached your viewing limit for this book.



You have either reached a page that is unavailable for viewing or reached your viewing limit for this book.



You have either reached a page that is unavailable for viewing or reached your viewing limit for this book.



You have either reached a page that is unavailable for viewing or reached your viewing limit for this book.



You have either reached a page that is unavailable for viewing or reached your viewing limit for this book.



You have either reached a page that is unavailable for viewing or reached your viewing limit for this book.



You have either reached a page that is unavailable for viewing or reached your viewing limit for this book.



You have either reached a page that is unavailable for viewing or reached your viewing limit for this book.



You have either reached a page that is unavailable for viewing or reached your viewing limit for this book.

With $K_c = 9$, $\zeta = 0.5$ is obtained when K_D statisfies the following relations:

$$\omega_n = \sqrt{2 + 18} = = 4.47$$

$$3 + 2K_D = 2 \times 0.5 \times \omega_n$$

This gives $K_D = 0.736$

The zero of the closed-loop transfer function is at $s = -K_c/K_D = -9/0.736 = -12.23$. The magnitude of the zero is about 5.5 times the magnitude of the real part of the poles ($\zeta\omega_n = 2.235$). So the unit-step response of the system with the PD controller should closely resemble the response of a standard second-order system with $\zeta = 0.5$ and $\omega_n = 4.47$.

If static accuracy demand is very high, PI control would probably be necessary. With $D(s) = K_c + K_I/s$, the open-loop transfer function becomes

$$D(s)G(s) = \frac{sK_c + K_I}{s(s+1)(0.5s+1)}$$

The system has become a type-1 system and the steady-state error to step inputs is zero.

The velocity error constant $K_v = K_I$, and

$$e_{ss|\text{unit ramp}} = \frac{1}{K_I}$$

Thus, the steady-state error to ramp inputs reduces as the integral gain factor K_I is increased (note that the steady-state error to ramp inputs is infinity for the system with only proportional control or PD control). As one would expect, this improvement in static accuracy is limited by considerations of relative stability. The closed-loop transfer function

$$\frac{Y(s)}{R(s)} = \frac{sK_c + K_I}{0.5s^3 + 15s^3 + (1 + K_c)s + K_I}$$

shows a third-order characteristic equation. Design to determine suitable values of K_c and K_I can be carried out using the root-locus and frequency-response methods discussed in the following chapters. This will show that careful design is necessary to avoid oscillatory or slow system dynamic behaviour.

Review Example 6.5

The system shown in Fig. 6.36 is a unity-feedback control system with a minor rate-feedback loop.

(a) In the absence of rate feedback ($\alpha = 0$), determine the peak overshoot of the system to unit-step input, and the steady-state error resulting from a unit-ramp input.

(b) Determine the rate-feedback constant α which will decrease the peak overshoot of the system to unit-step input to 1.5%. What is steady-state error to unit-ramp input with this setting of the rate-feedback constant?

(c) Illustrate how in the system with rate feedback, the steady-state error to

Copyrighted material



You have either reached a page that is unavailable for viewing or reached your viewing limit for this book.



You have either reached a page that is unavailable for viewing or reached your viewing limit for this book.



You have either reached a page that is unavailable for viewing or reached your viewing limit for this book.

6.7 A unity feedback system has a plant

$$G(s) = \frac{K}{s(\tau s + 1)}$$

with a cascade controller

$$D(s) = K_c(1 + T_D s)$$

Describe the effects of K_c and T_D on steady-state error, settling time, and peak overshoot of the system response. (Help: pp 372-374, pp 445-448)

6.8 A unity feedback system has a plant

$$G(s) = \frac{K}{s(\tau s + 1)}$$

with a cascade controller

$$D(s) = K_c\left(1 + \frac{1}{T_I s}\right)$$

Describe the effects of K_c and T_I on steady-state error, settling time, and peak overshoot of the system response. (Help: pp 379-380, pp 451-453)

6.9 A unity feedback servosystem has the plant

$$G(s) = \frac{K}{s(\tau s + 1)}$$

Show how a cascade PD controller could be used to achieve acceptable performance. Compare the cascade PD compensation with that of minor-loop feedback compensation using a tachogenerator.(Help: Section 4.6, pp 376-377, pp 472-475)

6.10 (a) Desired dominant closed-loop poles are usually a complex-conjugate pair. Why? (Help: p 353)

(b) Transient performance is usually judged by only one test signal—step, while the steady-state performance is usually judged by more than one test signal—step, ramp, parabola. Why? (Help: pp 337-339, pp 341-343, p 351)

(c) The test signals are step, ramp and parabola. Actual control system will have different input. How is control system study using test signals useful? (Help: pp 337-339, p 341-343, p351)

(d) The formulas for t_r, t_p, M_p, t_s, etc., have been derived for second-order feedback system with plant transfer function of the form $G(s) = \omega_n^2/(s^2 + 2\zeta\omega_n s)$. However, we also apply these formulas for designing controllers when a plant is higher than second-order and/or has finite zeros. Justify. (Help: pp 364-365, pp 459-460)

(e) We know that K_p, K_v, and K_a are defined for unity-feedback systems. How do you describe steady-state performance of a non-unity feedback system? (Help: pp 370-371)

6.11 (a) A feedback system has a PD compensator in the forward path. What will happen if the proportional term of the PD compensator becomes zero? (Help: p 273, p 472)

Copyrighted material



You have either reached a page that is unavailable for viewing or reached your viewing limit for this book.



You have either reached a page that is unavailable for viewing or reached your viewing limit for this book.



You have either reached a page that is unavailable for viewing or reached your viewing limit for this book.

the unit-step response? If not, why?

6.8 A control system with a type-0 process and a PI controller is shown in Fig. P6.8.

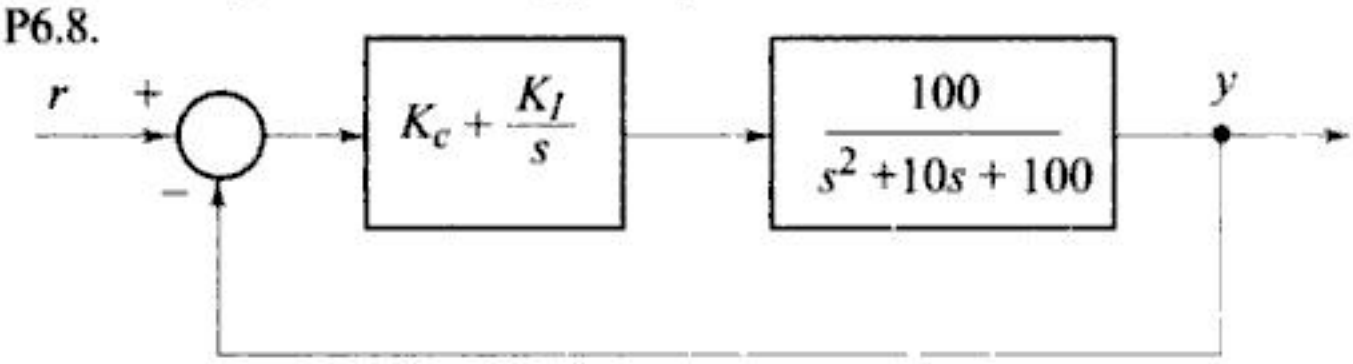


Fig. P6.8

(a) Find the value of K_I so that the velocity error K_v is 10.
(b) With the value of K_I found is part (a), determine the value of K_c so that the real part of the conjugate pair of complex roots of the characteristic equation of the closed-loop system is −1.
(c) Find the conjugate pair of complex roots and therefrom obtain the value of ζ.
(d) Is ζ a reasonably accurate estimate on peak overshoot of the unit-step response? Give reasons.

6.9 A three-term controller with transfer function

$$D(s) = 20\left[1 + \frac{1}{T_I s} + T_D s\right]$$

is used to control a process with transfer function

$$G(s) = \frac{4}{s^2 + 8s + 80}$$

The closed-loop system is a unity-feedback structure with $D(s)$ and $G(s)$ in cascade.

(a) If integral action is not employed, find the derivative time T_D required to make the closed-loop damping ratio unity.
(b) A simulation study on your design in part (a) shows overshoot in unit-step response. Give reasons.
(c) If the value of derivative time is maintained as in part (a), determine the minimum value of reset time T_I that can be used without instability arising.

6.10 (a) For the motor position servo shown in Fig. P6.10a without the rate feedback ($K_t = 0$), show that $K = 10$ will give a steady-state unit-ramp following error of 0.1. What is the corresponding damping ratio?
(b) With $K = 10$, what value of K_t will give a system damping ratio of 0.5? How does the steady-state error compare with that in part (a)?
(c) The system of Fig. P6.10a with $K = 10$ has been extended by including the amplifier K_A as shown in Fig. P6.10b. Determine whether it is now possible to achieve both the steady-state error of 0.1 and damping ratio of 0.5. If so, find the values of K_t and K_A required.

6.11 The block diagram of a control system is shown in Fig. P6.11.
(a) Find the values of K_1 and K_2 so that peak overshoot is 10% and settling time is 0.05 sec.
(b) For the values of K_1 and K_2 obtained in part (a), find the step, ramp and

Copyrighted material



You have either reached a page that is unavailable for viewing or reached your viewing limit for this book.



You have either reached a page that is unavailable for viewing or reached your viewing limit for this book.



You have either reached a page that is unavailable for viewing or reached your viewing limit for this book.

$$e_c(t) = K_A e(t) + K_A \int e(t)dt$$

where the value of K_A is same as that obtained in part (b). Compare the steady-state behaviour of the system with that of part (b).

(d) A simulation study on the system of part (c) shows that the transient behaviour of the third-order system resembles that of the standard second-order system with characteristic equation

$$s^2 + 99.4508s + 3514.6322 = 0$$

Give reasons. Also determine the peak overshoot and settling time of the system.

6.18 In a dc position control servomechanism, the load is driven by a motor, supplied with constant armature current. The motor field current is supplied from a dc amplifier, the input to which is the difference between the voltages obtained from input and output potentiometers. A tachogenerator is coupled to the motor shaft and a fraction K of tachogenerator output is fed back to produce a stabilizing effect. The following particulars refer to the system: moment of inertia of motor, $J_M = 2 \times 10^{-3}$ kg-m^2; moment of inertia of load, $J_L = 5$ kg-m^2; motor to load gear ratio, $(\dot{\theta}_L / \dot{\theta}_M) = 1/50$; load to potentiometer gear ratio, $\dot{\theta}_P / \dot{\theta}_L = 1/1$; motor torque constant, $K_T = 2$ N-m/amp; tachogenerator constant, $K_t = 0.2$ volt per rad/sec; sensitivity of error detector, $K_P = 0.6$ volt/rad, and amplifier gain = K_A amps/volt.

(a) Make a sketch of the system showing how the hardware is connected.

(b) Draw a block diagram of the system indicating the transfer function of each block.

(c) Determine the amplifier gain required and a fraction of the tachogenerator voltage fed back to give an undamped natural frequency of 4 rad/sec and damping ratio of 0.8.

6.19 The schematic diagram of a servomechanism is given in Fig. P6.19. The system constants are given below.

Sensitivity of error detector, $K_P = 1$ volt/rad; gain of dc amplifier = K_A volts/volt; resistance of armature of motor, $R_a = 5$ ohms; equivalent inertia at the motor shaft $J = 4 \times 10^{-3}$ kg-m^2; equivalent friction at the motor shaft, $B = 2 \times 10^{-3}$ N-m per rad/sec; torque constant of motor, $K_T = 1$ N-m/amp; and gear ratio$\left(\dot{\theta}_L / \dot{\theta}_M\right)$, $n = 1/10$.

(a) Draw a block diagram of the system indicating the transfer function of each block.

(b) Find amplifier gain K_A so that the steady-state error to unit-ramp input is less than 0.01 rad. For this value of amplifier gain, determine the damping ratio, and peak overshoot to unit-step input.

(c) To improve the system damping, the amplifier is modified by introducing an additional derivative term such that its output is given by

$$e_a(t) = K_1 e(t) + K_D \frac{de(t)}{dt}$$

where the value of K_1 is same as that obtained in part (b). Does this modification affect the steady-state error as in part (b)?

Copyrighted material



You have either reached a page that is unavailable for viewing or reached your viewing limit for this book.



You have either reached a page that is unavailable for viewing or reached your viewing limit for this book.



You have either reached a page that is unavailable for viewing or reached your viewing limit for this book.



You have either reached a page that is unavailable for viewing or reached your viewing limit for this book.



You have either reached a page that is unavailable for viewing or reached your viewing limit for this book.



You have either reached a page that is unavailable for viewing or reached your viewing limit for this book.



You have either reached a page that is unavailable for viewing or reached your viewing limit for this book.

$$\left|\sqrt{1-K}\right| = 1$$

which is true if $K = 2$.

Consider now the second-order system shown in Fig. 7.3 which represents a typical position control system with velocity feedback. It is a multi-loop system with closed-loop transfer function

$$M(s) = \frac{K}{s^2 + (0.2K + 2)s + K} \tag{7.5}$$

The characteristic equation is

$$\Delta(s) = s^2 + (0.2K + 2)s + K = 0 \tag{7.6}$$

which can be rearranged as

$$s^2 + 2s + K(0.2s + 1) = 0$$

or

$$1 + \frac{0.2K(s + 5)}{s(s + 2)} = 0 \tag{7.7}$$

Note that Eqn. (7.7) is also the characteristic equation of a unity feedback system with (open-loop) transfer function

$$F(s) = \frac{K'(s + 5)}{s(s + 2)};\ K' = 0.2K \tag{7.8}$$

which has two poles at $s = 0$ and $s = -2$, and a zero at $s = -5$. In Fig. 7.4, the open-loop poles (poles of $F(s)$) are indicated by $\times$ and the open-loop zero (zero of $F(s)$) is indicated by $\circ$.

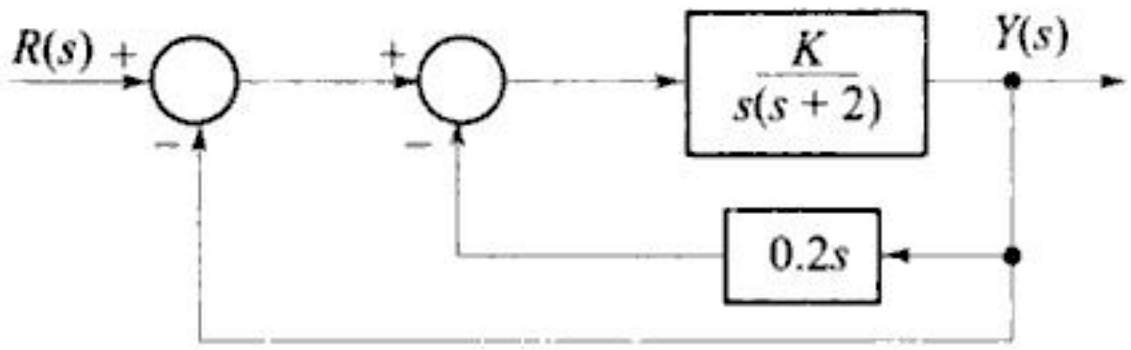


Fig. 7.3 *A position control system with velocity feedback*

Let us examine the nature of characteristic roots

$$s_{1,2} = -(0.1K + 1) \pm \sqrt{(0.1K + 1)^2 - K} \tag{7.9}$$

As K is varied from zero to infinity, the characteristic roots move in the s-plane as shown in Fig. 7.4. At $K = 0$, the root s_1 is equal to the open-loop pole at $s = 0$ and the root s_2 is equal to the open-loop pole at $s = -2$. As K increases, the roots move towards each other. The two roots meet at $s = -1.127$ for $K = 1.27$. As K is increased further, the roots break away from the real axis and become complex conjugate. It turns out that the complex roots move along a circle[2] of radius $\sqrt{15}$ with centre at $s = -5$.

2. This can easily be proved as we shall see later in Example 7.1.

Copyrighted material



You have either reached a page that is unavailable for viewing or reached your viewing limit for this book.



You have either reached a page that is unavailable for viewing or reached your viewing limit for this book.



You have either reached a page that is unavailable for viewing or reached your viewing limit for this book.



You have either reached a page that is unavailable for viewing or reached your viewing limit for this book.



You have either reached a page that is unavailable for viewing or reached your viewing limit for this book.



You have either reached a page that is unavailable for viewing or reached your viewing limit for this book.



You have either reached a page that is unavailable for viewing or reached your viewing limit for this book.

The root locus plot for this case is shown in Fig. 7.8. The two root loci are *A-C-D-F-G* and *B-C-E-F-H*; the locus *A-C-D-F-G* starts at open-loop pole $s = -2$ with $K = 0$ and terminates at open-loop zero $s = -5$ with $K = \infty$; and the locus *B-C-E-F-H* starts at open-loop pole $s = -1$ with $K = 0$ and goes off to infinity along the negative real axis as $K \to \infty$.

The value of K corresponding to least damping may be obtained by applying the magnitude criterion (7.21a) at the point P where OP is a straight line tangential to the circular locus.

$$K = \frac{\text{length of the vector } AP \times \text{length of the vector } BP}{\text{length of the vector } GP}$$

$$= \frac{2.6 \times 2.9}{3.45} \cong 2.2;\ \zeta_{\min} = \cos\theta = 0.72$$

The closed-loop poles corresponding to this value of damping are (read from Fig. 7.8): $s_{1,2} = -2.6 \pm j2.5$.

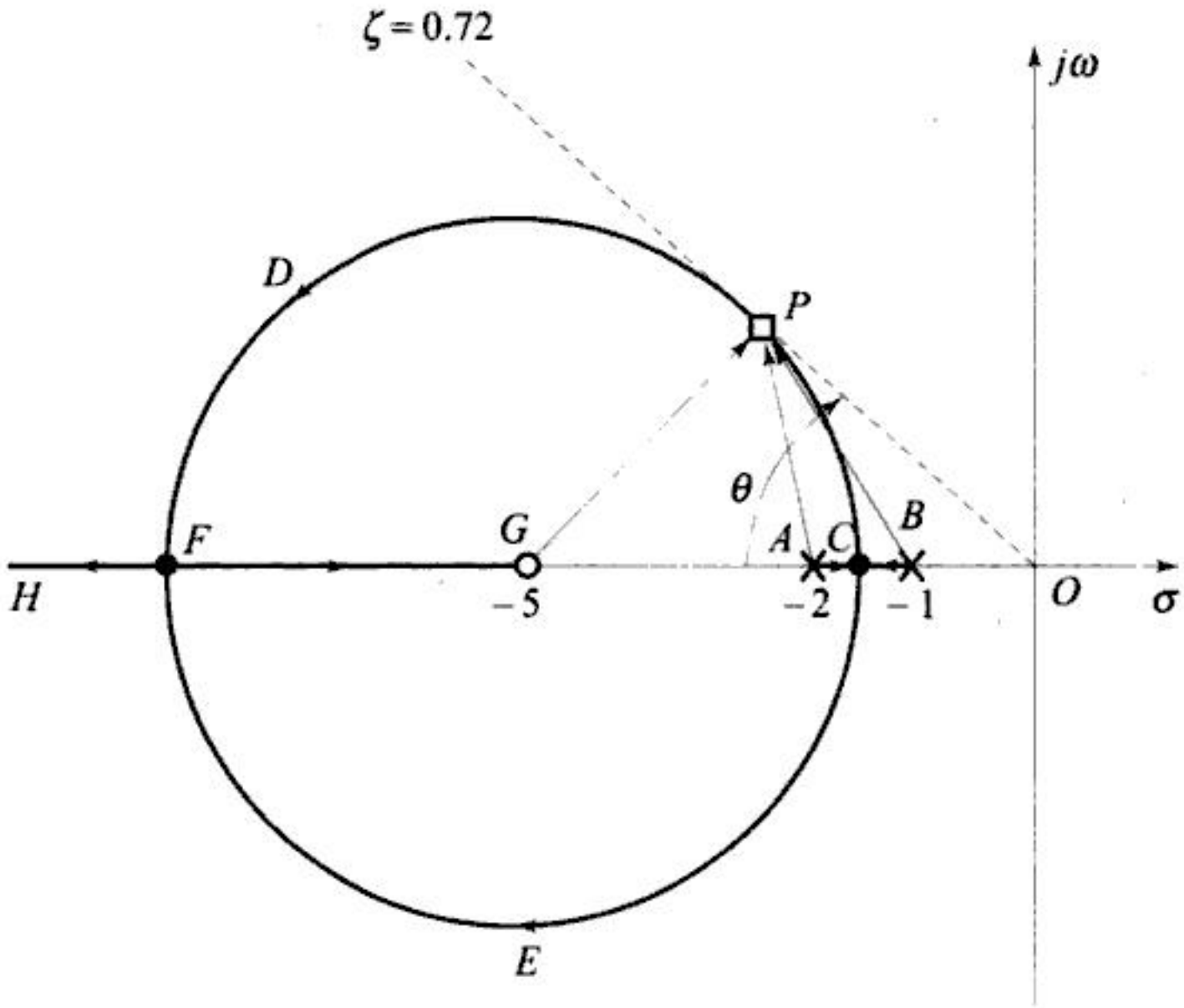


Fig. 7.8 *A root locus plot (Example 7.1)*

Example 7.2

Consider the second-order characteristics equation

$$1 + F(s) = 0$$

with $$F(s) = \frac{K(s+b)}{(s+\alpha+j\beta)(s+\alpha-j\beta)};\ K \geq 0$$

having pole-zero configuration shown in Fig. 7.9.

Copyrighted material



You have either reached a page that is unavailable for viewing or reached your viewing limit for this book.



You have either reached a page that is unavailable for viewing or reached your viewing limit for this book.



You have either reached a page that is unavailable for viewing or reached your viewing limit for this book.



You have either reached a page that is unavailable for viewing or reached your viewing limit for this book.



You have either reached a page that is unavailable for viewing or reached your viewing limit for this book.



You have either reached a page that is unavailable for viewing or reached your viewing limit for this book.



You have either reached a page that is unavailable for viewing or reached your viewing limit for this book.

For the point s_0 in Fig. 7.11b to be on the root locus,

$$-(n-m)\phi = -(2q+1)\,180°;\ q = 0, 1, \ldots$$

or
$$\phi = \frac{(2q+1)180°}{n-m};\ q = 0, 1, \ldots$$

The $(n-m)$ angles given by this equation divide 360° equally and are symmetric with respect to real axis. The $(n-m)$ root loci, therefore, tend to infinity along $(n-m)$ asymptotes radiating out from $s = -\sigma_A$ given by Eqn. (7.26a) at angles ϕ_A given by Eqn. (7.26b).

The pole-zero map of Fig. 7.11a corresponds to

$$F(s) = \frac{K(s+2)}{(s+1+j4)(s+1-j4)(s+3)(s+4)} \tag{7.28a}$$

The root locus plot of

$$1 + F(s) = 0 \tag{7.28b}$$

will consist of four root loci, each starting from an open-loop pole with $K = 0$. One root locus will terminate on open-loop zero with $K = \infty$. The other three loci will terminate on infinity as $K \to \infty$ along the asymptotes radiating out from $s = -\sigma_A$

where
$$-\sigma_A = \frac{-1-1-3-4-(-2)}{4-1} = -7/3$$

at angles 60°, 180°, and 300° respectively. Figure 7.12 shows the asymptotes. Note that asymptotes are developed for large s; thus the root loci will *approach* them for large s or large K.

Rule 4 On-Locus Segments of the Real Axis

A point on the real axis lies on the locus if the number of open-loop poles plus zeros on the real axis to the right of this point is odd.

For the fourth-order example under consideration (refer Eqns (7.28)), open-loop pole-zero configuration is shown in Fig. 7.13a. Let us examine any point s_0 on the real axis. As this point is joined by phasors to all the open-loop poles and zeros, it is easily seen that (i) the poles and zeros on the real axis to the right of this point contribute an angle of 180° each, (ii) the poles and zeros on the real axis to the left of this point contribute an angle of 0° each, and (iii) the net angle contribution of a complex conjugate pole or zero pair is always zero.
Therefore,

$$\angle F(s) = (m_r - n_r)180° = \pm(2q+1)180°,\ q = 0, 1, 2, \ldots$$

where

m_r = number of open-loop zeros on the real axis to the right of s_0; and
n_r = number of open-loop poles on the real axis to the right of s_0.

Copyrighted material



You have either reached a page that is unavailable for viewing or reached your viewing limit for this book.



You have either reached a page that is unavailable for viewing or reached your viewing limit for this book.



You have either reached a page that is unavailable for viewing or reached your viewing limit for this book.

Therefore the total phase of $F(s)$ at s_0 is $\phi - \phi_p$. In order for s_0 to be on the root locus, the total phase must be $\pm 180°$. Thus we have $\phi_p = 180° + \phi$. This is the angle of departure from the complex open-loop pole.

If the point s_0 is very close to the pole at $-1 + j4$, then the vectors drawn from the zero and all other open-loop poles to s_0 can be approximated by the vectors drawn to the pole at $-1 + j4$, i.e., we consider the point s_0 to be at $-1 + j4$ for measurement of angles θ_1, θ_2, θ_3, and θ_4. Under this approximation, $\theta_1 = 90°$, $\theta_2 = 76°$, $\theta_3 = 63°$, and $\theta_4 = 53°$. Therefore

$$\phi = \theta_2 - (\theta_1 + \theta_3 + \theta_4) = -130°; \quad \phi_p = 180° + \phi = 50°$$

We can now sketch a rough root locus plot for the fourth-order example under consideration. The plot is shown in Fig. 7.15. The information given in Figs 7.12–7.14 has been used to construct this plot.

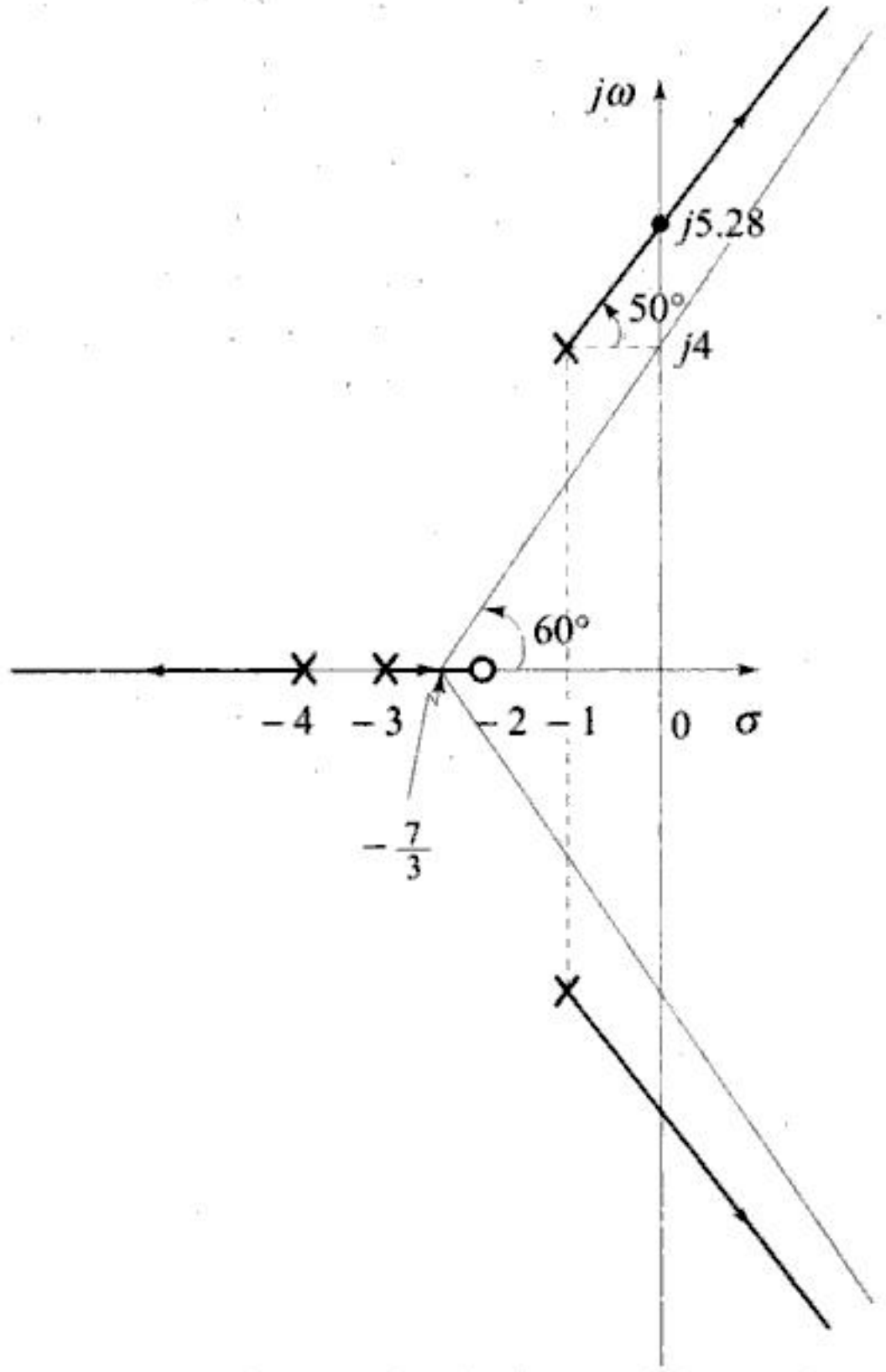


Fig. 7.15 *Root locus plot for the characteristic equation (7.28)*

There are four open-loop poles; so there are four loci. One locus departs from the real pole at -3 and terminates on the zero at -2 along the real axis. The second locus departs from another real pole at -4 and moves along the asymptote on the negative real axis. The third locus departs from the complex pole at $-1 + j4$ with a departure angle of $\phi_p = 50°$, and moves toward the

Copyrighted material



You have either reached a page that is unavailable for viewing or reached your viewing limit for this book.



You have either reached a page that is unavailable for viewing or reached your viewing limit for this book.



You have either reached a page that is unavailable for viewing or reached your viewing limit for this book.



You have either reached a page that is unavailable for viewing or reached your viewing limit for this book.



You have either reached a page that is unavailable for viewing or reached your viewing limit for this book.



You have either reached a page that is unavailable for viewing or reached your viewing limit for this book.



You have either reached a page that is unavailable for viewing or reached your viewing limit for this book.

Differentiating this equation, we get

$$\frac{dK}{ds} = -(3s^2 + 6s + 2)$$

The roots of the equation $dK/ds = 0$, are $s_{1,2} = -0.4226, -1.5774$

From Fig. 7.18, we see that the breakaway point must lie between 0 and -1. Therefore $s = -0.4226$ corresponds to the breakaway point. The other solution of the equation $dK/ds = 0$ is $s = -1.5774$. This solution is not on the root locus (it does not satisfy Eqn. (7.38) for any $K \geq 0$) and therefore does not represent a breakaway point. The derivative condition $dK/ds = 0$ is therefore necessary but not sufficient to indicate a breakaway, or multiple-root situation.

If two loci breakaway from a breakaway point, then their tangents will be 180° apart. In general, as we shall see in other illustrative examples, if r loci breakaway from a breakaway point, then their tangents will be $360°/r$ apart, i.e., the tangents will equally divide 360°.

With the information obtained through the use of these rules, the root locus is sketched in Fig. 7.18 from where it is seen that for $K > 6$, the system has two closed-loop poles in the right half of the s-plane and is thus unstable.

It is important to note that the root locus plot given in Fig. 7.18 is only a rough sketch; it gives qualitative information about the behaviour of the closed-loop system when the parameter K is varied. For quantitative analysis, the loci or specific segments of the loci need be constructed with sufficient accuracy.

Suppose it is required to determine dominant closed-loop poles with damping ratio $\zeta = 0.5$. A closed-loop pole with $\zeta = 0.5$ lies on a line passing through the origin and making an angle $\cos^{-1}\zeta = \cos^{-1}0.5 = 60°$ with the negative real axis. The point of intersection of the ζ-line with the rough sketch of the root locus plot gives the first guess. In the region where the rough root locus sketch intersects the ζ-line, a trial-and-error procedure is adapted along the ζ-line by applying the angle criterion to determine the point of intersection accurately. From Fig. 7.18, we see that the point $-0.33 + j0.58$, which lies on the ζ-line, satisfies the angle criterion. Therefore the dominant closed-loop poles of the system are $s_{1,2} = -0.33 \pm j0.58$.

The value of K that yields these poles is found from the magnitude criterion as follows:

$$K = \{|s|\ |s+1|\ |s+2|\}_{s\ =\ -0.33\ +\ j0.58}$$

= Product of the distances from the open-loop poles to the point $-0.33 + j0.58$

$$= 0.667 \times 0.886 \times 1.768 = 1.04$$

The third closed-loop pole will lie on the third locus which is along the negative real axis. We need to guess a test point, compute a trial gain, and correct the guess until we found the point where $K = 1.04$. Using this trial-and-

Copyrighted material



You have either reached a page that is unavailable for viewing or reached your viewing limit for this book.



You have either reached a page that is unavailable for viewing or reached your viewing limit for this book.



You have either reached a page that is unavailable for viewing or reached your viewing limit for this book.

points $s = -1.4$ and $s = -2.85$ have gain $K = 2.91$. Thus the closed-loop transfer function of the system under consideration is

$$M(s) = \frac{2.91}{(s+0.4+j0.7)(s+0.4-j0.7)(s+1.4)(s+2.85)}$$

Example 7.5

In this example, we illustrate multiple roots of multiplicity more than two. Consider the root locus of $1 + F(s)$,

where $$F(s) = \frac{K(s+1)}{s^2(s+9)}; K \geq 0$$

The pole-zero configuration is shown in Fig. 7.20.

Rule (i) tells us that the root locus plot consists of three root loci as K is varied from 0 to ∞.

Rule (ii) tells us that the three root loci originate from open-loop poles with $K = 0$; one of these terminates on the zero at $s = -1$ with $K = \infty$, and the other two terminate on infinity with $K = \infty$.

Rule (iii) tells us that the two root loci tend to infinity along asymptotes radiating out from

$$s = -\sigma_A = \frac{-9-0-(-1)}{3-1} = -4$$

with angles

$$\phi_A = \frac{(2q+1)180^\circ}{3-1}; q = 0, 1$$
$$= 90^\circ, 270^\circ$$

The asymptotes are shown by dotted lines in Fig. 7.20.

Rule (iv) tells us that root loci exist on the real axis for $-9 \leq s \leq -1$; shown by thick line on the real axis in Fig. 7.20.

Rule (v) tells us to check by use of the Routh criterion if the root loci will intersect the imaginary axis. It is found that the root loci do not cross the imaginary axis.

The characteristics equation under consideration does not require application of rules (vi) and (vii).

Rule (viii) is used below to determine the breakaway points.

From the characteristic equation of the system,

$$K = -\frac{s^2(s+9)}{s+1} = -\frac{s^3+9s^2}{s+1}$$

Differentiating this equation, we get

Copyrighted material



You have either reached a page that is unavailable for viewing or reached your viewing limit for this book.



You have either reached a page that is unavailable for viewing or reached your viewing limit for this book.



You have either reached a page that is unavailable for viewing or reached your viewing limit for this book.

$$K = -s(s+2)(s^2+2s+5) = -(s^4+4s^3+9s^2+10s)$$

Differentiating this equation, we get

$$\frac{dK}{ds} = -4(s^3+3s^2+4.5s+2.5)$$

We could find solutions to the cubic

$$s^3+3s^2+4.5s+2.5=0,$$

but from the application of rule (vi) we know that the entire line $s = -1 + j\omega$ is on the locus; so there must be a breakaway at $s = -1$. Therefore $(s+1)$ is one of the factors of the cubic. We can now easily show that

$$(s^3+3s^2+4.5s+2.5) = (s+1)(s+1+j1.22)(s+1-j1.22)$$

Since the solutions $-1 \pm j1.22$ are on the line between the complex poles, they are true points of multiple roots on the locus.

The complete root locus plot is sketched in Fig. 7.21. Notice that here we have complex multiple roots of multiplicity 2. Segments of the root loci come together at $-1 \pm j1.22$ and break away; tangents to the loci breaking away will be 180° apart.

7.5 RESHAPING THE ROOT LOCUS

A simple control-system configuration of Fig. 7.22 is created by providing feedback around the plant $G_p(s)$ and adding an error signal amplifier with gain K_c. The amplifier gain is adjusted to provide acceptable performance, if possible. The system of Fig. 7.22 is often referred to as having *proportional compensation.*

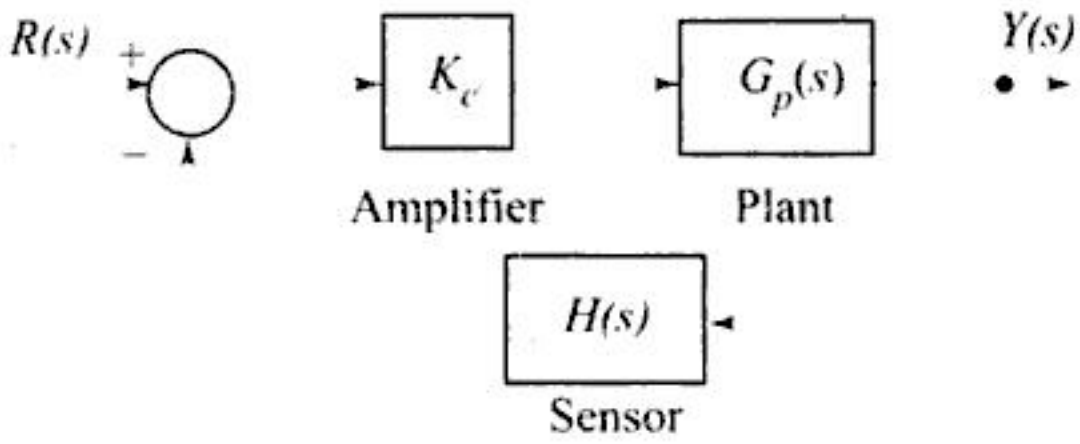


Fig. 7.22 *A simple control system configuration*

If the plant dynamics are of such a nature that a satisfactory design *cannot* be obtained by a gain adjustment alone, some dynamic compensation for the plant dynamics is required. A simple control-system configuration that includes dynamic compensation is shown in Fig. 7.23; the compensator $D_c(s)$ is placed in cascade with the forward-path transfer function $G_p(s)$. The system of Fig. 7.23 is often referred to as having *cascade compensation.*[5]

5. The term 'cascade compensation' used in Chapters 7–10 refers to the use of compensator (controller) in cascade (series) with the forward-path transfer function. It may be pointed out here that in process field, the term 'cascade control' is frequently used for feedback configurations having 'loop within a loop'.

Copyrighted material



You have either reached a page that is unavailable for viewing or reached your viewing limit for this book.



You have either reached a page that is unavailable for viewing or reached your viewing limit for this book.



You have either reached a page that is unavailable for viewing or reached your viewing limit for this book.

addition to the dominant complex-root pair is always located to the left of the open-loop ploe at $s = -5$. On the other hand, in the presence of compensating zero, this root moves over to the right of $s = -5$ and the dominance condition is therefore weakend. Since the real root (which is the closed-loop pole) will be located close to the compensating zero, the amplitude of the response term due to this root will be small. Also, the time-constant of the real root will be comparable to that of complex dominant root-pair; therefore, its effect on settling time may be tolerable.

An acceptable transient response can generally be obtained by trial-and-error adjustments of the compensating zero on the real axis. It can easily be verified that if we place the compensating zero too far to the left (say, near the open-loop pole at $s = -5$), the dominance condition is improved but complex branches of the root locus are pressed toward the right and the dynamic response becomes poor. If, on the other hand, the zero is placed close to the origin (say, to the right of the open-loop pole at $s = -1$), the complex branches are advantageously far into the left, but a real root close to the origin appears. This root will also be close to the compensating zero; therefore amplitude of the response term due to this root may be small. However, since the real root will have a large time-constant compared to that of dominant complex root pair, its effect on settling time may be appreciable.

No general rule can be laid down for selecting the location of compensating zero that satisfactorily meets all the design requirements. Trial-and-error procedure is the best tool in hand. However, the following *guidelines* can be of considerable help.

Place the compensating zero on the real axis in the region below the desired closed-loop pole location such that it lies close to the left of any open-loop pole in this region. This technique ensures that the closed-loop pole on the real axis caused by the introduction of the compensating zero will be located close to it with a time-constant comparable to that of desired dominant closed-loop pole-pair, and would therefore make a negligible contribution to system dynamics. In case the uncompensated system does not have any open-loop pole in the region below the desired closed-loop poles, the dominance condition must be checked by locating the real-axis closed-loop pole created by the compensating zero.

The addition of a zero in the open-loop transfer function can be achieved by placing a compensator

$$D(s) = s + z = s + 1/\tau \tag{7.44}$$

in cascade with the forward path transfer function.

It is seen that the compensator given by Eqn. (7.44) is a form of proportional plus derivative (PD) controller

$$D(s) = K_c(1 + T_D s) = K_c T_D(s + 1/T_D) = K_c T_D(s + z)$$

The problem with PD compensation is that the inevitable high-frequency noise present at the input to the $D(s)$ will be greatly amplified. The usual method

Copyrighted material



You have either reached a page that is unavailable for viewing or reached your viewing limit for this book.



You have either reached a page that is unavailable for viewing or reached your viewing limit for this book.



You have either reached a page that is unavailable for viewing or reached your viewing limit for this book.



You have either reached a page that is unavailable for viewing or reached your viewing limit for this book.

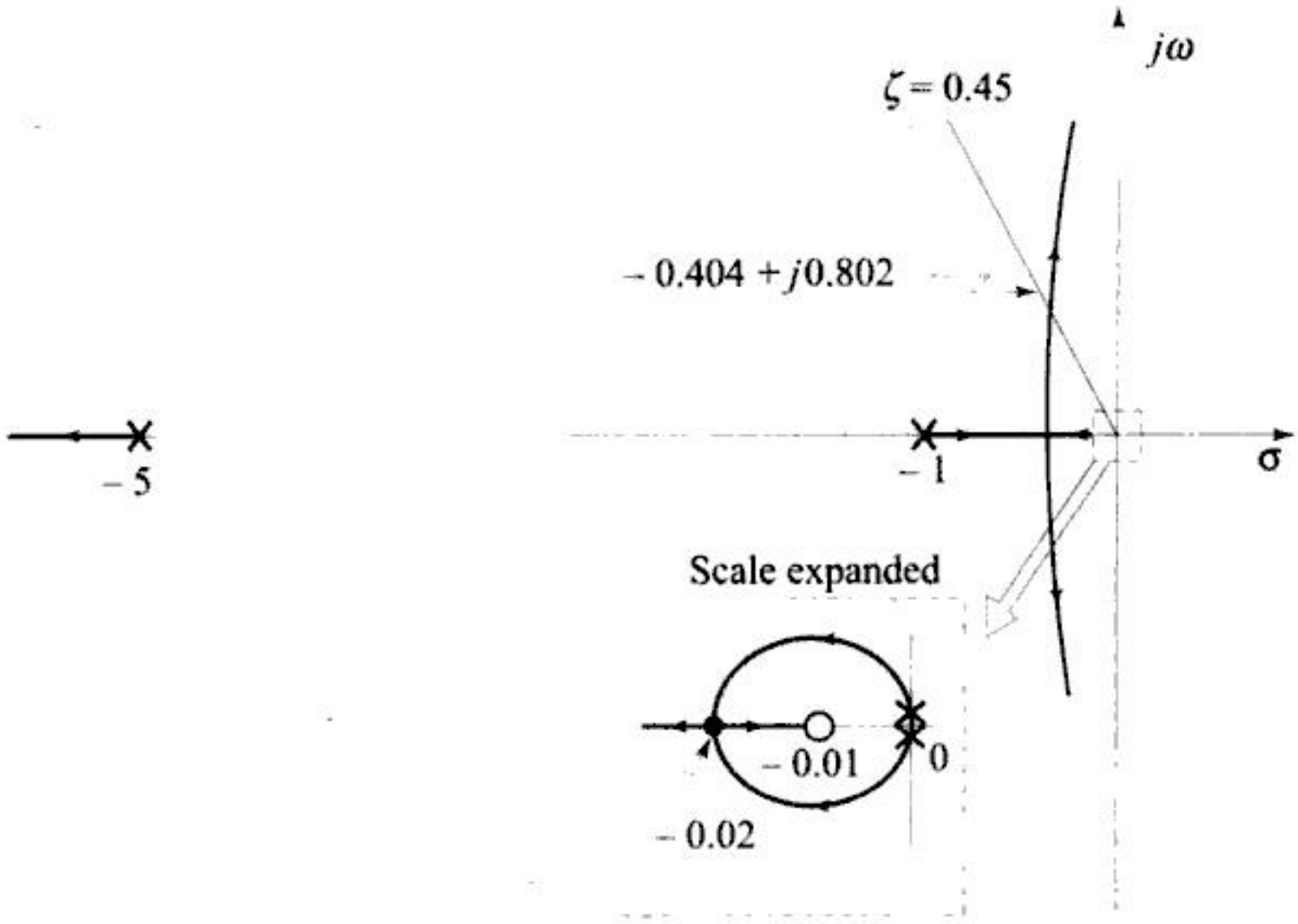


Fig. 7.29 *Root locus plot of* $1+\dfrac{K(s+0.01)}{s^2(s+1)(s+5)}$

It can easily be verified that if the compensating pole-zero pair is placed too far to the left (say, on the real-axis segment to the left of desired dominant complex closed-loop poles), no significant improvement in the steady-state response is possible.

Figure 7.30 shows the root locus plot in the presence of compensating pole at $s = -0.005$ and the compensating zero at $s = -0.05$. The angle contributed by the compensator pole-zero pair at $s = -0.404 + j0.802$, which is the desired dominant root, is about 2.6° and is therefore acceptable. For the damping ratio $\zeta = 0.45$, the new locus is close to the locus of uncompensated system. The new dominant roots are $s_{1,2} = -0.384 \pm j0.763$; thus the roots are essentially unchanged.

For the compensated system adjusted to a damping ratio of 0.45, the following results are obtained.

Dominant roots: $s_{1,2} = -0.384 \pm j0.763$

Root locus gain at s_1: $$K = \frac{|s_1||s_1+1||s_1+5||s_1+0.005|}{|s_1+0.05|} = 4.01$$

Velocity error constant: $$K_v = \lim_{s \to 0} s\left\{\frac{K(s+0.05)}{s(s+1)(s+5)(s+0.005)}\right\}$$

Copyrighted material



You have either reached a page that is unavailable for viewing or reached your viewing limit for this book.



You have either reached a page that is unavailable for viewing or reached your viewing limit for this book.



You have either reached a page that is unavailable for viewing or reached your viewing limit for this book.

If the angle criterion at s_d is not met, i.e., $\angle G(s_d) \neq \pm 180°$, the uncompensated root locus with variable open-loop gain will not pass through the desired root location, indicating the need for compensation. Let us introduce a first-order lead compensator with zero and pole in the left half of the complex plane:

$$D(s) = \frac{s+z}{s+p} = \frac{s+1/\tau}{s+1/\alpha\tau};\ \alpha = \frac{z}{p} < 1,\ \tau > 0 \tag{7.49}$$

in cascade with the forward-path transfer function $G(s)$ as shown in Fig. 7.32.

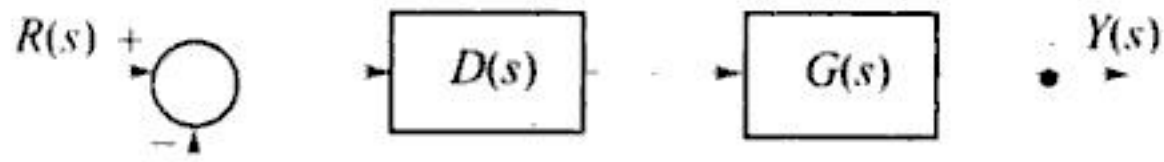


Fig. 7.32 *A feedback system with cascade compensator*

The compensator $D(s)$ has to be so designed that the compensated root locus passes through s_d. In terms of the angle criterion, this requires that

$$\angle D(s_d)G(s_d) = \angle D(s_d) + \angle G(s_d) = \pm 180°$$

or

$$\angle D(s_d) = \phi = \pm 180° - \angle G(s_d) \tag{7.50}$$

Thus, for the root locus of the compensated system to pass through the desired root location, the lead compensator pole-zero must contribute an angle ϕ given by Eqn. (7.50) and shown in Fig. 7.33. For a given angle ϕ for lead compensation, there is no unique location for the pole-zero pair. Out of many possible solutions, we select the one that satisfies the following additional requirements:

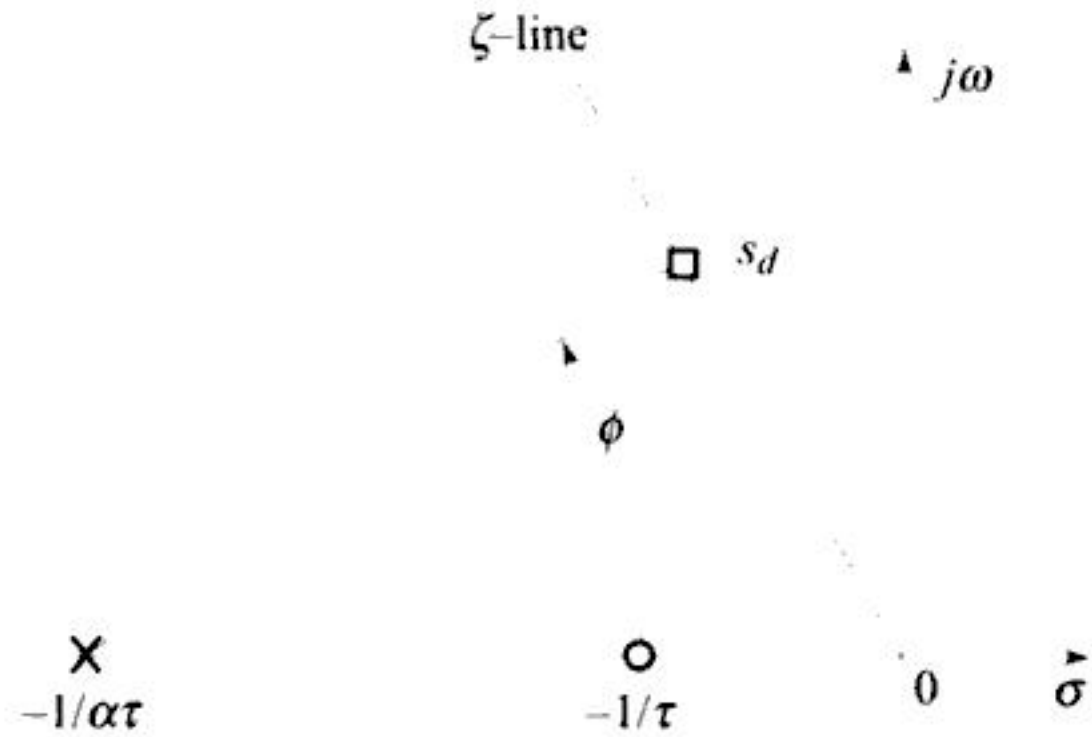


Fig. 7.33 *Angle contribution of lead compensator*

Copyrighted material



You have either reached a page that is unavailable for viewing or reached your viewing limit for this book.



You have either reached a page that is unavailable for viewing or reached your viewing limit for this book.



You have either reached a page that is unavailable for viewing or reached your viewing limit for this book.



You have either reached a page that is unavailable for viewing or reached your viewing limit for this book.



You have either reached a page that is unavailable for viewing or reached your viewing limit for this book.



You have either reached a page that is unavailable for viewing or reached your viewing limit for this book.



You have either reached a page that is unavailable for viewing or reached your viewing limit for this book.



You have either reached a page that is unavailable for viewing or reached your viewing limit for this book.



You have either reached a page that is unavailable for viewing or reached your viewing limit for this book.



You have either reached a page that is unavailable for viewing or reached your viewing limit for this book.



You have either reached a page that is unavailable for viewing or reached your viewing limit for this book.



You have either reached a page that is unavailable for viewing or reached your viewing limit for this book.

Chapter 11). With $\beta = 1/\alpha$, the transfer function (7.57) of the lag-lead compensator reduces to

$$D(s) = \underbrace{\left(\frac{s + 1/\tau_2}{s + \alpha/\tau_2}\right)}_{\text{Lag Section}}\underbrace{\left(\frac{s + 1/\tau_1}{s + 1/\alpha\tau_1}\right)}_{\text{Lead Section}}; \tau_2, \tau_1 > 0 \tag{7.58}$$

We first design the lead section to realize the required ζ and ω_n for the dominant closed-loop poles. The error constant is then determined for the lead-compensated system, say it is K_e^{lc}. If K_e^{lc} is sufficiently high to give the desired steady-state response, we need not go further. Lead compensation is all that is required. If, however, K_e^{lc} is not large enough, we consider adding the lag section with $\beta = 1/\alpha$. This results in an error constant

$$K_e^{llc} \cong \frac{1}{\alpha} K_e^{lc} \tag{7.59}$$

If K_e^{llc}, as given in Eqn. (7.59), is not large enough to meet steady-state specifications, we choose $\beta > 1/\alpha$ and redesign the lag section.

Example 7.11

Consider a plant with transfer function

$$G(s) = \frac{4}{s(s + 0.5)}$$

Design a feedback system to meet the following specifications:

1. Damping ratio of dominant closed-loop poles, $\zeta = 0.5$.
2. Undamped natural frequency of dominant closed-loop poles, $\omega_n = 5$ rad/sec.
3. Velocity error constant = 80 sec.$^{-1}$

We choose the unity-feedback control configuration shown in Fig. 7.39. Root locus plot of the system with $A > 0$ and $D(s) = 1$ is shown by dashed line in Fig. 7.40. The $\zeta = 0.5$ line intersects the root locus at the point $s = -0.25 + j0.433$. The undamped natural frequency corresponding to this root is 0.5 rad/sec. Therefore the configuration in Fig. 7.39 with $D(s) = 1$ cannot meet the specifications.

We introduce a cascade lead compensator. From the performance specifications we find that the dominant closed-loop poles must be at $s = -2.5 \pm j4.33$. Consider the desired location

$$s_d = -2.5 + j4.33$$

Since (refer Fig. 7.40) $\angle G(s_d) = -120° - 115° = -235°$, the lead compensator must contribute 55° so that the root locus passes through the desired root s_d. To design the lead compensator, we first determine the location of the compensator zero. There are many possible choices, but we shall here choose the zero at $s = -z = -0.5$ so that it cancels the open-loop pole at $s = -0.5$. Once the compensator zero is chosen, the compensator pole can be located such that

Copyrighted material



You have either reached a page that is unavailable for viewing or reached your viewing limit for this book.



You have either reached a page that is unavailable for viewing or reached your viewing limit for this book.



You have either reached a page that is unavailable for viewing or reached your viewing limit for this book.

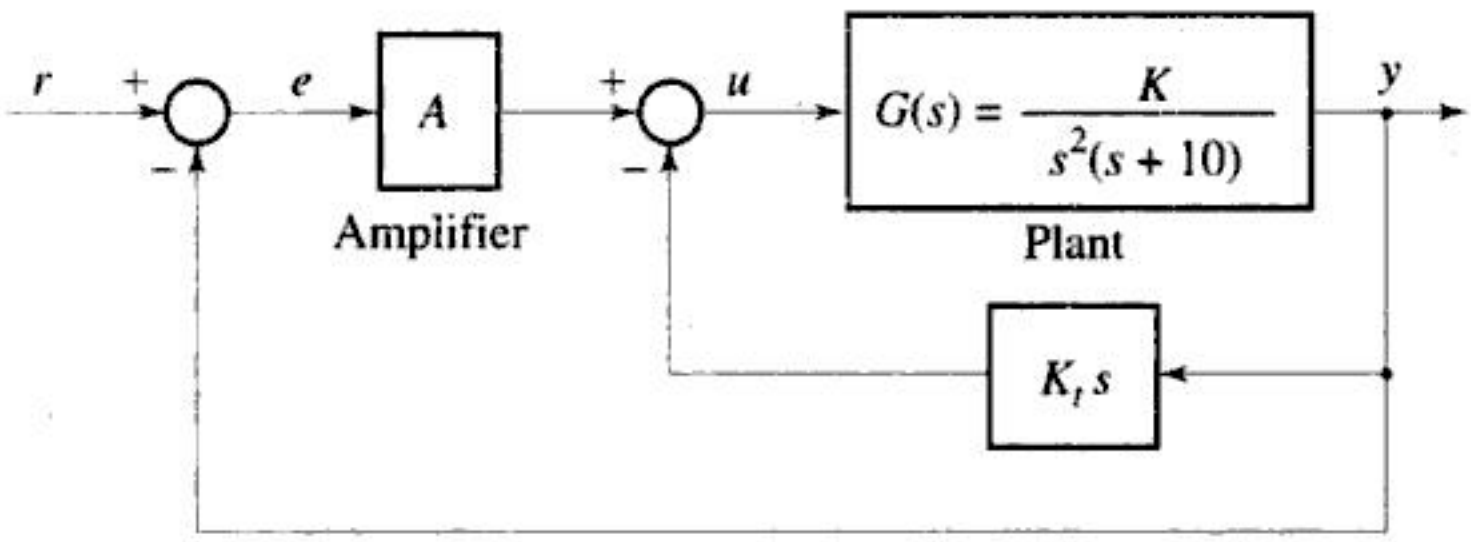


Fig. 7.42 *Rate feedback compensation*

We shall discuss two methods for the design of control systems with rate feedback; one is based on single-parameter loci and the other on multiple-parameter loci.

Single-Parameter Loci

The characteristic equation of the given system is (refer Fig. 7.42)

$$1 + \frac{AG(s)}{1 + sK_t G(s)} = 1 + \frac{AK}{s^2(s+10) + KK_t s} = 0 \tag{7.62}$$

Rearranging, we get

$$s^3 + 10s^2 + KK_t s + AK = 0$$

There are three variable parameters: A, K, and K_t. By appropriate partitioning of the characteristic equation, we can use single-parameter root loci for the design of three parameters (A, K, K_t) of the given system.

Consider the following partitioning:

$$1 + \frac{KK_t(s + A/K_t)}{s^2(s+10)} = 0 \tag{7.63a}$$

This equation shows that the net effect of rate feedback is to add a zero at $s = -A/K_t$. Now the design procedure calls for a search for suitable location for this additional zero to satisfy the specifications.

Assume that the system is to be compensated to meet the following specifications:

Per cent peak overshoot	$\leq 10\%$
Settling time	≤ 4 sec

The damping ζ and natural frequency ω_n of the dominant roots, obtained from the relations

$$e^{-\pi\zeta/\sqrt{1-\zeta^2}} \cong 0.1; \quad \text{and} \quad \frac{4}{\zeta\omega_n} = 4$$

are $\zeta = 0.6,\ \omega_n = 1.67$ rad/sec.

The desired dominant roots are then given as $s_d = -1 \pm j1.34$.

From Fig. 7.43, we see that the angle contribution of the open-loop poles at s_d is $-2(127°) - 8° = -262°$. Therefore, for the point s_d to be on the root locus,

Copyrighted material



You have either reached a page that is unavailable for viewing or reached your viewing limit for this book.



You have either reached a page that is unavailable for viewing or reached your viewing limit for this book.



You have either reached a page that is unavailable for viewing or reached your viewing limit for this book.



You have either reached a page that is unavailable for viewing or reached your viewing limit for this book.



You have either reached a page that is unavailable for viewing or reached your viewing limit for this book.



You have either reached a page that is unavailable for viewing or reached your viewing limit for this book.



You have either reached a page that is unavailable for viewing or reached your viewing limit for this book.



You have either reached a page that is unavailable for viewing or reached your viewing limit for this book.



You have either reached a page that is unavailable for viewing or reached your viewing limit for this book.



You have either reached a page that is unavailable for viewing or reached your viewing limit for this book.



You have either reached a page that is unavailable for viewing or reached your viewing limit for this book.



You have either reached a page that is unavailable for viewing or reached your viewing limit for this book.



You have either reached a page that is unavailable for viewing or reached your viewing limit for this book.



You have either reached a page that is unavailable for viewing or reached your viewing limit for this book.



You have either reached a page that is unavailable for viewing or reached your viewing limit for this book.



You have either reached a page that is unavailable for viewing or reached your viewing limit for this book.



You have either reached a page that is unavailable for viewing or reached your viewing limit for this book.



You have either reached a page that is unavailable for viewing or reached your viewing limit for this book.

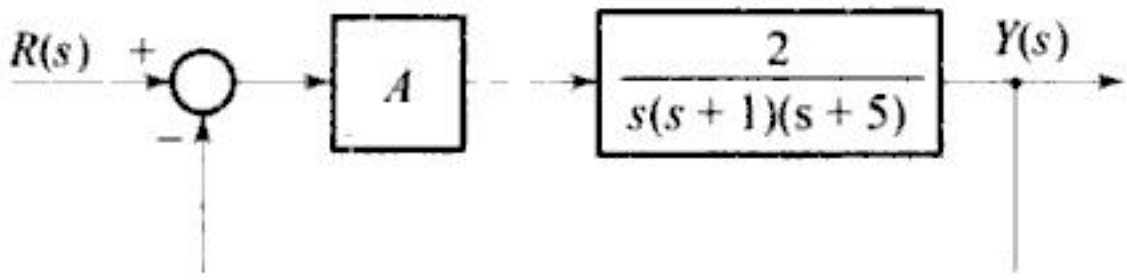


Fig. 7.59 *A control configuration (Review Example 7.4)*

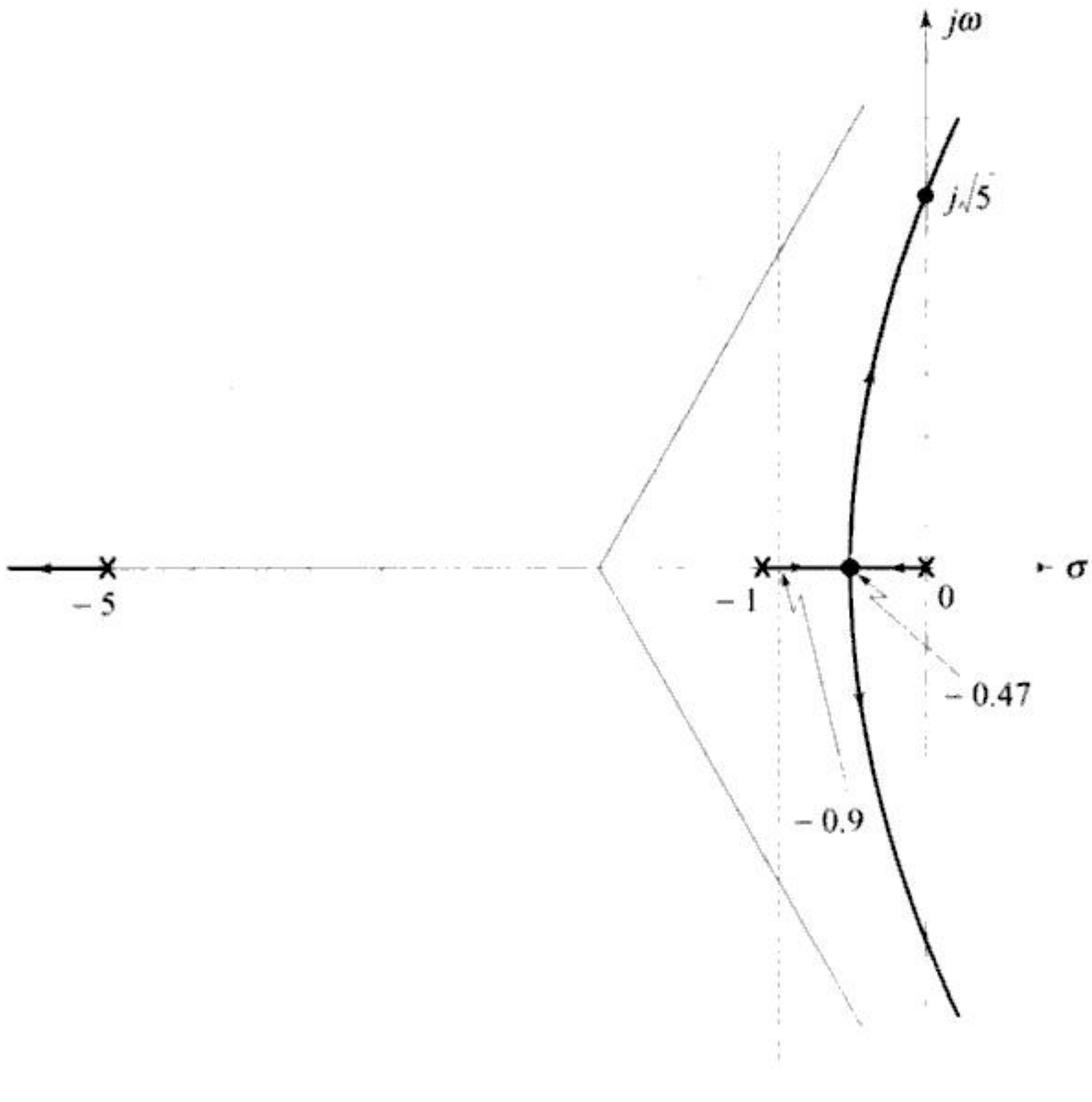


Fig. 7.60 *Root locus plot for the system of Fig. 7.59*

As a next try, we introduce an additional tachometer feedback as shown in Fig. 7.61. The characteristic equation of the system becomes

$$1 + \frac{AG(s)}{1 + sK_t G(s)} = 0 \tag{7.88}$$

where $$G(s) = \frac{2}{s(s+1)(s+5)}.$$

Rearranging, we get

$$s^3 + 6s^2 + (5 + 2K_t)\, s + 2A = 0$$

There are two variable parameters: A and K_t. We can use single-parameter root loci for the design by choosing a value for A. First we choose $A = 5$ and carry out the design. We will change the value of A appropriately if we find that the design is not possible with $A = 5$.

Copyrighted material



You have either reached a page that is unavailable for viewing or reached your viewing limit for this book.



You have either reached a page that is unavailable for viewing or reached your viewing limit for this book.



You have either reached a page that is unavailable for viewing or reached your viewing limit for this book.



You have either reached a page that is unavailable for viewing or reached your viewing limit for this book.



You have either reached a page that is unavailable for viewing or reached your viewing limit for this book.



You have either reached a page that is unavailable for viewing or reached your viewing limit for this book.



You have either reached a page that is unavailable for viewing or reached your viewing limit for this book.



You have either reached a page that is unavailable for viewing or reached your viewing limit for this book.



You have either reached a page that is unavailable for viewing or reached your viewing limit for this book.



You have either reached a page that is unavailable for viewing or reached your viewing limit for this book.

cally, the frequency-domain technique was the first method developed to design control systems. Harry Nyquist in 1932 published his study of stability theory, which is the foundation of the frequency-domain approach to control system analysis and design. The Nyquist criterion is a graphical procedure for illustrating system stability, or lack thereof. The complex plots (Nyquist plots) required can usually be sketched quickly without extensive mathematical calculations. System stability and the margins by which that stability is obtained (relative stability) are readily apparent from the sketch.

The general objective in all the frequency-domain design procedures is to shape the Nyquist plot to achieve acceptable closed-loop response characteristics. Direct use of the Nyquist plot for design is not particularly convenient, since changes in parameters other than gain require extensive plot revisions. The work of Hendrik W. Bode during the 1930s led to a more efficient design procedure: the general characteristics of the Nyquist plot can be visualized with reasonable accuracy in most cases of interest from the Bode plot shape, and the Bode plot is easily constructed and modified. The frequency-domain design procedures are reduced to orderly graphical trial-and-error processes carried out using the Bode plot. Thus, although the Nyquist plot characteristics form the basis for all of our designs, the mechanics of the design procedures are readily established on the Bode plot without requiring the construction of Nyquist plot.

A preview of the frequency-domain design procedure is as follows.

Step 1: Construct transfer function models for the controlled process, actuator, and the sensor. Validate the models $G(s)$ and $H(s)$ (refer Fig. 8.1) with experimental data where possible. Compute $G(j\omega)$ and $H(j\omega)$; $\omega \geq 0$.

Major strength of frequency-domain methods is that it does not need precise mathematical models. It uses only $G(j\omega)$ and $H(j\omega)$ which, for stable devices, can be obtained by direct measurement. Once $G(j\omega)$ and $H(j\omega)$ are measured, we may proceed directly to the design without computing the transfer functions $G(s)$ and $H(s)$.

Step 2: Investigate stability properties of a feedback structure of the form shown in Fig. 8.1.

Given the data $G(j\omega)$ and $H(j\omega)$; $\omega \geq 0$, computed from $G(s)$ and $H(s)$ with s replaced by $j\omega$, or obtained by experimental measurement, the stability of the closed-loop system can be determined by the Nyquist stability criterion using Nyquist plots/Bode plots.

Step 3: Translate the performance requirements into frequency-domain specifications.

There is a definite correlation between the time-domain and frequency-domain modes of behaviour. A common procedure is to interpret desired time-domain behaviour (step response with specified limits on rise time, peak overshoot, and settling time) in terms of frequency-domain characteristics. Design is carried out in the

Copyrighted material



You have either reached a page that is unavailable for viewing or reached your viewing limit for this book.



You have either reached a page that is unavailable for viewing or reached your viewing limit for this book.



You have either reached a page that is unavailable for viewing or reached your viewing limit for this book.

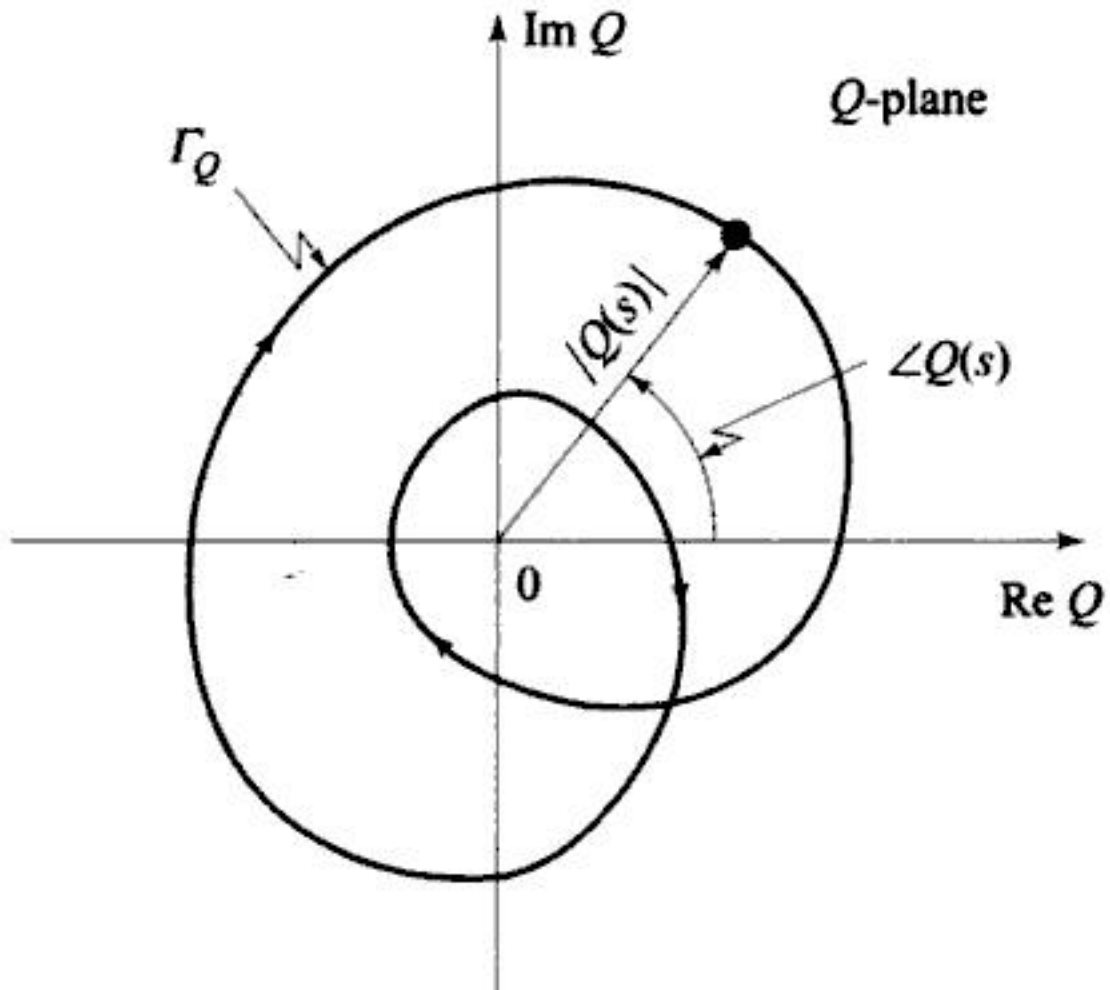


Fig. 8.4 *Q(s) evaluated on the contour Γ_s in Fig. 8.3*

where N is the number of clockwise encirclements of the origin that Γ_Q makes in the Q-plane. It may be noted that we are not interested in the exact shape of the $Q(s)$-plane contour. The important fact that concerns us is the encirclements of the origin by the $Q(s)$-plane contour.

The Principle of Argument

The relation (8.6) between the enclosure of poles and zeros of $Q(s)$ by the s-plane contour and the encirclements of the origin by the $Q(s)$-plane contour is commonly known as the *principle of argument* which may be stated as follows (refer Appendix A).

Let $Q(s)$ be a ratio of polynomials in s. Let P be the number of poles and Z be the number of zeros of $Q(s)$ which are enclosed by a simple closed contour in the s-plane, multiplicity accounted for. Let the closed contour be such that it does not pass through any poles or zeros of $Q(s)$. The s-plane contour then maps into the $Q(s)$-plane contour as a closed curve.

The number N of clockwise encirclements of the origin of the $Q(s)$-plane, as a representative point s traces out the entire contour in the s-plane in the clockwise direction, is equal to $Z - P$.

Since $$Q(s) = 1 + G(s)H(s),$$

we can obtain $Q(s)$-plane contour from the $G(s)H(s)$-plane contour simply by adding +1 to each point of $G(s)H(s)$-plane contour. Figure 8.5 shows a typical $G(s)H(s)$-plane contour Γ_{GH}. The effect of adding +1 to each point of Γ_{GH} to obtain $Q(s)$-plane contour Γ_Q is accomplished simply by adding +1 to the scale

Copyrighted material



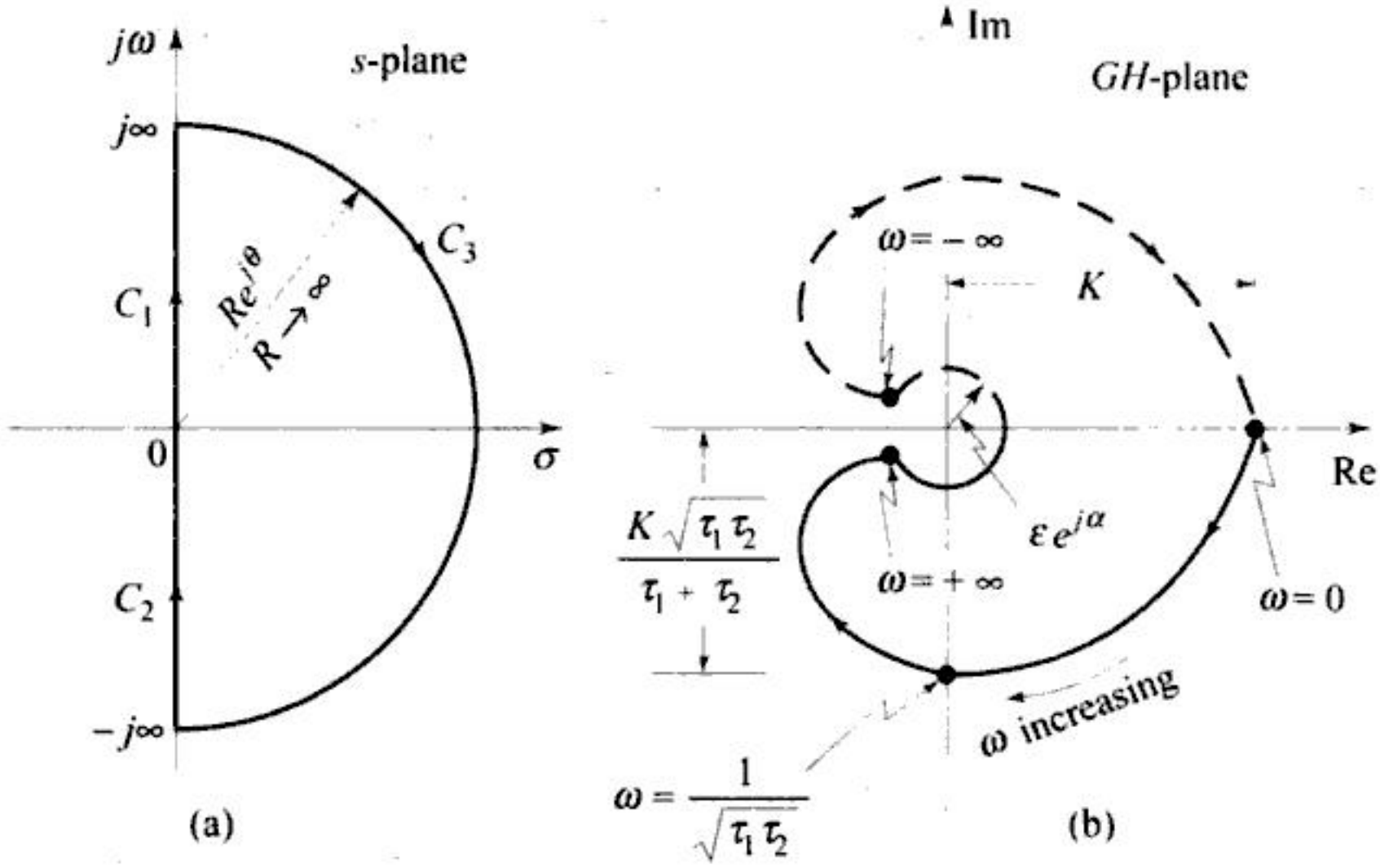
You have either reached a page that is unavailable for viewing or reached your viewing limit for this book.



You have either reached a page that is unavailable for viewing or reached your viewing limit for this book.



You have either reached a page that is unavailable for viewing or reached your viewing limit for this book.



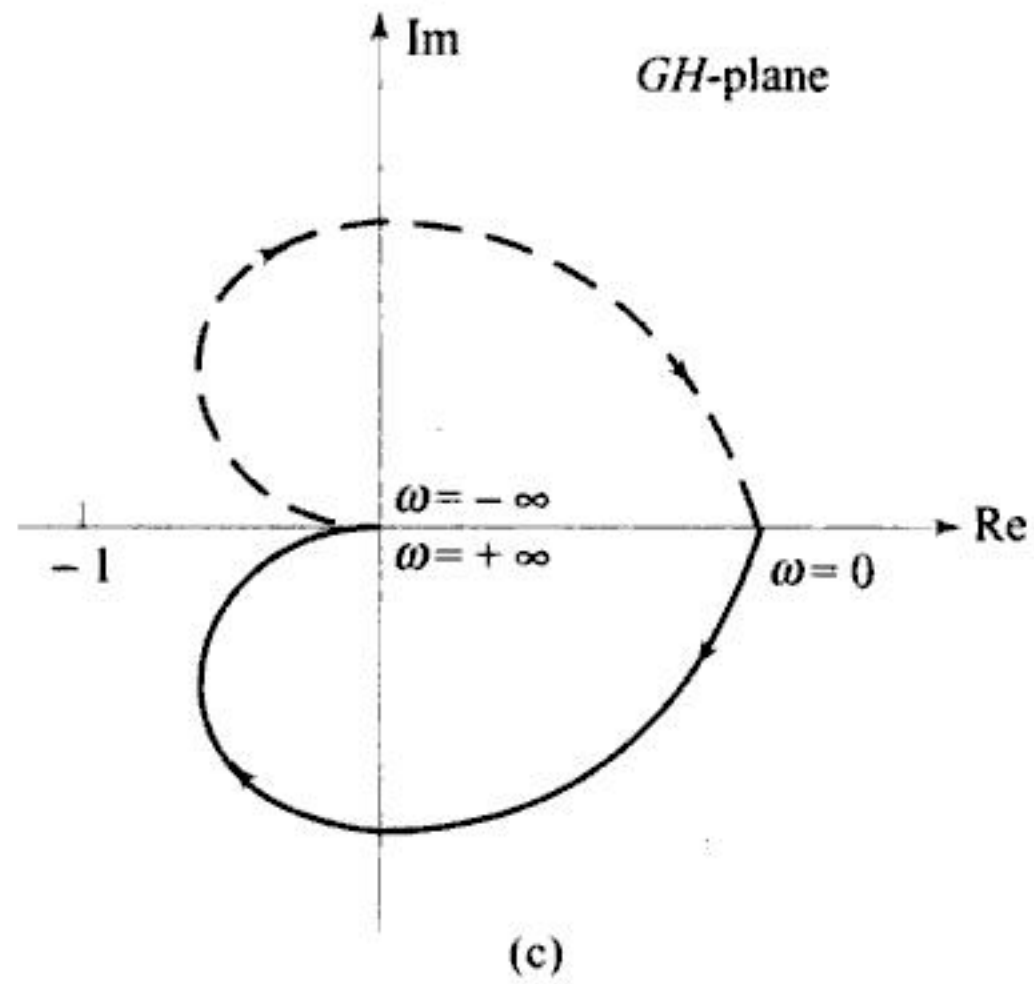


Fig. 8.9 *(a) Nyquist contour; (b) Nyquist plot of G(s)H(s) of Eqn. (8.9); (c) Simplified Nyquist plot*

For $G(j\omega)H(j\omega)$ given by Eqn. (8.10), the magnitude and phase at $\omega = 0$ and $\omega = \infty$ are calculated as follows:

$$\left|G(j\omega)H(j\omega)\right|_{\omega=0} = K$$

$$\angle G(j\omega)H(j\omega)\Big|_{\omega=0} = 0°$$

$$\left|G(j\omega)H(j\omega)\right|_{\omega\to\infty} = \left|\frac{K}{j^2\omega^2\tau_1\tau_2}\right|_{\omega\to\infty} = 0$$

Copyrighted material



You have either reached a page that is unavailable for viewing or reached your viewing limit for this book.



You have either reached a page that is unavailable for viewing or reached your viewing limit for this book.



You have either reached a page that is unavailable for viewing or reached your viewing limit for this book.



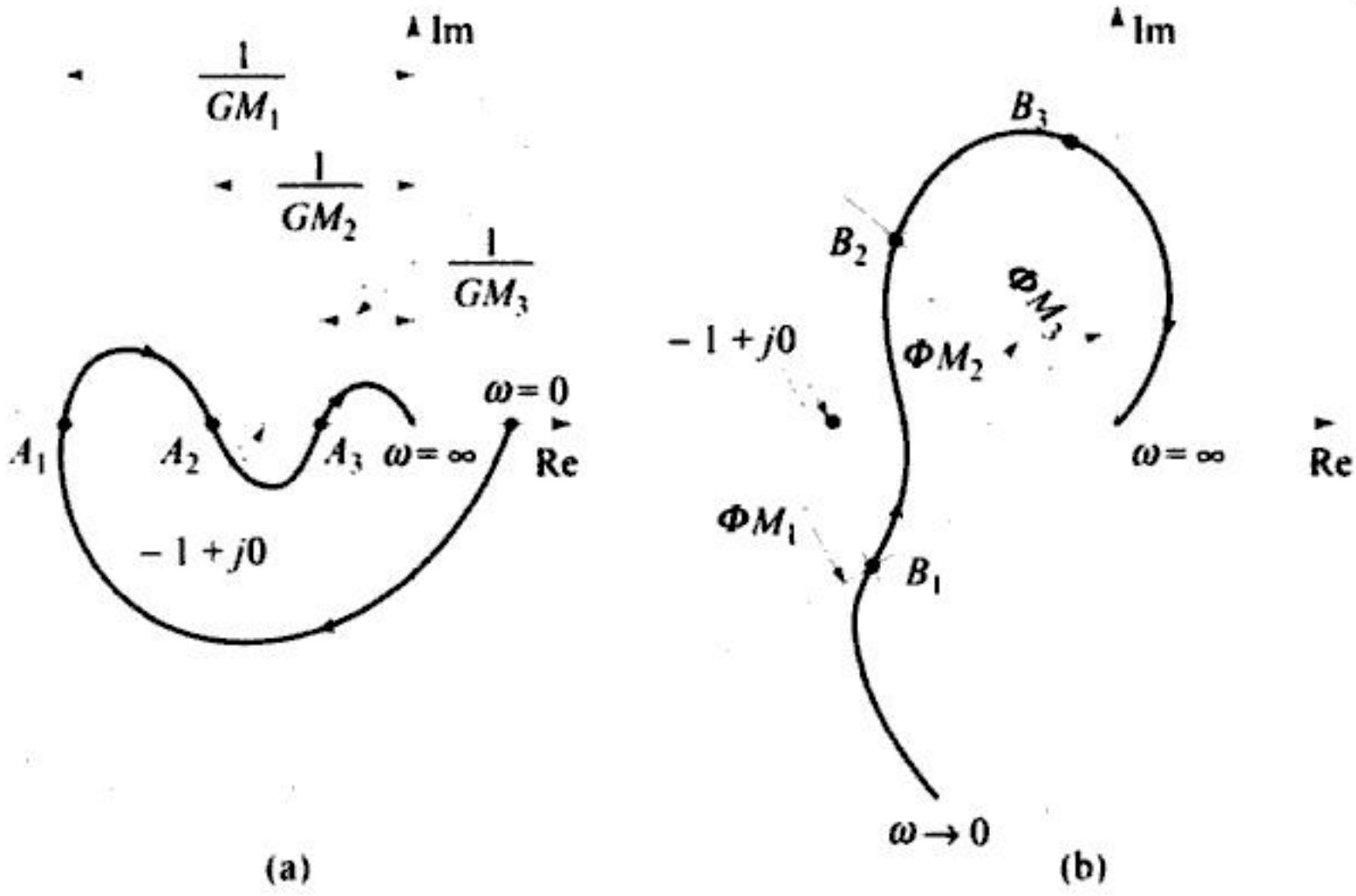
You have either reached a page that is unavailable for viewing or reached your viewing limit for this book.

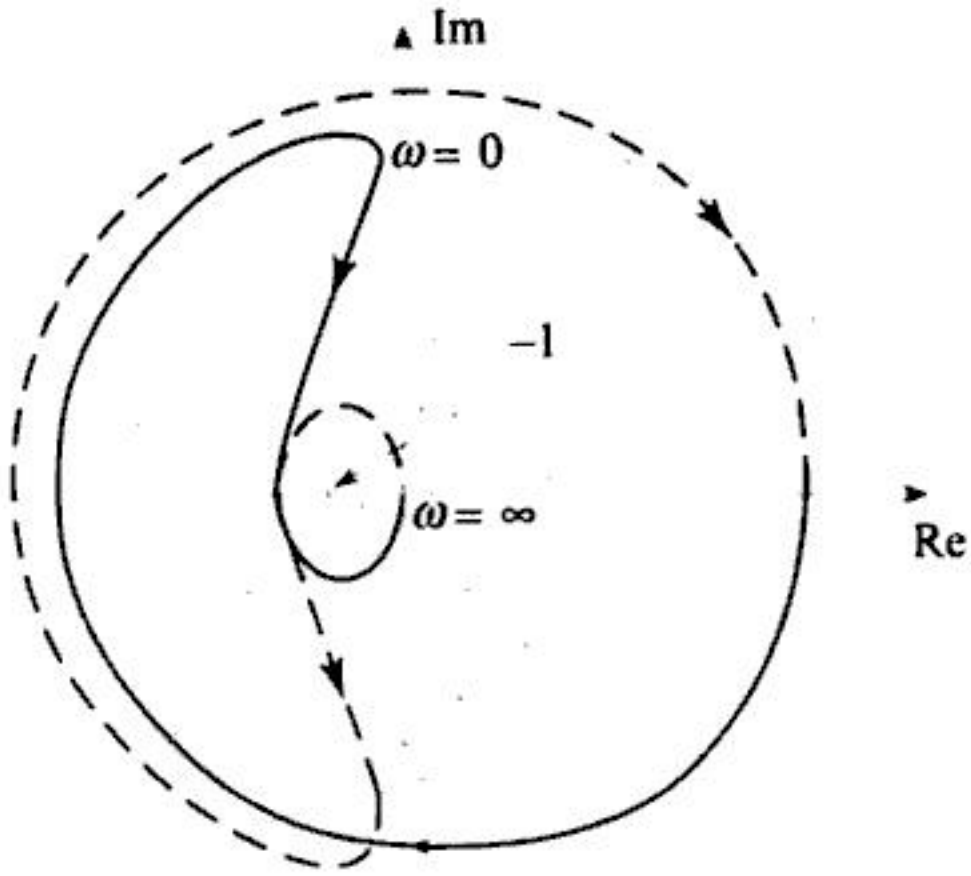


You have either reached a page that is unavailable for viewing or reached your viewing limit for this book.



You have either reached a page that is unavailable for viewing or reached your viewing limit for this book.





(c)

Fig. 8.21 *Nyquist plots requiring careful interpretation of GM and ΦM*

Example 8.7

A unity-feedback system has open-loop transfer function

$$G(s) = \frac{6}{(s^2 + 2s + 2)(s + 2)} \tag{8.25}$$

Since the open-loop poles are only in the left half s-plane, the Nyquist criterion tells us that we want no encirclement of $-1+j0$ point for stability. In such cases closed-loop stability can be evaluated from Nyquist $G(j\omega)$-plot.

$$G(j\omega)|_{\omega = 0} = 1.5\angle 0°; \quad G(j\omega)|_{\omega \to \infty} = 0\angle 90°$$

$$G(j\omega) = \left.\frac{6}{(s^2 + 2s + 2)(s + 2)}\right|_{s = j\omega}$$

Copyrighted material



You have either reached a page that is unavailable for viewing or reached your viewing limit for this book.



You have either reached a page that is unavailable for viewing or reached your viewing limit for this book.



You have either reached a page that is unavailable for viewing or reached your viewing limit for this book.



You have either reached a page that is unavailable for viewing or reached your viewing limit for this book.



You have either reached a page that is unavailable for viewing or reached your viewing limit for this book.



You have either reached a page that is unavailable for viewing or reached your viewing limit for this book.



You have either reached a page that is unavailable for viewing or reached your viewing limit for this book.

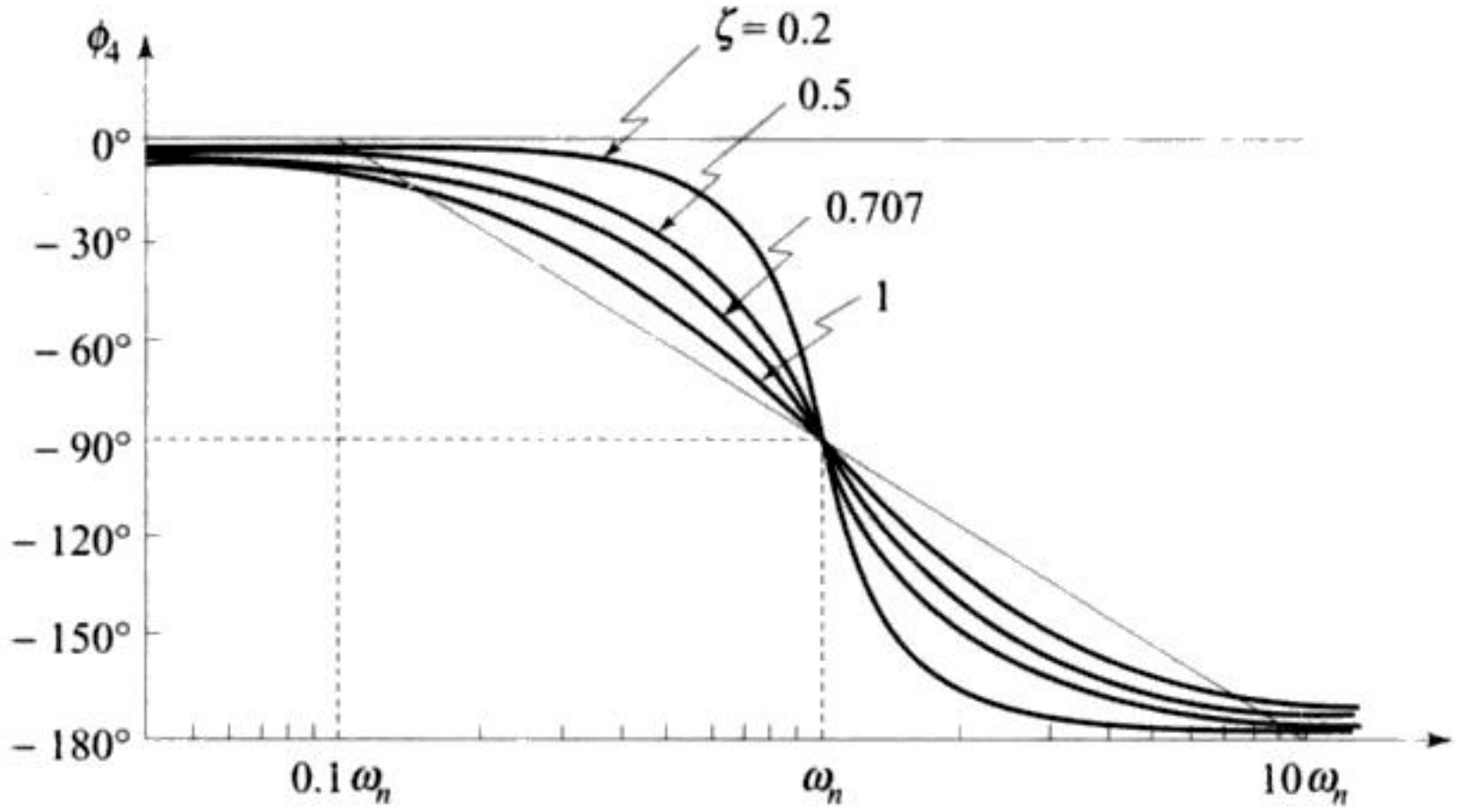


Fig. 8.34 *Phase characteristics of* $1/[1 + (j\,2\zeta/\omega_n)\omega - \omega^2/\omega_n^2\,]$

phase angle plot of any other factor. In this case, the phase angle plots for the various factors can be superimposed on each other to obtain the overall phase.

For a general case, it is usually advisable to make a table of phase angle against frequency for each factor and then obtain the total phase as the algebraic sum of these. Better accuracy is obtained by using the exact values in the table instead of those obtained through the asymptotic approximation. The computational effort to achieve this accuracy is not heavy.

Example 8.12

Consider the transfer function given in Eqn. (8.48) for which the magnitude plot was obtained in Fig. 8.32. We shall now plot the phase curve.

The phase angle due to each factor for different values of ω is given in Table 8.6. The plot of the total phase is shown in Fig. 8.35.

Table 8.6 *Phase angle due to different factors of the transfer function given by Eqn. (8.48)*

ω (rad/sec)	Poles at the origin	Zero at $s = -2$	Complex conjugate poles	Total phase angle, ϕ
0.1	– 90°	2.86°	– 0.57°	– 87.71°
0.2	– 90°	5.71°	– 1.15°	– 85.44°
0.5	– 90°	14.04°	– 2.87°	– 78.33°
1	– 90°	26.57°	– 5.77°	– 69.20°
2	– 90°	45.00°	– 11.77°	– 56.77°
5	– 90°	68.20°	– 33.69°	– 55.49°
10	– 90°	78.69°	– 90.00°	– 101.32°
20	– 90°	84.29°	– 146.31°	– 152.02°
50	– 90°	87.71°	– 168.23°	– 170.52°
100	– 90°	88.85°	– 174.22°	– 175.68°

Copyrighted material



You have either reached a page that is unavailable for viewing or reached your viewing limit for this book.



You have either reached a page that is unavailable for viewing or reached your viewing limit for this book.



You have either reached a page that is unavailable for viewing or reached your viewing limit for this book.

ω_ϕ = phase crossover frequency = 7 rad/sec
GM = gain margin = – 16.5 dB
ω_g = pain crossover frequency = 16 rad/sec
ΦM = phase margin = – 40°

The closed-loop system is thus unstable.

8.7 STABILITY ANALYSIS OF SYSTEMS WITH DEAD-TIME

Figure 8.38 shows the block diagram of a system with dead-time elements in the loop. Open-loop transfer function of the system is

$$G(s)H(s) = G_1(s)e^{-s\tau_D} \tag{8.52}$$

where $G_1(s)$ is a rational function.

Root locus analysis of systems with dead-time elements is possible, but the method is quite complex. In Section 7.11, root locus analysis was carried out using the following approximation:

$$e^{-s\tau_D} \cong \frac{1 - s\tau_D/2}{1 + s\tau_D/2}$$

This approximation works fairly well as long as the dead-time τ_D is small in comparison to the system time-constants.

The frequency-domain graphical methods provide a simple yet exact approach to handle the dead-time problem since the factor $e^{-s\tau_D}$ is readily interpreted in terms of either the Nyquist or the Bode plot.

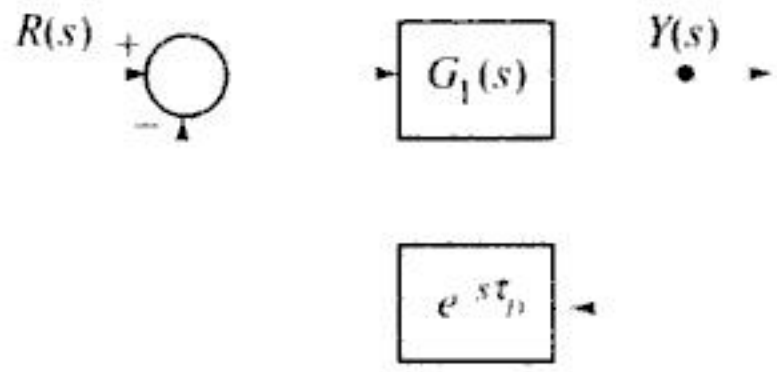


Fig. 8.38 *A closed-loop system with dead-time elements in the loop*

Assume that $G_1(s)$ in Fig. 8.38 is an integrator. Then the open-loop transfer function of the system becomes

$$G(s)H(s) = \frac{e^{-s\tau_D}}{j\omega}$$

The sinusoidal transfer function is

$$G(j\omega)H(j\omega) = \frac{e^{-j\omega\tau_D}}{j\omega}$$

Copyrighted material



You have either reached a page that is unavailable for viewing or reached your viewing limit for this book.



You have either reached a page that is unavailable for viewing or reached your viewing limit for this book.



You have either reached a page that is unavailable for viewing or reached your viewing limit for this book.



You have either reached a page that is unavailable for viewing or reached your viewing limit for this book.



You have either reached a page that is unavailable for viewing or reached your viewing limit for this book.



You have either reached a page that is unavailable for viewing or reached your viewing limit for this book.



You have either reached a page that is unavailable for viewing or reached your viewing limit for this book.



You have either reached a page that is unavailable for viewing or reached your viewing limit for this book.



You have either reached a page that is unavailable for viewing or reached your viewing limit for this book.



You have either reached a page that is unavailable for viewing or reached your viewing limit for this book.



You have either reached a page that is unavailable for viewing or reached your viewing limit for this book.



You have either reached a page that is unavailable for viewing or reached your viewing limit for this book.



You have either reached a page that is unavailable for viewing or reached your viewing limit for this book.



You have either reached a page that is unavailable for viewing or reached your viewing limit for this book.



You have either reached a page that is unavailable for viewing or reached your viewing limit for this book.



You have either reached a page that is unavailable for viewing or reached your viewing limit for this book.



You have either reached a page that is unavailable for viewing or reached your viewing limit for this book.



You have either reached a page that is unavailable for viewing or reached your viewing limit for this book.

content. Thus, if the control system is to faithfully follow a command that is changing rapidly, it must be capable of reproducing inputs at high frequencies, i.e., it must have a large bandwidth. On the other hand, if the command is slowly varying, the control system does not need a high bandwidth. A step change (i.e., a discontinuity) in the input has a large amount of high frequency content; to reproduce it faithfully (with a short rise time) requires a high bandwidth. If a short rise time is not required, then neither is a high bandwidth. Furthermore, all control systems are subject to noise during operation. Therefore, in addition to responding to the input signal, the system should be able to suppress noise and unwanted signals. The phase characteristics of the frequency response of a control system is also of importance, as it plays an important role in the stability of closed-loop systems. Shaping the frequency-response characteristics is the objective of the frequency-domain design methods.

When one has the frequency-response curves (obtained experimentally, or analytically using Eqn. (9.1b)) for any stable system, evaluation of the steady-state response to a sinusoidal input is straightforward. What is not obvious, but is extremely important, is that the frequency-response curves are really a *complete* description of the system's dynamic behaviour and allow one to compute the response to *any* input, not just sine waves.

The behaviour in the frequency domain of a given driving function $r(t)$ can be determined by the Fourier transform (refer Eqn. (A.26a) in Appendix A) as

$$R(j\omega) = \int_{-\infty}^{\infty} r(t)e^{-j\omega t}dt \tag{9.3a}$$

For a given control system, the frequency response of the controlled variable is

$$Y(j\omega) = \frac{G(j\omega)}{1 + G(j\omega)\,H(j\omega)}\,R(j\omega) = M(j\omega)R(j\omega) \tag{9.3b}$$

Inverse Fourier transformation (refer Eqn. (A.26b) in Appendix A) of $Y(j\omega)$ then gives the response

$$y(t) = \frac{1}{2\pi}\int_{-\infty}^{\infty} Y(j\omega)e^{j\omega t}d\omega \tag{9.3c}$$

Therefore, if we know the frequency response of a stable linear system, we can compute the dynamic response to any form of input. It should thus not be surprising that the control system performance can be (and is) described in frequency-response terms.

The correlation between transient response and frequency response through the Fourier integral forms an important basis of most design procedures and criteria. Usually the desired time-domain behaviour is interpreted in terms of

Copyrighted material



You have either reached a page that is unavailable for viewing or reached your viewing limit for this book.



You have either reached a page that is unavailable for viewing or reached your viewing limit for this book.



You have either reached a page that is unavailable for viewing or reached your viewing limit for this book.



You have either reached a page that is unavailable for viewing or reached your viewing limit for this book.



You have either reached a page that is unavailable for viewing or reached your viewing limit for this book.



You have either reached a page that is unavailable for viewing or reached your viewing limit for this book.



You have either reached a page that is unavailable for viewing or reached your viewing limit for this book.



You have either reached a page that is unavailable for viewing or reached your viewing limit for this book.



You have either reached a page that is unavailable for viewing or reached your viewing limit for this book.

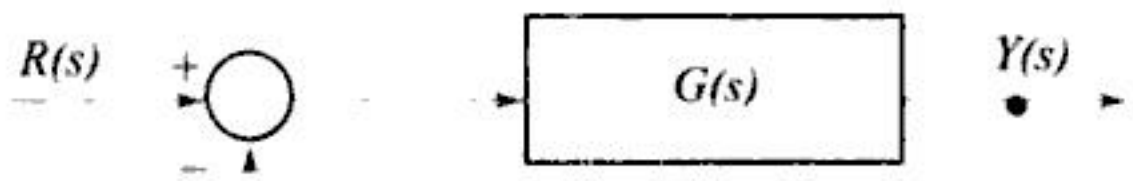


Fig. 9.19 *A unity-feedback system*

$$M(s) = \frac{G(s)}{1 + G(s)}$$

The frequency response of the closed-loop transfer function is given by

$$M(j\omega) = \frac{G(j\omega)}{1 + G(j\omega)} \tag{9.19}$$

Figure 9.20 shows a typical plot of $G(j\omega)$ in polar coordinates. Consider the point A on this plot associated with frequency ω_1. $G(j\omega_1)$ is a vector from the origin to the point A; and $1 + G(j\omega_1)$ is a vector from $-1 + j0$ point to the point A. One point on the closed-loop frequency response can be calculated by measuring lengths and angles of these vectors:

$$|M(j\omega_1)| = \frac{|G(j\omega_1)|}{|1 + G(j\omega_1)|}$$

$$\angle M(j\omega_1) = \angle G(j\omega_1) - \angle(1 + G(j\omega_1))$$

Obviously, this calculation can be repeated at many points on the $G(j\omega)$-curve, and the entire closed-loop frequency response can be calculated in this manner.

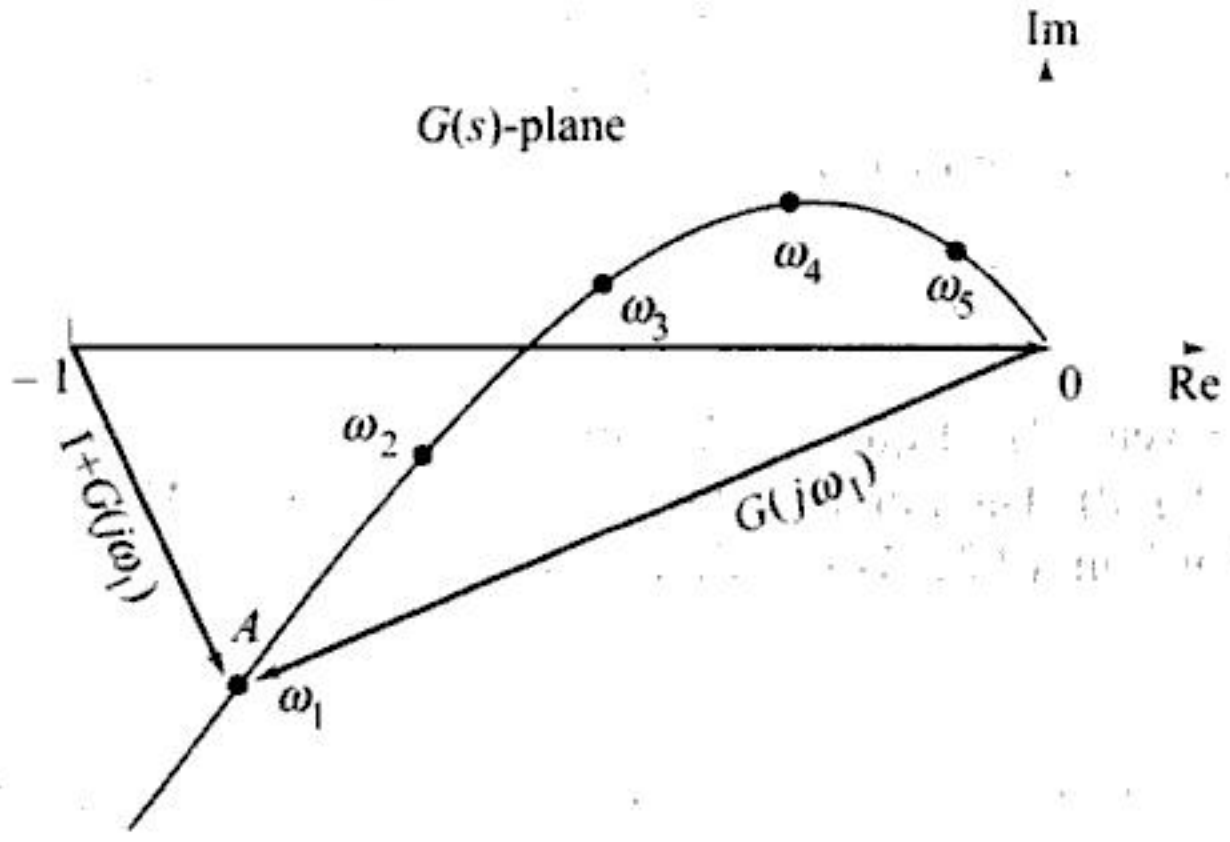


Fig. 9.20 *Polar relationship between open-loop and closed-loop frequency responses*

It is easier to prepare nomographs so that the results can be read off without additional calculations. Consider the graphical configuration of Fig. 9.20 as a

Copyrighted material



You have either reached a page that is unavailable for viewing or reached your viewing limit for this book.



You have either reached a page that is unavailable for viewing or reached your viewing limit for this book.



You have either reached a page that is unavailable for viewing or reached your viewing limit for this book.



You have either reached a page that is unavailable for viewing or reached your viewing limit for this book.



You have either reached a page that is unavailable for viewing or reached your viewing limit for this book.



You have either reached a page that is unavailable for viewing or reached your viewing limit for this book.



You have either reached a page that is unavailable for viewing or reached your viewing limit for this book.



You have either reached a page that is unavailable for viewing or reached your viewing limit for this book.



You have either reached a page that is unavailable for viewing or reached your viewing limit for this book.



You have either reached a page that is unavailable for viewing or reached your viewing limit for this book.



You have either reached a page that is unavailable for viewing or reached your viewing limit for this book.



You have either reached a page that is unavailable for viewing or reached your viewing limit for this book.



You have either reached a page that is unavailable for viewing or reached your viewing limit for this book.



You have either reached a page that is unavailable for viewing or reached your viewing limit for this book.



You have either reached a page that is unavailable for viewing or reached your viewing limit for this book.

margin, given by the open-loop frequency response, are indicators of relative stability. The objective of the frequency-response design is to reshape, by means of a compensator, the frequency-response plot of the basic system and achieve the performance specifications in terms of M_r, ω_r, ω_b, gain margin, phase margin, etc. We can obtain the transient-response parameters from the frequency-response parameters using the correlations developed in the previous chapter. These correlations are, however, approximate and give only qualitative information about the transient response.

The root-locus design provides very good indicators of the transient response of a system. However, we do need a relatively accurate model of the system to obtain these benefits from the root locus plots. In fact, various design techniques supplement each other, rather than one method excluding others; the control engineer must therefore be familiar with all the design methods.

This chapter is concerned with the changes that can be made in the frequency-response characteristics of a given system by various types of compensators. Design procedures to obtain improvement in the system performance are described.

10.2 RESHAPING THE BODE PLOT

The performance of a closed-loop system may be described in terms of the following frequency-domain specifications:

1. Phase margin ΦM/resonance peak M_r—indicative of relative stability.
2. Gain crossover frequency ω_g/bandwidth ω_b/resonance frequency ω_r—indicative of speed of response.
3. Error constants $K_p/K_v/K_a$—indicative of steady-state error to step/ramp/parabolic input.

In case the transient-response specifications are given in time domain, we must first translate these into frequency domain to carry out frequency-domain compensation. This translation is carried out by using the explicit correlations between the two domains for the standard second-order system. These correlations are valid approximations for higher-order systems dominated by a pair of complex conjugate poles. The correlations, developed earlier in chapter 9, are reproduced below for convenience of use.

$$\Phi M = \tan^{-1}\frac{2\zeta}{\sqrt{\sqrt{4\zeta^4+1}-2\zeta^2}} \cong 100\zeta \tag{10.1}$$

$$\omega_g = \omega_n\sqrt{\sqrt{4\zeta^4+1}-2\zeta^2} \tag{10.2}$$

$$M_r = \frac{1}{2\zeta\sqrt{1-\zeta^2}} \tag{10.3}$$

$$\omega_r = \omega_n\sqrt{1-2\zeta^2} \tag{10.4}$$

$$\omega_b = \omega_n\sqrt{\left[(1-2\zeta^2)+\sqrt{4\zeta^4-4\zeta^2+2}\right]} \tag{10.5}$$

Copyrighted material



You have either reached a page that is unavailable for viewing or reached your viewing limit for this book.



You have either reached a page that is unavailable for viewing or reached your viewing limit for this book.



You have either reached a page that is unavailable for viewing or reached your viewing limit for this book.



You have either reached a page that is unavailable for viewing or reached your viewing limit for this book.



You have either reached a page that is unavailable for viewing or reached your viewing limit for this book.



You have either reached a page that is unavailable for viewing or reached your viewing limit for this book.



You have either reached a page that is unavailable for viewing or reached your viewing limit for this book.



You have either reached a page that is unavailable for viewing or reached your viewing limit for this book.



You have either reached a page that is unavailable for viewing or reached your viewing limit for this book.



You have either reached a page that is unavailable for viewing or reached your viewing limit for this book.



You have either reached a page that is unavailable for viewing or reached your viewing limit for this book.



You have either reached a page that is unavailable for viewing or reached your viewing limit for this book.



You have either reached a page that is unavailable for viewing or reached your viewing limit for this book.



You have either reached a page that is unavailable for viewing or reached your viewing limit for this book.



You have either reached a page that is unavailable for viewing or reached your viewing limit for this book.



You have either reached a page that is unavailable for viewing or reached your viewing limit for this book.



You have either reached a page that is unavailable for viewing or reached your viewing limit for this book.



You have either reached a page that is unavailable for viewing or reached your viewing limit for this book.



You have either reached a page that is unavailable for viewing or reached your viewing limit for this book.



You have either reached a page that is unavailable for viewing or reached your viewing limit for this book.



You have either reached a page that is unavailable for viewing or reached your viewing limit for this book.



You have either reached a page that is unavailable for viewing or reached your viewing limit for this book.



You have either reached a page that is unavailable for viewing or reached your viewing limit for this book.



You have either reached a page that is unavailable for viewing or reached your viewing limit for this book.



You have either reached a page that is unavailable for viewing or reached your viewing limit for this book.



You have either reached a page that is unavailable for viewing or reached your viewing limit for this book.



You have either reached a page that is unavailable for viewing or reached your viewing limit for this book.



You have either reached a page that is unavailable for viewing or reached your viewing limit for this book.

Lead Compensator Implementation

Consider the RC network shown in Fig. 11.1. Assume that this network sees a small source impedance and that the output load impedance is large. Sometimes an isolating amplifier is inserted to ensure the validity of this assumption.

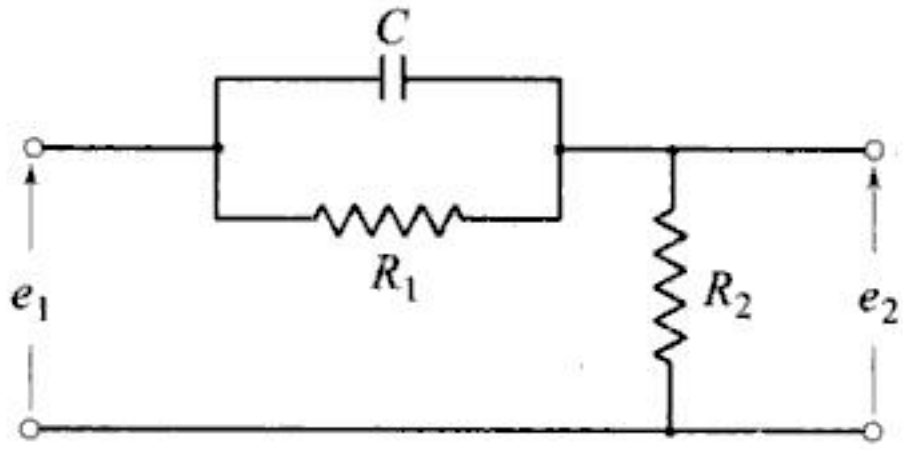


Fig. 11.1 *A lead network*

Taking these impedances to be zero and infinity, respectively, the transfer function of the network is derived as follows.

The equivalent impedance of R_1 and C is

$$Z(s) = \frac{R_1\left(\frac{1}{Cs}\right)}{R_1 + \frac{1}{Cs}} = \frac{R_1}{R_1Cs + 1}$$

The transfer function between the output $E_2(s)$ and the input $E_1(s)$ is

$$\frac{E_2(s)}{E_1(s)} = \frac{R_2}{Z(s) + R_2} = \frac{R_2}{R_1 + R_2}\left(\frac{R_1Cs + 1}{\frac{R_1R_2}{R_1 + R_2}Cs + 1}\right)$$

Define

$$R_1C = \tau \tag{11.2a}$$

$$\frac{R_2}{R_1 + R_2} = \alpha < 1$$

Then the transfer function becomes

$$\frac{E_2(s)}{E_1(s)} = \alpha\left(\frac{\tau s + 1}{\alpha\tau s + 1}\right) = \frac{s + 1/\tau}{s + 1/\alpha\tau} \tag{11.2b}$$

This transfer function has a real zero at $s = -1/\tau$ and a real pole at $s = -1/\alpha\tau$ with the pole to the left of the zero, as is shown in Fig. 11.2. The network of Fig. 11.1 thus realizes a lead compensator. The values of the three parameters R_1, R_2, and C are determined from the two compensator parameters τ and α using Eqns (11.2a). There is an additional degree of freedom in the choice of the values of the network components which is used to set the impedance level of the network.

Copyrighted material



You have either reached a page that is unavailable for viewing or reached your viewing limit for this book.



You have either reached a page that is unavailable for viewing or reached your viewing limit for this book.



You have either reached a page that is unavailable for viewing or reached your viewing limit for this book.

$$D(s) = \underbrace{\left(\frac{\tau_1 s + 1}{\beta\tau_1 s + 1}\right)}_{\text{Lag section}} \underbrace{\left(\frac{\tau_2 s + 1}{\alpha\tau_2 s + 1}\right)}_{\text{Lead section}}; \beta > 1,\ \alpha < 1,\ \tau_1,\ \tau_2 > 0 \qquad (11.6)$$

The attenuation factor α of the lead compensator is not included in the equation assuming that adequate loop gain is available in the system to compensate for this attenuation.

A lag-lead compensator can be realized by cascading the lead and the lag networks. However, a single network can be used to realize the transfer function in Eqn. (11.6) if α and β need not be specified independently.

Let us examine the RC network shown in Fig. 11.8, to see whether it realizes a lag-lead compensator. With the usual impedance assumptions, the transfer function of the network is derived as follows.

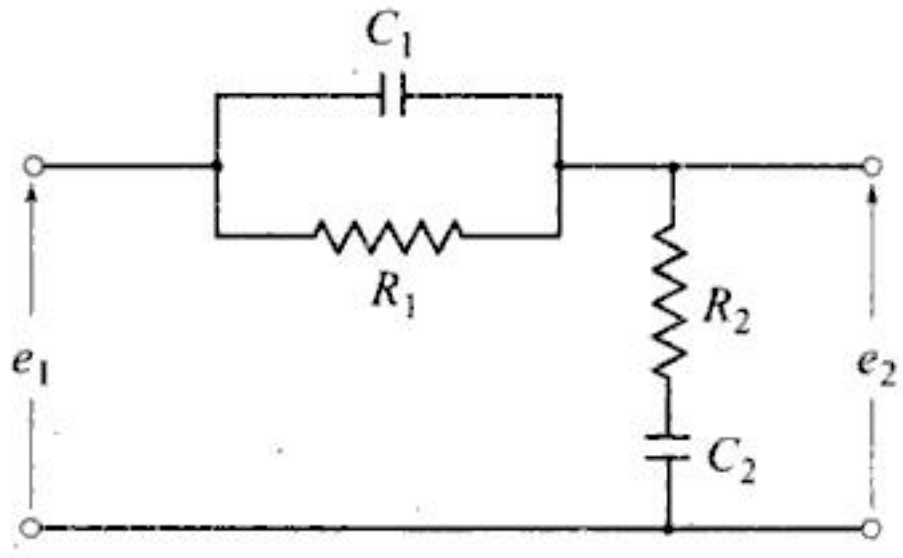


Fig. 11.8 *A lag-lead network*

The equivalent impedance of R_1 and C_1 is

$$Z_1(s) = \frac{R_1\left(\frac{1}{C_1 s}\right)}{R_1 + \frac{1}{C_1 s}} = \frac{R_1}{R_1 C_1 s + 1},$$

and the equivalent impedance of R_2 and C_2 is

$$Z_2(s) = R_2 + \frac{1}{C_2 s}$$

The transfer function between the output $E_2(s)$ and the input $E_1(s)$ is

$$\frac{E_2(s)}{E_1(s)} = \frac{Z_2(s)}{Z_1(s) + Z_2(s)} = \frac{(R_1 C_1 s + 1)(R_2 C_2 s + 1)}{(R_1 C_1 s + 1)(R_2 C_2 s + 1) + R_1 C_2 s}$$

The denominator of the transfer function can be factored into two real terms. Let us define

$$R_1 C_1 = \tau_1; \quad R_2 C_2 = \tau_2$$

$$R_1 C_1 + R_2 C_2 + R_1 C_2 = \beta\tau_1 + \frac{1}{\beta}\tau_2; \beta > 1 \qquad (11.7a)$$

Copyrighted material



You have either reached a page that is unavailable for viewing or reached your viewing limit for this book.



You have either reached a page that is unavailable for viewing or reached your viewing limit for this book.



You have either reached a page that is unavailable for viewing or reached your viewing limit for this book.



You have either reached a page that is unavailable for viewing or reached your viewing limit for this book.



You have either reached a page that is unavailable for viewing or reached your viewing limit for this book.



You have either reached a page that is unavailable for viewing or reached your viewing limit for this book.



You have either reached a page that is unavailable for viewing or reached your viewing limit for this book.



You have either reached a page that is unavailable for viewing or reached your viewing limit for this book.



You have either reached a page that is unavailable for viewing or reached your viewing limit for this book.



You have either reached a page that is unavailable for viewing or reached your viewing limit for this book.



You have either reached a page that is unavailable for viewing or reached your viewing limit for this book.



You have either reached a page that is unavailable for viewing or reached your viewing limit for this book.



You have either reached a page that is unavailable for viewing or reached your viewing limit for this book.



You have either reached a page that is unavailable for viewing or reached your viewing limit for this book.



You have either reached a page that is unavailable for viewing or reached your viewing limit for this book.



You have either reached a page that is unavailable for viewing or reached your viewing limit for this book.



You have either reached a page that is unavailable for viewing or reached your viewing limit for this book.



You have either reached a page that is unavailable for viewing or reached your viewing limit for this book.



You have either reached a page that is unavailable for viewing or reached your viewing limit for this book.



You have either reached a page that is unavailable for viewing or reached your viewing limit for this book.



You have either reached a page that is unavailable for viewing or reached your viewing limit for this book.



You have either reached a page that is unavailable for viewing or reached your viewing limit for this book.



You have either reached a page that is unavailable for viewing or reached your viewing limit for this book.



You have either reached a page that is unavailable for viewing or reached your viewing limit for this book.



You have either reached a page that is unavailable for viewing or reached your viewing limit for this book.



You have either reached a page that is unavailable for viewing or reached your viewing limit for this book.



You have either reached a page that is unavailable for viewing or reached your viewing limit for this book.



You have either reached a page that is unavailable for viewing or reached your viewing limit for this book.



You have either reached a page that is unavailable for viewing or reached your viewing limit for this book.



You have either reached a page that is unavailable for viewing or reached your viewing limit for this book.



You have either reached a page that is unavailable for viewing or reached your viewing limit for this book.



You have either reached a page that is unavailable for viewing or reached your viewing limit for this book.



You have either reached a page that is unavailable for viewing or reached your viewing limit for this book.



You have either reached a page that is unavailable for viewing or reached your viewing limit for this book.



You have either reached a page that is unavailable for viewing or reached your viewing limit for this book.



You have either reached a page that is unavailable for viewing or reached your viewing limit for this book.



You have either reached a page that is unavailable for viewing or reached your viewing limit for this book.



You have either reached a page that is unavailable for viewing or reached your viewing limit for this book.



You have either reached a page that is unavailable for viewing or reached your viewing limit for this book.



You have either reached a page that is unavailable for viewing or reached your viewing limit for this book.



You have either reached a page that is unavailable for viewing or reached your viewing limit for this book.



You have either reached a page that is unavailable for viewing or reached your viewing limit for this book.



You have either reached a page that is unavailable for viewing or reached your viewing limit for this book.



You have either reached a page that is unavailable for viewing or reached your viewing limit for this book.



You have either reached a page that is unavailable for viewing or reached your viewing limit for this book.



You have either reached a page that is unavailable for viewing or reached your viewing limit for this book.



You have either reached a page that is unavailable for viewing or reached your viewing limit for this book.



You have either reached a page that is unavailable for viewing or reached your viewing limit for this book.



You have either reached a page that is unavailable for viewing or reached your viewing limit for this book.



You have either reached a page that is unavailable for viewing or reached your viewing limit for this book.



You have either reached a page that is unavailable for viewing or reached your viewing limit for this book.



You have either reached a page that is unavailable for viewing or reached your viewing limit for this book.



You have either reached a page that is unavailable for viewing or reached your viewing limit for this book.



You have either reached a page that is unavailable for viewing or reached your viewing limit for this book.



You have either reached a page that is unavailable for viewing or reached your viewing limit for this book.



You have either reached a page that is unavailable for viewing or reached your viewing limit for this book.



You have either reached a page that is unavailable for viewing or reached your viewing limit for this book.



You have either reached a page that is unavailable for viewing or reached your viewing limit for this book.



You have either reached a page that is unavailable for viewing or reached your viewing limit for this book.



You have either reached a page that is unavailable for viewing or reached your viewing limit for this book.



You have either reached a page that is unavailable for viewing or reached your viewing limit for this book.



You have either reached a page that is unavailable for viewing or reached your viewing limit for this book.



You have either reached a page that is unavailable for viewing or reached your viewing limit for this book.



You have either reached a page that is unavailable for viewing or reached your viewing limit for this book.



You have either reached a page that is unavailable for viewing or reached your viewing limit for this book.



You have either reached a page that is unavailable for viewing or reached your viewing limit for this book.



You have either reached a page that is unavailable for viewing or reached your viewing limit for this book.



You have either reached a page that is unavailable for viewing or reached your viewing limit for this book.



You have either reached a page that is unavailable for viewing or reached your viewing limit for this book.



You have either reached a page that is unavailable for viewing or reached your viewing limit for this book.



You have either reached a page that is unavailable for viewing or reached your viewing limit for this book.



You have either reached a page that is unavailable for viewing or reached your viewing limit for this book.



You have either reached a page that is unavailable for viewing or reached your viewing limit for this book.



You have either reached a page that is unavailable for viewing or reached your viewing limit for this book.



You have either reached a page that is unavailable for viewing or reached your viewing limit for this book.



You have either reached a page that is unavailable for viewing or reached your viewing limit for this book.



You have either reached a page that is unavailable for viewing or reached your viewing limit for this book.



You have either reached a page that is unavailable for viewing or reached your viewing limit for this book.



You have either reached a page that is unavailable for viewing or reached your viewing limit for this book.



You have either reached a page that is unavailable for viewing or reached your viewing limit for this book.



You have either reached a page that is unavailable for viewing or reached your viewing limit for this book.



You have either reached a page that is unavailable for viewing or reached your viewing limit for this book.



You have either reached a page that is unavailable for viewing or reached your viewing limit for this book.



You have either reached a page that is unavailable for viewing or reached your viewing limit for this book.



You have either reached a page that is unavailable for viewing or reached your viewing limit for this book.



You have either reached a page that is unavailable for viewing or reached your viewing limit for this book.



You have either reached a page that is unavailable for viewing or reached your viewing limit for this book.



You have either reached a page that is unavailable for viewing or reached your viewing limit for this book.



You have either reached a page that is unavailable for viewing or reached your viewing limit for this book.



You have either reached a page that is unavailable for viewing or reached your viewing limit for this book.



You have either reached a page that is unavailable for viewing or reached your viewing limit for this book.



You have either reached a page that is unavailable for viewing or reached your viewing limit for this book.



You have either reached a page that is unavailable for viewing or reached your viewing limit for this book.



You have either reached a page that is unavailable for viewing or reached your viewing limit for this book.



You have either reached a page that is unavailable for viewing or reached your viewing limit for this book.



You have either reached a page that is unavailable for viewing or reached your viewing limit for this book.



You have either reached a page that is unavailable for viewing or reached your viewing limit for this book.



You have either reached a page that is unavailable for viewing or reached your viewing limit for this book.



You have either reached a page that is unavailable for viewing or reached your viewing limit for this book.



You have either reached a page that is unavailable for viewing or reached your viewing limit for this book.



You have either reached a page that is unavailable for viewing or reached your viewing limit for this book.



You have either reached a page that is unavailable for viewing or reached your viewing limit for this book.



You have either reached a page that is unavailable for viewing or reached your viewing limit for this book.



You have either reached a page that is unavailable for viewing or reached your viewing limit for this book.



You have either reached a page that is unavailable for viewing or reached your viewing limit for this book.



You have either reached a page that is unavailable for viewing or reached your viewing limit for this book.



You have either reached a page that is unavailable for viewing or reached your viewing limit for this book.



You have either reached a page that is unavailable for viewing or reached your viewing limit for this book.



You have either reached a page that is unavailable for viewing or reached your viewing limit for this book.



You have either reached a page that is unavailable for viewing or reached your viewing limit for this book.



You have either reached a page that is unavailable for viewing or reached your viewing limit for this book.



You have either reached a page that is unavailable for viewing or reached your viewing limit for this book.



You have either reached a page that is unavailable for viewing or reached your viewing limit for this book.

23. For the negative feedback system shown in Fig. Q23, the effective time-constant is

(A) L/R
(B) Less than L/R
(C) more than L/R
(D) zero

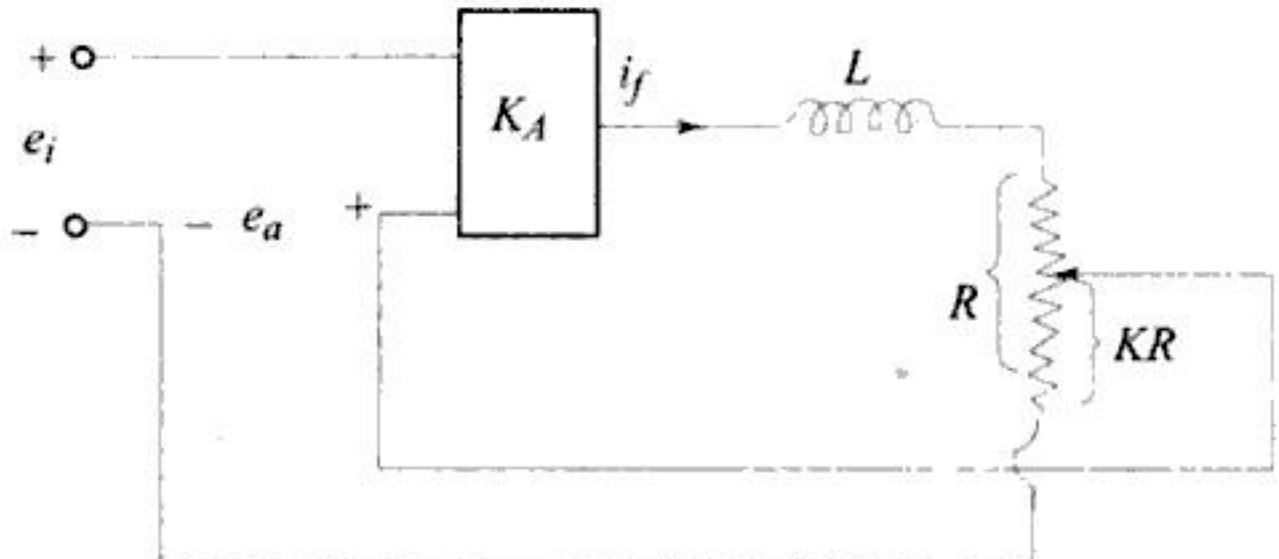
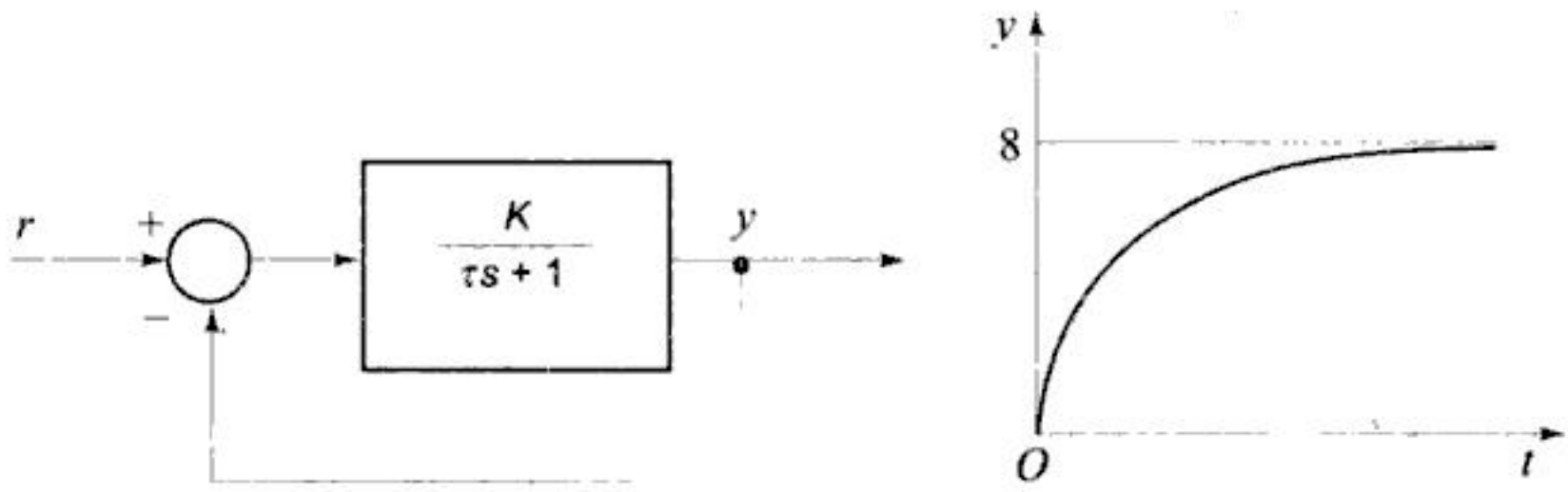


Fig. Q23

24. The time response of the system of Fig. Q24a to an input $r(t) = 10\ \mu(t)$ is shown in Fig. Q24b. The gain K is equal to

(A) 10
(B) 8
(C) 4
(D) None of the answers in (A), (B), and (C) is correct



(a) (b)

Fig. Q24

25. An inertial and a frictional load are driven by a dc motor with torque T_M. The dynamic model of the system is

$$T_M(t) = J\frac{d\omega(t)}{dt} + B\omega(t)$$

The steady-state speed of the motor for step input will be doubled when

(A) inertia J is doubled
(B) friction B is doubled
(C) both the inertia J and friction B are doubled
(D) None of the answers in (A), (B), and (C) is correct

Copyrighted material



You have either reached a page that is unavailable for viewing or reached your viewing limit for this book.



You have either reached a page that is unavailable for viewing or reached your viewing limit for this book.



You have either reached a page that is unavailable for viewing or reached your viewing limit for this book.



You have either reached a page that is unavailable for viewing or reached your viewing limit for this book.



You have either reached a page that is unavailable for viewing or reached your viewing limit for this book.



You have either reached a page that is unavailable for viewing or reached your viewing limit for this book.



You have either reached a page that is unavailable for viewing or reached your viewing limit for this book.



You have either reached a page that is unavailable for viewing or reached your viewing limit for this book.



You have either reached a page that is unavailable for viewing or reached your viewing limit for this book.



You have either reached a page that is unavailable for viewing or reached your viewing limit for this book.



You have either reached a page that is unavailable for viewing or reached your viewing limit for this book.



You have either reached a page that is unavailable for viewing or reached your viewing limit for this book.



You have either reached a page that is unavailable for viewing or reached your viewing limit for this book.



You have either reached a page that is unavailable for viewing or reached your viewing limit for this book.



You have either reached a page that is unavailable for viewing or reached your viewing limit for this book.



You have either reached a page that is unavailable for viewing or reached your viewing limit for this book.



You have either reached a page that is unavailable for viewing or reached your viewing limit for this book.

Control Systems

Principles and Design

Second Edition

Retaining the basic foundation of the first edition, the revised edition is updated by the coverage on MATLAB. The balance between mathematical rigour and physical interpretation has been maintained.

SALIENT FEATURES

- Includes a new section on MATLAB 6 (the latest version) offers a computer- aided learning environment. This section provides 16 MATLAB based projects, with tested outputs.
- Emphasises the frequency-domain design methods using root locus and Nyquist/Bode/Nichols plots.
- Details important hardware and software aspects of implementation of controllers, including tunable PID controllers.
- Provides delightful range of real-world applications from manufacturing industry and process industry.
- Presents state variable methods for control system analysis.
- Includes a comprehensive quiz on control systems having 120 multiple-choice questions with answers – the questions follow the pattern of treatment in the book and enable a comprehensive revision of the material.
- Includes a Question Bank on Control Theory (105 questions) added to the book, with hints to the answers.

http://www.mhhe.com/gopal/controlsystems

Tata McGraw-Hill
A Division of The McGraw-Hill Companies

Visit us at: www.tatamcgrawhill.com

ISBN 0-07-048289-6



Copyrighted material